

ANALYSIS OF THE DEVELOPMENTAL AND PHYSIOLOGICAL
ROLES OF HISTONE DEACETYLASES 1 AND 2.

Thesis submitted for the degree of
Doctor of Philosophy
at the University of Leicester

by

Oliver M. Dovey

College of Medicine, Biological Sciences, and Psychology
/Department of Biochemistry

University of Leicester

February 2012

Oliver M. Dovey.

Analysis of the developmental and physiological roles of histone deacetylases 1 and 2.

Abstract

Histone deacetylases (HDAC) 1 and 2 are highly similar enzymes that help regulate chromatin structure as the core catalytic components of co-repressor complexes. Although tissue specific deletion of HDAC1 and HDAC2 has demonstrated functional redundancy, germline deletion of HDAC1 in the mouse causes early embryonic lethality, whereas HDAC2 does not. To address the unique requirement for HDAC1 in early embryogenesis I have generated conditional knock-out mouse embryonic stem (mES) cells in which HDAC1 or HDAC2 genes can be inactivated. Deletion of HDAC1, but not HDAC2, causes a significant reduction in the HDAC activity of Sin3A, NuRD and CoREST co-repressor complexes. This reduced co-repressor activity results in a specific 1.6-fold increase in histone H3 K56 acetylation, providing genetic evidence that H3K56Ac is a substrate of HDAC1. In culture, loss of HDAC1 but not HDAC2 leads to precocious mES cell differentiation. This genetic study of HDAC1 and HDAC2 in mES cells, which mimic the embryonic epiblast, has identified a unique requirement for HDAC1 in the optimal activity of HDAC1/2 co-repressor complexes and cell fate determination during differentiation.

Given previous demonstrations of the roles of HDAC1/2 known co-repressor complexes in T cell development and the functional redundancy between HDAC1 and -2 in a number of tissues, a conditional knock-out approach was undertaken in murine T cells. I have demonstrated that HDAC1 and -2 exert pleiotropic effects on T-cell development. I have also shown, for the first time in a physiological system, that HDAC1/2 activity is critical for maintaining genome stability. The occurrence of tumours (and the developmental block) is dose dependent, occurring in cells with the least amount of deacetylase activity, indicating that regulation of the acetyl-proteome, a balance between HAT and HDAC enzymes is crucial for normal cell development and viability.

Acknowledgements

I wish to thank my supervisor, Dr Shaun Cowley, for his faith and endless encouragement. He has been a real tutor and given me the freedom and environment to explore, within reason, my scientific potential to its fullest. I'd also like to express my gratitude to my friend and colleague of the last four or so years, Dr Charles Foster the undisputed king of "Chrombobs". He has been a great pal and to have shared this experience with a human, whose head is strikingly magnificent, has been a competitive, hilarious and wonderful time in my life. With the deepest sincerity, I'll miss them both a great deal. I'd also like to express my gratitude to Professors John Schwabe and Ian Eperon for their time as part of my Thesis committee. My thanks also to Bipin Patel, Dr Neil Bate, Samantha Carrera and Nico Portolano. I'd especially like to thank Dr Kayoko Tanaka and Dr Salvador Macip for their frequent shoulders to cry on and support throughout our shared time in the lab, I wish them all great things.

Without the support of friends and family this would not have been possible and I'm deeply indebted to my Mum and Tony in particular. An extra special thanks to the Shawes, Christopher-Frimley and Nicola, likewise the Vivienne-Nelsons, Mark and Alison, for sharing the load.

Finally, and most importantly, I'd like to thank my wife, Eirini, for her endless patience and the occasional motivational rally.....it's almost over!!

List of Contents

Abstract	ii
Acknowledgements	iii
List of Contents	iv
List of Figures	xii
List of Tables	xix
Abbreviations	xx
Chapter One: Introduction.	1
1.1 Histones, the nucleosome core particle and chromatin.	1
1.2 Functional divides between chromatin structures.	3
1.3 Altering chromatin accessibility.	5
1.3.1 <i>Post translational histone modifications.</i>	6
1.3.2 <i>Mechanisms and functional consequences of histone modifications.</i>	8
1.3.3 <i>Direct structural disturbance by histone PTMs.</i>	8
1.3.4 <i>Indirectly altering chromatin via “reading” histone PTMs.</i>	12
1.4 HDACs and transcriptional activation.	17
1.5 Non-histone substrates of HDACs.	21
1.6 The KDAC/HDAC family of enzymes.	22
1.7 Class I HDAC co-repressor complexes.	25
1.8 Functions of class 1 and II HDACs in mammals.	28
1.8.1 <i>Germ-line deletion of class I and II HDACs.</i>	28
1.8.2 Tissue specific deletion of HDACs 1 and -2.	30
1.9 Intra-thymic T cell development.	33

1.10	Transcription factors and co-repressor complexes in T cell development.	39
1.10.1	<i>Key transcription factors in T cell development.</i>	40
1.10.2	<i>The roles of co-repressors complexes and chromatin modifying enzymes in T cell development.</i>	44
1.10.3	<i>Histone deacetylases in thymic T cell development.</i>	46
	Chapter Two: Materials and Methods.	48
2.1	Chemicals and reagents.	48
2.2	Culture and manipulation of mouse embryonic stem cells.	48
2.2.1	<i>Thawing and seeding mES cells.</i>	48
2.2.2	<i>Passage of mES cells.</i>	49
2.2.3	<i>Freezing and storage of mES cell stocks.</i>	50
2.2.4	<i>Population doubling, colony formation and alkaline phosphatase assays.</i>	51
2.2.5	<i>In vitro differentiation of mES cells, embryoid body formation.</i>	52
2.2.7	<i>Neuronal lineage differentiation of mES cells.</i>	52
2.2.7	<i>Media and reagents used for the culture and manipulation of mouse embryonic stem cells.</i>	53
2.3	mES cell gene targeting and molecular cloning.	54
2.3.1	<i>Targeting vector/DNA electroporation.</i>	54
2.3.2	<i>Transient transfection of mES cells by lipofection.</i>	55
2.3.3	<i>Positive and negative selection of targeted/transfected mES cells.</i>	55
2.3.4	<i>Recombineering.</i>	56

2.3.5	<i>Induction of LoxP recombination in targeted mES cells.</i>	58
2.3.6	<i>Generation of FLAG-tagged Hdac1 expression construct.</i>	59
2.3.6.1	<i>Introduction of FLAG epitopes to the C' of Hdac1.</i>	59
2.3.6.2	<i>Enzymatic digestion of pcDNA3.1(+) vector.</i>	60
2.3.6.3	<i>PCR fragment insert/vector ligation.</i>	61
2.3.7	<i>Plasmids and recombineering reagents.</i>	62
2.3.7.1	<i>HDAC1-cKO-Neo.</i>	62
2.3.7.2	<i>HDAC2-cKO-Neo.</i>	62
2.3.7.3	<i>HDAC2-cKO-Neo.</i>	63
2.3.7.4	<i>pCAGGS-FLPe.</i>	63
2.3.7.5	<i>pcDNA3.1(+).</i>	64
2.4	<i>gDNA, mRNA, protein and histone sample extraction.</i>	64
2.4.1	<i>HotSHOT preparation of mouse ear DNA for PCR genotyping.</i>	64
2.4.2	<i>gDNA extraction.</i>	65
2.4.3	<i>Total mRNA extraction.</i>	66
2.4.4	<i>Protein extraction.</i>	67
2.4.5	<i>Histone extraction and post translational modification analysis.</i>	68
2.4.6	<i>Lysis buffers.</i>	69
2.4.7	<i>Co-immunoprecipitation.</i>	70
2.4.8	<i>Deacetylase assays.</i>	71
2.5	<i>Molecular biology.</i>	72
2.5.1	<i>gDNA polymerase chain reaction (PCR).</i>	72
2.5.2	<i>Reverse transcription and quantitative real time PCR.</i>	73
2.5.3	<i>Storage and revival of bacterial strains.</i>	74
2.5.4	<i>Culture of bacterial strains for “mini” and “maxi-preparation”.</i>	74

2.5.5	<i>Plasmid purification, gel extraction and PCR/enzymatic digest column purification.</i>	75
2.5.6	<i>DNA sequencing.</i>	75
2.5.7	<i>Southern blotting.</i>	76
2.5.7.1	<i>Southern blotting gel electrophoresis.</i>	76
2.5.7.2	<i>Neutral transfer of nucleic acid to nylon membranes.</i>	76
2.5.7.3	<i>DNA Southern blot probe labelling.</i>	77
2.5.7.4	<i>Membrane washing and development.</i>	78
2.5.7.5	<i>Global DNA methylation analysis by Southern blot.</i>	78
2.6	<i>Fluorescence activated cell sorting (FACS).</i>	79
2.6.1	<i>Isolation of mouse thymocytes and splenocytes.</i>	79
2.6.2	<i>Positive isolation of CD4/CD8 cells from total splenocytes.</i>	79
2.6.3	<i>Staining of mouse cells for T cell development analysis by FACS.</i>	80
2.6.4	<i>Apoptosis detection in mouse thymocytes by FACS.</i>	81
2.7	<i>Histological and immunohistochemical analysis.</i>	82
2.7.1	<i>Immunohistochemistry of ATRA treated EBs.</i>	83
2.7.2	<i>Immunohistochemistry of paraffin embedded tissues.</i>	83
2.7.2.1	<i>Antigen retrieval.</i>	83
2.7.2.2	<i>Immuno-staining.</i>	84
2.8	<i>Global transcriptome and DNA copy number variation analysis.</i>	85
2.8.1	<i>Global gene expression profiling using Illumina MouseWG-6 v2 Expression BeadChip microarrays.</i>	85
2.8.2	<i>Comparative genomic hybridisation using the Agilent Mouse Genome Comparative Genomic Hybridisation 244K Microarray.</i>	86

Chapter Three: Generation of inducible HDAC1 and HDAC2 conditional knock-out mouse ES cell-lines and T cell specific HDAC1 and HDAC2

knock-out mice.	88
3.1 Chapter aims.	88
3.2 Strategy for generating homozygous conditional knock-out HDAC1 and HDAC2 mES cell lines.	90
3.2.1 <i>Targeting the 1st wild type allele of Hdac1 and Hdac2 in E14 CreER-T mES cells.</i>	91
3.2.2 <i>Generation of the second Hdac1 and Hdac2 targeting vector.</i>	95
3.2.3 <i>Targeting the 2nd wild type allele of Hdac1 or Hdac2 in E14 CreER-T mES cells.</i>	99
3.2.4 <i>FLPe-mediated deletion of selection markers in Hdac1^{Neo/HygΔTk} and Hdac2^{Neo/HygΔTk} double targeted E14 CreER-T mES cells.</i>	100
3.3 Ligand inducible deletion of HDAC1 and HDAC2 in Hdac1 ^{Lox/Lox} and Hdac2 ^{Lox/Lox} E14 CreER-T mES cell lines.	103
3.4 Generation of HDAC1 ^{Lox/Lox} rescue mES cells lines.	108
3.4.1 <i>Generation of an Hdac1 C' FLAG-tagged expression construct (Hdac1-C-FLAG-Resc).</i>	108
3.4.2 <i>Generation of transient and stably transfected HDAC1^{Lox/Lox} and HDAC1^{Δ2/Δ2} mES cell lines.</i>	109
3.5 Generation of T cell specific conditional HDAC1 and knock-out mice.	114
3.5.1 <i>Strategy for generating T cell specific Cre-mediated conditionally inactivated Hdac1 and Hdac2 alleles.</i>	114

3.5.2	<i>Generation of targeted HD1^{Neo/+} and HD2^{Neo/+} mice harbouring a knocked-in Gt(Rosa)26Sor-FLPe allele.</i>	115
3.5.3	<i>Germ-line transmission of Hdac1^{Lox} and Hdac2^{Lox} alleles.</i>	117
3.5.4	<i>Generation of heterozygous and homozygous Hdac1^{Lox} and Hdac2^{Lox} mice carrying the T cell specific LckCre transgene.</i>	119
3.5.5	<i>Conditional deletion of HDAC1 or HDAC2 in HD1^{L/L:LckCre} and HD2^{L/L:LckCre} mice.</i>	120
3.5.6	<i>Generation of compound heterozygous HD1^{L/L}HD2^{L/+LckCre} and HD1^{L/+}HD2^{L/L:LckCre}, double homozygous HD1^{L/L}HD2^{L/L:LckCre} T cell specific knock-out mice.</i>	123
3.6	Conclusions.	125
3.6.1	<i>Successful generation of homozygous conditional knock-out HDAC1 and HDAC2 mES cell lines.</i>	125
3.6.2	<i>Generation of HDAC1^{Lox/Lox} rescue mES cell lines.</i>	126
3.6.3	<i>Successful Generation of T cell specific conditional knock-out HDAC1 and HDAC2 mouse lines.</i>	128

Chapter Four: HDAC1, but not HDAC2, Controls Embryonic Stem

	Cell Differentiation.	130
4.1	Chapter aims.	130
4.2	HDAC1/2 complexes have reduced HDAC activity in the absence of HDAC1.	130
4.3	Proliferation and differentiation capacity of mES cells is not inhibited by loss of HDAC1 or HDAC2.	135

4.4	Loss of HDAC1, but not HDAC2, causes enhanced differentiation of embryoid bodies.	140
4.4.1	<i>Increased expression of cardiomyocyte, muscle and neuronal specific markers in embryoid bodies lacking HDAC1.</i>	145
4.4.2	<i>Differentiation of EBs lacking HDAC1 into neuronal lineages is further enhanced upon treatment with ATRA.</i>	149
4.4.3	<i>Serum dependent and serum independent enhanced differentiation of EBs lacking HDAC1.</i>	153
4.5	Stable transfection of the Hdac1-C-FLAG-Resc construct fails to prevent the established differentiation phenotype of HDAC1 ^{Δ2/Δ2} EBs.	159
4.6	Conclusions.	161

Chapter Five: HDAC1 and 2 are required for normal thymocyte development and are major contributors to the maintenance of thymocyte genomic stability. **162**

5.1	Chapter aims.	162
5.2	The LckCre transgene does not affect normal T cell development.	162
5.3	Incomplete deletion of HDAC2 in HD1&2 ^{Δ2/Δ2} double knock-out thymocytes from 6-8 week old mice.	163
5.4	HDAC1 and -2 are required for normal thymocyte development.	166
5.4.1	<i>Mutant-CD8 cells are immature thymocytes that fail to express CD4 at the DP stage.</i>	173

5.4.2	<i>De-repression of CD8 in HD1^{Δ2/Δ2};HD2^{WT/Δ2} immature double negative thymocytes.</i>	180
5.4.3	<i>Deletion of HDAC 1 and -2 in HD1&2^{Δ2/Δ2} neonatal thymocytes reveals a delay during β-selection and an increase in apoptosis during the DN-DP transition.</i>	182
5.4.4	<i>HDAC1 and -2 deficient thymocytes exhibit positive selection defects and reduced CD4 lineage commitment post selection.</i>	184
5.4.5	<i>The maturation block in HD1^{Δ2/Δ2};HD2^{WT/Δ2} mutant thymocytes is independent of TCR complex formation.</i>	192
5.5	<i>Reduced HDAC activity and co-repressor complex integrity in HDAC1 and -2 knock-out thymocytes.</i>	195
5.6	<i>HD1^{Δ2/Δ2};HD2^{WT/Δ2} and HD1&2^{Δ2/Δ2} conditional knock-out mice exhibit a lethal pathology as a result of intra-thymic T cell neoplastic transformation.</i>	201
5.6.1	<i>T cell lymphomas in HD1^{Δ2/Δ2};HD2^{WT/Δ2} mice are associated with chromosomal instability.</i>	209
5.6.2	<i>Global gDNA methylation levels are unaltered in T cell lymphomas of HD1^{Δ2/Δ2};HD2^{WT/Δ2} mice.</i>	212
5.6.3	<i>Gene expression profiling of pre-lymphomic HD1^{Δ2/Δ2};HD2^{WT/Δ2} thymocytes.</i>	214
5.7	<i>Global histone hyperacetylation of T cells in the absence of HDAC1 but not HDAC2.</i>	220
5.8	<i>Conclusions.</i>	223

Chapter Six: Discussion **225**

6.1	HDAC1, but not HDAC2, regulates H3K56ac and is required for optimal deacetylase activity of HDAC1/2 complexes in mES cells.	225
6.2	Loss of HDAC1 or HDAC2 does not affect cell cycle in mES cells.	226
6.3	HDAC1 is required for the controlled re-programming of mES cells upon differentiation.	227
6.3.1	<i>HDAC1 mediates neuronal and cardiac cell differentiation of mES cells.</i>	229
6.4	Putative mechanisms of precocious differentiation in HDAC1 deficient mES cells: HDAC1 is required for the control of SRF centred cardiomyocyte differentiation.	233
6.5	Optimal levels of HDAC1 are required to maintain controlled mES cell differentiation.	239
6.6	mES cell summary.	239
6.7	HDAC1 is required for optimal deacetylase activity in developing thymocytes.	240
6.8	HDAC1 and -2 are required for expression of CD4 at the double positive stage of development.	242
6.9	HDAC1 and -2 are required for the progression of T cells from the DN-DP stage of thymocyte development and repression of CD8 at the double negative stage of T cell development.	247
6.10	HDAC1 and -2 are required for positive selection and post selection lineage commitment of thymocytes.	249
6.11	HDAC1 and -2 maintain normal levels of global acetylation which contributes to chromosomal stability in developing thymocytes.	251

6.12 Summary: HDACs 1 and -2 are required for normal T cell development and maintenance of genome stability.	255
--	-----

APPENDIX ONE: PCR PRIMERS AND RESTRICTION ENZYMES	256
--	------------

APPENDIX TWO: CHAPTER 3 SEQUENCING RESULTS	260
---	------------

APPENDIX THREE: ANTIBODIES	263
-----------------------------------	------------

APPENDIX FOUR: ARRAY COMPARATIVE GENOMIC HYBRIDISATION RESULTS	265
---	------------

APPENDIX FIVE: PRE-LYMPHOMIC COMPARATIVE MICROARRAY ANALYSIS	275
---	------------

References	282
-------------------	------------

List of Figures

Figure 1.1 *Chromatin consists of DNA, histones and non-histone protein.*

Figure 1.2 *The reversible acetylation and deacetylation of lysine residues.*

Figure 1.3 *The “classic” binary model for the mutually exclusive utilisation of HDAC associated co-repressor and HAT associated co-activator complexes, based on the function of un-liganded and ligand bound nuclear hormone receptors.*

- Figure 1.4. *A model for the utilization of histone deacetylases (HDAC) during the process of transcriptional activation.*
- Figure 1.5. *Schematic depiction of mammalian histone deacetylases.*
- Figure 1.6. *Germ-line HDAC loss-of-function phenotypes in mice.*
- Figure 1.7. *Overview of T cell developmental sub-populations as defined by the expression of cell surface markers.*
- Figure 1.8. *Overview of intra-thymic T cell development.*
- Figure 1.9. *Kinetic signalling model of T cell lineage commitment.*
- Figure 1.10. *Key transcriptional factors, corepressors and chromatin modifiers in intra-thymic T cell development.*
-
- Figure 2.1 *Diagrammatic representation of capillary transfer apparatus.*
- Figure 3.1 *Strategy for generating conditional HDAC1 and HDAC2 knock-out mES cell lines.*
- Figure 3.2 *Strategy for generating conditional HDAC1 knock-out mES cell lines.*
- Figure 3.3 *Strategy for generating conditional HDAC2 knock-out mES cell lines.*
- Figure 3.4 *Successful targeting of the 1st wild type allele of Hdac1 and Hdac2.*
- Figure 3.5 *Generation of the HDAC1-cKO-Hyg Δ Tk targeting vector.*
- Figure 3.6 *Generation of the HDAC2-cKO-Hyg Δ Tk targeting vector.*
- Figure 3.7 *Successful targeting of the 2nd wild type allele of Hdac1 and Hdac2.*
- Figure 3.8 *FLPe-mediated excision of selection markers.*

- Figure 3.9 *Generation of inducible HDAC1 conditional knock-out mES cell lines.*
- Figure 3.10 *Generation of inducible HDAC2 conditional knock-out mES cell lines.*
- Figure 3.11 *Ligand inducible deletion of HDAC1 and HDAC2 in multiple $Hdac1^{Lox/Lox}$ and $Hdac2^{Lox/Lox}$ mES cell lines.*
- Figure 3.12 *Strategy for generating $Hdac1$ -C'-FLAG-Resc constructs.*
- Figure 3.13 *Generation of transient and stably transfected $HDAC1^{Lox/Lox}$ and $HDAC1^{\Delta2/\Delta2}$ mES cell lines.*
- Figure 3.14 *Generation of T cell specific conditional HDAC1 knock-out mice.*
- Figure 3.15 *PCR genotyping strategies used for generating of T cell specific conditional HDAC1 and HDAC2 knock-out mice.*
- Figure 3.16 *$LckCre$ induced site specific recombination of $Hdac1^{Lox}$ and $Hdac2^{Lox}$ alleles.*
- Figure 3.17 *Generation of HDAC1 and HDAC2 T cell specific conditional knock-out mice.*
- Figure 3.18 *HDAC1 and HDAC2 T cell specific experimental cohorts.*
- Figure 4.1 *Deletion of HDAC1 results in an increased level of HDAC2 protein.*
- Figure 4.2 *Loss of HDAC1 results in decreased deacetylase activity associated with HDAC1/2 complexes.*
- Figure 4.3 *Loss of HDAC1 results in an increase H3K56Ac.*

- Figure 4.4 *H3K56Ac is regulated by HDAC1 in addition to other zinc-dependent HDAC enzymes.*
- Figure 4.5 *Conditional deletion of HDAC1 or 2 does not inhibit the growth of mES cells.*
- Figure 4.6 *Conditional deletion of HDAC1 or 2 does not inhibit the differentiation potential of mES cells.*
- Figure 4.7 *Loss of HDAC1 enhances embryoid body differentiation.*
- Figure 4.8 *Expression of the prototypical HDAC1 target gene p21 is unaltered in HDAC1^{Δ2/Δ2} mES cells.*
- Figure 4.9 *Loss of HDAC1 causes precocious differentiation into mesodermal and ectodermal lineages at the expense of endoderm in EBs.*
- Figure 4.10 *Treatment of EBs with ATRA promotes differentiation and inhibits formation of mesoderm.*
- Figure 4.11 *Differentiation into neuronal lineages in EBs lacking HDAC1 is further enhanced upon treatment with ATRA*
- Figure 4.12 *Serum free culture of HDAC1^{Lox/Lox} and HDAC1^{Δ2/Δ2} EBs.*
- Figure 4.13 *Serum dependent and serum independent differentiation of HDAC1^{Δ2/Δ2} EBs.*
- Figure 4.14 *HDAC1^{Resc} mES cell lines fail to “rescue” the phenotype observed in HDAC1^{Δ2/Δ2} embryoid bodies.*
- Figure 5.1 *Presence of the LckCre transgene does not affect normal thymocyte development.*
- Figure 5.2 *Incomplete deletion of HDAC2 in HD1&2^{Δ2/Δ2} double knock-out thymocytes.*

- Figure 5.3 *Increased thymocyte cellularity in HD1^{Δ2/Δ2};HD2^{WT/Δ2} and HD1&2^{Δ2/Δ2} in 6-8 week old mice.*
- Figure 5.4 *HDAC1 and -2 are required for normal thymocyte development.*
- Figure 5.5 *Neonatal thymocytes exhibit similar intra-thymic developmental defects as observed in 6-8 week old mice.*
- Figure 5.6 *Mutant-CD8 thymocytes exhibit an immature T cell profile.*
- Figure 5.7 *De-repression of CD8 in immature double negative HD1^{Δ2/Δ2};HD2^{WT/Δ2} thymocytes.*
- Figure 5.8 *Analysis of HDAC1 and -2 in neonatal HD1&2^{Δ2/Δ2} thymocytes reveals a delay at the β-selection checkpoint and increased cell death at the DN-DP transition.*
- Figure 5.9 *Cell surface expression of CD8α and CD8β is unaffected in HD1^{Δ2/Δ2};HD2^{WT/Δ2} thymocytes.*
- Figure 5.10 *Reduced numbers of “selection” thymocytes in HD1^{WT/Δ2};HD2^{Δ2/Δ2} and HD1^{Δ2/Δ2};HD2^{WT/Δ2} mice.*
- Figure 5.11 *The developmental block in thymocytes of HD1^{Δ2/Δ2};HD2^{WT/Δ2} mutant mice is independent of TCR complex formation.*
- Figure 5.12 *Reduced deacetylase activity associated with HDAC1 and -2 complexes.*
- Figure 5.13 *Increased apoptosis detected in mutant-CD8 thymocytes of HD1^{Δ2/Δ2};HD2^{WT/Δ2} mice.*
- Figure 5.14 *Development of pathological diseased state in HD1^{Δ2/Δ2};HD2^{WT/Δ2} and HD1&2^{Δ2/Δ2}.*

- Figure 5.15 *Thymocytes of diseased secondary lymphatic organs are immature mutant-CD8 cells.*
- Figure 5.16 *Diseased tissues exhibit characteristics of increased proliferation.*
- Figure 5.17 *HD1^{Δ2/Δ2};HD2^{WT/Δ2} and HD1&2^{Δ2/Δ2} thymocytes are increasingly clonal.*
- Figure 5.18 *HD1^{Δ2/Δ2};HD2^{WT/Δ2} T cell tumours are associated with chromosomal instability.*
- Figure 5.19 *Global gDNA methylation levels are unaffected in T cell lymphomas of HD1^{Δ2/Δ2};HD2^{WT/Δ2} mice.*
- Figure 5.20 *Gene expression profiling of pre-lymphomic HD1^{Δ2/Δ2};HD2^{WT/Δ2} thymocytes.*
- Figure 5.21 *Global histone hyperacetylation of T cells in the absence of HDAC1 but not HDAC2.*
- Figure 6.1 *Summary of putative mechanisms of precocious differentiation in HDAC1 deficient mES cells: HDAC1 is required for the control of SRF centred cardiomyocyte differentiation.*

List of Tables

- Table 1.1 *Mammalian histone-modifying enzymes and their histone substrates.*
- Table 1.2 *Functional outcomes of histone modifications.*
- Table 1.3 *Histone post-translational modifications and their protein domain binding partners.*
- Table 1.4. *The composition of class I HDAC complexes.*

Abbreviations

4-OHT	4-hydroxytamoxifen
ac	acetyl
<i>Actc</i>	<i>alpha, cardiac muscle actin</i>
<i>Afp</i>	<i>alpha fetoprotein</i>
Amp	ampicillin
<i>Apex1</i>	<i>apurinic/aprimidinic endonuclease 1</i>
ATP	adenosine triphosphate
ATRA	all-trans retinoic acid
aCGH	array comparative genomic hybridisation
B220	CD45R
BAC	bacterial artificial chromosome
BAF	BRG1- or hbrm-associated factors
BF-GO terms	biological function gene ontology term
BGH	bovine growth hormone
<i>bet</i>	<i>bacteriophage lambda bet gene</i>
<i>brachyury</i>	<i>T box transcription factor</i>
BSA	bovine serum albumin

<i>Cad</i>	<i>carbamoyl-phosphate synthetase 2, aspartate transcarbamylase, and dihydroorotase</i>
CCB	cell collection buffer
CD4	cluster of differentiation 4
CD4 ^{Int}	CD4 intermediate thymocytes
CD5	cluster of differentiation 5
CD8 α	cluster of differentiation 8 alpha
CD8 β	cluster of differentiation 8 beta
CD8 ^{ISP}	CD8 intermediate single positive thymocytes
CD25	cluster of differentiation 25, IL-2 receptor alpha chain
CD44	cluster of differentiation 44
CD69	cluster of differentiation 69
CDK	cyclin dependent kinase
<i>Cdk4</i>	<i>cyclin dependent kinase 4</i>
cDNA	complimentary deoxyribonucleic acid
Cdt1	chromatin licensing and DNA replication factor 1
ChIP	chromatin immunoprecipitation
cKO	conditional knock-out
C-MYC/ <i>c-myc</i>	myelocytomatosis oncogene

CMV	cytomegalovirus
CNS	Central Nervous System
CNV	copy number variation
Co-IP	coimmunoprecipitation
CoREST	co-repressor to REST (RE1 silencing transcription factor/neural restrictive silencing factor)
CreER-T	cre recombinase, estrogen receptor, tamoxifen inducible
Ct	cross threshold
Cy3	cyanine 3
Cy5	cyanine 5
Cy5.5	cyanine 5.5
DAB	3,3'-Diaminobenzidine
DAPI	4, 6-diamidino-2-phenylindole
DAVID	database for annotation, visualization and integrated discovery
<i>Dclre1c</i>	<i>DNA cross-link repair 1C, PSO2 homolog (S. cerevisiae)</i>
dCTP	deoxycytosine triphosphate
dNTP	deoxyribonucleotide triphosphate
ddH ₂ O	double distilled H ₂ O

DEPC	diethylpyrocarbonate
<i>Deltex</i>	<i>protein deltex 1</i>
DMEM	Dulbecco's modified eagle medium
DN	double negative thymocytes
DNA	deoxyribonucleic acid
DNMT1/ <i>Dnmt1</i>	DNA (cytosine-5)-methyltransferase 1
DNMT3b/ <i>Dnmt3b</i>	DNA (cytosine-5)-methyltransferase 3b
DP	double positive thymocytes
EASE	expression analysis systematic explorer
EBs	embryoid bodies
E. Coli	Escherichia coli
EDTA	ethylenediaminetetraacetic acid
<i>Egr-1</i>	<i>early growth response 1</i>
EPL	early progenitor
ERK1/2	Extracellular signal-regulated kinase 1/2
<i>exo</i>	<i>bacteriophage lambda exo gene</i>
FACS	Fluorescence-activated cell sorting
FAM	6-carboxyfluorescein
<i>Fas</i>	<i>tumour necrosis factor receptor superfamily member 6</i>

Fc	fold change
FCS	foetal calf serum
FSC	forward scatter
<i>Fgf5</i>	<i>fibroblast growth factor 5</i>
FIAU	1-(2-deoxy-2-fluoro-1-β-D-arabinofuranosyl)-5-iodouracil
FITC	Fluorescein isothiocyanate
FLPe	enhanced Flippase recombination enzyme
<i>Foxa2</i>	<i>forkhead box A2</i>
FRT	FLP recombination target site
Fyn	tyrosine protein kinase FYN
<i>Gata4</i>	<i>GATA binding protein 4</i>
<i>Gata6</i>	<i>GATA binding protein 6</i>
gDNA	genomic deoxyribonucleic acid
<i>Gam</i>	<i>bacteriophage lambda gam gene</i>
<i>Gapdh</i>	<i>glyceraldehyde 3-phosphate dehydrogenase</i>
H2	histone 2
H3	histone 3
H4	histone 4
H and E	haematoxylin and eosin

HAT	histone acetyltransferase
HBSS	Hank's balance salt solution
HDAC/ <i>Hdac</i> /HD	histone deacetylase
HEB	basic helix-loop-helix protein 20
HEPES	4-(2-hydroxyethyl)-1-piperazineethanesulfonic acid
<i>Hes1</i>	<i>hairy and enhancer of split1</i>
HEX	hexachlorofluorescein
<i>Hopx</i>	<i>homeodomain-only protein</i>
HP-1	heterochromatin protein 1
HSA	heat stable antigen, CD24a
Hyg	hygromycin B
Hyg Δ TK	hygromycin, delta thymidine kinase
IAP	interstitial A particle
Ikaros	Ikaros family zinc finger protein 1
I.M.A.G.E.	integrated molecular analysis of genomes and their expression
IRDye	infrared dye
<i>Itk</i>	<i>IL-2 inducible T cell kinase</i>
Ki67	antigen KI-67

<i>LAT</i>	<i>linker of activated T cells</i>
LB	Luria-Bertani
<i>LCK/Lck</i>	<i>lymphocyte protein tyrosine kinase</i>
<i>LckCre</i>	<i>Cre recombinase transgene under the control of the lymphocyte protein tyrosine kinase promoter</i>
LIF	leukaemia inhibitory factor
<i>Lig1</i>	<i>ATP dependent DNA ligase I</i>
LMC	litter mate control
LoxP	locus of X over P1
LSD-1	lysine specific demethylase-1
MAPK	mitogen activated protein kinase
MBD3	methyl-CpG binding domain protein 3
<i>Mcm 3, 6, 7, 10</i>	<i>mini-chromosome maintenance genes 3, 6, 7 and 10</i>
me3	trimethylation
MEF	mouse embryonic fibroblast
<i>Mef2c</i>	<i>myocyte enhancer factor 2C</i>
mES	mouse embryonic stem
MHC I/II	major histocompatibility complex I/II
MITR	Mef-2 interacting transcriptional repressor

Mi2 β	chromodomain helicase DNA binding protein 3
MOZ	monocytic leukaemia zinc finger homologue
mRNA	messenger ribonucleic acid
mSin3a	paired amphipathic helix protein Sin3a (<i>Mus musculus</i>)
MTA-1	metastasis associated 1
MTA-2	metastasis associated 2
<i>Myl2</i>	<i>myosin, light polypeptide 2, regulatory, cardiac, slow</i>
<i>MyoD</i>	<i>myogenic differentiation 1</i>
NAD	nicotinamide adenine dinucleotide
<i>Nanog</i>	<i>nanog homeobox</i>
<i>Ncl</i>	<i>nucleolin</i>
NE	nuclear extract
NEBA	nuclear extract buffer A
NEBB	nuclear extract buffer B
Neo	neomycin
<i>Nkx2.5</i>	<i>homeobox protein NK-2 homolog E</i>
NODE	nanog and oct4-associated deacetylase repressor complex

<i>Notch 1</i>	<i>notch homolog 1, translocation-associated (Drosophila)</i>
NP-40	nonyl phenoxypolyethoxylethanol
NuRD	nucleosome remodelling and histone deacetylase complex
<i>Oct4</i>	<i>POU domain, class 5, transcription factor 1</i>
ORF	open reading frame
p21/p21	<i>cyclin dependent kinase inhibitor 1A</i>
p27	cyclin dependent kinase inhibitor 1B
p300	histone acetyltransferase p300
PBS	phosphate buffered saline
PCR	polymerase chain reaction
PE	phycoerythrin
Pgk	phosphoglycerate kinase
PI	propidium iodide
PNACL	protein and nucleic acid chemistry laboratory at the University of Leicester
<i>Polδ</i>	<i>DNA polymerase delta</i>
<i>Polλ</i>	<i>DNA polymerase lambda</i>
<i>Prim1</i>	<i>DNA primase, p49 subunit</i>
PS	phosphatidylserine

<i>Pten</i>	<i>phosphatase and tensin homolog</i>
PTM	post-translational modification
Q-RT PCR	quantitative reverse transcription polymerase chain reaction
RAD51	RecA-like, RAD51 homolog (<i>S. cerevisiae</i>)
<i>Rad54l</i>	<i>RecA-like, RAD54-like homolog (S. cerevisiae)</i>
<i>Rag1</i>	<i>recombination activating gene 1</i>
<i>Rag2</i>	<i>recombination activating gene 2</i>
Rb	retinoblastoma
RbAp46/48	Histone-binding protein RBBP7/4
RBCLB	red blood cell lysis buffer
RNA	ribonucleic acid
<i>Rory</i>	<i>RAR-related orphan receptor gamma</i>
RT	room temperature
RT-PCR	reverse transcription polymerase chain reaction
Runx1/3	runt-related transcription factor 1/3
<i>Satb1</i>	<i>special AT-rich sequence binding protein 1</i>
SSC	side scatter
SDS	sodium dodecyl sulphate

SDS-PAGE	sodium dodecyl sulphate polyacrylamide gel electrophoresis
S.E.M.	standard error of mean
shRNA	short hairpin RNA
SIN3	SWI-independent 3
siRNA	small interfering RNA
SIRT/ <i>sirt</i>	sirtuin
SKY	spectral karyotyping
SMARCAD1	SWI/SNF-related matrix-associated actin-dependent regulator of chromatin subfamily A containing DEAD/H box 1
SP	single positive thymocytes
Spl	splenocytes
Src	tyrosine protein kinase Src
<i>Srf</i>	<i>serum response factor</i>
SSC	saline-sodium citrate
Suv39h1/2	Suppressor of variegation 3-9 homolog 1/2
SWI/SNF	SWItch/Sucrose non-fermentable
Syk	tyrosine protein kinase SYK
T-ALL	T cell acute lymphoblastic leukaemia/lymphoma

TAFIID	transcription initiating factor TFIID subunit
TCA	trichloroacetic acid
TCR	T cell receptor
TCR α	T cell receptor alpha chain
TCR β	T cell receptor beta chain
T.E.	10mM Tris-HCl/1mM EDTA
<i>Tec</i>	Tec protein-tyrosine kinase
TGF β	transforming growth factor β
TgN	transgene
<i>Themis</i>	<i>thymocyte expressed molecule involved in selection</i>
Thy	thymocytes
TSA	trichostatin A
UPL	Universal ProbeLibrary
VEGA	vertebrate genome annotation
WCE	whole cell extract
Wnt	wingless-integration 1
WT	wildtype

ZAP-70

Tyrosine-protein kinase ZAP-70

Chapter One: Introduction

Eukaryotic chromosomes are compacted in the nucleus in the form of chromatin, a highly organised and dynamic protein-DNA complex remarkably well conserved across eukaryotes (Turner, B.M., 2005). Cytologically, chromatin can be classified into distinct conformations during interphase, relatively uncondensed regions of euchromatin and a much denser form, heterochromatin (Heitz, E., 1928). In addition to, or as a consequence of its fundamental role in DNA packaging, chromatin conformation acts as an instructive DNA scaffold for many basic DNA-templated biological processes such as replication, repair, recombination, and gene transcription, as described below.

1.1 Histones, the nucleosome core particle and chromatin.

Chromatin compaction of DNA follows a strict hierarchical structure. At the simplest level, the basic unit of chromatin is a repetitive link of nucleosome core particles. Viewed under electron microscopy, they appear as 10nm “beads on a string” at 200 base pair (bp) intervals along DNA (Thomas, J.O. and Kornberg, R.D., 1974; Olins, A.L. and Olins, D.E., 1974). The crystal structure of the core particle reveals 146bp of DNA is wound around a histone octamer consisting of two of each class of the “core” histone proteins, that is, two H2A-H2B dimers combined with an H3-H4 tetramer (Luger, K., *et al.*, 1997a; Luger, K., *et al.*, 1997b) (Fig 1.1). Protruding from the nucleosome, are the unstructured N-terminal “tails” of each of the “core” histones (Luger, K., *et al.*, 1997b).

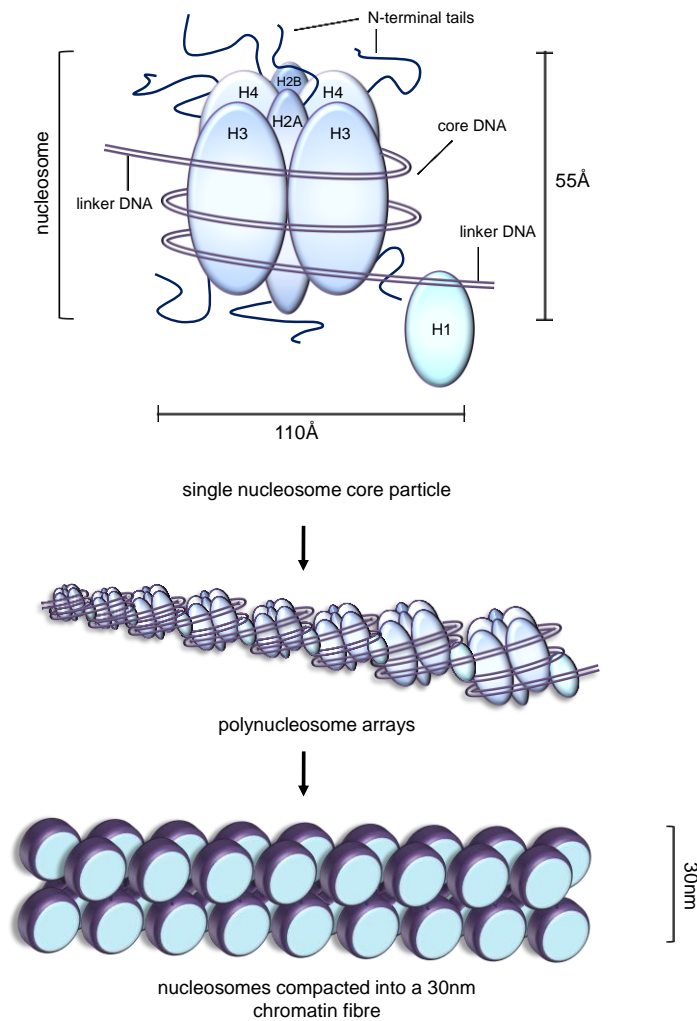


Figure 1.1. *Chromatin consists of DNA, histones and non-histone protein.* The DNA helix is wrapped around the nucleosome, an octamer of histone proteins, approximately 1.8 times. Each nucleosome has two copies each of Histone H2A, H2B, H3 and H4. Linker DNA and H1 form polynucleosome arrays which in turn further compact to form the “30nm” chromatin fibre during metaphase.

At the next level of chromatin organisation, adjacent nucleosomes are joined together by approximately 40-70bp of linker DNA to form polynucleosome arrays. Critical to the formation of nucleosome arrays is an interaction between linker-DNA, non-histone proteins and another histone, H1 (Zhou, Y.B., *et al.*,

1998; Thoma, F., *et al.*, 1979). During metaphase, nucleosome arrays have been identified as forming helical structures with approximately 6 nucleosomes per turn, commonly known as the 30nm chromatin fibre (Finch, J.T. and Klug, A., 1976; Thoma, F., *et al.*, 1979). Electron micrographs of HeLa cells during metaphase have provided the basis for a third level of higher ordered organisation, in which 30nm fibres form loops which emanate out from and return to the same point of the metaphase chromosome similar to petals of a flower (Marsden, M.P. and Laemmli, U.K., 1979). As cells make the transition to interphase, the presence of chromatin fibres greater than 10nm have yet to be visualised and rather than compaction of chromatin into 30nm fibres, variable chromatin condensation (into the distinct “open” euchromatic or “condensed” heterochromatic regions) arises as a result of variations in chromatin packing density achieved via bending of the 10nm fibre back on itself (Fussner, E., *et al.*, 2011).

1.2 Functional divides between chromatin structures.

The cytological distinctions between euchromatin and heterochromatin also correlate with a number of distinct molecular and functional characteristics. As far back as 1963, Alfrey and colleagues were able to show that histone depleted nuclei have an increased rate of RNA synthesis and that RNA synthesis is more active in diffuse euchromatin compared to condensed heterochromatin (Alfrey, V.G., *et al.*, 1963; Littau, V.C., *et al.*, 1964). Typically, constitutive heterochromatin is transcriptionally inactive and concentrated in gene poor territories, particularly in regions containing high density repetitive

DNA such as transposons (found at centromeres and telomeres) (Weintraub, H. and Groudine, M., 1976; Grewal, S.I.S., and Jia, S., 2007). DNA CpG dinucleotides, within heterochromatin, are usually methylated and the DNA itself refractory to digestion with nucleases (Bellard, M., *et al.*, 1980; Bird, A., 2002). Repression of these regions is critical in promoting genomic stability via prevention of spurious recombination between repetitive DNA elements (Peng, J.C. and Karpen, G.H., 2008). Facultative heterochromatin refers to regions of the genome which are poised for expression or differentially expressed during cell differentiation which, upon differentiation, are silenced by their incorporation into heterochromatin. Examples of this include X inactivation and large scale heterochromatinisation of the genome in terminally differentiated cells (Goto, T. and Monk, M., 1998). In contrast to heterochromatin, regions of euchromatin correspond to gene rich, transcriptionally active genomic loci (Gilbert, N., *et al.*, 2004), regulatory sequences (such as gene promoters) are more disposed to nuclease digestion and DNA CpG islands are largely un-methylated (Bird, A.P., 1986).

The chromatin landscape is also characterised by its effects on the timing of DNA replication during mitosis, with euchromatin first to replicate early during S-phase followed by facultative, and finally, constitutive heterochromatin (O'Keefe, R.T., *et al.*, 1992 and Weidtkamp-Peters, S., *et al.*, 2006). Of note is the ability for these distinct chromatin characteristics to be stably inherited by daughter cells post replication including; overall levels of chromatin condensation, CpG methylation status and the localisation of chromatin associated proteins, including histone post translational modifications, such as acetylation, introduced below (Holliday, R. and Pugh, J.E., 1975, Turner, B.M.,

et al., 1992, Pradhan, S., *et al.*, 1999, Craig, J.M., 2005, Bird, A., 2002; Goll, M.G., and Bestor, T.H., 2005). This aspect of heritability has opened up an era of intense interest in “The study of mitotically and/or meiotically heritable changes in gene function that cannot be explained by changes in DNA sequence”, commonly known as epigenetics (Russo, V.E.A, *et al.*, 1996).

1.3 Altering chromatin accessibility.

As described above, chromatin compaction affects DNA accessibility and has had long associations with a number of biological functions and DNA-templated processes (i.e. transcription and replication). The ability of a cell to either maintain or alter, a particular chromatin state, is therefore key to normal function. A number of key mediators and mechanisms of chromatin-state regulation have now been identified which include; DNA CpG di-nucleotide methylation, histone post translational modifications (PTMs) (Strahl B.D. and Allis, C.D., 2000; Jenuwein, T, and Allis, C.D., 2001), chromatin remodelling (Saha, A., *et al.*, 2006) non-histone protein-chromatin associations (Eissenberg, J.C, *et al.*, 1990), temporal or site specific incorporation of histone variants (Li, B., *et al.*, 2005; Jin, C. and Felsenfeld, G., 2007; Ray-Gallet, D. and Almouzni, G., 2010) and even histone tail “clipping” (Duncan, E.M., *et al.*, 2007; Santa-Rosa, H., *et al.*, 2009). The majority of studies thus far have focused on their roles in the control of transcription but importantly their effects are applicable to any DNA-template mediated process.

1.3.1 Post translational histone modifications.

Allfrey and colleagues first demonstrated, almost 50 years ago, that histones are post translationally modified and in particular that histone acetylation has a positive effect on transcription (Allfrey, V.G., *et al.*, 1964). However, not until the high resolution X-ray structure of the nucleosome, by Luger in 1997, was it possible to gain an insight into how these modifications may affect chromatin structure. Luger *et al* were able to demonstrate that the mainly globular histone proteins of the nucleosome, each had an unstructured basic N-terminal tail that could potentially make contact with adjacent nucleosomes. Summarily, it seemed that modification of histones could interfere with inter-nucleosomal interactions. We now know this to be true and that covalent histone modifications not only mediate chromatin conformation by their physical presence but also recruit remodelling enzymes, as well as other non-histone proteins or enzymes, which in turn have chromatin/histone modifying activities. Furthermore, the advent of chromatin immunoprecipitation (ChIP), followed by hybridisation to genomic microarrays (ChIP-chip) (Weber, M., *et al.*, 2005; ENCODE project consortium, 2004) or direct sequencing (ChIPseq) (Wang, Z., *et al.*, 2009), has permitted the large-scale identification of the temporal, genome-wide distribution of histone PTMs and chromatin associated proteins to be linked with functional outcomes (Barski, A., *et al.*, 2007; Mikkelsen, T.S., *et al.*, 2007).

More than 70 different sites and 8 different types of histone PTM have been identified, and include; lysine-acetylation (Kac), lysine-methylation (Kme), arginine-methylation (Rme), serine/tyrosine phosphorylation, lysine-ubiquitylation (K-ub), lysine-sumoylation (K-su), arginine and glutamine ADP-

ribosylation (R/E-ar), arginine to citrulline deimination (R-Cit), serine and threonine β -N-actylglucosamine (S/T-O-GlcNac) and finally proline isomerisation (Bannister, A.J and Kouzarides, T., 2011).

Table 1.1. *Mammalian histone-modifying enzymes and their histone substrates.* (Adapted or results summarised from Sterner, D.E. and Berger, S.L., 2000; Johnson, C.A., *et al.*, 2002; Kouzarides, T., 2007; Lee, K.K. and Workman, J.L., 2007; Voss, A.K. and Thomas, T., 2009).

Histone-modifying enzyme	Histone residues modified	Histone-modifying enzyme	Histone residues modified
Acetyltransferases		Arginine methyltransferases	
HAT1	H4 (K5/12)	CARM1	H3 (R2/17/26)
CBP/P300	H3 (K14/18), H4 (K5/8), H2A (K5), H2B (K12/15)	PRMT4	H4 (R3)
PCAF/GCN5	H3 (K9/14/18)	PRMT5	H3 (R8), H4(R3)
TIP60	H4 (K5/8/12/16), H3 (K14)	Serine/threonine kinases	
HBO1	H4 (K5/8/12)	MSK1/MSK2	H3 (S28)
MOF	H4 (K16)	CKII	H4 (S1)
TAF _i 250	H3 (K14)	Mst1	H2B (S14)
Deacetylases		Ubiquitilases	
HDAC1*	Pan-H2/3/4 K-residues H3K14	Bmi/Ring1A	H2A (K119)
HDAC2*	Pan-H2/3/4 K-residues but not H3 (K14)	RNF20/RNF40	H2B (K120)
HDAC3*	Pan-H2/3/4 K-residues ; preference for H2A (K5) and H4 (K5/12)	<p>HAT1, histone acetyltransferase 1; CBP, CREB binding protein; PCAF, P300/CBP-associated factor; TIP60, Tat interacting protein-60kDa; HBO1, histone acetyltransferase binding to ORC1; MOF, MYST histone acetyltransferase 1; TAF_i250 TATA box binding protein (TBP)-associated factor, RNA polymerase II, A, 250kD; HDAC, histone deacetylase; SIRT2, sirtuin 2; SUV39H1/2, suppressor of variegation 3-9 homolog 1/2; SETDB1, SET domain, bifurcated 1; SUV420H1/2, suppressor of variegation 4-20 homolog 1/2; EZH2, nhancer of zeste homolog 2; LSD1, lysine (K)-specific demethylase 1; JHMD, jumonji C domain-containing histone demethylase; JMJD, jumonji domain containing 2; CARM1, coactivator-associated arginine methyltransferase 1; CKII, casein kinase II; PRMT4/5, protein arginine methyltransferase 4/5; MSK1/2, mitogen and stress-activated protein kinase; Mst1, macrophage stimulating 1; Ring1A, really interesting new gene 1 protein; Ring finger protein. *inferred from co-immunoprecipitation of known co-repressor complexes.</p>	
SIRT2	H4K16		
Lysine methyltransferases			
SUV39H1/SUV39H2	H3 (K9)		
G9a	H3 (K9)		
ESET/SETDB1	H3 (K9)		
MLL1,2,3,4 and 5	H3 (K9)		
SET1A/SET1B	H3 (K4)		
ASH1	H3 (K4)		
SET2	H3 (K36)		
DOT1	H3 (K79)		
SUV420H1/SUV20H2	H4 (K20)		
EZH2	H3 (K27)		
Lysine demethylases			
LSD1	H3 (K4)		
JHDM1a/JHDM1b	H3 (K36)		
JHDM2a/JHDM2b	H3 (K9)		
JMJD2A	H3 (K9/36)		
JMJD2B	H3 (K9)		
JMJD2C	H3 (K9/36)		
JMJD2D	H3 (K9)		

Importantly, these modifications are readily reversible and the enzymes responsible have been established. Table 1.1 details a number of these histone modifiers and their known substrates. Table 1.2 summarises some of the biological outcomes and genome wide locations of these histone modifications.

Table 1.2. *Functional outcomes of histone modifications.* (Adapted or results summarised from Berger, S.L., 2007; Kouzarides, T., 2007; Millar, C.B. and Grunstein, M., 2006; Bernstein, B.E., *et al.*, 2007; Bernstein, B.E., *et al.*, 2006; Bernstein, B.E., *et al.*, 2005; Barski, A., *et al.*, 2007; Wang, Z., *et al.*, 2008; Martin, C. and Zhang, Y., 2005)

Modification	Histone	Residue	Effect on transcription/functional association	Common location
DNA methylation	-	CpG di-nucleotides	Repression	Heterochromatin
Acetylation	H2A H2B H3 H4	K5 K5/12/15/K20 K4/9/14/18/56 K5/8/13/16	Activation Activation Activation Activation	Euchromatin Euchromatin
Methylation	H3 H4	K4/36/79 K9/27 K36 K4/K27* R17/23 K20	Activation Repression Elongation Poised Activation Repression	Euchromatin Heterochromatin/Facultative heterochromatin Gene bodies Bi-valent domains in stem cells
Phosphorylation	H2A H2AX H3 H4	S1, T119 S139 T3, S10, T11, S28 S10 S1	Mitosis DNA repair Mitosis Activation Mitosis	-
Ubiquitination	H2A H2B	K119 K120	Repression Activation	-

H, histone; K, lysine; R, arginine; S, serine; T, threonine. *Co-occurring histone modifications, termed “bi-valent”.

1.3.2 Mechanisms and functional consequences of histone modifications.

Mechanistically, the consequence of N-terminal histone modifications, either directly disturb local chromatin structure or act to mediate secondary events via the recognition of a particular PTM by non-histone multi-protein complexes. In the latter instance, the consequence and functional outcome, with regards local chromatin structure, is determined by the constituents of these large multi-protein complexes, which may contain nucleosome remodelers, histone modifying enzymes or site-specific recruitment of proteins with well established roles in DNA-templated processes.

1.3.3 Direct structural disturbance by histone PTMs.

The major histone PTM associated with a direct affect on local chromatin compaction is acetylation of the ϵ -amino group of lysine residues, steady state levels of which are directed by the opposing actions of HAT/KATs (histone acetyltransferases/ lysine acetytransferases) and HDAC/KDACs (histone deacetylases/ lysine deacetylases) (which, in mammals are grouped into four classes, discussed later) (Sterner, D.E and Berger, S.L., 2000; Yang, X.J. and Seto, E., 2008) (Fig 1.2). Addition of an acetyl moiety restores a negative charge to the N-terminal tail and thus loosens the interaction between nucleosomes and adjacent negatively charged DNA. Consistent with this, acetylation of the nucleosome core increases the DNase I sensitivity of linker DNA (Simpson, R.T., 1978), as does treatment with the deacetylase inhibitor sodium butyrate, indicating a relaxation of histone-DNA contacts with increased

histone acetylation. Conversely, deacetylation restores the positive charge and thus potentially stabilises local chromatin architecture. The number of potential sites of acetylation (see Table 1.1) indicates hyper- or hypoacetylation of histone tails could impose drastic effects on chromatin compaction. More recently, use of homogeneous recombinant histone 4 acetylated at lysine 16 (H4K16ac), demonstrated this modification alone is able to negatively affect higher order chromatin compaction. As described in the early experiments by Allfrey, histone acetylation has long been associated with increased rates of RNA synthesis. More recently, genome-wide mapping of over 18 H-Kac modifications, using ChIPseq, indicates that all sites of acetylation correlate positively with gene expression, albeit at distinct sites of actively transcribed genes. For example, acetylated H3K9/14/18/27 and 36 peak at areas around gene transcriptional start sites (TSSs), whereas acetylated H4K4/8/12 and 16 are elevated in the promoter and transcribed regions of active genes. Moreover, heterochromatin, devoid of active gene transcription, is hypoacetylated (2002; Millar, C.B. and Grunstein, M., 2006; Wang, Z., *et al.*, 2008).

Combined, these data act to form a well accepted dogma with regards histone acetylation and access to DNA in the context of chromatin. That is, histone acetylation confers a relaxed chromatin state so that processes which require access to DNA, such as binding of the pre-initiation complex (PIC) during gene transcription, is facilitated.

Like acetylation, phosphorylation of serines, threonines and tyrosines by kinases (Nowak, S.J. and Corces, V.G., 2004), restores a negative charge to

histone tails and it is assumed, loosens DNA-histone interactions. Similarly to acetylation, phosphorylation of histone 3 at serine 10 (H3S10p) has been

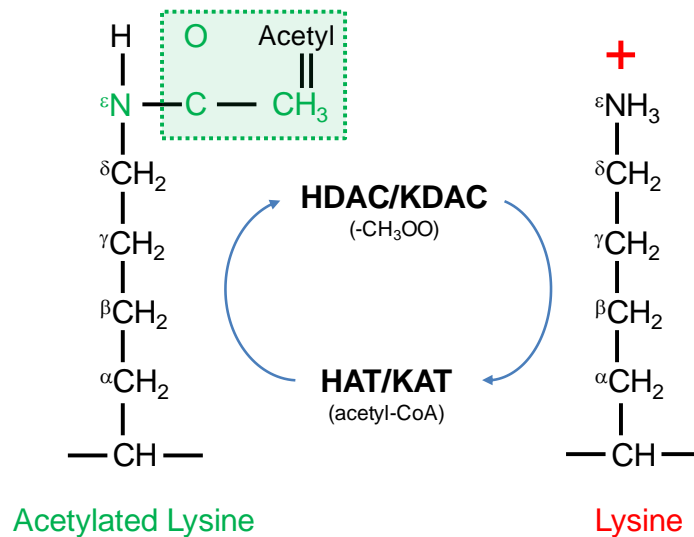


Figure 1.2. *The reversible acetylation and deacetylation of lysine residues.* Reaction catalysed by the respective histone or lysine acetyltransferases (HAT/KAT) and histone or lysine deacetylases (HDAC/KDAC). (Adapted from Yang, X.J. and Seto, E., 2008; Turner, B.M., 1991).

shown to correlate with transcriptionally active gene loci (i.e. in response to heat shock treatment) (Nowak, S.J. and Corces, V.G., 2000). However, mutation of the same phosphorylation site impairs chromosome condensation and segregation, providing a causal link between H3S10p and the initiation of chromosome condensation during mitosis, Wei, Y., *et al.*, 1999). As such, these data provide an example of context dependent functional outcomes of the same histone tail PTM.

Ubiquitylation of lysines, itself a large 76-amino acid polypeptide, is thought to act as a “wedge”, prising chromatin into an open configuration by virtue of its relatively large size. Although evidence exists for ubiquitylation in transcriptional activation of HOX genes (i.e. H2BK120 monoubiquitylation) (Zhu, B., *et al.*, 2005), deletion of Ring1B, an E3 ubiquitin ligase, in mouse embryonic stem (mES) cells causes de-repression of lineage specific genes and again demonstrates the effect of context on functional outcome as Ring1B forms part of polycomb repressive complex-1, PRC1, responsible for maintaining chromatin compaction (Margeuron, R. and Reinberg, D., 2011).

1.3.4 Indirectly altering chromatin via “reading” histone PTMs.

Methylation of histone tails is more diverse than lysine acetylation and occurs at both lysine and arginine residues. Lysines can be un-modified (me0), mono-methylated (me1), di-methylated (me2) or tri-methylated (me3), with arginines mono- (Rme1) and symmetrically (Rme2s) or asymmetrically (Rme2as) di-methylated. Of the lysine methyltransferases, all except DOT-1 contain a SET (suppressor of variegation-enhancer of zeste-trithorax) domain, responsible for the methyltransferase enzymatic activity which catalyses the transfer of S-adenosylmethionine (SAM) to a lysine’s ϵ -amino group (Dillon, S.C., *et al.*, 2005). These enzymes, unlike HDACs, seem to be relatively specific for the lysine residue (see Table 1.1) and the degree of methylation (i.e., mono-, di- or tri- methylated). Two classes of arginine methyltransferase have been identified, the type I (Rme1 and Rme 2as) and type II (Rme1 and Rme2s) group of proteins, referred to as PRMTS (protein arginine

methyltransferases). All of these enzymes transfer a methyl group from SAM to ω -guanidino group of arginine (Bedford, M.T., *et al.*, 2009).

Initially, lysine methylation was thought to be irreversible, due in part to the absence of any known histone demethylases. However, in 2004 the first lysine demethylase was identified, LSD-1, which catalyses the removal of methyl moieties from H3K4me1/2 but not K4me3 (Shi, Y., *et al.*, 2004). Two years later the first enzyme identified as a tri-methyl lysine demethylase was discovered, JMJD2, which demethylates both H3K9me3 and H3K36me3 (Tsukada, Y., *et al.*, 2006). Since this initial discovery, identification of a number of other demethylase enzymes has followed suit (see Table 1.1). As with methyltransferases, they also exhibit a high level of substrate specificity with respect to their target lysine and are sensitive to the degree of lysine methylation (Whetstine, J.R., *et al.*, 2006; Klose, R.J., *et al.*, 2006; Hong, S., *et al.*, 2007). Globally, lysine methylation has been well studied and a number of methylated lysine marks have been associated with distinct forms of chromatin (see table 1.2). Functionally, histone lysine methylation has been correlated with both transcriptional silencing (H3K9me3/H3K27me3) and activation (H3K4me3). Whilst in mES cells (Bernstein, B.E., *et al.*, 2006), and more recently in developing thymocytes (Harker, N., *et al.*, 2011), bivalent domains have been identified at gene promoters which are resolved upon lineage specification.

Although histone methylation occurs in a multitude of forms and the enzymes responsible for either adding or removing this mark are many, histone methylation is not thought to mediate a direct effect on nucleosome-DNA interactions, as is the case with acetylation. Rather methylation (as well as

acetylation and phosphorylation) of histone tails provides potential binding sites for enzymes with other catalytic or chromatin restructuring capabilities (Table 1.4). A classic example of this is the recruitment of the non-histone protein HP1 (heterochromatin protein 1) which co-localises with H3K9me3 at heterochromatin (Jacobs, S.A., *et al.*, 2001). HP1 is thought to passively stabilise dense chromatin conformations by cross linking nucleosomes (Nielsen, A.L., *et al.*, 2001), and a stable interaction with H3K9me3 via its chromodomain has been shown in mice (Lachner, M., *et al.*, 2001). Moreover, HP1 has been shown to interact with Suv39H1, a known H3K9me3 methyltransferase, providing a mechanism for long range, self perpetuating maintenance of heterochromatin. Histone modifying enzymes are often found in large multi-subunit complexes. Suv39H1 has also been shown to interact with methyl-CpG-binding domain protein, MBD1, and histone deacetylases, HDACs to repress transcription (Fujita, N., *et al.*, 2003), presumably through recruiting the deacetylase potential of HDACs.

Other histone methyl marks such as H3K4me3 can act as positive mediators of transcription/open chromatin. Di-methyl H3K4 acts as a binding site for the MLL tri-methyltransferase containing complex, COMPASS (Complex Proteins Associated with Set 1) (Miller, T., *et al.*, 2001) through virtue of a WD40-repeat protein, WDR5, resulting in the conversion of H3K4me2 to -me3 (Wysocka, J., *et al.*, 2005), a histone methylation mark present at the 5' ends of ORFs and positively associated with gene transcription (Barski, A., *et al.*, 2007). In turn, the BPTF sub-unit of NURF contains an H3K4me3 reading PHD domain and a K-ac reading bromodomain. The combination of which, acts to localise the nucleosome remodelling factor, NURF (Wysocka, J., *et al.*, 2006), the

founding member of the imitation switch remodelling complexes, ISWI (Tsukiyama, T., *et al.*, 1995). Nucleosome remodelers catalyse energy-dependent nucleosome mobilisation, sliding or repositioning and in the context of NURF disrupt the ordered periodicity of nucleosomes around TSSs, resulting in transcriptional activation both *in vitro* and *in vivo* (Mizuguchi, G., *et al.*, 1997; Badenhorst, P., *et al.*, 2002). Keeping with H3K4me3, this modification also recruits transcriptional co-repressor complexes, such as Sin3 (SWI-independent 3) (Laherty, C.D., *et al.*, 1997) and N-CoR (nuclear receptor co-repressor) (Li, J., *et al.*, 2000) via the PHD domain of ING2 (Sin3a) and the tandem tudor domains of JMJD2A (N-CoR). In response to DNA damage, Sin3 is actively recruited to sites of H3K4me3 resulting in the active repression of genes involved in the progression of cell cycle (Shi, X., *et al.*, 2006; Huang, Y., *et al.*, 2006). Presumably, Sin3/ N-CoR mediated repression occurs through their associations with HDACs (see table 1.4). H3K4me3 exemplifies the promiscuity of a single histone modification on functional outcome, which is likely dependent on a number of extrinsic, context dependent factors, such as DNA damage and complex recruitment.

Histone PTM “readers” can also serve as adaptors to recruit factors which have direct roles in DNA-templated activities, some of which include; TFIID (TAF₂₅₀, a general transcription factor) which recognises K-ac and H3K4me3 (Vermeulen, M., *et al.*, 2010), recombination activating protein, RAG2, recognises H3K4me3, which in combination with RAG1 mediates somatic re-arrangement of the T cell receptor (Ji, Y., *et al.*, 2010) and MRG15, which recognises K36me3 and recruits the splicing regulator polytrimidine tract binding protein, PTB (Luco, R.F., *et al.*, 2010).

Table 1.3. *Histone post-translational modifications and their protein domain binding partners.*
(Adapted or summarised from Taverna, S., *et al.*, 2007; Lee, J. S., *et al.*, 2010; Yun, M., *et al.*, 2011).

Modification recognition protein domain	Post Translational Marks	Example of domain containing protein	Functional role
Bromodomain	K-ac	PCAF	Transcriptional co-activator
Chromodomain	H3K9me2/3, H3K27me2/3	HP1	Regulator of chromatin structure
Double chromodomain	H3K4me1/2/3	CHD1	ATP-dependent chromatin remodeller
Double/tandem tudor	H3K4me3, H4K20me1/2/3,	JMJD2A TP53BP1	Lysine demethylase. Binds TP53 transcription factor
PHD finger	H3K4me3, H3K4me0, H3K9me3, H3K36me3	BPTF TAF3	Subunit of NURF, ATP-dependent chromatin remodelling complex. Subunit of the basal transcription factor TAFIID
WD40 repeat	H3R2/K4me2	WDR5	Common component of SET-1 family of histone methyltransferase complexes
14-3-3	H3S10p, H3S28p	14-3-3 ϵ/ζ	Histone acetyltransferase (MOF) recruitment.

Abbreviations: PCAF, p300/CBP-associated factor; HP1, heterochromatin protein-1; CHD1, chromohelicase DNA-binding 1; JMJD2, jumonji domain-containing protein-2A; TP53BP1, tumour protein p53 binding protein 1; PHD, plant homeo domain; BPTF, bromodomain PHD finger transcription factor; NURF, nucleosome remodelling factor; TAF3, TATA box binding protein-associated factor; TAFIID, transcription factor II D; WD40 repeat, tryptophan-aspartate 40 repeat; WDR5, WD repeat domain 5; SET, Su(var)3-9, Enhancer of Zeste, Trithorax; MOF, males-absent on the first protein. K-ac (lysine acetylation, me1/2/3 (mono-, di- and tri-methylation), H (histone), R (arginine), S (serine), p (phosphorylation).

Factors which effect the deposition of histone PTMs (other than the groups of enzymes in Table 1.1) have also been identified and include most obviously the prior deposition of PTMs themselves. This phenomenon is also apparent for neighbouring or flanking PTMs, such as has been described for H3S10p, catalysed by the kinase AuroraB. This particular modification disrupts the HP1 H3K9me3 interaction, releasing HP1 from chromosomes during mitosis in MEFs (Hirota, T., *et al*, 2005) and counter-intuitive to the direct charge effect of H3S10p. Other studies have shown that “cross-talk” between H3S10p and

the recruitment of acetyltransferases provides binding sites for kinases which facilitate transcriptional elongation (Zippo, A., et al., 2009).

Originally it was postulated that patterns of histone PTMs constitute a code which is determinant of transcriptional outcomes. Accumulation of knowledge of these marks, it was assumed, would eventually lead to this code being deciphered (Strahl, B.D. and Allis D.C., 2000). More recently evidence has suggested a more complex, context dependent interplay between histone PTMs, with layers of subtlety more akin to a language with particular grammatical and context dependent nuances.

1.4 HDACs and transcriptional activation.

Typical dogma surrounding the precise mechanistic switch between transcriptional repression or activation, as mediated by local acetylation status, comes from the fact that un-liganded nuclear hormone receptors repress transcription through interactions with co-repressor complexes such as N-CoR/SMRT, which also associate with mSin3a (Xu, L., et al., 1999). Upon ligand binding, the receptor alters its conformation such that it exchanges the co-repressor complex (containing HDACs) for a co-activating complex (containing HATs). This simplistic model has formed the basis for the “classical” and mutually exclusive model of acetylation-mediated repression or activation; whereby HDACs are associated with repressed genes and HATs are associated with active genes (Perissi, V., *et al.*, 2010) (Fig 1.3). Yet, despite the overwhelming weight of evidence in favour of HDAC mediated transcriptional

repression (presented already), there has always been a hint that HDACs might also positively influence transcription.

Deletion of Rpd3, the HDAC1 orthologue, results in the downregulation of more genes than are upregulated, an effect that can be recapitulated using the (class I and II) HDAC inhibitor, trichostatin A (TSA) (Bernstein, B.E., *et al.*, 2000). Treatment of yeast with TSA for as little as 15 minutes recapitulates the downregulation of certain genes, suggesting a function for Rpd3 in gene activation. Similar treatment of mammalian MCF-7 cells also produces a pattern of up- and downregulated genes (Reid G., *et al.*, 2005). However, the strongest evidence for a positive role in transcription comes from two separate studies by the Grunstein and Zhao laboratories, which used chromatin-immunoprecipitation to define the genome-wide loci of Rpd3 and HDAC1 in yeast (Kurdistani S.K., *et al.*, 2002) and human CD4 T cells (Wang Z., *et al.*, 2009) cells respectively. Surprisingly, both groups found that Rpd3/HDAC1 are predominantly localised at active gene loci, with binding centred on the transcriptional start site (TSS) in humans. Indeed, the more active the gene, the stronger the association (see Fig. 1.4A for schematic). This paradoxical result is compounded by the co-localization of many histone acetyltransferase (HAT) enzymes, including, p300, CBP, GCN5, P/CAF and MOF in a subset of H3K4me enriched genes (Wang Z., *et al.*, 2009). One potential explanation is that transcriptional activation involves a 'cyclical' utilization of HATs, and then HDACs, to initiate and reset chromatin between rounds of RNA polymerase II (RNAP-II) recruitment. This idea fits well with the pronounced cycling of histone

A.

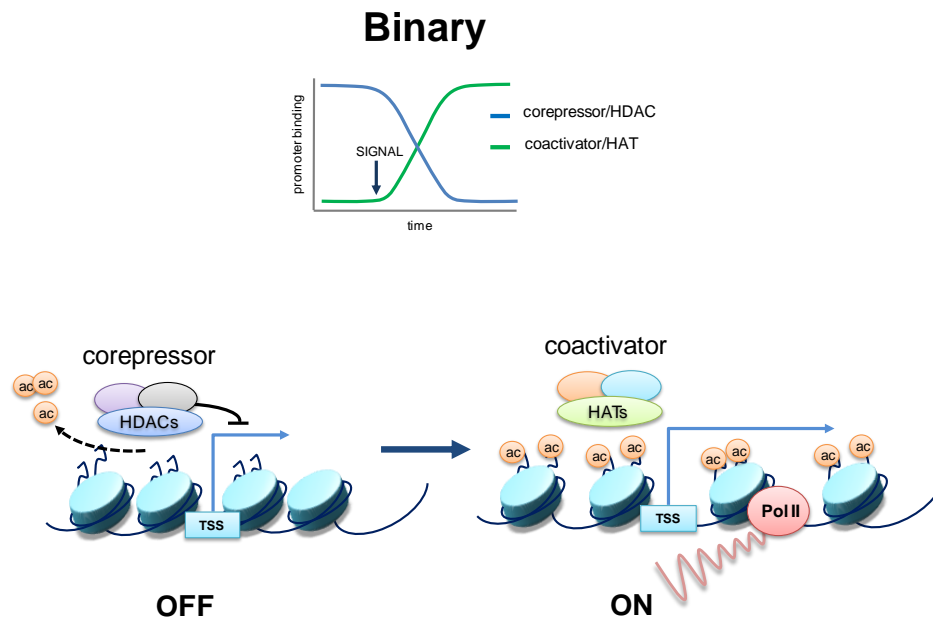


Figure 1.3. The “classic” binary model for the mutually exclusive utilisation of HDAC associated co-repressor and HAT associated co-activator complexes, based on the function of un-liganded and ligand bound nuclear hormone receptors. Deacetylation, mediated by the co-repressor complex bound to a gene promoter, mediates a transcriptionally repressive environment. Upon an extrinsic signal (or ligand binding), the co-repressor is replaced by a co-activator, increased acetylation and a transcriptionally permissive environment.

modifications observed during gene activation at the estrogen responsive gene, PS2. By first synchronizing transcription (using pre-treatment with α -amanitin) and then stimulating PS2 expression (with estradiol) RNAP-II recruitment and histone acetylation occurs in a pattern reminiscent of a ‘sine’ wave (Metivier R., et al., 2003) (Fig. 1.4A). Under these conditions, HDAC1 recruitment occurs during a period of reduced histone acetylation and RNAP-II binding, suggesting that HDACs have a role in promoter “clearance”, which may be necessary to

“reinitialize” the promoter before a second round of transcriptional initiation can begin (Fig. 1.4B).

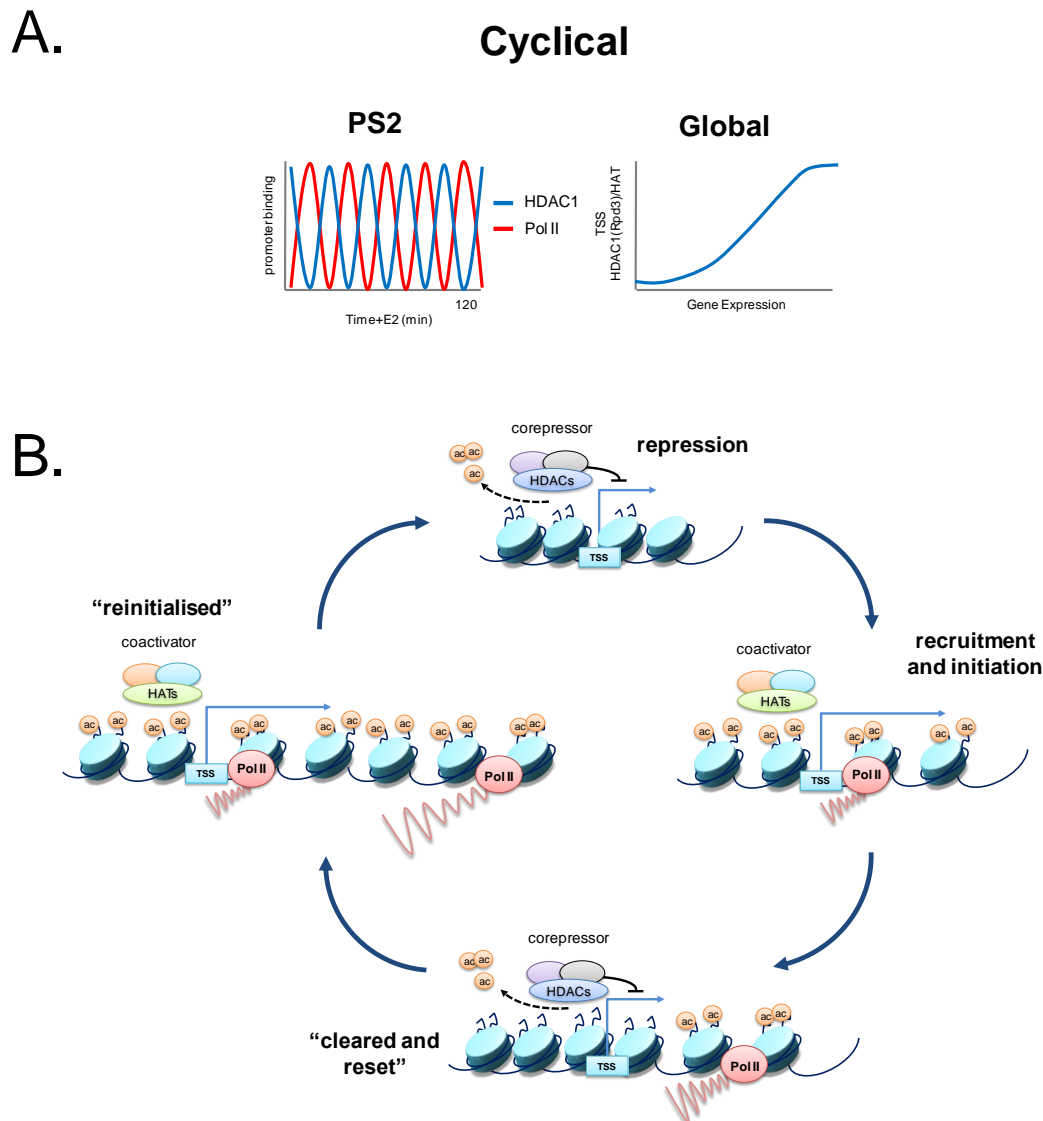


Figure 1.4. A model for the utilization of histone deacetylases (HDAC) during the process of transcriptional activation. (A) Transcriptional activation of the estrogen (E2) responsive gene, PS2, results in the ‘cyclical’ association of RNA polymerase II (Pol II) and HDAC1. The reciprocal association of Pol II and HDAC1 suggests that the deacetylation process may play a role in promoter ‘clearance’. Chromatin immunoprecipitation experiments in yeast (Rpd3) and human (HDAC1) cells demonstrate that, the more active the gene, the greater the association with HDACs. (C) A model for the ‘cyclical’ utilization of histone acetyltransferases (HAT) and HDACs during transcriptional activation of H3K4me3 marked genes.

1.5 Non-histone substrates of HDACs.

Since the initial discovery of histone lysine acetylation and latterly the identification of the enzymes responsible for this modification, there is increasing evidence that the function of several other proteins is also regulated by their acetylation status. For example, many proteins involved in the regulation of transcription such as p53 and GATA1 are targets for acetylation which acts to enhance their activity (Gu, W. and Roeder, R.G., 1997; Boyes, J., *et al.*, 1998). Also, HDAC6 has been shown to regulate microtubule dependent cell mobility via its direct deacetylation of α -Tubulin (Hubert, C., *et al.*, 2002), while acetylation of DNMT1 protein acts as a marker for degradation, a process reversed by HDAC1 dependent deacetylation (Du, Z., *et al.*, 2010). These data suggest that altering the acetylation status of protein lysine residues may be a general mechanism for altering protein structures or protein-protein interactions. Using high-resolution mass spectrometry, Choudhary, *et al* have demonstrated that lysine acetylation is an abundant post-translational modification, occurring at approximately 3,500 sites in 1,750 proteins and targets proteins involved in diverse molecular processes, such as chromatin remodelling, cell cycle, splicing and nuclear transport (Choudhary, C., *et al.*, 2009). This study confirmed previously muted thoughts that the acetylome is potentially a post translational modification to rival phosphorylation (Kouzarides, T., 2000).

1.6 The KDAC/HDAC family of enzymes.

The fact that the reversible acetylation of histones is a key component in the regulation of gene expression has stimulated the study of lysine deacetylases (KDACs or as they will be referred to exclusively from here, HDACs).

Histones were first identified as the substrates of lysine deacetylase enzymes in 1969 by Inoue and Fujimoto. Latterly, Butyrate and more recently Tricostatin A (TSA) were demonstrated as inhibitors of histone deacetylation (Vidali, G., *et al.*, 1978; Yoshida, M., *et al.*, 1990) and as such the “moniker” HDAC has prevailed until recently. Using an inhibitor affinity tag, the first mammalian HDAC was purified and discovered to be an orthologue of the established global gene regulator in yeast (*S. cerevisiae*), reduced potassium dependency-3, Rpd3 (Taunton, J., *et al.*, 1996; Vidal, M. and Gaber, R.F., 1991) which accelerated the discovery of additional family members and also supported evidence (described in early sections) of their roles in the control of gene transcription. The discovery of NAD⁺-dependent sirtuin (or Sir2-like) family of histone deacetylases (Haigis, M.C. and Guarente, L.P., 2006) resulted in the definition of the Rpd3-like (Zinc-dependent) family of proteins to be the “classical” HDACs. Subsequently, the 18 mammalian histone deacetylases are classed into four main groups (I-IV) as depicted in figure 1.3. (Note that the class III enzymes, absent from Fig 1.3, constitute the sirtuin family.)

As depicted in figure 1.5, the catalytic domain of class I HDACs is extremely conserved when compared to their yeast ancestors and spans the

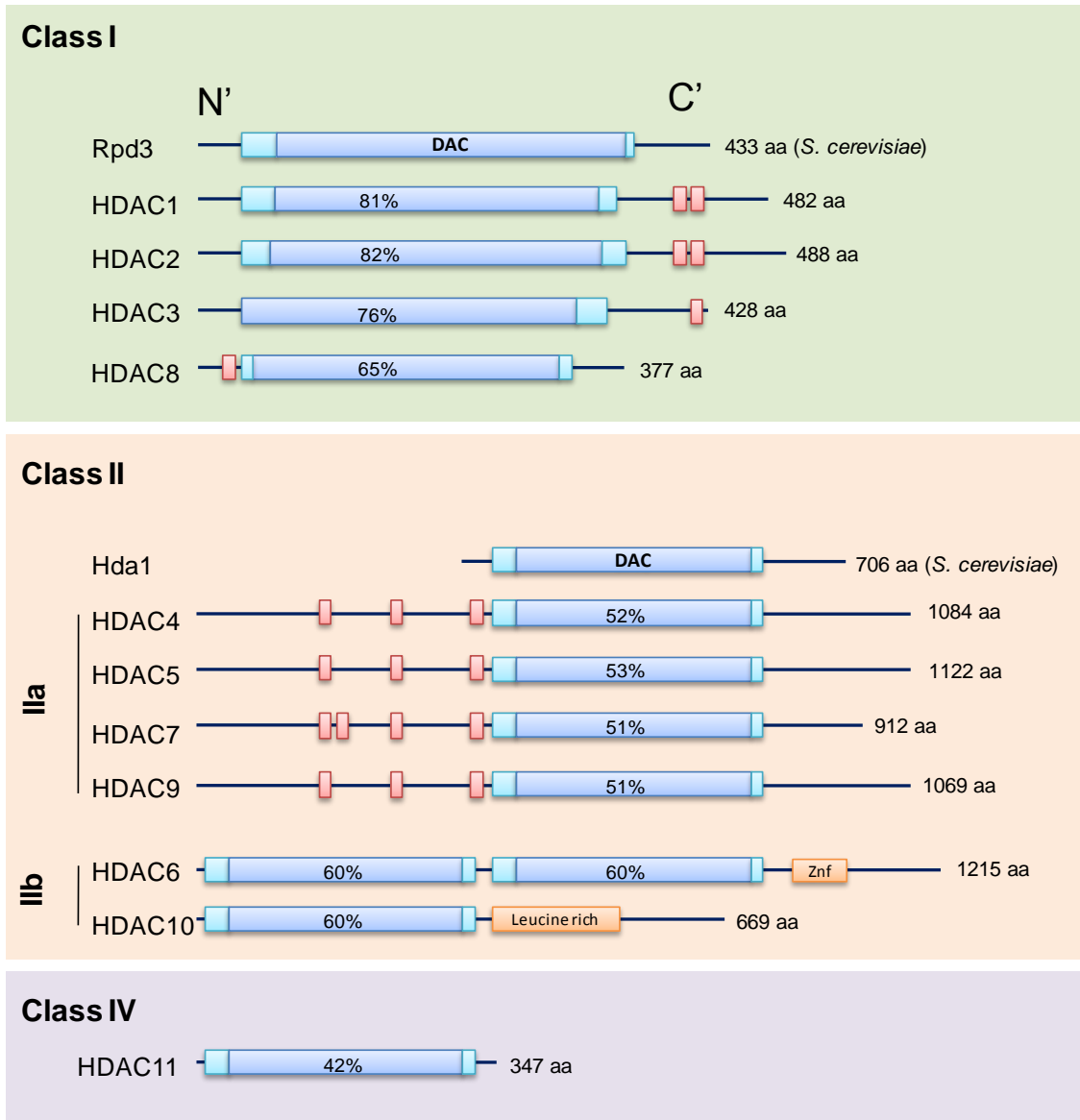


Figure 1.5. *Schematic depiction of mammalian histone deacetylases.* Mammalian histone deacetylases are grouped into four different classes according to their sequence similarity to their yeast counterparts. Dark blue bars indicate the deacetylase domain (DAC), percentages within indicate the percentage of sequence homology between Rpd3 (Class I) and Hda1 (Class II). The class II HDACs are further sub-classed into IIa and IIb. Homology of HDAC11 is compared to Hda1. Red bars indicate serine phosphorylation sites. N' (N-terminal), C' (C-terminal) and Znf (zinc finger). (Adapted from Yang, X-J. and Seto, E., 2008; Haberland, M, *et al.*, 2009; De Ruijter, A.J.M., *et al.*, 2003).

majority of these proteins (approximately 300 amino acids). Crystal structure data obtained from HDAC8 and the class II HDAC7, reveal that the tertiary structure of the catalytic domains are shared and comprise a pocket containing two adjacent histidine residues, two aspartic acid residues and one tyrosine residue forming a charge-relay system with a Zn^{2+} ion as an essential component (Vannini, A., *et al.*, 2004; Nielsen, T.K., *et al.*, 2005). This catalytic domain partly overlaps with an N-terminal HDAC association domain (HAD; residues 1 to ~50) which is essential for homo- and heterodimerisation (Taplick *et al.*, 2001). As histones are the predominant substrate of HDACs, it is essential that they be localised to the nucleus. This is achieved by class I enzymes by either the presence of a nuclear localisation motif or the absence of a nuclear export signal (HDACs 1 and -2 respectively) (Brunmeir, R., *et al.*, 2009) and in the instance of HDAC3, by its association with numerous class II HDACs when localised to DNA (Fischle, W., *et al.*, 2001). Nuclear localisation of the weakly expressed HDAC8 is also detected when over-expressed (Van den Wyngaert, I., *et al.*, 2000). HDACs 1 and 2 are almost identical proteins that appear to be the result of a duplication event (Gregoretta, I.V., *et al.*, 2004), share 86% sequence homology and two tandem casein kinase-2 (CK2) phosphorylation sites which can be modified post translationally, loss of which reduce enzymatic activity and complex formation (Pflum, M.K., *et al.*, 2001).

The class II HDACs -4, -5, -7 and -9 belong to the class IIa HDAC family and share between 51 and 60% with Hda1. They also have shared (but not evolutionary conserved) long N-terminal domains that contain binding sites for the transcription factor myocyte enhancer factor 2 (MEF2) and the chaperone protein 14-3-3 (Lu, J., *et al.*, 2000). Upon phosphorylation by the

Ca²⁺/calmodulin-dependent kinase (CaMK), these HDACs are shuttled from the nucleus to the cytoplasm by their interaction with chaperone protein 14-3-3, providing a direct link between extracellular signalling and transcription as has been shown in both cardiac, skeletal muscle and T cell development (Zhang, C.L., *et al.*, 2002; Chang, S., *et al.*, 2004; Kasler, H.G., *et al.*, 2011). In comparison to the ubiquitously expressed nature of class I enzymes, the class II HDACs have more tightly controlled patterns of expression, specifically enriched in endothelial and developing T cells (HDAC7) or muscle, heart and brain tissues (HDAC4, -5 and -9) (De Ruijter, A.J.M., *et al.*, 2003; Zhang, C.L., *et al.*, 2002; Chang, S., *et al.*, 2004; Vega, R.B., *et al.*, 2004; Chang, S., *et al.*, 2006).

Of the remaining “classical” HDACs, -6 and 10 form the class IIb family and HDAC11 is the sole class IV HDAC family member, of which little is known. HDAC6 is distinct from all other HDACs as it contains two deacetylase domains and in the main cytoplasmic where it effects the acetylation of cytoskeletal proteins such as α -Tubulin (Zhang, Y., *et al.*, 2008; Zhang, X., *et al.*, 2007).

1.7 Class I HDAC co-repressor complexes.

Common to their yeast ancestors, the mammalian class I HDACs are non-DNA binding and with the exception of HDAC8, are required to be recruited to specific co-repressor complexes, in order to be localised to histone substrates (Rundlett, S.E., *et al.*, 1996). The main mammalian class I HDAC containing complexes include Sin3 (Laherty, C.D., *et al.*, 1997), NuRD (Zhang, Y., *et al.*, 1999), CoREST (You, A., *et al.*, 2001), and N-CoR/SMRT (Fischle,

W., et al., 2002). HDAC1 and -2 form a heterodimer and constitute the catalytic sub-unit of all but the N-CoR/SMRT complex (Table 1.5). Of note is the presence of a number of proteins that contain DNA-methyl binding or PTM “reader” domains of the types discussed in 1.3.2 (and summarised in Table 1.3). These, combined with the presence of chromatin remodelers, form platforms which co-ordinate the deacetylase activities of HDAC1 and -2 with other modifiers of chromatin structure. It should be noted that these complexes can often exhibit similar although different, cell specific components. An example of which is the NODE complex (Nanog and Oct4 associated deacetylase, identified in mES cells) in which the key pluripotent transcription factors Nanog and Oct4 replace MBD3 and Rbbp7 of the canonical NuRD complex (Liang, J., *et al.*, 2008).). A common feature of these complexes is their direct interaction with DNA-sequence specific transcription factors such as; the RE1-silencing transcription factor, REST (Sin3, CoREST) (Andres, M.E., *et al.*, 1999; Naruse, Y., *et al.*, 1999), Ikaros (NuRD, Sin3) (Knoepfler, P.S. and Eisenman, R.N., 1999) and the Runt-domain transcription factors 1 and 2, RUNX1/2 (Sin3) (Lutterbach, J.J., *et al.*, 2000). Equally, HDAC1 is directly recruited to directly to gene promoters by individual transcription factors such as Yin Yang 1, (YY1) (Yang, W.M., et al., 1996).

Table 1.4. *The composition of class I HDAC complexes.* Listed are only interactions which have been biochemically purified (Adapted from Grozinger, C.M. and Schreiber, S.L., 2002; Yang, X. J. and Seto, E., 2008)

Complex	Component	Enzymatic activity/ modification recognition domain
Sin3	HDAC1	deacetylase
	HDAC2	deacetylase
	RbAp46, RbAp48	WD40 repeat
	Sin3A	PAH motifs
	Sds3	
	RBP1	
	SAP30	
	SAP18	ubiquitin fold
	ING1/2	PHD finger
	NuRD	HDAC1
HDAC2		deacetylase
RbAp46, RbAp48		WD40 repeat
Mi2 α/β		Chromo domain/ATP-dependent helicase
MTA1/2/3		SANT domain
MBD2/3		methyl CpG binding
P66 α/β		
CoREST	HDAC1	deacetylase
	HDAC2	deacetylase
	CoREST	SANT domain
	LSD-1	histone lysine demethylase/ SWIRM domain
	BHC80	PHD finger
	CtBP	dehydrogenase
N-CoR/SMRT	HDAC3	Deacetylase
	N-CoR/SMRT	SANT domain
	TBL1/TBLR1	WD40 repeat
	GPS2	
	JMJD2A	histone lysine demethylase/ PHD finger/Tudor domain
	Kaiso	methyl CpG binding

Abbreviations: BHC80, an 80-kDa subunit of the BRAF-histone deacetylase complex; CoREST, corepressor of REST (repressor element 1 silencing transcription factor); CtBP1, E1A C-terminal binding protein 1; ING1/2, inhibitor of growth 1 or 2; JMJD2A, jumonji demethylase D group member 2A; LSD1, lysine-specific demethylase 1; MBD3, methyl CpG-binding domain 3; MTA1, metastasis-associated protein 1; Mi2, dermatomyositis-specific autoantigen; NuRD, nucleosome remodelling deacetylase complex; PHD finger, plant homeodomain-linked zinc finger; PAH motif, paired amphipathic helix motif; RBP1, Rb-binding protein 1; SANT domain: Swi3, Ada2, N-CoR, and TFIIIB homologous domain; SAP30, Sin3-associated polypeptide of 30 kDa; SDS3, suppressor of defective silencing 3; N-CoR, nuclear receptor co-repressor; Sin3, SWI-independent 3; SMRT, silencing mediator of retinoic acid and thyroid hormone receptors; SWIRM domain, Swi3p, Rsc8p and Moira homologous domain; TBL1, transducin β -like protein 1; WD40 repeat, tryptophan-aspartate 40 repeat.

1.8 Functions of class I and II HDACs in mammals.

1.8.1 Germ-line deletion of class I and II HDACs.

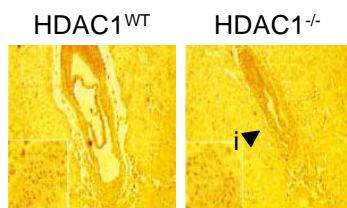
Unlike methylation, it is difficult to ascertain which HDACs is responsible for what modification, given that they co-occur in many co-repressor complexes. However it has been possible, through the use of reverse genetics, to determine which enzymes are required for a given physiological process.

In the mouse, germ-line deletion of all but HDAC10 and -11 has been performed (the results of which are summarised in Fig 1.6.). The embryonic lethality in HDAC1 null mice is reported to be as a result of developmental retardation, in part due to proliferation defects (Lagger, G., *et al.*, 2002). Likewise, HDAC3 knock-out mice die at a similar age reportedly due to gastrulation defects (Bhaskara, S., *et al.*, 2008; Montgomery, R.L., *et al.*, 2008). constitutive HDAC2 knock-out mice survive embryogenesis and either die perinatally in one model, due to a spectrum of cardiac defects (Montgomery, R.L., *et al.*, 2007), or survive to adulthood in others (Trivedi, C.M., *et al.*, 2007; Zimmerman, S., *et al.*, 2007), albeit at reduced Mendelian frequencies. The cardiac defects have been linked to the disruption of the function of the homeodomain-only protein (HOPx), previously established to interact with HDAC2, deletion of which results in a similar hyperproliferation of developing cardiomyocytes. These data implicate HOPx-HDAC2 co-repressive interactions in the negative regulation of cardiac differentiation. Deletion of HDAC8 results in severe craniofacial defects, a result phenocopied upon tissue specific deletion in the neural crest due to de-repression of a sub-set of homeobox transcription factors (Haberland, M., *et al.*, 2009). These data demonstrate that despite their

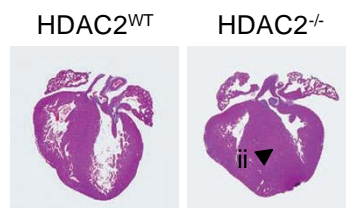
A.

Deacetylase	Time of lethality	Phenotype	Reference
HDAC1	E10.5	Proliferation defects	Lagger, G., <i>et al</i> , 2002.
HDAC2	Perinatal/ 50% neonatal	Cardiac malformation/ hypertrophy	Montgomery, R.L., <i>et al</i> , 2007, Trivedi, C.M., <i>et al</i> , 2007.
HDAC3	E9.5	Gastrulation defects	Montgomery, R.L., <i>et al</i> , 2008, Bhaskara, S. <i>et al.</i> , 2007.
HDAC8	Perinatal	Cranio-facial defects	Haberland, M., <i>et al</i> , 2009.
HDAC4	Perinatal	Chondrocyte hypertrophy	Vega, R.B., <i>et al</i> , 2004.
HDAC5	Viable	Stress induced cardiac hypertrophy	Chang, S., <i>et al</i> , 2004.
HDAC7	E11	Endothelial cell adhesion defects resulting in impaired vascular integrity	Chang, S., <i>et al</i> , 2007.
HDAC9	Viable	Stress induced cardiac hypertrophy	Zhang, C.L., <i>et al</i> , 2002.
HDAC6	Viable	Global tubulin hyperacetylation	Zhang, Y., <i>et al</i> , 2008.
HDAC10	-	-	
HDAC11	-	-	

B.



C.



D.

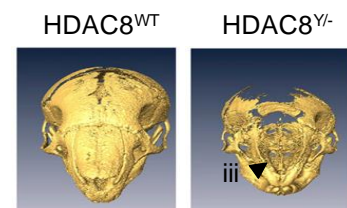


Figure 1.6. *Germ-line HDAC loss-of-function phenotypes in mice.* (A) Deacetylase enzymes in which germ-line loss of function studies have been carried out and the indicated phenotype. (B-D) Are selected results from germ-line loss-of-function studies of the class I HDACs 1, 2 and 8. (B) Immuno-histochemical analysis of the proliferation marker, Ki67 antigen, in mouse embryos at E7.5; i, highlights reduction in size of E7.5 embryos and reduced Ki67 staining in HDAC1 deficient embryos. (C) Hematoxylin and eosin stained sections of hearts from neonatal mice; ii, highlights an excess of cardiomyocytes of the left and right ventricles of HDAC2 mutant mice. (D) Three-dimensional reconstruction of micro-CT scans of newborn mouse skulls; iii, highlights the severe ossification defects in HDAC8 mutant mice. (B-D taken from Lagger, G., *et al.*, 2002, Montgomery, R.L., *et al.*, 2007 and Haberland, M., *et al.*, 2009, respectively.

common substrate specificity, nuclear localisation and high sequence homology, HDACs have unique, non-redundant roles in development and potentially control unique gene expression programmes or biological functions.

1.8.2 Tissue specific deletion of HDACs 1 and -2.

To overcome the embryonic lethality of HDAC1 and HDAC2 germ-line deficient mice, conditional alleles in combination with various Cre-expressing strains have been generated permitting the analysis of HDACs 1 and -2 in a tissue specific manner. Unsurprisingly, given that HDAC1 and -2 are co-expressed and present in the same co-repressor complexes, tissue specific deletion reveals functional redundancy between the two enzymes. Often deletion of both enzymes are required to develop a phenotype as is the case in B Cell development, haematopoiesis and the epidermis (Yamaguchi, T., et al., 2010; Wilting, R.H., et al., 2010; LeBoeuf, M., et al., 2010). However, in many tissue specific knock-outs, singular deletion of either HDAC, often results in a compensatory increase in its counterpart, notably in the absence of a change in mRNA levels. This enforces the fact that these enzymes share common functional roles. Data from these studies supports an overwhelming implication that HDAC1 and -2 have critical roles in the regulation of cell cycle. HDAC1 null mES cells (derived from the HDAC1 germ-line knock-out mice) have a much reduced proliferation capacity and an increase in the levels of the negative cell cycle regulator, p21. ChIP assays at the p21 promoter, in the absence of HDAC1, revealed increases in both H3 and H4 acetylation, and in WT mES cells, HDAC1 does indeed bind to the promoter of p21 (Lagger, G., et al., 2002).

Ablation of p21 in HDAC1 null mES cells “rescued” the reduced proliferation phenotype but intriguingly failed to rescue the developmental phenotype in p21/HDAC1 double knock-out mice, indicating that the developmental block in this model is not due to defective proliferation (Zupkowitz, G., *et al.*, 2010). Deletion of HDAC1 in primary mouse embryonic fibroblasts (MEFs) has a subtle effect on the G1/S transition, exacerbated upon combined deletion of HDAC2 and paralleled with up regulation of the cell cycle inhibitors (p21, p27) as well as radical apoptosis. Again, HDAC1 and -2 were shown to directly bind to the promoters of p21 and p27. Significantly, functional knock-down of these proteins reverted the block in cell cycle (Yamaguchi, T., *et al.*, 2010). In line with these data, knock down of HDAC1 and -2 in primary MEFs, transformed with large T antigen, and a number of tumour cell lines (but interestingly not all) also results in G1 cell cycle arrest and profound cell death (Wilting, R.H., *et al.*, 2010). Due to their function as positive regulators of cell cycle, as well as the anti-proliferative properties of HDAC inhibitors (Mann, B.S., *et al.*, 2007), HDACs have become the focus of intense research as targets for cancer therapy. HDAC1 and -2 fulfil many of the criteria required of effective anti-cancer targets. They are an essential cellular component, common to all cancer types, whose inhibition induces growth arrest or apoptosis.

Other than effects on cell cycle, deletion of HDAC1 and -2 has shown the requirement for either enzyme in development of the central nervous system (CNS), and in particular neuronal and oligodendrocyte development, via a mechanism which results in the stabilisation of β -catenin and thus activation of Wnt (wingless-integration 1) signalling (Montgomery, R.L., *et al.*, 2009; Ye, F., *et al.*, 2009). Yet despite this redundancy in CNS, development loss of HDAC2

in adults leads to aberrant Sox2 expression and an increased rate of proliferation in neuronal progenitors (Jawerka, M., et al., 2010).

Returning to the cardiac defects in HDAC2 knock-out mice, these defects cannot be phenocopied by conditional inactivation of HDAC2 in cardiomyocytes and smooth muscle (Montgomery, R.L., *et al.*, 2007). This suggests that the cardiac specific defects may occur in a number of cell types rendered defective by the absence of HDAC2 during embryogenesis. Thus, it appears that HDAC1 and -2 have distinct and as yet undefined roles in gastrulation in the developing embryo. In Chapter Four, using mouse embryonic stem cells, the *in vitro* counterpart of the developing blastocyst, I aim to decipher the unique roles of these enzymes during differentiation from the stem cell programme.

1.9 Intra-thymic T cell development.

Two major subsets of T lymphocytes in the peripheral immune system exist, helper and cytotoxic, which together form major arms of the specialised adaptive, cell-mediated immune response to pathogen. All helper and cytotoxic T cells express a clonotypic, cell surface T cell receptor (TCR) that recognises antigen as presented in the context of either class I or class II major histocompatibility complex (MHC) molecules (Jorgensen, J. L., *et al.*, 1992). These clonotypic receptors are generated earlier in T cell development through a process of selecting variably recombined, germ-line encoded gene segments of the α/β chains of the TCR (discussed later), which generates the diverse array of T cell receptors required for a functional adaptive immune response (Whitehurst, C. E., Chattopadhyay, S. and Chen, J., 1999, Hodges, E., *et al.*, 2003 and Murphy, K., *et al.*, 2008). Helper and cytotoxic T cells can be identified respectively, by their mutually exclusive expression of the cell surface glycoproteins CD4 and CD8, which aid in the TCR recognition of antigen/MHC by acting as co-receptors for either MHC class II (CD4) or MHC class I (CD8) molecules (Swain, S. L. 1983 and Janeway, C. A. Jr. 1992). Both subsets of T cells are derived from a common early lymphocyte precursor (ELP), with its prenatal and postnatal origins in the foetal liver and bone marrow respectively. ELPs circulate from the bone marrow to the thymus via the blood where their development into T cells takes place (the name “T” cell owed to their development in the thymus) (Medina, K. L., *et al.*, 2001). From here, “naive” CD4 or CD8 single positive (SP) cells exit to the periphery to further mature into “effector” cells upon contact with their cognate antigen, as presented by cells of secondary lymphoid organs such as the spleen and lymph

nodes (the primary lymphoid organs being the bone marrow and thymus) (Adkins, B., *et al.*, 1987).

Normal intra-thymic T cell development follows one of the best defined and well characterised pathways of somatic cell development, with individual stages defined by the relative expression of cell surface markers including CD4, CD8, CD44 and CD25, markers readily detected by fluorescence-activated cell sorting (Fig 1.7) (Godfrey, D. I., *et al.*, 1993, Starr, T. K., *et al.*, 2003). An overview of intra-thymic T cell development is depicted in figure 1.8. The most immature T cells, denoted double negative (DN), express neither CD4 nor CD8 and are also negative for the expression of the TCR. DN cells pass through four developmental stages (DN1-4), defined by the expression of CD44 and the α -chain of the IL-2 receptor, CD25. DN cells give rise to α/β TCR expressing cells (destined to become CD4⁺ or CD8⁺ single positive T cells) or cells expressing γ/δ TCRs (a small subset of T cells which lie at the interface between innate and adaptive immunity), a decision made at the DN3 stage of development (Robey, E. and Fowlkes, B. J., 1994). During this stage, the majority of cells, destined to become α/β T cells, begin to express a re-arranged TCR β chain, the product of successful, in-frame, somatic DNA V(D)J recombination, an event mediated by the recombination activating genes 1 and 2 (RAG1 and RAG2) (Mombaerts, P., *et al.*, 1992, Shinkai, Y., *et al.*, 1993). This is coupled with expression of a germ line configured pre-TCR α . Expression of a viable TCR β chain suppresses further TCR β gene locus rearrangement, ensuring the clonal expression of only a single rearranged β chain (allelic exclusion). On the cell surface, the pre-TCR α /TCR β chain pair forms the pre-TCR complex by associating with the

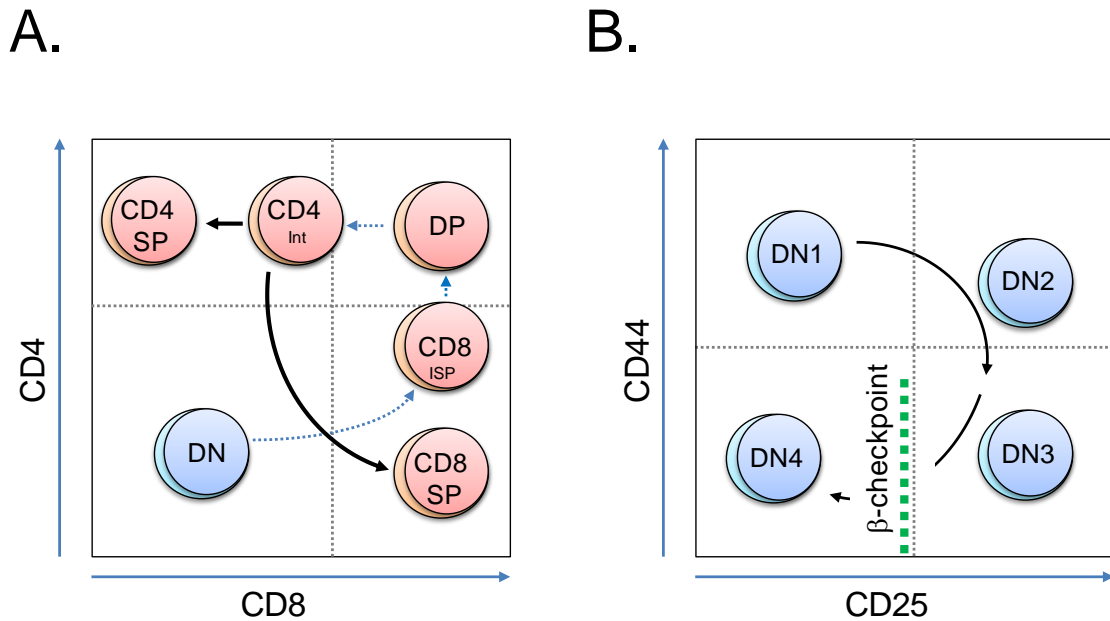


Figure 1.7. Overview of T cell developmental sub-populations as defined by the expression of cell surface markers. (A) Schematic of DN to SP thymocyte development. **DN**: $CD4^-/CD8^-$, **CD8^{ISP}**: $CD4^{low}/CD8^+$, **DP**: $CD4^+/CD8^+$, **CD4^{Int}**: $CD4^+/CD8^{low}$, **CD4SP**: $CD4^+/CD8^-$ and **CD8SP**: $CD4^-/CD8^+$. SP: single positive. (B) Schematic of DN1 to 4 thymocyte development. **DN1**: $CD44^+/CD25^-$, **DN2**: $CD44^+/CD25^+$, **DN3**: $CD44^-/CD25^+$ and **DN4**: $CD44^-/CD25^-$. Schematics depict positions of thymocyte populations (when plotted as dot-plots) as analysed for cell surface expression of CD4/CD8 and CD44/CD25 by FACS.

transmembrane CD3/ ζ complex (van Oers, N. S., *et al.*, 1995, von Boehmer, H., *et al.*, 1997). Signal transduction via the TCR complex propels DN3 cells to the DN4 stage (i.e. through the β -selection checkpoint) (Negishi, I., *et al.*, 1995). DN4 cells then undergo substantial cellular proliferation and activate CD8 transcription to become a short lived population of immature single positive (CD8^{ISP}) cells. De-repression of CD4 leads to the development of a bipotential subset of CD4 and CD8 expressing double positive (DP) cells, which make up approximately 80% of total thymocytes (Germain, R. N., *et al.*, 2002). During

this time, the pre-TCR α is replaced as DP cells begin to rearrange the TCR α gene locus, again by RAG mediated V(D)J recombination. DP thymocytes come into contact with epithelial and dendritic cells, of the cortical and medullary stroma (cells abundant in the expression of MHC class I and II presenting “self-peptide” ligands). The cell fate of a DP cell at this stage is determined by the strength of signalling mediated by the specificity of the MHC “self-peptide”-TCR complex interaction (specificity of the interaction conferred by the variably configured α/β -chains of the TCR) (von Boehmer, H.*et al.*, 1989). In the absence of a TCR mediated signal (as a consequence of weakly interacting, non-functional TCR α/β -chain rearrangement) DP cells undergo apoptosis in a process known as death by neglect. Conversely, too strong a TCR-complex mediated signal, results in apoptosis and a process known as negative selection. Death by neglect and negative selection are means by which the thymus mediates the elimination of T cells preventing the maturation of both non-reactive and dangerous self-reacting T cell populations (approximately 95-97% of DP cells are thought to die at this stage (Surh, C.D., and Sprent, J., 1994). Those cells that receive an adequate, intermediate TCR complex “survival” signal are positively selected for survival and briefly terminate transcription of CD8, which manifests as an intermediate subpopulation of cells phenotypically CD4⁺/CD8^{low} (CD4^{Int}) (Singer, A., *et al.*, 2008). Signalling via the TCR-MHC interaction activates lymphocyte specific protein tyrosine kinase (LCK) (Anderson, S.J., *et al.*, 1994). Once activated a sequential cascade of phosphorylation events occurs whereby LCK phosphorylates immunoreceptor tyrosine based activation motifs (ITAMs) of the CD3 ζ chain which in turn act as

binding sites for the paired SRC-homology domains (SH2) of ZAP-70 (ζ -chain associated protein).

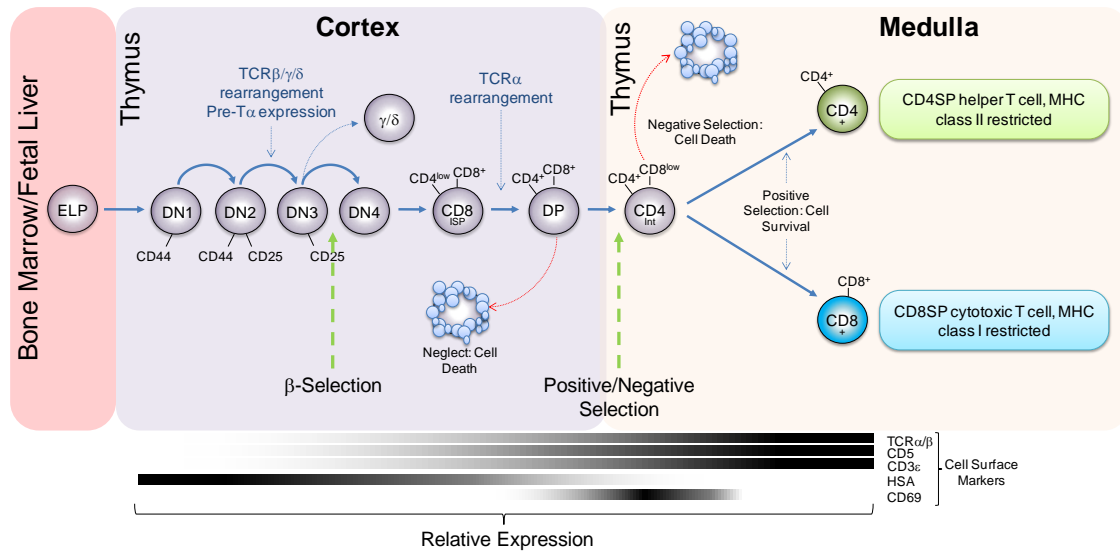


Figure 1.8. *Overview of intra-thymic T cell development.* Early lymphoid progenitor (ELP) cells enter the thymus from the bone marrow as double negative (DN) cells, the most immature cells of the thymus and exit to the periphery as either CD4SP helper, MHC class II restricted or CD8SP cytotoxic, MHC class I restricted T cells. DN1, DN2, DN3, and DN4 stages of DN cell differentiation are distinguished by the relative expression levels of CD44 and CD25. Likewise, stages of DN to CD4⁺ or CD8⁺ T cell differentiation are distinguished by the relative expression levels of CD4 and CD8. Bottom Panel: expression of other cell-surface markers, in combination with the expression of CD4/8, used to distinguish compartments of intra thymic development of T cells of the TCR α/β lineage. **TCR $\alpha\beta$** (α and β chains of the T cell receptor), **CD3 ϵ** (CD3 ϵ chain of the CD3 complex) and **CD5** (T cell surface glycoprotein) all exhibit gradual increases in expression from low (DN) to high (SP). **HSA** (heat stable antigen) expression is gradually decreased from high (DN) to low (SP). **CD69** (early activation antigen) is expressed on activated T cells during positive/negative selection (Mekenschlager, M., *et al.*, 1997, Star, T. K., *et al.*, 2003). SP: Single Positive CD4⁺ or CD8⁺ T cells.

kinase, 70kDa) (Weiss, A. and Littman, D.R., 1994 and Kane, L.P., *et al.*, 2000) Lck associated with the proximal MHC interacting CD4 or CD8 coreceptors, then activates bound ZAP-70 which in turn phosphorylates the adaptor protein, LAT (linker for activation of T cells)(Zhang, W., *et al.*, 1998). Several other enzymes and adaptor proteins are activated which ultimately directs gene expression required for T cell survival and lineage commitment via activation of the MAPK (mitogen-activated protein kinase) pathway, nuclear translocation of NFAT (nuclear factor of activated T cells) and activation of the transcription factor NF- κ B(Wang, L., *et al.*, 2010). The duration of TCR signalling mediated by the TCR-MHC-coreceptor interaction (the kinetic signalling model), is widely becoming accepted as the determining factor in CD4 or CD8 lineage commitment in positively selected T cells. That is sustained TCR signalling in CD4^{Int} T cells results in CD4 commitment with attenuated signalling resulting in reversal of coreceptor expression and CD8 commitment (Fig 1.9).

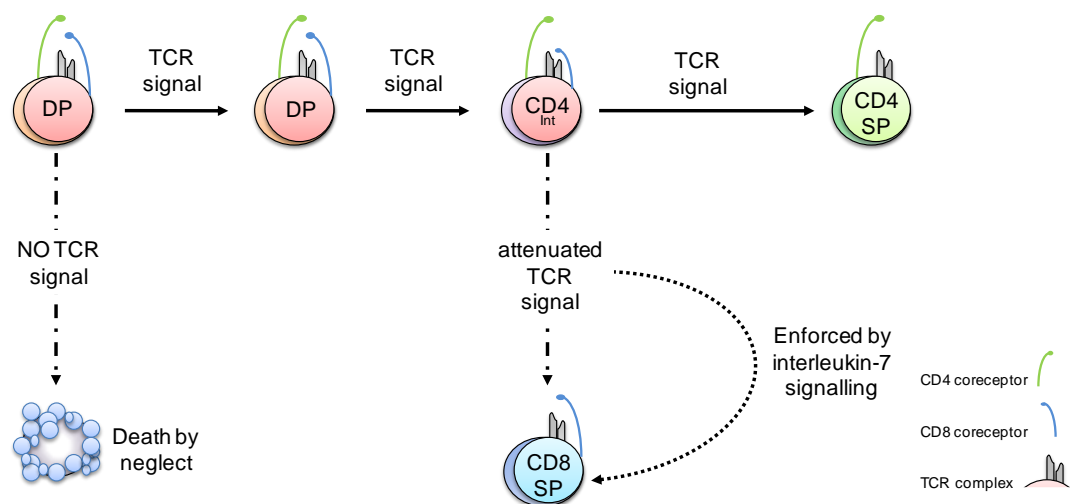


Figure 1.9. *Kinetic signalling model of T cell lineage commitment.* From right to left, no TCR signalling results in death by neglect, appropriate TCR signalling results in positive selection of uncommitted DP cells and downregulation of CD8 (CD4^{Int}). Sustained or persistent signalling results in CD4 lineage commitment, whereas attenuated TCR signalling results in coreceptor

expression reversal and CD8 lineage commitment. Attenuation of TCR signalling also permits transduction of IL-7 (interleukin-7) signalling which acts to enforce CD8 specification (Yu, Q., *et al.*, 2003).

1.10 Transcription factors and co-repressor complexes in T cell development.

Due to the well defined pathways of development, T cell differentiation presents a paradigm in which to study not only the many aspects of T cell developmental biology, which include cellular proliferation, survival, apoptosis, signal transduction and migration, but also the underlying changes in gene expression brought about as a requirement or a reflection of lineage commitment. With the exception of the TCR, which is assembled by a process of V(D)J gene segment recombination, lineage commitment is not resolved by changes in DNA sequence. Rather, commitment is imposed by alterations in the patterns of gene transcription that are enforced in a heritable, epigenetic manner. In particular the expression of CD4 and CD8, while acting as stage specific markers, present ideal candidates for studying the mechanisms by which epigenetic changes are dynamically regulated during development. That is, expression of CD4 and CD8 is down regulated or repressed in DN cells, derepressed or expressed in DP cells and dependent on lineage commitment, terminally expressed or silenced in single positive CD4⁺ or CD8⁺ cells. Thus, the expression of CD4/8 in T cell development in particular, represents a system to examine factors involved in both the permanent and reversible control of gene expression. Mice, housed under standard laboratory conditions, present a physiological model system in which to study T cell development as in these

animals the thymus is rendered a non-essential tissue (ordinarily these animals are not immunologically challenged). Applying reverse genetics has already established roles for a number of key transcriptional activators, repressors, corepressors and chromatin modifying enzymes in T cell development.

1.10.1 Key transcription factors in T cell development.

Runx transcription factor complexes consist of two Core Binding Factors (CBFs), a DNA binding Runx/AML family protein and a non-DNA binding subunit, CBF β , which dependent on context act as repressors or activators of transcription (de Bruin, M. F. T. R. and Speck, N.A., 2004, Ito, Y., 2008). The three mammalian forms of Runx; Runx1, Runx2 and Runx 3 are all expressed during T cell development (Sato, T., *et al.*, 2005). Conditional knock-out studies have shown that Runx2 is dispensable during T cell development (or has a redundant function compensated by the presence of Runx1/3) (Tanuichi, I., *et al.*, 2002a). Conversely, deletion of Runx1 and -3 has revealed non-redundant roles in the regulation of CD4 expression. Disruption of Runx3 leads to derepression of CD4 in CD8SP cells but not in the DN subpopulation. This contrasts with disruption of Runx1 where precocious expression of CD4 is observed in the DN compartment but unaffected in CD8SP T cells. Stage specific transcription of the *Cd4* locus is conferred by a region known as the CD4 silencer, deletion of which leads to cell surface expression of CD4 in both DN and CD8SP thymocytes (Zou, Y. R., *et al.*, 2001, Taniuchi, I. and Littman, D. R., 2004). Deletion of Runx binding motifs, within the CD4 silencer, confirmed that Runx transcription factor binding was critical for silencer activity

and thus CD4 repression (Tanuichi, I., *et al.*, 2002b). In contrast to their roles in CD4 repression, the association of Runx proteins with *Cd8* gene loci enhancer elements suggests a positive role in *Cd8* expression (Sato, T., *et al.*, 2005). This view is further supported by the reduced levels of CD8 expression in CBF β depleted developing thymocytes (Naoe, Y., *et al.*, 2007).

In addition to its role in CD4 repression, conditional deletion of Runx1, at a variety of developmental stages, has revealed roles in T cell proliferation and or survival (blocked transition from DN2-3 compartments, reduced proliferation post β -selection, as well as defective survival in the periphery) (Growney, J.D., *et al.*, 2005, Ichikawa, M., *et al.*, 2004 and Egawa, T., *et al.*, 2007). Deletion of the common Runx transcriptional subunit, CBF β (at the DN3 and DP stage of development), results in similar developmental defects to Runx 1 and -3 conditional knock-outs, confirming Runx transcription factors to be key mediators of T cell development (Naoe, Y., *et al.*, 2007).

Gata3 is a zinc-finger transcriptional regulator, crucial for the development of the earliest T cell progenitors (Hendriks, R.W., *et al.*, 1999). Retroviral transduction of GATA3 in thymic organ cultures revealed overexpression of GATA3 biased T cell differentiation towards the CD4 lineage. Reduced GATA3 expression in the same assays, using RNA interference (RNAi), had the opposing effect, a result confirmed *in vivo* by deleting GATA3 protein at the DP stage of T cell differentiation (Hernandez-Hoyos, G., *et al.*, 2003 and Pai, S Y., *et al.*, 2003).

Identification of a spontaneous, deficient CD4SP mutant mouse strain, subsequently named HD (“helper deficient”), was the beginning of identifying a

“master” regulator of CD4/CD8 lineage commitment (Dave, V. P., *et al.*, 1998). Lack of CD4 T cells in the periphery was identified as a consequence of redirected cells expressing MHC class II restricted TCRs to the CD8 lineage, a finding that indicated CD4/CD8 lineage choice to be an independent event of positive selection and not a stochastic process based on the expression of the co-receptor (Keefe, R., *et al.*, 1999). Subsequently, the molecular mechanism responsible for the HD phenotype was elucidated as being a single base pair point mutation in the DNA binding domain of a zinc-finger transcription factor encoded by the *ThPOK* gene. Gain (and loss) of function studies have demonstrated that ThPOK expression is necessary to direct CD4 expression in MHC II restricted cells but also sufficient to redirect class I MHC T cells into the CD4 T helper lineage (He, X., *et al.*, 2005). ThPOK is part of the BTB-ZF (Broad-complex, Tramtrack and Bric-a-brac zinc finger) family of transcription factors (generally thought to be repressors of transcription), of which MAZR (Myc-associated zinc-finger related factor) is another expressed during T cell development (Billic, I. and Ellmeier, W., 2007). In contrast to ThPOK, MAZR deficient MHC I cytotoxic T cells are redirected to the CD4 lineage likely through derepression of ThPOK expression (MAZR was demonstrated to bind to a region of the ThPOK locus, termed *ThPOK* silencer, upstream of the ATG translational start site, in controls) (Sakaguchi, S., *et al.*, 2010).

Mutation of another zinc-finger transcription factor, Ikaros, has shown it to be required for the differentiation of haematopoietic pre-cursors into cells of the lymphoid lineage (Georgopoulos, K., *et al.*, 1994). Moreover, mice expressing a functionally inactive form of Ikaros develop aggressive lymphoma (Winandy, S. P., *et al.*, 1995). Thymic cellularity of Ikaros null mice is reduced

up to 9-fold. The few T cells that develop to the SP stage also exhibit a bias towards the CD4 lineage (Wang, H., *et al.*, 1996 and Urban, J.A. and Winandy, S., 2004) demonstrating a role for Ikaros in CD8 lineage commitment.

In summary, key transcription factors required for CD4 commitment include Gata3 and ThPOK. Those which appear to be required for CD8 commitment include Runx 1/3 (via direct repression of *CD4* transcription as well as active expression of *CD8*), MAZR (via the repression of ThPOK) and Ikaros (Fig 1.10). Notably, a substantial amount of evidence points to a collaborative or antagonistic relationship between the roles of these transcription factors, especially with regards CD4/CD8SP lineage commitment, centred on the control of *ThPOK* expression. Analysis of double mutant Runx1 and -3 mice revealed a reduced number of peripheral CD8 SP thymocytes due to redirection of class I-MHC T cells into CD4SP thymocytes and was concomitant with de-repression of ThPOK at a critical pre-selection stage during development (in WT thymocytes the earliest detection of ThPOK is in a subsequent post-selection stage of development) (Setoguchi, R., *et al.*, 2008). The same study utilised ChIP-on-chip (DNA enriched by chromatin immunoprecipitation hybridised to tiling arrays) to identify two Runx binding sites, one of which was the *ThPOK* silencer and confirmed a direct role for Runx mediated repression of ThPOK. Similar studies have also identified an opposing role for Gata3 as an upstream activator of ThPOK expression (Wang, L.K.F., *et al.*, 2008).

1.10.2 The roles of co-repressors complexes and chromatin modifying enzymes in T cell development.

Many of the transcription factors discussed above have known associations with co-repressors complexes. In particular, Runx proteins associate with transcriptional repressors TLE (transducin-like enhancer), as well as several HDAC enzymes and also with the co-repressor mSin3a. The association of Runx1-TLE has been shown to be vital for T cell development (aberrant CD4 expression) by mutating the Runx-TLE binding motif at the C' terminus of the Runx1 (an interaction site not shared with HDACs or mSin3a) (Aronson, B. D., *et al.*, 1997 and Levanon, D., *et al.*, 1998, Lutterbach, B., *et al.*, 2000, Wheeler, J. C., *et al.*, 2000 and Durst, K.I., *et al.*, 2004). Conditional deletion of mSin3a results in a partial block in α/β development at the DN3 stage and subsequently reduced DP and SP thymocyte cellularity, putatively due to a block in pre-TCR induced proliferation and not TCR signalling (which appeared intact). Additionally, mSin3a depleted thymocytes cultured *in vivo*, exhibited a higher apoptotic index (as measured by AnnexinV staining) which may also contribute to the decreased cellularity (Cowley, S.M., *et al.*, 2005). It is possible, given the requirement of Runx proteins for CD8 T cell development that the decrease in CD8 cells could be due to the disruption of a Runx-mSin3a interaction. Importantly in this study, mSin3b is up-regulated upon deletion of mSin3a and may, in part, compensate for loss of mSin3a. To date, examination of the role of mSin3b in T cell development has not been assessed.

Like Runx proteins, a small amount of Ikaros associates with mSin3a in T cells, with the remaining majority associated with Mi2 β , a core component of the HDAC1 and -2 containing NuRD co-repressor complex (Kim, J., *et al.*, 1999).

Conditional inactivation of Mi2 β results in an accumulation of DP-like thymocytes that fail to express CD4. In particular, Mi2 β was shown to be required for the active recruitment of the transcription factor HEB and p300 (a HAT enzyme) to the proximal *Cd4* enhancer region in order to facilitate *Cd4* transcription. Co-immunoprecipitation of p300 demonstrated interactions between Mi2 β , HEB and p300 but notably, not HDAC2, revealing a putative role for the NuRD complex as a positive regulator of transcription in the absence of HDACs (Williams, C., *et al.*, 2004). The same group, revealed an antagonistic interaction between Ikaros and Mi2 β in determining CD4 expression, using double Ikaros/Mi2 β knock-out mice the opposing individual knock-out developmental phenotypes reverted to those similar to WT (Sridharan and Smale, 2007, Naito, T., *et al.*, 2007). Intricate analysis of the chromatin landscape at the *Cd4* locus in Ikaros and Mi2 β knock-out thymocytes demonstrated that Ikaros is required for the repression of CD4 from the DN stage by laying down a repressive chromatin state, marked at the *Cd4* silencer by comparative histone hypoacetylation. During the DN-DP transition this repressive state at the *Cd4* silencer is antagonised by the Mi2 β dependent, active recruitment of MOZ and the TFIID component of the basal transcriptional machinery, which results in *Cd4* silencer histone hyperacetylation and expression of CD4. In their analysis, HDAC2 was present at the CD4 silencer in ChIP experiments performed on total thymocytes (the majority of which express CD4) and deletion of Mi2 β or Ikaros did not change this association or dramatically affect the localisation of other corepressor proteins which were also present (Runx1 or mSin3a), suggesting that the antagonistic interactions of Ikaros and Mi2 β at the *Cd4* silencer are independent of these corepressor

proteins (Naito, T., *et al.*, 2007). Intriguingly, given the altered acetylation status of the *CD4* silencer in these experiments, HDAC1 occupancy was not assayed.

Other chromatin remodelling complexes have also been implicated in T cell development, including; the BAF complex (a mammalian homologue of the yeast SWI/SNF ATPase chromatin remodelling complex) (Chi, T., *et al.*, 2002); NCoR (nuclear receptor corepressor), (Jepsen, K., *et al.*, 2000); and the nucleosome remodelling factor NURF (the founding member of imitation switch remodelling complexes, ISWI) (Landry, J.W., *et al.*, 2011) (Fig 1.10).

1.10.3 Histone deacetylases in thymic T cell development.

Although HDACs are core components of corepressor complexes (essential for normal T cell development) analysis of their specific roles has been limited, due in part to the embryonic lethality observed in HDAC null mice or the expression of functionally redundant family members. To date, only the roles of HDAC1 and HDAC7 have been assessed. Conditional inactivation of HDAC7 at the DN3 and DP stages of development resulted in a block in differentiation at the DP stage and an accumulation of immature CD8^{ISP} cells. Viability of HDAC7 deficient DP cells was reduced due to upregulation of a pro-apoptotic pathway, which subsequently impaired the efficiency of TCR α chain rearrangement in mutant DP thymocytes. As well as a role in T cell survival, global expression analysis revealed HDAC7 mediates repression of a subset of genes involved in TCR signalling transduction to the nucleus (Kasler, H.G., *et al.*, 2011). Deletion of HDAC1 at the DP stage of T cell development has not revealed any obvious phenotype. As is common with ablation of HDAC1 protein, upregulation of HDAC2 was observed which may compensate for the

loss of its corepressor partner and infers that combined deletion of the two proteins would provide a better understanding of their roles. Given the importance and frequency of key corepressor complexes and transcription factors in T cell development, with HDAC1/2 associations, genetic assessment of these enzymes in T cell development would be a means to confirm their often inferred classical repressive functions, which has until now, been surprisingly overlooked. As such, combinatorial deletion of HDAC1 and -2 in T cell development is the subject of Chapter Five.

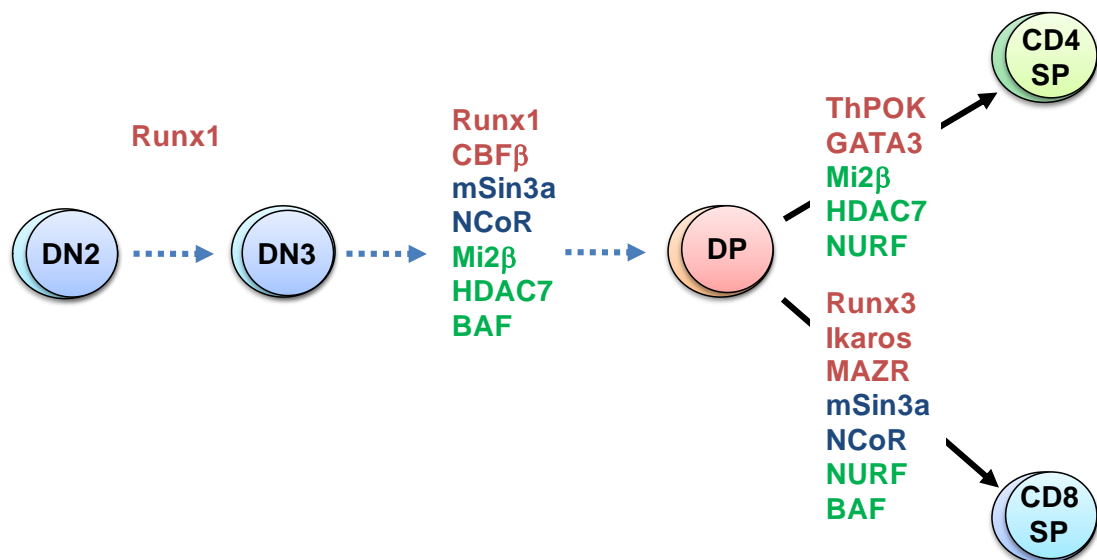


Figure 1.10. *Key transcriptional factors, corepressors and chromatin modifiers in intra-thymic T cell development.* Shown is a schematic of T cell development, listing negative regulators of transcription required at different stages of T cell development as demonstrated by null or conditional knock-out mice. The names of **transcription factors** are shown in red, **co-repressors** shown in blue, and **chromatin modifiers** shown in green.

Chapter Two: Materials and Methods.

2.1 Chemicals and reagents.

All commonly used stocks, solutions and buffers were prepared as described in *Current Protocols in Molecular Biology* (Ausubel, F. M., *et al.*, 2007, Wiley). Unless otherwise stated, all chemicals and reagents were of analytical grade or higher and supplied by Sigma Aldrich or Fisher Scientific. Enzymes, unless otherwise stated were supplied by New England Biolabs (NEB).

2.2 Culture and manipulation of mouse embryonic stem cells.

The E14 CreER-T mouse embryonic stem (mES) cell line, exclusively used for all experimental work described in this thesis, was a kind gift from David Adams and Jos Jonkers. All standard mES cell culture procedures and reagents are described in *Gene Targeting, A Practical Approach* (Joyner, A.L., 2000, Oxford University Press). The constituents of all mES cell culture reagents are listed in 2.2.7.

2.2.1 Thawing and seeding mES cells.

Individual vials of mES cells (typically containing $5-8 \times 10^6$ cells in a total volume of 1ml) were thawed rapidly at 37°C and seeded onto 1 x 10cm² culture plates coated with 0.1% gelatin solution in PBS (prepared at least 1hr prior to

thawing mES cells). Routine culture of mES cells was maintained by daily changes with standard mES cell medium (M15+LIF) with cells grown in a 5% CO₂ incubator at 36.8°C.

mES cells frozen in 96-well plates were revived from -80°C storage by the addition of 100µl/well of pre-warmed (36.8°C) standard culture media and mixed thoroughly by pipetting up and down several times. 50-75µl/well of the cell suspension was then split between 3 x 96-well plates pre-coated with 0.1% gelatin solution before adding a further 125µl/well of standard mES cell culture medium to all plates.

2.2.2 Passage of mES cells.

Once plates of mES cells had achieved ~80% confluency, cells were passaged (or split) 1:4. Prior to passaging, mES cells were fed with fresh media at least 1hr before, followed by two washes at room temperature (RT) with PBS. After the final wash, PBS was aspirated and mES cell dissociation achieved by incubation at 36.8°C for 5' in pre-warmed trypsin solution (1/5 volume of normal culture medium). To quench the dissociation reaction, an equal volume of standard mES cell medium was added and cells suspended by pipetting back and forth several times. Cells were aspirated, pelleted by centrifugation for 5' at 1,200rpm, re-suspended in fresh media and divided between 4 newly 0.1% gelatin coated culture dishes.

mES cells cultured in 96-well plates that had achieved ~80% confluency, were washed in PBS as above and incubated at 36.8°C for 5' in 50µl/well of

pre-warmed trypsin solution. 100µl/well of standard mES cell culture medium was added and cells re-suspended. 50µl/well of the cell suspension was then split between 3 x 96-well plates pre-coated with 0.1% gelatin solution before adding a further 125µl/well of standard mES cell culture medium to all plates.

2.2.3 Freezing and storage of mES cell stocks.

mES cells from tissue culture dishes were dissociated as described (2.2.2) and re-suspended in equal volumes of standard mES cell culture medium and 2X freezing media (up to 4mls total volume). Typically an 80% confluent 10cm² plate yields 2-3 x 10⁷ mES cells, as such 1ml aliquots of cell suspensions were transferred to 1.5ml cryovials. Cells were frozen slowly, to prevent the formation of ice-crystals, by transferring vials to freezer pots containing iso-propanol and placed at -80C for 24hrs, after which cryovials were transferred to long term storage in liquid nitrogen.

mES cells cultured in 96-well plates were dissociated as previously described (2.2.2) with the following exception to the protocol. 50µl of trypsin solution/ well was added to dissociate cells at 36.8°C for 5' and directly followed by the addition of 50µl of 2X freezing media. Cells were suspended by pipetting back and forth several times before wrapping the plates in cling film and blue roll. The wrapped plate was then placed in a sealed plastic box and transferred, for long term storage, to a -80°C freezer.

2.2.4 Population doubling, colony formation and alkaline phosphatase assays.

To assess the proliferative potential of mES cell lines 1.5×10^6 cells were seeded in triplicate in 6 well culture plates, trypsinised and counted every 2-3 days for a period of 18 days.

Population doublings were calculated as follows:

$$\text{PD} = \frac{\log \text{CICnt} - \log \text{INoCI}}{\log T}$$

PD: population doublings

CICnt: actual cell count on a given day

INoCI: initial number of cells seeded

T: number of days between seeding cells and counting cells

Colony formation was assessed by seeding 7×10^2 cells in triplicate in 6 well plates followed by culture for 8 days. Colonies were stained with methylene blue (to aid in identification) and counted by eye.

For alkaline phosphatase assays cells were plated at 7×10^2 cells per well in 6-well plates in the presence of LIF. After overnight culture, cells were cultured in the presence or absence of LIF for 6 days, fixed with 4% formaldehyde for 2', washed 2 x in PBS/0.1% Tween and stained with a commercial Alkaline Phosphatase Assay Kit (Millipore, Watford). This required prior combination of Fast Red Violet, Napthol and water in a ratio of 2:1:1. Cells were incubated at RT in the dark for 15min followed by a final wash in PBS/0.1% Tween. Cells were viewed by light microscopy and scored as follows;

undifferentiated (strong purple staining), mixed (intermediate purple staining) and differentiated (absence of purple staining).

2.2.5 *In vitro* differentiation of mES cells, embryoid body formation.

mES cell differentiation was evoked by culturing cells as embryoid bodies (EBs) according to the hanging drop method for two days (Valamehr, B., *et al.*, 2008). Drops of differentiation medium, containing 7×10^2 mES cells, were plated onto the lids of 15cm² culture dishes. After 48h, EBs were transferred to culture plates coated with a hydrophobic coating (Sylgard184, Dow Corning Corporation, Midland MI, USA) and cultured in suspension under constant rotation for a further 10 days. For serum free differentiation of EBs, formation of EBs was carried out as above with differentiation medium replaced with the commercially available serum free ESGRO® Complete Basal Medium (Millipore, Watford). EBs were visualised daily by light microscopy and diameters measured using the Leica Application Suite software.

2.2.6 *Neuronal lineage differentiation of mES cells.*

In vitro differentiation of mES cells into cells of neuronal lineage was achieved using a variation on published methods (Ying, Q.L., *et al.*, 2003) and depicted in figure 4.10A. Briefly, EBs were generated as in 2.2.4 and on day 4 differentiation medium was supplemented with 10^{-6} M all-trans retinoic acid (ATRA). On day 8 EBs were dissociated into a single cell suspension with 5X trypsin solution and seeded (2×10^5 cells/slide) onto glass slides coated with

50µg/ml laminin (Sigma, #L2020). Culture of cells on coated slides continued for a further 4 days in standard differentiation media without ATRA prior to preparation for immunocytochemistry.

2.2.7 Media and reagents used for the culture and manipulation of mouse embryonic stem cells.

Standard mES cell medium (M15+LIF)

Knockout DMEM + L-Glucose –Pyruvate (GIBCO, Life Technologies, Paisley)	500ml
Foetal Calf Serum (Hyclone, Thermo Scientific, Hemel Hempsted)	90ml
100X Glutamine/Penicillin/Streptomycin	6ml
100mM β-mercaptoethanol	600µl
Leukaemia Inhibitory Factor (LIF, Synthesised In House)	50µl

2.5% trypsin solution (1X Trypsin solution)

PBS (GIBCO, Life Technologies, Pasiley)	500ml
0.5M EDTA	500µl
Trypsin solution (Invitrogen, Life Technologies, Pasiley)	20ml
Chicken serum (Invitrogen, Life Technologies, Pasiley)	5ml

0.1% gelatin

PBS	500ml
2% Bovine gelatin solution	25ml

2X freezing media

Knockout DMEM (GIBCO, Life Technologies, Pasiley)	60%
Foetal Calf Serum (Hyclone, Thermo Scientific, Hemel Hempsted)	20%
DMSO	20%

Differentiation medium

Knockout DMEM + L-Glucose –Pyruvate (GIBCO, Life Technologies, Pasiley)	500ml
Fetal Calf Serum (Hyclone, Thermo Scientific, Hemel Hempsted)	90ml
100X Glutamine/Penicillin/Streptomycin	6ml

2.3 mES cell gene targeting and molecular cloning.

Specifics of enzymes and polymerase chain reaction (PCR) primers used in gene targeting/molecular cloning are described in detail in Chapter 3, as are Southern blot screening strategies (for a complete list of PCR primers and enzymes used see APPENDIX tables A1 and E1 respectively).

2.3.1 Targeting vector/DNA electroporation.

Approximately 10 μ g of targeting vector plasmid DNA was linearised by restriction digest, electrophoresed and visualised on a 1% agarose gel. The linearised fragment was then gel purified and eluted in 50 μ l of T.E. Two separate aliquots of 1 x 10⁷ E14 CreER-T mES cells were washed 2 x in PBS and resuspended in 0.9ml of PBS. 10 μ l and 30 μ l of eluted linearised targeting vector were added to each of the mES cell aliquots and allowed to incubate at RT for 5'. The cell/DNA vector mixture was then transferred into electroporation cuvettes and electroporation performed using a Biorad GenePulser with the following settings; 230V, 500 μ F. Cells were seeded onto 10cm² plates and cultured for 24hrs before proceeding to drug selection.

2.3.2 Transient transfection of mES cells by lipofection.

Lipofection was used for the transient transfection of pCAGGS FLPe and Hdac1-C-FLAG-Resc plasmid DNA. 1×10^6 mES cells were seeded the night before transfection. Media was changed the following morning and transfection reagents prepared as follows; 6-10 μ l of Lipofectamine (Invitrogen, Life Technologies, Paisley) was added to 250 μ l of knockout DMEM in 1.5ml tube and incubated at RT for 5'. Meanwhile, 2-2.5 μ g of plasmid DNA was added to 250 μ l DMEM in a separate 1.5ml tube. The two volumes were combined together and mixed by gentle tapping. Lipofection complexes were left to form over 20' at RT before the mixture was pipetted drop-wise into culture media of plated mES cells. 48hrs post addition of the lipofection complexes; cells were trypsinised and plated at quantities of 20,000 and 5,000 before proceeding to drug selection as required.

2.3.3 Positive and negative selection of targeted/transfected mES cells.

Post electroporation of targeting vectors, mES cells were subjected to positive drug selection for 10 days to enrich for successfully targeted events. mES cells electroporated with Hdac1/2-cKO-Neo or Hdac1/2-cKO-Hyg Δ Tk targeting vectors were selected using G418 (180 μ g/ml) and Hygromycin B (100 μ g/ml) respectively (Invitrogen, Life Technologies, Paisley). After 10 days, drug selection ceased and mES cells grown for a further 10 days without selection. Plates were washed 2 x in PBS and individual colonies picked into pre-coated gelatin 96-well plates containing 25 μ l of 1X trypsin solution (1

colony/well). Plates were incubated at 36.8°C for 10' prior to the addition of 150µl of standard culture medium/well and returned to the incubator for expansion and 3 copies of each plate made. Two of the replicate plates were frozen down; the remaining plate was grown to ~80% confluency and used for Southern blot screening to identify correctly targeted alleles as detailed in 3.2.2 and 3.2.4. This process was repeated with individual colonies, identified as successfully targeted (i.e. single cell cloned).

To remove the selection cassettes from double targeted clones, cells were transiently transfected with pCAGGS-FPLe plasmid as detailed in 2.3.2 and negative selection applied using 1-(2-deoxy-2-fluoro-1-β-D-arabinofuranosyl)-5-iodouracil (FIAU) to identify loss of the thymidine-kinase portion of the -cKO-HygΔTk cassette (FIAU final concentration of 0.2µM). As detailed with positive selection, individual colonies post selection, were picked into 96-well plates, expanded, replicated and screened by Southern blot for successful excision of selection cassettes as detailed in 3.2.5.

2.3.4 Recombineering.

In order to generate the second targeting vector required for the generation of double targeted mES cells, the Hdac1/2-cKO-HygΔTk targeting vectors were generated from the initial Hdac1/2-cKO-Neo targeting vectors (2.3.7.1 and 2.3.7.2) as outlined in Chapter 3. Briefly the -pgkHyg/ΔTk cassette was amplified by PCR (primers detailed in 3.2.3 and listed in APPENDIX table A1) using 10ng of pSC5 plasmid DNA (2.3.5.3) using primers that introduced 5' and 3' 66bp arms of homology to the -pgkNeo selection cassette of the

Hdac1/2-cKO-Neo targeting vectors. The PCR product was *Dpn* I treated by the addition of 2 μ l of enzyme directly to the PCR reaction for 1hr at 37°C and gel purified.

Meanwhile, a 5ml o/n culture of frozen stocks of the recombineering strains, DY380, already containing the Hdac1/2-cKO-Neo targeting vectors, were grown at 32°C in Luria-Bertani media (LB). The o/n culture was diluted 1/50 and a larger, 25ml, culture inoculated and cultured for 3-5hrs at 32°C in a shaking waterbath until the density reached an OD₆₀₀ of 0.6. 10ml of this culture was then transferred to a fresh 50ml flask and incubated at 45°C (heat shocked) for 15' to induce expression of recombineering genes (*exo*, *bet* and *gam*) (Lui, P., *et al.*, 2003). Following heat shock, the bacterial cultures were chilled immediately on ice for 2', transferred to a 50ml tube and centrifuged for 5' at 5,000rpm. Supernatant was poured off and cells washed 3 x in ice cold ddH₂O. After the final wash all supernatant was removed, cells transferred to a pre-chilled 1.5ml tube and mixed with 1-5 μ l of the purified DNA PCR amplified product, described above. The bacteria/DNA mixture was then transferred to a 0.4ml cuvette and electroporation performed using a Biorad GenePulser with the following settings; 230V, 500 μ F. Bacteria were subsequently transferred to a tube containing 1ml LB medium and incubated for 1hr at 32°C with constant agitation before being streaked on LB agar medium supplemented with hygromycin B (100 μ g/ml) (InvivoGen, Toulouse) and incubated for 24-48hrs at 32°C. Surviving colonies were PCR screened using the primers HD1/2 3'sc5Cap and SC5_Hyg_seq2. 5ml inoculations of colonies positive for a 1kb band were grown o/n, plasmid DNA "mini-prepped" and sequenced using the following primers; HD1For2 or 5'neogen and Hyg_SC5_seq2 (APPENDIX table

A1, for primers). “Maxi-preps” of verified clones with the predicted sequence were made in readiness for mES cell electroporation.

Luria-Bertani media (LB)

ddH ₂ O	800ml
Bacto-tryptone	10g
yeast extract	5g
NaCl	10g
adjusted to pH7.5 with NaOH	
volume made up to 1L with dH ₂ O and sterilized by autoclaving	

2.3.5 Induction of LoxP recombination in targeted mES cells.

At least 5 targeted Hdac1/2^{Lox/Lox} clones were revived into wells of 24-well plates and cultured for generation of stocks. Once sufficient stocks had been generated for freezing and analysis, cells were plated 6-well plates for assessment of deletion of the LoxP site-flanked (floxed) region over a 10 day time course. Induction of LoxP site recombination required the addition of 1 μ M 4-OHT (4-hydroxytamoxifen) to the culture media over a period of 10 days. Genomic DNA and protein was harvested from mES cells at specific time points after the addition of 4-OHT (as described in 2.4) and screened by both Southern and western blotting for deletion of exon 2 or the targeted protein.

2.3.6 Generation of FLAG-tagged Hdac1 expression construct.

The overall strategy for generating transiently and stably transfected HDAC1^{Lox/Lox} and HDAC1^{Δ2/Δ2} mES cell lines is detailed in Chapter 3 (3.3). An Hdac1 PCR insert fragment was cloned into the pcDNA3.1(+) vector (2.3.7.5) (Invitrogen, Life Technologies, Pasiley) designed for high-level stable and transient expression in mammalian hosts.

2.3.6.1 Introduction of FLAG epitopes to the C' of Hdac1.

To generate the Hdac1-C'-FLAG-Resc PCR fragment, murine full length Hdac1 cDNA, obtained from an I.M.A.G.E. clone (I.M.A.G.E. ID: 4217199, Source BioScience, LifeSciences), was PCR amplified using the primers 5'*Bam*HI-Hdac1 Resc cDNA and 3'Hdac1 Resc cDNA-FLAG-*Eco*R I (APPENDIX table A1). It was projected that amplification of the Hdac1 cDNA using these primers would introduce a 5'*Bam*H I and a 3'*Eco*R I restriction enzyme site (with the 3' *Eco*R I site preceded by a sequence that replaces the original stop codon with sequence encoding two FLAG peptide motifs followed by a new stop codon). The PCR product was gel purified and 1μg digested in a total reaction volume of 50μl as follows:

PCR insert digest

ddH ₂ O	16μl
<i>Eco</i> R I buffer	5μl
<i>Eco</i> R I	1μl
<i>Bam</i> H I	1μl
Vector plasmid	27μl of

33ng/μl

Incubated for 2hrs at 37°C

Digestions were *Dpn* I treated by the addition of 2µl of enzyme directly to the PCR reaction for 1hr at 37°C. The PCR insert/digestion reaction was column purified and re-quantified using a Nanodrop 2000 spectrophotometer.

2.3.6.2 Enzymatic digestion of *pcDNA3.1(+)* vector.

A 5ml inoculation of the *pcDNA3.1(+)* vector was grown o/n at 37°C in LB supplemented with 50µg/ml of ampicillin. Plasmid DNA was “mini-prepped” and 2µg digested in a total reaction volume of 50µl as follows:

Vector digest

ddH ₂ O	38µl
<i>EcoR</i> I buffer	5µl
<i>EcoR</i> I	1µl
<i>BamH</i> I	1µl
Vector plasmid	5µl of
400ng/µl	

Incubated for 2hrs at 37°C

Digested DNA was gel purified and the 5' phosphatase groups removed by 30' incubation with Antarctic phosphatase as follows:

Antarctic phosphatase digest of *EcoR* I/*BamH* I digested vector

10X Antarctic phosphatase reaction buffer	5µl
Antarctic phosphatase (5,000U/ml)	1µl
Digested vector	44µl

Incubated for 30' at 37°C

The vector/digestion reaction was column purified and re-quantified using a Nanodrop 2000 spectrophotometer.

2.3.6.3 PCR fragment insert/vector ligation.

A standard 10 μ l ligation reaction of DNA fragments was carried out o/n at 16°C with a ratio of digested PCR insert to vector DNA in a molar ratio of 3:1 calculated as follows:

$$\text{Amount of insert (ng)} = \text{insert: vector ratio} \times \left(\frac{\text{ng of vector} \times \text{kb of insert}}{\text{kb of vector}} \right)$$

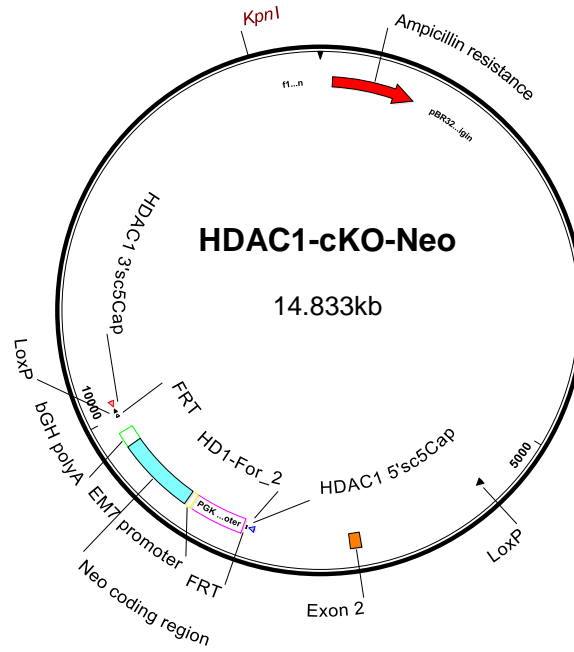
Ligation reaction

10X T4 ligation buffer	1 μ l
T4 ligase	1 μ l
Digested vector	4.3 μ l
Digested insert	1.3 μ l
ddH ₂ O	2.4 μ l
Incubated o/n at 16°C	

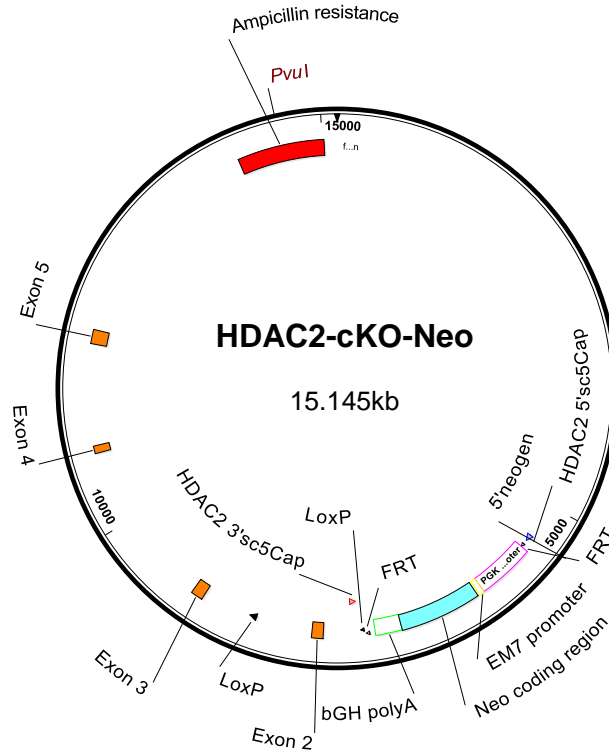
2 and 8 μ l of this reaction was then transformed into DH5 α TM chemically competent *E. coli* (Invitrogen, Life Technologies, Pasiley) and streaked on LB agar medium supplemented with ampicillin (50 μ g/ml) (InvivoGen, Toulouse). 5ml inoculations of positive colonies were “mini-prepped” screened by *Stu* I digest and sequenced using the T7 and BGH-Rev (APPENDIX table A1). Plasmid DNA “Maxi-preps” of verified colonies were generated ready for either transient or stable transfection (as described in 2.3.1-3 and Chapter 3).

2.3.7 Plasmids and recombineering reagents.

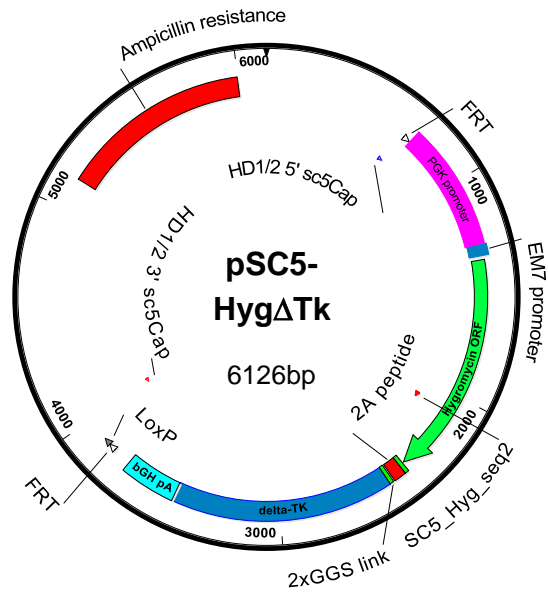
2.3.7.1 HDAC1-cKO-Neo.



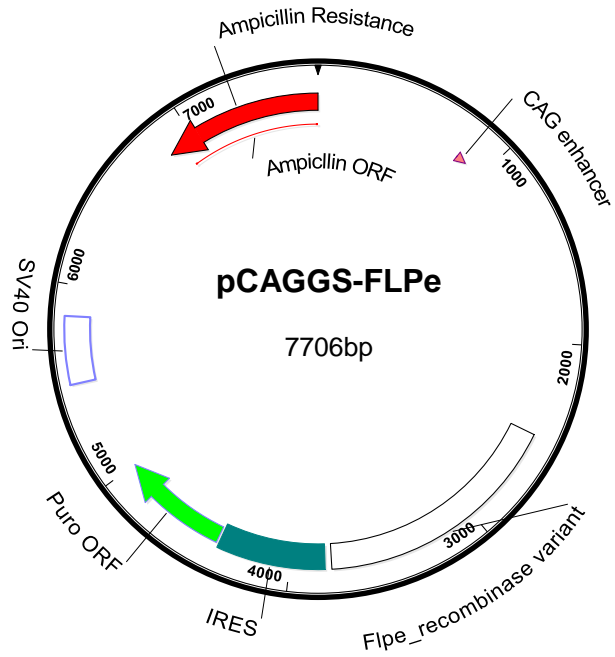
2.3.7.2 HDAC2-cKO-Neo.



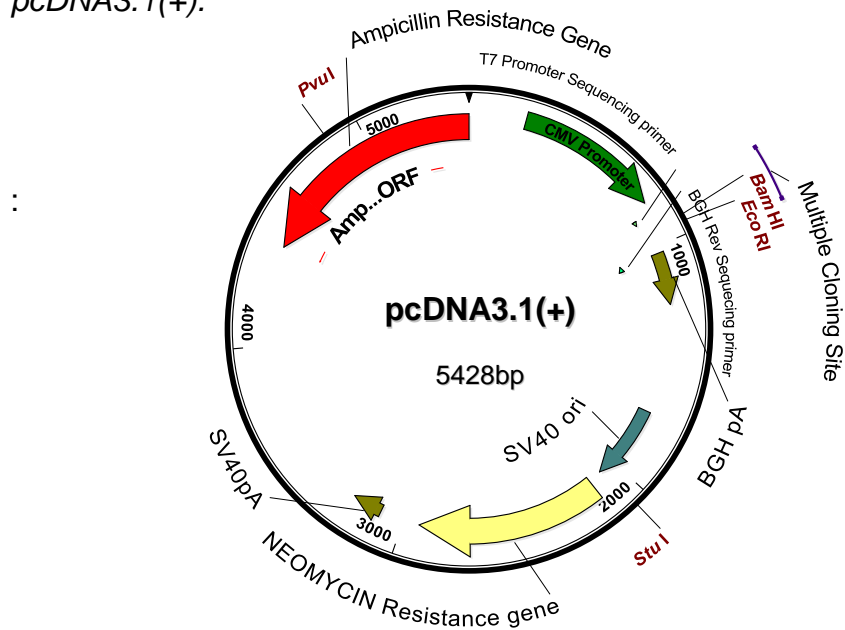
2.3.7.3 pSC5-HygΔTk.



2.3.7.4 pCAGGS-FLPe.



2.3.7.5 pcDNA3.1(+).



2.4 gDNA, mRNA, protein and histone sample extraction.

2.4.1 HotSHOT preparation of mouse ear DNA for PCR genotyping.

75µl of 1X base solution was added to mouse ear punches in 0.6ml PCR tubes and heated for 30' at 95°C. Samples were cooled to RT and 75µl of 1X neutralisation solution was added. Samples were vortexed for 1'. 2µl of this mixture was used for subsequent PCR genotyping reactions.

50X base solution

5N NaOH 5ml

0.5M EDTA 20ml

Made up to 1000ml with ddH₂O

50X neutralisation solution

Tris-HCl 315.2g

Made up to 1000ml with ddH₂O

For a full list of PCR genotyping primer sequences see APPENDIX table C1. General polymerase chain reaction (PCR) conditions are detailed in 2.5.1.

2.4.2 gDNA extraction.

Extraction of gDNA, total mRNA and protein was performed on mES cells grown to ~80% confluency. For gDNA extraction from tissue culture plates and mouse thymocytes, cells were washed twice in 5mls of PBS. After the last wash, PBS was aspirated and 1ml of PBS added to the culture plate. Cells were then scraped and the resulting suspension transferred to a 1.5ml tube, pelleted by centrifugation (1' at 1,200rpm) and incubated overnight (o/n) at 55°C with constant rotation, re-suspended in 200µl of cell lysis buffer. The following day, an equal volume of iso-propranol was added to precipitate DNA which was spooled on glass rods and transferred to 1.5ml tubes containing 1ml 70% ethanol for 15', followed by a transfer to 1.5ml tubes containing 1ml 90% ethanol for a further 15'. DNA was then air dried and re-suspended in 50-200µl of T.E.

For gDNA extraction from mES cells cultured in 96-well plates for Southern blot screening, cells were washed twice with PBS. Following the final wash in PBS, and the plate incubated o/n at 55°C with cells re-suspended in 50µl of cell lysis buffer supplemented with 200µg/ml proteinase K. The following day an equal volume/well of iso-propranol was added and the plate mixed at 200rpm on a flat bed rotating platform for 25'. Plates were spin to pellet the gDNA at 1,200rpm for 5' and washed twice with 200µl 70% ethanol. Plates were air dried and gDNA re-suspended in 50µl of T.E.

2.4.3 Total mRNA extraction.

All reagents, equipment and plasticware for the isolation of total mRNA was either certified ribonuclease free or treated with RNase Zap (Ambion, Life Technologies, Paisley), in order to maintain RNA integrity. Total mRNA from mES cells was harvested from tissue culture dishes. mRNA from embryoid bodies (EBs) was harvested from a single 15cm² plate containing approximately 70-120 individual EBs. mES cells were washed twice with pre-warmed (36.8°C) PBS. Following the final wash, 1ml/1 x 10⁷ mES cells of TRIzol® was added to each plate and mES cells lysed using a pipette until the solution achieved a smooth consistency. For EBs, total medium (containing EBs) was transferred from a single 15cm² culture plate into a 50ml conical tube. EBs were allowed to gather by gravity at the bottom of the tube before aspirating media and washing EBs twice in pre-warmed PBS (allowing EBs to settle at the bottom of the tube prior to aspiration). Following the final wash PBS was aspirated leaving approximately 1ml in which to transfer the EBs to a 1.5ml tube. Samples were left for 3' and the remainder of the PBS aspirated. 1ml of TRIzol® was added to each sample tube and EBs disrupted and cells lysed using a polytron until the solution achieved a smooth consistency. Thymocyte mRNA was extracted from pelleted cell suspensions as above.

The TRIzol®/lysed cell suspension was transferred to a 1.5ml tube and incubated for 3' at RT. Chloroform (1/5 volume of Trizol reagent) was added to the samples and mixed vigorously by inversion and left at RT for 15'. Samples were then transferred to pre-spun (2' at 13,000rpm) 2ml Phase Lock Gel Heavy Tubes (5 Prime, Hamburg, GmbH) and centrifuged for 15' at 13,000rpm to separate the aqueous phase which was transferred to a fresh tube and ½

volume of iso-propanol added to samples which were then mixed by inversion several times prior to chilled 4°C centrifugation at 13,000rpm for 15'. The supernatant was aspirated and the pellets washed once in 70% ethanol followed by a further 80% ethanol wash, before allowing total mRNA sample pellets to air dry. Samples were re-suspended in 20-50µl of DEPC treated H₂O and quantified using a Nanodrop 2000 spectrophotometer (Thermo Scientific, Hemel Hempsted).

2.4.4 Protein extraction.

The following steps were carried out at 4°C or on ice. Lysis buffer constituents are detailed in 2.4.6. Whole cell extracts (WCE), of mES cells, were prepared by washing cells twice in ice cold PBS before scrapping cells in a total volume of 1ml PBS and transferring samples to 1.5ml tubes. Samples were pelleted by chilled 4°C centrifugation for 2' at 1,200rpm PBS removed, re-suspended in 100-500µl of WCE buffer and placed on a rotator for 2-4hrs at 4°C with intermittent vortexing. Debris was pelleted by chilled 4°C centrifugation for 15' at 12,000rpm and the supernatant transferred to a fresh 1.5ml tube. Mouse tissue extracts were obtained as above from pelleted cell suspensions.

Nuclear extracts (NE) were prepared as above but following washing with PBS, cells were re-suspended in 1000µl of nuclear extract buffer A (NEBA) and placed on a rotator for 2-4hrs at 4°C with intermittent vortexing. 10% NP-40 (1/10 volume of NEBA) was added to the tubes and samples vortexed for 30s, before pelleting nuclei by chilled 4°C centrifugation for 2' at 2,00rpm. Supernatants were aspirated and cell nuclei re-suspended in 10-250µl nuclear

extract buffer B (NEBB) for 30' on ice with intermittent vortexing. Nuclear debris was pelleted by centrifugation for 10' at 12,000rpm and supernatant transferred to a fresh, pre-chilled 1.5ml tube.

Protein concentrations were quantified using Bradford reagent (Amresco, Solon, USA) and a standard spectrophotometer. Western blotting was performed on 10-20 μ g of protein extracts and resolved by 4-12% gradient SDS-PAGE. A list of antibodies used for western blots is presented in Appendix Table A3. Membranes were scanned using the Odyssey Infrared Imaging System and quantification of proteins achieved using the appropriate IRDye conjugated secondary antibodies (Li-COR Biosciences, Nebraska, USA).

2.4.5 Histone extraction and post translational modification analysis.

Acid extraction of histones was performed as previously described (Shecter *et al.*, 2007). All steps were carried out at 4°C or on ice. Nuclei were extracted from cells as described in 2.4.4, re-suspended in 400 μ l of 0.2M H₂SO₄ by pipetting and left o/n on a rotator. The following day, debris was pelleted by centrifugation at 16,000rpm for 10' and supernatant transferred to a fresh 1.5ml tube. Histones were precipitated by the drop-wise addition of 133 μ l of trichloroacetic acid (TCA) and incubated for 2hrs. Histones were pelleted by centrifugation at 16,000rpm for 30' followed by a series of washes in 1ml of acetone. Histones were pelleted once more at 16,000rpm, supernatant aspirated and allowed to air dry before re-suspending in 50-100 μ l of H₂O. Protein concentrations were quantified using Bradford reagent (Amresco, Solon, USA) and a standard spectrophotometer. Western blotting was performed on

5 μ g of protein extracts resolved by 4-12% gradient SDS-PAGE. Membranes were probed using a panel of antibodies raised against a number of histone modifications. A list of antibodies used for western blots is presented in Appendix Table B3. Membranes were scanned using the Odyssey Infrared Imaging System and quantification of proteins achieved using the appropriate IRDye conjugated secondary antibodies (Li-COR Bioscience, Nebraska, USA).

2.4.6 Lysis buffers.

Cell lysis buffer

50mM Tris-HCl

100mM NaCl

10mM EDTA

1% SDS

Whole cell extract (WCE) lysis buffer

50mM Tris-HCl

100mM NaCl

10mM EDTA

1% SDS

1 X Protease inhibitor cocktail (Sigma, #P8340)

1mM Dithiothreitol

Nuclear extract buffer A (NEBA)

10mM KCl

20mM HEPES pH7.9

1mM EDTA

1 X Protease inhibitor cocktail (Sigma, #P8340)

1mM Dithiothreitol

Nuclear extract buffer B (NEBB)

400mM NaCl

10mM EDTA

25% glycerol

1 X Protease inhibitor cocktail (Sigma, #P8340)

1mM Dithiothreitol

2.4.7 Co-immunoprecipitation.

Co-immunoprecipitation assays were performed on 70 μ g of nuclear extracts incubated overnight at 4°C with the 2 μ g of the appropriate antibody made up to a total volume of 1ml with Co-IP buffer (see table A3 for a complete list of antibodies used). Simultaneously, 50 μ l of protein-G agarose beads (GE Life Sciences, Buckinghamshire) were washed 2 x in pre-chilled PBS and blocked o/n in PBS/1% BSA. The following day, protein-G agarose beads were washed 3 x in Co-IP buffer, the nuclear extract-antibody mix added to the protein-G beads and incubated o/n at 4°C. After 3 x washes in Co-IP buffer, beads were resuspended in 100 μ l of Co-IP buffer and then split into two aliquots: one aliquot (80 μ l) was used to assess the enzymatic activity of the immunoprecipitates using a commercially available deacetylase assay (see 2.2.14) (Active Motif, La Hulpe, Belgium); the remaining aliquot (20 μ l) was resolved by SDS-PAGE and probed with antibodies raised against known components of the immunoprecipitated complexes (see table A3 for a complete list of antibodies used).

Co-IP Buffer

250mM NaCl

10mM HEPES pH7.9

1mM EDTA

1 X Protease inhibitor cocktail (Sigma, #P8340)

1mM Dithiothreitol

2.4.8 Deacetylase assays.

The deacetylase potential of immune precipitates was assayed using a commercially available colorimetric kit (Active Motif, La Hulpe, Belgium). This colorimetric assay utilises a short peptide substrate that contains an acetylated lysine residue. Once the substrate is deacetylated, the lysine residue reacts with the “developing” solution and releases the chromophore from the substrate resulting in a yellow coloured product that absorbs maximally at 405nm. 80µl of the immune precipitates, generated as in 2.4.7, were divided into 20µl triplicates in 96-well plates and 25µl of “HDAC” assay buffer was added to each well. Upon the addition of 5µl of the colorimetric “HDAC assay substrate”, samples were mixed at 200rpm on a flat bed rotator for 20’ at RT before proceeding with the reaction assay at 37°C. The reaction was stopped after 2hrs by the addition of 50µl of HDAC assay “stop/developer” solution, incubated for 15’ and read using a microtiter plate reader at 405nm. 2µg of nuclear extract incubated ± 2µM trichostatin A (TSA) was used as intra-assay positive and negative controls.

2.5 Molecular biology.

2.5.1 gDNA polymerase chain reaction (PCR).

Polymerase chain reaction (PCR) was performed to amplify DNA fragments for a number of purposes including; mouse genotyping, generation of Southern blot probes, screening transformed bacteria and molecular cloning. For mouse genotyping, Southern probe generation and screening bacterial transformants standard *Taq* polymerase was used (Thermo, #AB0192, Thermo Scientific, Hemel Hempsted). High Fidelity Platinum *Taq* polymerase (Invitrogen, Life Technologies, Pasiley) was used in all molecular cloning. A typical DNA PCR reaction is outlined below.

95°C 2min	} 35 cycles
95°C 30s	
Annealing temp 60s	
72°C 90s	
72°C 5'	
12°C ∞	

A typical 25 μ l PCR reaction mix consisted of;

10X Buffer	2.5 μ l
MgCl ₂	1.5 μ l
dNTPs	0.5 μ l
5'primer	0.5 μ l
3'primer	0.5 μ l
<i>Taq</i>	0.1 μ l
ddH ₂ O	17.4 μ l
Template	2.0 μ l

2.5.2 Reverse transcription and quantitative real time PCR.

Total RNA was isolated using the methods outlined in 2.4.3. Prior to reverse transcription synthesis of cDNA, 2 µg of total RNA (as assessed using a Nanodrop 2000) was electrophoresed on a 2% agarose gel to check sample integrity. A total of 2µg of total mRNA was reverse transcribed in a 40µl Q-Script One-Step Supermix reaction (Quanta Biosciences, Gaithersburg, MD, USA). cDNA synthesis was carried out in a thermocycler with the following conditions;

25°C 5'

42°C 30'

85°C 5'

4°C Hold

The resulting cDNA was diluted with an equal amount of DEPC treated H₂O. Multiplex assays (using *Gapdh* as an internal control) were designed using the Universal ProbeLibrary Assay Design Centre (www.roche-applied-science.com, see APPENDIX table D1, for primers and probes). Primers were designed based on theoretical algorithms to ensure close to 100% efficiency. Probes consisted of Lock Nucleic Acid technology, which upon binding of the reaction amplicon, released a HEX or FAM fluorophore. For each reaction, 2µl of diluted cDNA was used for all multiplex qRT-PCR reactions using Light Cycler Probes Master (Roche Applied Science) as per the manufacturer's instructions.

Reactions were carried out on a Roche LightCycler 480 under the following conditions;

94°C 10'	initial denaturing	
94°C 10s		} 40 cycles
55°C 20s		
72°C 5s		
4°C	Hold	

Advanced relative quantification analysis using the Roche LightCycler software generated a relative expression value based on the comparative Ct calculations ($[\Delta][\Delta]Ct = [\Delta]Ct_{\text{sample}} - [\Delta]Ct_{\text{reference}}$).

2.5.3 Storage and revival of bacterial strains.

Transformed bacterial strains were prepared as glycerol stocks for long-term storage at -80°C. 500µl of bacteria grown overnight with the appropriate antibiotic in LB media, was added to 500µl sterile 50% glycerol, in a screw-top 1.5ml cryovials and stored at -80°C. Revival of bacterial strains was achieved by picking a small quantity of the glycerol stock with a pipette tip and inoculating an agar plate or 5ml LB starter culture o/n at 37°C.

2.5.4 Culture of bacterial strains for “mini” and “maxi-preparation”.

Bacterial colonies were picked from agar plates with a sterile pipette tip and used to inoculate 5ml of LB media containing the appropriate antibiotic. These were incubated o/n in a 37°C shaker before either harvesting plasmid

DNA by “mini-prep” or inoculation a larger culture volume for plasmid “maxi-preps”.

2.5.5 Plasmid purification, gel extraction and PCR/enzymatic digest column purification.

All extraction methods are adapted from the original alkaline lysis plasmid purification method described in (Birnboim, H.C. and Doly, J., 1979) , followed by binding of DNA to an anion-exchange resin under appropriate salt and pH conditions and subsequent elution in ddH₂O or T.E. “Mini-preps” were prepared using Qiagen Plasmid Miniprep kits as per manufacturer’s instructions (Qiagen, Crawley). Endotoxin-free “maxi-preps” were prepared using NucleoBond EF kits (Macherey-Nagel GmbH) according to manufacturer’s instructions. Eluted “maxi-prep” plasmid DNA was further purified by isopropanol precipitation, ethanol wash and re-dissolving in endotoxin-free H₂O (2.3.5). Gel and PCR/enzymatic digest purification was performed using QIAquick Spin columns as per the manufacturer’s instructions (Qiagen, Crawley).

2.5.6 DNA sequencing.

DNA sequencing was performed by The Protein and Nucleic Acid Chemistry Laboratory at the University of Leicester (PNACL) using Applied Biosystems Big-Dye Ver 3.1 chemistry on an Applied Biosystems model 3730 automated capillary DNA sequencer. 0.5µg of plasmid DNA and primers at a concentration of 1.0pmol/µl were submitted to PNACL as required.

2.5.7 Southern blotting.

Southern blotting was routinely used for the detection of gene targeting events as well as excision of targeting vector selection cassettes and LoxP mediated deletion of exon 2, in both mES cells and mutant mouse strains. Chapter 3 details the precise strategies used for distinguishing between the various potential alleles subsequent to gene targeting. Details of PCR primers used to generate Southern blot probes, using wild-type mES cell gDNA as template, are detailed in APPENDIX table B1.

2.5.7.1 Southern blotting gel electrophoresis.

gDNA (as isolated in 2.4.2) was digested o/n with the appropriate restriction enzymes for a given strategy (detailed in Chapter 3), in a total reaction volume of 50 μ l. 10 μ l of 6X DNA loading buffer (60mM Tris pH7.5, 30% glycerol, 0.3% bromophenol blue) was added to the digested samples, loaded onto a 0.8% agarose gel and resolved o/n at 20V. The following day the gel was washed 1 x in ddH₂O, and 2 x in alkaline transfer buffer for 30' (1M NaCl, 0.4M NaOH).

2.5.7.2 Neutral transfer of nucleic acid to nylon membranes.

Charged nylon membrane, Hybond XL, (GE Healthcare Life Sciences, Buckinghamshire) was equilibrated in alkaline transfer buffer before capillary transfer apparatus was set up (Fig 2.1). The transfer was performed o/n. The following day the membrane was neutralised with 2 x 15' washes in

neutralisation buffer (1M NaCl, 0.5M Tris-HCl pH 6.8). The membrane was then dried in a 65°C incubator before a 1hr pre-hybridisation at 65°C in 15ml of Rapid-hyb buffer (GE Healthcare Life Sciences, Buckinghamshire) in hybridisation tubes under constant rotation.

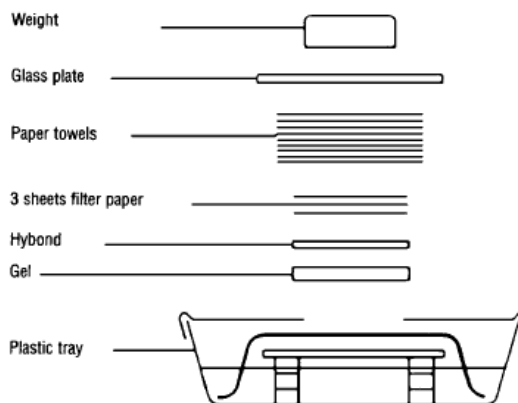


Figure 2.1. *Diagrammatic representation of capillary transfer apparatus* (image from Hybond-XL application handbook).

2.5.7.3 DNA Southern blot probe labelling.

25ng of double stranded DNA probes were radiolabelled by the incorporation of dCTP³². Probes were diluted in 45µl of T.E., denatured by boiling at 95°C for 5', rapidly chilled on ice for 2' and transferred to an aliquot of Amersham Rediprime II DNA labelling system (GE Healthcare Life Sciences, Buckinghamshire). 1.85Bq (5µl) of dCTP³² was added to the denatured probe/labelling mixture and incubated for 45' at 37°C. Unincorporated nucleotides were removed by centrifuging the labelled probe through Illustra ProbeQuant G-50 Micro Columns (GE Healthcare Life Sciences,

Buckinghamshire). Radiolabelled probes were boiled at 95°C prior to addition to 15ml fresh Rapid-hyb buffer and added directly to the hybridisation tube containing the charged membrane and incubated o/n at 65°C.

2.5.7.4 Membrane washing and development.

Following o/n hybridisation, membranes were washed 2 x in 2X SSC/0.2% SDS buffer at RT and then 2 x in 0.2X SSC/0.1% SDS buffer at 65°C. Membranes were exposed to X-ray film in a cassette placed at -80°C overnight, and the film developed the following day.

2.5.7.5 DNA methylation analysis by Southern blot.

gDNA from samples was extracted as described (2.4.2) and 2 aliquots of exactly 5µg of gDNA digested with either the methylation sensitive *Hpa* II or the *Hpa* II methylation insensitive isoschizomer, *Msp* I. Samples were transferred to nylon charged membranes as described in 2.5.7.1-2 and interstitial A particle (IAP) or a major satellite repeat fragment probe labelled and hybridised as in 2.5.7.3-4 to assess the status of global or pericentromeric genomic DNA respectively. Primer sequences for the IAP and major satellite repeat probes were supplied by Dr Christine Armstrong or taken from Yan, Q., *et al.*, 2003 respectively.

2.6 Fluorescence activated cell sorting (FACS).

2.6.1 Isolation of mouse thymocytes and splenocytes.

Mice were culled by cervical dislocation in accordance with schedule 1 home office guidelines. Thymus, spleen and lymph nodes were taken immediately from mice after they were culled and collected in ice chilled cell collection buffer (CCB). Tissues were disrupted and forced through a 0.4 μ m cell strainer and collected into 15ml conical tubes. Cells were spun down at 1,200rpm at 4°C for 5' and resuspended in 5ml of red blood cell lysis buffer (RBCLB), incubated at RT for 5', pelleted and resuspended in CCB. Cells were then counted using a haemocytometer.

2.6.2 Positive isolation of CD4/CD8 cells from total splenocytes.

Isolation of CD4/CD8 (Chapter 3) was achieved by positive magnetic isolation using a commercially available kit from Invitrogen according to the manufacturer's instructions (Dynabeads® FlowComp™ Mouse CD4 Cat. No. 114-61D and Dynabeads® FlowComp™ Mouse CD8 Cat. No.114-62D). Splenocytes were isolated as in 2.6.1 and divided into two aliquots. Cell aliquots were resuspended in 500ml of isolation buffer (PBS/0.5% BSA) and 25ml of either FlowComp™ Mouse CD4 or CD8 antibody. Cells were mixed and incubated for 10' on ice before being washed in cold isolation buffer and pelleted for 3' at 350xg. Supernatant was discarded, cell pellets resuspended in 1ml isolation buffer and 75 μ l of FlowComp™ Dynabeads added. Cells were incubated for 15' under constant agitation at 4°C and placed on a magnetic rack

for 1' before removing supernatant. Tubes were removed from the magnetic rack and washed in 1ml isolation buffer before incubating bead/cell mixtures in 1ml FlowComp™ Release Buffer for 10'. Tubes were placed in the magnetic rack for 1', supernatant transferred to fresh pre-chilled 1.5ml tubes and pelleted at 350xg for 5'. Protein was isolated as in 2.4.4. Prior to pelleting cells and protein extraction a small aliquot of cells was stained with α -CD4-PE and α -CD8-FITC conjugated antibodies to assess purity of isolated populations by FACS, which were typically >90% pure.

2.6.3 Staining of mouse cells for T cell development analysis by FACS.

3 x 10⁶ cell aliquots of each sample per FACS experiment were seeded into V bottom 96-well plates, spun down at 1,200rpm at 4°C for 5' and buffer aspirated. Fluorochrome conjugated antibody mixes (including single stain controls) were diluted in staining buffer (SB) (see APPENDIX table C3 for a full list of antibodies and concentrations used). 50 μ l of antibody mix/well were used to stain cells for 30' at 4°C, followed by 2 x washes with 200 μ l of SB. Between washes cells were spun down at 1,200rpm at 4°C for 5' and SB aspirated. If cells were stained with a biotin antibody conjugate cells were incubated with a secondary staining using a fluorochrome conjugated antibody (streptavidin-Cy5.5) for a further 20', washed 2 x as before. After the final wash, stained cells were transferred to standard FACS tubes, resuspended in 500 μ l of PBS and samples processed immediately for FACS analysis using a BD FACSCanto II flow cytometer (BD Biosciences). FCS 2.0 files generated by the FACS Diva software (BD Biosciences) were exported and analysed using VenturiOne

software (Applied Cytometry, Sheffield). Samples for mRNA extraction were stained as above and collected into cold PBS using a high speed Beckman Coulter MoFlo Legacy cell sorter. Cells were pelleted at 1,200rpm and mRNA extracted as described in 2.4.3.

2.6.4 Apoptosis detection in mouse thymocytes by FACS.

Annexins are a family of calcium-dependent phospholipid-binding proteins that preferentially bind phosphatidylserine (PS). Under normal physiologic conditions, PS is predominantly located in the inner leaflet of the plasma membrane. Upon initiation of apoptosis, PS loses its asymmetric distribution across the phospholipid bilayer and is translocated to the extracellular membrane leaflet marking cells as targets of phagocytosis. Once on the outer surface of the membrane, PS can be detected by fluorescently labelled Annexin V in a calcium-dependent manner. In combination with Annexin V staining, a viability dye, such as propidium iodide (PI), can be used to resolve late-stage apoptotic and necrotic cells (Annexin V, viability dye-positive) from the early-stage apoptotic cells (Annexin V positive, viability dye-negative).

Thymocytes were extracted, processed and counted as in 2.6.2. If cells were stained with CD4 or CD8 antibodies this was performed prior to Annexin V staining which was carried out as follows using a commercially available kit in accordance with the manufactures instructions (BD Biosciences). Cells were washed 2 x with cold PBS and resuspended in 100 μ l of 1X Annexin V binding buffer. 5 μ l of flouochrome conjugated Annexin V, 5 μ l of PI and incubated in the

dark for 15' at RT. The solution was then transferred to standard FACS tubes. A further 400µl of 1X Annexin V binding buffer was added and samples processed immediately for FACS analysis using a BD FACSCanto II flow cytometer (BD Biosciences).

Cell collection buffer (CCB)

HBSS (GIBCO, Life Technologies, Paisley)	485ml
Foetal Calf serum	15ml

Red blood cell lysis buffer (RBCLB)

NH ₄ Cl	8.3g
KHCO ₃	1.0g
5% EDTA	1.8ml

Made up to 1000ml with ddH₂O

Staining buffer (SB)

HBSS (GIBCO, Life Technologies, Paisley)	485ml
Bovine serum albumin	5g

2.7 Histological and immunohistochemical analysis.

For histological examination of EBs and mouse tissues samples were fixed for 24hrs in 4% paraformaldehyde and embedded in paraffin blocks using standard histological techniques and 5µm serial sections cut. EB and mouse tissue sections were stained with haematoxylin and eosin (H AND E) using a Shandon Varistain automated processor. Embedding, sectioning and H AND E staining were performed by Jennifer M. Edwards of the MRC Toxicology Unit, Leicester.

2.7.1 Immunohistochemistry of ATRA treated EBs.

Immunofluorescence of single cell suspensions derived from ATRA treated EBs seeded on laminin coated eight-well chamber glass slides (see Chapter 4), was performed using a previously published method (Cowley, S.M., *et al.*, 2005). Primary and secondary antibodies are as detailed in APPENDIX tables D3 and E3. Cells were seeded at a concentration of 5×10^4 , fixed in 2% paraformaldehyde for 1hr, permeabilized with 0.5% Triton X-100, and then probed with the indicated antibodies in PBS/ 5% normal goat serum (abcam, #ab7481, Cambridge) and 0.05% Tween 20 o/n at 4°C. Slides were washed 2 x in PBS, and incubated with the following secondary antibodies (i.e. Alexa Fluor 568 anti-mouse or Alexa Fluor 488 anti-rabbit) (Invitrogen, Life Technologies, Pasiley) for 4 hours at RT in the dark. Slides were washed 2 x in PBS, cell nuclei counterstained with 4, 6-diamidino-2-phenylindole (DAPI) (Invitrogen, Life Technologies, Pasiley) and slides mounted in ProLong Gold Antifade Reagent (Invitrogen, Life Technologies, Pasiley). Images were captured and mean intensity values of positively stained cells identified and quantified using a fully automated Olympus Cell[^]R/Scan[^]R imaging system.

2.7.2 Immunohistochemistry of paraffin embedded tissues.

2.7.2.1 Antigen retrieval.

Antigen retrieval of mouse tissue sections, prepared as in 2.7, was achieved as follows; sections were de-waxed in 2 changes of xylene (10'), dehydrated in 2 changes of 100% ethanol (10'), blocked with endogenous

peroxidise (10') and incubated in pre-boiled 10mM citrate buffer pH6 (10'), for heat-induced antigen retrieval.

Endogenous peroxidise block

30% H₂O₂ 2.4ml

Methanol 400ml

10mM citrate buffer pH6 (antigen retrieval buffer)

Tri-sodium citrate 2.94g

ddH₂O 800ml

Adjust to pH6 with 1M acetic acid

Made up to 1000ml with ddH₂O

2.7.2.2 Immuno-staining.

Slides were placed in humid chambers for immuno-staining. Sections were blocked for 2hrs with PBS/4% normal goat serum, followed by o/n incubation at 4°C with α -Ki67 (see APPENDIX table D3 and E3 for details) primary antibody diluted in with PBS/4% normal goat serum. The following day slides were washed 3 x for 5' in PBS with gentle agitation, before incubation with biotinylated swine anti-rabbit secondary antibody, diluted in PBS/4% normal goat serum for 30' at RT. Slides were washed 3 x for 5' in PBS and incubated with streptavidin-peroxidase, diluted 1:500 in PBS/4% normal goat serum for 30'. Slides were washed again, 3 x for 5' in PBS, incubated for 5' in DAB peroxidise (DakoCytomation, Ely), washed in H₂O and counterstained with eosin. Sections were dehydrated in a series of 10' incubations in 70%, 90% and 100% ethanol, cleared in xylene, mounted with DPX and visualised by bright field microscopy.

2.8 Global transcriptome and DNA copy number variation analysis.

Comparative gene expression profiles of pre-lymphomic HD1^{Δ2/Δ2};HD2^{WT/Δ2} thymocytes was compared to that of wild type litter mate controls using the Illumina MouseWG-6 v2 Expression BeadChip platform (Illumina, Little Chesterford). DNA copy number variation in diseased thymocytes was assessed using the Mouse Genome Comparative Genomic Hybridisation 244K Microarray (Agilent Technologies UK Limited, Stockport). Total mRNA and gDNA, for the respective analysis, were extracted as in 2.4.2 and 2.4.3. Processing of samples for microarray analysis was carried out by Christopher McGee. Bioinformatics was performed by Ruben Bautista of the Wellcome Trust Sanger Institute Microarray Facility and Nathalie Conte of the Sanger Institute Mouse Genomics Team.

2.8.1 Global gene expression profiling using Illumina MouseWG-6 v2 Expression BeadChip microarrays.

The MouseWG-6 v2.0 BeadChip platform covers 45,200 different mouse transcripts. The probe content is derived from the NCBI RefSeq database (Build 36, release 22) supplemented with probes from Mouse Exonic Evidence Based Oligonucleotide (MEEBO) set, as well as exemplar protein-coding sequences described in the RIKEN FANTOM2 database. Quality control of total mRNA was performed using a 2100 Bioanalyser (Agilent). Only samples that had an RNA integrity number (RIN) of 8.6 or higher were selected for processing and array hybridisation. Processing of samples followed the manufacturer's instructions. Raw data was uploaded to Illumina BeadStudio software for microarray quality

control. Probe summaries were performed prior to normalisation and analysis using BeadStudio, using the method: Making Probe Summary Data, in BeadStudio and quantile normalised. Using limma, a linear model fit was applied and the top differentially expressed genes were tabulated for each contrast using the method of Benjamini and Hochberg to correct the p-values. Detection P values <0.01 were used to filter all data. Significant differential expression between sample sets was defined as probes that exhibited a robust fold change of ≥ 2 ($F_c \geq 2$) with an adjusted P value of <0.005 .

An analysis of functionally related gene groups among deregulated genes and chromosomal distribution of deregulated genes was carried out using the Database for Annotation, Visualization and Integrated Discovery (DAVID) v6.7 (Huang, D. W., *et al*, 2009a and Huang, D. W., *et al*, 2009b).

2.8.2 Comparative genomic hybridisation using the Agilent Mouse Genome Comparative Genomic Hybridisation 244K Microarray.

Array comparative genomic hybridisation (aCGH) is a microarray-based technique to detect gains and losses in DNA, otherwise known as copy number variations (CNVs). aCGH utilises a two-colour assay, in which two DNA samples, a test (diseased state thymus) and a reference (sample matched tail), are labelled with different fluorescent dyes and then co-hybridised to the array. Dual colour fluorescence detection allows calculation of the relative intensity of both dyes, highlighting differences in copy number between the samples. The advantage of dual colour labelling is the elimination of inter-array variability, thereby ensuring tight data sets. The Agilent 244K microarray uses 60-mer

probes which have a median spacing of <9kb, designed to represent the whole mouse genome. DNA was labelled with Cy3 or Cy5 according to BioPrime aCGH genomic labelling protocol (Invitrogen, Paisley) and cleaned using purelink PCR purification kit (Invitrogen). Hybridization was performed using mouse genome CGH microarray244K from Agilent Technologies (Santa Clara, CA) according to the manufacturer's protocol. Slides were hybridized for 48 hours, washed, and scanned with an Agilent microarray scanner; the data were analyzed using Feature Extraction (Agilent Technologies), aCGH Spline (Tomas Fitzgerald, <http://cran.rproject.org/web/packages/aCGH.Spline/aCGH.Spline.pdf>) and Genomic workbench software packages (Agilent Technologies). Data normalization was done using the R Package aCGH.Spline. This algorithm allows robust spline interpolation normalization on dual colour aCGH data. CGH calls were made with Genomic workbench software using the ADM2 algorithm (6.0 threshold), with a minimum of 4 probes in the region as a filter.

Chapter Three: Generation of inducible HDAC1 and HDAC2 conditional knock-out mouse ES cell-lines and T cell specific HDAC1 and HDAC2 knock-out mice.

3.1 Chapter aims.

The class I HDACs, HDAC1 and 2 share 85% sequence homology and are present in the same co-repressor complexes Sin3, NuRD, Co-REST and NOD1 (Laherty, C.D., *et al.*, 1997, Zhang, Y., *et al.*, 1999, You, A., *et al.*, 2001 and Liang, J., *et al.*, 2008). Germ-line deletion of HDAC1 results in early embryonic lethality around embryonic day e9.5, although aberrant development occurs as early as e7.5 (Zupkovitz, G., *et al.*, 2006). In contrast to these early embryonic phenotypes, constitutive HDAC2 knockout mice survive embryogenesis and either die shortly after birth in one model after succumbing to a spectrum of cardiac defects (Montgomery, R. L., *et al.*, 2007), or survive to adulthood in others (Guan, J.S., *et al.*, 2009, Trivedi, C.M., *et al.*, 2007 and Zimmermann, S., *et al.*, 2007), albeit at reduced Mendelian frequencies. These defects cannot be phenocopied by conditional inactivation of HDAC2 in cardiomyocytes and smooth muscle (Montgomery, R.L., *et al.*, 2007), suggesting the cardiac specific defects may occur in a number of cell types rendered defective by the absence of HDAC2 during embryogenesis. In a number of cell types, deletion of both HDAC1 and HDAC2 is required to generate a phenotype (Montgomery, R.L., *et al.*, 2007, Haberland, M., *et al.*, 2009 and Montgomery, R.L., *et al.*, 2009). This result suggests that the activity of HDAC1 and HDAC2 is mostly redundant, with the requirement for both

HDAC1 and HDAC2 occurring only at certain key developmental periods, such as gastrulation.

To investigate the essential roles of HDAC1 and -2, during early embryogenesis, a strategy in which inducible inactivation of either enzyme in mouse embryonic stem (mES) cells was decided upon. mES cells are the *in vitro* counterpart of epiblast cells of the early post implantation embryo and their differentiation mimics many of the changes in gene expression associated with embryonic development (Smith, A.G., 2001). Allied to this, subsequent to the addition of precise stimuli, the pluripotent nature of mES cells permits *in vitro* differentiation into many derivatives of the three primary germ layers (endoderm, ectoderm and mesoderm) (Munsie, M., *et al.*, 2000). Conditional inactivation, permitting precise, temporal deletion of either HDAC1 or -2, prior to, or during mES cell differentiation, would permit the examination of the role of these enzymes at a variety of stages throughout a given differentiation process.

Given that germ-line deletion of HDAC1 results in embryonic lethality (preventing analysis of its roles in somatic tissues) and the ambiguity of the effects of germ-line deletion of HDAC2, a similar conditional inactivation strategy, as with mES cells, was decided upon to further define the developmental and physiological roles of HDAC1 and -2 *in vivo*. In mice housed under standard laboratory conditions, the thymus is rendered a non-essential tissue as ordinarily these animals are not immunologically challenged. Moreover, intra-thymic T cell development follows one of the best defined and well characterised pathways of somatic cell development. To date, the roles of HDAC1 and -2 in T cell development have not been determined. As such, ablation of HDAC1 and -2 during T cell development presents an attractive

means in which to study their involvement in the many aspects of T cell developmental biology which include; cellular proliferation, differentiation, survival, apoptosis, signal transduction and migration.

3.2 Strategy for generating homozygous conditional knock-out HDAC1 and HDAC2 mES cell lines.

To generate HDAC1 and HDAC2 mouse ES cells lines a strategy in which deletion of a “critical” 5’ exon, common to all transcripts, was decided upon. In the instances of both HDAC1 and -2, deletion of exon 2 was chosen. Deletion of exon 2 creates a frameshift mutation so that any residual transcript is subjected to nonsense-mediated decay and also results in the generation of a premature stop codon. Should nonsense-mediated decay not occur this ensures that any residual protein products are non-functional (Fig 3.1) (that is, lack the catalytic deacetylase domain which spans exons 2-9 of both HDAC1 and -2).

The same two step targeting strategy, for both Hdac1 and Hdac2 was designed and summarised in figures 3.2 and 3.3. The 1st wild type allele is targeted by homologous recombination with a targeting vector in which exon 2 is flanked (“floxed”) by Cre-recombinase recognition sites (LoxP sites). In addition, this targeting vector also contains a -pgkNeo expression cassette (for positive selection and enrichment of successfully targeted events), flanked by FLPe recombinase recognition sites (FRT sites). The 2nd wild type allele is targeted using a similar targeting vector as in the first instance, but the -pgkNeo expression cassette is exchanged for a -pgkHyg Δ Tk expression cassette.

Vectors are targeted to an E14 mES cell line (Hooper, M., *et al.*, 1987) that have an integrated inducible Cre recombinase, fused to a mutant oestrogen receptor ligand-binding domain, targeted to the endogenous ROSA26 locus (CreER-T) (Vooijs, M., *et al.*, 2001). Expression of Cre can be induced by the addition of the synthetic oestrogen antagonist 4-hydroxytamoxifen (4-OHT) to culture media. Cre induced recombination between the exon 2 flanking LoxP sites, results in excision of exon 2 from the mES cell genome and deletion of HDAC1 or HDAC2 protein as appropriately targeted.

3.2.1 Targeting the 1st wild type allele of Hdac1 and Hdac2 in E14 CreER-T mES cells.

At the beginning of the project, plasmid DNA of targeting vectors, Hdac1-cKO-Neo (Materials and Methods 2.3.7.1 and Fig 3.2) and Hdac2-cKO-Neo (Materials and Methods 2.3.7.2 and Fig 3.3) had previously been generated. Hdac1-cKO-Neo and Hdac2-cKO-Neo plasmid DNAs were linearised by restriction enzyme digest (*Kpn* I and *Pvu* I respectively) and used to target the endogenous loci in E14 CreER-T mES cells using standard gene targeting methods. Following selection, colonies were expanded and correctly targeted clones were detected by Southern blot screening as follows. To detect successful targeting of the Hdac1-cKO-Neo targeting vector the 5' probe (5'pr Fig 3.2), hybridised to *Stu* I digested gDNA, detects either a 10kb fragment (Hdac1^{WT}) or the 7kb targeted fragment (Hdac1^{Neo}) (Fig 3.4A). To detect successful targeting of the Hdac2-cKO-Neo targeting vector the 3'external probe (3'extpr Fig 3.3), hybridised to *Bam*HI, digested gDNA detects either a 24kb fragment (Hdac2^{WT}) or the 7kb targeted fragment (Hdac2^{Neo}) (Fig 3.4B).

HDAC1 Strategy

Allele:

Hdac1^{WT}
 10kb: *Stu* I-5'pr
 14kb: *Hind* III-3'pr

Targeting Vectors:
 1st Hdac1-cKO-Neo
 2nd Hdac1-cKO- HygΔTk

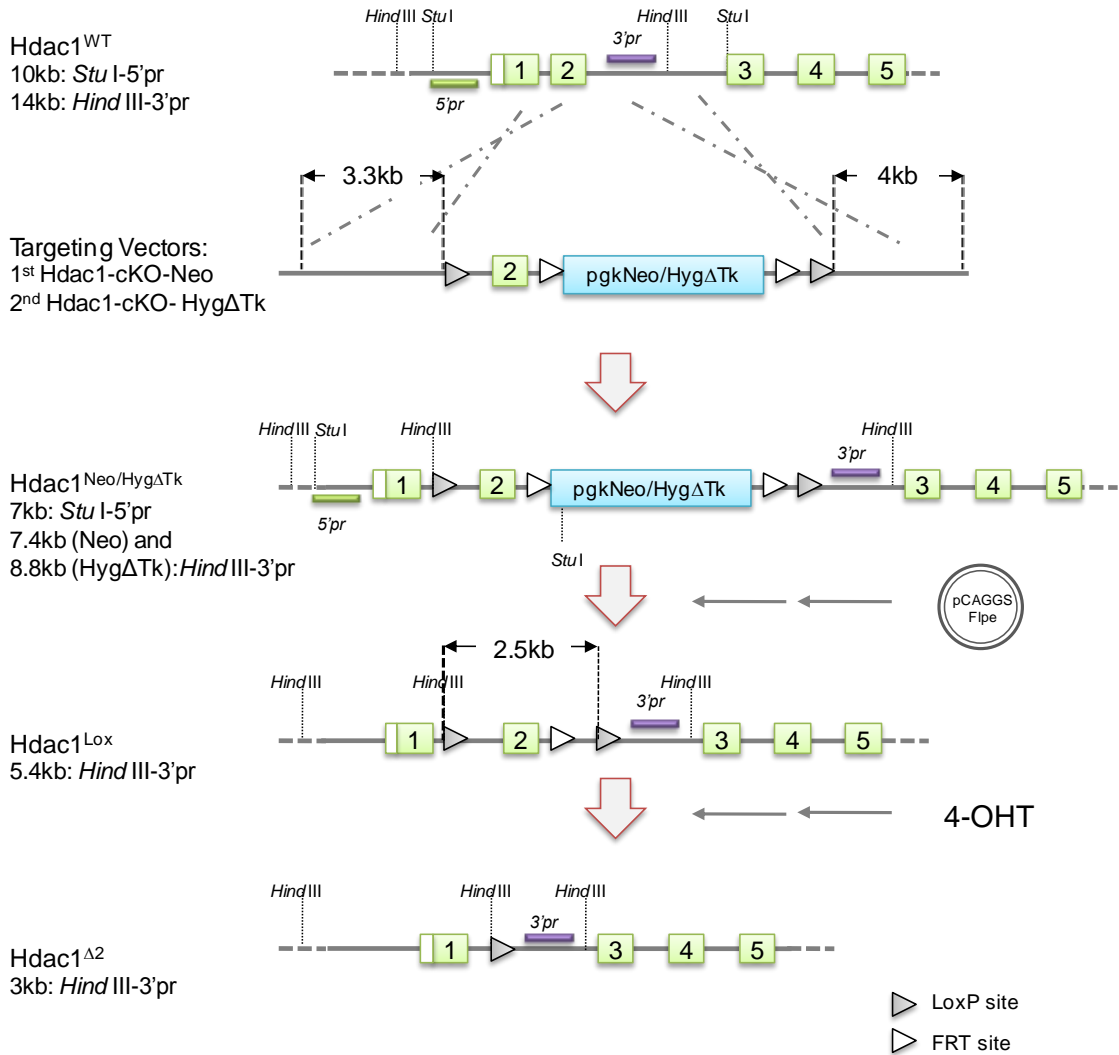


Figure 3.2. Strategy for generating conditional HDAC1 knock-out mES cell lines. Outline of sequential two step strategy to generate homozygous conditional knock-out Hdac1 alleles in mES cells. Southern Blot strategies to confirm successful integration of the targeting vectors into E14 mES cell line constitutively expressing a Cre/Estrogen Receptor (CreER-T) fusion from the *ROSA26* locus are detailed, including probes, digests and expected fragment sizes. The size of homology arms of the targeting vectors and position of LoxP (including distance between) and FRT sites in the final Hdac1 targeting vectors are also outlined.

HDAC2 Strategy

Allele:

Hdac2^{WT}
 17kb: *Bgl*I-5'pr
 24kb: *Bam*H I 3'extpr

Targeting Vectors:
 1st Hdac2-cKO-Neo
 2nd Hdac2-cKO- HygΔTk

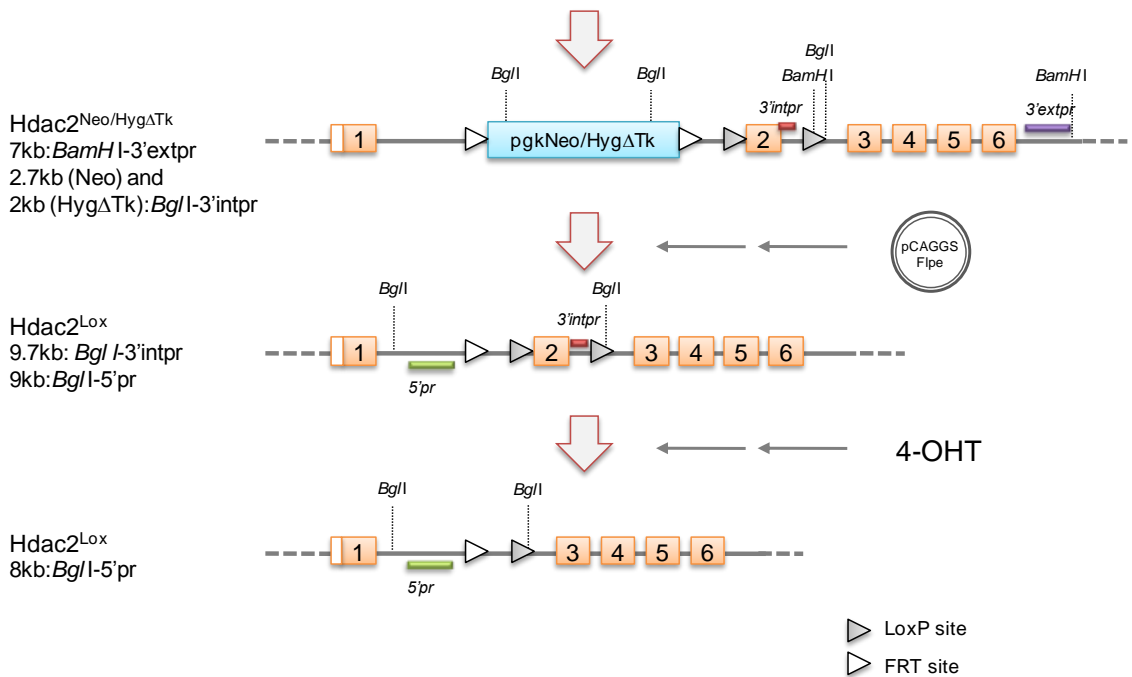


Figure 3.3. Strategy for generating conditional HDAC2 knock-out mES cell lines. Outline of sequential two step strategy to generate homozygous conditional knock-out Hdac2 alleles in mES cells. Southern Blot strategies to confirm successful integration of the targeting vectors into E14 mES cell line constitutively expressing a Cre/Estrogen Receptor (CreER-T) fusion from the *ROSA26* locus are detailed, including probes, digests and expected fragment sizes. The size of homology arms of the targeting vectors and position of LoxP (including distance between) and FRT sites in the final Hdac2 targeting vectors are also outlined.

3.2.2 Generation of the second *Hdac1* and *Hdac2* targeting vector.

In order to target the second wild type allele of *Hdac1* or *Hdac2* the -pgkNeo cassette from the initial *Hdac1/2*^{Neo} targeting vector was replaced with a -pgkHyg/ Δ TK expression cassette using Red/ET recombination (Liu, P.*et al* 2003). Targeting the second allele, using a different selectable, marker permits double drug selection following electroporation, using G418 and hygromycin B, to select for double targeted events.

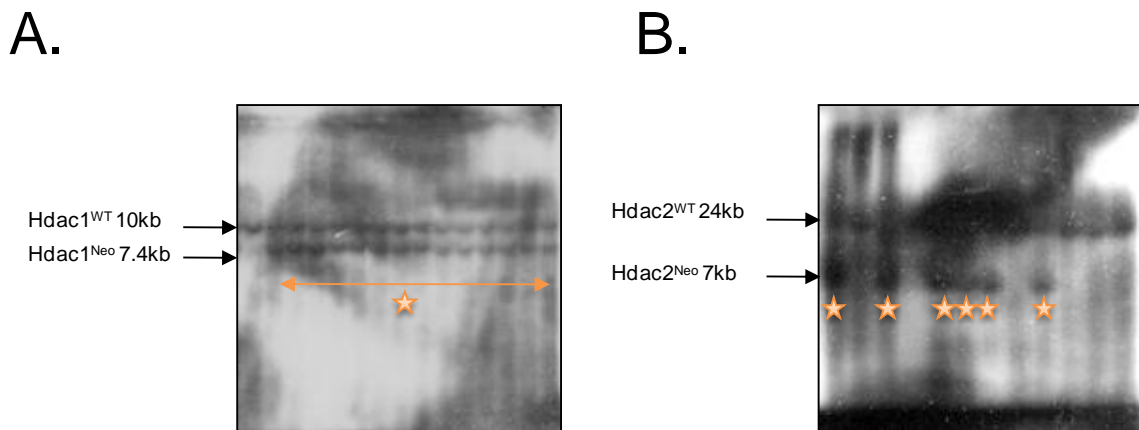


Figure 3.4. Successful targeting of the 1st wild type allele of *Hdac1* and *Hdac2*. (A) Confirmation of successful gene targeting of the *Hdac1*-cKO-Neo targeting vector into E14 CreER-T mES cells was assessed by Southern blot. Using the 5' probe (5'pr), on *Stu* I digested gDNA, yields either a 10kb fragment (*Hdac1*^{WT}) or a 7kb targeted fragment (*Hdac1*^{Neo}). Representative blot of at least 96 individual clones grown under positive selection conditions in G418 supplemented M15 culture media. (B) Confirmation of successful gene targeting of the *Hdac2*-cKO-Neo targeting vector into E14 CreER-T mES cells was assessed by Southern blot. Using the 3'external probe (3'extpr), on *Bam*H I digested gDNA, yields either a 24kb fragment (*Hdac2*^{WT}) or a 7kb targeted fragment (*Hdac2*^{Neo}). Representative blot of at least 48 individual clones grown under positive selection conditions in G418 supplemented M15 culture media. Orange star denotes successfully targeted clones.

The outline for generating both the Hdac1-cKO-Hyg Δ Tk and Hdac2-cKOHyg Δ Tk targeting vectors are depicted in figures 3.5 and 3.6 respectively. To generate the Hdac1/2-cKO-Hyg Δ Tk targeting vector the-pgkHyg/ Δ tk cassette was amplified from pSC5 using the following primer pairs; Hdac1 5'sc5Cap and Hdac1 3'sc5Cap (Hdac1-cKO-Hyg Δ Tk) and Hdac2 5'sc5Cap and Hdac2 3'sc5Cap (Hdac2-cKO-Hyg Δ Tk) (Materials and Methods 2.3.7.3). These PCR primers consist of a 66bp sequence homologous to the 5' and 3' sequence flanking the -pgkNeo selection cassette of Hdac1-cKO-Neo as well as shorter 20bp sequence used to amplify the -pgkHyg/ Δ TK fragment from pSC5. These fragments were gel purified and electroporated as appropriate into the DY380 recombineering bacterial strain, containing Hdac1-ckO-Neo or Hdac2-cKO-Neo and heat shocked to initiate recombination, followed by hygromycin selection on LB agar plates. Genomic DNA from positively selected clones was then sequenced to ensure the recombined fragment was in the correct orientation and matched the predicted sequence (APPENDIX Fig A1-D1). The size of homology arms, position of LoxP and FRT sites in the final Hdac1/2-cKO-Hyg Δ Tk targeting vectors are outlined in Figures 3.2 and 3.3.

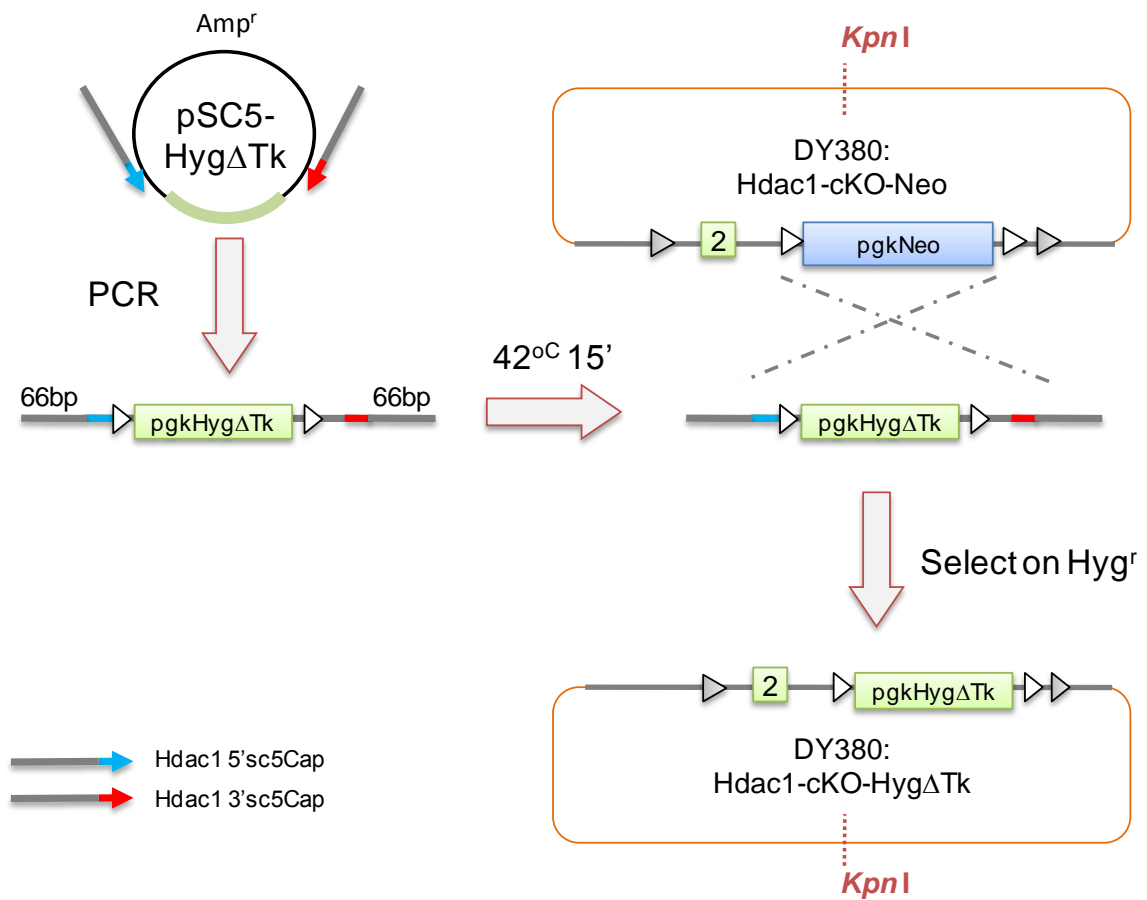


Figure 3.5. *Generation of the HDAC1-cKO-HygΔTk targeting vector.* Outline of strategy to generate HDAC1-cKO-HygΔtk from the Hdac1-cKO-Neo targeting vector using recombineering. The -pgkHygΔTk cassette was amplified from pSC5 using the primers Hdac1 5'sc5Cap and Hdac1 3'sc5Cap (66bp of homology with 5' and 3' target Hdac1-cKO-Neo are shown in grey, red and blue portions indicate sequences used to prime the amplification of the -pgkHygΔTk selectable marker fragment) and electroporated into DY380 bacteria containing HDAC1-cKO-Neo and heat shocked to initiate recombination, followed by hygromycin selection. Also shown is the unique restriction site (*Kpn* I) used to linearise both targeting vectors prior to electroporation into single targeted E14 CreER-T mES cells.

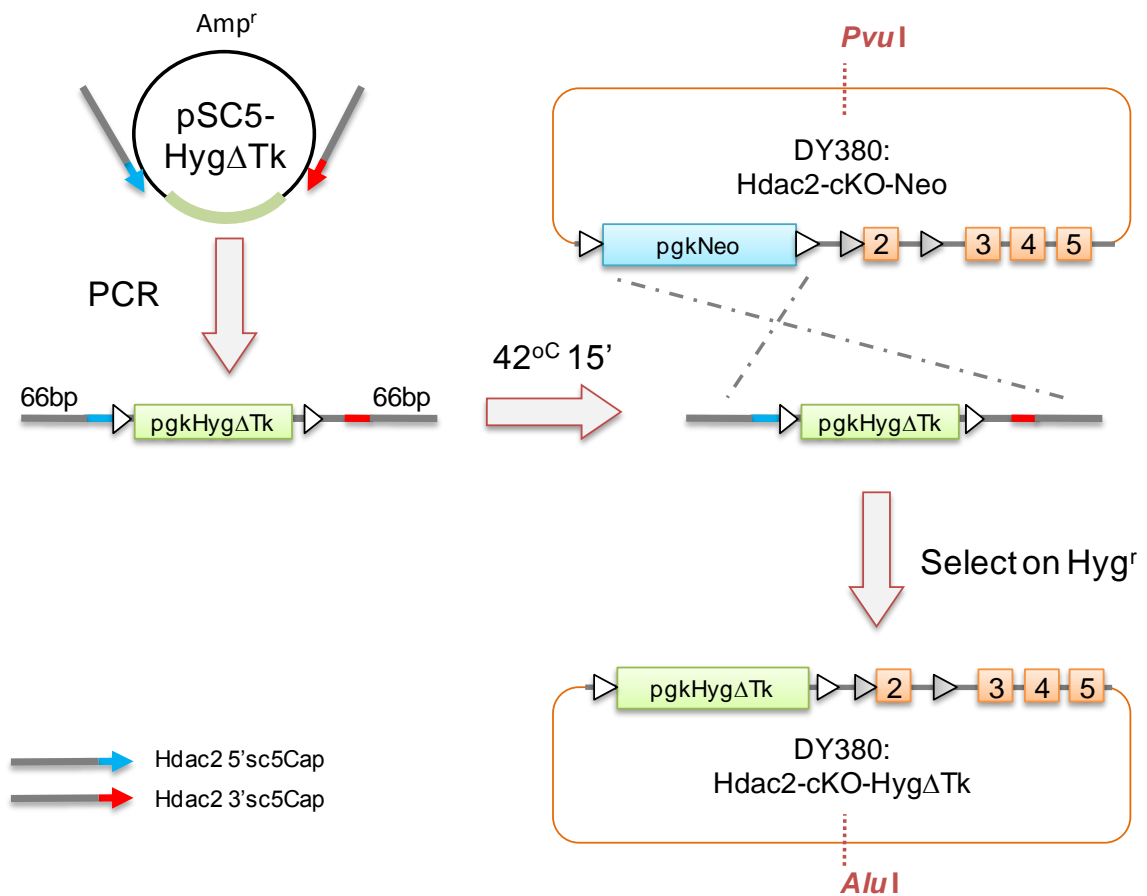


Figure 3.6. *Generation of the HDAC2-cKO-HygΔTk targeting vector.* Outline of strategy to generate HDAC2-cKO-HygΔtk from the Hdac2-cKO-Neo targeting vector using recombineering. The -pgkHygΔTk cassette was amplified from pSC5 using the primers Hdac2 5'sc5Cap and Hdac2 3'sc5Cap (66bp of homology with 5' and 3' target Hdac2-cKO-Neo are shown in grey, red and blue portions indicate sequences used to prime the amplification of the -pgkHygΔTk selectable marker fragment) and electroporated into DY380 bacteria containing HDAC2-ckO-Neo and heat shocked to initiate recombination, followed by hygromycin selection. Also shown are the unique restriction sites (*Pvu* I and *Alu* I) used to linearise the targeting vectors prior to electroporation into single targeted E14 CreER-T mES cells.

3.2.3 Targeting the 2nd wild type allele of Hdac1 or Hdac2 in E14 CreER-T mES cells.

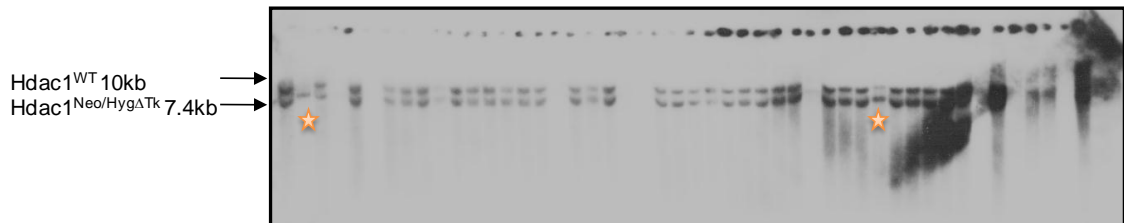
To target the 2nd Hdac1 or Hdac2 wild type allele, Hdac1-cKO-Hyg Δ Tk or Hdac2-cKO-Hyg Δ Tk targeting vector plasmid DNA was linearised by restriction enzyme digest (*Kpn* I or *Alu* I respectively) and electroporated as appropriate into single cell cloned, single targeted Hdac1^{Neo/+} or Hdac2^{Neo/+} mES cells. Positive clones were identified by hygromycin B. Following selection, surviving colonies were expanded and identification of double targeted (Hdac1/2^{Neo/Hyg Δ Tk}) mES cells detected by Southern blot screening as follows. To detect successful targeting of the Hdac1-cKO-Hyg Δ Tk targeting vector the 5' probe (5'pr Fig 3.2), hybridised to *Stu* I digested gDNA, detects either a 10kb fragment (Hdac1^{WT}) or the 7kb targeted fragment (Hdac1^{Neo/Hyg Δ Tk}) (Fig 3.7A). To detect successful targeting of the Hdac2-cKO-Hyg Δ Tk targeting vector the 3' external probe (3'extpr Fig 3.3), hybridised to *BamH* I digested gDNA, detects either a 24kb fragment (Hdac2^{WT}) or the 7kb targeted fragment (Hdac2^{Neo/Hyg Δ Tk}) (Fig 3.7B). Note that detection of a single targeted fragment identifies double targeted colonies. Single cell double targeted clones were expanded, re-screened using the same Southern strategy (to remove any low level contamination of un-recombined cells) and frozen stocks generated.

3.2.4 FLPe-mediated deletion of selection markers in *Hdac1*^{Neo/HygΔTk} and *Hdac2*^{Neo/HygΔTk} double targeted E14 CreER-T mES cells.

The presence of selectable markers associated with targeted alleles carry promoter and enhancer sequences which can interfere with expression of genes linked to the targeted locus (Buchholz, F. *et al.*, 1998 and Lakso, M. *et al.*, 1996). Long-range disruptions of gene expression at distances greater than 100kb have been reported which could potentially confound the analysis of any observed mutant phenotype (Dymecki, S.M. and Tomaszewicz, H. 1998). To circumnavigate any potential concerns over integration of the selectable markers into the mES cell genome, they were flanked by FRT sites (Fig 3.2 and 3.3) permitting excision of the selectable portion of the integrated targeting vector cassette (i.e. -pgkNeo and -pgkHygΔTk) via Flpe induced recombination between flanking FRT sites. To achieve recombination, double-targeted (single cell) clones were transiently transfected with a pCAGGS-FLPe plasmid (Materials and Methods 2.3.7.4, Beard C., *et al.*, 2006) and negative selection applied using 1-(2-deoxy-2-fluoro-1-D-arabinofuranosyl)-5-iodouracil (FIAU) to identify loss of the thymidine-kinase portion of the -pgkHygΔTk cassette. Finally, surviving mES cell clones in which loss of the selection cassettes had been achieved were identified by Southern blot screening as follows. To detect successful excision of the selectable markers, in double targeted *Hdac1*^{Neo/HygΔTk} CreER-T mES cells, the 3' internal probe (3'pr Fig 3.2), hybridised to *Hind* III digested gDNA, detected either an 8.8kb targeted fragment (*Hdac1*^{HygΔTk}), a 7.4kb targeted fragment (*Hdac1*^{Neo}) or the 5.4kb FLPe recombined fragment (*Hdac1*^{Lox}) (Fig 3.8A). For detection of successful

excision of selectable markers in double targeted $Hdac2^{Neo/Hyg\Delta Tk}$ mES cells (Fig 3.8B), the 3' internal probe (3'intpr Fig

A.



B.

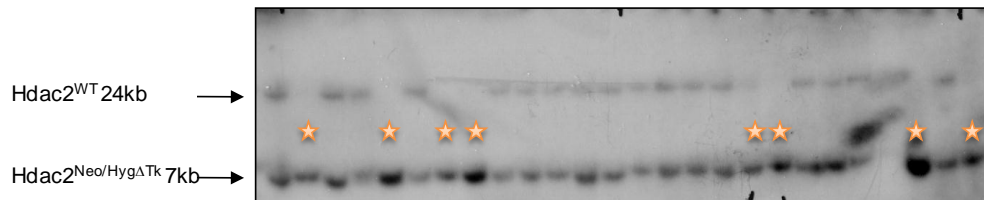


Figure 3.7. Successful targeting of the 2nd wild type allele of *Hdac1* and *Hdac2*. (A) Confirmation of successful gene targeting of the *Hdac1*-cKO-Hyg Δ Tk targeting vector into E14CreER-TmES cells was assessed by Southern blot. Using the 5' probe (5'pr), on *Stu* I digested gDNA, yields either a 10kb fragment ($Hdac1^{WT}$) or a 7kb targeted fragment ($Hdac1^{Neo/Hyg\Delta Tk}$). (B) Confirmation of successful gene targeting of the *Hdac2*-cKO-Hyg Δ Tk targeting vector into E14 CreER-T mES cells was assessed by Southern blot. Using the 3' external probe (3'extpr), on *Bam*H I digested gDNA, yields either a 24kb fragment ($Hdac2^{WT}$) or a 7kb targeted fragment ($Hdac2^{Neo/Hyg\Delta Tk}$). Blots are representative of at least 96 individual clones grown under positive selection conditions in hygromycin B supplemented M15 culture media. Orange star denotes successfully targeted clones.

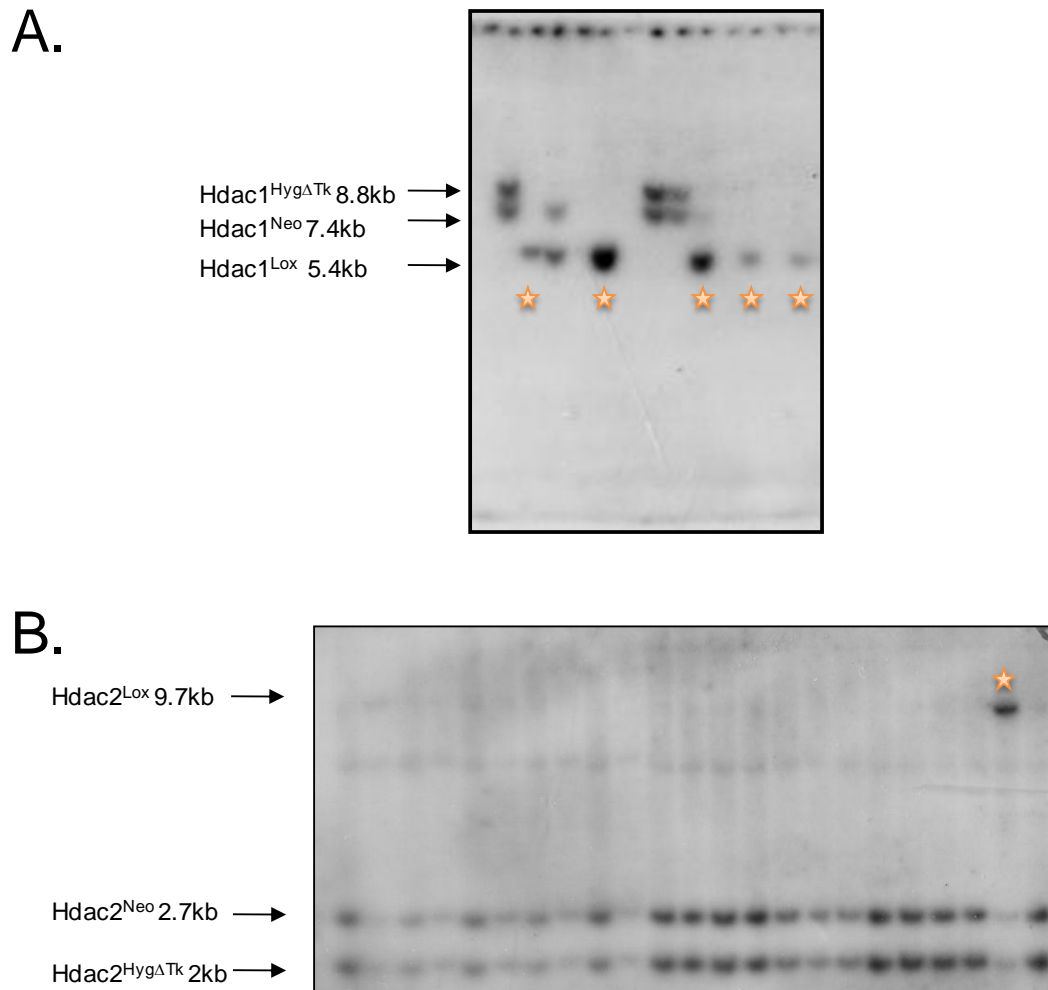


Figure 3.8. *FLPe-mediated excision of selection markers.* (A) Confirmation of successful FLPe mediated excision of the $-\text{pgkNeo}/\text{Hyg}\Delta\text{Tk}$ selection cassettes from homozygous conditional targeted Hdac1 alleles in E14 CreER-T mES cells was assessed by Southern blot. Using the 3' internal probe (3'pr), on *Hind* III digested gDNA, yielded either an 8.8kb targeted fragment (Hdac1^{HygΔTk}), a 7.4kb targeted fragment (Hdac1^{Neo}) or a 5.4kb FLPe recombined fragment (Hdac1^{Lox}). (B) Confirmation of successful FLPe mediated excision of the $-\text{pgkNeo}/\text{Hyg}\Delta\text{Tk}$ selection cassettes from homozygous conditional targeted Hdac2 alleles in E14 CreER-T mES cells was assessed by Southern blot. Using the 3' internal probe (3'intpr) on *Bgl* I digested genomic DNA, yielded either a 2kb targeted fragment (Hdac2^{HygΔTk}), a 2.7kb targeted fragment (Hdac2^{Neo}) or a 9.7kb Flpe recombined fragment (Hdac2^{Lox}). Blots are representative of at least 48 individual clones grown under negative selection conditions in FIAU supplemented M15 culture media.

3.3) hybridised to *Bgl* I digested gDNA detected either a 2kb targeted fragment ($Hdac2^{Hyg\Delta Tk}$), a 2.7kb targeted fragment ($Hdac2^{Neo}$) or the 9.7kb FLPe recombined fragment ($Hdac2^{Lox}$) (Fig 3.8B). Single cell $Hdac1^{Neo/Hyg\Delta Tk}$ and $Hdac2^{Neo/Hyg\Delta Tk}$ CreER-T mES cell clones detected as having successfully excised both selection cassettes were expanded, re-screened using the same Southern strategy (to remove any low level contamination of non re-recombined cells) and frozen stocks generated. These cells are henceforth denoted as $Hdac1^{Lox/Lox}$ or $Hdac2^{Lox/Lox}$ mES cell lines.

3.3 Ligand inducible deletion of HDAC1 and HDAC2 in $Hdac1^{Lox/Lox}$ and $Hdac2^{Lox/Lox}$ E14 CreER-T mES cell lines.

Activation of CreER, by addition of 1 μ M 4-OHT to the growth media, was used to induce LoxP recombination and deletion of exon 2 which was assessed by Southern blot as follows. To detect successful CreER recombinase inducible deletion of exon 2 in double targeted $Hdac1^{Lox/Lox}$ mES cells, the 3' internal probe (3'pr Fig 3.2), hybridised to *Hind* III digested gDNA, detected either a 14kb WT fragment ($Hdac1^{WT}$), a 5.4kb targeted fragment ($Hdac1^{Lox}$) or the 3kb LoxP recombined fragment ($Hdac1^{\Delta 2}$) (Fig 3.9A). To detect successful, CreER recombinase inducible deletion of exon 2 in double targeted $Hdac2^{Lox/Lox}$ mES cells, the 5' internal probe (5'pr Fig 3.3), hybridised to *Bgl* I digested gDNA, detected either a 17kb WT fragment ($Hdac2^{WT}$), a 9kb targeted fragment ($Hdac2^{Lox}$) or the 8kb LoxP recombined fragment ($Hdac2^{\Delta 2}$) (Fig 3.10A). Addition of 4-OHT resulted in complete recombination of floxed alleles and deletion of exon 2 within 24hr (note no deletion of exon 2 is detectable in

control, CreER WT, cells) (Fig 3.9A and 3.10A). Loss of exon 2 disrupts the open reading frame (ORF) of both Hdac1 and Hdac2 such that a premature stop codon is introduced in exons 3 and 5 respectively. Following deletion of exon 2 a further 4–5 days of culture are required before HDAC1 and HDAC2 protein levels are reduced below 10% of those of CreER WT cells (Fig 3.9B and 3.10B). In order to perform biological replicates in future experiments, to ensure robustness of the conditional knock-out strategy, up to 5 individual Hdac1^{Lox/Lox} or Hdac2^{Lox/Lox} mES cell lines were treated with 4-OHT and the protein levels of HDAC1 and HDAC2 screened by quantitative western blot. Figure 3.11 shows representative results of the screens revealing complete deletion in all clones tested. Using these multiple, individually targeted cell lines in future experiments (i.e. using biological replicates as opposed to technical replicates) adds confidence and improves validity of any observed experimental outcomes or conclusions. In subsequent experiments Hdac1^{Lox/Lox} and Hdac2^{Lox/Lox} E14 CreER mES cells are henceforth referred to as HDAC1^{Lox/Lox} or HDAC2^{Lox/Lox} mES cells. Hdac1^{Lox/Lox} and Hdac2^{Lox/Lox};E14 CreER mES cells 10–24 days post recombination are hence referred to as HDAC1^{Δ2/Δ2} and HDAC2^{Δ2/Δ2}.

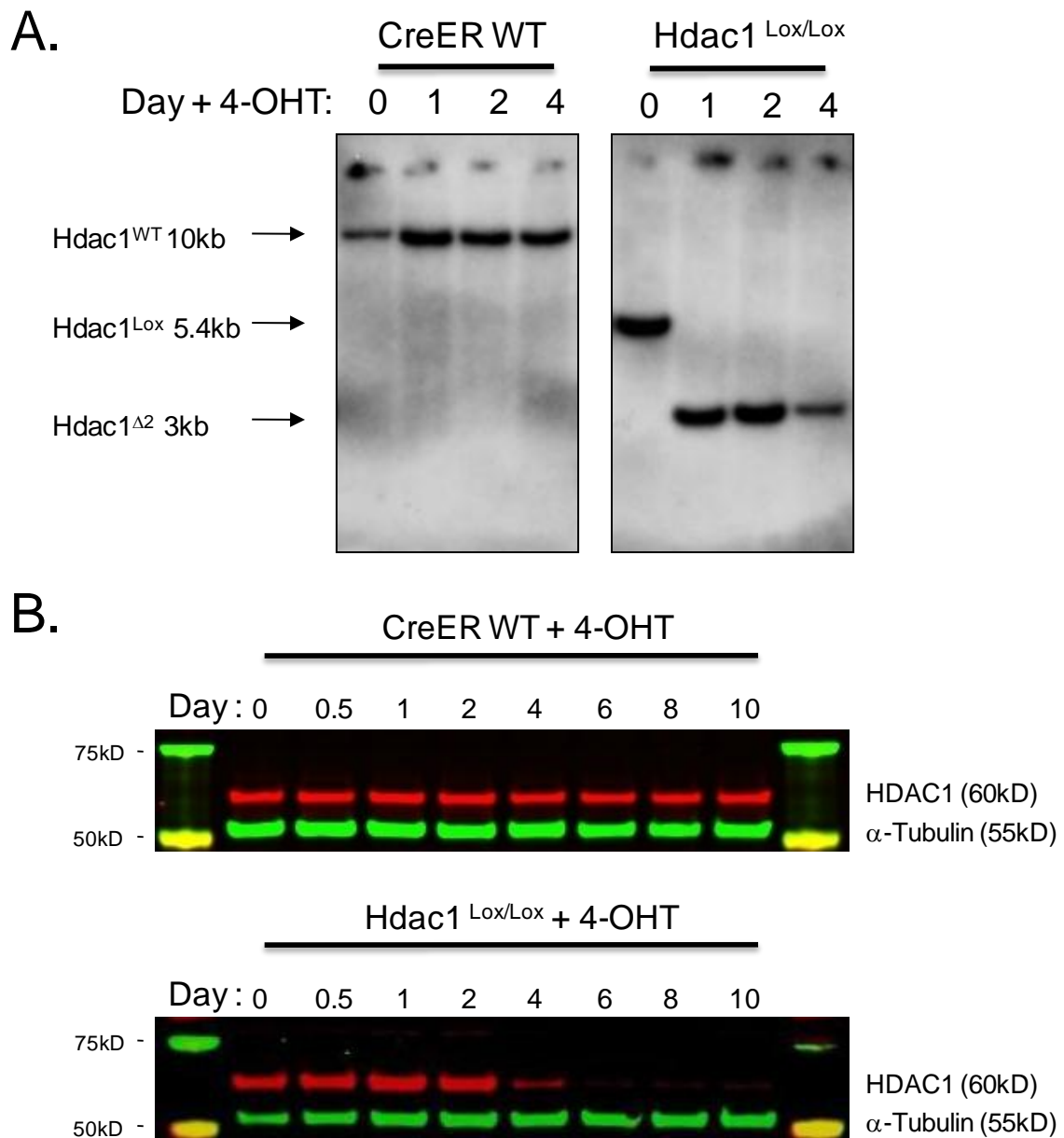


Figure 3.9. *Generation of inducible HDAC1 conditional knock-out mES cell lines.* (A) Southern blots on gDNA isolated from CreER WT and Hdac1^{Lox/Lox} mES cells. Addition of 4-hydroxy tamoxifen (4-OHT) activates the CreER fusion protein and induces deletion of exon2 (HDAC1^{Δ2/Δ2}) in Hdac1^{Lox/Lox} mES cells, >95% recombination is observed after 24h. (B) Quantitative western blot shows ligand-inducible deletion of HDAC1 protein in whole cell extracts from HDAC1^{Lox/Lox} mES cells. Cells were cultured for up to 10 days (0-3 days in the presence of 4-OHT). α-Tubulin was used to normalize protein loading. Blots were visualized and quantified using a LiCOR scanner.

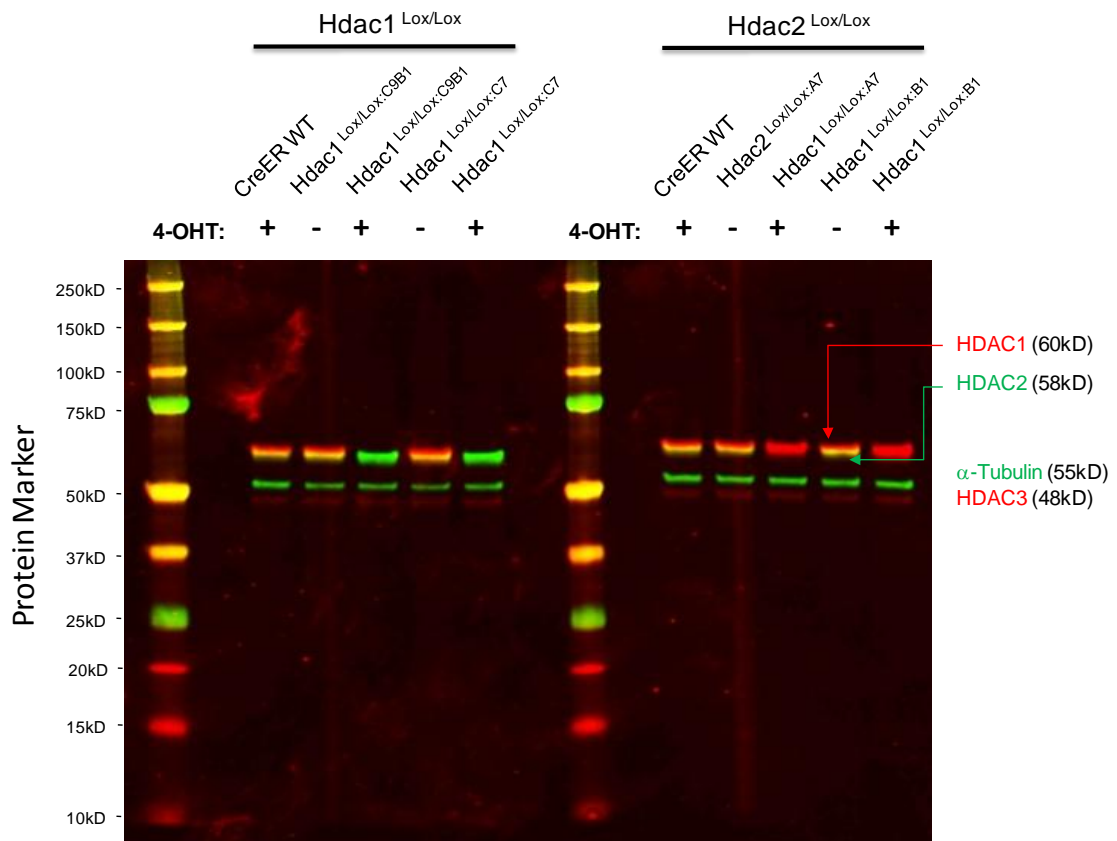


Figure 3.11. *Ligand inducible deletion of HDAC1 and HDAC2 in multiple Hdac1^{Lox/Lox} and Hdac2^{Lox/Lox} mES cell lines.* Representative quantitative western blot shows ligand-inducible deletion of HDAC1 or HDAC2 protein in whole cell extracts from 2 clones of each HDAC1^{Lox/Lox} and Hdac2^{Lox/Lox} mES cell line. Cells were cultured for up to 10 days (0-3 days in the presence of 4-OHT). CreER WT and untreated cell lines are loaded as controls. α-Tubulin was used to normalize protein loading. Blots were visualized and quantified using a LiCOR scanner.

3.4 Generation of HDAC1^{Lox/Lox} rescue mES cells lines.

In order to “rescue” any potential phenotype, following ligand-induced deletion of HDAC1 in HDAC1^{Lox/Lox} cell lines, attempts were made to generate Hdac1-C'-FLAG-tagged expression constructs which could be stably transfected into HDAC1^{Lox/Lox} mES cell lines. Fusion of FLAG epitopes to the C-terminus of the transfected HDAC1 protein would be useful in verifying expression of protein from the transfected construct over the endogenous. C' FLAG-tagged proteins are readily detected using an antibody (M2) raised against the FLAG epitope DYKDDDDK (Brizzard, B.L., *et al.*, 1994).

3.4.1 Generation of an Hdac1 C' FLAG-tagged expression construct (Hdac1-C-FLAG-Resc).

To generate the Hdac1-C'-FLAG-Resc construct, murine full length Hdac1 cDNA, obtained from an I.M.A.G.E. clone (I.M.A.G.E. ID: 4217199, Source BioScience, LifeSciences), was PCR amplified using the primers 5'*Bam*HI-Hdac1 Resc cDNA and 3'Hdac1 Resc cDNA-FLAG-*Eco*R I. It was projected that amplification of the Hdac1 cDNA using these primers would introduce a 5'*Bam*HI and a 3'*Eco*R I restriction enzyme site (with the 3' *Eco*R I site preceded by a sequence that replaces the original stop codon with sequence encoding two FLAG peptide motifs followed by a new stop codon) (Fig 3.12A). The resulting PCR (insert) fragment, as well as vector plasmid DNA from pcDNA3.1(+), was restriction enzyme digested with *Bam*HI and *Eco*R I to facilitate complementary ligation via generation of cohesive ends. PCR fragments were dephosphorylated, ligated and transformed into chemically

competent *E. coli.*, followed by ampicillin selection on TB agar plates (resistance conferred by the ampicillin gene present in the backbone of pcDNA3.1(+)). Positively selected transformants were screened using *Stu* I restriction enzyme digests to determine the presence of the insert. The pcDNA 3.1 vector has a single *Stu* I site that in the absence of the insert results in a single fragment of 5.4kb (Materials and Methods 2.3.7.5). However, if the insert has been successfully cloned into the vector, subsequent *Stu* I digestion would result in two fragments of 2kb and 5kb due to the presence of an additional *Stu* I site in the insert (Fig 3.12B). Figure 3.12C shows the results of 4 *Stu* I enzymatic digests, 3 of which contain the insert (c21-23). Positively screened clones identified by restriction digest, were then sequenced using primers from within the pcDNA 3.1 vector and flanking the insertion site (T7 and BGH-Rev, see Materials and Methods 2.3.7.5), verifying consensus of cloned insert sequences with predicted sequence and confirming that the insert fragment was cloned in the correct orientation (APPENDIX Fig E1 and F1).

3.4.2 Generation of transient and stably transfected HDAC1^{Lox/Lox} and HDAC1^{Δ2/Δ2} mES cell lines.

Prior to the generation of stable cell lines with the Hdac1-C-FLAG-Resc construct, transient transfection of a single HDAC1^{Lox/Lox} mES cell line was carried out to confirm the expression of FLAG-tagged HDAC1 protein using unlinearised Hdac1-C-FLAG-Resc DNA from maxi preps of previously correctly identified transformants. Profiling transfected cells by probing western blots, 3 days post transfection, with antibodies raised in two different species i.e. anti

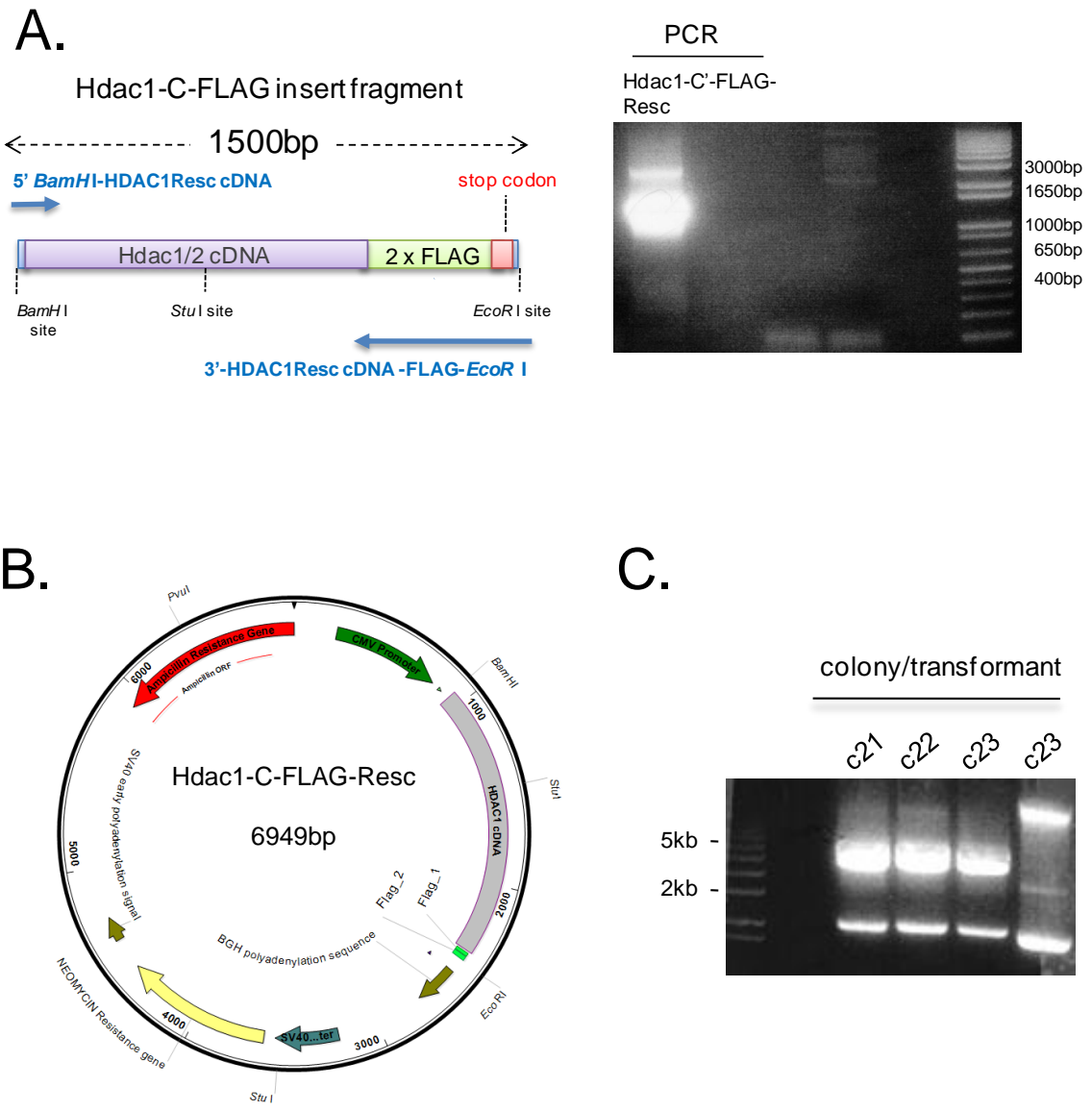
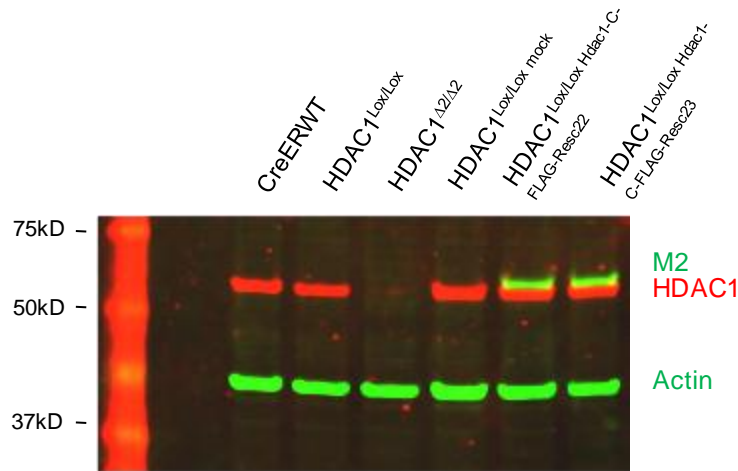


Figure 3.12. Strategy for generating *Hdac1* -C'-FLAG-Resc constructs. (A) The 1.5kb *Hdac1*-C'-FLAG-Resc insert fragment was PCR amplified using full length *Hdac1* cDNA template to incorporate 5'*BamH* I sites, 3'*EcoR* I sites (for cloning into a *BamH* I/ *EcoR* I pcDNA3.1(+) vector fragment) and a 3' sequence encoding for two FLAG epitopes as well as a newly defined stop codon. (B) Predicted *Hdac1*-C-FLAG-Rescue plasmid map. Map shows position of resistance genes (*Amp* and *Neo*) as well as unique cloning sites (C) Successful insertion of the insert was identified by agarose electrophoresis of *Stu* I plasmid DNA digests. Correct insertion profiles are indicated by two bands of 2 and 5kb.

A.



B. Plasmid DNA

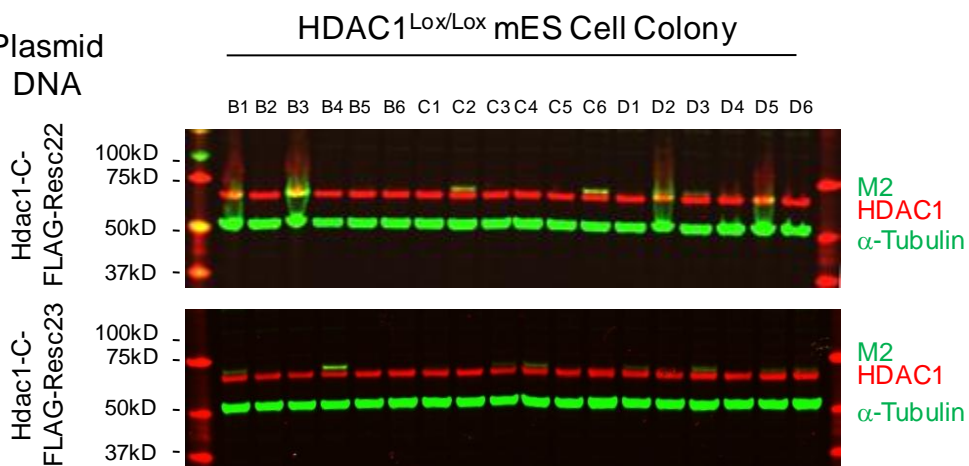


Figure 3.13. Generation of transient and stably transfected $HDAC1^{Lox/Lox}$ and $HDAC1^{\Delta2/\Delta2}$ mES cell lines. (A) A single $HDAC1^{Lox/Lox}$ mES cell line was transiently transfected with either mock (transfection reagent alone) or *Hdac1-C-FLAG-Resc* expression construct plasmid DNA (c22 and c23). Whole cell extracts were obtained 3 days post transfection and analysed by western blotting for HDAC1 C'-FLAG-tag protein and HDAC1 with mouse monoclonal M2 and HDAC1 rabbit polyclonal antibodies respectively. CreER WT, $HDAC1^{Lox/Lox}$ and $HDAC1^{\Delta2/\Delta2}$ extracts were loaded as controls. (B) A single $Hdac1^{Lox/Lox}$ mES cell line was transfected using *Pvu I* linearised plasmid DNA from the same *Hdac1-C-FLAG-Resc* expression constructs as in A. Quantitative western blot for C'-FLAG-tag and endogenous HDAC1 obtained from whole cell extracts of 18 G418 resistant colonies was used to identify stable expression of HDAC1-C'-FLAG-tag protein.

C.

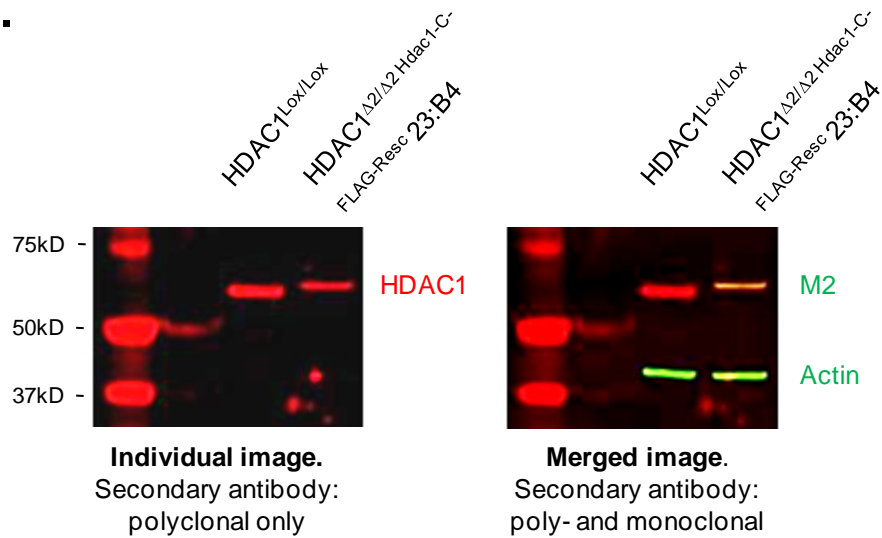


Figure 3.13 continued. *Generation of transient and stably transfected HDAC1^{Lox/Lox} and HDAC1^{Δ2/Δ2} mES cell lines.* (C) A stably transfected HDAC1^{Lox/Lox} mES cell line was treated with 4-OHT, to induce ligand mediated deletion of endogenous HDAC1 and probed by western blotting for HDAC1 and C'FLAG-tag. Shown is the individual, 700nm channel and the merged, 700/800nm channel images. All blots were visualised and quantified using a LiCOR scanner and normalised against the loading controls, Actin or α -Tubulin as appropriate.

rabbit polyclonal HDAC1 and anti mouse monoclonal FLAG epitope (using the M2 antibody) permits multiplex western assays and confirms the presence of a FLAG-tagged protein of the expected size (i.e. approximately 2.5kD larger than endogenous HDAC1) (Fig 3.13A).

Having confirmed the presence of a FLAG-tagged protein of the predicted size, attempts to generate a stably transfected Hdac1^{Lox/Lox} mES cell line were made by transfection of two different *Pvu* I linearised Hdac1-C-FLAG-Resc plasmid DNAs (C-FLAG-Resc c22 and c23), followed by positive selection of colonies in sustained culture under G418 selection (resistance of transfected cells to G418 conferred by the -Neo resistance portion of the Hdac1-C-FLAG-

Resc construct (Fig 3.12B). Following selection, surviving colonies were selected and seeded into 96 well plates, expanded and replicated. Whole cell extracts from one of the replicate plates were made and analysed by western blot for the presence of the FLAG-tagged protein identified previously in transient transfected cells using the M2 antibody (Fig 3.13B). HDAC1^{Lox/Lox} mES cell lines that revealed the highest expression of FLAG-tagged protein were identified by western blotting (i.e. HDAC1^{L/L-C'-FLAG-Resc}22:B3/C6 and HDAC1^{L/L-C'-FLAG-Resc}23:B4) and treated with 4-OHT to induce deletion of endogenous HDAC1, thus generating HDAC1^{Δ2/Δ2:Hdac1-C-FLAG-Resc} mES cell lines (Fig 3.13C). Confirmation that the FLAG-tagged protein identified by the M2 antibody was HDAC1 is demonstrated by western blotting using an antibody against endogenous/WT HDAC1 in HDAC1^{Δ2/Δ2:Hdac1-C-FLAG-Resc} mES cells (note that both the endogenous HDAC1 antibody signal and that of the M2 antibody overlap producing a yellow band in the merged image). Additionally, control protein from an HDAC1^{Lox/Lox} mES cell line also indicates that endogenous HDAC1 is identifiably smaller than that HDAC1-C'-FLAG-Resc protein and is absent in HDAC1^{Δ2/Δ2:Hdac1-C-FLAG-Resc} mES cells. These cells will be used in Chapter 4 to rescue any potential phenotypes associated with the deletion of HDAC1 in mES cells. However, quantification of protein expression of HDAC1-C'-FLAG-tag and WT HDAC1 in HDAC1^{Δ2/Δ2:Hdac1-C-FLAG-Resc} and HDAC1^{Lox/Lox} mES cell lines respectively, reveals that expression levels of FLAG-tagged HDAC1, despite prior selection, are much lower, approximately 25% of endogenous HDAC1 levels. As such, HDAC1-C'-FLAG-tag protein may not be sufficiently expressed to rescue any potential phenotypes caused by deletion of endogenous HDAC1 in future experiments.

3.5 Generation of T cell specific conditional HDAC1 and 2 knock-out mice.

3.5.1 Strategy for generating T cell specific Cre-mediated conditionally inactivated Hdac1 and Hdac2 alleles.

In order to generate mice with Hdac1 and Hdac2 conditional knock-out alleles the same targeting constructs used to target Hdac1 and Hdac2 in mES cells (namely Hdac1/2-cKO-Neo) were used to target AB1.1;129S5 mES cells using standard gene targeting methods. Successfully targeted heterozygous Hdac1^{Neo} and Hdac2^{Neo} AB1.1;129/Sv mES cells were used to generate mice heterozygous for the targeted-cKO-Neo alleles by blastocyst injection and chimera germ line transmission. These mice are henceforth denoted as HD1^{Neo/+} and HD2^{Neo/+}.

A four step breeding strategy (outlined in Fig 3.14) was applied in order to generate cohorts of homozygous Hdac1^{Lox/Lox} or Hdac2^{Lox/Lox} mice that also carried a T cell restricted *Cre recombinase* expressing transgene, TgN(*LckCre*) (Hennet, T., *et al.*, 1995 and Lee, P.P., *et al.*, 2001). These mice are henceforth denoted as HD1^{L/L:LckCre} and HD2^{L/L:LckCre} respectively. *Cre* expression from this particular transgene is under the control of the *Lck* promoter. Expression of *Lck* is restricted to T cells and expressed early in T cell development (<http://biogps.org/#goto=genereport&id=3932>, Alberts, B., *et al.*, 2002). In particular the *LckCre* transgene has been shown to be T cell specific and active early in T cell differentiation at the double negative stage (Williams, C.J., *et al.*, 2004). As with Hdac1 and Hdac2 conditional knock-out mES cell lines, expression of *Cre* is expected to result in LoxP recombination, deletion of the “floxed” exon 2, a frame shift mutation, generation of an early stop codon and

deletion of HDAC1 or HDAC2 protein as targeted. (Note for simplicity Figure 3.14 details the strategy for the generation of conditional HDAC1 knock-out mice only; however, the breeding strategy remains the same for the generation of the conditional HDAC2 knock-out mouse cohorts.)

3.5.2 Generation of targeted HD1^{Neo/+} and HD2^{Neo/+} mice harbouring a knocked-in Gt(Rosa)26Sor-FLPe allele.

As previously discussed, to avoid selection marker interference and genetic ambiguity of targeted mouse cohorts, heterozygous HD1^{Neo/+} and HD2^{Neo/+} mice were inter-crossed to a germline FLPe deleter mouse strain WTc57bl6^{Gt(Rosa)26Sor-FLPe} (Farley, F. W., *et al.*, 2000) (Fig 3.14, STEP1). This strain harbours a FLPe knock-in allele gene driven by the *Gt(ROSA)26Sor* promoter driving ubiquitous FLPe expression, which should result in FRT site specific recombination and removal of the “flrtd” -pgkNeo selection cassette from targeted alleles. gDNA from ear samples of pups was extracted and subjected to PCR genotyping. Transmission of the Hdac1^{Neo} allele was determined by the presence of the 5' LoxP site of the targeting vector using the primers HDAC1_Fwd and HDAC1_Rev (Fig 3.15A). Likewise, transmission of the Hdac2^{Neo} allele was determined by the presence of the 3' LoxP site of the targeting vector using the primers HDAC2_Fwd and HDAC2_Rev (Fig 3.15B). Mice positive for the cKO-Neo allele were also screened for the presence of the knocked in *Gt(Rosa)26Sor-FLPe* allele using the primers R26R GT1, R26R GT2 and R26R GT3 (Fig 3.15C). Pups that had both alleles were denoted

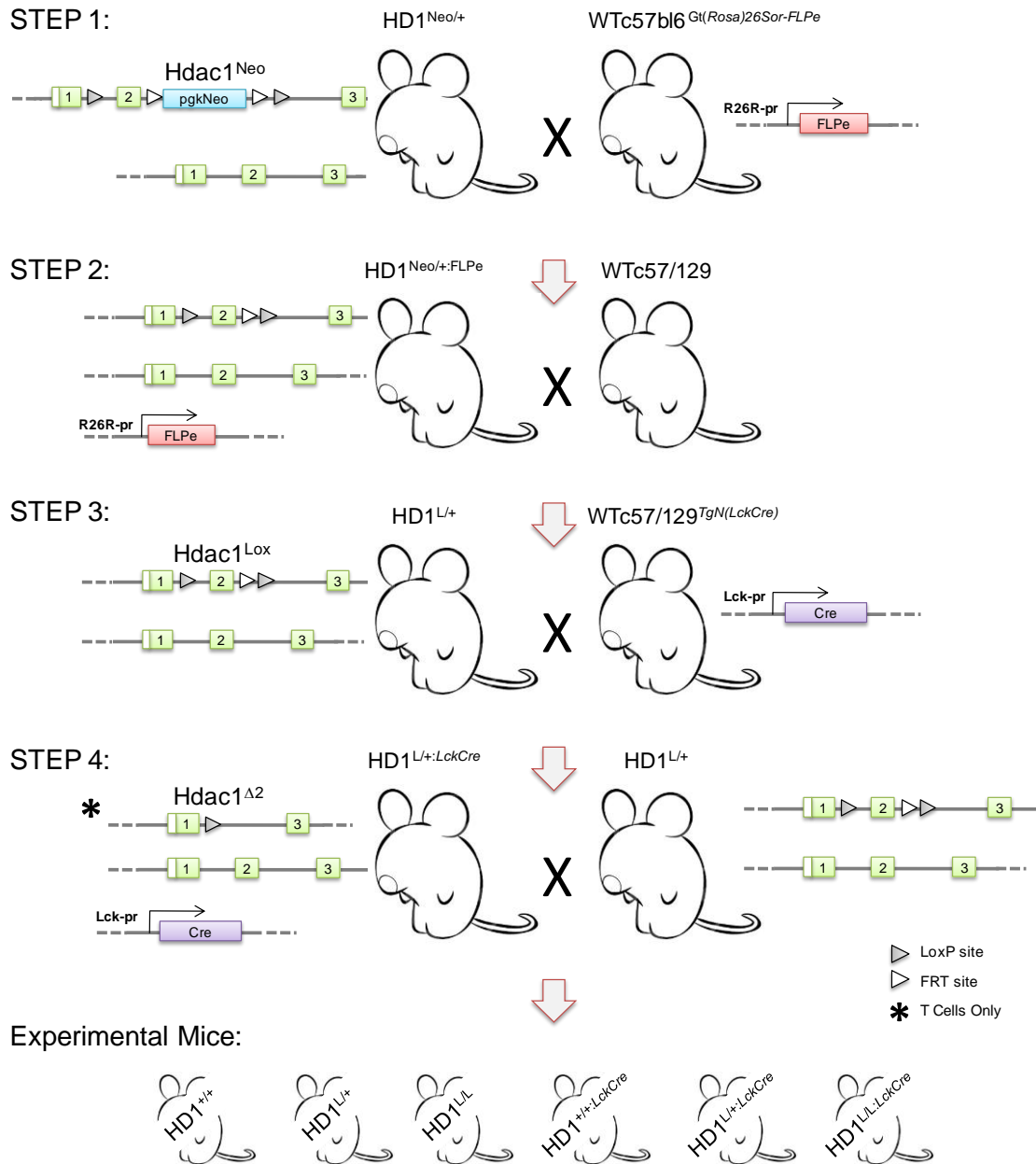


Figure 3.14. *Generation of T cell specific conditional HDAC1 knock-out mice.* Four step breeding strategy to generate T cell specific homozygous conditional knock-out HD1^{L/L;LckCre} mice. **STEP 1.**FLPe mediated removal of selection markers. **STEP 2.**Germline transmission of Hdac1^{Lox} allele and loss of *Gt(Rosa)26Sor-FLPe* allele. **STEP 3.**Generation of HD1^{L/+;LckCre} cohorts, introduction of TgN(*LckCre*). **STEP 4.**Generation of experimental mice including homozygous HD1^{L/L;LckCre} and WT litter mate controls (LMCs).

HD1^{Neo/+;FLPe} or HD2^{Neo/+;FLPe} and used for the next intercross (Fig 3.14, STEP 2).

3.5.3 Germ-line transmission of *Hdac1*^{Lox} and *Hdac2*^{Lox} alleles.

HD1^{Neo/+;FLPe} or HD2^{Neo/+;FLPe} generated by the STEP 1 intercross were bred to WTc57bl6 mice (Fig 3.14.STEP 2) for two reasons; firstly to “breed-out” the *Gt(Rosa)26Sor-FLPe* allele (again to avoid gene interference and genetic ambiguity of targeted mouse cohorts), and secondly to determine germline transmission of the floxed *Hdac1*^{Lox} and *Hdac2*^{Lox} alleles (i.e. post FLPe-mediated deletion of the –pgkNeo selection marker). Again, subsequent pups were PCR genotyped. Transmission of the *Hdac1*^{Lox} allele was determined in pups screened for the presence of the 5’LoxP site as before. Mice positive for the 5’ LoxP site (i.e. transmission of the targeted allele) were then screened using primers flanking the 3’ LoxP site using the primers HDAC1_For2 and HDAC1_Mut (Fig 3.15A). This 3’ LoxP assay distinguishes the *Hdac1*^{Neo} allele from the *Hdac1*^{Lox} allele by the presence of a 680bp band. Likewise transmission of the *Hdac2*^{Lox} allele was determined in pups screened for the presence of the 3’LoxP site as before. Mice positive for the 3’ LoxP site (i.e. transmission of the targeted allele) were then screened using primers flanking the 5’ LoxP site using the primers HDAC2_5’neogen and HDAC2_3’neogen (Fig 3.15B). This 5’ LoxP assay distinguishes the *Hdac1*^{Neo} allele from the *Hdac1*^{Lox} allele by the presence of a 462bp band. Mice positive for “FLPe’d” *Hdac1*^{Lox} or *Hdac2*^{Lox} alleles were also screened for the absence of the knocked-in

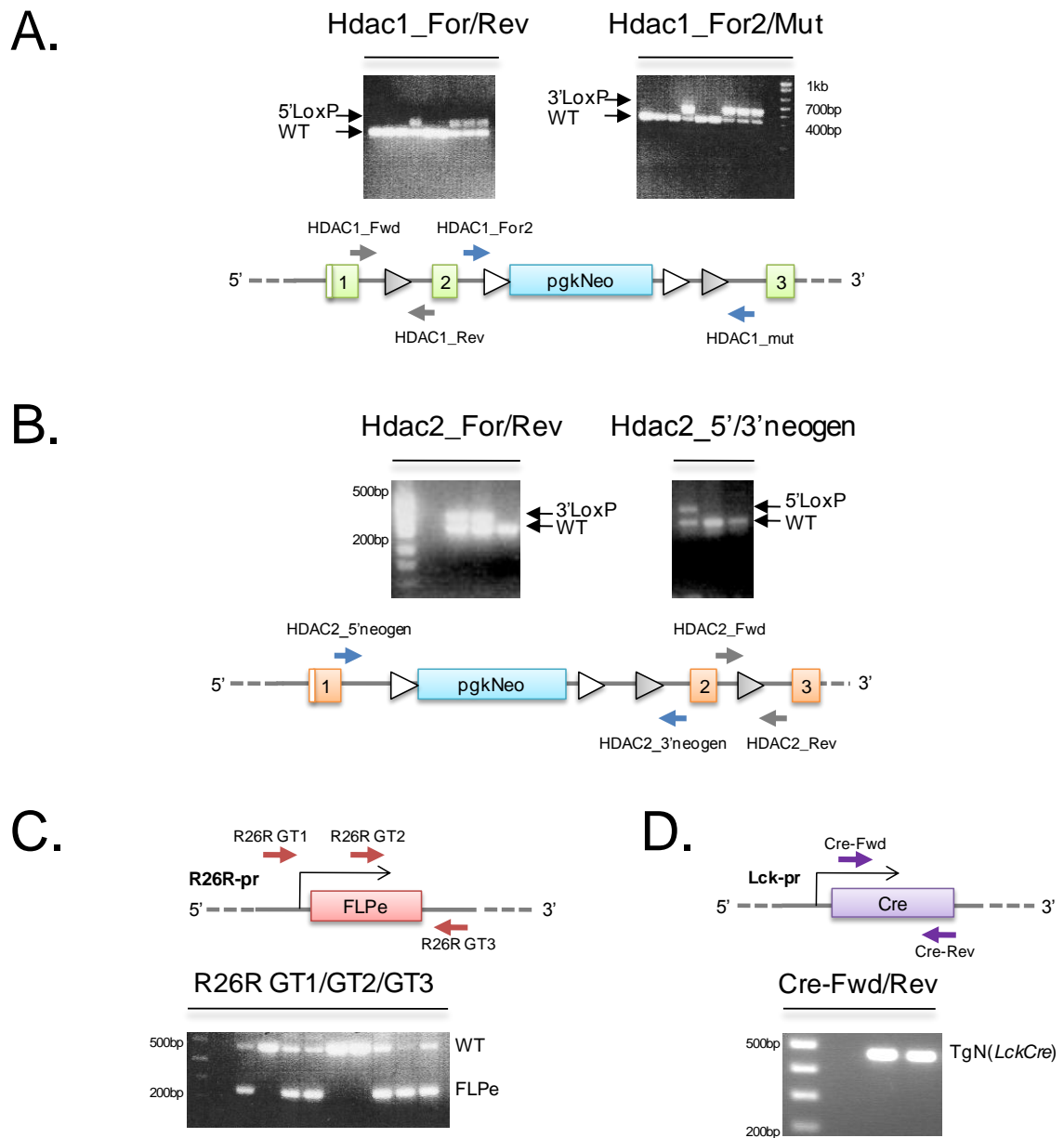


Figure 3.15. *PCR genotyping strategies used for generating of T cell specific conditional HDAC1 and HDAC2 knock-out mice.* (A) The targeted Hdac1 locus, position of PCR primers used for genotyping and representative results of genotyping screens; HDAC1_For/Rev (5'LoxP=462bp, WT=342bp) and HDAC1_For2/Mut (3'LoxP= 680bp, WT=560bp). (B) The targeted Hdac2 locus, position of PCR primers used for genotyping and representative results of genotyping screens; HDAC2_For/Rev (3'LoxP=330bp, WT=259bp) and HDAC2_Fo5'/3'neogen (5'LoxP= 352bp, WT=266bp). (C) The knocked in Gt(*Rosa*)26Sor-FLPe allele and(D) the TgN(*LckCre*) transgene, position of PCR primers used for genotyping and representative results of genotyping screens.

Gt(Rosa)26Sor-FLPe allele (Fig3.15C). This was to rule out the possibility that the detected recombination event was not as a result of somatic expression of FLPe from a transmitted *Gt(Rosa)26Sor-FLPe* allele. Pups positive for the *Hdac1^{Lox}* or *Hdac2^{Lox}* allele, in the absence of the *Gt(Rosa)26Sor-FLPe* allele are denoted as HD1^{L/+} or HD2^{L/+} and used for the next intercross (Fig 3.14, STEP 3).

3.5.4 Generation of heterozygous and homozygous *Hdac1^{Lox}* and *Hdac2^{Lox}* mice carrying the T cell specific *LckCre* transgene.

HD1^{L/+} or HD2^{L/+} mice were bred to WTc57/129^{TgN(*LckCre*)} (Fig 3.14, STEP 3). Subsequent generations were PCR genotyped for the floxed alleles (either *Hdac1^{Lox}* or *Hdac2^{Lox}*, using the same primers as in 3.3.3 for the 3' and 5' LoxP sites respectively) and for the presence of the *LckCre* transgene using primers Cre_Fwd and Cre_Rev (Fig 3.15D). Pups that were positive for the *Hdac1^{Lox}* or *Hdac2^{Lox}* and positive for the *LckCre* transgene were denoted as HD1^{L/+;*LckCre*} or HD2^{L/+;*LckCre*} and used for the next intercross (Fig 3.14, STEP 4). The full panel of experimental mouse genotypes for single conditional HDAC1 or HDAC2 knock-out cohorts include; WT, heterozygous floxed and homozygous floxed, all with or without the *LckCre* transgene (Fig 3.14, Experimental Mice). Examples of systematic genotyping results are shown in figure 3.16A.

3.5.5 Conditional deletion of HDAC1 or HDAC2 in HD1^{L/L:LckCre} and HD2^{L/L:LckCre} mice.

Induction of Cre expression in T cells early in their development, via the *LckCre* transgene, should result in conditional LoxP recombination and deletion of exon 2. T cell specific deletion of exon 2 was assessed in thymocytes and splenocytes of WT^{LckCre}, HD1^{L/L:LckCre} and HD2^{L/L:LckCre} mice by Southern blot, using the same strategy as described in 3.1.6, as follows. To detect successful, Cre recombinase inducible excision of exon 2 in homozygous, HD1^{L/L:LckCre} mice, the 3' internal probe (3'pr Fig 3.2) hybridised to *Hind* III digested gDNA detected either a 14kb WT fragment (Hdac1^{WT}), a 5.4kb targeted fragment (Hdac1^{Lox}) or the 3kb LoxP recombined fragment (Hdac1^{Δ2}) (Fig3.16B). To detect successful, Cre recombinase inducible excision of exon 2 in homozygous, HD2^{L/L:LckCre} mice, the 5' internal probe (5'pr Fig3.4) hybridised to *Bgl* I digested gDNA detected either a 17kb WT fragment (Hdac2^{WT}), a 9kb targeted fragment (Hdac2^{Lox}) or the 8kb LoxP recombined fragment (Hdac2^{Δ2}) (Fig3.16B). Greater than 95% recombination (deletion of exon 2) is detected in thymocytes from both HD1^{L/L:LckCre} and HD2^{L/L:LckCre} mice with no apparent deletion of exon 2 detectable in WT^{LckCre} litter mate controls (LMCs), revealing that deletion of exon 2 is dependent upon the presence of the Hdac1^{Lox} and Hdac2^{Lox} alleles. A lesser degree of recombination, and thus deletion of exon 2, is detected in total splenocytes of both HD1^{L/L:LckCre} and HD2^{L/L:LckCre} mice, consistent with the fact that although the spleen consists mainly of B cells, macrophages, dendritic cells, natural killer cells and red blood cells, approximately 25-35% of the cellular compartment are T cells (Thomas, J.*et al.*, 2006 and Alberts, B.*et al.*, 2002), thus indicating the T cell specificity of the

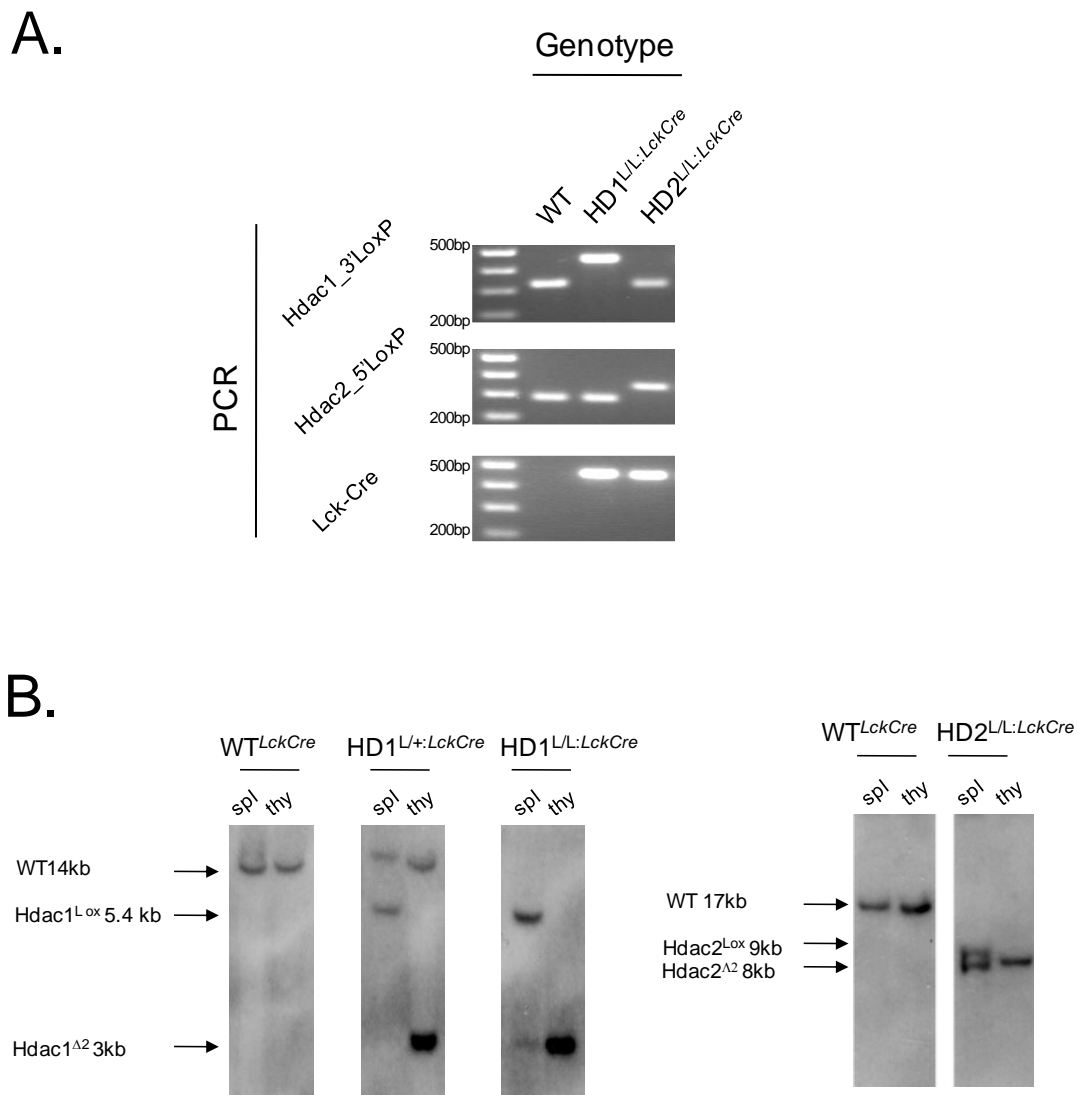


Figure 3.16. *LckCre* induced site specific recombination of *Hdac1^{Lox}* and *Hdac2^{Lox}* alleles. (A) Examples of systematic PCR genotyping of ear gDNA from WT, HD1^{L/L:LckCre} and HD2^{L/L:LckCre} mice. (B) Southern blots performed on gDNA extracted from splenocytes (**spl**) and thymocytes (**thy**) of HD1^{L/+LckCre}, HD1^{L/L:LckCre}, HD2^{L/L:LckCre} and WT LMCs. Presence of the TgN(*LckCre*) transgene induces deletion of exon2 in HD1^{L/L} and HD2^{L/L} thymocytes where >95% recombination is observed, but not in untargeted WT^{LckCre} thymocytes. Targeted splenocytes exhibit a lesser degree of recombination consistent with the proportion of T cells within splenocytes and exemplifies the restricted expression of the *LckCre* transgene.

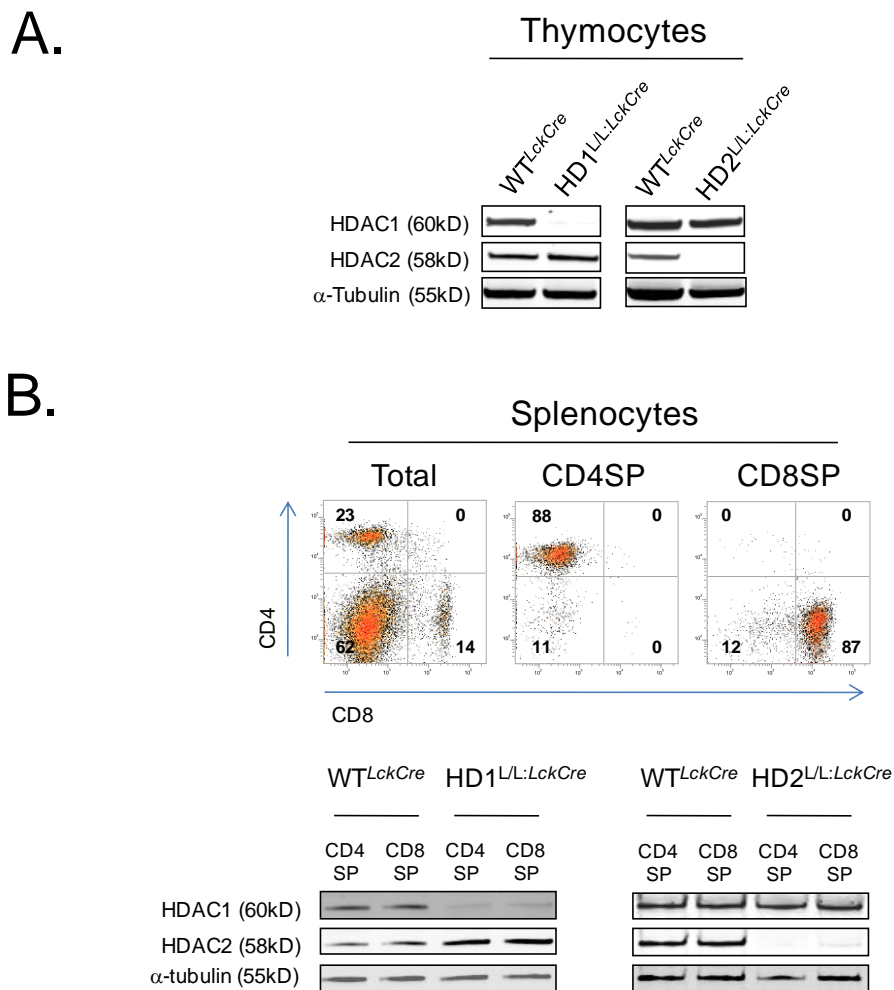


Figure 3.17. *Generation of HDAC1 and HDAC2 T cell specific conditional knock-out mice.* (A) Quantitative western blot shows that presence of the TgN(*LckCre*) transgene induces complete deletion of HDAC1 or HDAC2 protein in whole cell extracts of $HD1^{L/L;LckCre}$ and $HD2^{L/L;LckCre}$ total thymocyte preparations respectively. (B) Mature CD4 and CD8SP T cells were positively isolated using magnetic beads coated with monoclonal antibodies against the T cell specific cell surface markers CD4 and CD8 from $HD1^{L/L;LckCre}$, $HD2^{L/L;LckCre}$ and WT LMC splenocytes, typically with >85% purity (as assessed by FACS). Whole cell extracts were analysed by quantitative western blot revealing >90% deletion of HDAC1 or HDAC2 in mature circulating T cells. Mice were between 6-8 weeks old. α -Tubulin was used to normalize protein loading. Blots were visualized and quantified using a LiCOR scanner.

LckCre transgene. As previously discussed, loss of exon 2 disrupts the ORF of both HDAC1 and HDAC2 such that a premature stop codon is introduced in exons 3 and 5 respectively. Deletion of HDAC1 and HDAC2 protein was shown to be complete in whole cell protein extracts of total thymocyte populations extracted from HD1^{L/L:LckCre} and HD2^{L/L:LckCre} mice (Fig 3.17A) with almost complete deletion (<10% of LMC protein levels) in mature T cells positively isolated from splenocyte populations of the same animals (Fig 3.17B).

3.5.6 Generation of compound heterozygous HD1^{L/L}HD2^{L/+LckCre}, HD1^{L/+}HD2^{L/L:LckCre} and double homozygous HD1^{L/L} HD2^{L/L:LckCre} T cell specific knock-out mice.

Given the reported degree of redundancy between the activities of HDAC1 and 2, double conditional knock-out mice were generated by inter-crosses between the two separate HD1^{L/L:LckCre} and HD2^{L/L:LckCre} mouse cohorts. Following confirmation of the success of the conditional targeting strategy, HD1^{L/L-LckCre} and HD2^{L/L:LckCre} mice were inter-crossed to generate compound heterozygous HD1^{L/+}:HD2^{L/+LckCre} pups. Subsequently, these compound heterozygous mice were bred to litter mates to generate a cohort of mice with genotypes consisting of; single homozygous HD1^{L/L:LckCre} or HD2^{L/L:LckCre} mice, compound heterozygous HD1^{L/+}:HD2^{L/+LckCre}, homozygous-heterozygous mice that have a single copy of the *Hdac2*^{WT} or *Hdac1*^{WT} allele (HD1^{L/L}HD2^{L/+LckCre} or HD1^{L/L} HD2^{L/L:LckCre}), double homozygous HD1^{L/L} HD2^{L/L:LckCre} mice and WT LMCs (WT^{LckCre}) (Fig 3.18). These mice were PCR genotyped systematically 14

days after birth and would form the experimental cohort to be analysed in Chapter 5.

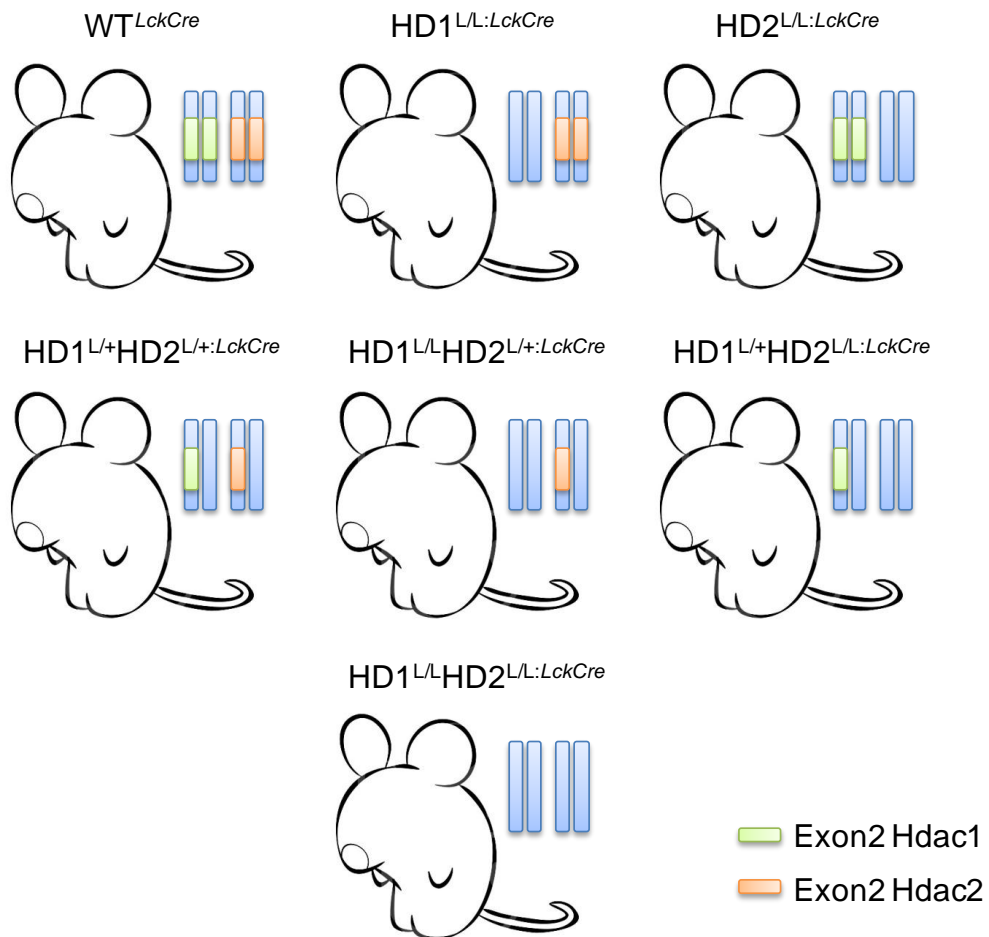


Figure 3.18. *HDAC1 and HDAC2 T cell specific experimental cohorts*. Potential genotypes resulting from inter-crosses between HD1^{L/+}:HD2^{L/+} and HD1^{L/+}:HD2^{L/+}:*Lck* mice. Depicted genotypes all harbour the TgN(*LckCre*) transgene, note however the same genotypic outcomes that do not carry *LckCre* are possible thus doubling the number of potential genotypes from 7 to 14.

3.6 Conclusions.

3.6.1 Successful generation of homozygous conditional knock-out HDAC1 and HDAC2 mES cell lines.

Sections 3.2.1– 3.2.6 outlines the successful gene targeting of both alleles of Hdac1 and Hdac2 of separate CreER-T mES cell lines based on evidence provided by Southern blot (Figs 3.4 and 3.7). Transfection of these targeted clones with FLPe successfully mediated the excision of selectable markers used in the gene targeting strategy in a number of individual colonies, but not all (Fig 3.8), presumably due to either inefficient pCAGGS-FLpe plasmid transfection or sub optimal FIAU selection conditions. Individual Hdac1^{Lox/Lox} and Hdac2^{Lox/Lox} colonies, with selection cassettes excised, were tested for ligand-dependent mediated recombination of the floxed exon 2 by the induction of Cre activity via the addition of 4-OHT. Southern blot analysis indicates >95% recombination of the floxed alleles occurs in targeted cells but none in non-targeted CreER WT mES control cells upon the addition of 4-OHT. Furthermore prior to the addition of 4-OHT and the activation of Cre in targeted Hdac1^{Lox/Lox} and Hdac2^{Lox/Lox} cells (i.e. Day 0) no recombination is detected (Figs. 3.9A and 3.10A), confirming that recombination (deletion) of exon 2 is dependent on the presence of the targeted (floxed) allele and the ligand dependent induction of Cre activity. Western blot analysis for HDAC1 and 2 proteins indicates that the overall targeting strategy used (i.e. deletion of exon 2) does indeed result in the deletion of HDAC1 or HDAC2 in the appropriately targeted cells lines. Complete loss of HDAC1 or HDAC2 protein in targeted mES cells does not occur until 4-5 days post recombination, suggestive of a combination of a long-lived mRNA and recruitment of these proteins into stable protein complexes

resulting in relatively slow protein turnover. Notably, deletion of exon 2 does not result in visibly detectable truncated forms of the proteins which could potentially confound future analysis (Fig 3.11), again suggesting that the overall targeting strategy was a success.

In summary, I can report the successful generation of novel ligand inducible conditional knock-out HDAC1 and HDAC2 E14 CreER-T mES cell lines. In the subsequent experiments described in Chapter 4, due to the use of multiple rounds of drug selection required for the targeting process, untreated HDAC1^{Lox/Lox} or HDAC2^{Lox/Lox} mES cells (that essentially went through the same selection process) will be used in conjunction with CreER WT mES cells as controls.

3.6.2 Generation of HDAC1^{Lox/Lox} rescue mES cell lines.

On the somewhat presumptive view that deletion of HDAC1 or 2 in mES cells would result in a detectable phenotype, I attempted to make transfectable reagents that could potentially rescue an HDAC1 dependent phenotype, at the same time as generate the ligand dependent conditional knock-out HDAC1 and -2 mES cell systems. On the whole this endeavour was met with mixed results. Generation of the Hdac1-C-FLAG-Resc construct was a success (Fig 3.12A) and both transient and stable expression of a FLAG-tagged HDAC1 protein detectable at the predicted size, in HDAC1^{Lox/Lox} and HDAC1^{Δ2/Δ2} mES cells (Fig 3.13). Notably however, expression of the FLAG-tagged protein in stably transfected cell lines was much lower than that of endogenous HDAC1 (even when selecting clones that exhibit the highest expression of the tagged versions of HDAC1), raising concerns as to how successful these cell lines may be in

“rescuing” any potential HDAC1 dependent phenotype. One reason for the poor expression of the construct could be the use of the CMV promoter in mES cells. A number of groups have reported conflicting evidence on the suitability of the CMV promoter for heterologous transgene expression in mES cells (Ward, C. M. and Stern, P. L., 2002, Chung, S., *et al.*, 2002 and Kawabata, K., *et al.*, 2005). However, expression of tagged HDAC1 (notwithstanding potential differences in the affinity and detection differences between the M2 and C-terminal HDAC1 antibody) is appreciably higher in transient versus stably transfected cell lines (compare Fig 3.13A and C). This could be suggestive of progressive shut down or silencing of the stably integrated Hdac1-C-FLAG-Resc construct (possibly due to its integration into heterochromatin) and not necessarily due to the intrinsic activity of the CMV promoter itself (Mutskov, V. and Felsenfeld, G., 2004 and Pikaart, M. J., *et al.*, 1998) but more likely due to plasmid copy number differences in transient versus stably transfected mES cells. Given that detection of the FLAG epitope in stably transfected HDAC1^{Lox/Lox} mES cell lines is relatively more comparable with endogenous HDAC1 expression than in stably transfected HDAC1^{Δ2/Δ2} mES cells (Compare detectable M2 signals from clone 23:B4 Fig 3.13B and that detected in Fig 3.13C.), another potential reason for the reduced expression could be that, either directly or indirectly, endogenous expression of HDAC1 is required for optimal CMV promoter activity. Essentially, only future experiments will determine if HDAC1^{Δ2/Δ2:Hdac1-C-FLAG-Resc} mES cells are a useful reagent, dependent, of course, on a detectable HDAC1 mES cell dependent phenotype.

3.6.3 Successful Generation of T cell specific conditional knock-out HDAC1 and HDAC2 mouse lines.

Sections 3.4.1– 3.4.4 outline the consecutive rounds of breeding in order to attain two individual TgN(*LckCre*) mouse lines, where the endogenous alleles of either Hdac1 or -2 have been replaced with gene targeted alleles in which exon 2 is “floxed”. PCR genotype screening (Fig 3.15) distinguished targeted from endogenous alleles by virtue of the addition of LoxP sites as a consequence of successful gene targeting. Germ line transmission of Hdac1^{Lox} and Hdac2^{Lox} alleles in which FLPe mediated excision of selectable markers had occurred (via inter-crossing Hdac1 and -2^{Neo} mice with WTc57bl6^{Gt(Rosa)26Sor-FLPe} mice) was also confirmed by PCR genotyping screens, as was the presence of the TgN(*LckCre*) transgene (Fig 3.15). TgN(*LckCre*) mediated recombination of the “floxed” alleles was assessed in thymocytes from WT^{LckCre}, HD1^{L/L:LckCre} and HD2^{L/L:LckCre} mice by Southern blot and revealed recombination of the “floxed” alleles (deletion of exon 2) was >95% (Fig 3.16B). Subsequent assessment of HDAC1 and -2 protein levels in total thymocytes confirms that deletion of exon 2 in HD1^{L/L:LckCre} and HD2^{L/L:LckCre} mice results in complete deletion of the targeted protein, suggesting that the overall targeting strategy was a success. As with mES cells, deletion of exon 2 does not result in visibly detectable truncated forms of either targeted protein in thymocytes, removing a potential variable which could confound future analysis (Fig 3.17A). The degree of recombination of the “floxed” allele in total splenocytes was a fraction of that seen in thymocytes (Fig 3.17B), reflecting the reduced number of T cells present in this compartment and thus the relative number of targeted cells predicted to undergo TgN(*LckCre*) mediated recombination and deletion of

exon 2. However, western blotting for HDAC1 and -2 in CD4⁺ and CD8⁺ single positive T cells, isolated from total splenocytes, reveals >90% reduction in protein when compared to LMCs (Fig 3.17B). Taken together, these results indicate that deletion of exon 2 and the subsequent deletion of either HDAC1 or -2 is dependent on the T cell specific expression of Cre, driven by the *LckCre* transgene.

In summary, I can report the successful generation of novel T cell specific conditional knock-out HDAC1 and HDAC2 mES mouse lines, namely HD1^{L/L:LckCre} and HD2^{L/L:LckCre} mice. Analysis of these mice is detailed in Chapter 5.

Chapter Four: HDAC1, but not HDAC2, Controls Embryonic Stem Cell Differentiation.

4.1 Chapter aims.

Having generated individual conditional knock-out HDAC1 and HDAC2 mES cell lines (Chapter 3.2) I aimed to characterise the roles of HDAC1 and HDAC2 in a number of cellular processes. As previously discussed, use of this inducible system in mES cells (the in vitro counterpart of epiblast cells of the early post implantation embryo), may provide new insights as to the requirements of HDAC1 and HDAC2 during embryogenesis. Initial assessment of the basic characteristics of mES cells lacking either HDAC1 or -2, will be coupled with a more intricate analysis of mES cell differentiation potential. Allied to this, analysis of the biochemical properties of knock-out cell lines, as relates to their enzymatic function, will also be performed, which may shed some new light on the mainly redundant nature of these enzymes.

4.2 HDAC1/2 complexes have reduced HDAC activity in the absence of HDAC1.

Consistent with previous reports (Lagger G., *et al.*, 2002, Zupkovitz G., *et al.*, 2006), deletion of HDAC1 results in an increased level of HDAC2 protein (Fig 4.1A). However, no increase in *hdac2* mRNA is detected (Fig 4.1C), suggesting that increased protein levels may occur from changes in HDAC2 translation and/or degradation in the absence of HDAC1. Interestingly, there is no change in HDAC1 protein levels in the absence of HDAC2 (Fig 4.1B). Most, if not all cellular HDAC1 and 2 is associated with higher order protein

complexes in the nucleus (Yang X.J. and Seto E. 2008). Co-immunoprecipitation of individual components of the Sin3A, NuRD and CoREST complexes was used to assess the associated HDAC activity and complex integrity in cells lacking either HDAC1 or HDAC2. In the absence of HDAC1 we observe a decrease in the deacetylase activity associated with each of the Sin3A, NuRD and CoREST complexes, with the largest reduction in the CoREST complex (Fig 4.2A, left panel). This decrease in activity occurs despite the fact that we detect increased amounts of HDAC2 in each of these same complexes (Fig 4.2B, compare levels of HDAC2 in lanes 3, 4, 5 with 10, 11 and 12). The increased incorporation of HDAC2 into HDAC1/2 complexes in the absence of HDAC1 may account for the increased abundance of HDAC2 protein (Fig 4.1A). In contrast, there is no significant alteration in the amount of deacetylase activity associated with the three HDAC1/2 complexes in the absence of HDAC2 (Fig 4.2A, right panel). These data argue that loss of HDAC1, but not HDAC2, causes a reduction in the HDAC activity of HDAC1/2 containing complexes. However, in the absence of either enzyme, deacetylase activity is still measurable and a physical association still remains, suggesting that the integrity of each complex is retained.

Next, the global acetylation levels of histones H3 and H4 in the absence of either HDAC1 or HDAC2 were examined (Fig 4.3). We detected a slight increase in the acetylation status of H3K9/14, H4K5 and H4K8 in the absence of HDAC1. However, the only significant difference in HDAC1^{Δ2/Δ2} cells was a 1.6 fold increase in the level of H3K56 acetylation (H3K56Ac) (Fig 4.3, left panel), a modification associated with DNA damage (Das C., *et al.*, 2009,

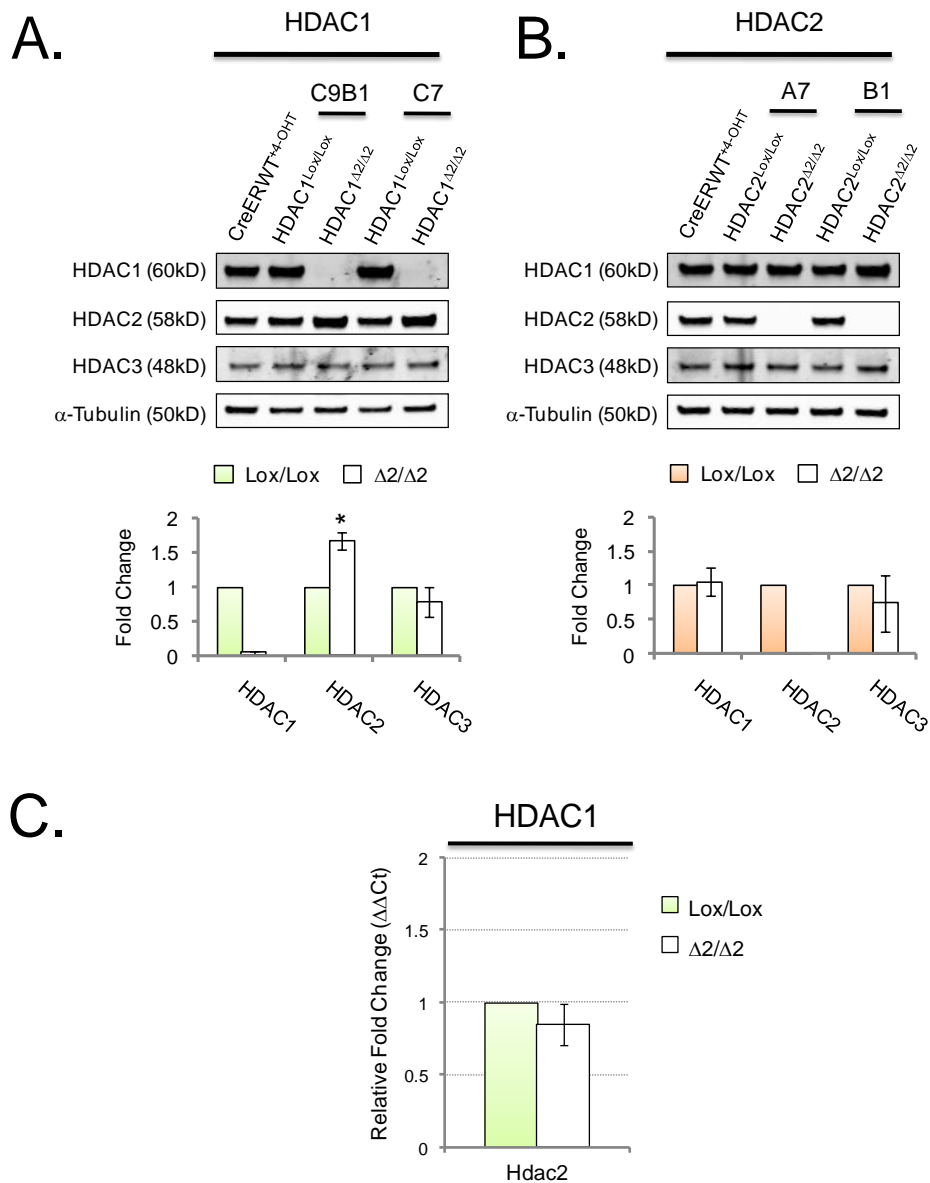


Figure 4.1. *Deletion of HDAC1 results in an increased level of HDAC2 protein.* (A) Quantitative Western blot of HDAC1, 2, and 3 obtained from nuclear extracts of the indicated cell types. Representative blots from 2 individual mES cell lines for each genotype are shown. Protein levels were quantified using a LiCOR scanner and normalized to the level of α -tubulin. Data represent 3 independent experiments. Mean values \pm S.E.M. are plotted ($n = 3$). (* $P < 0.05$, paired T-Test). (C) Relative fold change in *Hdac2* mRNA upon deletion of HDAC1, as detected by quantitative RT-PCR analysis. Levels of *Hdac2* mRNA was measured in a multiplex PCR assay and normalised to levels of *Gapdh* mRNA, using Universal ProbeLibrary hydrolysis probes. Normalised expression of *Hdac2* mRNA is expressed as a fold change in HDAC1^{Δ2/Δ2} (sample) relative to HDAC1^{Lox/Lox} (reference) cells. Mean values \pm S.E.M. are plotted ($n = 4$).

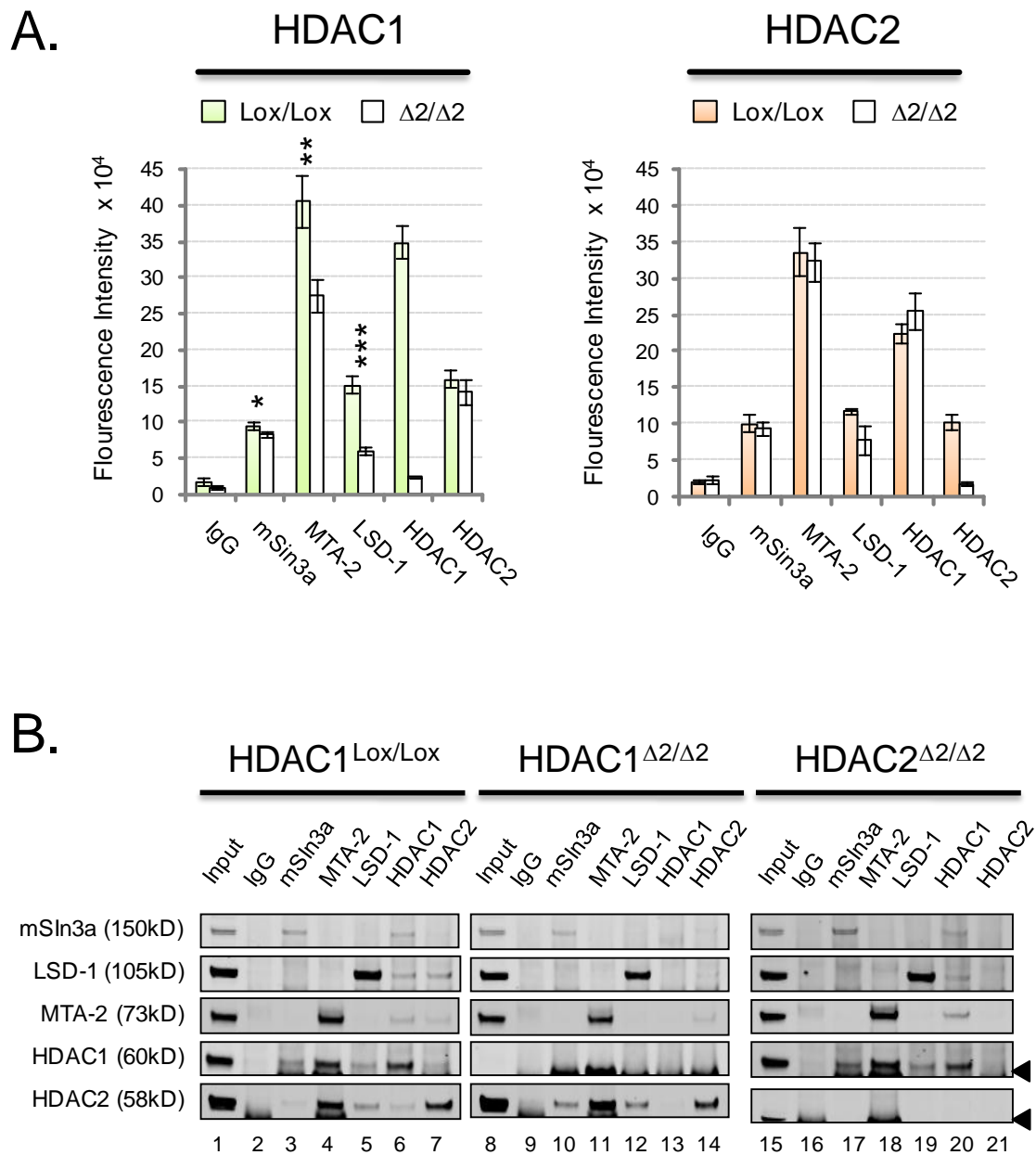


Figure 4.2. Loss of HDAC1 results in decreased deacetylase activity associated with HDAC1/2 complexes. (A) Specific antisera to the indicated proteins were used to coimmunoprecipitate Sin3A, NuRD (α -MTA-2), and CoREST (α -LSD1) complexes from the indicated mES cell lines. The amount of associated deacetylase activity was measured using a commercially available kit. Mean values \pm S.E.M. are plotted ($n = 3$) (* $P < 0.05$, ** $P < 0.01$, *** $P < 0.001$, paired T-Test). (B) The remaining material from the co-immunoprecipitation was run on an SDS-PAGE gel and then analyzed by Western blotting using the indicated antibodies. Black arrows indicate a nonspecific band.

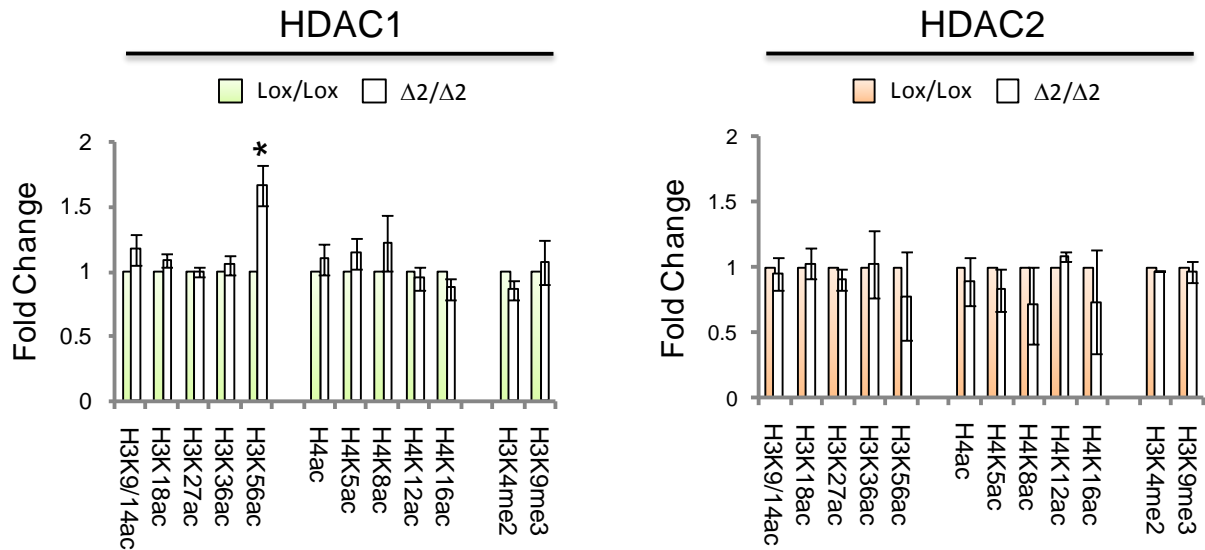


Figure 4.3. *Loss of HDAC1 results in an increase H3K56ac.* The acetylation status of core histones was detected using quantitative Western blotting. Histones were acid extracted from HDAC1^{Lox/Lox}, HDAC1 ^{$\Delta 2/\Delta 2$} , HDAC2^{Lox/Lox}, and HDAC2 ^{$\Delta 2/\Delta 2$} cell lines. The signal of specific acetylated lysines was normalized to the total amount of H3 or H4 as appropriate and quantified using a LiCOR scanner. Mean values \pm S.E.M. are plotted (n = 3) (*P < 0.01, paired T-Test). Data represent independent experiments using three different clones.

Tjeertes J.V., *et al.*, 2009 and Miller K.M., *et al.*, 2010), nucleosome assembly (Das C., *et al.*, 2009) and the activity of stem cell factors Xie W., *et al.*, 2009) in higher eukaryotes. This is the first demonstration that H3K56Ac may be a substrate for HDAC1. Global histone acetylation levels were (unchanged by loss of HDAC2 (Fig 4.3, right panel), consistent with an unchanged level of deacetylase activity associated with HDAC1/2 complexes in cells lacking HDAC2 protein. Treatment of HDAC1^{Lox/Lox} ES cells with the class I and II HDAC inhibitor trichostatin A (TSA) for 12 hours produces a 7 fold increase in H3K56ac levels, compared to the 1.6 fold change associated with loss of HDAC1, suggesting that additional class I and class II HDACs participate in its regulation (Fig 4.4A compare lanes 7 and 8). In contrast to H3K56ac which

occurs in the histone core, the acetylation status of lysines within the tails of histones H3 and H4 (H3K9/K14 and H4K5/K8/K12/K16) were changed by less than 1.5 fold in response to TSA. Similar increases in acetylation of the same lysine residues were detected upon treatment of WT mES cells with TSA (Fig 4.4B). Notably however, TSA treatment of mouse embryonic fibroblasts (MEFs) produces a robust 5 fold increase in lysine tail acetylation (H3K9/K14ac, Fig 4.4C), suggesting that histone tails are hyperacetylated in ES cells and thus potentially masks a detectable increase in histone acetylation in HDAC1^{Δ2/Δ2} cells. It has been shown previously that H3K56ac is a substrate for the NAD⁺-dependent deacetylases SIRT1 and SIRT2 (Das C., *et al.*, 2009). It is possible that deletion of HDAC1 negatively affects the levels of these enzymes, mediating the observed increase in H3K56ac associated with HDAC1 deletion indirectly. In the absence of antibodies raised against SIRT 1 and 2 I performed Q-RT PCR for *sirt1* and *sirt2* mRNA in 4 HDAC1 mES cells lines upon ligand induced deletion of HDAC1 and reveal, at least transcriptionally, that deletion of HDAC1 does not affect the levels of either *sirt1* or -2 (Fig 4.4D).

4.3 Proliferation and differentiation capacity of mES cells is not inhibited by loss of HDAC1 or HDAC2.

HDAC1 has been implicated in cell cycle progression (Lagger G., *et al.*, 2002, Glaser K.B., *et al.*, 2003 and Senese S., *et al.*, 2007), I therefore compared the growth ability of HDAC1^{Δ2/Δ2} and HDAC2^{Δ2/Δ2} cells to the appropriate control cells. Deleting HDAC1 or HDAC2 had no effect on colony

formation when plating mES cells at low density (Fig 4.5A), or on their population doubling time

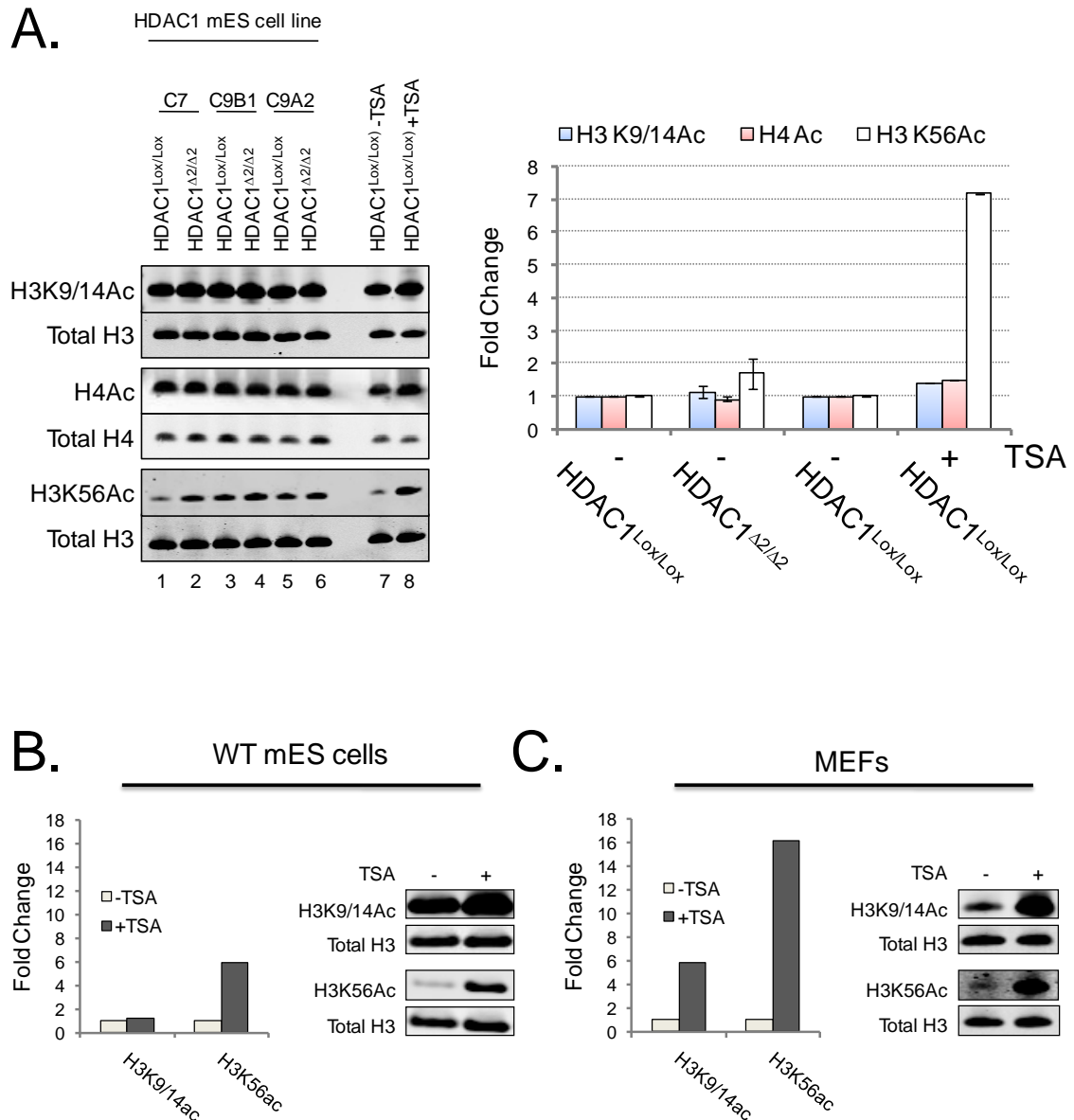


Figure 4.4. *H3K56Ac* is regulated by *HDAC1* in addition to other zinc-dependent *HDAC* enzymes. The acetylation status of core histones was detected using quantitative Western blotting. (A) Histones were acid extracted from three independent, treatment-matched *HDAC1*^{Lox/Lox} or *HDAC1*^{Δ2/Δ2} clones. Trichostatin A (TSA, 150nM) was added, as indicated, for 12h before histone extraction. The signal of specific acetylated lysines was normalized to the total amount of H3 or H4 as appropriate using a LiCOR scanner and plotted in the histogram in the right panel. Note, the antibody used to detect acetylated H4 recognises acetylated lysine

residues H4K5, K8, K12 and K16. (B and C) The acetylation status of histones extracted from wild-type mES cells and MEFs was compared with and without TSA treatment as in (A).

D.

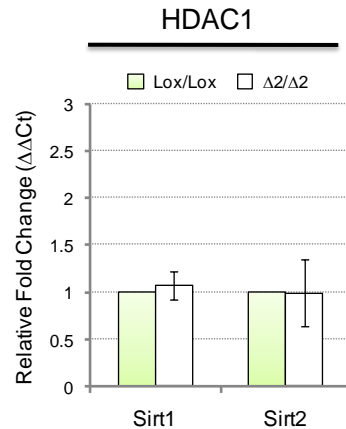


Figure 4.4. *H3K56Ac* is regulated by *HDAC1* in addition to other zinc-dependent *HDAC* enzymes. (D) The relative levels of *sirt1* and *sirt2* mRNA was measured in a multiplex PCR assay normalised to levels of *Gapdh* mRNA, using Universal ProbeLibrary hydrolysis probes. Normalised expression of *sirt1* and *-2* mRNA is expressed as a fold change in $HDAC1^{\Delta2/\Delta2}$ (sample) relative to $HDAC1^{Lox/Lox}$ (reference) cells. Mean values \pm S.E.M. are plotted ($n = 4$).

(Fig 4.5B). Loss of MBD3, a central component of the NuRD complex (Kaji K., *et al.*, 2006), or treatment with HDAC inhibitors (Lee J.H., *et al.*, 2004) has been demonstrated to inhibit ES cell differentiation. I therefore assessed the capacity of $HDAC1^{\Delta2/\Delta2}$ and $HDAC2^{\Delta2/\Delta2}$ cells to differentiate when grown in the absence of LIF compared to controls (Fig 4.6). The indicated mES cells were grown in the presence and absence of LIF for 6 days and then assayed for alkaline phosphatase activity, a stem cell marker. CreER WT cells treated with 4-OHT, untreated homozygous targeted cells ($HDAC1^{Lox/Lox}$ and $HDAC2^{Lox/Lox}$), and homozygous deleted cells ($HDAC1^{\Delta2/\Delta2}$ and $HDAC2^{\Delta2/\Delta2}$), all showed comparable levels of differentiation (i.e. similar reduction in the percentage of undifferentiated colonies). These data demonstrate that the growth

characteristics of ES cells lacking either HDAC1 or HDAC2 are similar to wild-type cells.

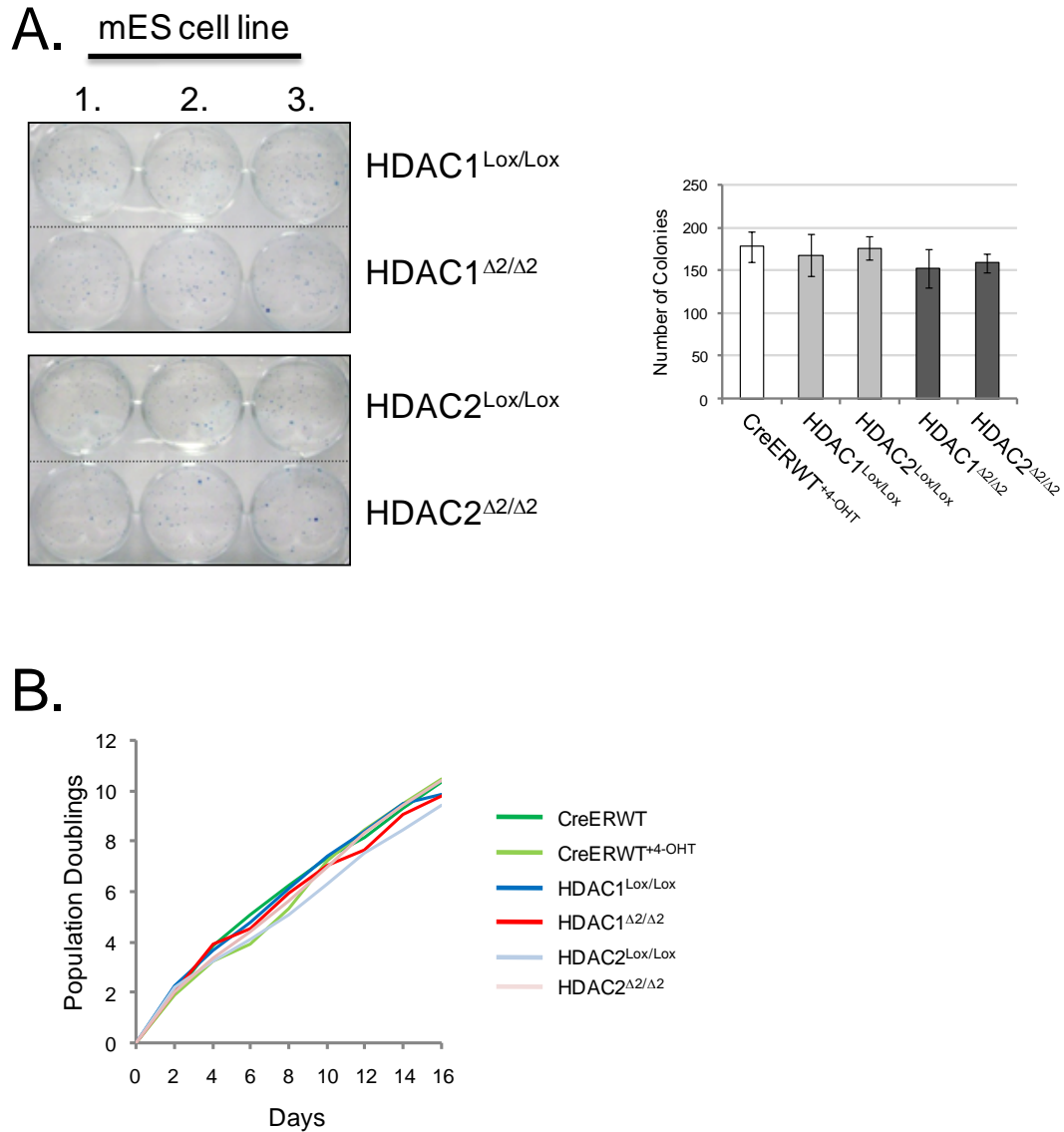


Figure 4.5. *Conditional deletion of HDAC1 or 2 does not inhibit the growth of mES cells.* (A) Colony formation assay: mean values and SDs of cells of the indicated genotype plated at low density, cultured for 8 days and stained with methylene blue making colonies readily observable (left panel) before counting. Mean values \pm S.E.M. are plotted (right panel) ($n = 3$). (B) The population doubling times of the indicated cell types were calculated by counting and then replating cells every 2 days for an 18-day period. Data represent three independent experiments using two individual clones of each genotype.

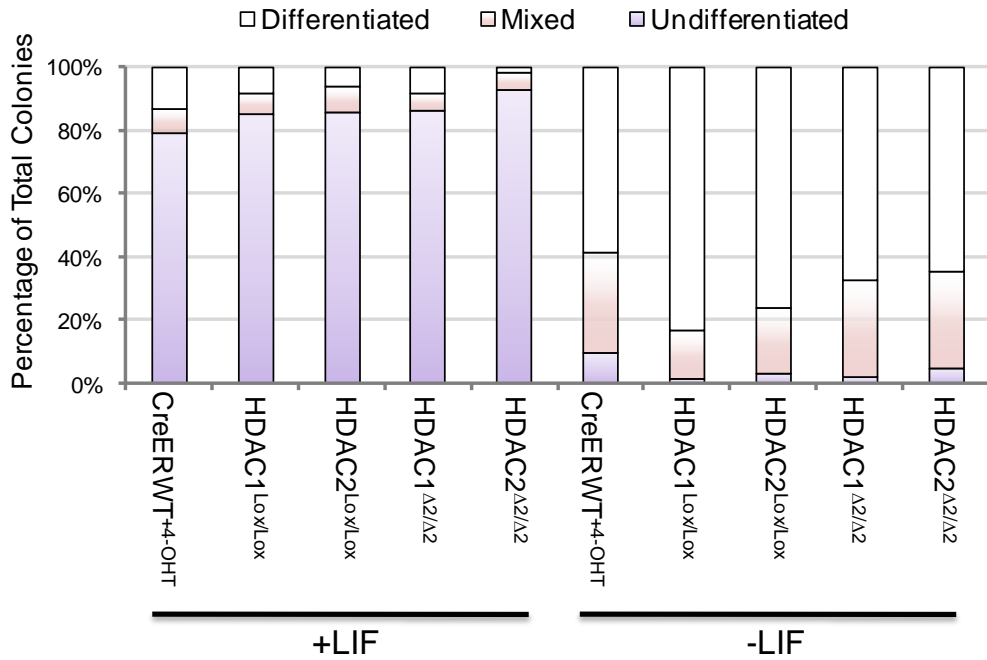
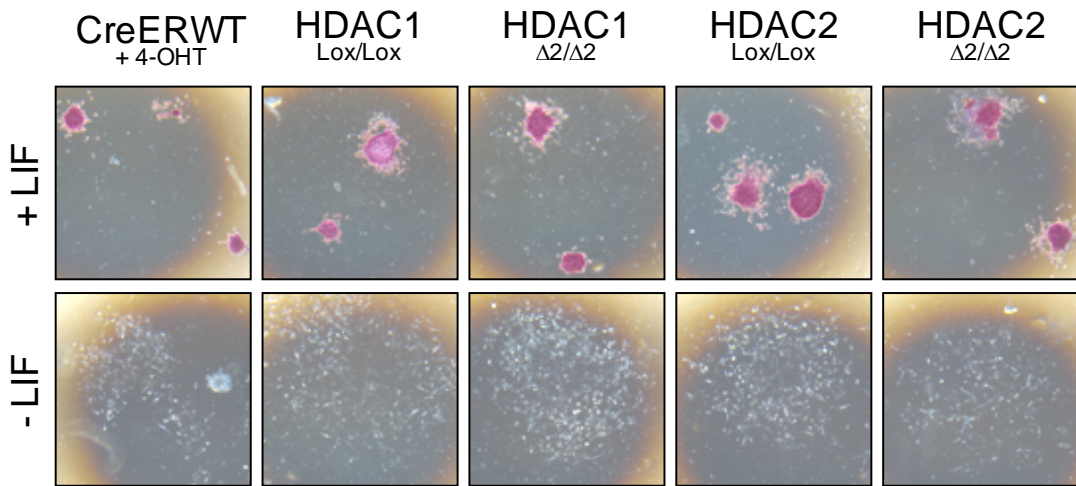


Figure 4.6. *Conditional deletion of HDAC1 or 2 does not inhibit the differentiation potential of mES cells.* Cells of the genotype indicated were plated at low density in the presence (+) or absence (-) of LIF and cultured for 6 days before staining for the presence of alkaline phosphatase. Colonies were scored as undifferentiated (purple), differentiated (white), or mixed. Representative bright-field images are shown in the top panel. Data in histogram (bottom panel) represents three independent experiments using two individual clones of each genotype.

4.4 Loss of HDAC1, but not HDAC2, causes enhanced differentiation of embryoid bodies.

To examine the differentiation capacity of HDAC knock-out cells in greater detail HDAC1^{Δ2/Δ2} and HDAC2^{Δ2/Δ2} mES cells were used to generate embryoid bodies (EB) which recapitulate many of the changes associated with gastrulation, including generation of the three primary germ layers, ectoderm, endoderm and mesoderm (Keller G.M., *et al.*, 1996, Desbaillets I., *et al.*, 2000 and Boheler K.R., *et al.*, 2002). As previously described, it is presumably during gastrulation, or just prior, that HDAC1 null embryos begin to accrue developmental defects that are apparent phenotypically at e7.5 days and beyond (Lagger G., *et al.*, 2002 and Montgomery R.L., *et al.*, 2007). mES cells lacking either HDAC1 or HDAC2 were able to form EBs over a two day period using the hanging drop method (Desbaillets I., *et al.*, 2000) (Fig 4.7.A, day2). Continued culture revealed that EBs lacking HDAC1 become irregular, rather than uniformly spherical, and are much reduced in size compared to EBs derived from control cells (Fig 4.7.A, day 12 and 4.7.B). By contrast, EBs lacking HDAC2 (HDAC2^{Δ2/Δ2}) were uniformly spherical and grew to a similar size as wild-type and HDAC2^{Lox/Lox} controls. HDAC1 and HDAC2 have been linked to cell cycle regulation by their association with the tumour suppressor, Rb (Brehm A., *et al.*, 1998, Luo R.X., *et al.*, 1998 and Magnaghi-Jaulin L., *et al.*, 1998) and transcriptional repression of the CDK inhibitor, *p21* (Lagger G., *et al.*, 2002, Zupkovitz G., *et al.*, 2006 and Senese S., *et al.*, 2007). Having established that HDAC1^{Δ2/Δ2} EBs appeared to have a reduction in growth potential, RNA was collected at time points from day 0 (cycling mES cells), up to day 12 (mature EBs) and Q-RT PCR performed for *p21* expression

(increased expression of *p21* may account for the decrease in growth potential of HDAC1^{Δ2/Δ2} EBs). However, Figure 4.8 reveals no change in p21 expression upon deletion of HDAC1 (although its expression is increased in cycling CreER WT mES cells by treatment with TSA, Fig 4.8.A and B)

At day 8, 100% of HDAC1^{Δ2/Δ2} EBs had developed a spontaneous rhythmic contraction phenotype, compared to less than 10% for HDAC1^{Lox/Lox} controls (Fig 4.7.C), indicative of differentiation into cardiomyocytes and pacemaker cells (Boheler K.R., *et al.*, 2002). Only a limited number of HDAC2^{Δ2/Δ2} EBs were observed to spontaneously contract. The reduction in HDAC1^{Δ2/Δ2} EB size, their irregular shape and spontaneous contraction suggested that increased differentiation was occurring. To visualize the differentiation and examine the cell types produced, day 12 EBs of the indicated genotype were embedded in paraffin, sectioned laterally and then stained with haematoxylin and eosin (Fig 4.7.D and E). Histological examination of HDAC2^{Δ2/Δ2} and undeleted control EBs (HDAC1^{Lox/Lox} and HDAC2^{Lox/Lox}) revealed a relatively uniform organization consisting mainly of mesenchyme surrounded by ground substrate. HDAC1^{Δ2/Δ2} EBs in contrast, have a large number of organised cellular structures, including epithelial rosettes with associated basement membrane and many regions of cell death, indicative of profound differentiation (Fig 4D, compare left and right panels).

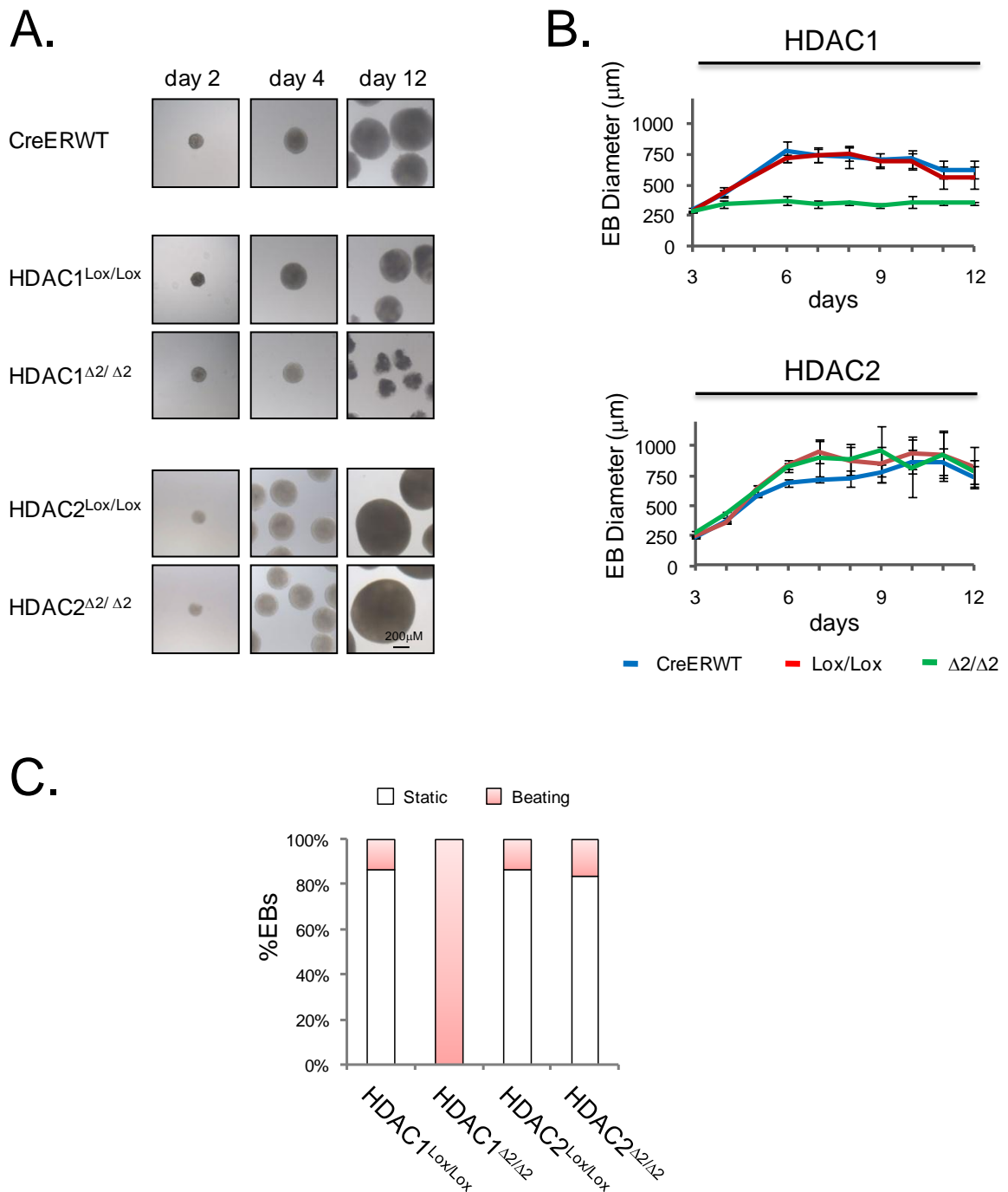


Figure 4.7. *Loss of HDAC1 enhances embryoid body differentiation.* (A) Representative examples of EBs at the indicated time points. (B) Mean size and SDs of EBs during a 12-day experiment. Different genotypes are indicated. Mean values \pm S.E.M. are plotted ($n = 3$). (C) Percentage of EBs with a rhythmic beating phenotype. Individual genotypes are indicated. Data are representative of three independently tested clones of each genotype.

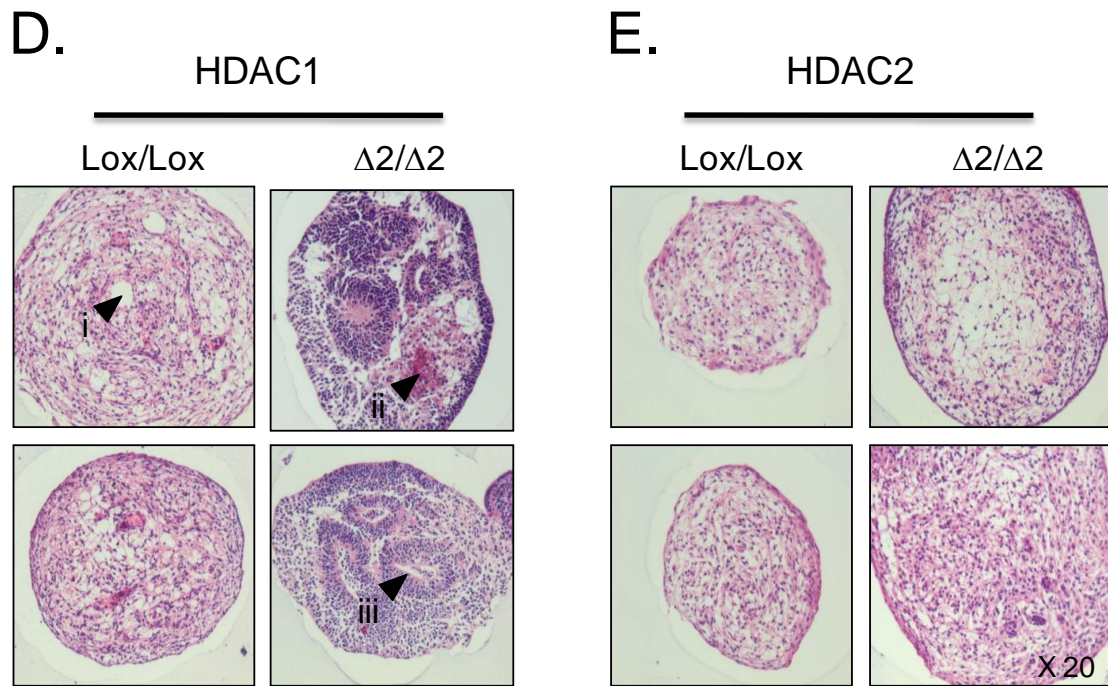


Figure 4.7. *Loss of HDAC1 enhances embryoid body differentiation.* (D and E) Hematoxylin and eosin-stained sections of day 12 EBs of the indicated genotypes. (i) Regions of mesenchyme, unstained areas demark ground substance; (ii) structured region of organised epithelium (epithelial rosette) on basement membrane; (iii) region of cell death and apoptosis. Both ii and iii are characteristic of EBs derived from HDAC1 ^{$\Delta 2/\Delta 2$} ES cells. Data are representative of three independently tested clones of each genotype.

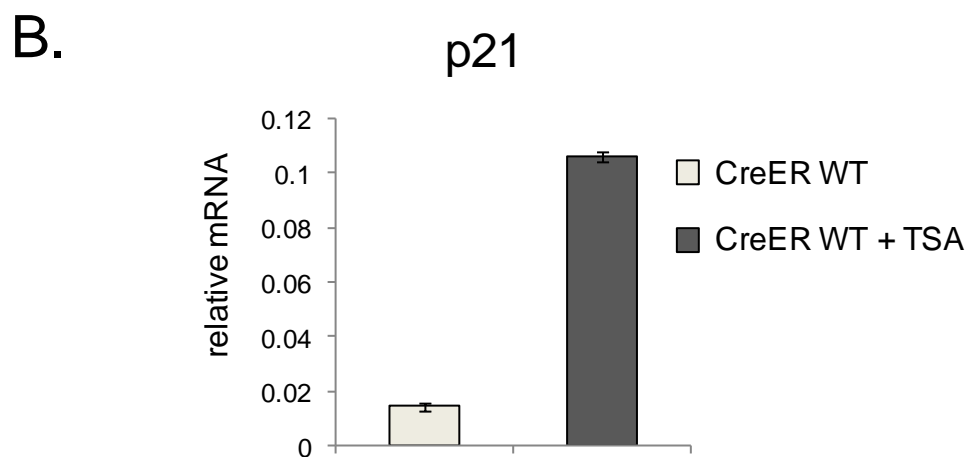
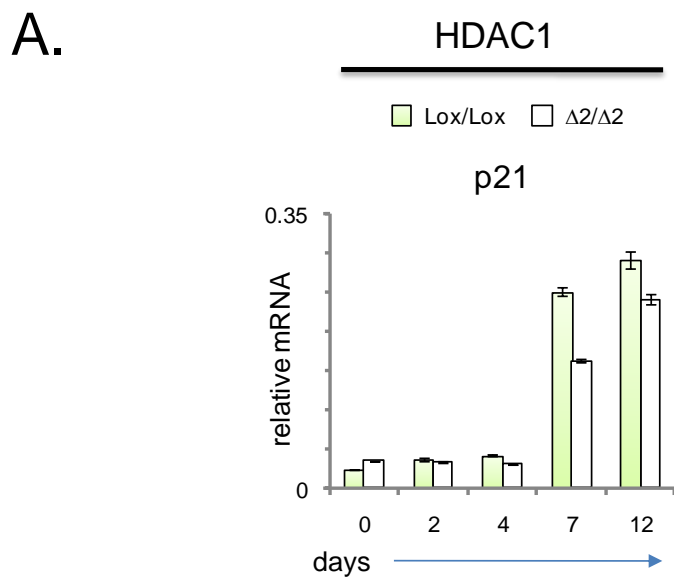


Figure 4.8. Expression of the prototypical HDAC1 target gene *p21* is unaltered in HDAC1 ^{$\Delta 2/\Delta 2$} mES cells. Quantitative RT-PCR analysis of *p21* mRNA (A) in embryoid bodies at the indicated time points and (B) in cycling ES cells with and without trichostatin A treatment (TSA, 30mM for 24 h). The level of *p21* mRNA was measured in a multiplex PCR assay relative to *Gapdh* mRNA, using Universal ProbeLibrary hydrolysis probes. Data in A is representative of two independently tested clones for each genotype, mean values \pm S.E.M. are plotted (n = 3). Data in B is from treatment of a single CreER WT clone, mean values \pm S.E.M. are plotted (n = 3).

4.4.1 Increased expression of cardiomyocyte, muscle and neuronal specific markers in embryoid bodies lacking HDAC1.

To identify the cell types present during wild-type and mutant EB differentiation, RNA was collected at time points from day 0 (cycling ES cells) to day 12 (mature EBs) and Q-RT PCR performed for lineage specific markers. Consistent with the process of mES cell differentiation, the pluripotency markers Oct4 and Nanog are repressed in both HDAC1^{Δ2/Δ2} and HDAC2^{Δ2/Δ2} EBs (Fig 4.9.A). Also, HDAC1^{Δ2/Δ2} and HDAC2^{Δ2/Δ2} EBs show a similar induction (day 2), and then repression (day 7), of Fgf5 (Fig 4.9.B) suggesting that loss of either HDAC does not adversely affect primitive ectoderm formation, a critical intermediate in the formation of the three primary germ-layers (Hebert J.M., et al., 1991). A key regulator of mesodermal specification is the T-box transcription factor, brachyury. Induction of *brachyury* gene expression during EB differentiation is enhanced in EBs lacking HDAC1 compared with HDAC2 deleted cells and undeleted controls (Fig 4.9.A). Consistent with increased *brachyury* levels and the spontaneous 'beating' phenotype of HDAC1^{Δ2/Δ2} EBs, increased expression of the cardiomyocyte specific markers *Nkx2-5* and *Mef2c* (critical transcription factors required for cardiomyocyte commitment and normal heart development) (Yan, F.Y., et al., 1998, Lin, Q., et al., 1997 and Grow, M. W. & Kreig, P. A., 1998), is detected. Focusing on transcriptional profiling of HDAC1^{Δ2/Δ2} EBs, increased expression of cardiac specific genes, *Hopx* (a crucial regulator of cardiomyogenesis and direct downstream target of the transcription factor NKX2-5), *Myf2*, and *Actc* is also observed in HDAC1^{Δ2/Δ2} EBs (Chen, F., et al., 2002 and Shin, C.H., et al., 2002) (Fig 4.9.C). Additionally, and again consistent with the up-regulation of the mesoderm marker *brachyury*,

the skeletal muscle marker, *MyoD*, is also over expressed in HDAC1^{Δ2/Δ2} EBs (Fig 4.8.A, left panel).

Neuronal cell markers, *nestin* and *βIII-tubulin* are similarly elevated in day 12 HDAC1^{Δ2/Δ2} EBs (Fig 4.9.B, left panel). Noticeably however, *Afp* and *Gata-6*, markers of endodermal differentiation, are reduced by loss of HDAC1 (Fig 4.9.A, left panel). Altogether, under these differentiation conditions, results from transcriptional profiling of HDAC1^{Δ2/Δ2} EBs indicate preferential differentiation towards mesodermal and ectodermal lineages at the expense of endoderm.

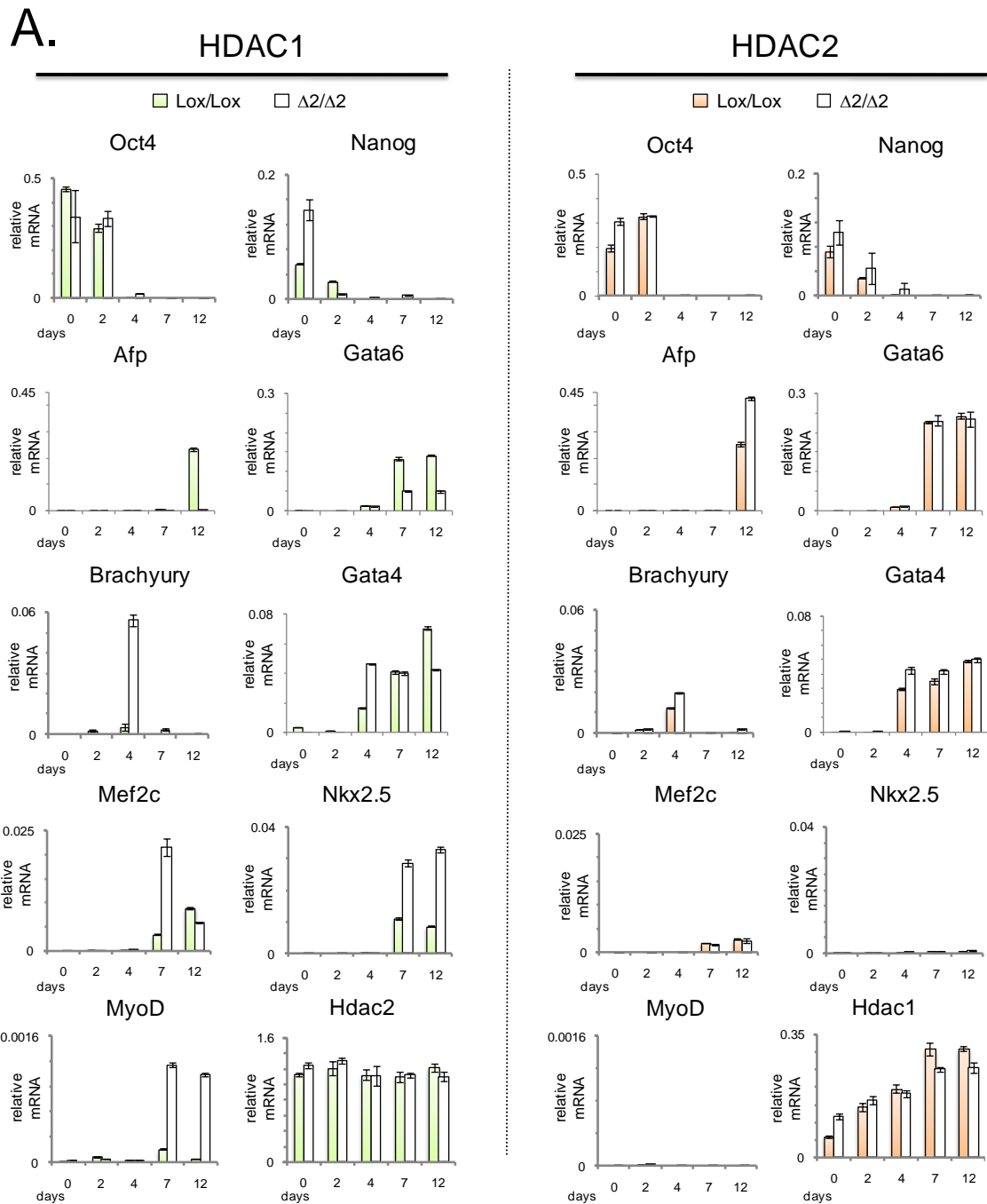


Figure 4.9. Loss of HDAC1 causes precocious differentiation into mesodermal and ectodermal lineages at the expense of endoderm in EBs. (A) Quantitative RT-PCR data for genes characteristic of undifferentiated stem cells (*Oct4*, *Nanog*), endoderm (*Gata6*, *Afp*), mesoderm (*brachyury*, *Nkx2-5*, *Mef2c*, and *MyoD*) was performed as indicated on mRNA collected at days 0, 2, 4, 7, and 12 during EB differentiation. Mean values \pm S.E.M. are plotted ($n = 3$). Values indicate expression of the specific gene relative to *Gapdh* measured using Universal ProbeLibrary hydrolysis probes. Data are representative of two independently tested clones for each genotype.

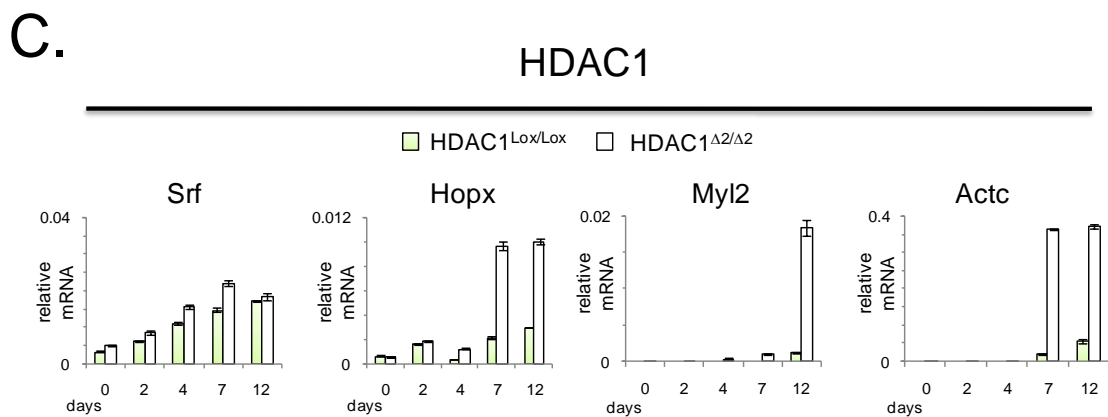
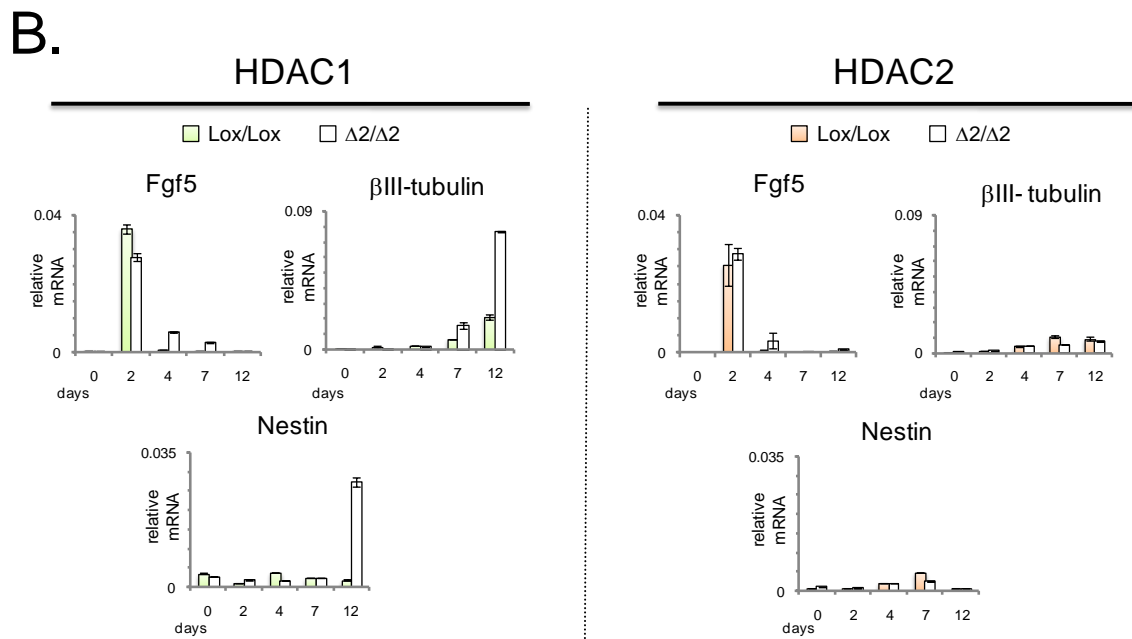


Figure 4.9. Loss of *HDAC1* causes precocious differentiation into mesodermal and ectodermal lineages at the expense of endoderm in EBs. (B) Quantitative RT-PCR data for regulators of cardiomyogenesis (*Srf*, *Hopx*) and cardiac specific genes (*Myl2* and *Actc*). (C) Quantitative RT-PCR data for genes characteristic of primitive ectoderm (*Fgf5*) and ectoderm (*Nestin*, *βIII-tubulin*). Quantitative RT-PCR was performed as indicated on mRNA collected at days 0, 2, 4, 7, and 12 during EB differentiation. Mean values ± S.E.M. are plotted (n = 3).

4.4.2 Differentiation of EBs lacking HDAC1 into neuronal lineages is further enhanced upon treatment with ATRA.

Treatment of Day 4 EBs with all-trans-retinoic acid (ATRA), a well known neuronal cell morphogen, has been shown to promote neural differentiation and repress mesoderm formation in mES cells (Carsten S., *et al.*, 1995, Bain G., *et al.*, 1996 and Okadaa Y., *et al.*, 2004). HDAC1^{Δ2/Δ2}, HDAC2^{Δ2/Δ2} and undeleted control EBs were treated from days 4-8 with ATRA before being dissociated into single cell suspensions on day 8. Cells were seeded on gelatin coated culture dishes and laminin coated glass slides and cultured up to day 12 (Fig 4.10.A). Again, to identify the cell types present during wild-type and mutant EB differentiation, RNA was collected at time points from day 0 (cycling mES cells), up to day 12 (differentiated cells) and Q-RT PCR performed for lineage specific markers. In accordance with previously published data (Bain G., *et al.*, 1996), comparing ATRA treated control (HDAC1^{Lox/Lox}) untreated EBs, formation of mesoderm is compromised whilst neural differentiation is enhanced (as observed by decreased brachyury and increased nestin mRNA expression in ATRA treated EBs, Fig 4.10.B). Moreover, the pluripotency marker *Oct4* is also repressed (and remains so upon ATRA treatment) suggesting cells have successfully exited from the pluripotent stem cell programme and entered a programme of differentiation (Fig 4.11.A). Further to the initial analysis of EBs lacking HDAC1, ATRA treatment of day 4 HDAC1^{Δ2/Δ2} EBs enhances neuronal differentiation as assessed by the elevated detection of nestin mRNA (a marker of undifferentiated neuronal progenitors) compared to HDAC2^{Δ2/Δ2} and control EBs (Fig 4.11.A). This is further supported by elevated immunohistochemical detection of NESTIN and βIII-TUBULIN in cells from dissociated ATRA treated

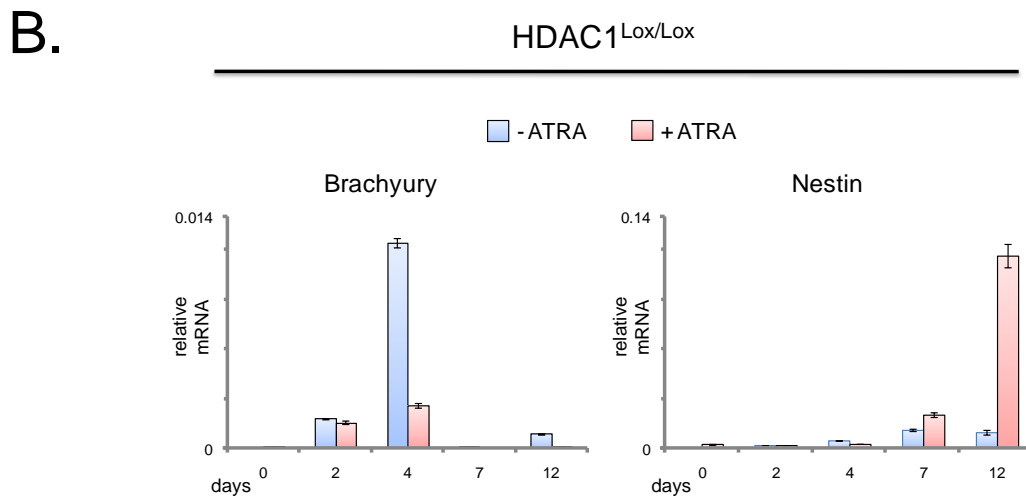
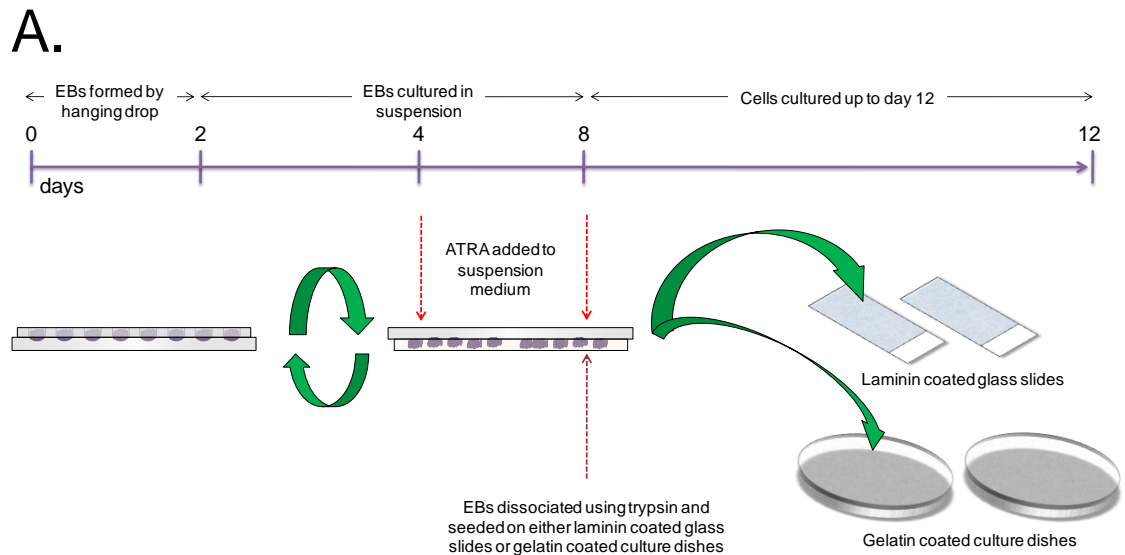


Figure 4.10. *Treatment of EBs with ATRA promotes differentiation and inhibits formation of mesoderm.* ATRA Treatment of EBs. (A) Control HDAC1^{Lox/Lox} EBs were formed by the hanging drop method from days 0-2. From day 2 EBs were maintained up to day 8 in normal differentiation media supplemented with or without 1×10^7 M ATRA from days 4-8. On day 8 EBs were dissociated into a single cell suspension and seeded on gelatin coated plates and laminin coated glass slides (for mRNA expression and immunohistochemical analysis respectively). (B) Quantitative RT-PCR data for genes characteristic of mesoderm (*brachyury*) and ectoderm (*nestin*) were measured by using Q-RT PCR, as in Figure 4.8). Further measurements were made in day 12 EBs that were trypsinised and plated on gelatin from day 8-12. Mean values \pm S.E.M. are plotted (n = 3).

A.

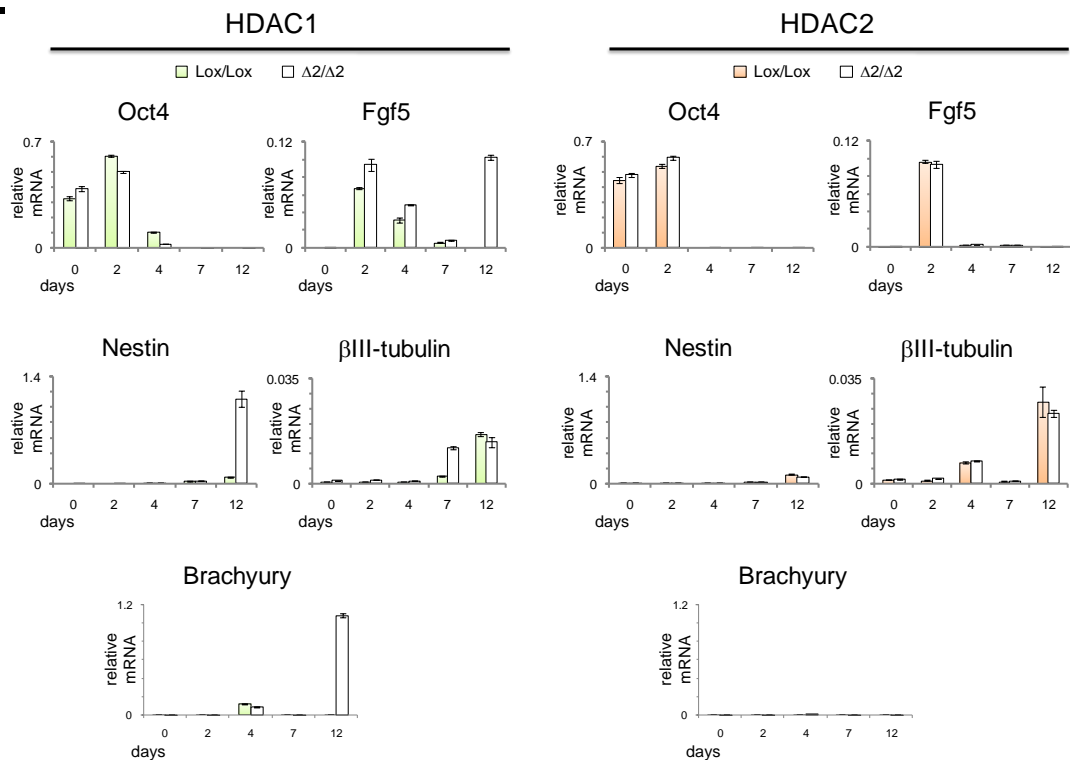


Figure 4.11. Differentiation into neuronal lineages in EBs lacking HDAC1 is further enhanced upon treatment with ATRA. Treatment of EBs with ATRA (B) Quantitative RT-PCR data for genes characteristic of undifferentiated stem cells (*Oct4*), primitive ectoderm (*Fgf5*), mesoderm (*brachyury*), neural progenitor (*nestin*) and differentiated neuron (β III-tubulin) were measured by using Q-RT PCR (as in Figure 4.8). Further measurements were made in day 12 EBs that were trypsinised and plated on gelatin from day 8-12. Mean values \pm S.E.M. are plotted (n = 3).

HDAC1 ^{$\Delta 2/\Delta 2$} EBs when plated on laminin coated glass slides (Fig 4.11.B). Notably, as with prior EB experiments, ATRA treated HDAC2 deficient EBs failed to yield any robust, detectable differences compared to controls in these assays (Fig4.11.A and B). *Brachyury* expression is elevated in HDAC1 ^{$\Delta 2/\Delta 2$} EBs at day 12, which will be discussed alongside other results later.

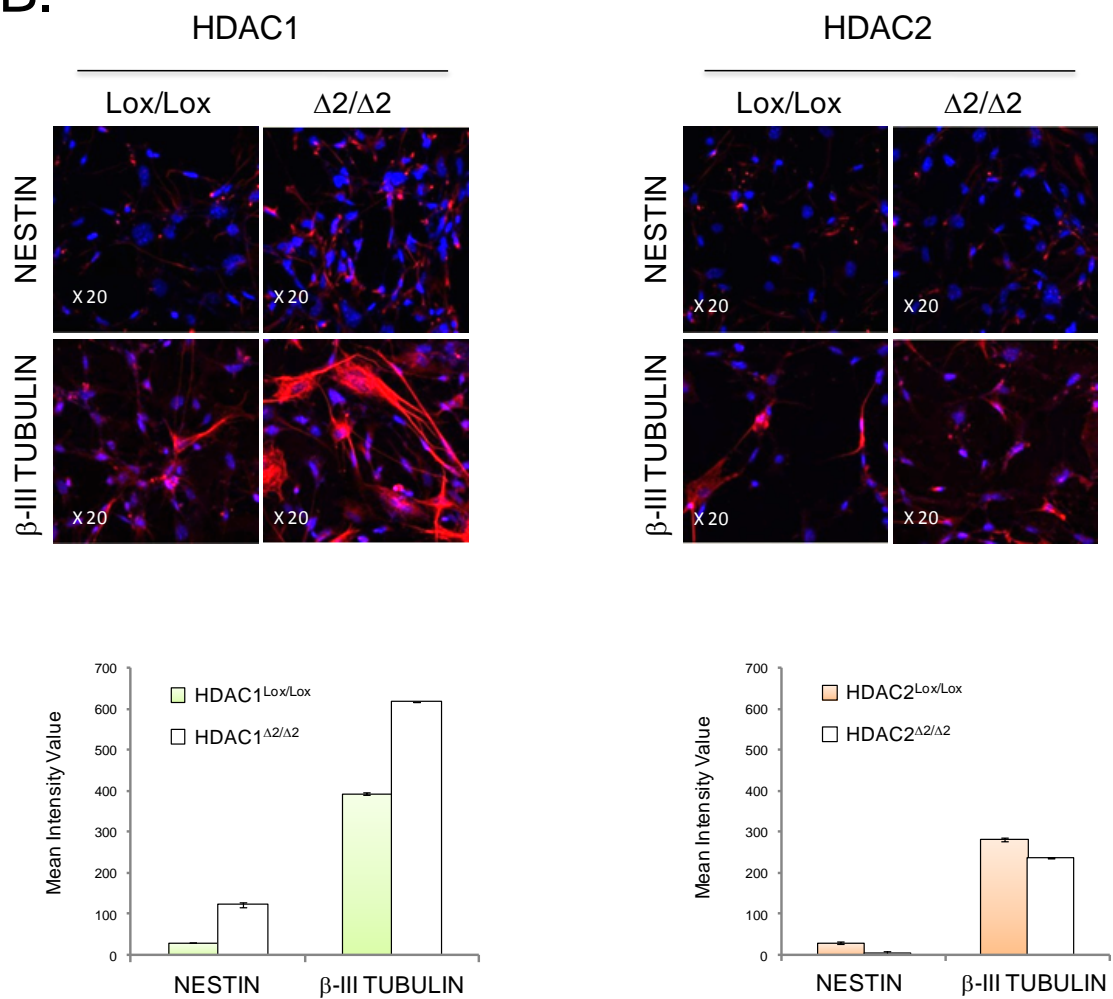
B.

Figure 4.11. *Precocious differentiation into neuronal lineages in EBs lacking HDAC1 is further enhanced upon treatment with ATRA.* Immunohistochemistry of ATRA treated EBs. (B) Approximately 1×10^5 cells from trypsinised/dissociated ATRA treated EBs were seeded on laminin coated glass slides, cultured up to day 12 and then stained with antisera for β III-TUBULIN (red) or NESTIN (red) and counterstained with DAPI (blue). Images were captured and mean intensity values of positively stained cells identified and quantified using the automated Cell^R/Scan^R imaging system. Mean intensity of >1500 positively stained cells \pm S.E.M. are plotted.

4.4.3 Serum dependent and serum independent enhanced differentiation of EBs lacking HDAC1.

Routine maintenance of mES cells *in vitro* (and their perpetual commitment to a programme of self renewal and maintenance of their pluripotent potential) requires the addition of serum to culture medium in combination with LIF. These two factors act respectively to induce Id proteins and activation of STAT3, which suppress mES cell differentiation as well as maintain pluripotency (Niwa, H., *et al.*, 1998 and Ying, Q.L., *et al.*, 2003a). Indeed, the importance of serum in ensuring mES cell maintenance is evidenced by the inability of LIF to block neuronal cell differentiation in serum free mES cell culture. In these conditions, addition of BMP4, a known inhibitor of neuronal differentiation, to serum-free, LIF-containing cell culture medium, is sufficient to prevent neuronal differentiation (Wilson, P.A. and Hemmati-Brivanlou, A., 1995, Ying, Q.L., *et al.*, 2003a). Note however, that in serum free culture, addition of BMP4 alone is insufficient to maintain mES cells in a state of pluripotent self renewal (mES cells differentiate along non-neuronal pathways) (Ying, Q.L., *et al.*, 2003b). Thus, BMP4 is an example of a potential constituent of serum that aids in preventing mES cell differentiation but also, in the absence of LIF, induces a defined process of cell differentiation. Therefore, additional growth factors and/or cytokines, ill-defined constituents of serum, help maintain mES cells in their pluripotent state. By extension, differentiation and lineage commitment of mES cells can be determined, or cued, by serum constituents upon withdrawal of LIF. To assess if the “spontaneous” contracting phenotype observed in HDAC1^{Δ2/Δ2} EBs is serum dependent, EBs derived from a single HDAC1^{Δ2/Δ2} clone and the undeleted counterpart, were cultured in a

commercially available, mES cell specific, serum free media. Parallel culture of the same EBs, in normal differentiation media, was also undertaken and comparative analysis of EB differentiation potential of the two culture conditions carried out as before.

EBs lacking HDAC1 and cultured in the absence of serum, become irregular in shape, rather than uniformly spherical, but do not exhibit the reduction in size at day 12 when compared to controls (Fig 4.12.A day 12 and 4.12.B), a contrasting result to culture in the presence of serum (Fig 4.7.A, day12 and 4.7.B). Measuring the percentage of EBs that developed rhythmic contraction reveals little difference between mutant and control EBs in the absence of serum; again, an observation which contrasts with observed results in the presence of serum where characteristics indicative of cardiomyocyte differentiation (i.e. “beating” EBs) are observed (compare Fig 4.7.C, in the presence of serum, with Fig 4.12.C, serum free culture). Histological examination of HDAC1^{Δ2/Δ2} EB sections, cultured in serum free conditions, reveal an increase in cell density and an increase in the presence of organised cellular structures (including epithelial rosettes with associated basement membrane) when compared to control sections (which again, mainly consist of uniform mesenchyme) (Fig 4.12.D). The disparity between the histological observations of control and HDAC1^{Δ2/Δ2} EBs cultured in the absence of serum, strongly resemble what can be observed in standard differentiation conditions (Fig 4.7.D). This suggests that despite the absence of a contractile phenotype, as previously observed, and irrespective of the presence of serum, EBs lacking HDAC1 are subject to enhanced differentiation.

Q-RT PCR performed for lineage specific markers reveals the process of mES cell differentiation, is unaltered in the absence of serum, as the pluripotency marker *Oct4* is repressed in both HDAC1^{Δ2/Δ2} and control EBs (Fig 4.13.A, Serum Free EBs). Moreover, HDAC1^{Δ2/Δ2} and control EBs show a similar induction (day 2), and then repression (day 7), of *Fgf5* (Fig 4.13.A Serum Free EBs) suggesting that loss of HDAC1, or the absence of serum, does not adversely affect primitive ectoderm formation and confirms an exit from the pluripotent stem cell programme. Consistent with the absence of a “beating” phenotype in either control or HDAC1 mutant EBs in serum free culture (Fig 4.12.C), no differential detection of cardiac specific genes (*Nkx2-5*, *Mef2c*, *Hopx*, *Myf2*, or *Actc*) is observed (Fig 4.13.A and B), this is despite a much larger relative induction of the mesoderm marker, brachyury, (Fig 4.13.A, compare brachyury expression in + serum EBs with serum free EBs). These results indicate that the differentiation of HDAC1^{Δ2/Δ2} EBs into cells characteristic of cardiomyocytes is serum dependent and that formation of mesoderm *per se*, although a pre-requisite, is not predictive of cardiomyogenesis under these culture conditions.

The neuronal cell marker, *nestin*, is similarly differentially elevated in day 12 HDAC1^{Δ2/Δ2} EBs in the absence of serum (Fig 4.13.A), indicating induction of neuronal cell lineages in EBs lacking HDAC1 is independent of serum. Finally, *Gata6*, a marker of endodermal differentiation, reduced by loss of HDAC1 in standard differentiation media, is similarly reduced in the absence of serum (Fig 4.13.A) and indicates a consistent reduction in endodermal lineage specification in EBs lacking HDAC1. Altogether, results from comparative transcriptional profiling combined with histological analysis of control and HDAC1^{Δ2/Δ2} EBs,

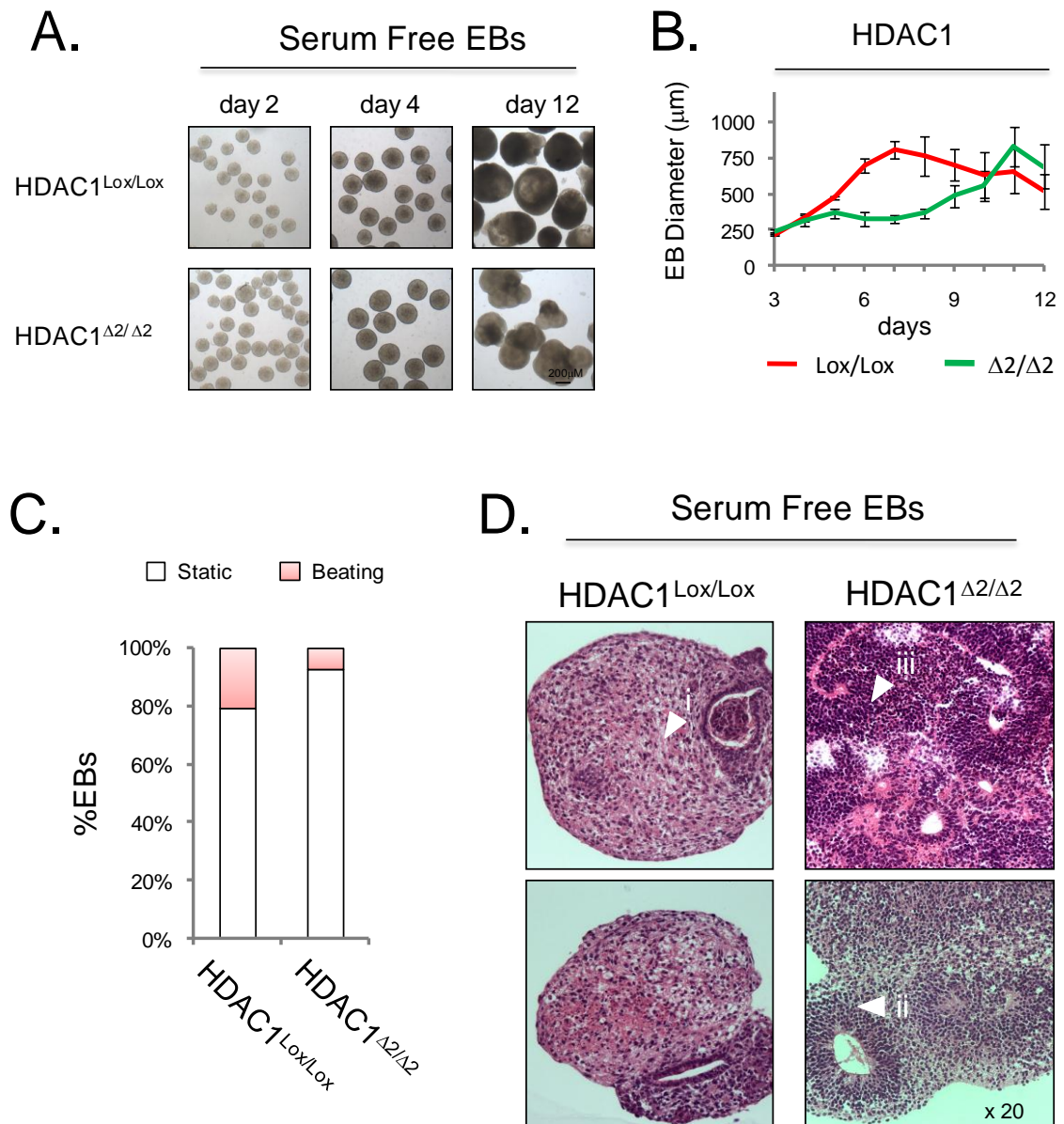


Figure 4.12. Serum free culture of HDAC1^{Lox/Lox} and HDAC1^{Δ2/Δ2} EBs. (A) Representative examples of EBs at the indicated time points. (B) Size of EBs during a 12-day experiment. Different genotypes are indicated. Mean values ± S.E.M. are plotted (n = 3). (C) Percentage of EBs with a rhythmic beating phenotype. Enhanced differentiation of EBs lacking HDAC1 is serum independent. (D) Hematoxylin and eosin-stained sections of day 12 EBs of the indicated genotype. (i) Regions of mesenchyme, unstained areas demark ground substance; (ii) structured region of organised epithelium (epithelial rosette) on basement membrane; (iii) cell dense regions. Both (ii) and (iii) are characteristic of EBs derived from HDAC1^{Δ2/Δ2} mES cells. Data are from a single HDAC1^{Δ2/Δ2} clone with the appropriate HDAC1^{Lox/Lox} clone as control.

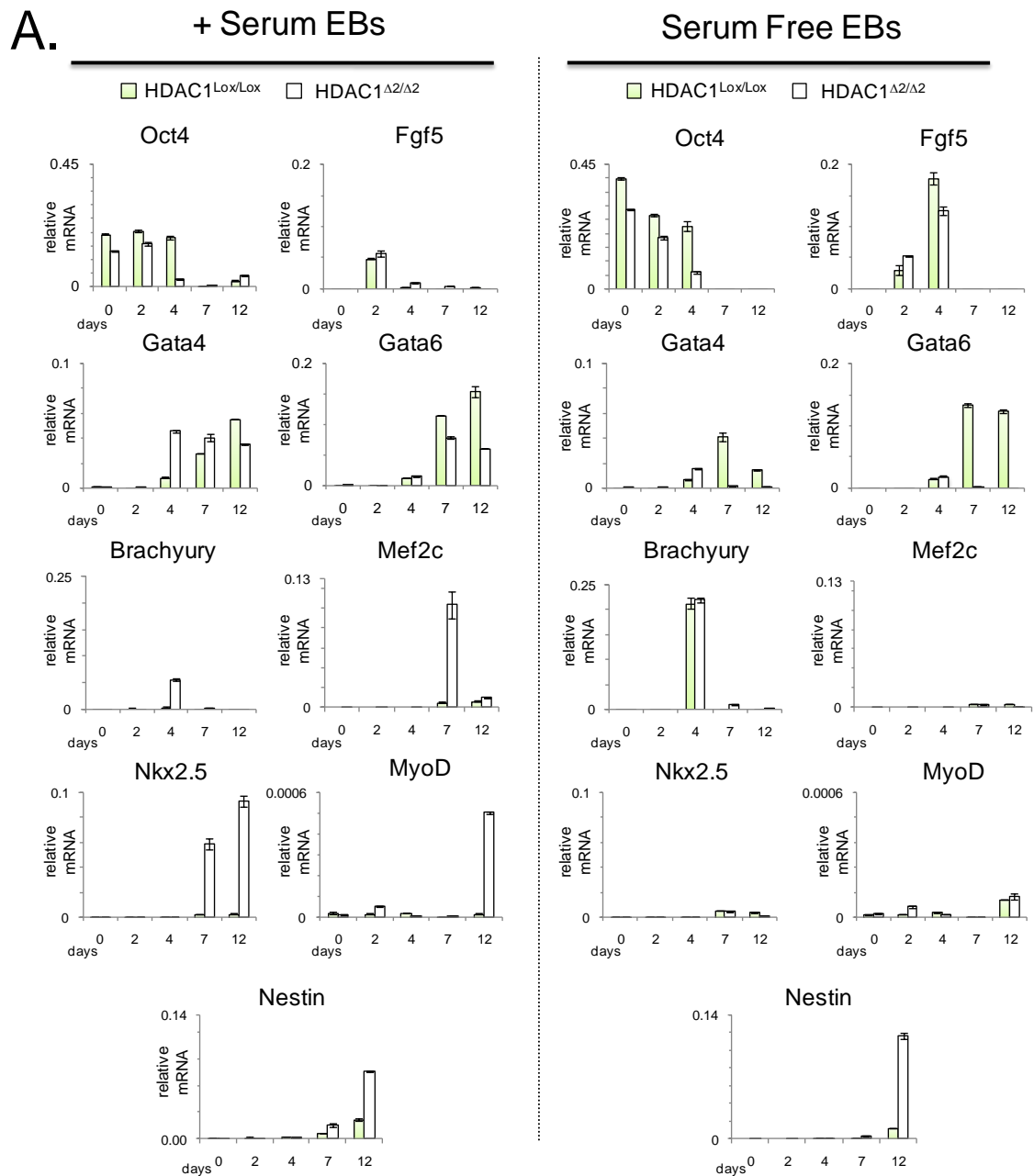


Figure 4.13. Serum dependent and serum independent differentiation of HDAC1^{Δ2/Δ2} EBs. (A) Quantitative RT-PCR data for genes characteristic of undifferentiated stem cells (*Oct4*), primitive endoderm (*Fgf5*), endoderm (*Gata6*) and mesoderm (*Brachyury*, *Nkx2-5*, *Mef2c*, and *MyoD*) was performed as indicated on mRNA collected at days 0, 2, 4, 7, and 12 during EB differentiation in the presence or absence of serum. Mean values \pm S.E.M. are plotted ($n = 3$). Values indicate expression of the specific gene relative to *Gapdh* measured using Universal ProbeLibrary hydrolysis probes. Data are from a single HDAC1^{Δ2/Δ2} clone with the appropriate HDAC1^{Lox/Lox} clone as control.

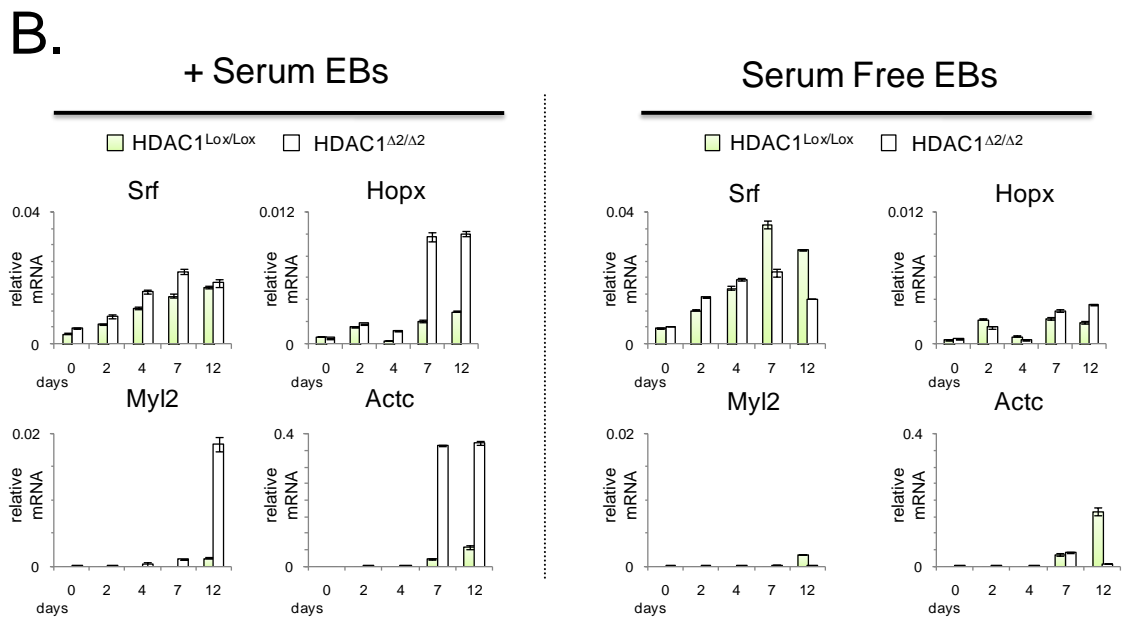


Figure 4.13. Serum dependent and serum independent differentiation of $HDAC1^{\Delta2/\Delta2}$ EBs. (B) Quantitative RT-PCR data for regulators of cardiomyogenesis (*Srf*, *Hopx*) and cardiac specific genes (*Myl2* and *Actc*) was performed as indicated on mRNA collected at days 0, 2, 4, 7, and 12 during EB differentiation in the presence or absence of serum. Mean values \pm S.E.M. are plotted ($n = 3$). Values indicate expression of the specific gene relative to *Gapdh* measured using Universal ProbeLibrary hydrolysis probes. Data are from a single $HDAC1^{\Delta2/\Delta2}$ clone with the appropriate $HDAC1^{Lox/Lox}$ clone as control.

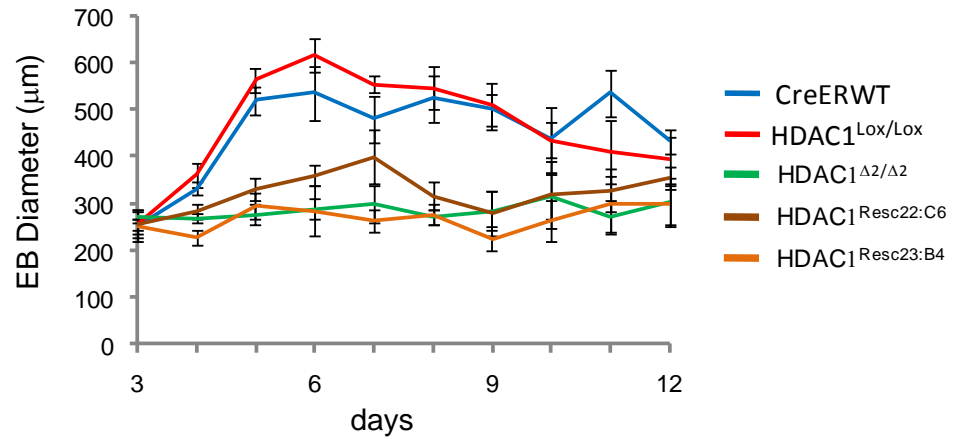
cultured in the presence or absence of serum reveal that precocious differentiation of $HDAC1$ mutant EBs, induction of neuronal lineage differentiation and a reduction in endodermal cell types is independent of serum. Conversely, induction of cardiomyocyte differentiation in $HDAC1^{\Delta2/\Delta2}$ EBs is serum dependent.

4.5 Stable transfection of the Hdac1-C-FLAG-Resc construct fails to prevent the established differentiation phenotype of HDAC1^{Δ2/Δ2} EBs.

Having established a robust phenotype in HDAC1^{Δ2/Δ2} mES cells upon differentiation, namely preferential differentiation into mesodermal and ectodermal cell lineages at the expense of endoderm, repeat experiments were performed using the “rescue” cell lines, HDAC1^{Δ2/Δ2}:Hdac1-C-FLAG-Resc (henceforth known as HDAC1^{Resc}) generated in section 3.3.3 (Fig 3.14.C). In standard differentiation culture medium containing serum, EBs lacking HDAC1 over a 12 day time course are marked phenotypically by their reduced size and increased contractility compared to controls (Fig 4.7). Using these readily detectable features of the HDAC1^{Δ2/Δ2} EB phenotype, initial assessment of the ability of HDAC1^{Resc} mES cell lines (i.e. HDAC1^{Δ2/Δ2} mES cell lines expressing a HDAC1-C’-FLAG-tag protein) to revert HDAC1^{Δ2/Δ2} EBs to the phenotype of control EBs, thus “rescuing” deletion of endogenous HDAC1, were undertaken using standard, serum containing, differentiation medium. For EB size assessment, two HDAC1^{Resc} mES cell lines were chosen based on their expression of exogenous HDAC1-C’-FLAG-tag protein (Fig 3.14B). Assessments of EB contractility were made using a single HDAC1^{Resc} mES cell line. Controls included the parental HDAC1^{Lox/Lox} clone used to derive the stably transfected mES cells, the subsequent ligand induced HDAC1^{Δ2/Δ2} clone and CreER WT mES cells. Comparison of EB diameter reveals the size of HDAC1^{Resc} EBs is similar to that of HDAC1^{Δ2/Δ2} EBs (Fig 4.14A). As with the results from comparing EB size, the percentage of HDAC1^{Resc} EBs with a beating phenotype (45%) was more comparable to the percentage of HDAC1^{Δ2/Δ2} (63%) than

controls (0%) (Fig 4.14B). Taken together these data affirm that HDAC1^{Resc} mES cells fail to “rescue” the established phenotype in HDAC1^{Δ2/Δ2} EBs, as such no further experiments using these cell lines were tasked.

A.



B.

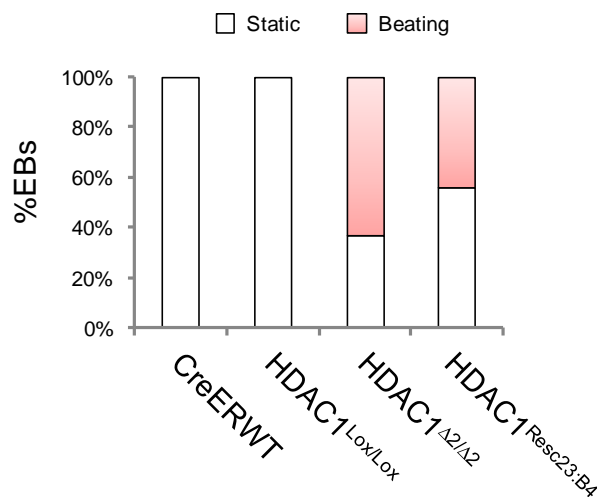


Figure 4.14. HDAC1^{Resc} mES cell lines fail to “rescue” the phenotype observed in HDAC1^{Δ2/Δ2} embryoid bodies. (A) Size of EBs during a 12-day experiment. Data from EBs derived from the following mES cell lines; single CreER WT, HDAC1^{Lox/Lox}, HDAC1^{Δ2/Δ2} clones and two individual HDCA1^{Resc} clones (HDAC1^{Resc22:C6}, HDAC1^{Resc23:B4}). Mean values ± S.E.M. are plotted (n = 3). (B) Percentage of EBs with a rhythmic beating phenotype at day 12. Data are from single CreER WT, HDAC1^{Lox/Lox}, HDAC1^{Δ2/Δ2} and HDAC1^{Resc23:B4} clones.

4.6 Conclusions.

Inducible knock-out of HDAC1 or HDAC2 in mES cells has provided new insights as to their requirements in mES cell proliferation and reveals non-redundant roles for these enzymes in mES cell differentiation. Assessment of the basic biochemical properties of mES cells, lacking either HDAC1 or -2, also reveals a degree of substrate specificity as well as differences in deacetylase potential between the two enzymes.

Singular deletion of either HDAC1 or -2 does not affect mES cell proliferation or the ability of mES cells to exit the pluripotent stem cell programme upon LIF withdrawal (Fig 4.5 and 4.6), instead differentiation of mES cells (via the formation of embryoid bodies, EBs) reveals a non-redundant role for these enzymes in the pace and control of differentiation (Fig 4.7). In particular HDAC1, and not HDAC2, mediates the control of neuronal and cardiac differentiation (Fig 4.7C, 4.9, 4.10 and 4.11). Biochemical analysis of deacetylase potential using *in vitro* deacetylase assays, reveals HDAC1 to be the more effective or prominent deacetylase of the two class I HDACs in co-repressor complexes (Fig 4.2). Analysis of histone extracts reveals very little change in the acetylation status in any of the histone lysine residues analysed in the absence of either enzyme, suggestive of redundant, compensatory or complementary roles for HDAC1 and -2 in global histone lysine deacetylation. An exception to this rule is H3K56 acetylation, which is increased in the absence of HDAC1 but not HDAC2 and reveals a novel, specific substrate for HDAC1 (Fig 4.3).

Chapter Five: HDAC1 and 2 are required for normal thymocyte development and are major contributors to the maintenance of thymocyte genomic stability.

5.1 Chapter aims.

Using T cell specific conditional knock-out HDAC1 and HDAC2 mice (Chapter 3.4) I aimed to characterise the roles of HDAC1 and -2 in intra-thymic T cell development. Analysis of the roles of HDAC1 and -2 in the many aspects of T cell maturation will be assessed by multi-coloured fluorescence activated cell sorting (FACS). Concomitant to this, biochemical analysis of thymocytes of conditional knock-out mice will also be performed. Combined, these studies may shed some new light on the mainly redundant nature of these enzymes.

5.2 The *LckCre* transgene does not affect normal T cell development.

As previously discussed, the *LckCre* transgene is active early in thymocyte development (Chapter 3.4.1). Expression of Cre recombinase has previously been reported to have cytotoxic effects on both mammalian cell lines and conditional mouse models (Loonstra, A., *et al.*, 2001 and Schmidt, E. E., *et al.*, 2000). Presence of the *LckCre* transgene in wild-type (WT) mice does not affect either total thymocyte cellularity or intra-thymic T cell development (that is, there is no change in the percentage of cells of developmental compartments when gated on expression of CD4 and CD8 coreceptors as analysed by FACS) (Figure 1A and B). Henceforth WT refers to WT, WT^{*LckCre*} or targeted mice (e.g. HD1^{L/L}). Conversely and for brevity, targeted mice that carry the *LckCre*

transgene are denoted as HD1^{Δ2/Δ2} or HD2^{Δ2/Δ2} (single), HD1^{WT/Δ2};HD2^{Δ2/Δ2} or HD1^{Δ2/Δ2};HD2^{WT/Δ2} (compound) and HD1&2^{Δ2/Δ2} (double) knock-out mice.

5.3 Incomplete deletion of HDAC2 in HD1&2^{Δ2/Δ2} double knock-out thymocytes from 6-8 week old mice.

I have already demonstrated almost complete recombination (thymocytes) and deletion of either HDAC1 or HDAC2 protein (thymocytes and splenocytes) in single targeted HD1^{Δ2/Δ2} and HD2^{Δ2/Δ2} mice (Chapter 3, Figs 3.17 and 3.18). Consistent with results obtained using HDAC1^{Δ2/Δ2} and HDAC2^{Δ2/Δ2} mES cells, Western blots performed on nuclear extracts obtained from thymocytes of 6-8 week old mice reveals deletion of HDAC1 results in an increase in HDAC2 (approximately 2 fold), a result not reciprocated upon deletion of HDAC2 (Fig 5.2, top panel, Fig 5.12B, quantified western blot). The same analysis performed on double targeted HD1&2^{Δ2/Δ2} mouse thymocytes reveals substantial and consistently detectable amounts of HDAC2, indicating incomplete deletion in thymocytes from these mice (Fig 5.2, bottom panel). Interestingly, analysis of HDAC1 and HDAC2 protein levels in compound knock-out mice (either HD1^{WT/Δ2};HD2^{Δ2/Δ2} or HD1^{Δ2/Δ2};HD2^{WT/Δ2}) do not reveal the decreases in HDAC1 or -2 protein levels that one might expect in heterozygous targeted mice (i.e. 50% reduction compared to WT controls). Similar to single HD1^{Δ2/Δ2} knock-out mice, an increase in HDAC2 protein upon HDAC1 deletion is detected in HD1^{Δ2/Δ2};HD2^{WT/Δ2} targeted mice (approximately 1.5 fold, Fig 5.12B, quantified western blot) and is reproducibly lower than the 2 fold increase in single HD1^{Δ2/Δ2} knock-outs. Notably, there is little change in HDAC1 protein in

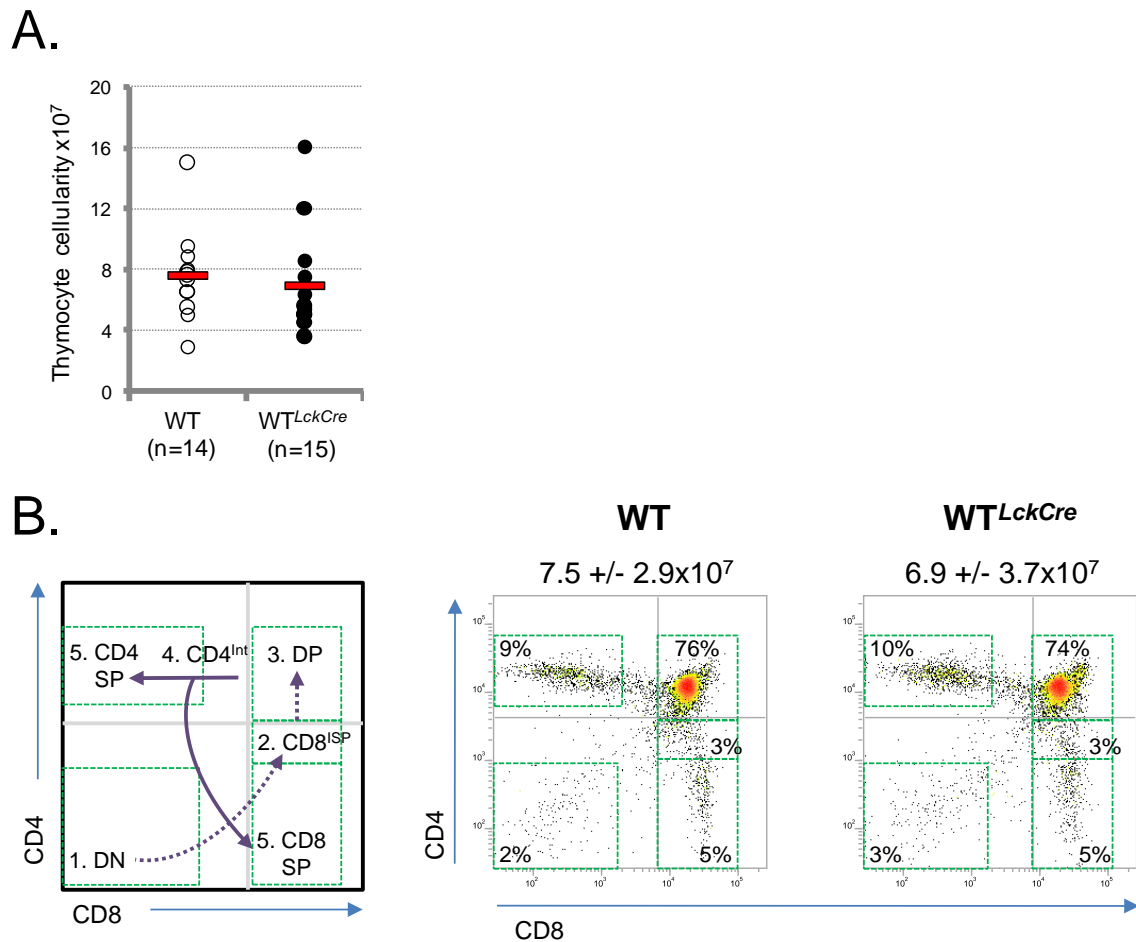


Figure 5.1. Presence of the *LckCre* transgene does not affect normal thymocyte development. (A) Total cellularity of thymocytes from WT and WT^{LckCre} mice. Circles represent cell counts obtained from individual 6-8 week old mice (open: WT, closed: WT^{LckCre}, red bar indicates mean value). (B) Example of two colour CD4/CD8 FACS analysis from the same mice in (A). Dot plots display CD4 versus CD8 expression profiles. Left panel (B) shows schematic representation of T cell maturation from immature double negative to mature single positive. Developmental progression and gates are depicted in top left panel as follows; 1. double negative (DN), 2. CD8 intermediate single positive (CD8^{ISP}), 3. double positive (DP), 4. CD4 intermediate (CD4^{Int}) and 5. CD4 or CD8 single positive (CD4SP and CD8SP). Total thymocyte cellularity is shown above dot plots (mean \pm S.E.M.) and average percentages of gated developmental populations are shown (WT n=14, WT^{LckCre} n=15).

HD1^{WT/Δ2};HD2^{Δ2/Δ2} mice compared to either WT litter mate controls (WT LMCs) or HDAC2 single knock-outs. No detectable change in protein levels of the remaining Class I HDACs, HDAC3 or -8 is observed in thymocytes derived from any of the genotypes analysed (Fig 5.2).

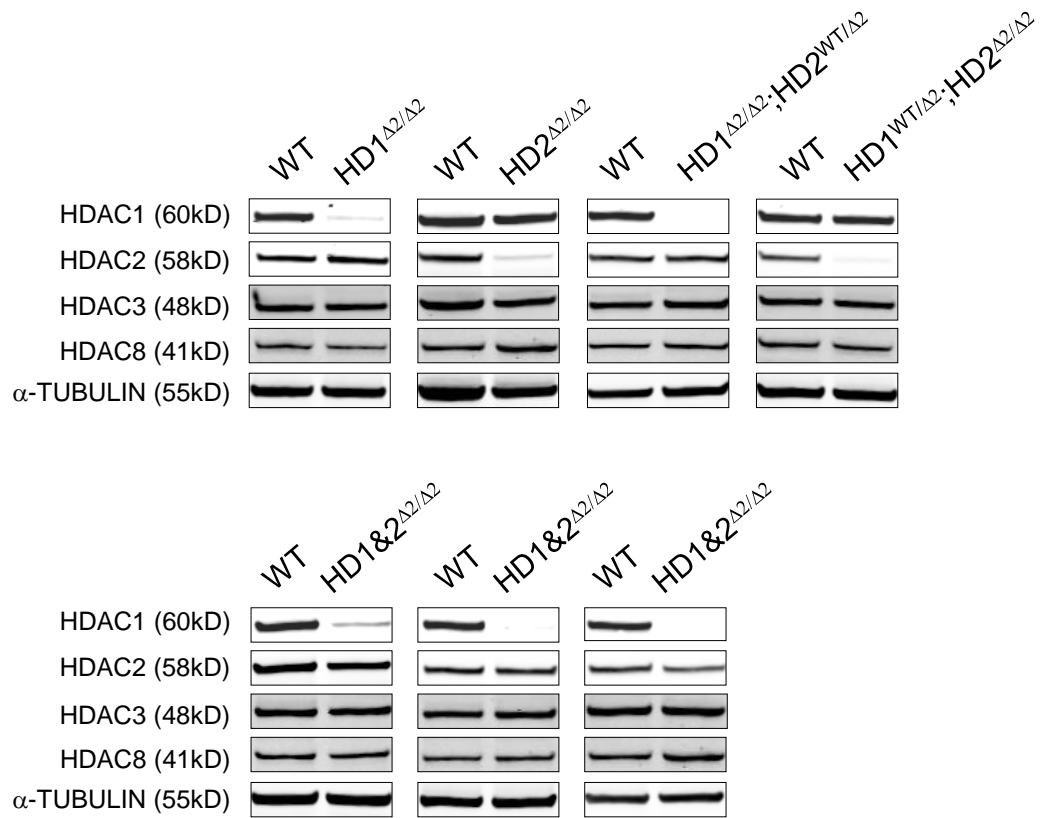


Figure 5.2. *Incomplete deletion of HDAC2 in HD1&2^{Δ2/Δ2} double knock-out thymocytes.* (A) Class I HDAC protein expression in thymocytes obtained from 6-8 week old mice. Representative Western blots performed on nuclear extracts obtained from all genotypes and WT litter mate controls (WT LMCs) for all four Class I HDACs. HDAC2 is consistently detected in HD1&2^{Δ2/Δ2} thymocytes (extracts from three double knock-out mice vs WT LMCs are shown). α -TUBULIN is used as a loading control.

5.4 HDAC1 and -2 are required for normal thymocyte development.

Notwithstanding incomplete deletion of HDAC2 protein in double knock-outs and increased detection of HDAC2 protein levels in both single HD1^{Δ2/Δ2} and compound HD1^{Δ2/Δ2};HD2^{WT/Δ2} knock-out mice, assessment of total thymocyte and splenocyte cellularity, in parallel with CD4/CD8 developmental profiling (using FACS) reveals a number of different phenotypes when comparing single, compound and double knock-out mice.

Total thymocyte cellularity is significantly increased in HD1^{Δ2/Δ2};HD2^{WT/Δ2} and HD1&2^{Δ2/Δ2} mice, although less so in double targeted mice when compared to WT LMCs (approximately 4 and 2 fold respectively) (Fig 5.3). No significant change in total thymocyte cellularity is observed in either single targeted HD1^{Δ2/Δ2} or HD2^{Δ2/Δ2} mice. Likewise, total thymocyte cellularity remains unaltered in mice carrying a single WT HDAC1 allele (HD1^{WT/Δ2};HD2^{Δ2/Δ2} mice). Interestingly, and despite the increase in thymocyte cellularity, no increase in overall splenocyte cellularity is observed in HD1^{Δ2/Δ2};HD2^{WT/Δ2} or HD1&2^{Δ2/Δ2} (where statistically there is a slight reduction). Two colour FACS analysis of intra-thymic T cell development, gating on CD4/CD8 coreceptor expression, reveals a number of abnormal developmental phenotypes when comparing mutant mice with WT LMCs. Consistent with total cellularity, no difference in thymocyte development is observed in single HD2^{Δ2/Δ2} knock-out mice (Fig 5.4A). In contrast, an increase in both the percentage and cellularity of the CD8 intermediate single positive (CD8^{ISP} or CD4^{low}/CD8^{high}) developmental population is observed for all other genotypes. Cellularity of this population ranges from almost 80 x10⁶ in HD1^{Δ2/Δ2};HD2^{WT/Δ2} to 5 x10⁶ in HD1^{Δ2/Δ2} mutants, equivalent to respective

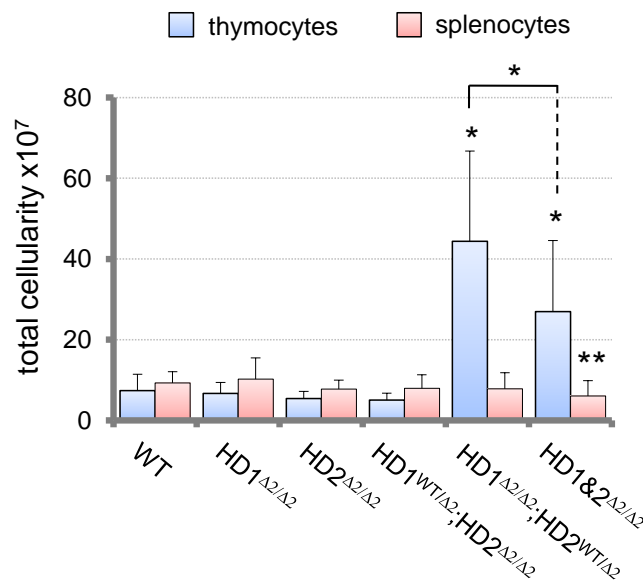
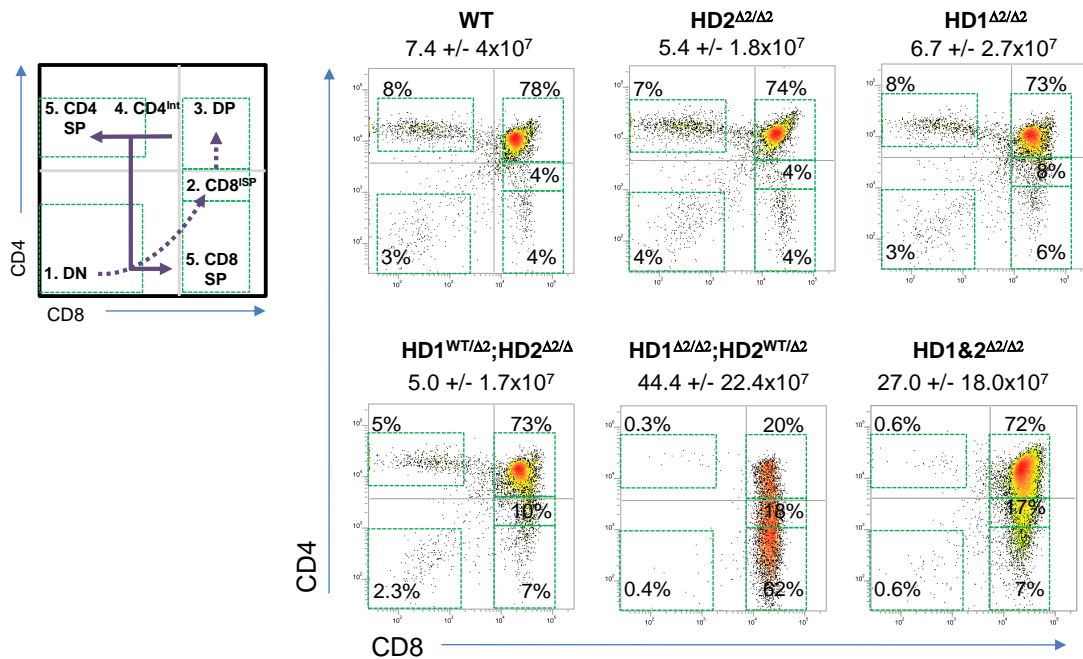


Figure 5.3. Increased thymocyte cellularity in HD1^{Δ2/Δ2};HD2^{WT/Δ2} and HD1&2^{Δ2/Δ2} in 6-8 week old mice. Total thymocyte and splenocyte cellularity of the genotypes indicated. Represented are mean cellularity ±S.E.M. of 6-8 week old mice. WT (n=13), HD1^{Δ2/Δ2} (n=13), HD2^{Δ2/Δ2} (n=22), HD1^{WT/Δ2};HD2^{Δ2/Δ2} (n=11), HD1^{Δ2/Δ2};HD2^{WT/Δ2} (n=16) and HD1&2^{Δ2/Δ2} (n=16). (*p<0.05, **p<0.01 paired T-Test).

increases of 32 and 2 fold when compared to WT LMCs (CD4^{low}/CD8^{high} cellularity with regards to all affected genotypes: HD1^{Δ2/Δ2};HD2^{WT/Δ2}>HD1&2^{Δ2/Δ2}>HD1^{WT/Δ2};HD2^{Δ2/Δ2}>HD1^{Δ2/Δ2}) (Fig 5.4A, percentages and Fig5.4C, CD4^{low}/CD8^{high} cellularity). These same mutant mice display observable decreases in CD4 single positive (CD4SP) cellularity, inverse to the increase in CD4^{low}/CD8^{high} cells. Cellularity of CD4SP thymocytes ranges from 1 x10⁶ in HD1^{Δ2/Δ2};HD2^{WT/Δ2} to 4 x10⁶ in HD1^{Δ2/Δ2} mutants, equivalent to respective decreases of 6 and 1.5 fold when compared to WT LMCs (Fig 5.4A, percentages and Fig5.4D, SP thymocytes cellularity) (CD4SP cellularity with regards to

A.



B.

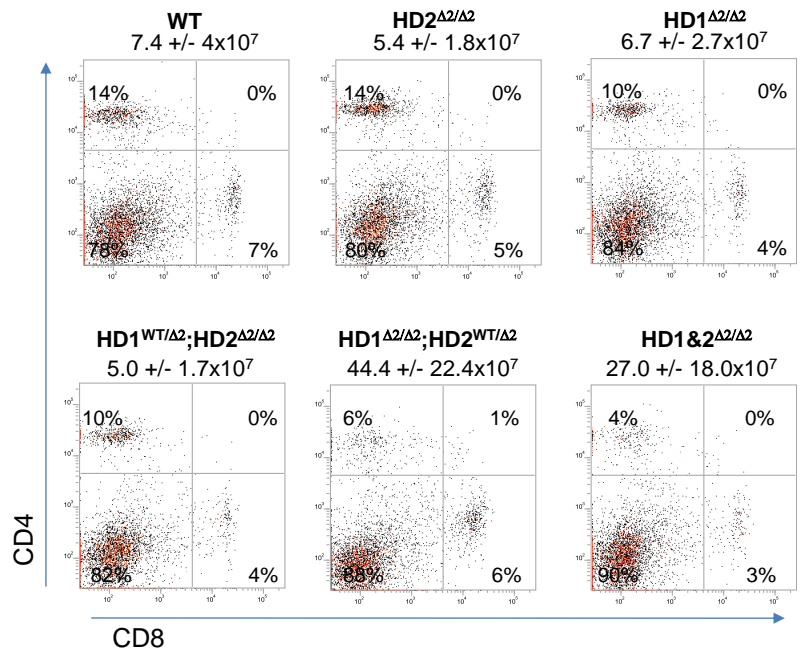


Figure 5.4. *HDAC1* and *-2* are required for normal thymocyte development. Two colour CD4/CD8 FACS analysis of (A) thymocytes and (B) splenocytes obtained from 6-8 week old mice of the indicated genotypes. Total thymocyte cellularity, mean \pm S.E.M. and average percentages of gated developmental populations are shown. (WT=20), (HD1^{Δ2/Δ2}=16), (HD2^{Δ2/Δ2}=11), (HD1^{WT/Δ2};HD2^{Δ2/Δ2}=11), (HD1^{Δ2/Δ2};HD2^{WT/Δ2}=16) and (HD1&2^{Δ2/Δ2}=15).

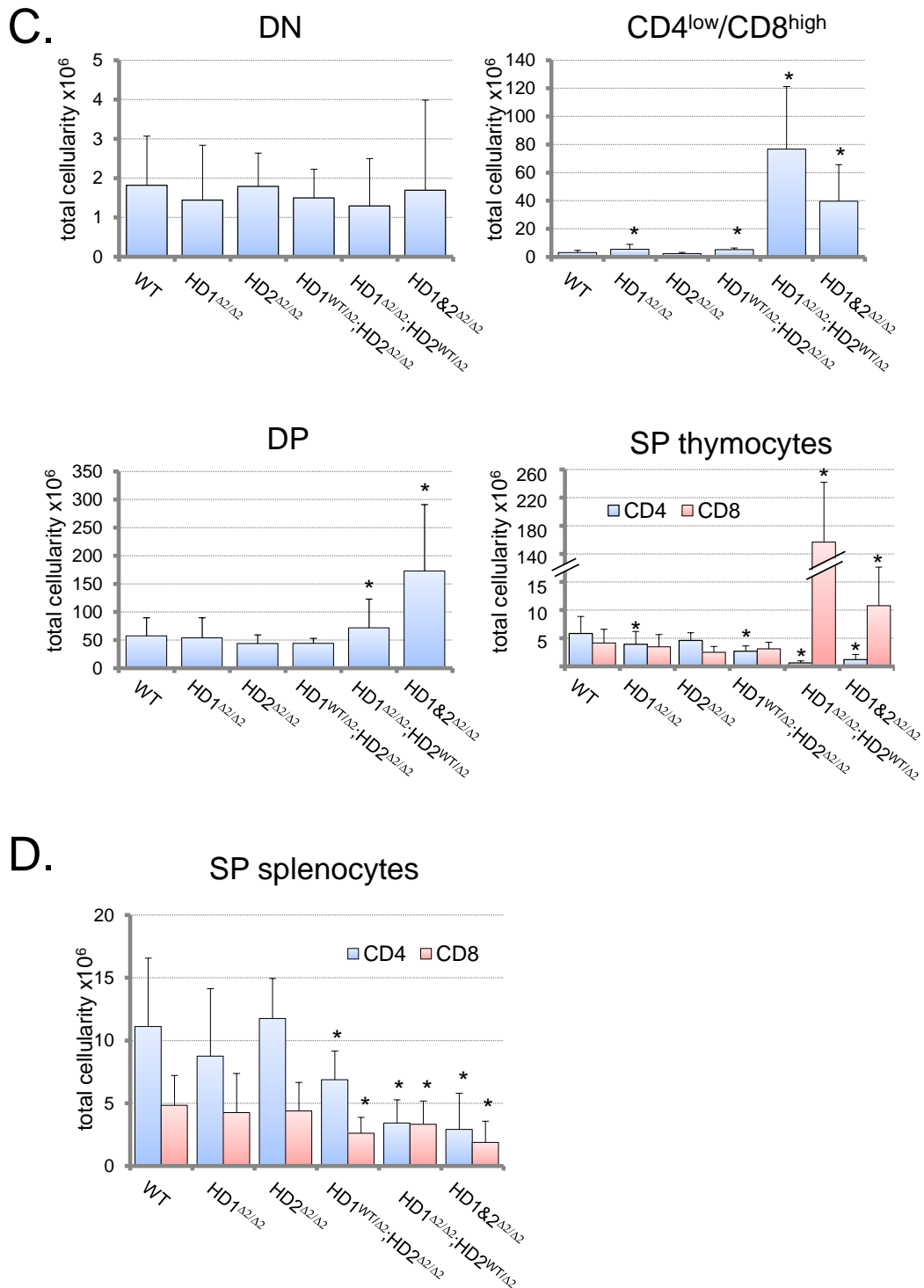


Figure 5.4 continued. *HDAC1* and *-2* are required for normal thymocyte development. Cellularity of intra-thymic maturation sub-populations (C) and of CD4/CD8 single positive splenocytes (D) of 6-8 week old mice. Represented are mean cellularity \pm S.E.M. (WT=20), (HD1^{Δ2/Δ2}=16), (HD2^{Δ2/Δ2}=11), (HD1^{WT/Δ2};HD2^{Δ2/Δ2}=11), (HD1^{Δ2/Δ2};HD2^{WT/Δ2}=16) and (HD1&2^{Δ2/Δ2}=15). (*p<0.05, paired T-Test.)

Genotype: HD1^{Δ2/Δ2};HD2^{WT/Δ2} < HD1&2^{Δ2/Δ2} < HD1^{WT/Δ2};HD2^{Δ2/Δ2} < HD1^{Δ2/Δ2}). A reduction in CD4SP (or an increase in CD4^{low}/CD8^{high}) thymocyte cellularity is also concomitant with a decrease in the percentage of double positive (DP) thymocytes (Fig 5.4A). A decrease in the percentage of DP and CD4SP cells (thymocyte sub-populations that, developmentally, are subsequent to CD4^{low}/CD8^{high} thymocytes) is suggestive of a block in T cell maturation and development. DP thymocytes make up the majority of developing thymocytes and the decrease in DP percentages of HD1^{Δ2/Δ2} or HD1^{WT/Δ2};HD2^{Δ2/Δ2} (percentage of DP thymocytes for both genotypes is 73%) appears to be too subtle to be translated into significant decreases in overall DP cellularity when compared to WT LMCs (the percentage of DP thymocytes in WT LMCs is 78%). In contrast, and despite larger reductions in the percentage of DP cells in HD1^{Δ2/Δ2};HD2^{WT/Δ2} and HD1&2^{Δ2/Δ2} thymocytes (almost a 75% reduction in HD1^{Δ2/Δ2};HD2^{WT/Δ2} mice), significant respective increases of 1.5 and 3 fold in DP cellularity are recorded (Fig 5.4C, DP), due to the overall increase in total thymocyte cellularity of these mice.

Subtle increases in the percentage of CD8SP thymocytes of HD1^{Δ2/Δ2} or HD1^{WT/Δ2};HD2^{Δ2/Δ2} mice (from 4% in WT LMCs to 6 and 7% respectively) are also not translated into significant increases in CD8SP thymocyte cellularity. In contrast, as a consequence of increased total thymocyte cellularity, a small increase in the percentage of CD8SP cells in double targeted HD1&2^{Δ2/Δ2} mice (from 4-7%) manifests as a 2 fold increase in CD8SP thymocyte cellularity. In HD1^{Δ2/Δ2};HD2^{WT/Δ2} thymocytes the majority of cells appear CD8SP (62%) resulting in an increase of approximately 25 fold more CD8SP thymocytes when

compared to WT LMCs, a striking result given that in the periphery (i.e. the spleen) both CD4SP and CD8SP cellularity is reduced (Fig 5.4A for gated percentages, Fig 5.4C for gated thymocyte cellularity and 5.4D for CD4/CD8SP splenocyte cellularity). This is also true in the instances of peripheral HD1^{WT/Δ2};HD2^{Δ2/Δ2} and HD1&2^{Δ2/Δ2} CD4 and CD8SP splenocytes (Fig 5.4D, SP splenocytes). The reduction in circulating CD4 and CD8SP T cells is consistent with a block in intra-thymic development and T cell maturation which may be linked to an increase in CD4^{low}/CD8^{high} thymocytes and a reduction in the percentage of DP cells. Thus far, all of the described phenotypes (due to their similarity) point to redundant and shared roles of HDAC1 and -2, however the severity of these developmental phenotypes appears to be dominantly conferred by the absence of HDAC1. Notably, the thymocyte cellularity and maturation phenotype of HD1^{Δ2/Δ2} mice, although similar to HD1^{WT/Δ2};HD2^{Δ2/Δ2}, differs in that deletion of HDAC1 alone does not affect the number of circulating SP thymocytes, suggesting that despite the dominant defects in development upon deletion of HDAC1, HDAC2 is not dispensable during thymocyte maturation or is able to compensate, at least in part, in the absence of HDAC1.

In order to determine the developmental nature of the aberrant CD8SP and CD4^{low}/CD8^{high} populations (henceforth denoted mutant -CD8 thymocytes) four colour FACS was performed, incorporating maturation markers whose expression is independent of CD4 or CD8 coreceptor expression. Potentially, the mutant -CD8 positive cells are DP cells that fail to express the CD4 coreceptor, CD8^{ISP} cells (CD4^{low}/CD8^{high}-DP precursors) or even CD8SP cells. These experiments were carried out in neonatal mice aged between 1-2 weeks old. As thymocyte maturation occurs in continuous, asynchronous waves and

peaks in mice around 6-8 weeks, I rationalised that performing these experiments on neonatal mice would provide clearer data, as potentially I would be examining the maturation process in a more homogeneous population, thus providing a clearer “snap-shot” of development. Also, I was intrigued to see if the increase in cellularity in HD1^{Δ2/Δ2};HD2^{WT/Δ2} and HD1&2^{Δ2/Δ2} mice was the result of an aberrant, long-lived, population of cells or the result of an increase in the proliferative capacity of these cells. Further to this, I felt there was the potential for revealing a more accurate analysis of HD1&2^{Δ2/Δ2} thymocyte development. Given that at 6-8 weeks the increase in HD1^{Δ2/Δ2};HD2^{WT/Δ2} total thymocyte cellularity is significantly more than HD1&2^{Δ2/Δ2} mice (Fig 5.3) and when compared to HD1^{Δ2/Δ2};HD2^{WT/Δ2} thymocytes, double knock-out thymocytes have comparable remaining levels of HDAC2 (Fig 5.2), I reasoned that the majority of HD1&2^{Δ2/Δ2} thymocytes acquired comparable levels of HDAC2 during the developmental process. HDAC1 and -2 appear to be essential for normal thymocyte development. An extended period in their absence increases the chances of HDAC1 and -2 expressing cells to be selected for survival during intra-thymic expansion (through the combination of the selective pressures during thymocyte development, on potentially a small sub-set of un-recombined cells and what seems to be the strong survival or proliferation advantage conferred in HD1^{Δ2/Δ2};HD2^{WT/Δ2} thymocytes). As such, earlier analysis of HD1&2^{Δ2/Δ2} mice may provide a sample set that exhibit a cleaner deletion of HDAC2 protein.

5.4.1 Mutant-CD8 cells are immature thymocytes that fail to express CD4 at the DP stage.

Examination of neonatal HDAC1 and -2 deleted thymocytes reveals equivalent reductions in HDAC1 and -2 protein levels as observed in 6-8 week old mice. Increases in HDAC2 protein levels in thymocytes lacking HDAC1 (i.e. HD1^{Δ2/Δ2} and HD1^{Δ2/Δ2};HD2^{WT/Δ2} mice) are similarly detected. Significantly, deletion of HDAC2 in thymocytes from HD1&2^{Δ2/Δ2} mice, although variable, is much improved in neonates (Compare Fig 5.5A far right panels with Fig 5.2 bottom panels). Interestingly, total thymic cellularity of HD1^{Δ2/Δ2};HD2^{WT/Δ2} mice is unaltered when compared to WT LMC suggesting, that in neonates, these mice have yet to exhibit the survival or growth advantage observed in older mice (Fig 5.5B). In contrast, neonatal double knock-out HD1&2^{Δ2/Δ2} thymocytes exhibit a striking decrease in total cellularity (25% of WT LMC, Fig 5.5B) with an almost 6 fold increase in the percentage of double negative (DN) cells (this phenotype is examined later in this chapter) (Fig 5.5C).

With the exception of double knock-outs (discussed in 5.1.6), FACS analysis of thymocyte development using CD4/CD8 coreceptor expression in neonates (gating cells as either positive or negative for coreceptor expression) reveals similar developmental profiles as observed for 6-8 week old mice (Fig 5.5C). Again we observe decreases in the number of CD4SP cells in HD1^{WT/Δ2};HD2^{Δ2/Δ2}, HD1^{Δ2/Δ2};HD2^{WT/Δ2} and HD1&2^{Δ2/Δ2} but not in HD1^{Δ2/Δ2} or HD2^{Δ2/Δ2} single targeted mice (Fig 5.5D). Concomitant with these decreases we see an increase in the percentage and total cellularity of the mutant-CD8 population (CD8 or CD4^{low}/CD8^{high}) of the same mice, as well as a significant

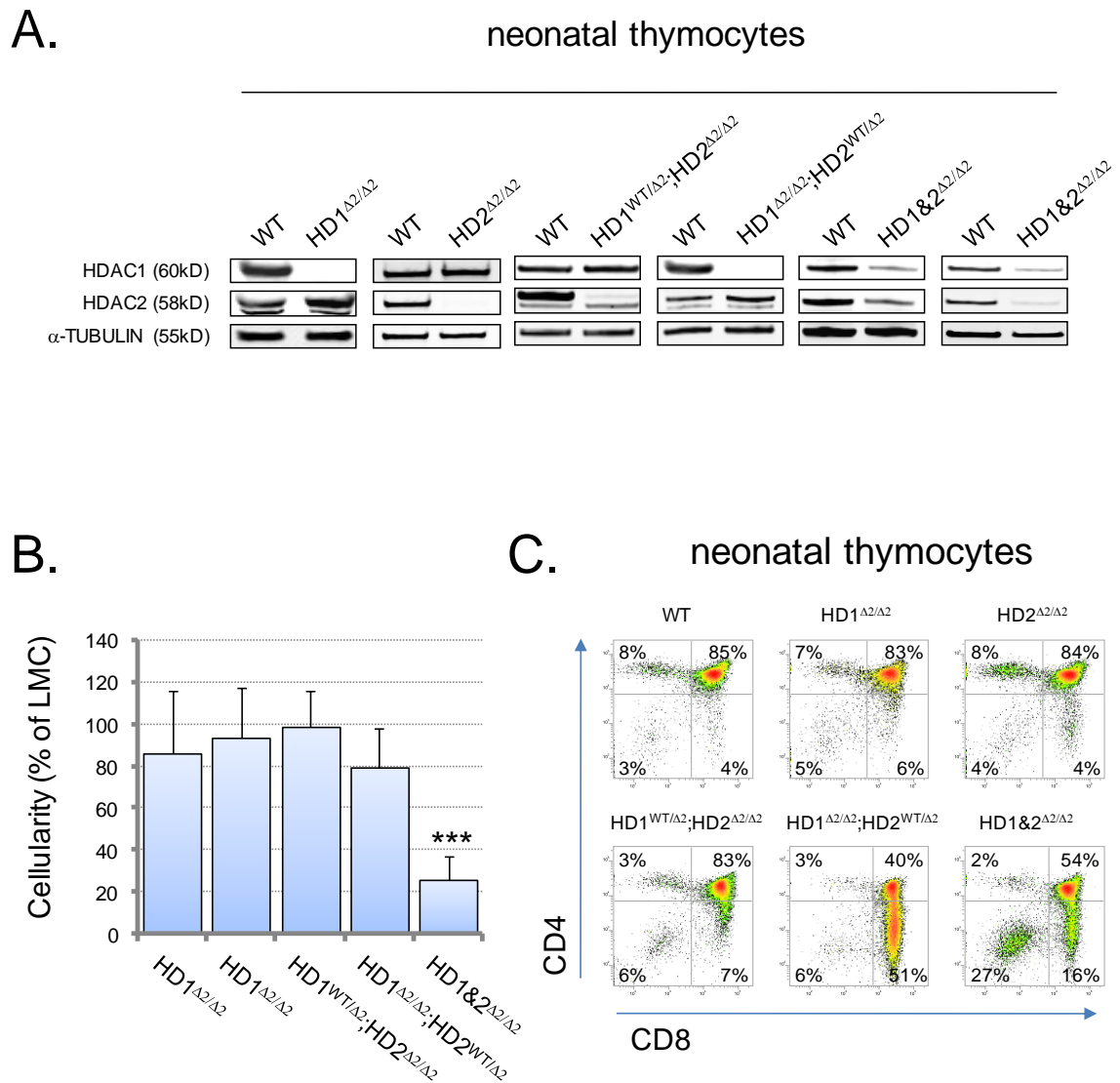


Figure 5.5. Neonatal thymocytes exhibit similar intra-thymic developmental defects as observed in 6-8 week old mice. (A) Western blots, performed as in Figure 5.2 shows improved deletion of HDAC1 and -2 in neonatal mice. (B) Comparative total thymocyte cellularity compared to LMCs of neonatal thymocytes from the genotypes indicated. (C) Two colour CD4/CD8 FACS of neonatal thymocytes from the genotypes indicated shows increase in the percentage of double negative cells in double knock-out mice and similar phenotypes for all other genotypes, as observed in 6-8 week old mice. Represented are mean \pm S.E.M. For (B) and (C) ($n > 6$) (***) $p < 0.001$, paired T-Test).

D.

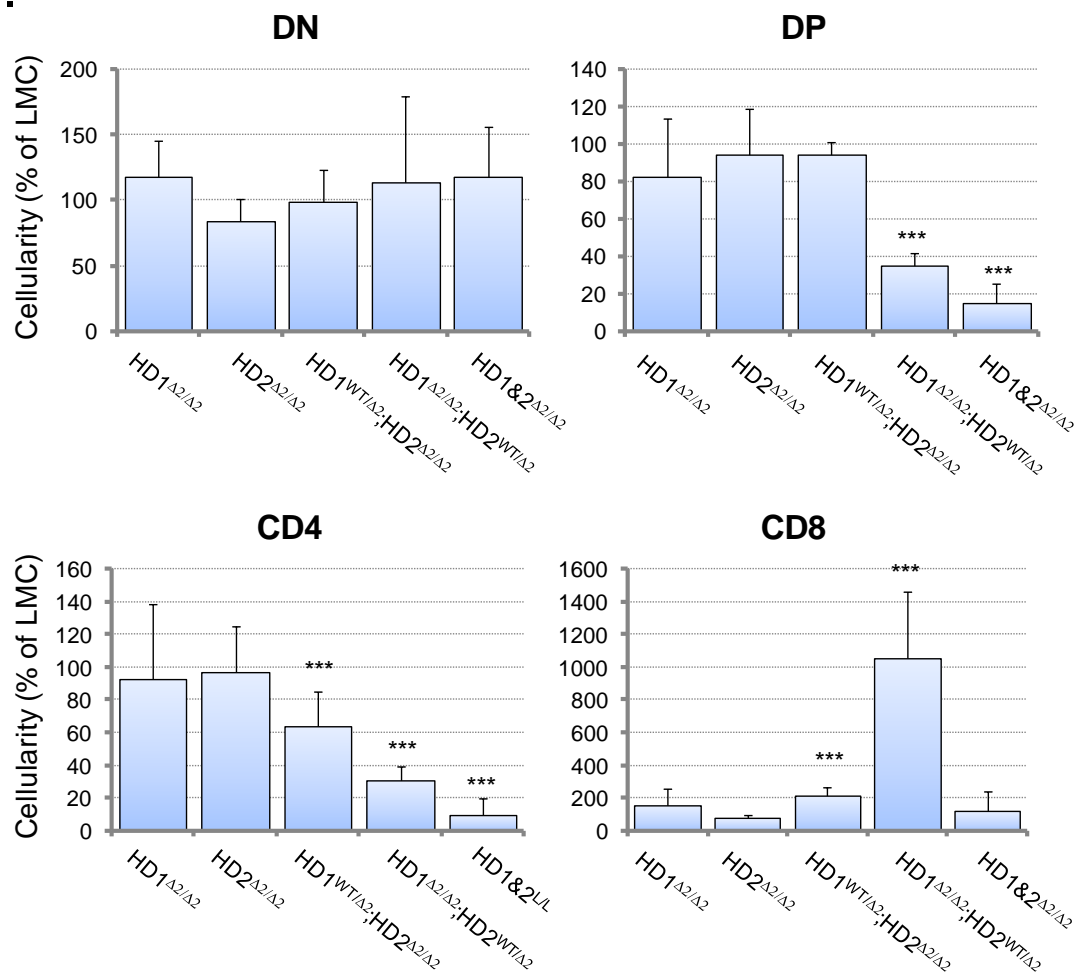


Figure 5.5 continued. Neonatal thymocytes exhibit similar intra-thymic developmental defects as observed in 6-8 week old mice. (D) Comparative cellularity of intra-thymic maturation subpopulations for the genotypes indicated expressed as a percentage of WT LMCs. Represented are mean \pm S.E.M. ($n \geq 6$ for all genotypes) (***) $p < 0.001$, paired T-Test).

decrease in the percentage, and in neonates, the number of HD1 $\Delta 2/\Delta 2$;HD2 $^{WT/\Delta 2}$ and HD1&2 $\Delta 2/\Delta 2$ DP thymocytes (Fig 5.5C, percentages and Fig 5.5D cellularity). An exception to these observations are thymocytes from HD1 $\Delta 2/\Delta 2$ mice which exhibit a subtler increase in the mutant-CD8 population than observed in older mice of the same genotype (Fig 5.5C, percentages and D, cellularity). Again, loss of HDAC1 correlates with the severity of this particular developmental phenotype. Expression of TCR β is progressively up-

regulated in developing thymocytes from negative/low in DN cells, low/intermediate in DP cells, to high in CD4 and CD8SP cells. Conversely, HSA is progressively down regulated in developing thymocytes from high in DN and DP cells, to low in CD4 and CD8SP cells. Using these maturation markers, focusing on HD1^{WT/Δ2};HD2^{Δ2/Δ2} and HD1^{Δ2/Δ2};HD2^{WT/Δ2} thymocytes, reveals a 50% reduction in the total number of SP cells when compared to WT LMCs (Fig 5.6A, TCRβ^{high}/HSA^{low}, green bar. Note the almost complete absence of these cells in HD1&2^{Δ2/Δ2} thymocytes which is discussed later). Analysis of the number of CD4SP or CD8SP TCRβ^{high}/HSA^{low} cells reveals the decrease is owed to a reduction in the CD4SP population, the magnitude of which correlates to deletion of HDAC1 (HD1^{WT/Δ2};HD2^{Δ2/Δ2} mice have 60% of WT LMC CD4SP cellularity versus 30% in HD1^{Δ2/Δ2};HD2^{WT/Δ2} mice) (Fig 5.6B and C, TCRβ^{high}/HSA^{low} SP). The number of CD8SP cells remains unchanged in both HD1^{WT/Δ2};HD2^{Δ2/Δ2} and HD1^{Δ2/Δ2};HD2^{WT/Δ2} mice, which points to either impaired CD4 lineage commitment or a reduced survival capacity of CD4SP cells in the absence of optimal levels of HDAC1 and -2 in neonates (Fig 5.6D). Furthermore, combined analysis of CD4/CD8 expression and TCRβ/HSA gating identifies that the mutant-CD8 population exhibits an immature profile, similar to WT DN, CD8^ISP (CD4^{low}/CD8^{high}) or DP cells (Fig 5.6B and C, TCRβ^{neg}/HSA^{high} and TCRβ^{low}HSA^{high} gated) and not mature CD8SP thymocytes (Fig 5.6B and C, TCRβ^{high}/HSA^{low} gated). Calculating the cellularity of individual CD4/CD8 sub-populations of TCRβ^{neg}/HSA^{high} and TCRβ^{low}HSA^{high} gated thymocytes reveals that the majority of mutant-CD8 cells are DP-like with regards to maturity (TCRβ/HSA expression) (Fig 5.6C) but fail to express the appropriate

cell surface levels of the CD4 coreceptor to be classed as *bona fide* DP (CD4/CD8 expressing) thymocytes.

A.

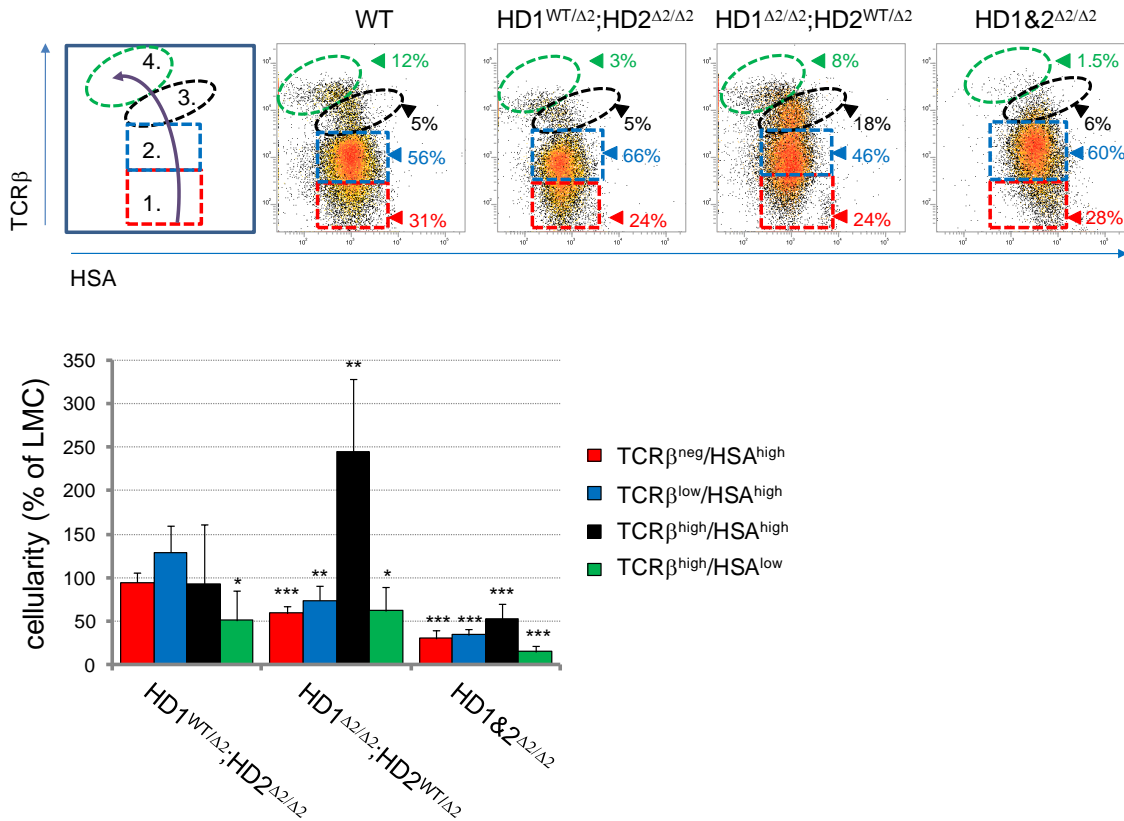


Figure 5.6. *Mutant-CD8 thymocytes exhibit an immature T cell profile.* (A) TCRβ/HSA maturation profiles and comparative cellularity of neonatal thymocytes of mice from the indicated genotypes. Top left panel shows schematic representation of T cell maturation from immature DN to mature SP. Developmental progression and gates are depicted in top left panel as follows; 1. TCRβ^{neg}/HSA^{high} (red); 2. TCRβ^{low}/HSA^{high} (blue); 3. TCRβ^{high}/HSA^{high} (black) and 4. TCRβ^{high}/HSA^{low} (green). Percentage cellularity of WT LMCs, mean ± S.E.M. are shown (HD1^{WT/Δ2};HD2^{Δ2/Δ2}=5) (HD1^{Δ2/Δ2};HD2^{LWT}=7) and HD1&2^{Δ2/Δ2}=10). (*p<0.05, **p<0.01, ***p<0.001, paired T-Test.)

B.

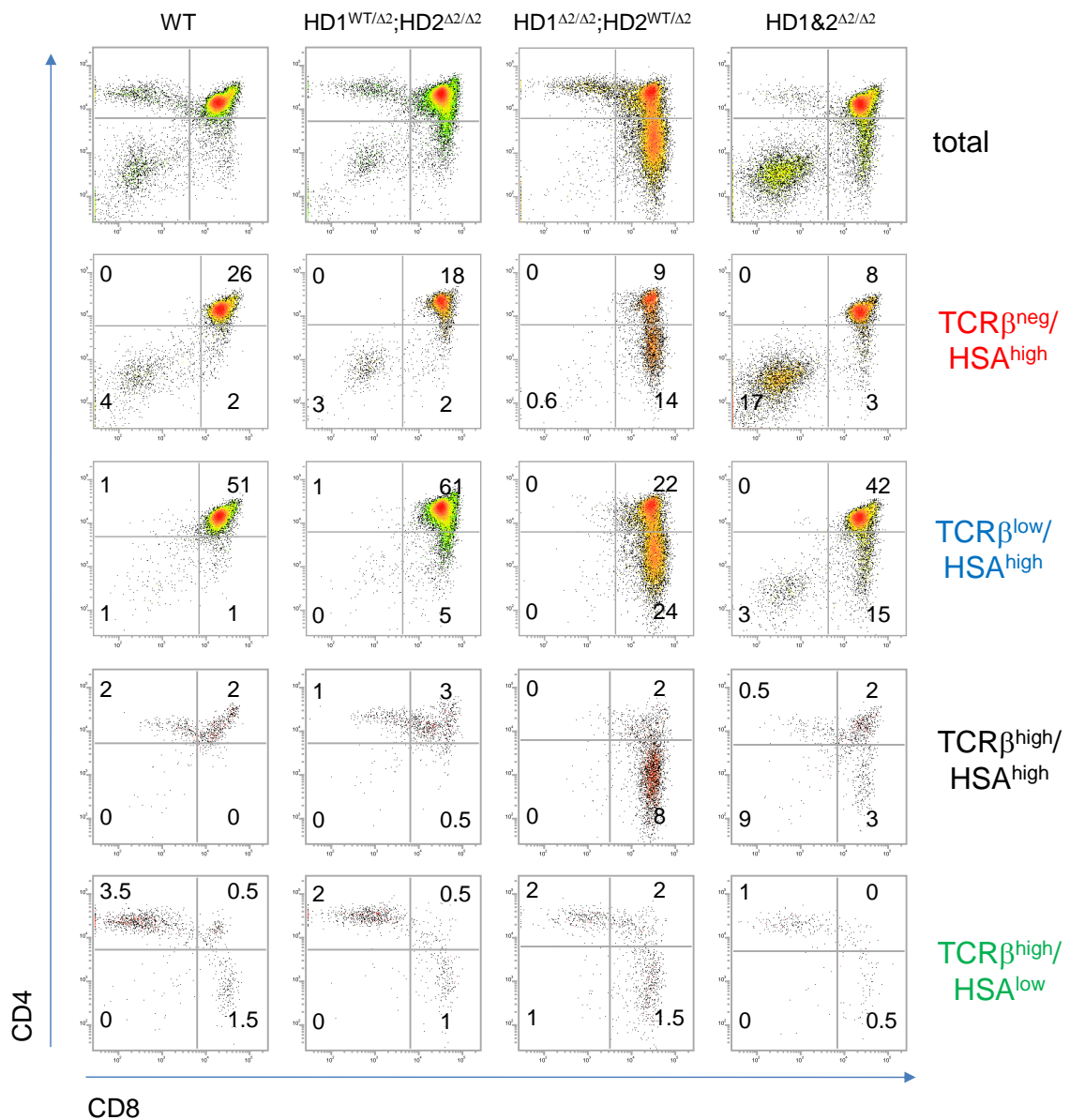


Figure 5.6 continued. *Mutant-CD8 thymocytes exhibit an immature T cell profile.* (B) Intra-thymic developmental sub-populations (as identified by CD4 and CD8 coreceptor expression) of the indicated genotypes, gated as in (A), identify the majority of mutant CD8 positive cells to be similar in maturation to WT double positive cells (TCR β^{low} HSA high) and not mature CD8SP thymocytes (TCR β^{high} /HSA low). Average percentage of DN, DP, CD4SP and CD8SP are shown for each individual TCR β /HSA maturation gate.

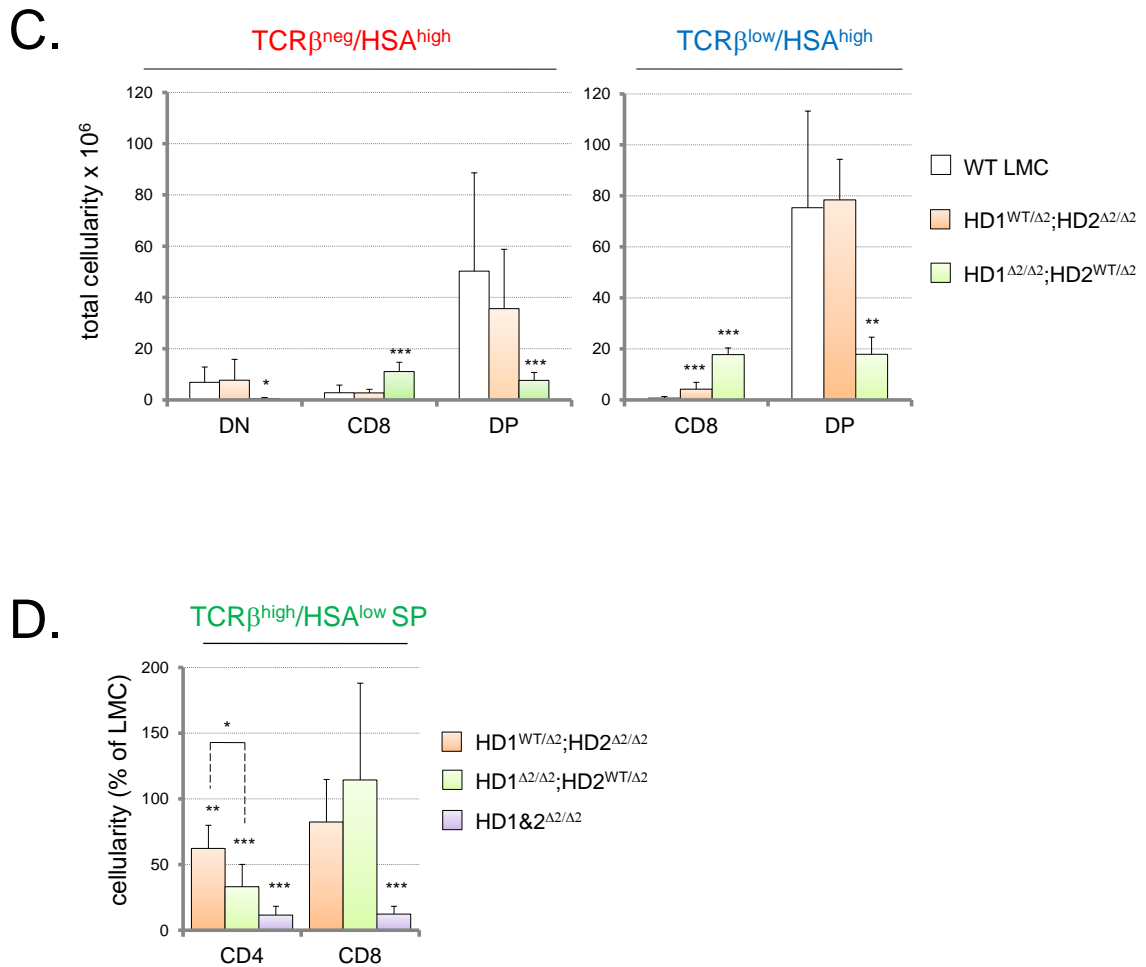


Figure 5.6 continued. *Mutant-CD8 thymocytes exhibit an immature T cell profile.*(C) Intra-thymic developmental sub-population cellularity (as identified by CD4 and CD8 coreceptor expression, as in (B) of the indicated genotypes, gated as in (A), identify the majority of mutant-CD8 positive cells to be similar in maturation to DP (TCR β ^{low}HSA^{high}) and not mature CD8SP (TCR β ^{high}/HSA^{low}SP) thymocytes, top panels. (D) Decreased SP thymocyte cellularity in HD1^{WT/Δ2};HD2^{Δ2/Δ2} and HD1^{Δ2/Δ2};HD2^{WT/Δ2} mice is due to a reduction in CD4SP and not CD8SP cells. Total cellularity (C) and comparative cellularity of LMCs (D) mean \pm S.E.M. are shown (HD1^{WT/Δ2};HD2^{Δ2/Δ2}=5) (HD1^{Δ2/Δ2};HD2^{WT/Δ2}=7) and HD1&2^{Δ2/Δ2}=10). (*p<0.05, **p<0.01, ***p<0.001, paired T-Test).

5.4.2 De-repression of CD8 in HD1^{Δ2/Δ2};HD2^{WT/Δ2} immature double negative thymocytes.

Of note is the apparent absence of any immature double negative (DN, CD4/CD8 negative, TCRβ^{neg}/HSA^{high}) thymocytes in HD1^{Δ2/Δ2};HD2^{WT/Δ2} mice (Fig 5.6B and C, TCRβ^{neg}/HSA^{high}, left panel) Further assessment of DN thymocytes in WT and HD1^{Δ2/Δ2};HD2^{WT/Δ2} mutants, was achieved by analysing thymocytes negative for the expression of TCRβ, CD4 and the B cell marker CD45R (B220). Using biotinylated conjugated versions of antibodies against all three cell surface markers permits the fractionation of a negatively stained (biotin-dump) population, akin to immature DN, TCRβ^{neg}/HSA^{high} thymocytes. Coupled with staining for CD25 and CD44, it is possible to delineate the four stages of immature DN thymocyte development (i.e. the DN1-4 sub-populations). Such analysis reveals the presence of only DN4 (CD25/CD44^{negative}) immature thymocytes in HD1^{Δ2/Δ2};HD2^{WT/Δ2} mice and the almost complete absence of any pre-cursor (DN1-3) sub-populations when compared to WT LMCs (Fig 5.7A). Normal DN thymocyte development is characterised by similarly equivalent DN3 and DN4 populations (Fig5.7A), with transition between the two marked by the β-selection checkpoint, mediated by signal transduction via the pre-TCR complex and requires successful in-frame somatic TCRβ-chain re-arrangement (propelling DN3 cells onto the DN4 stage (Negishi, I., *et al.*, 1995). Thus it appears that HD1^{Δ2/Δ2};HD2^{WT/Δ2} thymocytes are either devoid of, or accelerated through the normal β-selection checkpoint. Analysis of the remaining DN population for CD8 expression reveals precocious expression of the coreceptor when compared to WT LMCs (Fig 5.7B) indicating HDAC1 and -2 are required

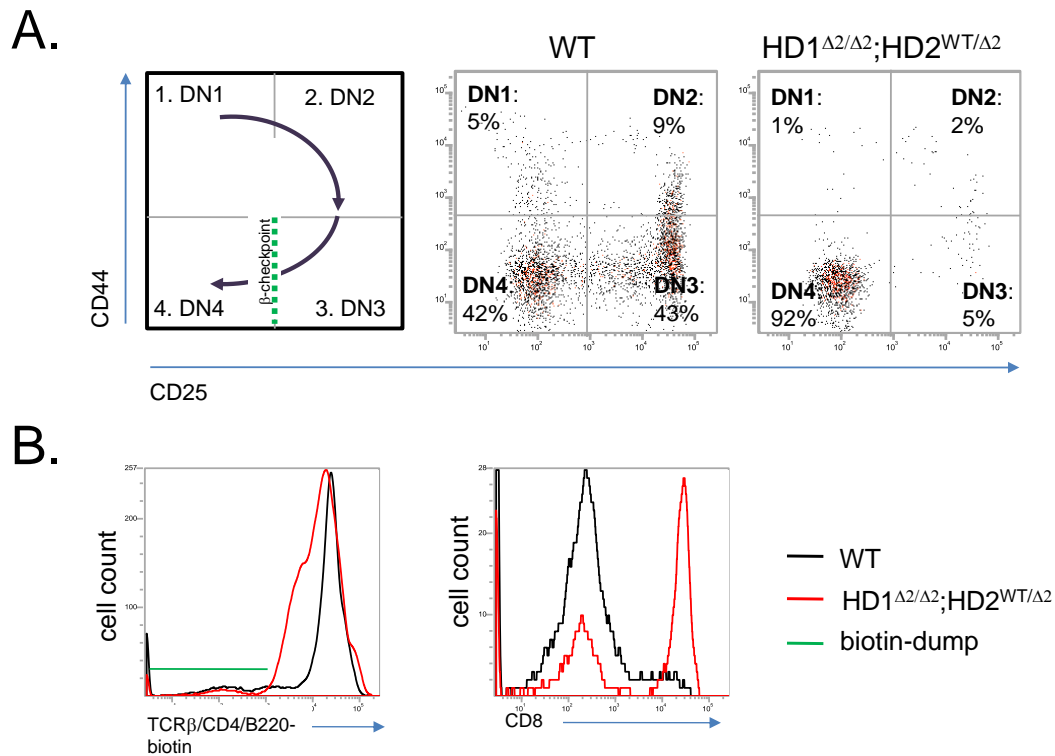


Figure 5.7. De-repression of CD8 in immature double negative $HD1^{\Delta2/\Delta2};HD2^{WT/\Delta2}$ thymocytes. CD25 and CD44 expression of biotinylated TCR β /CD4/B220 (biotin-dump) negative thymocytes were examined for expression of CD25 and CD44 and reveal an absence of the DN1, 2 and 3 subpopulations in $HD1^{\Delta2/\Delta2};HD2^{WT/\Delta2}$ mice. (A) Top left panel is a schematic representation of DN maturation. Developmental progression and gates are depicted in top left panel as follows; DN1, DN2, DN3 and DN4. Green dashed line represents the β -selection checkpoint at the DN3-4 transition. Average percentages of DN1-4 thymocyte sub-populations of WT and $HD1^{\Delta2/\Delta2};HD2^{WT/\Delta2}$ thymocytes are shown ($n>3$). (B) Expression of CD8 in biotin -dump cells was assessed and reveals precocious expression of CD8 at the DN4 stage.

to repress cell surface expression of CD8 during the early stages of thymocyte differentiation. Combined, the two results explain the apparent absence of traditional DN thymocytes in these mice (Fig 5.6B and C).

5.4.3 Deletion of HDAC1 and -2 in HD1&2^{Δ2/Δ2} neonatal thymocytes reveals a delay during β -selection and an increase in apoptosis during the DN-DP transition.

Improved deletion of HDAC1 and -2 in double targeted HD1&2^{Δ2/Δ2} neonates, results in decreased thymocyte cellularity. Gating HD1&2^{Δ2/Δ2} thymocytes on combined TCR β /HSA expression reveals the majority are early developmental, immature TCR β ^{low}/HSA^{high} T cells, at a stage of development similar to WT DN or DP cells (Fig 5.6B, compare far left and far right panels). Calculating the cellularity of DN, CD8^{ISP} (CD4^{low}/CD8^{high}) and DP cells within the TCR β ^{low}/HSA^{high} gate reveals no change in the number of DN cells but significant decreases in the number of CD8^{ISP} and DP cells (Fig 5.8A, to 50% and 15% of WT LMCs) indicating that the reduction in overall cellularity in double targeted mice occurs at the DN-DP stage of thymocyte development. As already described, T cell development at the DN stage can be further delineated by the cell surface expression of CD25 and CD44. Staining thymocytes using antibodies against the cell surface markers CD25, CD44 and biotinylated versions of TCR β /CD8 α /CD4/B220 (biotin-dump) permits the exclusive analysis of DN cells by gating on biotin-dump negative populations and reveals that HD1&2^{Δ2/Δ2} T cells appear to accumulate at the DN3 stage with a concomitant reduction in DN4 cells (Fig 5.8C). As previously described, signal transduction via the pre-TCR complex and propels DN3 cells through the β -selection checkpoint (Negishi, I., *et al.*, 1995). DN4 cells then undergo substantial cellular proliferation and activate CD8 transcription to become the short lived population of CD8^{ISP} (CD4^{low}/CD8^{high}) cells prior to transition to

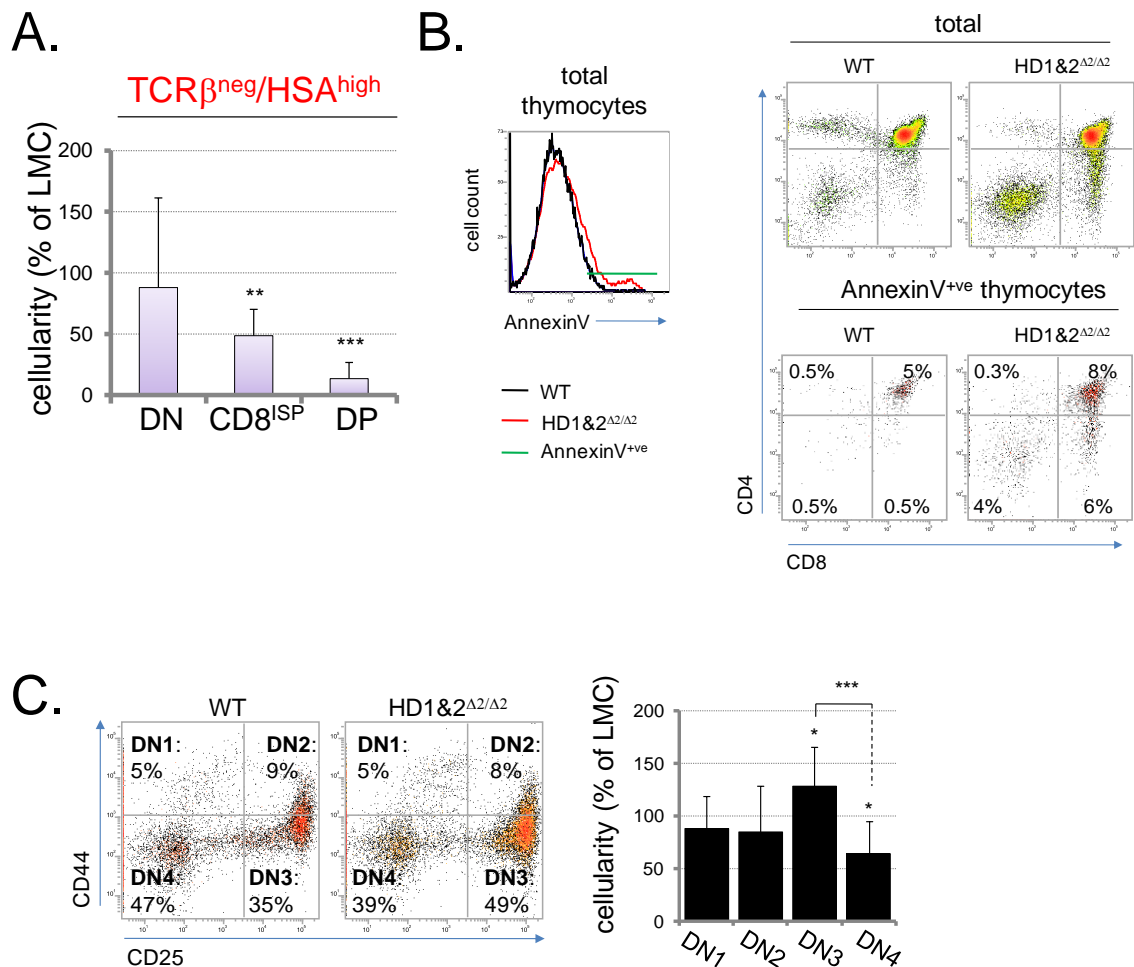


Figure 5.8. Analysis of HDAC1 and -2 in neonatal HD1&2 $\Delta 2/\Delta 2$ thymocytes reveals a delay at the β -selection checkpoint and increased cell death at the DN-DP transition. (A) Cellularity of TCR β ^{neg}/HSA^{high} gated CD4/CD8 intra-thymic developmental sub-populations of WT and HD1&2 $\Delta 2/\Delta 2$ neonatal thymocytes shows a decrease in the number of CD4^{low}/CD8^{high} and DP cells. (B) CD4/CD8 gated intra-thymic developmental distribution of total annexinV positive neonatal WT and HD1&2 $\Delta 2/\Delta 2$ thymocytes (histogram) reveals an increase in the percentage of apoptotic DN, CD8^{ISP}-like (CD4^{low}/CD8^{high}) and DP populations in HD1&2 $\Delta 2/\Delta 2$ mice compared to WT LMCs. Average percentages are shown (n>8). (C) CD25/CD44 expression of biotinylated TCR β /CD8 α /CD4/B220 (biotin-dump) negative thymocytes reveals an increase in DN3 and decrease in DN4 populations. Average percentages and percentage cellularity of WT LMC, mean \pm S.E.M. are shown (n=10), (*p<0.05, **p<0.01, ***p<0.001, paired T-Test)..

the DP stage. Apoptosis staining (using annexinV/propridium iodide) reveals that HD1&2^{Δ2/Δ2} mice have a higher percentage of apoptotic thymocytes compared to WT LMCs with increased apoptosis occurring in DN, CD8^{ISP}-like (CD4^{low}/CD8^{high}) and DP populations (Fig 5.8A and B). Thus, it appears that a full complement of HDAC1 and -2 are required for transition through the β-selection checkpoint. This developmental delay, in combination with increased susceptibility to cell death of DN, CD8^{ISP}(CD4^{low}/CD8^{high}) and DP cells marks a severe defect in the DN-DP transition and could explain the decrease in total numbers of viable DP cells and the subsequent reduction in mature (TCRβ^{high}/HSA^{low}) SP cells in mice deficient in HDAC1 and 2 (Fig 5.6D).

5.4.4 HDAC1 and -2 deficient thymocytes exhibit positive selection defects and reduced CD4 lineage commitment post selection.

The absolute number of TCRβ^{neg}/HSA^{high} and TCRβ^{low}/HSA^{high} thymocytes in HD1^{Δ2/Δ2};HD2^{WT/Δ2} mice is reduced to approximately 50 and 60% of WT LMCs respectively (Fig5.6A), resulting in decreased numbers of DP (or mutant-CD8 DP like) thymocytes (Fig5.6C). An increase of almost 2.5 fold in the TCRβ^{high}/HSA^{high} population maintains parity in overall cellularity with WT LMCs (Fig 5.6A). Thymocytes undergoing positive selection can be fractionated from total thymocyte populations by virtue of their intermediate-high cell surface expression of TCRβ. Typically, these cells are also CD4^{high}/CD8^{low} with regards coreceptor expression. Conspicuously, TCRβ^{high}/HSA^{high} gated HD1^{Δ2/Δ2};HD2^{WT/Δ2} neonatal thymocytes show an almost complete lack of CD4^{high}/CD8^{low} cells (compare the percentages of TCRβ^{high}/HSA^{high} gated

CD4SP cells in figure 5.6B, 0% for HD1^{Δ2/Δ2};HD2^{WT/Δ2} compared to 2% for WT LMCs) despite the relative increase in what appear to be either pre-selection or positively selected (TCRβ^{high}/HSA^{high}) thymocyte numbers (5% in WT LMCs compared to 18% in HD1^{Δ2/Δ2};HD2^{WT/Δ2} mice), (Fig 5.6A). In HD1^{WT/Δ2};HD2^{Δ2/Δ2} mice the number of TCRβ^{high}/HSA^{high} cells is comparative to WT LMCs. Furthermore a marked proportion of these cells are phenotypically CD4^{high}/CD8^{low} suggestive of thymocytes undergoing normal positive selection (Fig 5.6B). Given that there is an observable decrease in HD1^{WT/Δ2};HD2^{Δ2/Δ2} SP neonatal thymocyte cellularity (in particular CD4SPs, Fig 5.6C) suggests that a potential defect in positive selection in HD1^{WT/Δ2};HD2^{Δ2/Δ2} and HD1^{Δ2/Δ2};HD2^{WT/Δ2} mice may account for the reduction in mature SP cellularity.

As a first step in the analysis of positive selection in HDAC1 and -2 deficient mice, CD8 coreceptor expression was assayed. The CD8 coreceptor on most thymocytes is expressed as a disulphide-linked CD8α/CD8β heterodimer, isoforms encoded by the neighbouring CD8α/CD8β genes located on chromosome 6 (Ledbetter, J. A. and Seaman, W.E., 1982, Ledbetter, J.A., *et al.*, 1981). Previously, homozygous deletion of the CD8β gene showed its expression is required for positive selection and development of mature CD8SP thymocytes (Irie, H. Y., *et al.*, 1998 and Nakayama, K. K., *et al.*, 1994). FACS profiles of neonatal thymocytes analysed for cell surface expression of both isoforms reveals a linear relationship in their expression in WT mice and that this relationship is unaffected in mutant HD1^{Δ2/Δ2};HD2^{WT/Δ2} thymocytes (Fig 5.9A).

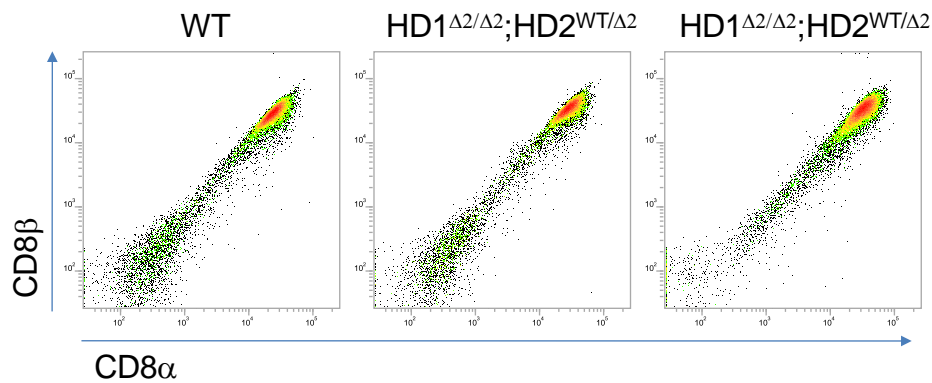


Figure 5.9. Cell surface expression of $CD8\alpha$ and $CD8\beta$ is unaffected in $HD1^{\Delta2/\Delta2};HD2^{WT/\Delta2}$ thymocytes. (A) Thymocytes from WT and $HD1^{\Delta2/\Delta2};HD2^{WT/\Delta2}$ mice were co-stained for $CD8\alpha$ and $CD8\beta$ and analysed by FACS. Dot plots are representative of 3 individual mice of each genotype.

Having established that the mutant-CD8 population have their origins at the DN-DP stage of development and no discernible defect in $CD8\alpha/CD8\beta$ expression in $HD1^{\Delta2/\Delta2};HD2^{WT/\Delta2}$ mice, fractionation of developing neonatal thymocytes, using expression of the maturation markers $CD5$ and $CD69$ (cell surface markers upregulated during positive selection) was performed. Cell surface expression of $CD5$ follows a similar expression pattern in developing thymocytes to that of $TCR\beta$, from negative/low in DN cells, low/intermediate in DP cells and high in SP cells. Thus, analysis of $TCR\beta/CD5$ expression permits an alternative method of delineating developmental sub-populations, especially DP cells that have been positively selected ($TCR\beta^{int}/CD5^{int}$) and terminally differentiated mature CD4 or CD8SP cells ($TCR\beta^{high}/CD5^{high}$) (Azzam, H. S., *et al.*, 1998). Cell surface expression of $CD69$ is transiently up-regulated on thymocytes during positive selection such that

TCR β /CD69 co-staining of thymocytes can be used to define a series of five distinct thymic developmental sub-populations, namely; immature thymocytes (TCR β^{low} /CD69 $^{\text{low}}$), pre-selection thymocytes (TCR β^{int}), thymocytes undergoing positive selection (TCR β^{int} /CD69 $^{\text{int}}$), post-positive selection immature SP thymocytes (TCR β^{high} /CD69 $^{\text{high}}$) and mature SP thymocytes (TCR β^{high} /CD69 $^{\text{low}}$) (Yamashita, I., *et al.*, 1993). With a focus on neonatal HD1 $^{\text{WT}/\Delta 2}$;HD2 $^{\Delta 2/\Delta 2}$ and HD1 $^{\Delta 2/\Delta 2}$;HD2 $^{\text{WT}/\Delta 2}$ mice, thymocyte development using TCR β /CD5/CD69 cell surface expression was assessed. TCR β /CD5 thymocyte profiles are unchanged in single knock-out HD1 $^{\Delta 2/\Delta 2}$ or HD2 $^{\Delta 2/\Delta 2}$ mice compared to WT LMCs and are presented as controls (Fig 5.10A). As discussed, double knock-out HD1&2 $^{\Delta 2/\Delta 2}$ mice show reduced cellularity post the DN stage of thymocyte development and data is presented as a control for a reduction in mature SP cellularity in figure 5.10A. The number of positively selected (TCR β^{int} /CD5 $^{\text{int}}$) and subsequent mature SP (TCR β^{high} /CD5 $^{\text{high}}$) thymocyte numbers are significantly decreased in HD1 $^{\text{WT}/\Delta 2}$;HD2 $^{\Delta 2/\Delta 2}$, HD1 $^{\Delta 2/\Delta 2}$;HD2 $^{\text{WT}/\Delta 2}$ and HD1&2 $^{\Delta 2/\Delta 2}$ thymocytes (75%, 40% and 12% respectively) when compared to LMCs (Fig 5.10A) and in agreement with reduced TCR β^{high} /HSA $^{\text{low}}$ SP cellularity. Despite a large increase in the detection of pre-selection (TCR β^{int}) thymocytes in HD1 $^{\Delta 2/\Delta 2}$;HD2 $^{\text{WT}/\Delta 2}$ mice (2.5 fold compared to WT), only 50% of these cells are CD5 positive, with a 20% reduction observed in the number of HD1 $^{\text{WT}/\Delta 2}$;HD2 $^{\Delta 2/\Delta 2}$ TCR β^{int} /CD5 $^{\text{int}}$ thymocytes (where the total number of TCR β^{int} pre-selection thymocytes is unaltered when compared to controls) (Fig5.10A, cellularity). Similarly the number of TCR β^{int} /CD69 $^{\text{int}}$ positively selected thymocytes are reduced by 20% in HD1 $^{\text{WT}/\Delta 2}$;HD2 $^{\Delta 2/\Delta 2}$ and 70% in

HD1^{Δ2/Δ2};HD2^{WT/Δ2} mice, despite increases in the number of pre-selection TCRβ^{int} thymocytes as defined in this assay (25% and 60% respectively) (Fig 5.10B, cellularity). Of the HD1^{Δ2/Δ2};HD2^{WT/Δ2} thymocytes that are positively selected, again, there are no characteristic CD4^{high}/CD8^{low} cells (indicative of thymocytes undergoing positive selection) as seen in WT LMCs. Note also, the visibly reduced number of these cells in HD1^{WT/Δ2};HD2^{Δ2/Δ2} mice when compared to controls (Fig 5.10C, TCRβ^{int}/CD5^{int} and TCRβ^{int}/CD69^{int} gates). These data provide evidence for reduced efficiency in the positive selection of HD1^{WT/Δ2};HD2^{Δ2/Δ2} and HD1^{Δ2/Δ2};HD2^{WT/Δ2} thymocytes. In agreement with data from 6-8 week old splenocytes and correlating with a decrease in positively selected thymocytes, the numbers of mature CD4 and CD8SP cells (defined as being TCRβ^{high}/CD5^{high}) in both neonatal HD1^{WT/Δ2};HD2^{Δ2/Δ2} and HD1^{Δ2/Δ2};HD2^{WT/Δ2} mice are reduced (Fig 5.10D). This result contrasts with TCRβ^{high}/HSA^{low} gated data in which CD8SP numbers are unaffected. The nature of the former fractionation strategy relies on the use of two positive markers to identify mature SP cells (as opposed to one positive and one negative, as is the case in the latter). Given the aberrant TCRβ expression profile of mutant thymocytes, the reduction in both CD4 and CD8 mature SP cells in neonates, identified as TCRβ^{high}/CD5^{high}, is a more reliable data set and reflects the observed reductions in CD4/CD8 SP cellularity in splenocytes of 6-8 week old mice of the same genotypes (Fig 5.4D). The observed reductions in CD4SP HD1^{WT/Δ2};HD2^{Δ2/Δ2} neonatal thymocytes and 6-8 week old splenocytes is 70% and 60% respectively. In HD1^{Δ2/Δ2};HD2^{WT/Δ2} mice reductions of CD4SP cells in the same compartments are respectively, 20% and 25% (Fig 5.4D and

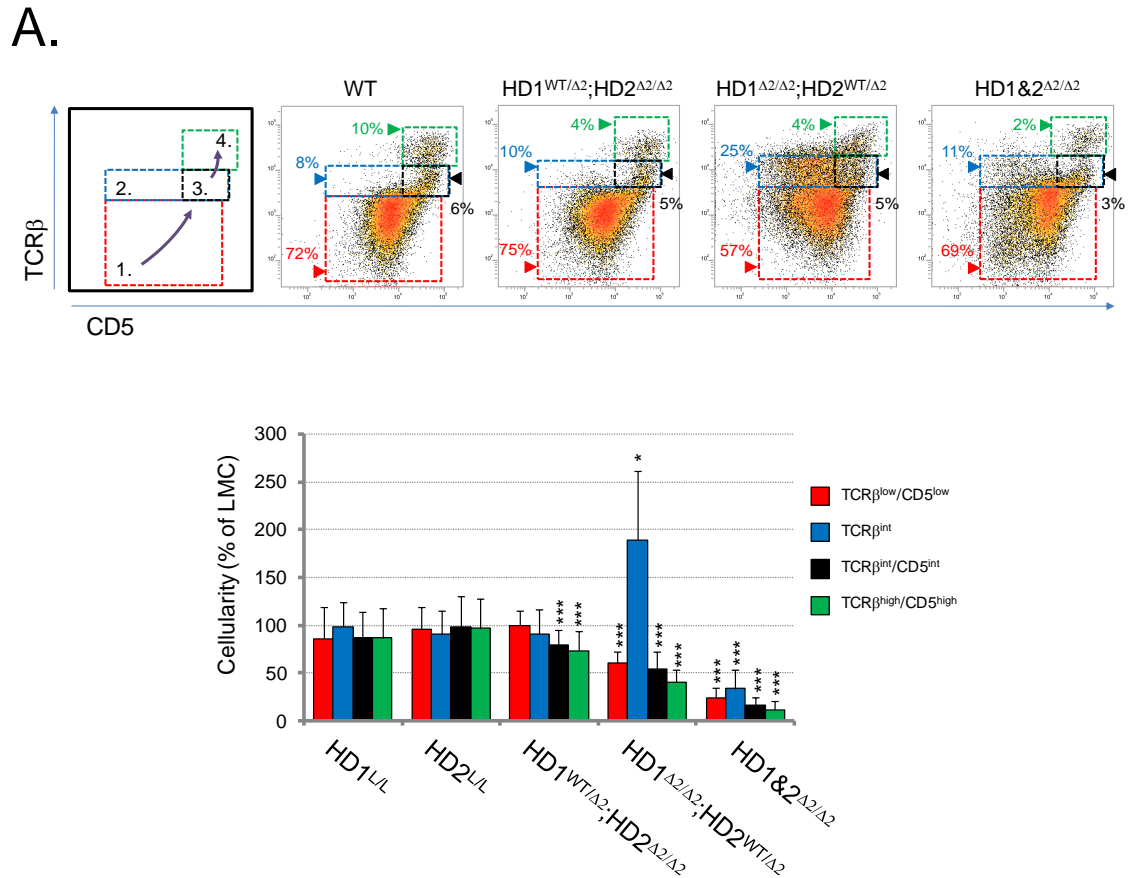


Figure 5.10. *Reduced numbers of “selection” thymocytes in HD1^{WT/Δ2};HD2^{Δ2/Δ2} and HD1^{Δ2/Δ2};HD2^{WT/Δ2} mice.* (A) TCRβ/CD5 maturation profiles and comparative cellularity of neonatal thymocytes of mice from the indicated genotypes. Developmental progression and gates are depicted in top left panel as follows; 1. TCRβ^{low}/CD5^{low} (red); 2. TCRβ^{int} (blue); 3. TCRβ^{int}/CD5^{int} (black) and 4. TCRβ^{high}/CD5^{high} (green). Percentage cellularity of LMCs, mean ± S.E.M. are shown (n>7 for all genotypes). (*p<0.05, **p<0.01, ***p<0.001, paired T-Test.)

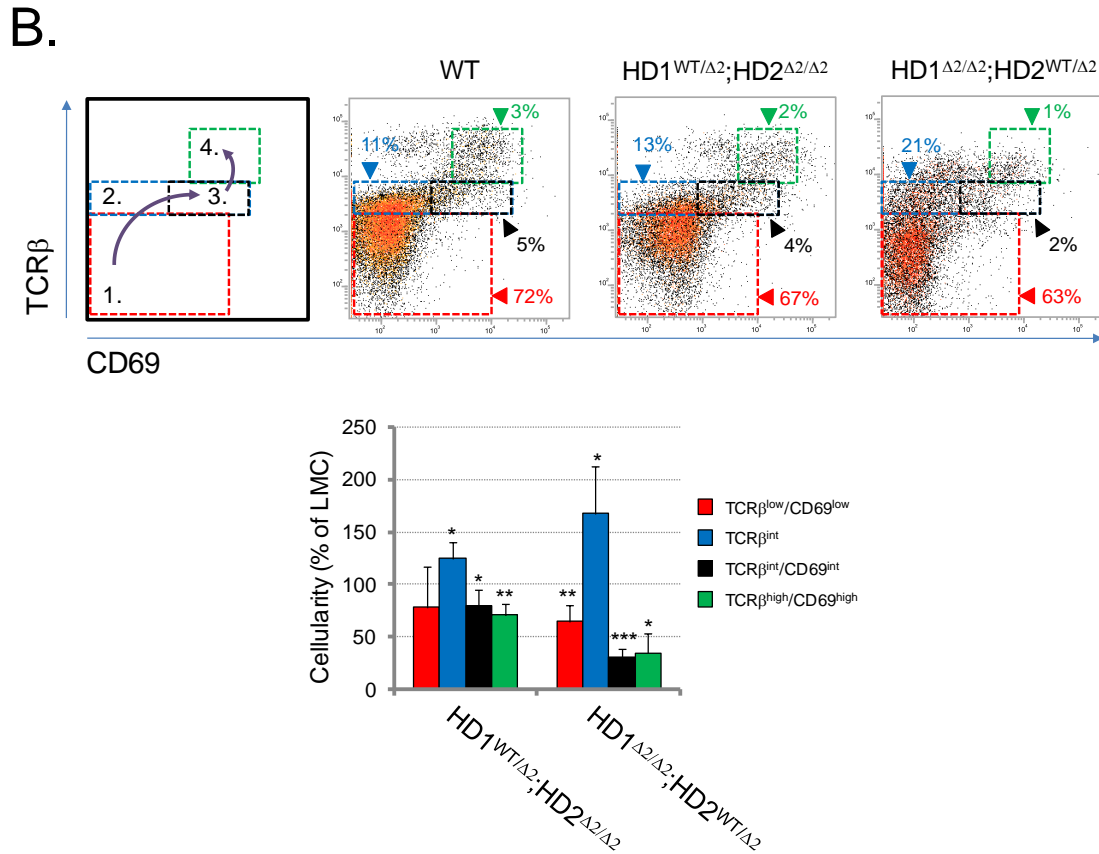


Figure 5.10 continued. *Decreased numbers of “selection” thymocytes in HD1^{WT/Δ2};HD2^{Δ2/Δ2} and HD1^{Δ2/Δ2};HD2^{WT/Δ2} mice.* (B) TCRβ/CD69 maturation profiles and comparative cellularity of neonatal thymocytes of mice from the indicated genotypes. Developmental progression and gates are depicted in top left panel as follows; 1. TCRβ^{low}/CD69^{low} (red); 2. TCRβ^{int} (blue); 3. TCRβ^{int}/CD69^{int} (black) and 4. TCRβ^{high}/CD69^{high} (green). Percentage cellularity of LMCs, mean ± S.E.M. are shown (n>7 for all genotypes). (*p<0.05, **p<0.01, ***p<0.001, paired T-Test.)

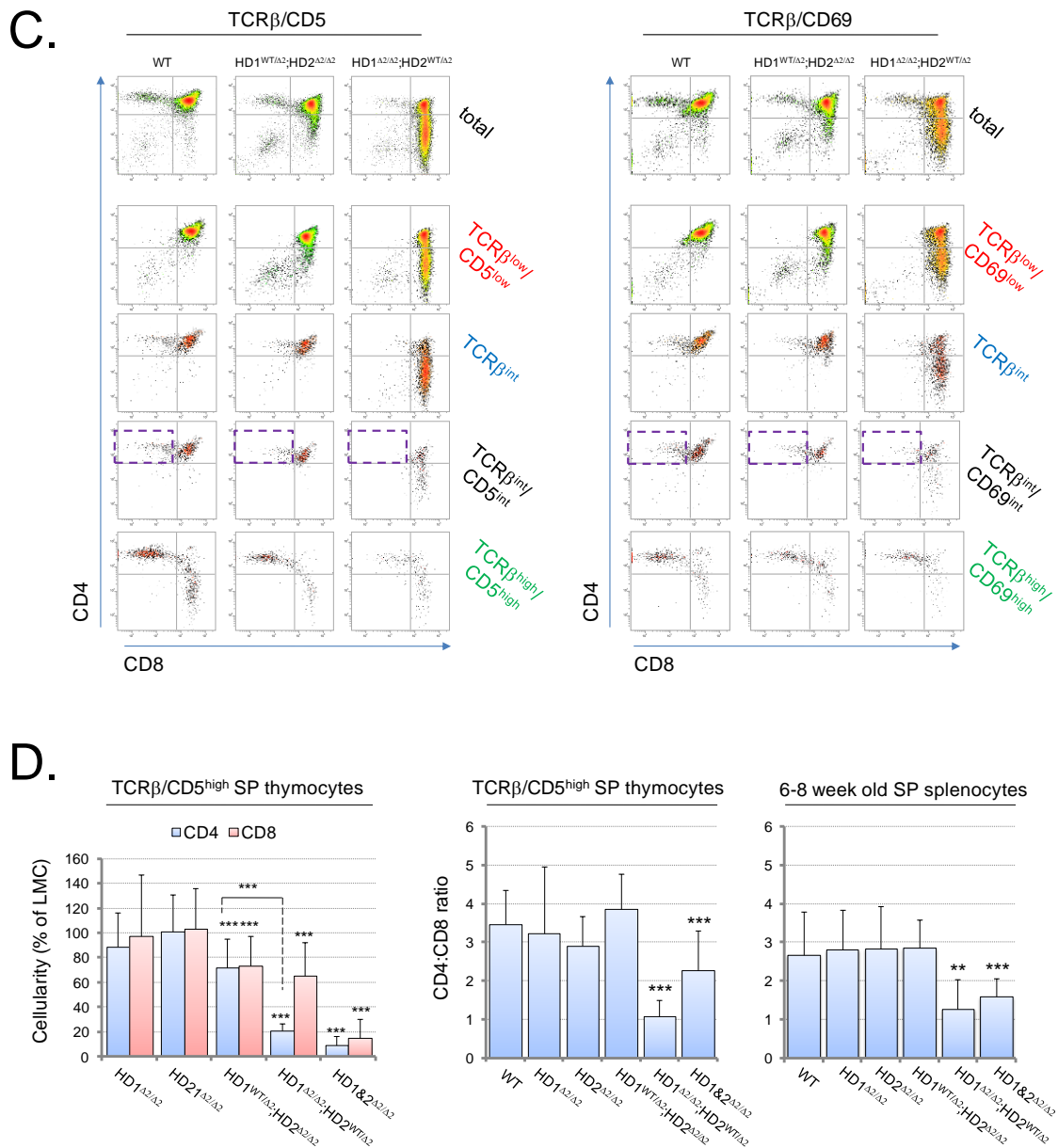


Figure 5.10 continued. *Decreased numbers of “selection” thymocytes in HD1^{WT/Δ2};HD2^{Δ2/Δ2} and HD1^{Δ2/Δ2};HD2^{WT/Δ2} mice.* (C) Intra-thymic developmental sub-populations (as identified by CD4 and CD8 coreceptor expression) of the indicated genotypes, gated as in (A and B), identify a reduction in “selection” thymocytes. Purple dashed box highlights CD4^{high}/CD8^{low} positively selected thymocytes. (D) Decreased cellularity of CD4 and CD8SP (TCRβ/CD5) cells in HD1^{WT/Δ2};HD2^{Δ2/Δ2}, HD1^{Δ2/Δ2};HD2^{WT/Δ2} and HD1&2^{Δ2/Δ2} mice. Ratio of CD4SP:CD8SP neonatal thymocytes and 6-8 week old splenocytes. Percentage cellularity of WT LMCs, mean ±S.E.M. are shown (n>7 for all genotypes). (**p<0.01, ***p<0.001, paired T-Test).

Fig 5.10D). Thus, the reduction in CD4SP cellularity correlates with the number of positively selected thymocytes which, in turn, are negatively correlated to the number of mutant-CD8 cells, dominantly conferred in compound heterozygous conditional knock-out mice by the absence of HDAC1. In contrast, the reduction of CD8SP cells, although reduced, in HD1^{Δ2/Δ2};HD2^{WT/Δ2} neonates is similar to that observed in HD1^{WT/Δ2};HD2^{Δ2/Δ2} mice (approximately 65%, Fig 5.10D). Calculating the ratios of CD4:CD8 post selection SP thymocytes (i.e. TCRβ^{high}/CD5^{high} gated cells) reveals significantly decreased ratios in HD1^{Δ2/Δ2};HD2^{WT/Δ2} mice (1.1) when compared to WT LMCs (3.4) or HD1^{WT/Δ2};HD2^{Δ2/Δ2} mice (3.8) (Fig 5.10D). A similar bias towards CD8SP differentiation is seen in SP splenocytes of 6-8 week old mice (Fig 5.10D, far right panel). Thus not only are HDAC1 and -2 required in maintaining the number of positively selected thymocytes, they are also required for CD4SP lineage commitment post-selection.

5.4.5 The maturation block in HD1^{Δ2/Δ2};HD2^{WT/Δ2} mutant thymocytes is independent of TCR complex formation.

To ascertain if the maturation defects and reduction of SP thymocytes (in particular CD4SP) in HD1^{Δ2/Δ2};HD2^{WT/Δ2} mutant mice was T cell receptor (TCR) dependent, I crossed hdac1 and -2 targeted mice to OT-II mice (Tg^{OT-II}-TCR) which express pre-arranged transgenic forms of the TCRα and β chains. Secondary to addressing issues regarding TCR dependency, the use of OT-II mice also serves as an attempt to rescue the mutant-CD8 phenotype. The pre-arranged α/β chains of OT-II mice are such that transgene expressing

thymocytes only interact with class II MHC molecules and as such the majority of mature thymocytes are CD4SP (Barnden, M. J., *et al.*, 1998). CD4/CD8 coreceptor expression analysis was performed on neonatal thymocytes of WT and HD1 ^{$\Delta 2/\Delta 2$} ;HD2^{WT/ $\Delta 2$} mice in the presence or absence of the transgene. As expected, the majority of SP cells of WT-Tg^{OT-II}-TCR mice are CD4SP (Fig 5.11A, CD4/CD8 dot plot, WT-Tg^{OT-II}-TCR). However, presence of the pre-arranged TCR failed to “rescue” the mutant-CD8 phenotype in total HD1 ^{$\Delta 2/\Delta 2$} ;HD2^{WT/ $\Delta 2$} -Tg^{OT-II}-TCR (Fig 5.11A, dot plots and Fig 5.11B, cellularity). TCRV $\alpha 2$ and V $\beta 5$ antibodies detect the transgenic OT-II TCR α and - β rearrangements. Assessment of CD4/CD8 sub-populations on total thymocytes, as gated on either TCR β ^{high}/CD5^{high} (non-transgenic mice) or on TCRV $\alpha 2$ ^{high}/TCRV $\beta 5$ ^{high} (in mice carrying the OT-II transgene) identifies mature SP thymocytes. In WT mice, presence of the transgene confers a bias in commitment to CD4SP cells when compared to non-transgenic WT LMCs (Fig 5.11B). In HD1 ^{$\Delta 2/\Delta 2$} ;HD2^{WT/ $\Delta 2$} mutant mice the absolute number of SP thymocytes (CD4 or CD8) is not significantly changed on the OT-II background, indicating that the reduction in positive selection and the mutant-CD8 phenotype is independent of TCR complex formation.

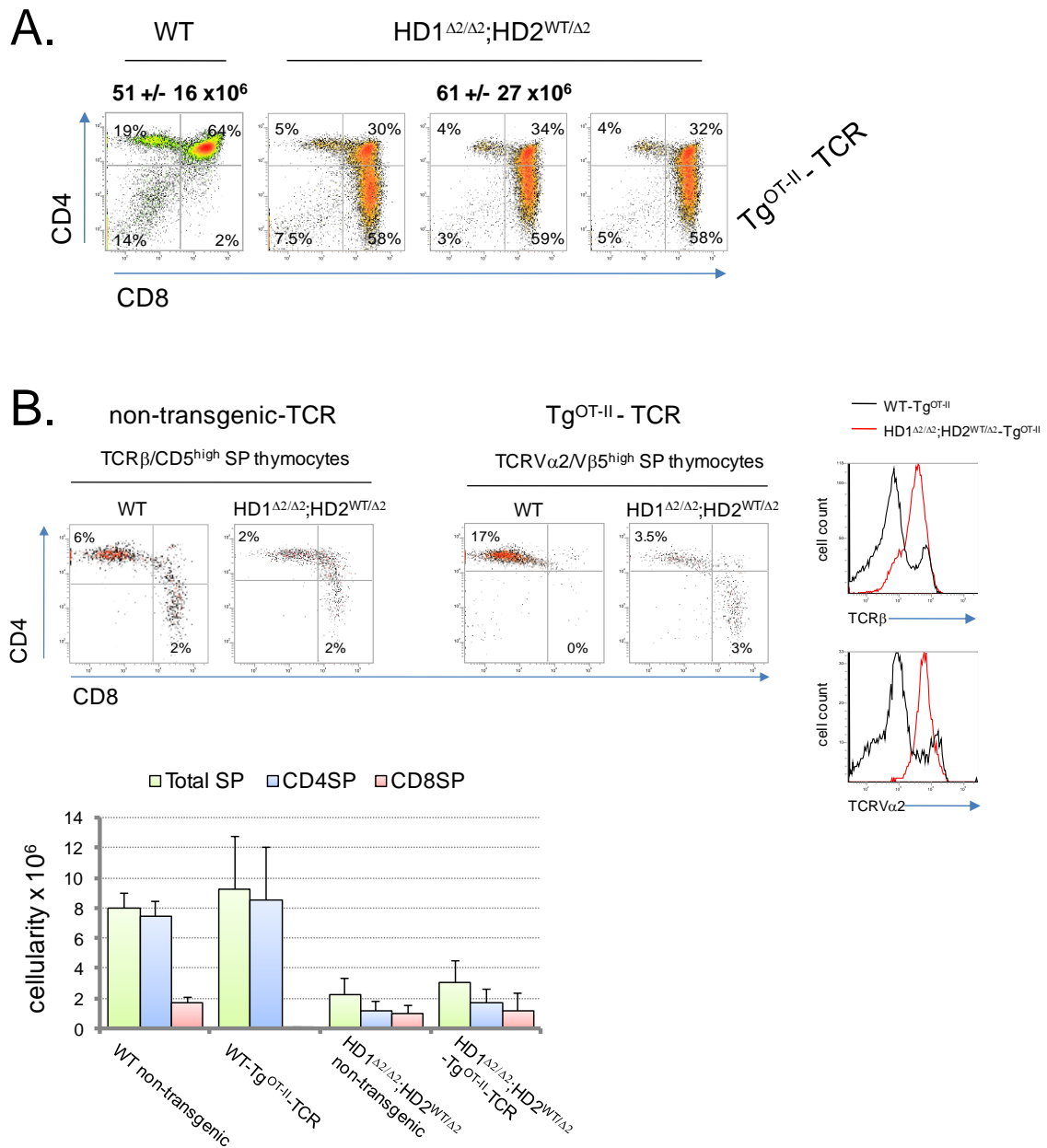
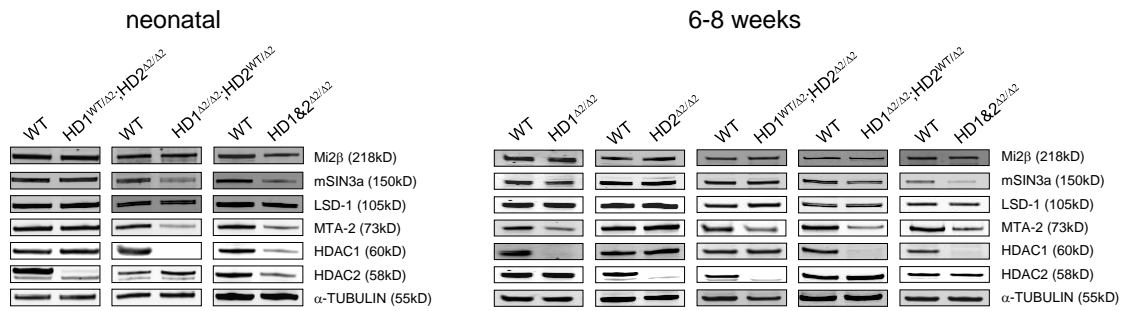


Figure 5.11. The developmental block in thymocytes of HD1^{Δ2/Δ2};HD2^{WT/Δ2} mutant mice is independent of TCR complex formation. Percentage and cellularity of intra-thymic developmental sub-populations (as identified by CD4 and CD8 coreceptor expression) of WT and HD1^{Δ2/Δ2};HD2^{WT/Δ2} mice on the Tg^{OT-II}-TCR background are unchanged compared to non-transgenic mice in either (A) total thymocytes or (B) CD4 and CD8SP thymocytes (non-transgenic, TCRβ/CD5^{high}; Tg^{OT-II} transgenic, TCRVα2/Vβ5^{high}). Total thymocyte cellularity mean ±S.E.M. are shown above dot plots. Average percentages of developmental sub-populations are shown. Cellularity of SP thymocytes, total, CD4SP and CD8SP ±S.E.M. are shown. (n=4 for all genotypes).

5.5 Reduced HDAC activity and co-repressor complex integrity in HDAC1 and -2 knock-out thymocytes.

Consistent with previous reports in mES cells, (Lagger G., *et al.*, 2002, Zupkovitz G., *et al.*, 2006, chapter 4.1.2) deletion of HDAC1 results in increased levels of HDAC2 in thymocytes from both neonates (Fig 5.5A) and 6-8 week old mice (Fig 5.2). Interestingly, when quantified, the increase in HDAC2 in HD1^{Δ2/Δ2} thymocytes (2 fold) is significantly greater than in HD1^{Δ2/Δ2};HD2^{WT/Δ2} mutants (1.5 fold) and permits a previously unobservable distinction to be made between these two genotypes in 6-8 week old mice with regards levels of HDAC1 and -2 protein (Fig 5.12B). As in mES cells, deletion of HDAC2 does not result in increased levels of HDAC1. Most cellular HDAC1 and -2 is associated with higher order protein complexes in the nucleus (Yang X.J. and Seto E., 2008). Western blotting for components of HDAC1 and -2 containing complexes; Sin3a (mSIN3a), NuRD (MTA-2) and CoREST (LSD-1), reveals observable decreases in mSIN3a and MTA-2 (Fig 5.12A, right panel and Fig5.12B). The decrease in mSIN3a correlates with deletion of HDAC1 whereas detectable decreases in MTA-2 are similar in HD1^{WT/Δ2};HD2^{Δ2/Δ2} and HD1^{Δ2/Δ2} thymocytes (~2 fold) with the greatest reduction observed in HD1^{Δ2/Δ2};HD2^{WT/Δ2} knock-outs (~3 fold). Of particular note are similar reductions in mSIN3a and MTA-2 in HD1^{Δ2/Δ2};HD2^{WT/Δ2} neonates (Fig 5.12A, left panel). Using coimmunoprecipitation of these co-repressor components I assessed the associated deacetylase activity and integrity of both Sin3a and NuRD complexes in 6-8 week old conditional knock-out thymocytes. Given that double targeted HD1&2^{Δ2/Δ2} thymocytes are typically HD1^{Δ2/Δ2};HD2^{WT/Δ2} with regards to

A.



B.

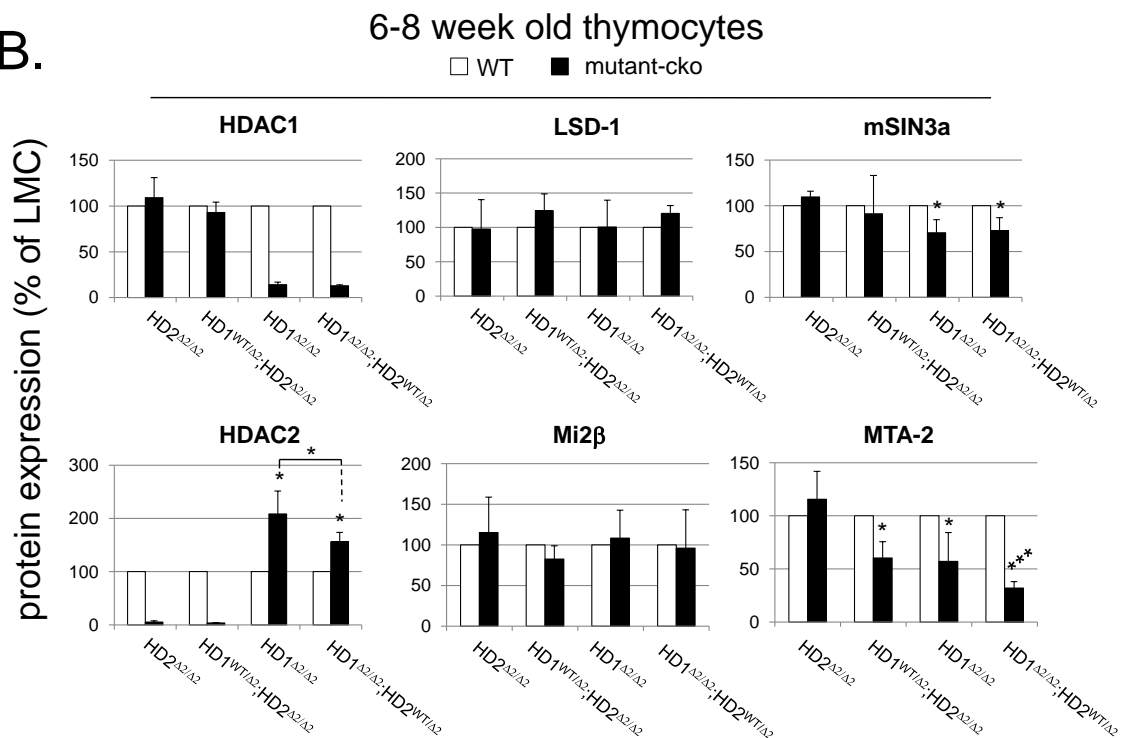


Figure 5.12. *Reduced deacetylase activity associated with HDAC1 and -2 complexes.* (A) Western blots of HDAC1, HDAC2, MTA-2, LSD-1, mSIN3a and Mi2 β of thymocyte nuclear extracts obtained from the genotypes indicated of 6-8 week old mice. (B) Protein levels probed for in (A) of 6-8 week old mice were quantitated using a LiCOR scanner and normalized to the level of α -TUBULIN. Relative protein expression is presented as % of LMCs. Mean values ($n = 3$) \pm S.E.M. are plotted. (* $p < 0.05$, *** $p < 0.001$, paired T-Test).

protein expression, these mice were excluded from the following analyses. Consistent with a reduction in mSin3a in thymocytes lacking HDAC1, a reduction in deacetylase activity is detected. Interestingly, HDAC2 is absent from the Sin3a complex in WT LMCs and only detectable upon deletion of HDAC1 (Fig 5.12C and Fig 5.12D, lanes 3, 7 and 15). In agreement with mES cell data (Chapter 4.2.1) loss of HDAC2 (HD2^{Δ2/Δ2} and HD1^{WT/Δ2};HD2^{Δ2/Δ2}) does not affect the deacetylase potential of the Sin3a complex (Fig 5.12C). Combined, these data provide evidence that in mouse thymocytes, HDAC1 is a preferred complex partner of Sin3a and contributes the majority of Sin3a deacetylase activity or is able to compensate for a loss of deacetylase potential in the absence of HDAC2. In line with reductions in the levels of the NuRD component MTA-2, a marked decrease in the deacetylase potential of MTA-2 immunoprecipitates is observed and correlates well with levels of total MTA-2 protein (Fig 5.12B, MTA-2 and 5.12C). Unlike the Sin3a complex, HDAC1 and -2 are detected in similar amounts in the NuRD complex of WT immunoprecipitates (Fig 5.12D, lane 4). However, similar to the Sin3a complex, loss of HDAC2 (HD2^{Δ2/Δ2}) does not affect the deacetylase potential of the NuRD complex and suggests that HDAC1 is able to compensate for the potential loss of deacetylase potential in the absence of HDAC2 in this complex. Notably, Mi2β, a major component of the NuRD complex (Reinberg, D., *et al.*, 1998) present in T cells (Williams, C., *et al.*, 2004) is absent in HD1^{Δ2/Δ2};HD2^{WT/Δ2} knock-out MTA-2 immunoprecipitates when compared to WT (Fig 5.12D, compare lanes 4 and 8). The amount of immunoprecipitated MTA-2 is reduced in HD1^{Δ2/Δ2};HD2^{WT/Δ2} 6-8 week old thymocytes and as such one would expect to detect reduced amounts of Mi2β.

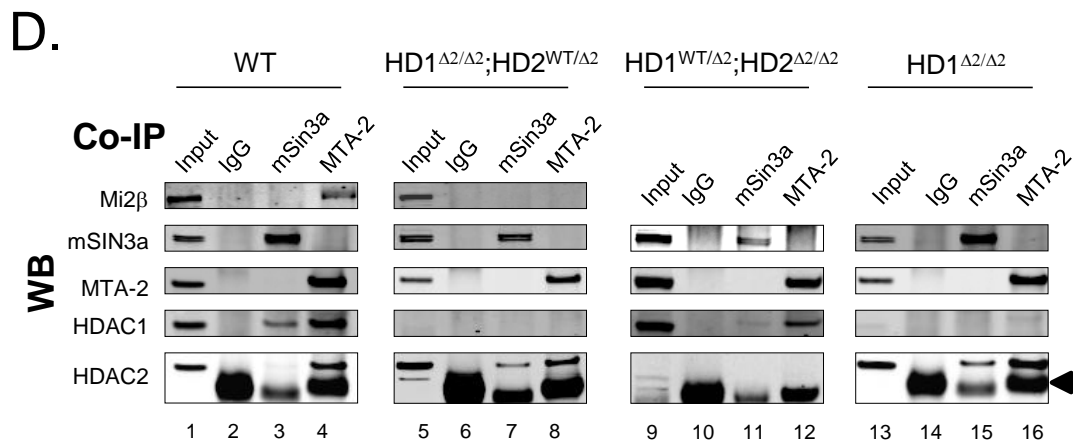
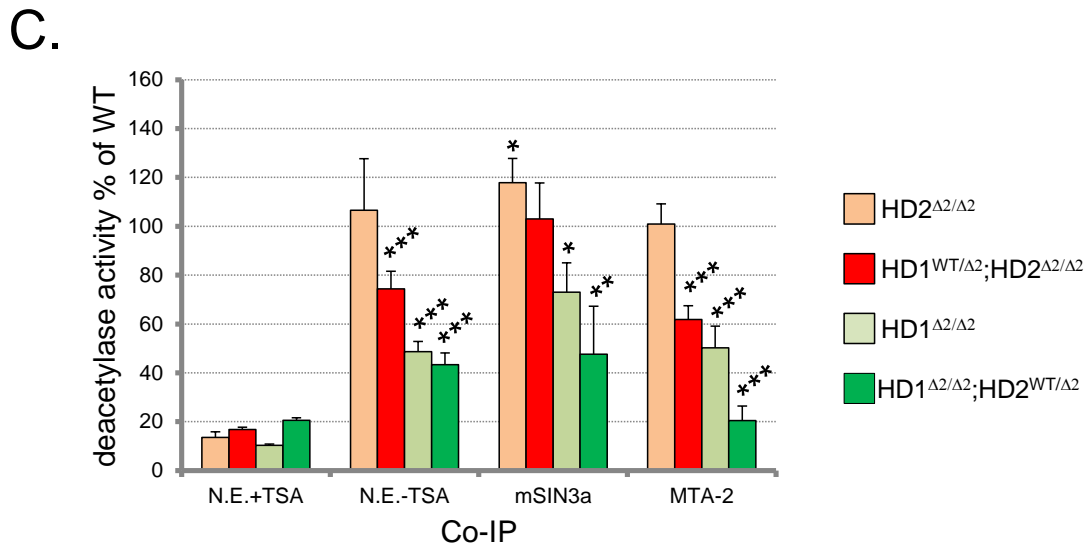


Figure 5.12 continued. *Reduced deacetylase activity associated with HDAC1 and -2 complexes.* (C) Specific antisera to the indicated proteins were used to coimmunoprecipitate (Co-IP) Sin3A (α -mSIN3a) and NuRD (α -MTA-2) complexes from the genotypes indicated. The amount of associated deacetylase activity was measured using a commercially available kit. 2 μ g of total nuclear extract (N.E.) used in the coimmunoprecipitates was placed in similar reactions and incubated with (+) or without (-) the class I and II HDAC inhibitor trichostatin A (TSA) and act as the respective negative and positive controls for this assay. Relative activity is presented as % of LMCs. Mean values (n = 4) \pm S.E.M. are plotted (*p<0.05, **p<0.01, ***p<0.001, paired T-Test). (D) The remaining material from coimmunoprecipitations was run on an SDS-PAGE gel and analyzed by Western blotting using the indicated antibodies. Arrow indicates a non-specific band.

E.

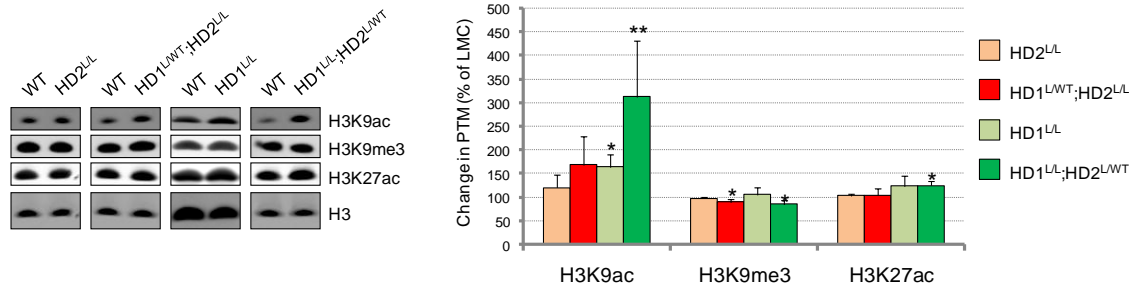


Figure 5.12. *Decreased deacetylase activity associated with HDAC1 and -2 complexes.* (E) The acetylation status of core histones was detected using quantitative Western blotting. Histones were acid extracted from thymocytes of 6-8 week old mice of the genotypes indicated. Detection of the indicated histone post translational modifications (PTM) were normalized to the total amount of H3 quantitated using a LiCOR scanner. Mean values (n = 3) ± S.E.M. are plotted. (*P < 0.05, **P < 0.01, paired T-Test).

Comparative analysis of global mRNA expression between 3-4 week old mouse thymocytes from HD1^{Δ2/Δ2};HD2^{WT/Δ2} and LMCs reveals no significant difference in mRNA expression of *mta-2*, *mSin3a* or *hdac2* (APPENDIX table E5). This suggests, as in the case of mES cells, increased HDAC2 protein in thymocytes may occur from changes in HDAC2 translation and (or) degradation in the absence of HDAC1. Likewise, this could also explain the reduction in MTA-2 and mSIN3a. Notably and unlike mSIN3a (or Sin3a deacetylase potential), reductions in MTA-2 protein and the subsequent reductions in deacetylase potential of NuRD immunoprecipitates correlate with the presence and severity of the mutant-CD8 developmental phenotype. Reductions in MTA-2 protein as a consequence or in combination with the absence of HDAC1 also appears to disrupt the integrity of the NuRD complex, as measured by the absence of Mi2β in HD1^{Δ2/Δ2};HD2^{WT/Δ2} thymocytes.

Due to decreases in thymocyte mSIN3a ($HD1^{\Delta2/\Delta2}$ and $HD1^{\Delta2/\Delta2};HD2^{WT/\Delta2}$) and MTA-2 ($HD1^{\Delta2/\Delta2}$, $HD1^{WT/\Delta2};HD2^{\Delta2/\Delta2}$ and $HD1^{\Delta2/\Delta2};HD2^{WT/\Delta2}$), direct comparisons of the deacetylase potential and contribution of HDAC1 and -2 to co-repressor complexes (beyond $HD2^{\Delta2/\Delta2}$ mice) are difficult to make. However, crude assessment of the deacetylase activity of total nuclear extracts reveals no change in the overall deacetylase potential of extracts which have a full complement of HDAC1 ($HD2^{\Delta2/\Delta2}$) as is the case in Sin3a and NuRD complexes (Fig 5.12C). In contrast, nuclear extracts which lack HDAC1 exhibit similar and comparable reductions in deacetylase activity despite the observed increase in HDAC2 ($HD1^{\Delta2/\Delta2}$ and $HD1^{\Delta2/\Delta2};HD2^{WT/\Delta2}$) and provides evidence that HDAC1 is the dominant deacetylase of the two enzymes. Importantly in $HD1^{WT/\Delta2};HD2^{\Delta2/\Delta2}$ nuclear extracts, where levels of HDAC1 are similar to WT controls (fig 5.12B, HDAC1), an observed decrease in HDAC activity is measured suggesting HDAC2 does contribute to the deacetylase activity of mouse thymocytes. Combined, these data suggest a non-redundant role for HDAC1 in mouse thymocytes as it appears that HDAC2 cannot compensate for the loss of deacetylase activity observed in the absence of HDAC1. Interestingly, these experiments also show that HDAC1 contributes a large portion of the total class I and II HDAC activity of mouse thymocytes. $HD1^{\Delta2/\Delta2}$ and $HD1^{\Delta2/\Delta2};HD2^{WT/\Delta2}$ extracts show a reduction in activity of ~40% when compared to WT controls. Treatment of protein extracts with the HDAC inhibitor, TSA, reduces activity to ~10-20% of control activity meaning that the presence of HDAC1 contributes roughly two thirds of all class I and II HDAC activity in mouse thymocytes. A brief analysis of the classic HDAC substrates, histones, reveals a similar pre-eminent, role for HDAC1 in the deacetylation of

histone tails (Fig 5.12E). Significant increases in the hyperacetylation of H3K27ac are only detected in HD1^{Δ2/Δ2};HD2^{WT/Δ2} extracts. Likewise, the acetylation status of H3K9 (H3K9ac) reveals a significant increase in the absence of HDAC1. Measurements of the heterochromatic marker, H3K9 trimethylation (H3K9me3) reveal significant, although slight, reductions in the levels of this histone modification in both HD1^{WT/Δ2};HD2^{Δ2/Δ2} and HD1^{Δ2/Δ2};HD2^{WT/Δ2} thymocytes and suggests that HDAC1 and -2 have a more even contribution to deacetylation of this particular modification.

In summary, HDAC1 appears to confer greater deacetylase potential to co-repressor complexes when compared to HDAC2, either as a direct consequence of its enzymatic activity or indirectly through maintaining adequate levels of co-repressor complex components. Also, upregulation of HDAC2 in thymocytes lacking HDAC1 does not compensate for the loss of the deacetylase potential in these cells.

5.6 HD1^{Δ2/Δ2};HD2^{WT/Δ2} and HD1&2^{Δ2/Δ2} conditional knock-out mice exhibit a lethal pathology as a result of intra-thymic T cell neoplastic transformation.

Staining thymocytes with annexinV (a positive marker of apoptosis) reveals a 10% increase in the number of neonatal thymocytes of HD1^{Δ2/Δ2};HD2^{WT/Δ2} mice undergoing apoptosis (Fig 5.13, bottom left neonatal dot plots comparing the sum of all percentages from each sub-population). Co-staining of annexinV^{+ve} cells for CD4/CD8 expression demonstrates that cells which exhibit a mutant-CD8 phenotype are responsible for the majority of

apoptosis in both neonates (15%) and older mice (36%). Despite the detected increase in cell death, we observe an almost 4 fold increase in thymocyte cellularity in 6-8 week old mice which suggests enhanced proliferation, as opposed to a putative defect in cell death, in establishing the increase in thymic cellularity of HD1^{Δ2/Δ2};HD2^{WT/Δ2} mice. A decrease in the number of mature SP thymocytes in both neonates and 6-8 week old HD1^{Δ2/Δ2};HD2^{WT/Δ2} mice, in combination with the expansion of the immature pre-selection neonatal thymocyte compartment, indicates the establishment of thymic dysplasia. To further investigate the increased cellularity in HD1^{Δ2/Δ2};HD2^{WT/Δ2} mice, the survival of small cohorts of all genotypes was ascertained over a period of 5 months. 100% of HD1^{Δ2/Δ2};HD2^{WT/Δ2} or double knock-out HD1&2^{Δ2/Δ2} mice became moribund (characterised by an enlarged chest or abdomen and rapid respiration) and were subsequently culled. The ages when culled were, 12 weeks (84 days) and 15 weeks (104 days) respectively (Fig 5.14A). Necropsy of these mice revealed they had developed a pathological diseased state characterised by massively enlarged thymi and spleens (the former likely accounting for the observed respiratory difficulties) (Fig 5.14B). Non-lymphatic tissue was fixed, embedded in paraffin, sectioned and stained with heamatoxylin and eosin (H and E) for further histological analysis. 43% of HD1^{Δ2/Δ2};HD2^{WT/Δ2} and HD1&2^{Δ2/Δ2} mice analysed (6/14) showed signs of non-lymphatic organ infiltration (Fig 5.14C) which may play a role in the observed lethality. No other genotypes, with the exception of a single HD1^{Δ2/Δ2} mouse (which succumbed to the same illness at a later stage), exhibited these reduced survival rates over this 5 month period. The lag of 3 weeks in median survival of

HD1 $\Delta 2/\Delta 2$ mice when compared to HD1 $\Delta 2/\Delta 2$;HD2 $^{WT/\Delta 2}$ mice could be attributed to the block

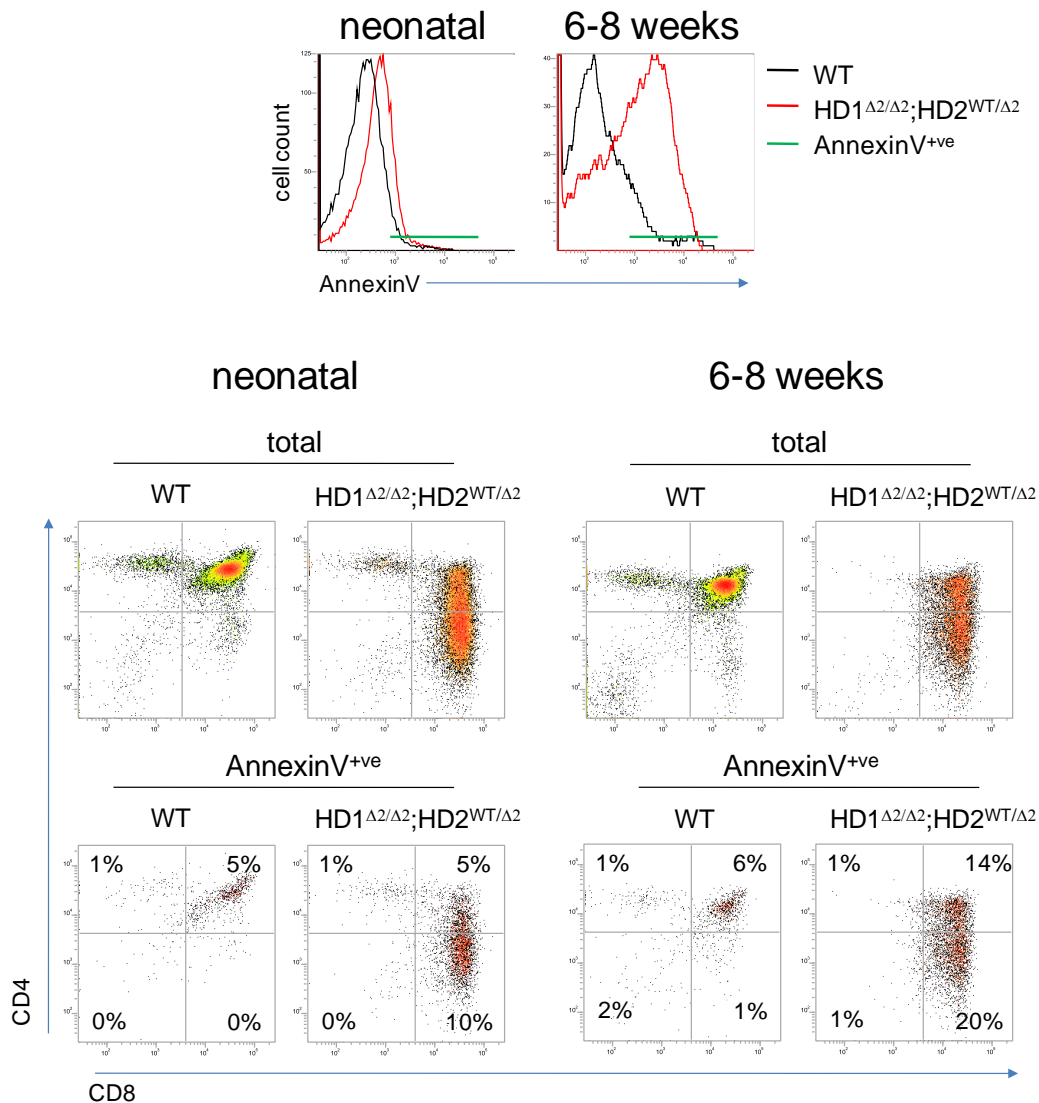


Figure 5.13. *Increased apoptosis detected in mutant-CD8 thymocytes of HD1 $\Delta 2/\Delta 2$;HD2 $^{WT/\Delta 2}$ mice.* CD4/CD8 gated intra-thymic developmental distribution of total annexinV positive neonatal and 6-8 week old thymocytes of WT and HD1 $\Delta 2/\Delta 2$;HD2 $^{WT/\Delta 2}$ mice (histograms, top panels) reveals an increase in the percentage of mutant-CD8 and DP populations compared to age matched LMCs. Mean average percentages are shown, (n=3).

in DN-DP transition observed in neonates (5.1.6). Analysis of thymus, spleen and lymph nodes of diseased and WT LMCs, reveals that the T cell compartment of secondary lymph organs, unlike 6-8 week old mice (spleen) is made up of the same developmentally blocked immature $\text{TCR}\beta^{\text{int}}/\text{CD5}^{\text{int}}$ T cells described section 5.1.7 (Fig 5.15). Side and forward scatter profiles of thymocytes from diseased mice exhibit a profile characteristic of a “blasting state” indicative of cellular proliferation (Fig 5.16A). Ki-67 staining (a marker of proliferation (Scholzen T. and Gerdes J., 2000) of paraffin embedded thymus sections confirms this to be the case (Fig 5.16B). The majority of cellular proliferation in the WT thymus occurs in the cortex with little or no proliferation in the medulla. Ki67 staining patterns of WT mice is indicative of the developmental processes which take place within each of these sub-compartments (i.e. in the cortex developing thymocytes undergo TCR receptor chain rearrangement and expansion, whereas in the medulla differentiated thymocytes undergo selection prior to their exit to the periphery, Fig 3.2). In the diseased thymus, sub-compartment structure is completely effaced; with Ki67 staining diffuse as opposed to being limited to a specific region. Given the infiltration characteristics of diseased mice, in combination with the lethal aggressive increase in thymocyte proliferation, one cannot rule out the possibility of a neoplastic transformation having occurred either dependent or independent of the apparent dysplasia observed in neonates, or in 6-8 week old mice. Somatic V(D)J recombination of the TCR chains occurs at the DN and DP stages of T cell development in which multiple non-contiguous variable (V), diversity (D), and joining (J) segments of the $\text{TCR}\beta$ locus are rearranged and brought together into a continuous V-D-J

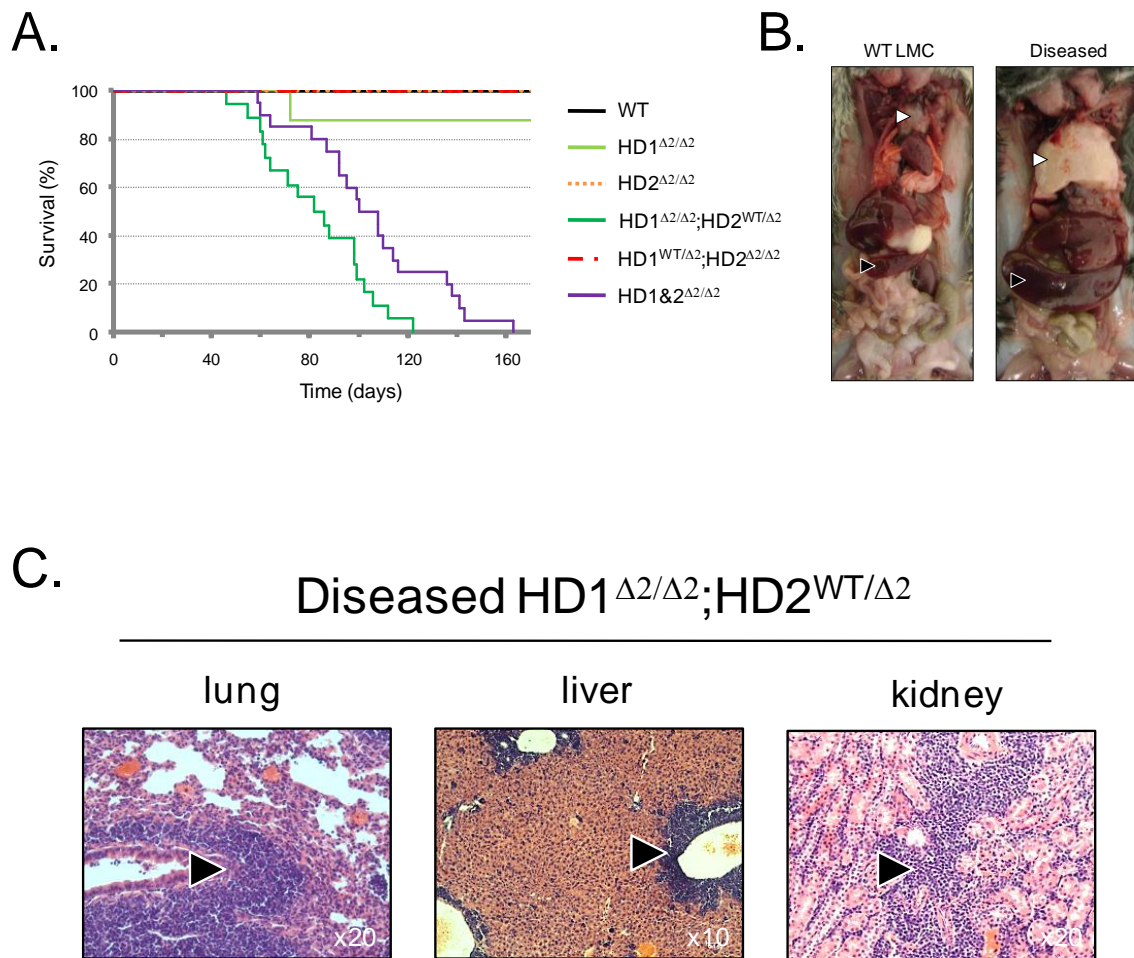


Figure 5.14. Development of pathological diseased state in HD1^{Δ2/Δ2};HD2^{WT/Δ2} and HD1&2^{Δ2/Δ2}. (A) Kaplan Meier survival curve. WT (n=13), HD1^{Δ2/Δ2}(n=8), HD2^{Δ2/Δ2}(n=11), HD1^{WT/Δ2};HD2^{Δ2/Δ2} (n=5), HD1^{Δ2/Δ2};HD2^{WT/Δ2}(n=18, median length of survival = 12 weeks) and HD1&2^{Δ2/Δ2} (n=20, median length of survival = 15 weeks.). (B) Enlarged thymus (white triangles) and spleens (black triangles) representative of HD1^{Δ2/Δ2};HD2^{WT/Δ2} and HD1&2^{Δ2/Δ2} diseased mice. Also shown are representative WT LMCs. (C) Heamatoxylin and eosin stained paraffin embedded sections show infiltration of lung, liver and kidney in diseased HD1^{Δ2/Δ2};HD2^{WT/Δ2} mice (6/14 cases analysed).

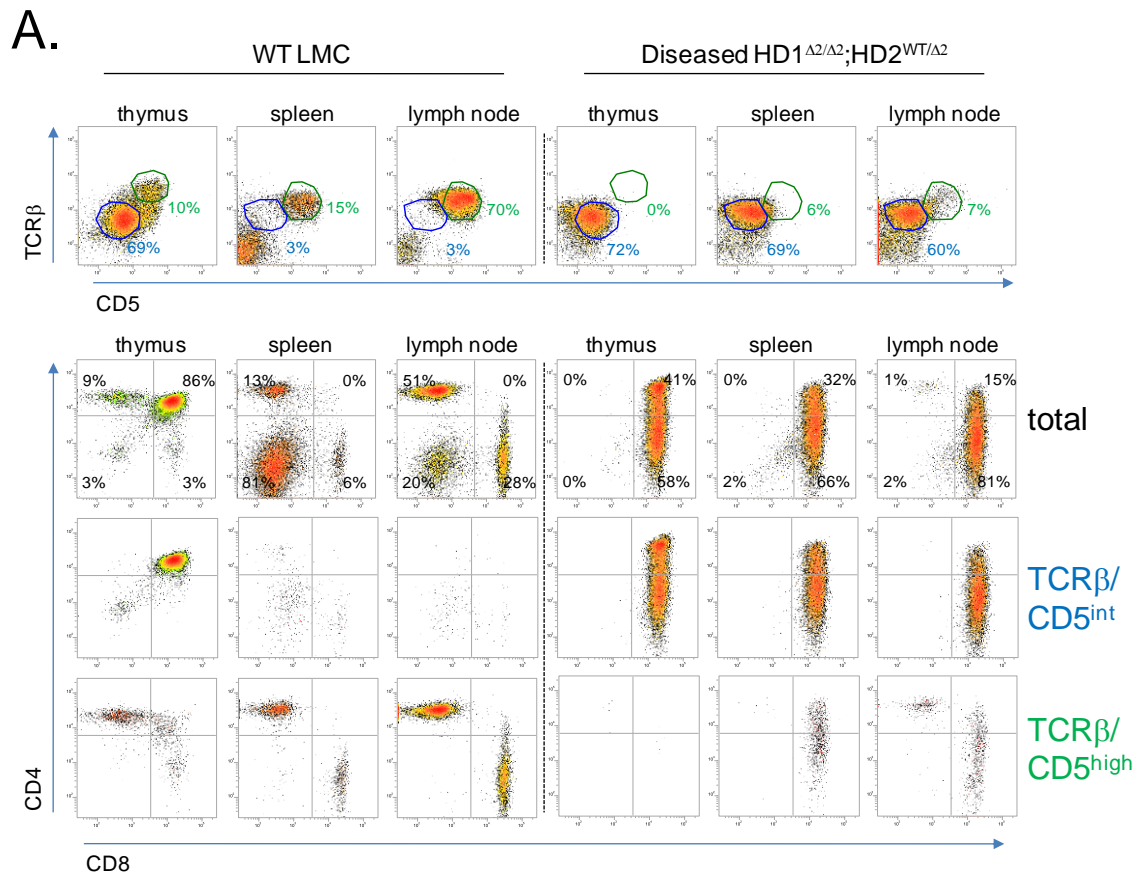


Figure 5.15. *Thymocytes of diseased secondary lymphatic organs are immature mutant-CD8 cells.* (A) Top row: TCRβ/CD5 expression profiles of thymocytes, splenocytes and lymphocytes from diseased and age matched WT LMCs reveals the majority of thymocytes are immature mutant-CD8 cells. Bottom 3 rows: intra-thymic developmental sub-populations (as identified by CD4 and CD8 coreceptor expression) of the same cell populations, fractionated on TCRβ/CD5 expression (TCRβ/CD5^{int} and TCRβ/CD5^{high}). Representative plots of at least 3 individual diseased and age matched WT LMC mice are shown.

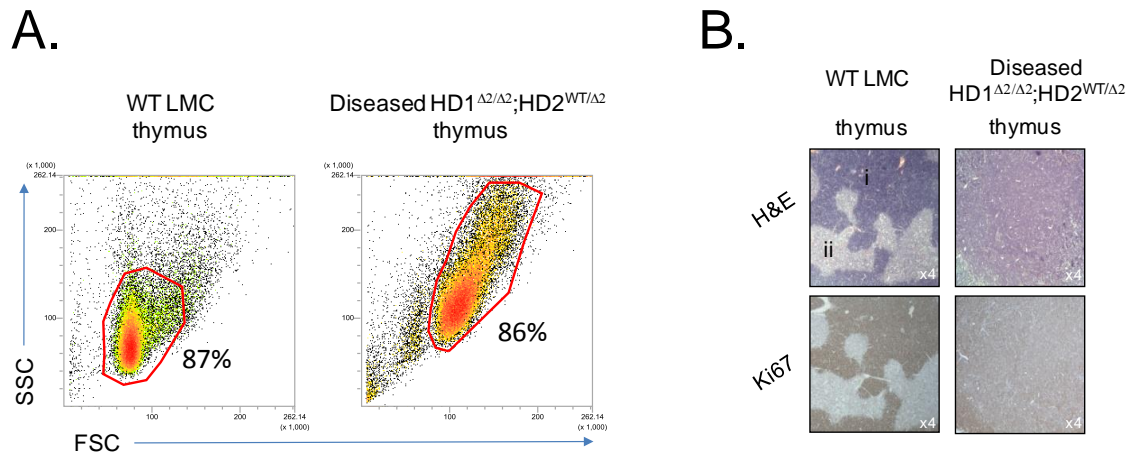


Figure 5.16. *Diseased tissues exhibit characteristics of increased proliferation.* (A) Side scatter (SSC) and forward scatter (FSC) plots of total thymocytes from diseased and WT LMCs analysed by FACS. (B) Serial thymic sections from WT LMCs and diseased HD1^{Δ2/Δ2};HD2^{WT/Δ2} mice stained with heamatoxylin and eosin or Ki67 counterstained with eosin. (i) cortex, (ii) medulla.

coding exon (Whitehurst, C. E., Chattopadhyay, S. and Chen, J., 1999 and Hodges, E., *et al.*, 2003). In order to assess thymocyte clonality, PCR of the TCR β variable chain was performed on thymocyte gDNA from 6-8 week old (and diseased HD1^{Δ2/Δ2};HD2^{WT/Δ2} and HD1&2^{Δ2/Δ2} mice as well as WT LMCs (Hodges, E., *et al.*, 2003, Gaudet, F., *et al.*, 2003), Figure 5.17 outlines this PCR strategy. Should the increase in cellularity be as a consequence of a general dysplasia one would expect to detect multiple recombined events, representative of a polyclonal and diverse T cell population. In fact thymocytes from 6-8 week old HD1^{Δ2/Δ2};HD2^{WT/Δ2} and HD1&2^{Δ2/Δ2} mice exhibit oligo-clonal TCR β rearrangements which appear progressively monoclonal in diseased mice of the same genotype (2/4 cases analysed have a single rearranged PCR

A.

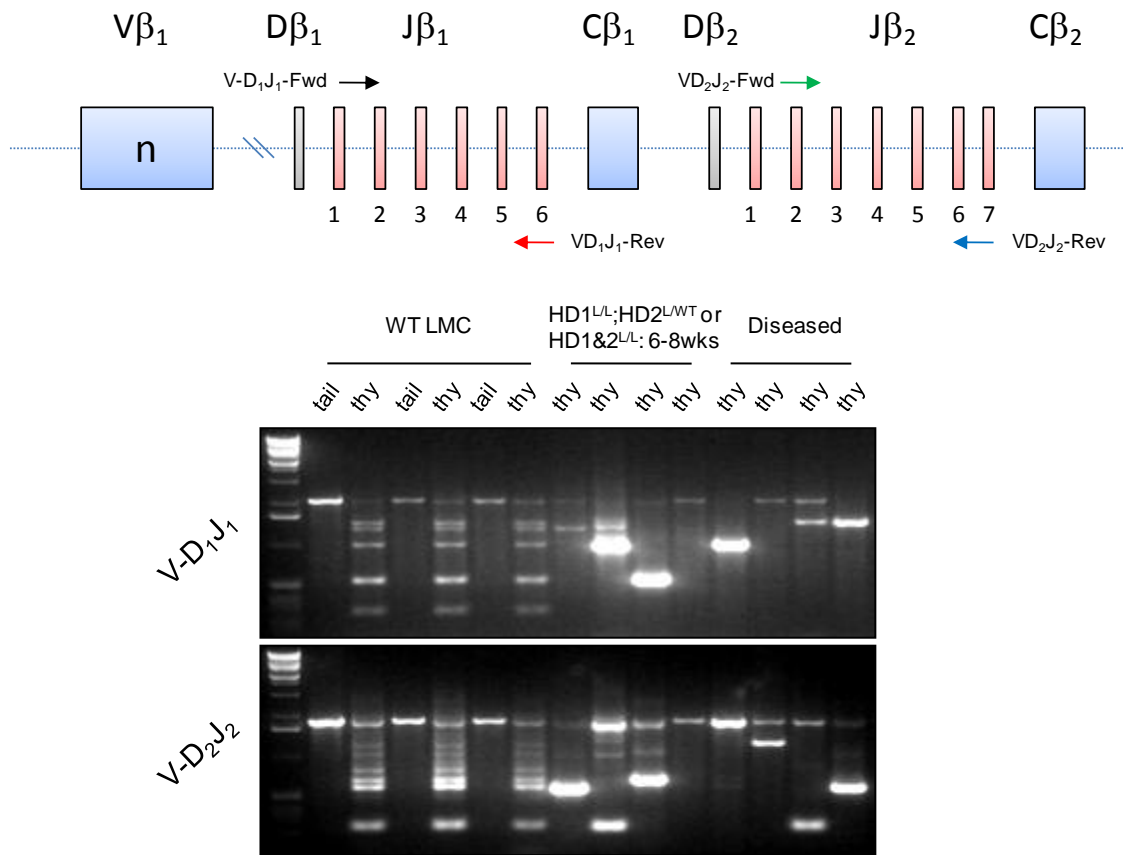


Figure 5.17. *HD1^{Δ2/Δ2};HD2^{WT/Δ2}* and *HD1&2^{Δ2/Δ2}* thymocytes are increasingly clonal. (A) Thymocyte clonality analysis: PCR strategy for determining Dβ₁-Jβ₁ and Dβ₂-Jβ₂ rearrangement at the TCRβ locus of tail and thy (thymus) gDNA. The V-D₁J₁ reaction was used to assess Dβ₁-Jβ₁ rearrangement using primers V-D₁J₁-Fwd and V-D₁J₁-Rev. The V-D₂J₂ reaction was used to assess Dβ₂-Jβ₂ rearrangement using primers V-D₂J₂-Fwd and V-D₂J₂-Rev. Germline configuration (see tail results, far left) results in a 2200bp or 1760bp fragment for the respective reactions. When rearranged, five and six different amplified fragments are possible ranging from approximately 1500bp-380bp (V-D₁J₁ PCR) or from 1200bp-350bp (V-D₂J₂ PCR) (see thy results of WT LMC thymus). Gene segments: V (variable), D (diversity), J (joining) and C (constant).

fragment, lanes 4 and 3 from the far right, Fig 5.17), indicating clonal expansion rather than a general dysplastic expansion of all immature T cells. Thus, as well

as a block in T cell maturation, sub-optimal levels of HDAC1 and 2 in T cells results in their neoplastic transformation and tumourigenesis.

5.6.1 T cell lymphomas in HD1^{Δ2/Δ2};HD2^{WT/Δ2} mice are associated with chromosomal instability.

Chromosomal instability, including chromosome translocations, deletions, amplifications and aneuploidy, are detected in most human malignancies (Lengauer, C., Kinzler, W. K. and Vogelstein, B., 1998) and has been shown to play a critical role in the initiation and progression of haematological malignancies (Nowicki, M., O., *et al.*, 2003, Skorski, T., 2007). A number of lymphoma prone mouse models display copy number alterations and mutations syntenic to those found in an array of human cancers (Winandy, P. M., Wu, P. and Georgopoulos, K., 1995, Masser, R. S., *et al.*, 2007 and de Keersmaecker, K., *et al.*, 2010). Using array comparative hybridisation on a small set of HD1^{Δ2/Δ2};HD2^{WT/Δ2} derived lymphomas (n=6) demonstrates that these tumours display both focal chromosomal deletions and whole chromosome gains or losses (aneuploidy) indicative of chromosomal instability (for full results see APPENDIX Fig A4-F4 and Tables A4). In total, 6 instances of aneuploidy and a total of 16 unique focal deletions or amplifications were detected (APPENDIX Table B4). With regards focal deletions, of particular note is a single instance of a homozygous deletion of the *Pten* locus (Fig 5.18A, Tumour 6). In humans, deletion or mutations of the *Pten* gene have been implicated in the development of T cell acute lymphoblastic

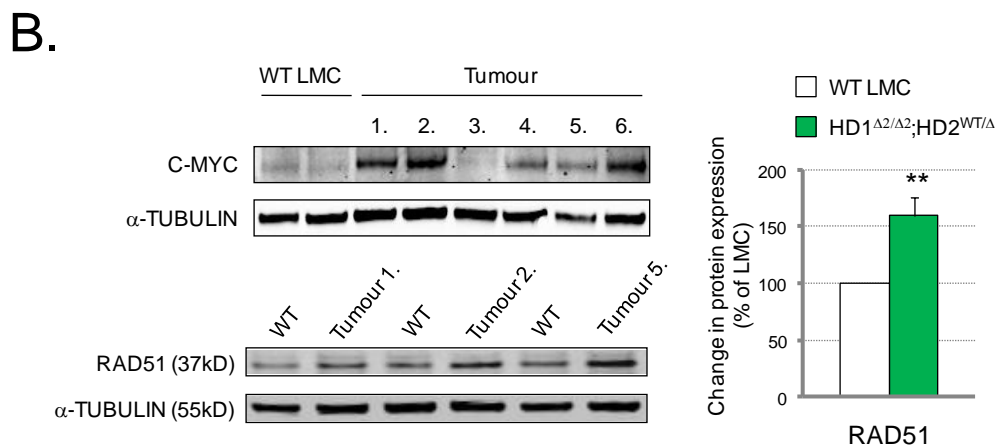
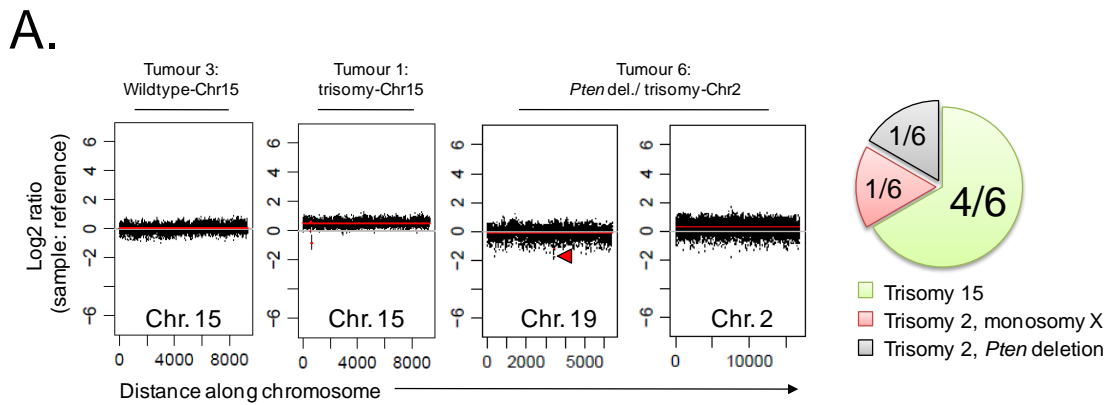


Figure 5.18. *HD1 ^{Δ 2/ Δ 2};HD2^{WT/ Δ}* T cell tumours are associated with chromosomal instability. (A) Representative aCGH plots of gDNA isolated from *HD1 ^{Δ 2/ Δ 2};HD2^{WT/ Δ}* T cell lymphomas (Tumour, sample) and tail matched (reference) mice. (B) C-MYC and RAD51 expression in thymocyte protein extracts of tumour samples analysed by aCGH and WT LMCs assessed by Western blotting. α -TUBULIN is used as a loading control with RAD51 levels quantified using the LiCOR scanner and normalised to levels of α -TUBULIN. Relative protein expression is presented as % of LMCs. Mean values (n = 3) + S.E.M. are plotted. (**P<0.01, paired T-Test). Grey lines in aCGH plots represent expected log₂ ratios of sample vs. reference samples which have an equal copy number. Red lines represent actual log₂ ratios observed for each profile. Log₂ ratios $>\pm 0.5$ indicate single copy gains or losses, log₂ ratios of $>\pm 1$ indicate multiple copy gains or losses. Red arrow indicates homozygous deletion (log₂ ratio >1) of the *Pten* locus.

leukaemia/lymphoma (T-ALL) (Masser, R. S., *et al.*, 2007) and conditional inactivation of *Pten* in a small subset of mouse haematopoietic stem cells results in the development of T-ALL with 100% penetrance (Guo, W., *et al.*, 2008). All tumours analysed displayed aneuploidy with 4/6 tumours revealing trisomy 15 and the remainder (2/6) presenting trisomy 2, coupled with either monosomy X or focal homozygous deletion of *Pten* (Fig 5.18A). The proto-oncogene, *c-myc* (located on chromosome 15 in mice), is frequently activated in tumours and when over expressed in mice results in T cell lymphomas (Selten, G., *et al.*, 1984). Indeed, trisomy 15 is a signature of mouse T cell tumours (Muto, M., *et al.*, 1996, Gaudet, F., *et al.*, 2003 and de Keersmaecker, K., *et al.*, 2010 and van Hamburg, J. P., *et al.*, 2001). Furthermore, *c-myc* is a direct target of signalling via Notch1 (Weng, A. P., *et al.*, 2006) which in mice is located on chromosome 2 (activating mutations of which are present in 50% of all human T cell acute lymphoblastic leukaemia/lymphoma, T-ALL) (Weng, A. P., *et al.*, 2004). Consistent with results assessing clonality (Fig 5.17), all tumour samples reveal deletions at the *tcr α* (chromosome 14) and *tcr β* loci (chromosome 6) providing evidence that the TCR α/β chains of HD1 $\Delta 2/\Delta 2$;HD2 $^{WT/\Delta 2}$ mice undergo somatic recombination (APPENDIX Fig A4-F4 and Table A4). Western blotting reveals C-MYC protein expression to be elevated in 5/6 tumour samples when compared to WT LMCs (Fig 5.18B) and in all tumours which exhibit trisomy 15 (APPENDIX Fig A4, B4, D4, and E4) Increase in *c-myc* gene dosage could, in part, explain the increase in C-MYC protein levels which may play a significant role in the transformation of HD1 $\Delta 2/\Delta 2$;HD2 $^{WT/\Delta 2}$ T cells. Notably, levels of RAD51, also found on chromosome 15, exhibits a near perfect relationship to a single copy gain in gene dosage (i.e.

a 50% increase) (Fig 5.18B). The variation in levels of C-MYC protein in 5/6 tumours (including Tumour 6 which is heterozygous for chromosome 15, see APPENDIX Fig F4 and H4) suggests that other factors may be responsible for the elevated levels of C-MYC in HD1^{Δ2/Δ2};HD2^{WT/Δ2} T lymphomas.

5.6.2 Global gDNA methylation levels are unaltered in T cell lymphomas of HD1^{Δ2/Δ2};HD2^{WT/Δ2} mice.

Genetically engineered mice carrying a hypomorphic *Dnmt1* allele display both global and centromeric DNA hypomethylation which leads to the development of clonal, thymic tumours which display a high frequency of genomic instability (in particular trisomy 15) (Gaudet, F., *et al.*, 2003). Post-translationally, HDAC1 mediated deacetylation has been shown to protect DNMT1 from proteasomal degradation (Du, Z., *et al.*, 2010) presenting a model by which alterations to the level of DNA methyltransferases could potentiate genomic instability in HD1^{Δ2/Δ2};HD2^{WT/Δ2} mice. Western blotting for both the “maintenance” and *de novo* DNA methyltransferases, DNMT1 and DNMT3b respectively, does not detect any change in the level of either enzyme in HD1^{Δ2/Δ2};HD2^{WT/Δ2} derived tumour protein extracts (Fig 5.19A), nor is there a detectable difference in global or pericentromeric gDNA methylation status (Fig 5.19B and C respectively), results which would seem to refute a causative role for genomic hypomethylation in HD1^{Δ2/Δ2};HD2^{WT/Δ2} lymphomas.

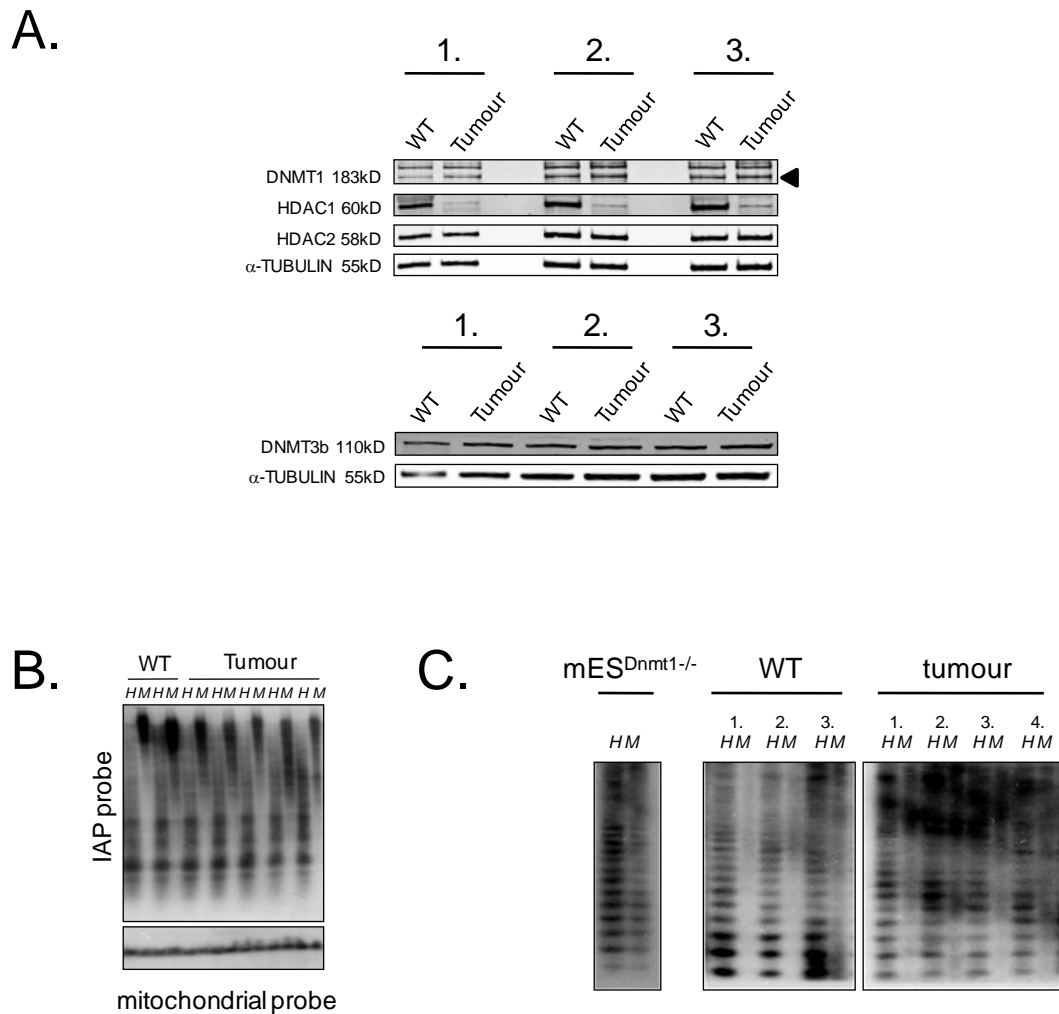


Figure 5.19. Global *gDNA* methylation levels are unaffected in *T* cell lymphomas of $HD1^{\Delta2/\Delta2};HD2^{WT/\Delta2}$ mice. (A) Protein extracts from aged matched WT LMC and $HD1^{\Delta2/\Delta2};HD2^{WT/\Delta2}$ T cell lymphoma (Tumour) samples probed for DNMT1 and DNMT3b by western blot. Sothern blotting was used to assess the level of methylation at interstitial A particle (IAP) and major satellite repeat elements. Genomic DNA from WT LMC and Tumour thymocytes digested with either *Hpa* II (*H*, methylation sensitive) or *Msp* I (*M*, methylation resistant) restriction enzymes was then hybridized with (B) an IAP probe or (C) a major satellite repeat fragment to assess the status of global and pericentromeric genomic DNA respectively. A mitochondrial probe in (B) was used as a control for complete digestion of genomic DNA. Genomic DNA from $Dnmt1^{-/-}$ mouse embryonic stem cells ($mES^{Dnmt1^{-/-}}$) was used as a hypomethylated control sample.

5.6.3 Gene expression profiling of pre-lymphomic HD1^{Δ2/Δ2};HD2^{WT/Δ2} thymocytes.

Having established that HD1^{Δ2/Δ2};HD2^{WT/Δ2} lymphomas have a recurring signature of chromosomal gains and losses common to other lymphoma/leukaemia prone mice, I aimed to determine if a particular transcriptional programme was activated in HD1^{Δ2/Δ2};HD2^{WT/Δ2} mice, which may account for the transformation of thymocytes acting either synergistically with, or independently and putatively causative of, the observed chromosomal instability. Transcriptional profiling of pre-lymphomic HD1^{Δ2/Δ2};HD2^{WT/Δ2} and age matched LMCs thymocytes from 2-3 week old mice was performed. Pre-lymphomic classification was crudely assessed by an absence of increased cellularity in HD1^{Δ2/Δ2};HD2^{WT/Δ2} mice when compared to WT LMCs (Fig 5.20A). TCRβ^{low}/CD5^{low} expressing cells were sorted, which are predominantly DP (CD4/CD8^{+ve}) in WT mice and a mixture of DP and mutant-CD8 thymocytes in HD1^{Δ2/Δ2};HD2^{WT/Δ2} conditional knock-outs (Fig 5.10A, for sorting gate and 5.10C for CD4/CD8 developmental sub-populations). RNA was isolated and comparative microarray analysis performed using an IlluminaBeadChip platform, which covers 45,200 different mouse transcripts. Transcripts up- or downregulated by ≥2-fold (Fc ≥2, adjusted P<0.005) were identified between WT (n=7) and HD1^{Δ2/Δ2};HD2^{WT/Δ2} (n=5) sorted thymocytes. Hierarchical clustering based on signal detection values of >8000 genes indicates the pre-lymphomic HD1^{Δ2/Δ2};HD2^{WT/Δ2} thymocyte transcriptional programme is distinct from the WT (Fig 5.20B). A total of 5954 transcripts are detected in either WT, HD1^{Δ2/Δ2};HD2^{WT/Δ2} mutant or in both sample groups. Of these, 892 transcripts

are deregulated. Consistent with the roles of HDAC1 and -2 in transcriptional repression more transcripts are upregulated (542) than down regulated (350) (Fig 5.20C, for a complete list see APPENDIX Table A5). An analysis of functionally related gene groups among deregulated genes, using DAVID (Huang, D. W., Sherman, B. T. and Lempicki, R. A., 2009a and Huang, D. W., Sherman, B. T. and Lempicki, R. A., 2009b), reveals that genes involved in chromatin organisation/assembly, DNA replication and T cell activation/differentiation were among the top 10 statistically significantly enriched annotational gene clusters (Fig 5.20D). Performing the same analysis on separate up- and downregulated gene lists reveals genes involved in DNA replication are upregulated, whereas genes with biological functions assigned to T cell activation/differentiation are downregulated in pre-lymphomic HD1^{Δ2/Δ2};HD2^{WT/Δ2} mutant thymocytes (Fig 5.20D, downregulated). Of the downregulated gene cluster are a number of genes involved in V(D)J recombination (*Rag1*, *Rag2*, and *Dclre1c* the gene that encodes ARTEMIS). This is consistent with evidence that suggests TCR V(D)J recombination has been completed in HD1^{Δ2/Δ2};HD2^{WT/Δ2} mutant thymocytes (Fig 5.17, and APPENDIX Table A4, see chromosome 14 results for *tcrα* rearrangements) and is ongoing in WT DP thymocytes where many cells have yet to rearrange their TCR α chain. Notably *Cd4* is down regulated in mutant thymocytes, reflective of the CD4 coreceptor expression in the mutant- CD8 population (i.e. CD4^{low}/CD8^{high}) and suggests that reduced cell surface expression of CD4 is a consequence of reduced *Cd4* gene transcription.

In agreement with FACS data and the developmental phenotype observed in HD1^{Δ2/Δ2};HD2^{WT/Δ2} neonatal thymocytes, the CD69 antigen

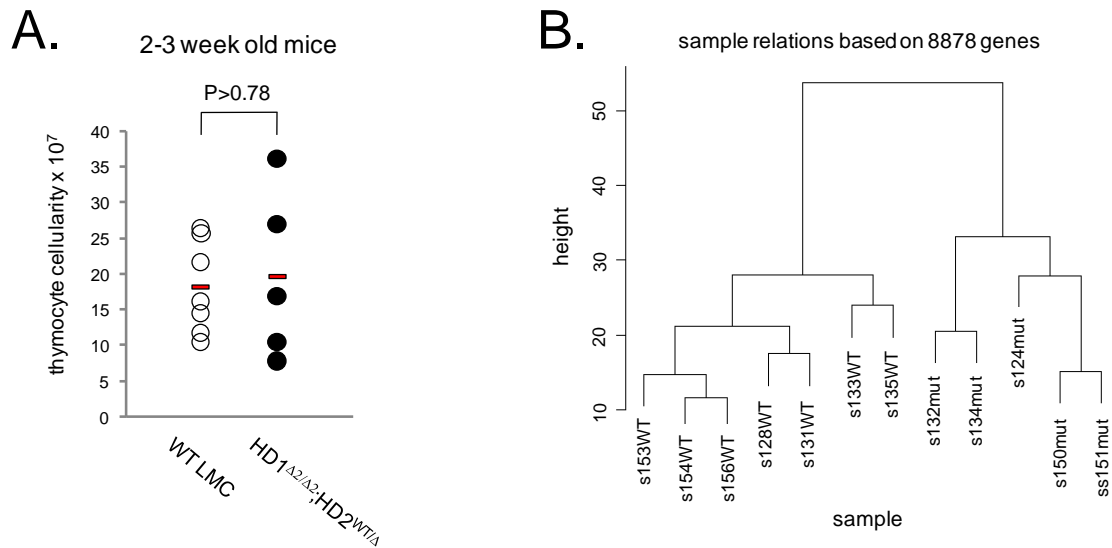


Figure 5.20. Gene expression profiling of pre-lymphomic $HD1^{\Delta2/\Delta2};HD2^{WT/\Delta2}$ thymocytes. (A) Total thymocyte cellularity is similar between $HD1^{\Delta2/\Delta2};HD2^{WT/\Delta2}$ and WT LMCs of 2-3 week old mice used for global transcription profiling. WT LMCs (n=7), $HD1^{\Delta2/\Delta2};HD2^{WT/\Delta2}$ (n=5). Red bar indicates mean. Cellularity for individual mice is represented as an open (WT) or closed ($HD1^{\Delta2/\Delta2};HD2^{WT/\Delta2}$) circle. ($P > 0.78$, Un-paired T-Test) (B) Hierarchical clustering of samples based on signal detection values of >8000 genes indicates the transcriptional programme in pre-lymphomic $HD1^{\Delta2/\Delta2};HD2^{WT/\Delta2}$ thymocytes is distinct from WT LMCs (s=sample, "number" = sample identifier, -WT or -mut post fix identifies samples from WT LMCs or $HD1^{\Delta2/\Delta2};HD2^{WT/\Delta2}$ genotypes respectively).

is identified as being downregulated (APPENDIX Table A5), as are key mediators of T cell signalling such as LAT (linker of activated T cells), *Themis* (thymocyte expressed molecule involved in selection), *Itk* (IL-2 inducible T cell kinase) and (see APPENDIX Table A5). Down regulation of these genes, befits a model whereby the absence of HDAC1 and -2, results in defective propagation of TCR signalling downstream of TCR complex formation and may

provide a rational mechanism for the reduction in positively selected thymocytes in HD1^{Δ2/Δ2};HD2^{WT/Δ2} mice. These results also suggest that the generation of T cell lymphoma in HD1^{Δ2/Δ2};HD2^{WT/Δ2} mice is independent of T cell signalling. Surprisingly, given the increase in apoptosis in both neonatal and 6-8 week old HD1^{Δ2/Δ2};HD2^{WT/Δ2} thymocytes, *Fas* (a cell surface mediator of apoptosis highly expressed in DP thymocytes) (Williams, C., *et al.*, 2004) is also downregulated in pre-lymphomic mutant thymocytes and suggestive that a FAS mediated extrinsic pathway of apoptosis is not activated in HD1^{Δ2/Δ2};HD2^{WT/Δ2} thymocytes.

The upregulated annotation cluster in Figure 5.20D, contains genes that encode DNA replication enzymes (*Polλ*, *Polδ2*, *Lig1*, *Prim2*) and DNA pre-replication complex proteins (*Cdt1*, *Mcm3*, -6, -7 and -10). Upregulation of genes involved in DNA replication and metabolism would suggest an increased demand for DNA replication in these cells. As total thymic cellularity is similar to WT in HD1^{Δ2/Δ2};HD2^{WT/Δ2} mice, one cannot easily attribute the increased expression of these DNA metabolic genes to a consequence of the demands of increased cellular proliferation. One could however, attribute these increases due to increased demand for DNA repair. Upregulation of *Apex1*, which has a major role in the base excision repair pathway of oxidative and single strand break DNA lesions, (Tall, G., *et al.*, 2009) as well as *RAD54l*, shown to have a role in homologous recombination repair of DNA double strand breaks (Ceballos, S. J. and Heyer, W.D., 2011) adds further support to suggest the increase in expression of DNA replication genes could potentially be due to increased DNA damage in these cells. This idea is supported by assessing the global levels of γ H2AX (the phosphorylated form of the histone 2A variant H2AX) in histone extracts from 6-8 week old thymocytes. γ H2AX is a marker of

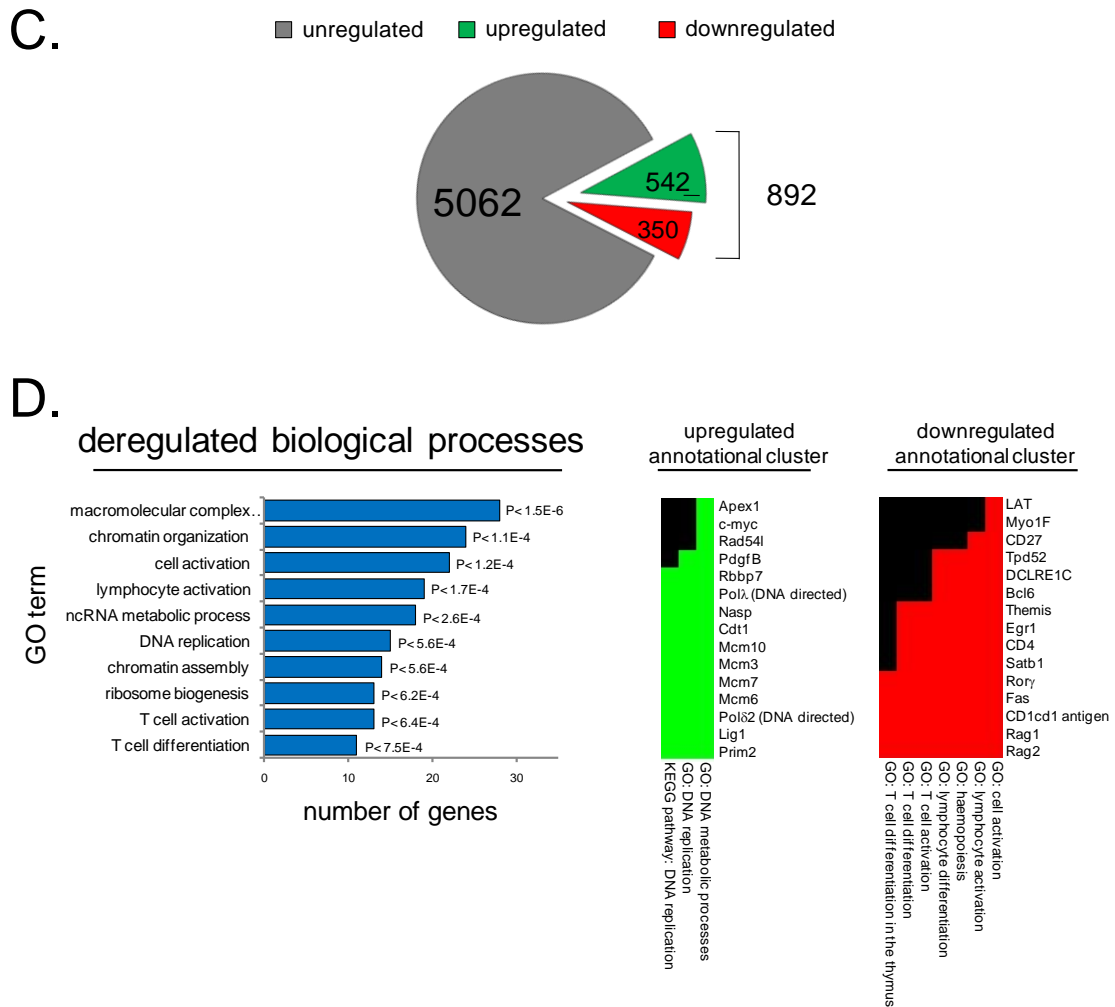


Figure 5.20 continued. *Gene expression profiling of pre-lymphomic HD1^{Δ2/Δ2};HD2^{Δ2/WT} thymocytes.* (C) Summary of expression profiling results. (C) Number of transcripts detected in HD1^{Δ2/Δ2};HD2^{WT/Δ2} or WT LMCs samples presented as unregulated, upregulated or downregulated (892 indicates the total number of deregulated transcripts i.e. the sum of both up- and downregulated transcripts). (D) Functional annotation clustering of all deregulated genes, using DAVID. Represented are the top 10 statistically enriched biological function gene ontology terms (BF-GO terms) and the number of deregulated genes of each annotational cluster. The same analysis performed on up- and downregulated genes identifies enrichment of gene clusters involved in DNA replication are upregulated and T cell activation/differentiation genes are downregulated in HD1^{Δ2/Δ2};HD2^{WT/Δ2} pre-lymphomic thymocytes. Gene names and associated BF-GO terms are listed; coloured blocks indicate a corresponding GO term association positively correlated. Gene enrichment P values are provided by DAVID; calculated using EASE Score (modified Fishers Exact P-value).

E.

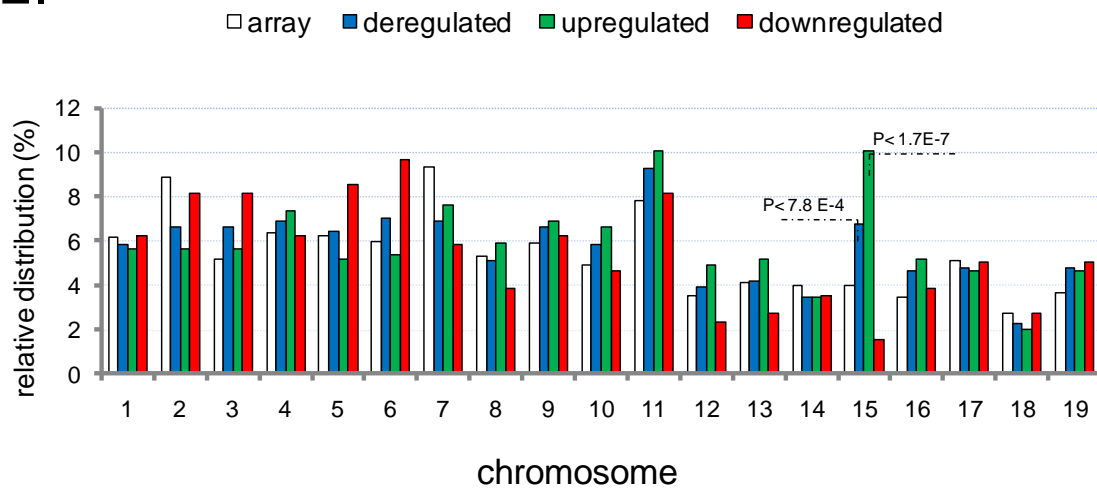


Figure 5.20 continued. *Gene expression profiling of pre-lymphomic HD1^{Δ2/Δ2};HD2^{WT/Δ2} thymocytes.* (E) Genome-wide distribution of deregulated genes shows a bias towards upregulation of genes on chromosome 15 in pre-lymphomic HD1^{Δ2/Δ2};HD2^{WT/Δ2} thymocytes. The total number of genes deregulated, upregulated and downregulated on a given chromosome is expressed as a percentage of the total number of deregulated genes. Also represented, the total number of genes located on a given chromosome, expressed as a percentage relative to the total number of genes represented on the array (array). Gene enrichment P-values are provided by DAVID; calculated using EASE Score (modified Fishers Exact P-value) comparing the fold enrichment of the relative percentages of deregulated, upregulated and down regulated genes with the total number of genes for a given chromosome. Chromosomes X and Y are not included as samples are not sex matched.

DNA damage double strand brakes (Stucki, M. and Jackson, S.P., 2006, Boner, W. M., *et al.*, 2008) and is greatly increased (4 fold) in HD1^{Δ2/Δ2};HD2^{WT/Δ2} extracts (Fig 5.21A). Similarly, another histone modification associated with sites of DNA damage, H4K16ac (Miller, M. K., *et al.*, 2010), is increased 2 fold in HD1^{Δ2/Δ2};HD2^{WT/Δ2} cells. Combined, these results point to an

increase in thymocyte DNA damage in the absence of optimal levels of HDAC1 and -2 which, putatively, could begat the chromosomal instability detected in HD1^{Δ2/Δ2};HD2^{WT/Δ2} T cell lymphomas.

One of the most intriguing results of comparative global expression profiling is the statistically significant bias towards deregulated genes on chromosome 15, in particular upregulated genes (Fig 5.20E). This may indicate that the aneuploidy observed in lymphomas of older HD1^{Δ2/Δ2};HD2^{WT/Δ2} mice is an early event in developing HD1^{Δ2/Δ2};HD2^{WT/Δ2} thymocytes. Notably, *c-myc* is also upregulated (~2.5 fold) as are verified *c-myc* target genes *Apex1*, *Cdk4*, *Cad* and *Ncl* (Zeller, K. I., *et al.*, 2003). Elevated levels of *c-myc* could potentially be a result of direct derepression in the absence of optimal levels of HDAC1 and -2. Of note is the downregulation of transcription factors *Satb1*, *Egr-1* and *Roryγ* (Fig 5.20D) which may play a role in the altered expression profiles of HD1^{Δ2/Δ2};HD2^{WT/Δ2} pre-lymphomic thymocytes and the derepression of *c-myc*, either through independent actions or synergistically in the absence of HDACs 1 and -2.

5.7 Global histone hyperacetylation of T cells in the absence of HDAC1 but not HDAC2.

Further analysis of histone substrates of acetylation in 6-8 week old mutant thymocytes reveals, as observed in *Hdac1* conditional knock-out mES cells, increased global H3K56ac in the absence of HDAC1 but not HDAC2. Focusing on HD1^{Δ2/Δ2};HD2^{WT/Δ2} thymocytes demonstrates histone hyperacetylation of all modifications tested. That is, H3K9 and -K27 (Fig 5.12);

H4K16 and H3K56 acetylation (Fig 5.21A); as well as H3K18, H4K12 and H4K14acetylation (Fig 5.21B). Hypoacetylation is required for faithful chromosome segregation and maintenance of constitutive heterochromatin through subsequent cell divisions (Grewal, S. I., Bonaduce, M. J. and Klar, A. J., 1998, Ekwall, K., et al., 1997). As such, the overall global hyperacetylation detected in HD1^{Δ2/Δ2};HD2^{WT/Δ2} thymocytes may well contribute to the degree of chromosomal instability associated with HD1^{Δ2/Δ2};HD2^{WT/Δ2} T cell lymphomas.

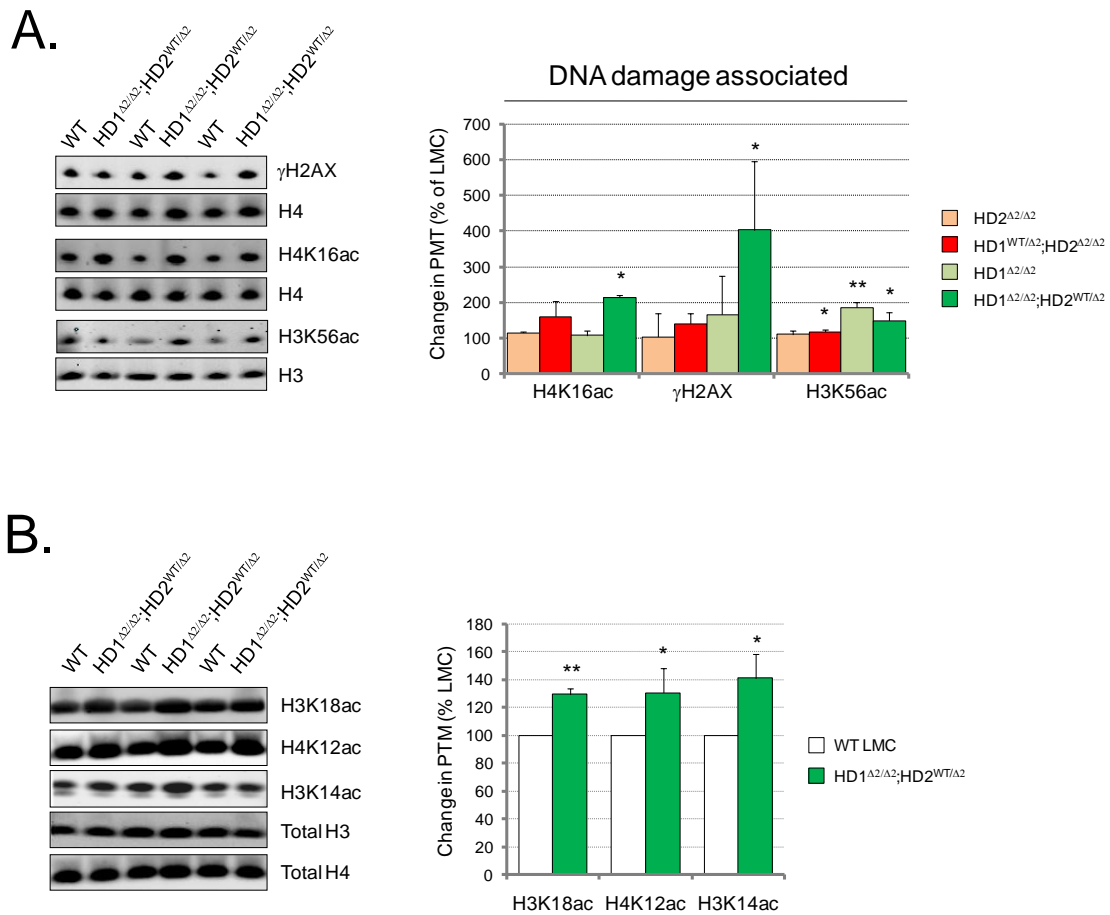


Figure 5.21. *Global histone hyperacetylation of T cells in the absence of HDAC1 but not HDAC2.* The global acetylation status of core histones from 6-8 week old mice was detected using quantitative Western blotting. Histone modifications associated with (A) DNA damage as well as (B) a number of other histone modifications are elevated in HD1 $\Delta 2/\Delta 2$;HD2 $^{WT/\Delta 2}$ thymocytes. Histones were acid extracted from thymocytes of 6-8 week old mice of the genotypes indicated. The signal of the indicated histone post translational modifications (PTM) were normalized to the total amount of H3 or H4 as appropriate and quantified using a LiCOR scanner. Mean values (n = 3) \pm S.E.M. are plotted. (*P<0.05, **P<0.01, paired T-Test). Western blots for HD1 $\Delta 2/\Delta 2$;HD2 $^{WT/\Delta 2}$ and WT LMCs (n=3) are shown on the left.

5.8 Conclusions.

The well defined process of T cell development provides a useful physiological tool in which to study the physiological roles of HDAC1 and -2. Conditional deletion of HDAC1 and -2 in mice reveals critical and combinatorial roles for these enzymes in the normal differentiation of early lymphocyte precursors, through to mature single positive (SP) CD4 helper or CD8 cytotoxic T cells. Namely, in order to maintain total thymocyte cellularity in neonates, a full complement of HDAC1 and -2 is required for the transition of immature thymocytes from the double negative (DN) to the DP stage of development (Fig 5.8). Conditional knock-out also demonstrates that optimal levels of HDAC1 and -2 are required for the repression of CD8 in immature DN thymocytes (Fig 5.7). Post DN development, using a combination of T cell surface markers, I was able to identify that mutant-CD8 thymocytes are DP cells that fail to express CD4, surprisingly, indicating a possible role for HDAC1 and -2 in the positive regulation of CD4 expression in DP thymocytes. Presence of mutant-CD8 thymocytes, correlated to the copy number of HDAC1 and -2, is dominantly conferred by an absence of HDAC1. Optimal levels of HDAC1 and 2 are also required to maintain the number of DP thymocytes which undergo positive selection, reduced in HD1^{WT/Δ2};HD2^{Δ2/Δ2} and HD1^{Δ2/Δ2};HD2^{WT/Δ2} mice and accounts for the subsequent decrease in mature CD4 and CD8 SP thymocytes. Cells which are positively selected show a bias towards CD8SP commitment (Fig 5.10), revealing a role for HDAC1 and -2 in thymocyte development both pre- and post-positive selection. By breeding HDAC mutant mice to the OT-II transgenic mouse line, demonstrates the profound block in thymocyte differentiation is downstream of TCR complex formation (Fig 5.11) and

suggestive of a block in TCR signal transduction. This is supported by transcriptional profiling which demonstrates decreased expression of genes which have roles in T cell activation, differentiation and in particular TCR mediated signalling. Analyses of deacetylase potential, using in vitro deacetylase assays and analysis of histone substrate acetylation, reveals HDAC1 to be the more effective, or prominent deacetylase of the two class I HDACs and also demonstrates that HDAC1 and -2 are required for normal thymocyte development in a dose dependent manner.

The use of compound targeted mice (i.e. HD1^{WT/Δ2};HD2^{Δ2/Δ2} and HD1^{Δ2/Δ};HD2^{WT/Δ2}) permitted the analysis of the roles of HDAC1 and -2 in T cell development beyond the DN stage in development and demonstrates a role for these enzymes in maintaining chromosomal instability. HD1^{Δ2/Δ};HD2^{WT/Δ2} mice, demonstrated as having the lowest deacetylase potential of mutant mice, develop a lethal pathology, characterised as T cell lymphoma (with 100% penetrance). These lymphomas are characterised by severe chromosomal abnormalities in all tumours analysed (in particular trisomy 15). Pre-lymphomic overexpression of the *c-myc* proto-oncogene is detected in HD1^{Δ2/Δ};HD2^{WT/Δ2} thymocytes, as are genes involved in DNA repair and replication. In 6-8 week old mice of the same genotype, a profound increase in DNA damage (as assessed by increased levels of γH2AX) and hyperacetylation of histones is also detected. These data suggest that in the absence of optimal levels of HDAC1 and -2 a combination of cellular and transcriptional defects cooperate in the malignant transformation of developing thymocytes.

Chapter Six: Discussion.

6.1 HDAC1, but not HDAC2, regulates H3K56ac and is required for optimal deacetylase activity of HDAC1/2 complexes in mES cells.

To assess the embryonic requirement for HDAC1, in relation to HDAC2, I have generated mouse embryonic stem (mES) cells in which each gene can be inactivated conditionally. Loss of HDAC1, but not HDAC2, reduces the amount of deacetylase activity associated with HDAC1/2 complexes, particularly NuRD and CoREST, despite a compensatory increase in HDAC2 protein and its incorporation into these complexes (Fig 4.2). Lager and colleagues (Lager G., *et al.*, 2002) noted a similar decrease in Sin3A and NuRD associated HDAC activity in their HDAC1^{-/-} mES cell system. Concordant with these data, one can report that loss of HDAC1 alone results in increased H3K56ac in mES cells (Fig 4.3). This solitary detected change in lysine acetylation may reflect that H3K56ac is a relatively rare modification in mammalian cells (approximately 1% of histone H3) (Das C.*et al.*, 2009 and Xie W., *et al.*, 2009). Whereas, histone tails appear to be hyperacetylated in mES cells (compare TSA induced acetylation in WT mES cells versus MEFs, Fig 4.4.B and C respectively), potentially masking the detection of increased acetylation due to the loss of HDAC1. It has been shown previously that H3K56ac is a substrate for the NAD⁺-dependent deacetylases SIRT1 and SIRT2 (Das C.*et al.*, 2009). Notably, no change in *sirt1* or *-2* mRNA expression in cells lacking HDAC1 is detected, thus ruling out reduced expression of these genes as a potential means of mediating the increase in H3K56ac observed in HDAC1^{Δ2/Δ2} mES cells (Fig 4.4D). Therefore, I have been able to demonstrate that H3K56ac levels are also regulated by HDAC1, in addition to other zinc-dependent HDACs (Fig 4.4.A).

Perhaps the most obvious explanation for a reduction in the deacetylase activity of HDAC1/2 complexes in the absence of HDAC1, is that HDAC1 is a slightly more effective deacetylase than HDAC2 in mES cells. It remains to repeat these experiments in somatic cells, particularly those cell types where HDAC1 and 2 are functionally redundant, to ask if this dependence for HDAC1 is embryonic specific. If so, then this may explain in part the post-gastrulation lethality of HDAC1-KO mice (Lager G., *et al.*, 2002 and Montgomery R.L., *et al.*, 2007), and the mES cell differentiation phenotype (discussed below).

6.2 Loss of HDAC1 or HDAC2 does not affect cell cycle in mES cells.

HDAC1 and HDAC2 have been linked to cell cycle regulation by their association with the tumour suppressor, Rb (Brehm A., *et al.*, 1998, Luo R.X., *et al.*, 1998 and Magnaghi-Jaulin L., *et al.*, 1998) and transcriptional repression of the CDK inhibitor, p21 (Lagger G., *et al.*, 2002, Zupkovitz G., *et al.*, 2006 and Senese S. *et al.*, 2007). However, I found no change in the growth potential of either HDAC1^{Δ2/Δ2}, or HDAC2^{Δ2/Δ2}mES cells (Fig 4.5A and B), nor could I observe any change in the level of *p21* mRNA (although its expression is increased by treatment with TSA, Fig 4.8A and B). Phenotypically therefore, HDAC1^{Δ2/Δ2} cells differ from the HDAC1^{-/-}mES cells used by Lagger *et al.*, which may reflect the difference in their derivation, either by sequential gene targeting followed by conditional deletion, or from blastocysts bearing a constitutive deletion. Although *p21* is the prototypical HDAC1 target gene, it is interesting to note that siRNA-mediated knockdown of HDAC1 produces a cell type specific up-regulation of *p21* (Senesse S., *et al.*, 2007). Rather than affecting cell cycle,

deletion of HDAC1 in HDAC1^{Lox/Lox} mES cells causes an increase in the amount and variety of cell types produced during mES cell differentiation.

6.3 HDAC1 is required for the controlled re-programming of mES cells upon differentiation.

mES cells contain a number of distinct HDAC1/2-containing complexes including Sin3A, NuRD, CoREST (Fig 4.2), and a recently described complex termed the Nanog and Oct-4-associated deacetylase (NODE) complex (Liang J., *et al.*, 2008). The NODE complex is similar in composition to NuRD, but lacks MBD3 and Rbbp7. Interestingly, perturbation of the NuRD complex by deletion of MBD3 causes a defect in mES cell differentiation, concomitant with a reduced Mta2-HDAC1 interaction (Kaji K., *et al.*, 2006). Conversely, disruption of NODE causes increased differentiation, associated with the activation of endodermal-specific markers (GATA6 and Foxa2) (Liang J., *et al.*, 2008). Therefore, two distinct HDAC1/2-containing complexes appear to have opposing functions in regard to mES cell fate and lineage commitment. Unlike deletion of the NuRD component MBD3 (Kaji K., *et al.*, 2006), deletion of either HDAC1 or HDAC2 did not affect the potential of mES cells to exit the pluripotent stem cell program upon LIF withdrawal (Fig 4.6.). Inactivation of Oct4 occurs concomitantly with deacetylation of its promoter region shortly after differentiation begins (Feldman N., *et al.*, 2006). However, the ability to switch off *Oct4* (and *Nanog*) expression is unperturbed by loss of either HDAC1 (serum, serum free and ATRA cultured EBs) or HDAC2 (serum and ATRA cultured EBs). Early differentiation of mES cells into primitive ectoderm, key to formation of the three primary germ layers, was also unaffected, as suggested

by the presence of *Oct4* and spike of *Fgf5* expression in day 2-4 EBs (Fig 4.9A and B, HDAC1^{Δ2/Δ2} and HDAC2^{Δ2/Δ2} serum cultured; Fig 4.11A, HDAC1^{Δ2/Δ2} and HDAC2^{Δ2/Δ2} ATRA cultured and Fig 4.13A, HDAC1^{Δ2/Δ2} serum free cultured). From days 4 to 12, in culture conditions containing serum, HDAC1^{Δ2/Δ2} EBs are distinct from either undeleted controls or HDAC2^{Δ2/Δ2} EBs, by their reduced size, irregular shape, substantially increased contractility and superior, more defined cellular organisation. Further analysis of transcriptional profiles of serum cultured HDAC1^{Δ2/Δ2} EBs indicates their preferential differentiation into mesoderm, particularly cardiomyocytes (*Nkx2-5*, *Mef2c*, *Hopx*, *Myl2*, *Actc*) and latterly neuroectoderm cell lineages (*nestin*, *βIII-tubulin*) possibly at the expense of endoderm (*Afp*, *Gata6*). In contrast, transcriptional differences have yet to be detected in HDAC2^{Δ2/Δ2} EBs, as might be expected since we observe no change in the deacetylase activity of co-repressor complexes in the absence of HDAC2. These results are consistent with results using shRNA-mediated knockdown of HDAC2 in mES (Liang J., *et al.*, 2008). In the absence of serum, despite the absence of a contractile phenotype and a gene expression profile endorsing the differentiation of mES cells into cells of the cardiomyocyte lineage, EBs lacking HDAC1 still display a greater degree of irregularity as well as exhibiting superior, more defined cellular organisation when compared to undeleted controls. Indeed, the differences in cellular organisation of HDAC1^{Δ2/Δ2} EBs cultured in standard differentiation media (containing serum) and those cultured serum free, compared to counterpart undeleted controls, are remarkably similar (compare Fig 4.7D with 4.12D, note the consistent presence of structured regions of organised epithelium in HDAC1^{Δ2/Δ2} EBs), revealing that HDAC1 consistently appears to moderate the overall degree, nature and pace of mES

cell differentiation, despite the absence of serum morphogens, in a generic fashion.

Notwithstanding a general bias towards neural lineage specification or the serum dependent differentiation into cardiomyocytes of HDAC1^{Δ2/Δ2}mES cells (discussed later), specific details with regards identification of a particular lineage, which may characterise the apparent generic enhancement of differentiation mediated by HDAC1 (as seen by basic histological analysis), remains to be formally accomplished. Potentially, this could be achieved by a more thorough immunohistochemical analysis on EB sections, in conjunction with global expression analysis using microarrays. Parallel to these analyses, generation of morphogen or signalling reporter mES cell lines could be used to identify signalling pathways (acting as predictors of tissue formation) specifically activated in HDAC1^{Δ2/Δ2}EB differentiation. Previously, a Wnt reporter mES cell line has been used to identify the role of Wnt signalling in formation of mesoderm progenitors in differentiating EBs (Berge, D., et al., 2008).

6.3.1 HDAC1 mediates neuronal and cardiac cell differentiation of mES cells.

One specific aspect of mES cell differentiation which appears to be consistently moderated by HDAC1, regardless of differentiation culture conditions, is neuroectodermal specification (in particular neuronal cells). Both in serum and serum free conditions overexpression of the neuronal precursor, *nestin*, is observed (Fig 4.13 A). Formal neural differentiation of EBs lacking HDAC1 using ATRA, increased detection of neuronal precursor and committed

neuronal cells, as defined by the expression of *nestin* and *β III-tubulin*, respectively (concomitant with increases in their relative gene expression) (Fig 4.11A and B). These data concur with studies in which HDAC inhibitors have been applied to neuronal precursors, resulting in a selective increase in neurons, but not oligodendrocytes or astrocytes (Balasubramaniyan V., et al., 2006, Hsieh J. *et al.*, 2004 and Siebzehnrubl F.A., *et al.*, 2007), which argues in favour of a specific, rather than general role for HDAC1 in differentiation.

In experiments using ATRA, although I demonstrate the formation of neuronal like cells that exhibit the expected expression of the neuronal and neurone specific proteins (NESTIN and β III-TUBULIN), these data would be more informative had I assessed the formation of other neuronal cell types, such as oligodendrocytes, by demonstrating the mutually exclusive expression of cell specific proteins in individual cells. Many of the assays performed here rely on the relative expression of one or two particular mRNAs, in what often appears to be heterogeneous population of cells, to identify the presence or absence of a particular cell lineage. It is entirely possible, for example, that the absence of HDAC1 is responsible for the direct derepression of a particular gene. When relying solely upon gene expression, without a wider ranging analysis incorporating detection of mutually exclusive cell type specific markers, I may simply be detecting global non-cell specific gene derepression and not differential lineage specification, per se. Indeed, expression of *nestin* in P19 embryonic carcinoma cell lines (early precursors to the use of ES cells) is concomitant with the acetylation status of its' regulatory elements alone (i.e. expression is induced by treatment with HDAC inhibitors and correlates with hyperacetylation of promoter/enhancer elements but not correlated with DNA

methylation) (Han, D. W., *et al.*, 2009). Also, HDAC1 is found in cells as part of a core complex with the co-repressor, CoREST, and LSD-1 which repress transcription by deacetylating histone tails (Humphrey, G.W., *et al.*, 2001 and Hakimi, M.A., *et al.*, 2002). The CoREST complex has been shown to repress neuronal genes in non-neuronal cells (Ballas, N.E., *et al.*, 2001). Thus, it is reasonable to speculate that the measured decrease in deacetylase potential of the co-repressor complexes CoREST, mSin3a and NuRD, in the absence of HDAC1 (demonstrated in Fig 4.2A), could be responsible for non lineage specific, derepression of a subset of co-repressor target genes, some of which may be genes I have used as lineage specific markers in Q-RT PCR analysis.

Identification of the serum dependent differentiation of mES cells lacking HDAC1 into cardiomyocytes, however, is much less ambiguous to interpret. The obvious rhythmic “beating” is accompanied with up regulation of a number of genes whose roles are well established in cardiomyocyte commitment and normal heart development (*Brachyury, Gata4, Nkx2-5, Mef2c, Hopx, Myl2, Actc*) (Heikinheimo, M *et al.*, 1994, Yan, F.Y., *et al.*, 1998, Lin, Q., *et al.*, 1997, Grow, M. W. & Kreig, P. A., 1998, Chen, F., *et al.*, 2002, Shin, C.H., *et al.*, 2002) and is consistent with a number of studies in which HDAC inhibitors have been applied to pluripotent cells. Treatment of day 7 EBs with TSA promotes cardiomyocyte differentiation (Kawamura T., *et al.*, 2005) as measured by an increase in *Nkx2-5* expression, which may be a direct target of HDAC1 (Liu Z., *et al.*, 2009).

The transcription factors GATA4, NKX2.5, MEF2C and SRF are all required for myocardial lineage commitment and normal heart development. All four are activators of cardiac specific genes individually or synergistically as co-

activators by binding to adjacent promoter or enhancer elements of target genes (Chen, F., *et al.*, 1996, Durocher, D., *et al.*, 1997, Morrin, S., *et al.*, 2000, Sepulveda, J., *et al.*, 2002, Niu, Z., *et al.*, 2005), with knock-out or systems biology studies pointing towards a SRF centric model of co-activation (Niu, Z., *et al.*, 2005, Schelsinger, J., *et al.*, 2011). Indeed, EBs formed from SRF null mES cells fail to contract or activate cardiac specific genes despite the expression of *Nkx2-5* and *Gata4* being unaltered (Niu, Z., *et al.*, 2005). HOPx is a novel homeodomain protein expressed by embryonic and postnatal cardiomyocytes which unusually does not interact with DNA (Chen, F., *et al.*, 2002, Shin C. H., *et al.*, 2002). HOPx, whose gene expression is positively regulated by NKX2-5, functions downstream of NKX2-5 during development and modulates cardiac growth and proliferation by inhibiting the transcriptional activity of SRF (Shin C. H., *et al.*, 2002). Significantly, the temporal pattern of gene expression of cardiac lineage transcriptional regulators in HDAC1^{Δ2/Δ2}EBs closely resembles what has been observed by in situ hybridisation, in developing cardiac tissue in the mouse embryo. *Brachyury*, required for mesoderm formation from which cardiac mesoderm is formed, is visible in the mouse embryo at E7.0 (Herrmann, B. G, 1991). This is followed shortly by expression of *Nkx2.5* and *Mef2c* in cardiac mesoderm (E7.5, Chen, F., *et al.*, 2002, Edmondson, D.G., *et al.*, 1994) and *Gata4* in myocardium (E8.0, Heikinheimo, M., *et al.*, 1994). Expression of *Hopx* and *Srf* expression is readily detected in the same tissue from day E8.5-E9.0 (Chen, F., *et al.*, 2002, Shin, C.H., *et al.*, 2002, Niu, Z., *et al.*, 2005). In HDAC1^{Δ2/Δ2}EBs that exhibit a contractile phenotype, formation of mesoderm, as detected by the expression of *brachyury*, occurs at day 4 of culture and is concomitant with detection of

Gata4. Consistent with the temporal expression patterns in developing mouse embryos, on day 7 of culture, expression of *Mef2c* and *Nkx2.5* is detected post detection of *brachyury* and *Gata4*. Further to this, expression of *Srf* (significantly detected in contacting HDAC1^{Δ2/Δ2} EBs, although not greatly over expressed compared to controls, Fig 4.9B) and over expression of *Hopx* is detected on days 7 and 12 of culture. This parallels with the detected expression levels of *Nkx2.5* and consistent with data suggesting *Hopx* to be a target of NKX2.5 (Shin, C.H., *et al.*, 2002). Finally, and consistent with the beating phenotype, expression of cardiac contractile genes *Actc* and *Myl2* are detected on days 7-12 (Fig 4.9A and B). Combined, the contractile phenotype and the temporal gene expression pattern of EBs lacking HDAC1 (which closely resembles that seen in the developing mouse embryo) indicate a role for HDAC1 in the specific control of mES cell differentiation into cells of the cardiac lineage.

6.4 Putative mechanisms of precocious differentiation in HDAC1 deficient mES cells: HDAC1 is required for the control of SRF centred cardiomyocyte differentiation.

Preceding the contractile phenotype and detection of cardiomyocyte gene expression profile, is the bias towards mesoderm formation (as detected by increased *brachyury* expression) in HDAC1^{Δ2/Δ2} EBs. As already noted, *brachyury* expression is key to mesoderm formation, which in turn is a prerequisite for formation of cardiac mesoderm and differentiation of cells into cardiomyocytes. A study utilising LSD-1 conditional knock-out mES cells, combined with mice homozygous for an *Lsd-1* gene trap insertion, infer that LSD1 is recruited directly to the *brachyury* locus in order to restrict its

expression prior to differentiation in mES cells and gastrulation in the developing embryo (Foster, C.T., *et al.*, 2010). LSD-1 forms part of a CoREST/HDAC1/2 co-repressor complex (Lee, M.G.C., *et al.*, 2006), integrity of which is compromised upon deletion of LSD-1 in mES cells, concomitant with a decrease in deacetylase potential of the complex and global increases in histone acetylation (H3K9ac and H3K56ac) (Foster, C.T., *et al.*, 2010). Given that deletion of HDAC1 in mES cells results in the reduced deacetylase potential of CoREST (Fig 4.2A) as well as similar increased global acetylation of H3K56ac (Fig 4.3), it is plausible that the reduction in deacetylase potential of this complex results in the increased expression of *brachyury*, mediated in part, by increased acetylation of the *brachyury* promoter. These associations, however, have yet to be formally correlated but suggest that HDAC1 may also be directly involved in the control of *brachyury* gene expression and provide a putative mechanism for the bias towards mesoderm formation observed in contracting HDAC1^{Δ2/Δ2}EBs. Notably, when compared to controls, *brachyury* over expression is also latterly detected in ATRA treated HDAC1^{Δ2/Δ2}EBs at day 12 of differentiation (4 days after withdrawal of ATRA from culture media) but not in serum free conditions (Fig 4.11B and 4.13A). This is suggestive of, in the presence of serum and the absence of an over-riding morphogenic signal, a general HDAC1-dependent mechanism of *brachyury* repression.

Serum free differentiation experiments indicate that formation of mesoderm per se is not predictive of cardiomyocyte differentiation (Fig 4.12C and 4.13). As already discussed, cardiomyocyte differentiation is dependent on the expression and activation of a number of transcription factors and mediators of transcription factor activity, which combine to generate a milieu of pro-

cardiomyocyte forming factors centred on SRF target gene activation. In contracting EBs deficient of HDAC1 a number of these factors are upregulated (*Nkx2.5* and *Mef2c*, Fig 4.9A). *Nkx2.5* has been shown to be a direct target of HDAC1 repression as has *Mef2c*. HDAC1 has been implicated in repressing *Nkx2-5* expression. Indeed, WNT signalling promotes *Nkx2-5* expression and early cardiomyogenesis via downregulation of Hdac1 (Kawamura T., *et al.*, 2005, Liu Z., *et al.*, 2009). Similarly, transcriptional repression of Mef2 has been shown to be mediated directly by the co-repressor MITR via its association with HDAC1 in *Xenopus* (Sparrow, D.J., *et al.*, 1999). Direct derepression of *Nkx2-5* and *Mef2c* expression by an HDAC1 associated complex may explain their elevated detection HDAC1 EBs. However, in skeletal muscle a large body of evidence has demonstrated that regulation of MEF2 target gene expression is mediated via the association of MEF2 with either Class II HDACs or HATs, associations that convert MEF2 into either a repressor or inducer of target gene expression imposed by respective localised alterations in the acetylation status of chromatin at MEF2 target gene loci (Lu, J., *et al.*, 2000, McKinsay, T. A., *et al.*, 2001, Potthoff, M.J., *et al.*, 2007). Current evidence also implicates a similar role for Class II HDACs in the regulation of MEF2 activity in cardiomyocytes and the regulation of cardiac hypertrophy. The MEF2-HDAC interaction is mediated by a sequence of 18aa conserved at the N-terminal of Class II but not Class I HDACs (Lu, J., *et al.*, 2000). This would seem to exclude a direct MEF2-HDAC1 association for providing a singularly mechanistic explanation for the increase in cardiomyocyte lineage commitment in HDAC1 EBs.

Unlike *Nkx2-5* or *Mef2c*, *Gata4* expression remains largely unchanged in contracting HDAC1 deficient EBs (Fig 4.9A), excluding over expression of

Gata4 mRNA as a possible mechanism for the cardiomyocyte phenotype. However, GATA4 activity and subsequent target gene transcription has been shown to be moderated via its' own acetylation status. Acetylation of GATA4 activates cardiac gene transcription which is reduced upon GATA4 deacetylation, possibly mediated by a GATA4-HDAC2 association, an interaction stabilised by the presence of HOPx (Trivedi, C.M., *et al.*, 2010). Given their shared sequence homology and co-occupancy of co-repressor complexes, it is possible (although not formally proven) this interaction is interchangeable between HDAC1 and 2, proposing another putative mechanism for the increase in cardiomyocyte lineage commitment in serum cultured HDAC1 deficient EBs. HOPx is known to mediate its repressive functions upon cardiac gene transcription by two methods; firstly by competing with known co-activators of SRF gene transcription, NKX2.5, GATA4, and MEF2C for association with SRF; and secondly via the recruitment of deacetylase activity to SRF target genes which is presumed to reduce the transcriptional permissiveness of chromatin associated around SRF target gene promoters (the latter mediated by a physical interaction between HDAC2, HOPx and SRF) (Chen, F., *et al.*, 2002, Shin, C.H., *et al.*, 2002). In addition, SRF target gene transcription is positively associated with H3 promoter acetylation (Schelsinger, J., *et al.*, 2011). Thus, one current opinion is of an auto-regulatory role for HOPx in cardiac gene transcription. NKX2.5 drives not only the expression of SRF target genes but also the expression of *Hopx* which in turn acts to temper the expression of SRF target genes during cardiomyocyte differentiation. As with the HDAC2-GATA4 interaction, a plausible case could be argued that the

deacetylase function of the HDAC2-HOPx-SRF interaction could be interchanged with HDAC1. Detection of *Srf* mRNA in contracting HDAC1^{Δ2/Δ2}

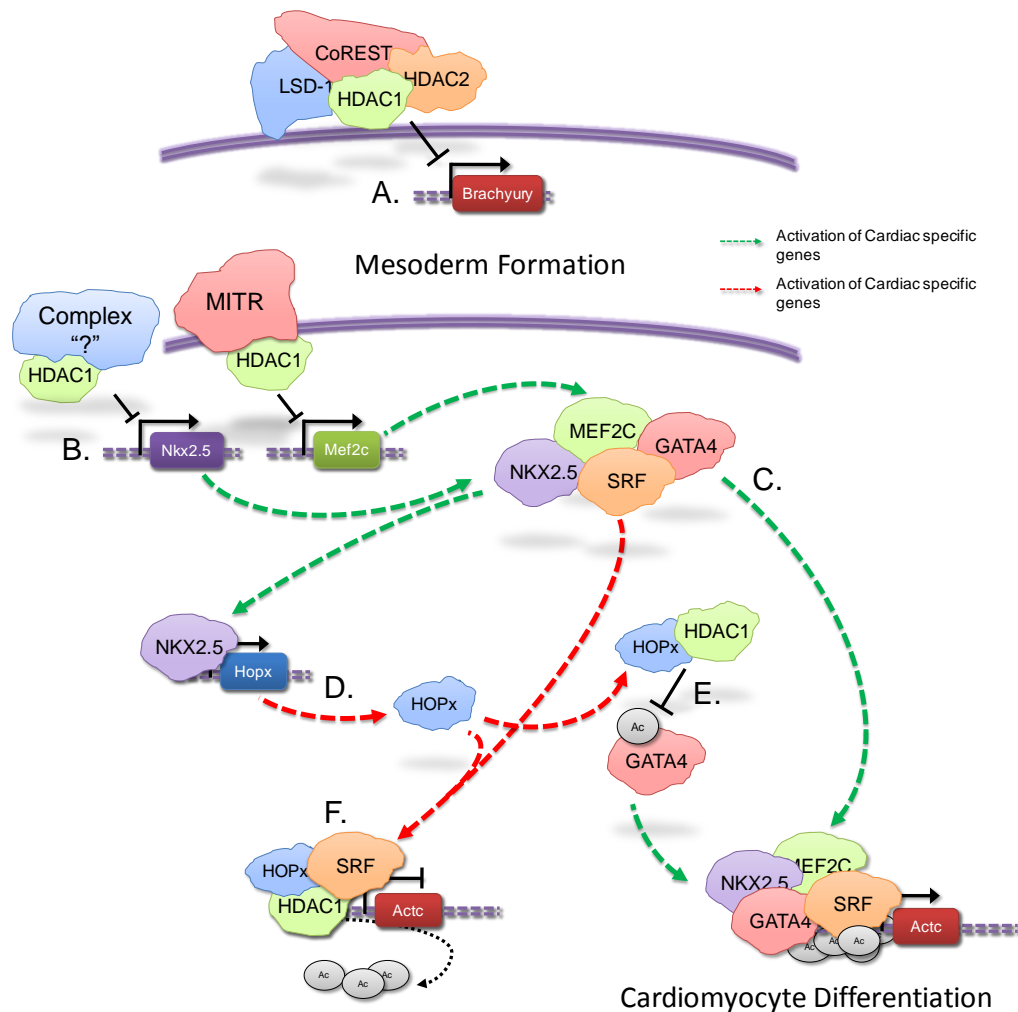


Figure 6.1. Summary of putative mechanisms of precocious differentiation in HDAC1 deficient mES cells: HDAC1 is required for the control of SRF centred cardiomyocyte differentiation. (A) *Brachyury* transcription, required for mesoderm formation, is a direct target of the HDAC1 containing co-repressor complex LSD-1/CoREST in mES cells. (B) *Nkx2-5* and *Mef2c*, required for direct and co-activation of cardiac specific genes, are directly repressed by an as yet unknown HDAC1 containing complex and the MITR-HDAC1 interaction respectively. (C) *NKX2.5*, *MEF2C*, *SRF* and *GATA4* are positive activators and transactivators of cardiac specific gene expression. Expression of these genes correlates with increased promoter H3 acetylation. (D) *Nkx2-5* positively regulates *Hopx* expression (E) In turn *HOPx* reduces the transcriptional activity of *GATA4* by direct deacetylation mediated formally by HDAC2

(putatively by HDAC1) and also (F) competitively associates with SRF reducing the association of co-activators whilst deacetylating SRF cardiac target gene promoter elements.

and control EBs is similar (slightly elevated in HDAC1 deficient EBs, Fig 4.9B). However, expression of *Hopx* is elevated in HDAC1^{Δ2/Δ2}EBs, presumably as a result of *Nkx2-5* expression. Expression of the cardiac specific genes *Actc* and *Myh2* has previously been shown to be negatively regulated by a HDAC2-HOPx-SRF (Shin, C.H., *et al.*, 2002) protein complex and are upregulated in contracting HDAC1 deficient EBs (Fig4.9.B) as would befit a model of combined HDAC1-HOPx-SRF mediated repression. Formal HDAC1-HOPx-SRF and HDAC1-HOPx-GATA4 protein interactions will need to be determined by co-immunoprecipitation experiments and assessment of their repressive capabilities confirmed using SRF responsive reporter expression assays in order for these models to hold true as singular mechanisms for the observed phenotype. Although I have been unable to formally identify a unique mechanism for the increased cardiomyocyte differentiation observed in serum cultured HDAC1 deficient EBs, I have identified a number of putative mechanisms which, based on the evidence presented here, I feel would warrant future investigation. Combined, the hypothesised mechanisms all centre around the induction of cardiac specific SRF genes and if proven correct would put HDAC1 at the centre of the SRF nexus of cardiomyocyte differentiation.

mES cell pluripotency and cell fate determination is profoundly affected by MAPK, Wnt and TGFβ signalling pathways (Murry C.E. and Keller G., 2008). It is interesting to note therefore that HDAC1 and -2 have been shown to be downstream effectors of Wnt signalling during cardiomyocyte (Liu Z., *et al.*, 2009) and oligodendrocyte (Ye F., *et al.*, 2009) differentiation. A more prudent

application of the conditional inactivation system using defined media (serum free supplemented with known amounts of particular morphogens), over prolonged periods, in conjunction with signalling molecule reporter mES cell lines could be used to identify the aberrant signalling pathways that lead to brachyury expression (in the instances of contracting HDAC1 deficient EBs) or the roles of HDAC1 and -2 in key lineage developmental pathways.

6.5 Optimal levels of HDAC1 are required to maintain controlled mES cell differentiation.

The requirement for HDAC1 for the control of mES cell differentiation, as illustrated in cardiomyocyte development, appears to be manifold, with HDAC1 involved in many key processes or pathways of transcriptional control (with both histone and non-histone substrates) and consequently cell differentiation and development. Thus it appears that cellular demands for HDAC1 protein are high (especially in differentiating mES cells), as such this may explain why in rescue experiments (Fig 4.15), the relatively low levels of stably transfected HDAC1 protein (Fig 3.14B) are insufficient to compensate for the loss of endogenous HDAC1 and a full complement of the protein is required to maintain normal HDAC1 function.

6.6 mES cell summary.

I have demonstrated that HDAC1 is necessary for the optimal deacetylase activity of HDAC1/2 co-repressor complexes and regulates the acetylation status of H3K56ac. This change in the biochemical activity of

HDAC1^{Δ2/Δ2}mES cells correlates with a precocious differentiation phenotype. The increased differentiation potential of these HDAC1^{Δ2/Δ2}mES (epiblast-like) cells may provide plausible *in vitro* evidence as to why HDAC2^{-/-} embryos survive at least until the perinatal stage and insight into why HDAC1^{-/-} embryos die shortly after gastrulation.

6.7 HDAC1 is required for optimal deacetylase activity in developing thymocytes.

In developing thymocytes, loss of HDAC1 reduces the amount of deacetylase potential of developing thymocytes via a direct reduction in deacetylase potential, or through the disruption of co-repressor complex integrity (Sin3, NuRD), this is despite compensatory increases in HDAC2 (HD1^{Δ2/Δ2} and HD1^{Δ2/Δ2};HD2^{WT/Δ2} thymocytes) (Fig 5.12). In the future, assessment of the deacetylase potential of co-repressor complex components, expression of which is unaffected by the loss of either HDAC1 or -2 (for example Mi2β), would be valuable with regards assessment of co-repressor deacetylase potential in the absence of either enzyme. Consistent with *in vitro* analysis of deacetylase activity, comparative analysis of histone modifications reveals that singular deletion of HDAC2 has no detectable effect on the global acetylation status of any of the histone lysine modifications analysed and reveals that HDAC1 is able to compensate for any loss of histone lysine deacetylase potential in the absence of HDAC2. Conversely, detectable increases in the acetylation of histone lysines only becomes apparent in thymocytes lacking HDAC1, where the increase in HDAC2 is able to partially

but not completely compensate for the loss of HDAC1 (Fig 5.12 and 5.21). Similar analysis of double targeted HDAC1 and -2 knock-out thymocytes would provide useful data with regards assessing the total contribution of HDACs 1 and -2 in the modification of the same lysine modifications. However, given the unsuitability of 6-8 week old HD1&2^{Δ2/Δ2} thymocytes (which have WT levels of HDAC2) and the low number for cells generated in HD1&2^{Δ2/Δ2} neonates, this was unachievable. Consistent with mES cell data (Fig 4.4), I am able to report that HDAC1 regulates H3K56ac in addition to all other histone lysine residues analysed. This data contrasts with data from human cell lines where knock down of both HDAC1 and -2 are required in order to detect hyperacetylation of H3K56 (Miller, M. K., *et al.*, 2010) but in agreement with a report in mouse embryonic fibroblasts (MEFs), where a combination of genetic and siRNA knock down of HDAC1 and -2, showed these enzymes to have preferred histone substrate specificities (Yamaguchi, T., *et al.*, 2010). The obvious explanation for a reduction in thymocyte deacetylase potential in the absence of HDAC1 is that it is a more effective deacetylase than HDAC2. Intriguingly, HDAC1 appears to be a preferred component of the Sin3a co-repressor complex and decreases in mSin3a protein are only apparent in thymocytes which lack HDAC1, this is despite an increase in the incorporation of HDAC2 into the Sin3a complex in the absence of HDAC1 (Fig 5.12). mRNA expression of *mSin3a* and *mta-2* is unchanged in 2-3 week old HD1^{Δ2/Δ2};HD2^{WT/Δ2} (pre-lymphomic) thymocytes (APPENDIX Table E5). Combined, these data suggest that the presence of HDAC1 also confers a greater degree of stability to co-repressor complexes. HDACs are non-DNA binding proteins and the hyperacetylation of histones in HD1^{Δ2/Δ2};HD2^{WT/Δ2} thymocytes could be compounded, not just by a global

reduction in enzymatic activity, but also a reduced capacity to recruit deacetylases to their enzymatic substrates as a result of complex degradation.

To address the issue of complex stability the generation of catalytic “dead” HDAC1 and -2 mutants would be extremely useful. The reduced deacetylase activity, reduction in the levels of co-repressor components and the global increase in histone acetylation, conferred mainly by an absence of HDAC1 in mouse thymocytes, are likely to contribute to the intra-thymic developmental phenotypes observed in HDAC1 and -2 deficient T cells (discussed below).

6.8 HDAC1 and -2 are required for expression of CD4 at the double positive stage of development.

Consistent with assessment of the deacetylase potential of mutant thymocytes lacking HDAC1, HDAC2 or combinations of HDAC1 and -2, deletion of HDAC2 does not affect normal T cell development. However, all other conditional knock-out mice analysed, exhibit an increase in an immature CD4^{low}/CD8^{high} or CD8 positive population and a decrease in mature CD4 or CD8SP thymocytes (Fig 5.4, 6-8 week old mice and Fig 5.5 and 5.10, neonates). Analysis of developing T cell populations identifies the mutant-CD8 cells to be DP thymocytes which fail to express cell surface CD4. *Cd4* mRNA expression is also downregulated in HD1^{Δ2/Δ2};HD2^{WT/Δ2} pre-lymphomic thymocytes and indicates a role for HDACs 1 and -2 in the positive regulation or maintenance of *Cd4* transcription. Intra-thymic T cell expression of CD4, at the gene level, is regulated in a stage specific manner and its regulation shows a

degree of plasticity. At the DN stage, *Cd4* expression is repressed with expression activated at the DP stage. In fully differentiated mature SP thymocytes, dependent upon either CD8 or CD4SP lineage commitment, *Cd4* expression must be either stably repressed or activated to permit mutually exclusive expression of either coreceptor. Thus, in the instance of CD8SP lineage commitment, the active transcription of *Cd4* at the DP stage of development is reversible (Kioussis, D., and Ellmeier, W., 2002). Positive *Cd4* transcription is driven by a number of constitutively active regulatory elements which include a promoter, two enhancers and a locus control region (Siu, G., et al., 1994, Sawada, S. and Littman, D. R., 1991, Adlam, M. and Siu, G., 2003), with stage specific transcription of the *Cd4* locus conferred by a region known as the CD4 silencer, deletion of which leads to cell surface expression of CD4 in both DN and CD8SP thymocytes (Zou, Y. R., et al., 2001, Taniuchi, I. and Littman, D. R., 2004). In mature CD8SP cells, transcriptional inactivation of *Cd4*, once established, is maintained independent of the *Cd4* silencer and mediated epigenetically by the incorporation of the *Cd4* locus into a heterochromatin-like structure, as marked by H3K9me3 and H3K27me3, with heterochromatin protein-1 (HP-1), one of the major structural components of heterochromatin, also implicated. (Zou, Y. R., et al., 2001, Taniuchi, I., et al., 2002b and Yu, M., et al., 2008). Thus, two different mechanisms in the *Cd4* silencer-mediated control of *Cd4* transcription has been established; active, reversible repression and epigenetic silencing. Several *trans*-acting factors are implicated in *Cd4* silencer function which include the Runt-domain proteins (Runx1 and -3) and the ATPase chromatin remodelling complex, BAF (a mammalian homologue of the yeast SWI/SNF complex) (Chi, T., et al., 2002). In

particular runt-domain proteins mediate either active repression in DN thymocytes (Runx1) or establishment of epigenetic silencing in CD8SP thymocytes (Runx3), through direct binding to the *Cd4* silencer (Taniuchi, I., *et al.*, 2002a, Taniuchi, I., *et al.*, 2002b) and thought to recruit HDACs via their interaction with mSin3a (Durst, K.I., *et al.*, 2004). Of note, at the DP stage of normal T cell development, histone acetylation of positive regulators of *Cd4* expression (i.e. the promoter and enhancers) positively correlates with cell surface expression of CD4 (Yu, M., *et al.*, 2008, Williams, C., *et al.*, 2004). By reducing levels of HDAC1 and -2, I have demonstrated that global hyperacetylation and decreased deacetylase potential in developing thymocytes correlates with the severity of the mutant-CD8 phenotype and reduced CD4 coreceptor expression. These results are paradoxical to the data presented thus far, whereby inducing a general status of global histone hyperacetylation at positive regulators of *Cd4* expression or by putatively reducing the deacetylase potential of Runx1 or -3 complexes, one might expect an increase in *Cd4* transcription and subsequent coreceptor expression. This indicates mechanisms of *Cd4* expression independent of background histone acetylation status, at promoter/enhancer elements, or impaired site-specific Runx recruitment of HDACs 1 and -2 to the *Cd4* silencer, as being responsible for the reduced *Cd4* expression in mutant-CD8 thymocytes. The Mi2 β component of the NuRD complex, an ATP-dependent chromatin remodeler, has been shown to be critical for normal intra-thymic T cell development. Indeed conditional inactivation of Mi2 β results in a developmental phenotype with characteristics strikingly similar to that observed in HD1 $\Delta 2/\Delta 2$;HD2^{WT/ $\Delta 2$} mice, that is, an accumulation of DP-like thymocytes that fail to express CD4. In particular,

Mi2 β was shown to be required for the active recruitment of the transcription factor HEB and the HAT (p300) to the proximal *Cd4* enhancer region in order to facilitate *Cd4* transcription. Co-immunoprecipitation of p300 demonstrated interactions between Mi2 β , HEB and p300 but not HDAC2, revealing a putative role for the NuRD complex as a positive regulator of transcription in the absence of HDACs (Williams, C., *et al.*, 2004). The same group, revealed an antagonistic interaction between Ikaros (the majority of which is associated with Mi2 β in T cells) and Mi2 β in determining CD4 expression mediated through alterations in the chromatin state of the *Cd4* silencer (Sridharan and Smale, 2007, Naito, T., *et al.*, 2007). Intricate analysis of the chromatin landscape at the *Cd4* locus in Ikaros and Mi2 β knock-out thymocytes demonstrated that Ikaros is required for the repression of CD4 from the DN stage by laying down a repressive chromatin state, marked at the *Cd4* silencer by comparative histone hypoacetylation. During the DN-DP transition this repressive state at the *Cd4* silencer is antagonised by the Mi2 β dependent, active recruitment of a HAT (MOZ) and the TAFIIID component of the basal transcriptional machinery, which results in *Cd4* silencer histone hyperacetylation and expression of CD4. In their analysis, HDAC2 was present at the CD4 silencer in ChIP experiments performed on total thymocytes (the majority of which express CD4) and deletion of either Mi2 β or Ikaros did not change this association or dramatically affect the localisation of other co-repressor proteins which were also present (Runx1 or mSin3a), suggesting that the antagonistic interactions of Ikaros and Mi2 β at the *Cd4* silencer are independent of these co-repressor proteins (Naito, T., *et al.*, 2007).

Decreases in protein levels of the NuRD component, MTA-2 (Fig 5.12), either through negative effects on MTA-2 translation or increased rates of post-translational turnover (note, no change in *mta-2* mRNA is detected in HD1^{Δ2/Δ2};HD2^{WT/Δ2} pre-lymphomic thymocytes using microarrays), correlates with the severity of the mutant-CD8 phenotype. Coimmunoprecipitation assays in HD1^{Δ2/Δ2};HD2^{WT/Δ2} thymocyte nuclear extracts show reduced amounts of MTA-2 associated with Mi2β and indicates reduced NuRD complex integrity (Fig 5.12). MTA-2 contains DNA binding protein motifs and has been shown to direct the formation of the NuRD deacetylase catalytic core (Zhang, Y., et al., 1998). Although admittedly a more thorough examination of the associations of other classic NuRD complex components such as MBD2/3 and RbAp46/48 or the HATs identified as interacting partners (above) would be more informative, reduced ability for functional NuRD complex formation, through loss of MTA-2 or MTA-2/Mi2β associations is likely to affect the recruitment of Mi2β to the *Cd4* silencer. Reductions in Mi2β silencer occupancy, a positive regulator of *Cd4* expression, are presented as a possible mechanism for reduced CD4 expression in the mutant-CD8 population. Performing CHIP for Mi2β and histone acetylation over the *Cd4* locus in HDAC1 and -2 knock-out thymocytes would reveal if Mi2β is still recruited and if the acetylation status is altered. Should the acetylation status be increased compared to WT mice, in the absence of Mi2β occupancy, one would have to conclude that the ATPase activity of Mi2β is also required for silencer mediated CD4 expression. Furthermore if merely background increased histone acetylation was required to mediate CD4 expression, one might imagine we would see a DN-like, CD4-positive mutant thymocyte population and not the DP-like, CD8-positive mutants

(as the authors revealed that Ikaros was present at the *Cd4* silencer and mediated repression of CD4 from the DN stage of T cell development). Alternatively, increased Ikaros recruitment or Ikaros protein levels (in absence of HDAC1 and -2) could mediate an overly repressive state through mechanisms independent of HDACs (note that although Ikaros protein levels have not been measured no significant change in *Ikaros* mRNA was detected in global transcriptional analysis).

6.9 HDAC1 and -2 are required for the progression of T cells from the DN-DP stage of thymocyte development and mediate repression of CD8 at the double negative stage of T cell development.

Double knock-out HDAC1 and -2 thymocytes show a dramatic 75% decrease in cellularity (Fig 5.5B). The DN-DP transition is marked not only by expression of the CD4/CD8 coreceptors but also by proliferative expansion, thus a block during this stage of development would result in a decrease in the subsequent DP and SP populations. Consistent with their role cellular proliferation and survival (Brehm A., *et al.*, 1998, Luo R.X., *et al.*, 1998, Magnaghi-Jaulin L., *et al.*, 1998, Lagger G., *et al.*, 2002, Zupkovitz G., *et al.*, 2006, Senese S., *et al.*, 2007 and Wilting, R.H., *et al.*, 2010) a decrease in cellularity is detected at this important transition, due in part to increased susceptibility to apoptosis and a subtle block or delay during the β -checkpoint (Fig 5.8). Conditional ablation of mSin3a in thymocytes results in a similar (although subtler) block at the DN stage and potentially is the complex through which HDAC1 and -2 mediate this transition in WT thymocytes (Cowley, S. M.,

et al., 2005). It would be interesting to analyse the levels of the cell cycle inhibitors, p21 and p27, known targets of HDAC mediated repression, in both mSin3a and HDAC1 and -2 double knock-out DN thymocytes, to assess if their derepression mediates this early block in T cell development. Likewise, analysis of DN cell cycle would be informative in confirming a block in cell proliferation. A single copy of HDAC2 is enough to circumnavigate this block at the DN stage and restore cellularity to WT levels as seen in HD1^{Δ2/Δ2};HD2^{WT/Δ2} neonatal mice (Fig 5.5B), where we actually observe an absence of traditional DN1-3 cells. Early re-arrangement of TCR genes may facilitate cells being driven through the β-checkpoint. PCR assays and aCGH results provide evidence that rearrangement does occur in HD1^{Δ2/Δ2};HD2^{WT/Δ2} thymocytes (Fig 5.17A). Furthermore, in pre-lymphomic mice TCR recombination genes (*Rag1/2* and *artemis*) are down regulated when compared to WT LMCs, suggesting that somatic recombination of the TCR locus has been achieved and they are no longer required (Fig 5.20D). The remaining DN4 cells exhibit precocious expression of CD8. Previously the Ikaros family of proteins have been shown to be involved in the activation of the CD8 locus, as has the activity of the chromatin remodelling complex BAF (Harker, N., T *et al.*, 2002, Chi, T., *et al.*, 2002). Repression of CD8 at the early DN stage of development correlates with co-occupancy of Ikaros, Mi2β and HP-1α at the CD8 gene locus. Upon transition to the DP stage, marked by CD8 expression, Ikaros remains bound to the CD8 locus, with Mi2β/HP-1α occupancy lost. Thus, recruitment of Mi2β to the CD8 locus, in particular, acts to repress CD8 expression. Putatively, a reduction in the deacetylase potential or integrity of the Mi2β co-repressor

complex, NuRD (Fig 5.12) could account for the derepression of CD8 during this stage of development in HD1^{Δ2/Δ2};HD2^{WT/Δ2} thymocytes.

6.10 HDAC1 and -2 are required for positive selection and post selection lineage commitment of thymocytes.

I have been able to demonstrate, consistently, using a panel of maturation markers, that HDAC1 and -2 are required for the maturation of thymocytes beyond the DP stage of development, due in part, to reduced efficiency in positive selection marked by reduced numbers of TCRβ^{int}/CD69^{int} positive (HD1^{WT/Δ2};HD2^{Δ2/Δ2} and HD1^{Δ2/Δ2};HD2^{WT/Δ2} mice, Fig 5.10.). A failed attempt to “rescue” the phenotype, using transgenic mice which express a pre-arranged TCR, provides evidence that this developmental block is independent of TCR complex formation and points to a potential defect in signalling mediated through TCR/MHC engagement. Thymocyte activation and development depends on TCR/MHC initiated cascades of signal transduction events, involving the action of several non-receptor protein tyrosine kinases and adaptor proteins which include the Syk family protein tyrosine kinase ZAP-70, Src family members LCK and FYN, as well as adaptor proteins such as LAT and SLP76. High signalling activity generated by the tyrosine kinase LCK or the MAP kinases ERK1/2, enhances CD4SP commitment, while low activity of LCK, ZAP-70 or ERK1/2 leads to CD8SP development (Hernandez-Hoyos, G., *et al.*, 2000, Sharp, L. L. and Hedrick, S. M., 1999). Transcriptional analysis of HD1^{Δ2/Δ2};HD2^{WT/Δ2} thymocytes (Fig 5.20D) reveals down regulation of a number of key mediators of T cell signalling and activation when compared to WT.

These include; *LAT* (linker of activated T cells), required for the transduction of TCR mediated signalling following TCR engagement (Zhang, W., *et al.*, 1998); *Themis*, shown to regulate positive and negative selection of thymocytes through the regulation or integration of TCR mediated signalling (Fu, G., *et al.*, 2009 and Lesourne, R., *et al.*, 2009)); and *Itk* (IL-2 inducible T cell kinase), shown to play multiple roles in T cell development and differentiation including, positive regulation of CD4 lineage commitment, (Jiangfang, H., Qian, Q. and August, A., 2010), amplification of TCR signalling (August, A., *et al.*, 2002) and a positive role in thymocyte positive selection (Lucas, J. A., Atherly L. O. and Berg L. J., 2002). In order to confirm reduced signalling via TCR engagement, ideally one would need to carry out assessment of the protein levels of the panel of adapter proteins and protein tyrosine kinases including the phosphorylation levels of their substrates. Both HD1^{WT/Δ2};HD2^{Δ2/Δ2} and HD1^{Δ2/Δ2};HD2^{WT/Δ2} mice have reduced numbers of positively selected thymocytes and as such reduced numbers of SP cells. However, in HD1^{Δ2/Δ2};HD2^{WT/Δ2} mice those cells that are positively selected show a bias towards CD8 lineage commitment (Fig 5.10D, CD4:CD8 ratios are greatly reduced), a phenotype shared with both *Itk* and *Themis* deficient thymocytes and suggests that the reductions in TCR signalling could well be mediated through down-regulation of a transcriptional programme, inclusive of these genes, prior to positive selection. Alternatively, having revealed precocious expression of CD8 in DN4 cells in HD1^{Δ2/Δ2};HD2^{WT/Δ2} mice, derepression of CD8 may render the majority of positively selected cells unable to make a commitment to the CD4 lineage. Notably there is an absence of CD4^{high}/CD8^{low}

cells (characteristic of cells undergoing positive selection, see purple boxes highlighted in Fig 5.10C).

6.11 HDAC1 and -2 maintain normal levels of global acetylation which contributes to chromosomal stability in developing thymocytes.

As already discussed, thymocytes depleted of HDAC1 and -2 do not progress past the early double negative (DN) stage of development. In contrast, HD1^{Δ2/Δ2};HD2^{WT/Δ2} mice develop a 4 fold increase in T-cell cellularity (at 6-8 weeks) which leads to the development of T lymphoma/lymphoblastic leukaemia at 12 weeks of age with 100% penetrance. All lymphomas from these mice exhibit chromosomal instability (either aneuploidy or focal chromosomal gains or deletions). Spectral karyotyping (using techniques such as SKY) of lymphomas may provide even more evidence of genomic instability through identification of balanced translocations, which would be undetectable by aCGH. Hypomorphic alleles of Dnmt1, the maintenance DNA methyltransferase, causes genomic instability and T-cell lymphoma due, in part, to trisomy of chromosome 15 which includes *c-myc* (Gaudet, F., *et al.*, 2003). Similarly, mice absent in the histone methyltransferases Suv39h1 and Suv39h2, which maintain the level of histone H3K9 methylation (a heterochromatic mark), also develop lymphoma (Peters, A. H. F. M, *et al.*, 2001). Global hypoacetylation has been shown to be required for faithful chromosome segregation and maintenance of constitutive heterochromatin through subsequent cell divisions (Grewal, S. I., *et al.*, 1998, Ekwall, K., *et al.*, 1997). SMARCAD1 (an ATPase nucleosome remodeler) has been shown to ensure

the propagation of heterochromatin (pericentric heterochromatin in particular) through cell division, mediated by modulating the interaction of HDAC1 to sites of DNA replication (Rowbotham, S. P., *et al.*, 2011). Specifically in lymphoid cells, the NuRD complex has also been implicated in the formation of heterochromatin (Helbling Chadwick, L., *et al.*, 2009) mediated by direct Ikaros recruitment (Kim, J., *et al.*, 1999). Mice lacking or expressing a dominant negative form of Ikaros develop T cell lymphomas (Winandy, S., *et al.*, 1995 and Wang, J., *et al.*, 1996). *In vitro* activated Ikaros mutant T cells exhibit high levels of aneuploidy, which may play a role in their malignant transformation. Thus, epigenetic mechanisms of gene silencing (DNA methylation, histone methylation and acetylation) are essential for the integrity of the mammalian genome. HD1^{Δ2/Δ2};HD2^{WT/Δ2} lymphomas exhibit chromosomal instability (in general trisomy 15) but notably no change in global or pericentromeric DNA methylation is detected. However, dramatic hyperacetylation and a slight but significant decrease in H3K9me3 is detected which correlates with tumour progression in these mice (Fig 5.12E and Fig 5.21), implicating global alterations in histone modifications (in particular global histone hyperacetylation) as a potential driver of chromosomal instability in HD1^{Δ2/Δ2};HD2^{WT/Δ2} thymocytes. To this end, performing immunohistological analysis on mutant thymocytes to assess heterochromatin formation and co-localisation of heterochromatin associated proteins (such as HP1 α and components of the NuRD complex) would be extremely informative.

In mES cells and mouse thymocytes, H3K56 acetylation levels are mediated by HDAC1 (Fig 4.4A and 5.12E). The enzymatic activity of HDAC1 and -2 has previously been linked to the reduction of H3K56 acetylation and a

pre-requisite for DNA damage repair. Cells depleted of both HDAC1 and -2 have defects in double strand break repair (Miller, K. M, *et al.*, 2010). Potentially, the inability for HD1^{Δ2/Δ2};HD2^{WT/Δ2} thymocytes to deacetylate H3K56 prevents repair of DNA damage. Increased DNA damage, as detected by elevated levels of γ H2AX detection in 6-8 week old thymocytes of HD1^{Δ2/Δ2};HD2^{WT/Δ2} thymocytes (above all other genotypes), would support this hypothesis (Fig 5.21A), as would the increased transcription of genes involved in DNA replication/metabolism which may indicate activation of the DNA damage response pathway (Fig 5.20D).

Overexpression of the proto-oncogene *c-myc* is detected in pre-lymphomic HD1^{Δ2/Δ2};HD2^{WT/Δ2} thymocytes (mRNA) and in fully developed tumours (protein) which could potentially be the source of chromosomal instability, given that mice which overexpress *c-myc*, develop thymic lymphomas, characterised by trisomy 15 (Marinkovic, D., *et al.*, 2004). Also *Satb1*, a global regulator of the thymocyte transcriptome that mediates its repressive functions through association with HDAC1 (Alvarez, J. D., *et al.*, 2000, Purbey, P. K., *et al.*, 2009), has been shown to repress *c-myc* expression in developing T cells and strengthens a case for tumourogenic transformation mediated by derepression of *c-myc* (*Satb1* is also detected as downregulated in pre-lymphomic HD1^{Δ2/Δ2};HD2^{WT/Δ2} thymocytes). However, a bias towards upregulated genes on chromosome 15, in pre-lymphomic thymocytes, indicates that the event which results in trisomy 15 (observed in 4/6 fully developed lymphomas analysed) may have already occurred and that chromosomal instability itself is the transformation initiating event in HD1^{Δ2/Δ2};HD2^{WT/Δ2} thymocytes (Fig 5.20E). A strong association exists between

activating *Notch1* mutations and human or mouse models of T-ALL (Weng, A. P., *et al.*, 2004, Malecke, M. J., *et al.*, 2006, De Keersmaecker, K., *et al.*, 2010). Global transcriptional analysis of pre-lymphomic HD1 ^{$\Delta 2/\Delta 2$} ;HD2^{WT/ $\Delta 2$} thymocytes does not reveal up-regulation of the classic *Notch1* target genes *Hes1* or *Deltex* (Kathrein, K. L., Chari, S. and Winandy, S., 2008, van Hamburg, J. P., *et al.*, 2008) and rules out a collaborative *c-myc-Notch1* pathway of transformation at this stage. Ultimately however, *Notch1* mutations may occur latterly which could participate in HD1 ^{$\Delta 2/\Delta 2$} ;HD2^{WT/ $\Delta 2$} thymocyte transformation, these could be identified by sequencing of the *Notch1* locus, coupled with transcriptional profiling, of HD1 ^{$\Delta 2/\Delta 2$} ;HD2^{WT/ $\Delta 2$} lymphomas. In summary I have been able to identify that HDAC1 and -2 are required for the maintenance of genomic stability and propose that in the absence of these enzymes a number of events take place which ultimately leads to tumour progression in T cells. Firstly a pre-malignant state is conferred by overexpression of the proto-oncogene *c-myc*, either as a consequence of direct derepression or through copy gain of chromosome 15 (the latter as a result of global hyperacetylation and unfaithful chromosome segregation). Thymocytes in which a pre-malignant state is established are then selected for expansion within the thymus. Global hyperacetylation and the inability to mediate the correct response to DNA damage (i.e. deacetylate H3K56), results in the accumulation of un-checked chromosomal or DNA abnormalities which leads to the subsequent gain of additional co-operating mutations and the consequent malignant transformation of HD1 ^{$\Delta 2/\Delta 2$} ;HD2^{WT/ $\Delta 2$} thymocytes.

6.12 Summary: HDACs 1 and -2 are required for normal T cell development and maintenance of genome stability.

A number of genetic studies have revealed critical functions of transcriptional repressors, co-repressors and chromatin modifying proteins throughout various stages of intra-thymic T cell development, many of which have been shown to associate with, and their repressor functions mediated by, an association with HDACs or known HDAC containing multi-protein complexes. I have been able to demonstrate, genetically, that HDAC1 and -2 play pleiotropic roles in normal T cell development. I have also been able to demonstrate, in a physiological system, a critical role for these enzymes in maintaining genome stability.

Appendices

APPENDIX ONE: PCR PRIMERS AND RESTRICTION ENZYMES.

A1. Cloning and recombineering primer sequences.

Primer	Primer Sequence
5' <i>Bam</i> HI-Hdac1 Resc cDNA	taaggatccatggcgcagactcagggcacc
3'Hdac1 Resc cDNA-FLAG- <i>Eco</i> R I	taggaattctcactgtcgatcatgctttgtagcaatgtcatgaccttgaatcgc gtcgtggccaacttgacctctcttga
5' <i>Bam</i> HI-Hdac2 Resc cDNA	taaggatccatggcgtacagtcaaggaggcggc
3'Hdac2 Resc cDNA-FLAG- <i>Eco</i> R I	taggaattctcactgtcgatcatgctttgtagcaatgtcatgaccttgaatcgc gtcgtgaggggtgctgagttgtctgact
T7	gtaatacactcactatagggc
BGH-Rev	tcagacaatgcatgcaatttc
HDAC1 5'sc5Cap	ttgtgaccctctcggtcccctctgaagagctgagctccatggtgcccgcaggc caccctcgaggctgcagggatcg
HDAC1 3'sc5Cap	acacgagcttacactgaggctggaagcatagcactggaagacaacgacagc ggtggcgggagcggataacaatttcacaca
HDAC2 5'sc5Cap	gcacaggctactactgtgtagctctgagaaatgaagacaagagtgtcttattac ctgaaaaatgccctcgaggctgcagggatcg
HDAC2 3'sc5Cap	tacataagaagtattctgaagtagcggagtaggatctaattgtcagctagtagtgc tcttgatccgctctagaactagtggatc
HD1For2	ctgaagagctgagctccatgg
HygSC5Seq2	ttggctgtatggagcagcag
5'neogen	tcaaacaccacagcatctaag
3'neogen	ttgtgtgtgttcatttgtaa

B1. Southern blot probe primer sequences.

Primer	Primer Sequence
HDAC1 5'pr 5'	gagagatggctcagtagttgg
HDAC1 5'pr 3'	gcaagctaaagtatcctcttc
HDAC1 3'pr 5'	gctgtcgtgtcttccagtgc
HDAC1 3'pr 3'	tccaggccttgaaggaggcagg
HDAC2 3'extpr 5'	gtttgttccggagatgtggc
HDAC2 3'extpr 5'	acatccactgcgccactctgg
HDAC2 5'pr 5'	tccttgaatgtgtgtacc
HDAC2 5'pr 5'	agtattatcactaccagc
HDAC2 3'intpr 5'	gttggcactgtgttttaac
HDAC2 3'intpr 5'	gcaacatttcatatgtatgt

C1. Mouse genotyping primer sequences.

Primer	Primer Sequence
HDAC1_For	aagcaggagctgatgcagagg
HDAC1_Rev	agtcagctcagaacatctcc
HDAC1_Mut	ggcttgattctcagtttgct
HDAC1_For2	ctgaagagctgagctccatgg
HDAC2_5'neogen	tcaaaccaccacagcatctaag
HDAC2_3'neogen	ttgttgttgttgcattttgtaa
HDAC2_For	ttaacatacatatgaaatgttgcc
HDAC2_Rev	ctgtctaccactgactttcatc
R26R GT1	aaagtcgctctgagttgttat
R26R GT2	gcgaagagttgtcctcaacc
R26R GT3	ggagcgggagaaatggatatg
Cre-Rev	attctcccaccgtcagtagc
Cre-Fwd	cgttttctgagcatacctgga
Tcr α Fwd	aaaggagaaaaagctctcc
Tcr α Rev	acacagcaggttctgggttc
Tcr β Fwd	gctgctgcacagacctact
Tcr β Rev	cagctcacctaacacgagga
Sin3_For	tggaggagaacatgtgctgttac
Sin3_Rev	ttaacagaagatcatccatgctc
Sin3_Mut	taacagtgttagttccctaactg
MRG15-For	cacatgctaaaggtgcatcaggaaca
MRG15-Rev	cttcagacataccagaagaggcatt
MRG15-Mut	ctagatgactccactaagtctgttca
VD1J1-Fwd	acctatgggagggtcctttttgtataaag
VD1J1-Rev	agactcctagactgcagactcag
VD2J2-Fwd	aaagctgtaacattgtggggacag
VD2J2-Rev	ccggagattccctaaccctggtc

D1. UPL Dual Hydrolysis ProbeLibrary; Q-RT PCR primer sequences, probe ID and amplicon size.

Primer	Direction	Universal Probe Library Primer Sequence	UPL Hydrolysis Probe	Amplicon Size (bp)
Oct3/4	F:	cacgagtgaaagcaactca	82	125
	R:	ctctgcagggttcatgt		
Nanog	F:	agcctccagcagatgcaa	25	76
	R:	ggtttgaaccagggtctaacc		
Fgf5	F:	gagccctgaaggaaactcg	89	76
	R:	gcgaacaaaatgacctgact		
Brachyury	F:	cgagatgattgaccaagaac	88	65
	R:	ggcctgacacattacctca		
Nkx2-5	F:	gacgtagcctggtctcg	53	70
	R:	gtgtggaatccgtcgaagt		
Mef2c	F:	tctccctcagtcattgg	77	63
	R:	cgtggtgtgtgtgggtatc		
MyoD	F:	ccaggacacgactgtcttct	52	76
	R:	cacaccgggtgtcctctac		
βIII-tubulin	F:	ggcaactatgtaggggactcag	78	87
	R:	cctgggcacatactgtgag		
Nestin	F:	tgcaggccactgaaaagt	2	89
	R:	ttccaggatctgagcgtct		
Gata6	F:	ggctctacagcaagatgatgg	40	94
	R:	tgccacagagacagtccaag		
Gata4	F:	ggaagacaccccaatctcg	13	75
	R:	catggccccacaattgac		
Hdac1	F:	gagtacctggagaagatcaagca	89	121
	R:	ctcatcccactctctcg		
Hdac2	F:	ctccacgggtgttctcagt	45	71
	R:	cccaattgacagccatatca		
p21	F:	tccacagcgatccagaca	21	90
	R:	ggcacactttgctcctgtg		
Hopx	F:	accacgctgtgcctatc,	68	72
	R:	gcgctgcttaaccatttct		
Srf	F:	cagcagtggggaaaccaa	10	91
	R:	gctgggtgctgtctggat		
Myl2	F:	cccagatccaggagtcaag	93	67
	R:	ttgtcgatgaagccgtctct		
Actc1	F:	gcttcgctgtccagaga	11	61
	R:	atgccagcagattccatacc		
sirt 1	F:	tctgcagtcaccagacct	41	56
	R:	aaaggaaggccttgagtttagg		
sirt 2	F:	cactacttcatccgcctgct	66	74
	R:	tcgttccagcgtctatgt		

Probes supplied by Roche Diagnostics. Intron spanning Primer sequences (forward (F) and reverse (R)), Universal ProbeLibrary hydrolysis probe and length of amplified product displayed above. Universal ProbeLibrary reference gene, GAPDH control probe and primers were used as reference gene in all multiplex reactions (product of Roche Applied Science, Cat# 05046211001).

E1. Restriction enzymes.

Enzyme	Company	Buffer
<i>EcoR</i> I	NEB	EcoR I
<i>BamH</i> I	NEB	NEB Buffer 2
HiFidelity Taq Polymerase	Invitrogen	HiFidelity Taq polymerase buffer
Antarctic Phosphatase	Promega	Antarctic Phosphatase reaction buffer
T4 DNA ligase	NEB	10X ligase buffer
<i>Pvu</i> I	NEB	NEB buffer 3
<i>Bgl</i> I	NEB	NEB buffer 3
<i>Stu</i> I	NEB	NEB buffer 1
<i>Hind</i> III	NEB	NEB buffer 2
<i>Kpn</i> I	NEB	NEB buffer 1
<i>Alu</i> I	NEB	NEB buffer 4

APPENDIX TWO: CHAPTER 3 SEQUENCING RESULTS.

```

1      10     20     30     40     50     60     70     80     90     100    110    120    130
Hyg_HDAC1_For2
Seq    CTGAAGAGCTGAGCTCCATGGTTGCCCGAGGCACACCCCTCGAGGTCGACGGTATCGATAGCCTCGAGTTCCTATCTCTAGAAAGTATAGGACTTCAGGCTCGAAGGAGTTTACGCTCAGCC
Consensus .....nACnG_ATCGAaa...TeCGAGTTCCTATCTCTAGAAAGTATAGGACTTCAGGCTCGAAGGAGTTTACGCTCAGCC
|-----|
131    140    150    160    170    180    190    200    210    220    230    240    250    260
Hyg_HDAC1_For2
Seq    AAGCTAGCTTGGCTGACGGTCTCGAARTCTACCGGGTAGGGGAGGGCGCTTTCCARAGGCGAGTCTGGAGCATGGCTTTAGCAGCCCGCTGGGACTTGGGCTACACAGTGGCTTGGCTCGC
Consensus AAGCTAGCTTGGCTGACGGTCTCGAARTCTACCGGGTAGGGGAGGGCGCTTTCCARAGGCGAGTCTGGAGCATGGCTTTAGCAGCCCGCTGGGACTTGGGCTACACAGTGGCTTGGCTCGC
|-----|
261    270    280    290    300    310    320    330    340    350    360    370    380    390
Hyg_HDAC1_For2
Seq    ACACATCCACATCCACCGTAGGGCCACCGGCTCGTTCTTTGGTGGCCCTTCGCGCCACCTTACTCTCCCTAGTCAGGAGTTCCCGCCCGCCCGAGCTCGGCTCGTGCAGGAGCTGAC
Consensus ACACATCCACATCCACCGTAGGGCCACCGGCTCGTTCTTTGGTGGCCCTTCGCGCCACCTTACTCTCCCTAGTCAGGAGTTCCCGCCCGCCCGAGCTCGGCTCGTGCAGGAGCTGAC
|-----|
391    400    410    420    430    440    450    460    470    480    490    500    510    520
Hyg_HDAC1_For2
Seq    AATGGAGTAGCAGCTCCTACTAGTCTCGTGCAGATGGACAGCCCGCTGAGCARTGGAGCGGGTAGGCCCTTTGGGCGAGCGCCAGTAGCAGCTTGGCTCTCGTTCTGGGCTCAGAGGCTGGG
Consensus AATGGAGTAGCAGCTCCTACTAGTCTCGTGCAGATGGACAGCCCGCTGAGCARTGGAGCGGGTAGGCCCTTTGGGCGAGCGCCAGTAGCAGCTTGGCTCTCGTTCTGGGCTCAGAGGCTGGG
|-----|
521    530    540    550    560    570    580    590    600    610    620    630    640    650
Hyg_HDAC1_For2
Seq    AAGGGGTGGCTCCGGGGCGGGCTCAGGGCGGGCTCAGGGCGGGCGGGCGCCGAGGCTCTCCGGAGGCCCGGATTCGACGCTTCARAGCGCAGCTTCCCGCGCTTCTCTCTCTCTCA
Consensus AAGGGGTGGCTCCGGGGCGGGCTCAGGGCGGGCTCAGGGCGGGCGGGCGCCGAGGCTCTCCGGAGGCCCGGATTCGACGCTTCARAGCGCAGCTTCCCGCGCTTCTCTCTCTCTCA
|-----|
651    660    670    680    690    700    710    720    730    740    750    760    770    780
Hyg_HDAC1_For2
Seq    TCTCCGGGCTTCGACCTGACGCTGTTGACATTAATCATCGCATAGTATATCGCATAGTATATCGCATAGTATTAATACGACAGGTGAGGACTTAACCATGAAAGAGCTGAACTCCCGCAGCTCTGTCAGAA
Consensus TCTCCGGGCTTCGACCTGACGCTGTTGACATTAATCATCGCATAGTATATCGCATAGTATATCGCATAGTATTAATACGACAGGTGAGGACTTAACCATGAAAGAGCTGAACTCCCGCAGCTCTGTCAGAA

```

A2. HDAC1-cKO-Hyg/ Δ Tk, HD1For2 predicted and sequence trace consensus.

```

391    400    410    420    430    440    450    460    470    480    490    500    510    520
HD1HygSC5seq2
Seq    ACTTCGAGCGAGGACATCCGGAGCTTGCAGATCGCCCGGCTCCGGGCTATATGCTCCGCTTGGCTTGCACACTCTATCAGAGCTTGGTTCAGGCAATTCGATGATGAGCTTGGGCGAGGG
Consensus .....nTTCGAGGAnCGCCCGGCTCCGGGCTATATGCTCCGCTTGGCTTGCACACTCTATCAGAGCTTGGTTCAGGCAATTCGATGATGAGCTTGGGCGAGGG
|-----|
521    530    540    550    560    570    580    590    600    610    620    630    640    650
HD1HygSC5seq2
Seq    TCGATCGAGCGCARTCGCCGATCCGGAGCCGGGACTGTCGGGCGTACACAAATCGCCCGAGAGCGCGGCGCTGGACCGATGGCTGTGAGAGTACCGCCGATGAGGAAACGACGCCCGAGC
Consensus TCGATCGAGCGCARTCGCCGATCCGGAGCCGGGACTGTCGGGCGTACACAAATCGCCCGAGAGCGCGGCGCTGGACCGATGGCTGTGAGAGTACCGCCGATGAGGAAACGACGCCCGAGC
|-----|
651    660    670    680    690    700    710    720    730    740    750    760    770    780
HD1HygSC5seq2
Seq    ACTCGTCCGAGGGCAAGGARGAATTCGGCGGTTCAAGTGGCTCTCTGCTGAACTTCGATCTGCTGAAACTGGCCGGCGATGGAAGGCAACCCAGGCCAGGATCCGGCGGTTCAAGTGACTTCCCA
Consensus ACTCGTCCGAGGGCAAGGARGAATTCGGCGGTTCAAGTGGCTCTCTGCTGAACTTCGATCTGCTGAAACTGGCCGGCGATGGAAGGCAACCCAGGCCAGGATCCGGCGGTTCAAGTGACTTCCCA
|-----|
781    790    800    810    820    830    840    850    860    870    880    890    900    910
HD1HygSC5seq2
Seq    CGCTACTGCGGGTTTATATAGACGCTCTACCGGATGGGAAACACACACACACACACCGCTCGACAGGGTGAATATCGCCCGGGAGCGCGGCTGGTATGACAGCGCCAGATACATGGCATGCTTATGCCG
Consensus CGCTACTGCGGGTTTATATAGACGCTCTACCGGATGGGAAACACACACACACACACCGCTCGACAGGGTGAATATCGCCCGGGAGCGCGGCTGGTATGACAGCGCCAGATACATGGCATGCTTATGCCG
|-----|
911    920    930    940    950    960    970    980    990    1000  1010  1020  1030  1040
HD1HygSC5seq2
Seq    GGGGGCTTCGAGACATCGGACATCTACACACACACACACCGCTCGACAGGGTGAATATCGCCCGGGAGCGCGGCTGGTATGACAGCGCCAGATACATGGCATGCTTATGCCG
Consensus GGGGGCTTCGAGACATCGGACATCTACACACACACACACCGCTCGACAGGGTGAATATCGCCCGGGAGCGCGGCTGGTATGACAGCGCCAGATACATGGCATGCTTATGCCG
|-----|
1041  1050  1060  1070  1080  1090  1100  1110  1120  1130  1140  1150  1160  1170
HD1HygSC5seq2
Seq    ACCGACGCGCTTCTGGCTCTCATATCGGGGGGAGGCTGGGAGCTCACATGCCCCCGCCCGCCCTCACCTCATCTTGACCGCCATCCCATCGCCGCTCTGTGCTACCGCCCGCGGATACC
Consensus ACCGACGCGCTTCTGGCTCTCATATCGGGGGGAGGCTGGGAGCTCACATGCCCCCGCCCGCCCTCACCTCATCTTGACCGCCATCCCATCGCCGCTCTGTGCTACCGCCCGCGGATACC
|-----|
1171  1180  1190  1200  1210  1220  1230  1240  1250  1260  1270  1280  1290  1300
HD1HygSC5seq2
Seq    TTATGGGACGATGACCCCCAGGCGGCTGGGCTTCTGGGCTCTATCCCGCGGCTTGGCCGCAACACATCGTGTGGGGCCCTTCGGAGGACAGACACATGACCGCTGGCCAGAGCCCA
Consensus TTATGGGACGATGACCCCCAGGCGGCTGGGCTTCTGGGCTCTATCCCGCGGCTTGGCCGCAACACATCGTGTGGGGCCCTTCGGAGGACAGACACATGACCGCTGGCCAGAGCCCA
|-----|
1301  1310  1320  1330  1340  1350  1360  1370  1380  1390  1400  1410  1420  1430
HD1HygSC5seq2
Seq    GCGCCCCGCGAGCGGCTTGGCTGCTTATGCTGGCCGATTCGCGGCTTATCCCGCGGCTTGGCCGCAACACATCGTGTGGGGCCCTTCGGAGGACAGACACATGACCGCTGGCCAGAGCCCA
Consensus GCGCCCCGCGAGCGGCTTGGCTGCTTATGCTGGCCGATTCGCGGCTTATCCCGCGGCTTGGCCGCAACACATCGTGTGGGGCCCTTCGGAGGACAGACACATGACCGCTGGCCAGAGCCCA

```

B2. HDAC1-cKO-Hyg/ Δ Tk, Hyg_SC5_seq2 predicted and sequence trace consensus.

HDAC2 seq
 Consensus
 HDAC2 seq
 Consensus

C2. HDAC2-cKO-Hyg/ Δ Tk, 5'neogen predicted and sequence trace consensus.

SC5 seq
 Consensus
 SC5 seq
 Consensus

D2. HDAC2-cKO-Hyg/ Δ Tk, Hyg_SC5_seq2 predicted and sequence trace consensus.

1 10 20 30 40 50 60 70 80 90 100 110 120 130
 HDAC1 HD1_23_17
 Consensus TARTACGACTCAGTATAGGGAGCCAGCTGGCTAGCGTTTAAACTTAGCTTGGTACCAGCTCGGATCCATGGCCAGACTCAGGGCCACRAGAGGAAAGTCTGTACTACACGCGGGATGTTG
 CTTGGTACCAGCTCGGATCCATGGCCAGACTCAGGGCCACRAGAGGAAAGTCTGTACTACACGCGGGATGTTG
 CTGGTACCAGCTCGGATCCATGGCCAGACTCAGGGCCACRAGAGGAAAGTCTGTACTACACGCGGGATGTTG

131 140 150 160 170 180 190 200 210 220 230 240 250 260
 HDAC1 HD1_23_17
 Consensus GAACTACTATTATGGACRAGGGCCACCCATGAGGCTCACCAGTCCGATGACTACATATTTGGTGCACACTATGGTCTACCCGAAARATGGAGATCACCCTCCACRAGGCCAATGCTGAGGA
 GAACTACTATTATGGACRAGGGCCACCCATGAGGCTCACCAGTCCGATGACTACATATTTGGTGCACACTATGGTCTACCCGAAARATGGAGATCACCCTCCACRAGGCCAATGCTGAGGA
 GAACTACTATTATGGACRAGGGCCACCCATGAGGCTCACCAGTCCGATGACTACATATTTGGTGCACACTATGGTCTACCCGAAARATGGAGATCACCCTCCACRAGGCCAATGCTGAGGA

261 270 280 290 300 310 320 330 340 350 360 370 380 390
 HDAC1 HD1_23_17
 Consensus GATGACCACTACCAAGTGTGACTACATTAATCTCGCTTCTATTCGCCAGATACATGCTGAATACAGCAGCAGATGCAGAGATTCARTGTTGGTGGAGGCTCCGGTATTGATGGCTG
 GATGACCACTACCAAGTGTGACTACATTAATCTCGCTTCTATTCGCCAGATACATGCTGAATACAGCAGCAGATGCAGAGATTCARTGTTGGTGGAGGCTCCGGTATTGATGGCTG
 GATGACCACTACCAAGTGTGACTACATTAATCTCGCTTCTATTCGCCAGATACATGCTGAATACAGCAGCAGATGCAGAGATTCARTGTTGGTGGAGGCTCCGGTATTGATGGCTG

391 400 410 420 430 440 450 460 470 480 490 500 510 520
 HDAC1 HD1_23_17
 Consensus TTTGAGTCTGTCAAGTTGTCACGGAGGCTGTGTCAGGCTGTGAGGCTTARTTAGCAGCAGCAGGACATCGTGTGAGCTGGGCTGGGGGCTGCACCATGCARAGAGTCTGAGCATCCGGCT
 TTTGAGTCTGTCAAGTTGTCACGGAGGCTGTGTCAGGCTGTGAGGCTTARTTAGCAGCAGCAGGACATCGTGTGAGCTGGGCTGGGGGCTGCACCATGCARAGAGTCTGAGCATCCGGCT
 TTTGAGTCTGTCAAGTTGTCACGGAGGCTGTGTCAGGCTGTGAGGCTTARTTAGCAGCAGCAGGACATCGTGTGAGCTGGGCTGGGGGCTGCACCATGCARAGAGTCTGAGCATCCGGCT

521 530 540 550 560 570 580 590 600 610 620 630 640 650
 HDAC1 HD1_23_17
 Consensus TCTGTACTCARTGACATCGCTTGGCCATCTGGAACTGCTAAGACTACCCAGAGGCTGCTTATATTGACATTAATTCACCATGGCAGTGGCTGGAGAGGCTCTATACACRAGCCGGT
 TCTGTACTCARTGACATCGCTTGGCCATCTGGAACTGCTAAGACTACCCAGAGGCTGCTTATATTGACATTAATTCACCATGGCAGTGGCTGGAGAGGCTCTATACACRAGCCGGT
 TCTGTACTCARTGACATCGCTTGGCCATCTGGAACTGCTAAGACTACCCAGAGGCTGCTTATATTGACATTAATTCACCATGGCAGTGGCTGGAGAGGCTCTATACACRAGCCGGT

651 660 670 680 690 700 710 720 730 740 750 760 770 780
 HDAC1 HD1_23_17
 Consensus CATGACTGTGCTTCTAATTAACGGAGTACTTCCAGGACTGGGACCTAGCGGACATAGGGCTGGCAGAGGCAAGTACTATGCTGTGACTACCCATGCARAGAGGCTGAGCATCCGGCT
 CATGACTGTGCTTCTAATTAACGGAGTACTTCCAGGACTGGGACCTAGCGGACATAGGGCTGGCAGAGGCAAGTACTATGCTGTGACTACCCATGCARAGAGGCTGAGCATCCGGCT
 CATGACTGTGCTTCTAATTAACGGAGTACTTCCAGGACTGGGACCTAGCGGACATAGGGCTGGCAGAGGCAAGTACTATGCTGTGACTACCCATGCARAGAGGCTGAGCATCCGGCT

781 790 800 810 820 830 840 850 860 870 880 890 900 910
 HDAC1 HD1_23_17
 Consensus TATGAGCCATCTTAAAGCAGTCTGTCARAGTATGGAGATGTTCCAGGCTAGTGCAGTGGCTTACAGTGTGGCTCAGATCCCTGCTGGGGCCGGTATGATGCTTCATCTGACCATCAAG
 TATGAGCCATCTTAAAGCAGTCTGTCARAGTATGGAGATGTTCCAGGCTAGTGCAGTGGCTTACAGTGTGGCTCAGATCCCTGCTGGGGCCGGTATGATGCTTCATCTGACCATCAAG
 TATGAGCCATCTTAAAGCAGTCTGTCARAGTATGGAGATGTTCCAGGCTAGTGCAGTGGCTTACAGTGTGGCTCAGATCCCTGCTGGGGCCGGTATGATGCTTCATCTGACCATCAAG

911 920 930 940 950 960 970 980 990 1000 1010 1020 1030 1040
 HDAC1 HD1_23_17
 Consensus GACACGCCAGTGTGTGGAGTTCTGTGAGAGTTTCAACTTGGCCATGCTGATGCTGGAGGAGTGGCTACACCATCCGGAAATGTTGCTGCTGGACTACGAAACAGCGGTGGCCCTGGACACGA
 GACACGCCAGTGTGTGGAGTTCTGTGAGAGTTTCAACTTGGCCATGCTGATGCTGGAGGAGTGGCTACACCATCCGGAAATGTTGCTGCTGGACTACGAAACAGCGGTGGCCCTGGACACGA
 GACACGCCAGTGTGTGGAGTTCTGTGAGAGTTTCAACTTGGCCATGCTGATGCTGGAGGAGTGGCTACACCATCCGGAAATGTTGCTGCTGGACTACGAAACAGCGGTGGCCCTGGACACGA

E2. HDAC1-C'-FLAG-Resc, T7promoter predicted and sequence trace consensus.

1 10 20 30 40 50 60 70 80 90 100 110 120 130
 HDAC1 HD1_23_BGH
 Consensus CTGATCAGCGGGTTTAAACGGCCCTCTGACCTGAGCGGGCCGCACTGTGCTGGATATCTCGAARATCTCACTTGTGCTCATCGCTTTGATGATCARTGATGATCTGTARTCCGCTGTGGG
 CTGACCTGAGCGGGCCGCACTGTGCTGGATATCTCGAARATCTCACTTGTGCTCATCGCTTTGATGATCARTGATGATCTGTARTCCGCTGTGGG

131 140 150 160 170 180 190 200 210 220 230 240 250 260
 HDAC1 HD1_23_BGH
 Consensus CAACTGACCTCTCTTGGCCCTTGGCTTCTGGCTTCTCCCTTGGTTTCTCTCTCTGACTCTTTTCTCTCAGGATCTTCTCTTCTCATCTCTGTTTAACTCTTTTGGCTTT
 CAACTGACCTCTCTTGGCCCTTGGCTTCTGGCTTCTCCCTTGGTTTCTCTCTCTGACTCTTTTCTCTCAGGATCTTCTCTTCTCATCTCTGTTTAACTCTTTTGGCTTT

261 270 280 290 300 310 320 330 340 350 360 370 380 390
 HDAC1 HD1_23_BGH
 Consensus TTAGAGTTAGAGAGTTCTTGGCCACCTTCTCCCTCTCATCTGAGTCCGAGACTCTCTCAGCGGCAATGCTTTATCAGAGGACAGATGGAGTGGCTTTGTCAGGGTCTTCTCATCTCAT
 TTAGAGTTAGAGAGTTCTTGGCCACCTTCTCCCTCTCATCTGAGTCCGAGACTCTCTCAGCGGCAATGCTTTATCAGAGGACAGATGGAGTGGCTTTGTCAGGGTCTTCTCATCTCAT
 TTAGAGTTAGAGAGTTCTTGGCCACCTTCTCCCTCTCATCTGAGTCCGAGACTCTCTCAGCGGCAATGCTTTATCAGAGGACAGATGGAGTGGCTTTGTCAGGGTCTTCTCATCTCAT

391 400 410 420 430 440 450 460 470 480 490 500 510 520
 HDAC1 HD1_23_BGH
 Consensus CCCCACCTCTTCCGGGATGGCTCTCAGGATGGCTGCATCTGACCCAGGGGATGGGGAGCATCTCAGGTTCTCAGAGAGCGTGTGATCTCTCAGGATCTGATGTTCTGGT
 CCCCACCTCTTCCGGGATGGCTCTCAGGATGGCTGCATCTGACCCAGGGGATGGGGAGCATCTCAGGTTCTCAGAGAGCGTGTGATCTCTCAGGATCTGATGTTCTGGT
 CCCCACCTCTTCCGGGATGGCTCTCAGGATGGCTGCATCTGACCCAGGGGATGGGGAGCATCTCAGGTTCTCAGAGAGCGTGTGATCTCTCAGGATCTGATGTTCTGGT

521 530 540 550 560 570 580 590 600 610 620 630 640 650
 HDAC1 HD1_23_BGH
 Consensus GGTATGTTAGAGGGCTGATGTGAGCTTGAATCCGGTCCAAAGTATCAAGTAGTCAATGAGGACAGCTCATTAGGGATCTGTGTCCAGGGCCACCGCTTTCTGATGCTCAGAGCAGCA
 GGTATGTTAGAGGGCTGATGTGAGCTTGAATCCGGTCCAAAGTATCAAGTAGTCAATGAGGACAGCTCATTAGGGATCTGTGTCCAGGGCCACCGCTTTCTGATGCTCAGAGCAGCA
 GGTATGTTAGAGGGCTGATGTGAGCTTGAATCCGGTCCAAAGTATCAAGTAGTCAATGAGGACAGCTCATTAGGGATCTGTGTCCAGGGCCACCGCTTTCTGATGCTCAGAGCAGCA

651 660 670 680 690 700 710 720 730 740 750 760 770 780
 HDAC1 HD1_23_BGH
 Consensus ACATCCGGATGGTGTAGCCACCTCTCCAGCATCAGATGGGCAAGTGAARCTCTCAGCACTCCACACACTTGGCTGTCTTTGATGGTCAATGAGCAGCTACCCGGTCCCGACAGGG
 ACATCCGGATGGTGTAGCCACCTCTCCAGCATCAGATGGGCAAGTGAARCTCTCAGCACTCCACACACTTGGCTGTCTTTGATGGTCAATGAGCAGCTACCCGGTCCCGACAGGG
 ACATCCGGATGGTGTAGCCACCTCTCCAGCATCAGATGGGCAAGTGAARCTCTCAGCACTCCACACACTTGGCTGTCTTTGATGGTCAATGAGCAGCTACCCGGTCCCGACAGGG

781 790 800 810 820 830 840 850 860 870 880 890 900 910
 HDAC1 HD1_23_BGH
 Consensus AATCTGAGCCACACTGTAGACCACTGCACATGCTGGACATCTCCATCTTGGACATGACTGCTTAAAGATGGCTTCAAGGATTCGCTGCTCATGCGCTCTGCAATGGTGTGACACATA
 AATCTGAGCCACACTGTAGACCACTGCACATGCTGGACATCTCCATCTTGGACATGACTGCTTAAAGATGGCTTCAAGGATTCGCTGCTCATGCGCTCTGCAATGGTGTGACACATA
 AATCTGAGCCACACTGTAGACCACTGCACATGCTGGACATCTCCATCTTGGACATGACTGCTTAAAGATGGCTTCAAGGATTCGCTGCTCATGCGCTCTGCAATGGTGTGACACATA

911 920 930 940 950 960 970 980 990 1000 1010 1020 1030 1040
 HDAC1 HD1_23_BGH
 Consensus GTACTTGGCTTGGCCAGCCCAATGTCCTGAGTCCCGAGTCTTCCGGATTTATGAGAGGACAGCTCATGCCCCGGTCTGATGATAGAGGGCTCTTCCAGCCATCCGCTAGG
 GTACTTGGCTTGGCCAGCCCAATGTCCTGAGTCCCGAGTCTTCCGGATTTATGAGAGGACAGCTCATGCCCCGGTCTGATGATAGAGGGCTCTTCCAGCCATCCGCTAGG

F2. HDAC1-C'-FLAG-Resc, BGH rev predicted and sequence trace consensus.

APPENDIX THREE: ANTIBODIES

A3. Western blot and Co-immunoprecipitation antibodies.

Antibody	Clonality	Source	Dilution	Company	Catalogue#	WB/IP
HDAC1	polyclonal	rabbit	1:2000	Santa Cruz	sc-7872	WB
HDAC1	monoclonal	mouse	1:2000	Abcam	ab46985	IP
HDAC2	polyclonal	rabbit	1:2000	Santa Cruz	sc-7899	IP
HDAC2	monoclonal	mouse	1:2000	Millipore	05-814	WB
HDAC3	polyclonal	rabbit	1:1000	Santa Cruz	sc-11417	WB
LSD-1	polyclonal	rabbit	1:2000	Abcam	ab37165	WB/IP
MSIN3A	polyclonal	rabbit	1:2000	Santa Cruz	sc-767	WB/IP
MTA-2	monoclonal	mouse	1:2000	Sigma	M-7569	WB/IP
ACTIN	monoclonal	mouse	1:3000	Sigma	A4700	WB
M2 ANTI FLAG	monoclonal	mouse	1:2000	Sigma	F1804-1MG	WB
A-TUBULIN	monoclonal	mouse	1:3000	Sigma	T5168	WB

WB: Western blot, IP: immunoprecipitation.

B3. Histone modification antibodies.

Antibody	Clonality	Source	Dilution	Company	Catalogue#	WB/IP
H3	monoclonal	mouse	1:2000	Millipore	05-499	WB
H4	monoclonal	mouse	1:2000	Abcam	ab31827	WB
H4ac	polyclonal	rabbit	1:1000	Millipore	06-866	WB
H4K5ac	polyclonal	rabbit	1:1000	Millipore	06-759MN	WB
H4K8ac	polyclonal	rabbit	1:1000	Millipore	06-760MN	WB
H4K12ac	polyclonal	rabbit	1:1000	Millipore	06-761	WB
H4K16ac	polyclonal	rabbit	1:1000	Millipore	06-762	WB
H3K9/14ac	polyclonal	rabbit	1:1000	Millipore	06-599	WB
H3K18ac	polyclonal	rabbit	1:1000	Millipore	07-354	WB
H3K27ac	polyclonal	rabbit	1:1000	Active Motif	39132	WB
H3K36ac	polyclonal	rabbit	1:1000	Millipore	07-540	WB
H3K56ac	polyclonal	rabbit	1:1000	Active Motif	39281	WB
H3K4me2	polyclonal	rabbit	1:1000	Abcam	ab32356	WB
H3K9me3	polyclonal	rabbit	1:1000	Abcam	Ab8898	WB

C3. FACS antibodies.

Antibody	Clonality	Source	Dilution	Company	Odering Code	Conjuagted Flourochrome
CD4	monoclonal	Rat anti mouse	1:500	CALTAG	MCD0404	R-PE
CD8 α	monoclonal	Rat anti mouse	1:500	CALTAG	MCD0801	FITC
CD25	monoclonal	Rat anti mouse	1:100	CALTAG	RM6004	PE
CD44	monoclonal	Rat anti mouse	1:100	CALTAG	RM5701	FITC
CD8 α	monoclonal	Rat-anti mouse	1:500	BD Biosciences	553028	Biotin
CD45R(B220)	monoclonal	Rat-anti mouse	1:500	CALTAG	RM2615	Biotin
CD5	monoclonal	Rat-anti mouse	1:500	BD Biosciences	550035	APC
TCRb-chain	monoclonal	Hamster-anti mouse	1:500	BD Biosciences	553169	Biotin
CD69	monoclonal	Hamster-anti mouse	1:500	eBioscience	17-0691	APC
CD24/HSA	monoclonal	Rat-anti mouse	1:500	Genway	20-787-275334	APC
Va2 TCR	monoclonal	Rat-anti mouse	1:500	BD Biosciences	560622	APC
Vb 5.1, 5.2 TCR	monoclonal	Rat-anti mouse	1:500	BD Biosciences	553189	FITC
CD8 β	monoclonal	Rat-anti mouse	1:500	BD Biosciences	554973	FITC
CD4	monoclonal	Rat-anti mouse	1:500	BD Biosciences	554836	Biotin
Streptavidin	-	-	1:1000	BD Biosciences	551419	Cy5.5
AnnexinV	monoclonal	Rat-anti mouse	1:500	eBioscience	88-8007	APC
Propidium Iodide	-	-	1:1000	eBioscience	88-8007	-

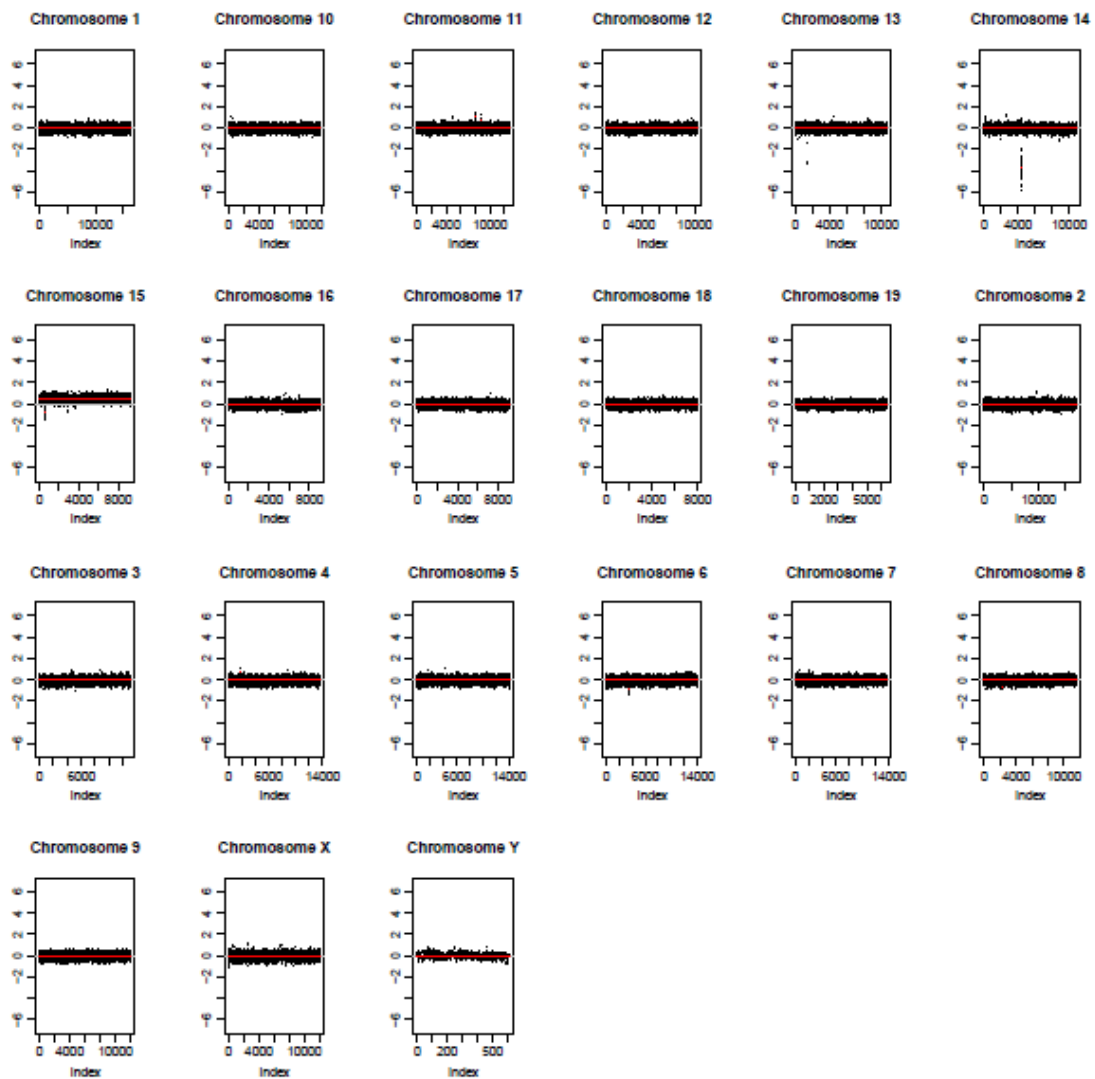
D3. Immunohistochemical primary antibodies.

Antibody	Clonality	Source	Dilution	Company	Odering Code
Ki67	polyclonal	rabbit	1:200	CALTAG	MCD0404
nestin	monoclonal	mouse	1:200	Abcam	ab6142
b-III tubulin	monoclonal	mouse	1:200	Millipore	MAB1637

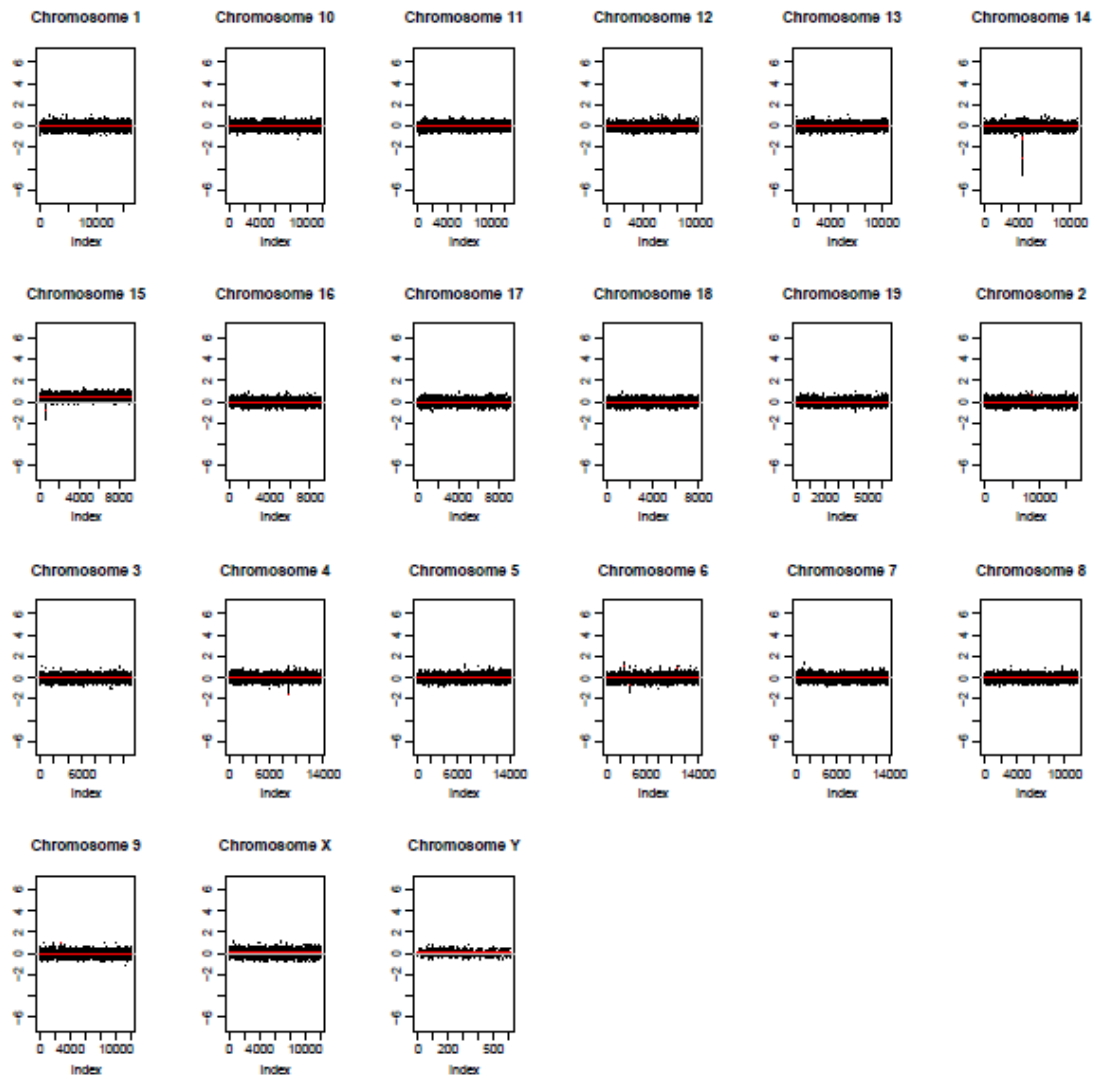
E3. Immunohistochemical secondary antibodies/ counterstains.

Antibody	Dilution	Company	Odering Code
Alexa Flour 568 goat anti-mouse	1:500	Invitrogen	A11004
Alexa Flour 488 goat anti-mouse	1:500	Invitrogen	A10667
Biotinylated polyclonal Swine anti-rabbit	1:200	DakoCytomation	E0353
DAPI	1:5000	Invitrogen	D3571

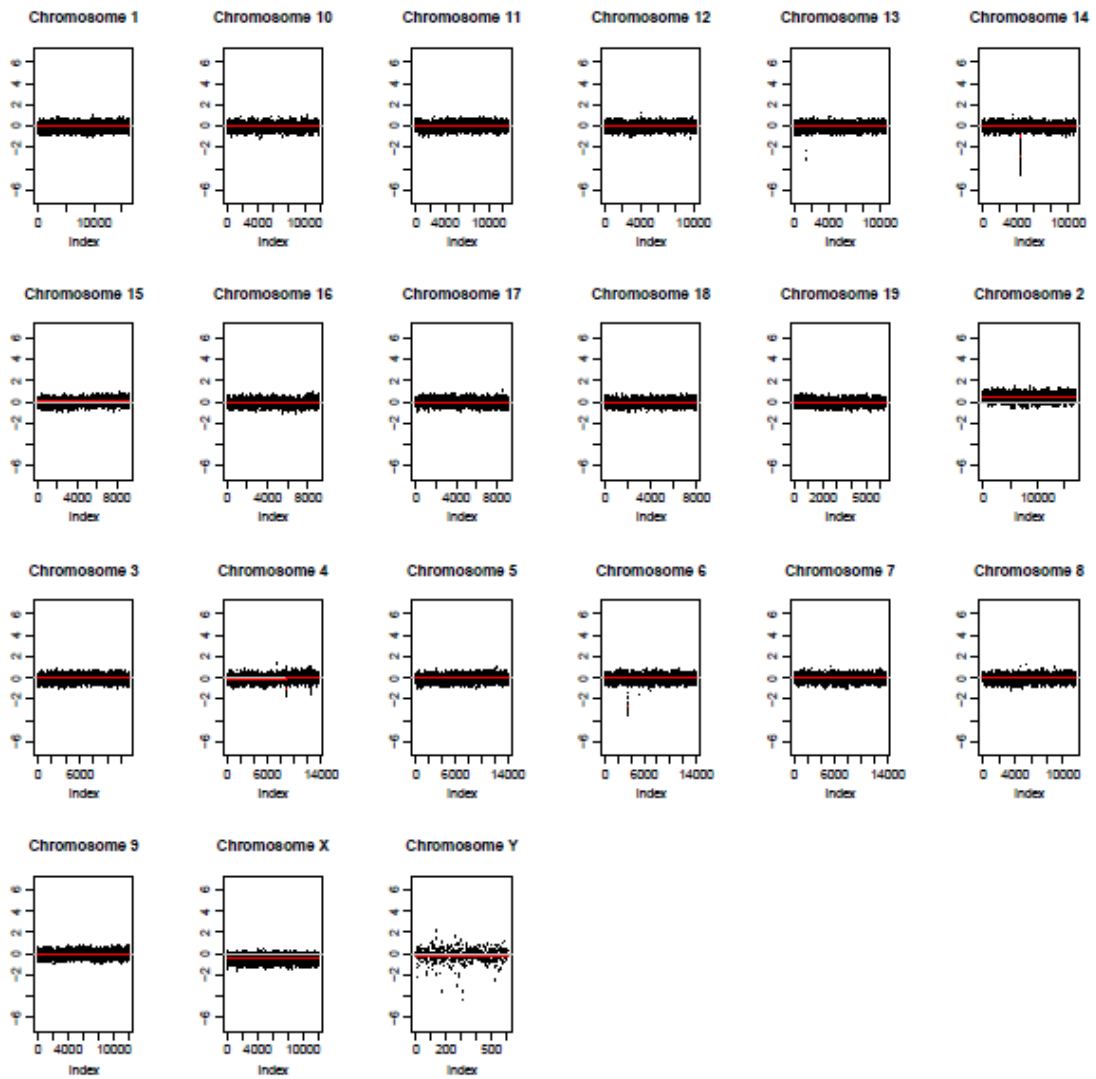
APPENDIX FOUR: ARRAY COMPARATIVE GENOMIC HYBRIDISATION RESULT PLOTS.



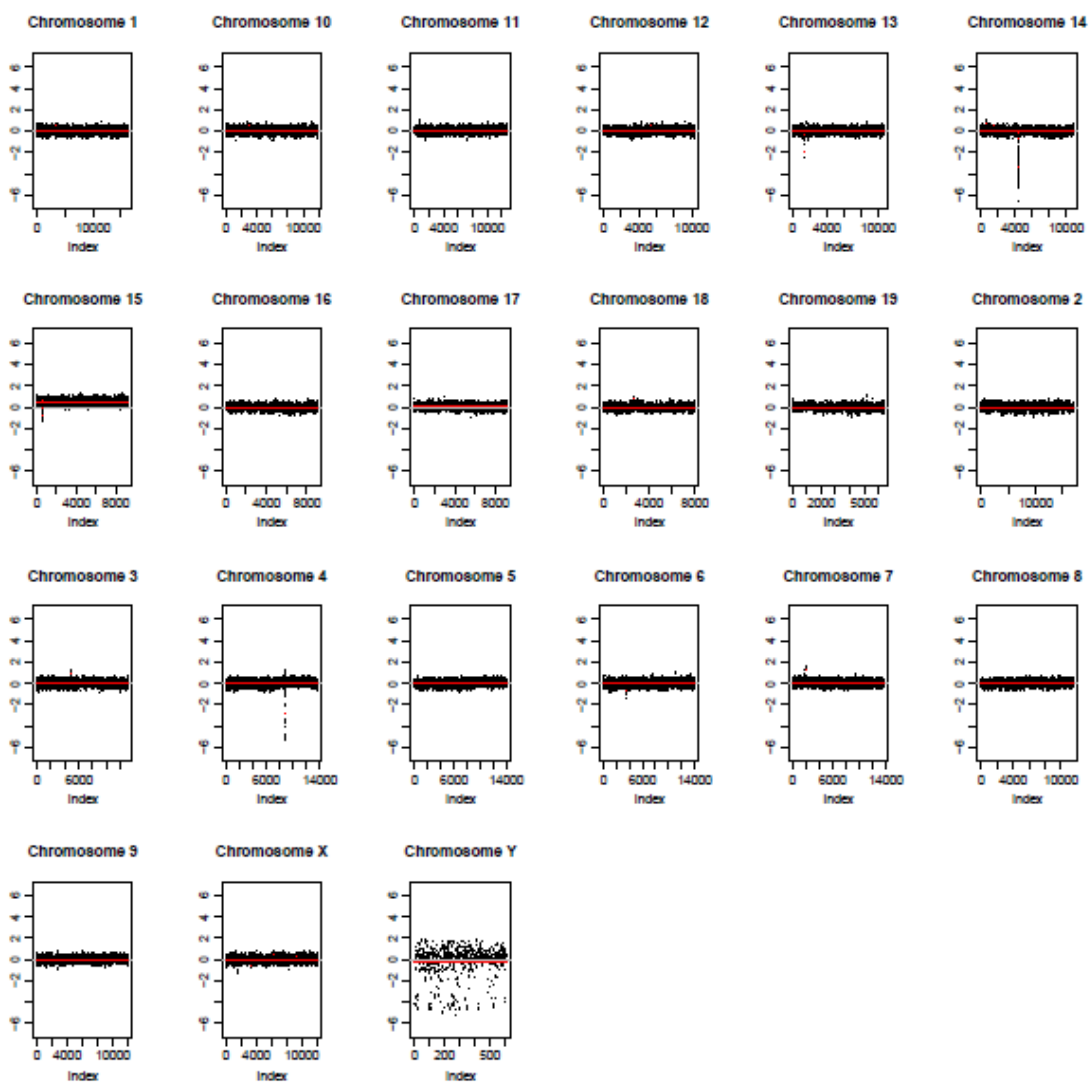
A4. aCGH results (Log2 ratios, individual chromosomes). Tumour sample 1.



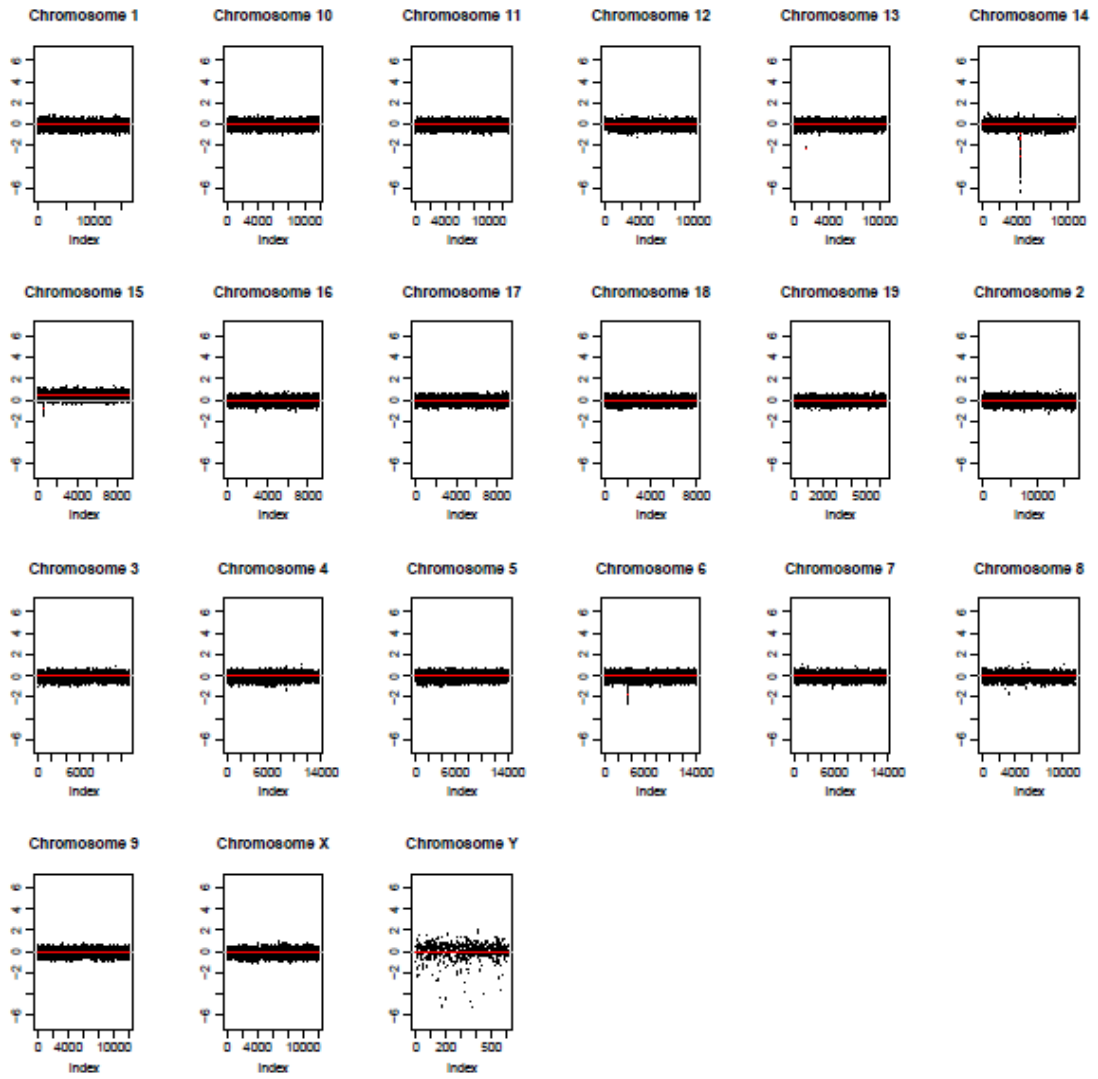
B4. aCGH results (Log2 ratios, individual chromosomes). Tumour sample 2.



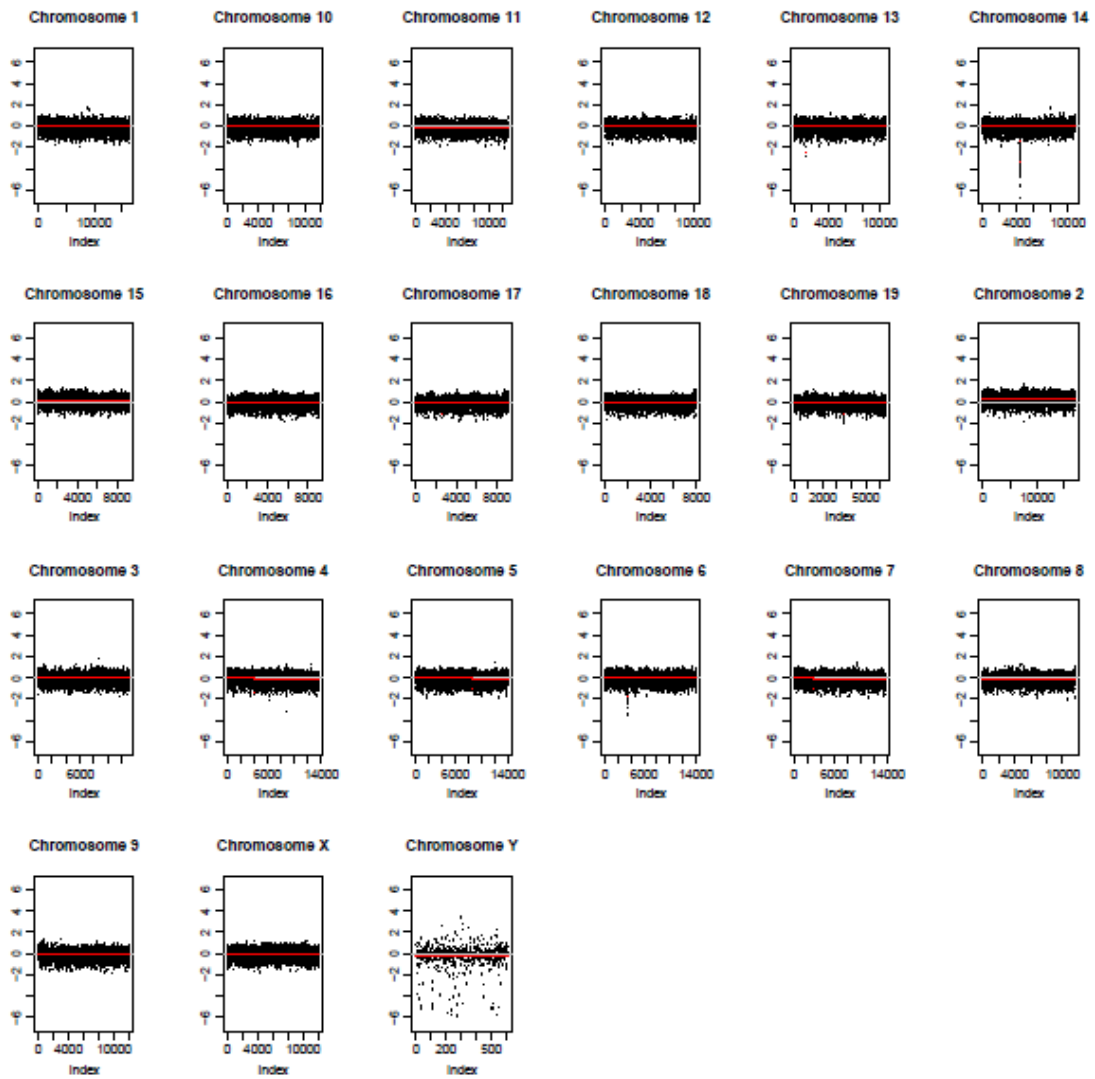
C4. aCGH results (Log2 ratios, individual chromosomes). Tumour sample 3.



D4. aCGH results (Log2 ratios, individual chromosomes). Tumour sample 4.



E4. aCGH results (Log2 ratios, individual chromosomes). Tumour sample 5.



F4. aCGH results (Log₂ ratios, individual chromosomes). Tumour sample 6.

A4. aCGH results: summary of all samples, gains and losses, chromosomal start and end.

Chromosome	Chromosome start	Chromosome end	Log2 Ratio					
			Tumour Sample 1	Tumour Sample 2	Tumour Sample 3	Tumour Sample 4	Tumour Sample 5	Tumour Sample 6
1	3002738	44299501	-0.0197	-0.0188	-0.0334	-0.0139	-0.0276	-0.0504
1	44299502	44317697	-0.0197	-0.0188	-0.0334	0	-0.0276	-0.0504
1	44317698	44368405	-0.0197	-0.0188	-0.0334	0.5261	-0.0276	-0.0504
1	44368406	44399794	-0.0197	-0.0188	-0.0334	0	-0.0276	-0.0504
1	44399795	197188227	-0.0197	-0.0188	-0.0334	-0.0206	-0.0276	-0.0504
2	3010301	91431760	-0.0099	-0.0063	0.4671	-0.0047	-0.0257	0.2782
2	91431761	91438103	-0.0099	0	0.4671	-0.0047	-0.0257	0.2782
2	91438104	91442966	-0.0099	0	0.4671	-0.0047	-0.0257	0.2782
2	91442967	181723517	-0.0099	-0.0201	0.4671	-0.0047	-0.0257	0.2782
3	3005504	69544385	-0.0295	-0.0264	-0.0382	-0.0362	-0.0312	-0.0357
3	69544386	69552800	-0.0295	-0.0264	-0.0382	0	-0.0312	-0.0357
3	69552801	159597973	-0.0295	-0.0264	-0.0382	-0.017	-0.0312	-0.0357
4	3012291	25205194	-0.0357	-0.0357	-0.0609	-0.0383	-0.0251	-0.0228
4	25205195	25214479	0	-0.0357	-0.0609	-0.0383	-0.0251	-0.0228
4	25214480	25220491	0.7926	-0.0357	-0.0609	-0.0383	-0.0251	-0.0228
4	25220492	25232469	0	-0.0357	-0.0609	-0.0383	-0.0251	-0.0228
4	25232470	54625921	-0.0233	-0.0357	-0.0609	-0.0383	-0.0251	-0.0228
4	54625922	54651974	-0.0233	-0.0357	-0.0609	-0.0383	-0.0251	0
4	54651975	54677848	-0.0233	-0.0357	-0.0609	-0.0383	-0.0251	-1.3812
4	54677849	54697110	-0.0233	-0.0357	-0.0609	-0.0383	-0.0251	0
4	54697111	111790950	-0.0233	-0.0357	-0.0609	-0.0383	-0.0251	-0.0872
4	111790951	111796995	-0.0233	-0.0357	0	-0.0383	-0.0251	-0.0872
4	111796996	111830630	-0.0233	-0.0357	-1.0321	-0.0383	-0.0251	-0.0872
4	111830631	111840897	-0.0233	-0.0357	0	-0.0383	-0.0251	-0.0872
4	111840898	112130091	-0.0233	-0.0357	0.0539	-0.0383	-0.0251	-0.0872
4	112130092	112145346	-0.0233	0	0.0539	-0.0383	-0.0251	-0.0872
4	112145347	112193921	-0.0233	-1.4951	0.0539	0	-0.0251	-0.0872
4	112193922	112213162	-0.0233	0	0.0539	-2.8814	-0.0251	-0.0872
4	112213163	112265745	-0.0233	0.0081	0.0539	-2.8814	-0.0251	-0.0872
4	112265746	112278851	-0.0233	0.0081	0.0539	0	-0.0251	-0.0872
4	112278852	155625629	-0.0233	0.0081	0.0539	0.0563	-0.0251	-0.0872
5	3008399	103868859	-0.017	-0.015	-0.0088	-0.0023	-0.022	-0.0523
5	103868860	103876796	-0.017	-0.015	-0.0088	-0.0023	-0.022	0
5	103876797	103891094	-0.017	-0.015	-0.0088	-0.0023	-0.022	-1.0351
5	103891095	103904853	-0.017	-0.015	-0.0088	-0.0023	-0.022	0
5	103904854	152536901	-0.017	-0.015	-0.0088	-0.0023	-0.022	-0.0736
6	3024849	33732691	-0.0325	-0.0356	-0.0479	-0.0412	-0.0367	-0.0465
6	33732692	33737392	-0.0325	0	-0.0479	-0.0412	-0.0367	-0.0465
6	33737393	40998689	-0.0325	0.0258	-0.0479	-0.0412	-0.0367	-0.0465
6	40998690	41004202	-0.0325	0.0258	-0.0479	-0.0412	0	-0.0465
6	41004203	41090809	-0.0325	0.0258	-0.0479	-0.0412	-1.7497	-0.0465
6	41090810	41100250	-0.0325	0	-0.0479	-0.0412	-1.7497	-0.0465
6	41100251	41128270	-0.0325	-0.7308	-0.0479	-0.0412	-1.7497	-0.0465
6	41128271	41138381	0	-0.7308	-0.0479	-0.0412	-1.7497	-0.0465
6	41144825	41164726	-0.8195	-0.7308	-2.6942	-0.0412	-1.7497	-1.6626
6	41164727	41174493	-0.8195	-0.7308	-2.6942	0	-1.7497	-1.6626
6	41174494	41480645	-0.8195	-0.7308	-2.6942	-0.7245	-1.7497	-1.6626
6	41480646	41489611	-0.8195	-0.7308	-2.6942	0	-1.7497	-1.6626
6	41495140	119116239	-0.024	-0.032	-0.0215	-0.0138	-0.0244	-0.0502
6	119121036	119126329	-0.024	0	-0.0215	-0.0138	-0.0244	-0.0502
6	119126330	149511955	-0.024	0.0174	-0.0215	-0.0138	-0.0244	-0.0502
7	3049177	26892214	-0.0186	-0.0149	0.0022	0.0805	-0.0232	-0.0344
7	26892215	26913981	-0.0186	-0.0149	0.0022	0	-0.0232	-0.0344
7	26913982	26973183	-0.0186	-0.0149	0.0022	1.2577	-0.0232	-0.0344
7	26973184	26987202	-0.0186	-0.0149	0.0022	0	-0.0232	-0.0344
7	26987203	38265873	-0.0186	-0.0149	0.0022	-0.0061	-0.0232	-0.0344
7	38265874	38270957	-0.0186	-0.0149	0.0022	-0.0061	-0.0232	0
7	38270958	38309701	-0.0186	-0.0149	0.0022	-0.0061	-0.0232	-1.0073
7	38309702	38316474	-0.0186	-0.0149	0.0022	-0.0061	-0.0232	0
7	38316475	152520688	-0.0186	-0.0149	0.0022	-0.0061	-0.0232	-0.0816

A4 continued. aCGH results: summary of all samples, gains and losses, chromosomal start and end.

Chromosome	Chromosome start	Chromosome end	Log2 Ratio					
			Tumour Sample 1	Tumour Sample 2	Tumour Sample 3	Tumour Sample 4	Tumour Sample 5	Tumour Sample 6
8	3111085	29124694	-0.0233	-0.0205	-0.0262	-0.0113	-0.0324	-0.0756
8	29124695	29133818	0	-0.0205	-0.0262	-0.0113	-0.0324	-0.0756
8	29133819	29160967	-0.6985	-0.0205	-0.0262	-0.0113	-0.0324	-0.0756
8	29160968	29172015	0	-0.0205	-0.0262	-0.0113	-0.0324	-0.0756
8	29172016	131735244	-0.0226	-0.0205	-0.0262	-0.0113	-0.0324	-0.0756
9	3088282	34877937	-0.0129	-0.0235	0.0037	0.0103	-0.0145	-0.0561
9	34877938	34899271	-0.0129	0	0.0037	0.0103	-0.0145	-0.0561
9	34899272	34907603	-0.0129	0.9503	0.0037	0.0103	-0.0145	-0.0561
9	34907604	34912142	-0.0129	0	0.0037	0.0103	-0.0145	-0.0561
9	34912143	124046731	-0.0129	-0.0021	0.0037	0.0103	-0.0145	-0.0561
10	3002742	38830169	-0.013	-0.0034	-0.0065	-0.0057	-0.0023	-0.0375
10	38830170	38837369	-0.013	-0.0034	-0.0065	0	-0.0023	-0.0375
10	38837370	38850163	-0.013	-0.0034	-0.0065	0.5531	-0.0023	-0.0375
10	38850164	38852068	-0.013	-0.0034	-0.0065	0	-0.0023	-0.0375
10	38852069	129970926	-0.013	-0.0034	-0.0065	0.0083	-0.0023	-0.0375
11	3026911	83485175	0.0015	0.0081	0.0364	0.0317	-0.0033	-0.0796
11	83485176	83492037	0	0.0081	0.0364	0.0317	-0.0033	-0.0796
11	83492038	83497710	1.0766	0.0081	0.0364	0.0317	-0.0033	-0.0796
11	83497711	83505065	0	0.0081	0.0364	0.0317	-0.0033	-0.0796
11	83505066	89880601	0.0255	0.0081	0.0364	0.0317	-0.0033	-0.0796
11	89880602	89884440	0	0.0081	0.0364	0.0317	-0.0033	-0.0796
11	89884441	89888640	0	0.0081	0.0364	0.0317	-0.0033	-0.0796
11	89888641	121841895	0.001	0.0081	0.0364	0.0317	-0.0033	-0.0796
12	3095298	75133943	-0.0114	-0.015	-0.0188	-0.0279	-0.025	-0.0545
12	75133944	75138112	-0.0114	-0.015	-0.0188	0	-0.025	-0.0545
12	75138113	75157465	-0.0114	-0.015	-0.0188	0.5468	-0.025	-0.0545
12	75157466	75167161	-0.0114	-0.015	-0.0188	0	-0.025	-0.0545
12	75167162	121252484	-0.0114	-0.015	-0.0188	0.0221	-0.025	-0.0545
13	3004789	19274779	-0.0177	-0.0125	-0.0213	-0.0074	-0.0175	0.0127
13	19274780	19281464	-0.0177	-0.0125	-0.0213	0	0	0
13	19281465	19297883	-0.0177	-0.0125	-0.0213	-1.8653	-2.2257	-2.4363
13	19297884	19314431	-0.0177	-0.0125	-0.0213	0	0	0
13	19314432	19429787	-0.0177	-0.0125	-0.0213	-0.4149	-0.0239	-0.0615
13	19429788	19436617	-0.0177	-0.0125	-0.0213	0	-0.0239	-0.0615
13	19436618	120276105	-0.0177	-0.0125	-0.0213	-0.007	-0.0239	-0.0615
14	3042998	15187282	-0.018	-0.018	-0.0264	-0.043	-0.0275	-0.0409
14	15187283	15197609	-0.018	-0.018	-0.0264	0	-0.0275	-0.0409
14	15197610	15214187	-0.018	-0.018	-0.0264	0.6757	-0.0275	-0.0409
14	15214188	15228961	-0.018	-0.018	-0.0264	0	-0.0275	-0.0409
14	15228962	25112301	-0.018	-0.018	-0.0264	-0.0105	-0.0275	-0.0409
14	25112302	25117469	-0.018	-0.018	-0.0264	0	-0.0275	-0.0409
14	25117470	25128981	-0.018	-0.018	-0.0264	0.5089	-0.0275	-0.0409
14	25128982	25147899	-0.018	-0.018	-0.0264	0	-0.0275	-0.0409
14	25147900	53397427	-0.018	-0.018	-0.0264	-0.0048	-0.0275	-0.0409
14	53397428	53415714	-0.018	-0.018	-0.0264	-0.0048	0	-0.0409
14	53533309	53536480	-0.018	-0.018	-0.0264	-0.0048	0	-0.0409
14	53536481	53548447	-0.018	-0.018	-0.0264	-0.0048	-2.2764	-0.0409
14	53548448	53553702	-0.018	-0.018	-0.0264	0	-2.2764	-0.0409
14	53553703	53673489	-0.018	-0.018	-0.0264	-0.7416	-2.2764	-0.0409
14	53673490	53714075	-0.018	-0.018	-0.0264	-0.7416	0	-0.0409
14	53714076	53759005	-0.018	-0.018	-0.0264	-0.7416	-1.2294	-0.0409
14	53759006	53961688	-0.018	-0.018	-0.0264	0	-1.2294	-0.0409
14	53961689	54157811	-0.018	-0.018	-0.0264	-0.1164	-1.2294	-0.0409
14	54157812	54163670	-0.018	0	-0.0264	-0.1164	-1.2294	-0.0409
14	54163671	54298700	-0.018	-1.0197	-0.0264	-0.1164	-1.2294	-0.0409
14	54298701	54304425	-0.018	-1.0197	0	-0.1164	-1.2294	-0.0409
14	54304426	54345365	-0.018	-1.0197	-0.8821	-0.1164	-1.2294	-0.0409
14	54345366	54358152	-0.018	-1.0197	-0.8821	-0.1164	0	-0.0409
14	54358153	54371162	-0.018	-1.0197	-0.8821	-0.1164	-3.074	-0.0409
14	54371163	54380572	-0.018	0	-0.8821	0	-3.074	0
14	54380573	54391011	-0.018	-2.9929	0	-3.3124	-3.074	-1.3336
14	54391012	54497009	-0.018	-2.9929	-2.8686	-3.3124	-3.074	-1.3336
14	54497010	54505165	0	-2.9929	-2.8686	-3.3124	-3.074	0
14	54505166	54763436	-3.7422	-2.9929	-2.8686	-3.3124	-3.074	-3.351
14	54763437	54783994	-3.7422	-2.9929	0	-3.3124	-3.074	-3.351
14	54783995	54792677	0	0	-1.1219	-3.3124	-3.074	0
14	54792678	54797444	-0.0356	-1.2107	-1.1219	-3.3124	0	0.0022
14	54797445	54805597	-0.0356	0	0	0	-0.8138	0.0022
14	54805598	54810415	-0.0356	-0.0262	-0.0299	-0.786	-0.8138	0.0022
14	54810416	54818532	-0.0356	-0.0262	-0.0299	0	-0.8138	0.0022
14	54818533	54827282	-0.0356	-0.0262	-0.0299	-0.028	0	0.0022

A4 continued. aCGH results: summary of all samples, gains and losses, chromosomal start and end.

Chromosome	Chromosome start	Chromosome end	Log2 Ratio					
			Tumour Sample 1	Tumour Sample 2	Tumour Sample 3	Tumour Sample 4	Tumour Sample 5	Tumour Sample 6
14	54827283	125164197	-0.0356	-0.0262	-0.0299	-0.028	-0.023	0.0022
15	3091692	8957124	0.5147	0.4942	0.0529	0.5408	0.5103	0.1736
15	8957125	8957628	0.5147	0.4942	0.0529	0	0.5103	0.1736
15	8957629	8977914	0.5147	0.4942	0.0529	-0.0139	0.5103	0.1736
15	8977915	8985039	0.5147	0.4942	0.0529	0	0.5103	0.1736
15	8985040	9454831	0.5147	0.4942	0.0529	0.624	0.5103	0.1736
15	9454832	9458823	0	0	0.0529	0	0	0.1736
15	9458824	9695478	-0.8499	-0.8334	0.0529	-0.8374	-0.7879	0.1736
15	9695479	9716192	-0.8499	-0.8334	0.0529	-0.8374	0	0.1736
15	9716193	9763805	-0.8499	-0.8334	0.0529	-0.8374	0.4749	0.1736
15	9763806	9772453	-0.8499	0	0.0529	-0.8374	0.4749	0.1736
15	9772454	9785836	-0.8499	0.4841	0.0529	-0.8374	0.4749	0.1736
15	9785837	9798688	-0.8499	0.4841	0.0529	0	0.4749	0.1736
15	9798689	9875899	-0.8499	0.4841	0.0529	0.5293	0.4749	0.1736
15	9875900	9891615	0	0.4841	0.0529	0.5293	0.4749	0.1736
15	9891616	103485012	0.516	0.4841	0.0529	0.5293	0.4749	0.1736
16	3013195	98303726	-0.0212	-0.0202	-0.0233	-0.0152	-0.0298	-0.0503
16	3013196	98303726	-0.0212	-0.0202	-0.0233	-0.0152	-0.0298	-0.0503
16	98303727	98303726	0	0	0	0	0	0
17	3006536	28148517	-0.0076	-0.0028	0.0138	0.0244	-0.0134	-0.0725
17	28148518	28159560	-0.0076	-0.0028	0.0138	0.0244	-0.0134	0
17	28159561	28175451	-0.0076	-0.0028	0.0138	0.0244	-0.0134	-1.1423
17	28175452	28185919	-0.0076	-0.0028	0.0138	0.0244	-0.0134	0
17	28185920	95265289	-0.0076	-0.0028	0.0138	0.0244	-0.0134	-0.0461
18	3181133	34684461	-0.0189	-0.0122	-0.0311	-0.0229	-0.0262	-0.0568
18	34684462	34689601	-0.0189	-0.0122	-0.0311	0	-0.0262	-0.0568
18	34689602	34695979	-0.0189	-0.0122	-0.0311	0.8195	-0.0262	-0.0568
18	34695980	34703043	-0.0189	-0.0122	-0.0311	0	-0.0262	-0.0568
18	34703044	90762590	-0.0189	-0.0122	-0.0311	-0.0091	-0.0262	-0.0568
19	3147156	32827300	-0.0076	-8.00E-04	0.0033	0.0048	-0.0175	-0.0792
19	32827301	32832966	-0.0076	-8.00E-04	0.0033	0.0048	-0.0175	0
19	32832967	33164302	-0.0076	-8.00E-04	0.0033	0.0048	-0.0175	-1.1733
19	33164303	33194356	-0.0076	-8.00E-04	0.0033	0.0048	-0.0175	0
19	33194357	61337201	-0.0076	-8.00E-04	0.0033	0.0048	-0.0175	-0.0756
X	56448916	56458374	-0.0138	0.0446	-0.4832	0	-0.0553	9.00E-04
X	56458375	56501318	-0.0138	0.0446	-0.4832	-0.5957	-0.0553	9.00E-04
X	56501319	56512129	-0.0138	0.0446	-0.4832	0	-0.0553	9.00E-04
X	56512130	93451785	-0.0138	0.0446	-0.4832	-0.0422	-0.0553	9.00E-04
X	93451786	93462123	-0.0138	0.0446	-0.4832	0	-0.0553	9.00E-04
X	93462124	93486599	-0.0138	0.0446	-0.4832	0.5165	-0.0553	9.00E-04
X	93486600	93496490	-0.0138	0.0446	-0.4832	0	-0.0553	9.00E-04
X	93496491	135170346	-0.0138	0.0446	-0.4832	-0.0148	-0.0553	9.00E-04
X	135170347	135174881	-0.0138	0.0446	-0.4832	0	-0.0553	9.00E-04
X	135174882	135228365	-0.0138	0.0446	-0.4832	0.3956	-0.0553	9.00E-04
X	135228366	135238003	-0.0138	0.0446	-0.4832	0	-0.0553	9.00E-04
X	135238004	166612158	-0.0138	0.0446	-0.4832	-0.0084	-0.0553	9.00E-04

B4. aCGH results: summary of gains and deletions, whole chromosomes and genes within focal gains and deletions.

Tumour Sample	Chromosome gains	Chromosome losses	Focal deletions	Focal gains
Tumour Sample 1	Trisomy 15	-	-	1 (Gm11438)
Tumour Sample 2	Trisomy 15	-	-	1 (St3gal4)
Tumour Sample 3	Trisomy 2	Monosomy X	1(Fgf13)	-
Tumour Sample 4	Trisomy 15	-	3 (Gm12814, Gm12819, Gm12821)	5 (Vsig4, Il1rapl2, syt16, Cyp2b9, RIKEN cDNA E330034G19)
Tumour Sample 5	Trisomy 15	-	-	-
Tumour Sample 6	Trisomy 2	-	5,(anks1,Pten,ptpn13, Zfp536, Gm 12478, Gm12480)	

APPENDIX FIVE: PRE-LYMPHOMIC COMPARATIVE MICROARRAY ANALYSIS

A5. Deregulated genes ($F_c \geq 2$, adjusted P value >0.005). For a given transcript positive F_c values indicate an increase and negative values indicate a decrease in expression in HD1^{L/L};HD2^{L/WT} samples compared to WT LMCs.

downregulated			upregulated			upregulated		
gene symbols	FC	adj.P.Val	gene symbols	FC	adj.P.Val	gene symbols	FC	adj.P.Val
F13a1	-15.57509285	7.5E-11	Pdlim4	35.12732823	3.2E-10	Mfap2	3.971160172	9.6E-09
Hsd11b1	-10.8051195	1.2E-09	Ly6c1	19.43049885	2.3E-09	Hist1h3a	3.968790178	1.1E-06
Hsd11b1	-10.21975701	1.2E-09	Cpsf4l	14.07896918	1.3E-06	Jazf1	3.87430275	2.6E-07
Hsd11b1	-8.977765901	4.2E-09	Prr13	12.89997109	7.5E-11	1500009L16Rik	3.866113219	9.2E-07
Cd52	-8.2447705	2.3E-07	Grb7	12.50609692	2.0E-11	Sdc1	3.823592272	7.5E-11
Ctnna1	-8.208575935	1.4E-09	Aif1l	10.00916646	1.2E-08	Cd9	3.807476054	1.7E-07
Gm6273	-7.691656618	1.4E-04	Mmp14	9.153031778	7.5E-08	Egfl7	3.711264126	2.0E-06
S100a11	-7.500375285	8.2E-06	Slc6a13	8.506891747	3.6E-08	Bag3	3.699210317	1.4E-07
Smoc1	-6.919971639	1.1E-05	Gm525	8.056011962	1.1E-08	Tagln2	3.659063361	2.9E-08
1190002H23Rik	-6.763732745	5.2E-08	Plac8	7.375515814	2.3E-05	Hlcs	3.651738357	7.8E-08
Fgf13	-6.329399085	8.1E-08	Trf	7.206013191	4.9E-09	Gm2179	3.563618424	5.3E-06
Mgst3	-6.054928062	7.5E-11	Hap1	6.998937276	7.5E-11	Myo6	3.558877417	1.3E-03
Prodh	-6.036673321	3.1E-07	1110008L16Rik	6.821345536	1.7E-08	Mcoln2	3.558068291	1.5E-09
Spo11	-5.606627	2.6E-05	Slc7a7	6.499276869	7.5E-11	Enc1	3.503256205	4.0E-07
Prnp	-5.249644349	5.4E-06	Sox12	6.454739798	4.1E-08	Tpi1	3.472222696	3.5E-07
Dnajc6	-5.095632714	6.2E-04	Gsto1	6.115466092	5.7E-09	Odz4	3.444934858	1.4E-03
Dnajc6	-5.092830653	3.0E-04	Fgfbp1	6.114462323	1.0E-06	Aldh2	3.429589215	9.6E-08
P2rx1	-5.088753116	6.5E-07	Aldh3a1	6.044461285	8.0E-06	Cpsf4l	3.379330978	3.2E-05
Dok2	-5.03127853	1.1E-06	Cd163l1	6.006688036	7.1E-04	Chd3	3.367877586	5.0E-08
Cd69	-5.010032584	4.4E-06	Litaf	5.888390821	3.8E-08	Bik	3.367669712	2.5E-06
Scn4b	-4.985569802	3.9E-05	Fxyd6	5.73263268	1.7E-03	Myh10	3.364367454	1.2E-06
Wdr78	-4.956262749	5.6E-05	Prelid2	5.685272292	7.7E-06	Ppm1e	3.364122645	1.5E-07
2610019F03Rik	-4.72397872	1.5E-09	Ddc	5.677155368	1.6E-06	Tcea3	3.355707381	7.0E-06
Abca3	-4.646363946	8.8E-07	Kctd17	5.48083404	3.5E-06	Dctpp1	3.342761689	7.0E-06
Prodh	-4.420446655	1.1E-06	Ddc	5.464057503	2.2E-06	Igf1bp7	3.326369508	7.4E-05
Ankrd50	-4.348273265	1.4E-07	Slc7a7	5.427061425	7.5E-11	Fkbp11	3.325817183	5.5E-05
P2rx1	-4.310789825	1.5E-07	Ldhd	5.22128405	2.2E-07	Cyth4	3.310775709	9.8E-05
Cd4	-4.128369063	2.5E-06	Rbpms	5.215278331	5.1E-07	Nt5dc2	3.299825322	5.3E-08
Samd9l	-4.083894724	2.0E-04	Srm	5.08549468	1.4E-07	Ppa1	3.297625481	2.3E-06
Txnip	-4.051246095	4.8E-05	Srm	4.878978979	1.9E-06	Slc29a1	3.282580634	7.5E-11
Cdk20	-4.030164525	5.5E-08	Fgf8	4.876347099	2.3E-06	Mapre2	3.281590034	1.4E-07
Txnip	-3.984765531	7.2E-05	Plxn2	4.853535217	8.5E-08	Igf2bp2	3.260992263	1.4E-05
Gbp2	-3.957897543	8.8E-08	Inpp1	4.851776695	6.0E-06	Gcat	3.260534667	2.1E-07
Bcl6	-3.927532009	9.9E-06	Gpr83	4.849527118	3.4E-04	Prdx4	3.259251711	5.3E-08
Zfp36	-3.876336463	3.1E-07	Pcbp4	4.847135785	2.7E-07	Hspa12b	3.25644266	4.8E-07
Arhgef6	-3.849096307	6.4E-10	Zfhx3	4.842969879	2.1E-09	Renbp	3.250144392	1.3E-09
A930003A15Rik	-3.784924651	3.1E-06	Cenpv	4.840676377	5.7E-07	Zbtb8b	3.244920489	2.0E-06
Obfc2a	-3.781143729	7.1E-08	Ly6a	4.822457342	1.3E-04	Lama5	3.237631243	3.8E-10
Insl5	-3.732906099	4.1E-07	Rhoj	4.820597967	1.1E-09	D11Bwg0517e	3.21790881	7.7E-05
Cdk20	-3.728374769	8.7E-09	Syde1	4.795648779	2.8E-08	Dclk2	3.216251093	1.9E-07
Abca3	-3.690989777	1.7E-07	Sdc1	4.753430544	7.5E-11	Acpl2	3.20540847	2.8E-08
St3gal6	-3.69006416	5.3E-07	Gm525	4.750089702	5.8E-08	Lcn4	3.19416355	1.0E-05
Rag2	-3.672219917	4.4E-08	Ldhd	4.732402441	8.5E-08	Ncf4	3.191888552	8.5E-04
Tpd52	-3.55675155	1.1E-06	Tspan17	4.561962482	1.2E-09	Polr2f	3.185569763	3.9E-07
Gpr177	-3.549807874	1.2E-06	Wdr86	4.494211287	1.8E-06	Gpr183	3.179735424	5.6E-05
Stat4	-3.546534744	1.2E-06	Odz4	4.479658477	5.7E-04	Shmt2	3.175574677	4.5E-06
Bop1	-3.54050659	5.2E-07	Inpp1	4.458309896	8.7E-06	Mthfd1	3.160768105	5.8E-06
Mllt4	-3.539669441	7.7E-05	Hist1h3d	4.422430117	2.5E-07	Dpcd	3.140987268	9.4E-08
Ankrd6	-3.518520745	2.3E-08	E330016A19Rik	4.322361151	2.8E-07	Als2	3.13388364	5.1E-06
Mgst3	-3.494334309	1.1E-08	Cacng4	4.292380502	6.8E-09	Rrp12	3.12643085	4.5E-07
Podxl2	-3.47917733	3.3E-05	Lsr	4.261341282	1.2E-06	Wnt8b	3.117185764	9.7E-07
Pdlim2	-3.478596482	1.1E-06	Wwc2	4.229029535	4.0E-06	S1pr2	3.115426157	1.1E-08
Gtf2h4	-3.467926972	5.9E-08	Hmgn3	4.210544866	8.4E-06	Rcl1	3.101467036	3.6E-07
Bin1	-3.446162652	6.4E-08	Sh3gl3	4.201679754	7.5E-08	Hspg2	3.100874096	1.1E-05
Ras11b	-3.402112067	3.2E-06	Cdkn1c	4.190215711	1.6E-04	Tcf7l1	3.082202656	1.0E-09
Cdc42ep3	-3.378138327	5.1E-06	Prpf40b	4.179844351	4.2E-09	Lmna	3.075224981	2.7E-06
Gngt2	-3.374410813	1.2E-07	Hmgn3	4.158306056	7.0E-06	Elov16	3.061272016	2.7E-06
Atp10a	-3.340371785	7.1E-08	Srm	4.149188311	7.8E-07	Hspg2	3.056613996	1.1E-05
Ras11b	-3.337024874	5.5E-07	Adk	4.142922209	5.9E-08	1110036O03Rik	3.055785777	7.8E-08
Dock10	-3.306217565	8.7E-07	Tpi1	4.010118715	3.6E-08	D11Bwg0517e	3.046974387	1.2E-04
Sit1	-3.274299217	1.1E-07	Klhdc2	3.986227496	9.7E-08	Scara3	3.029709165	1.6E-03

A5 continued. Deregulated genes ($F_c \geq 2$, adjusted P value <0.005). For a given transcript positive F_c values indicate an increase and negative values indicate a decrease in expression in HD1^{L/L};HD2^{L^{WT}} samples compared to WT LMCs.

downregulated			upregulated			upregulated		
gene symbols	FC	adj.P.Val	gene symbols	FC	adj.P.Val	gene symbols	FC	adj.P.Val
Jakmip1	-3.207889195	5.8E-09	Dfna5	3.028330142	4.5E-04	Polr1b	2.678034158	5.6E-08
Scn2b	-3.169567481	2.1E-04	Fam111a	3.026493006	9.6E-06	Ipo4	2.665783818	6.0E-07
B3gnt8	-3.138289312	2.5E-06	Abi2	3.018176732	8.5E-08	Tmem55b	2.663180338	1.2E-04
NA	-3.095647939	1.7E-07	Asprv1	3.016769729	2.1E-08	H2-Ab1	2.661052961	6.0E-07
NA	-3.074298675	8.3E-05	Adk	3.010676884	5.8E-07	Gstp1	2.660621061	5.9E-06
Camkk1	-3.069210528	3.3E-07	Dctd	3.006837233	1.3E-06	Vars	2.655434363	5.9E-06
Tec	-3.0691374	2.0E-07	Sort1	3.006810443	4.3E-07	Gstp1	2.653480905	2.5E-05
LOC625360	-3.045786568	1.3E-06	Hist1h2bf	3.00307324	1.6E-05	Lrrc50	2.651884086	4.6E-07
Abi3	-3.027399341	1.6E-06	Ipo5	2.997442588	2.5E-06	Hsp90ab1	2.636713522	2.9E-06
Mgat4a	-2.97376331	8.2E-09	Adk	2.995564393	2.3E-06	Ctnnal1	2.635144943	8.7E-08
Plcb2	-2.954403092	1.2E-06	Angptl4	2.994849955	4.8E-07	Epb4.115	2.623632639	4.2E-09
Arhgap24	-2.950726627	1.4E-07	Abhd14a	2.993702731	9.6E-09	9430038I01Rik	2.619284653	1.4E-07
Hchd2	-2.923987964	7.8E-08	Hist1h2bh	2.976760271	6.3E-06	Gale	2.617815641	3.7E-08
Hcst	-2.918074124	2.8E-07	Trmt61a	2.96209003	8.1E-07	Dos	2.614454695	8.8E-09
Snx15	-2.908668785	3.6E-08	Hist1h2bk	2.958023609	1.3E-05	Oxct1	2.609373285	1.2E-06
Cdk20	-2.903422811	1.2E-07	Cela1	2.956014663	3.1E-06	Gins2	2.606936216	1.4E-05
Dstn	-2.903115098	1.5E-07	Sort1	2.955597112	4.8E-07	Glipr2	2.586099452	7.7E-07
5830405N20Rik	-2.889083911	8.3E-08	Lmna	2.951876937	8.3E-07	Klhl5	2.580213054	8.6E-10
Cd96	-2.8822056	2.0E-07	Rab15	2.951808226	6.8E-05	Lmna	2.578173942	6.2E-06
Lpxn	-2.871246854	2.0E-07	Glipr2	2.951656334	3.9E-07	Suclg2	2.576060634	2.8E-06
F2r	-2.857917343	1.7E-04	Gm10355	2.948158914	8.7E-07	Prmt3	2.57463724	2.0E-07
Vamp1	-2.831461015	1.4E-05	Hist1h3c	2.924070023	7.0E-06	Adam12	2.57106018	2.4E-07
Sit1	-2.825256491	1.9E-08	Nhp2	2.921446923	1.2E-06	Zfp365	2.570705836	1.4E-06
Ets2	-2.798449588	1.9E-05	Lag3	2.91831917	4.3E-05	5730507C01Rik	2.566381259	1.8E-04
Errf1	-2.789169495	5.4E-05	Card10	2.909430111	1.1E-04	Gkap1	2.559940448	7.5E-07
Ift172	-2.788774331	1.9E-07	Rcl1	2.909418552	2.9E-07	Alpl	2.558234591	2.2E-04
Cd84	-2.783315204	4.6E-06	Abi2	2.897170138	2.0E-08	Mcm6	2.557555473	7.6E-06
Klf7	-2.745782664	9.3E-07	Rangrf	2.889142869	3.7E-07	Als2	2.557086483	6.6E-06
Sic37a2	-2.745289339	6.3E-07	AW555464	2.879230257	2.0E-08	Zfhx3	2.541316808	1.2E-08
Csrp1	-2.743131934	1.6E-04	Crtap	2.875169647	7.7E-07	E130012A19Rik	2.540512357	7.1E-08
Brdt	-2.742753128	1.7E-06	Gpc1	2.872748672	1.3E-06	Gnl3	2.540383171	6.0E-07
Ypel3	-2.739187836	2.6E-05	Nlgn2	2.863545402	2.0E-08	Ldhd	2.538536566	1.0E-05
Lxn	-2.721119115	7.9E-08	Psat1	2.860595746	2.7E-06	Mrto4	2.538028855	6.1E-07
Notch3	-2.676652422	2.4E-06	Isyna1	2.85343696	2.5E-07	Rpl22	2.529112269	6.1E-07
Ppp1r3b	-2.673828353	1.6E-05	Gar1	2.847691037	2.8E-07	Phlda1	2.521383738	1.8E-05
Gtdc1	-2.653975225	1.4E-09	Cad	2.846266494	1.3E-05	Apobec3	2.517559546	1.2E-07
Dgka	-2.645252827	2.9E-05	Csrp2	2.831155324	8.3E-07	Myc	2.515055297	4.0E-08
S100a8	-2.634761811	6.0E-06	Ifi30	2.829290357	2.2E-07	Rrp15	2.510179607	3.7E-07
Gm889	-2.630221668	6.6E-07	Mettl1	2.821224479	8.2E-07	Hist1h2bn	2.508674019	2.0E-05
Dennd1c	-2.624834728	3.2E-06	Ung	2.815778101	3.8E-06	Snx10	2.507277269	2.6E-05
Znf512b	-2.619350558	2.3E-06	Agrn	2.810603497	1.8E-08	Dennd2a	2.504135054	4.1E-10
Caena1d	-2.616246561	7.8E-06	Tmem97	2.806029969	4.7E-06	Pyclr1	2.498107411	2.9E-07
Gpr171	-2.611497307	3.1E-06	Stag3	2.802169897	4.3E-06	Sema6b	2.495044304	3.4E-07
Pitpnm2	-2.610688964	4.7E-05	C1qbp	2.79157143	1.7E-06	Prkca	2.494525509	1.5E-05
Arhgap4	-2.610432091	2.2E-07	Mettl1	2.79112577	3.3E-07	Pvrl2	2.493365927	4.0E-08
NA	-2.607883942	1.1E-06	Aimp2	2.781862072	8.1E-07	Cask	2.490210168	1.3E-08
Dusp6	-2.605590905	7.5E-05	Cd63	2.764898524	3.2E-04	Hint1	2.488213752	6.1E-06
Trp53inp1	-2.60471082	9.5E-05	NA	2.757813221	6.9E-06	Tfrc	2.485553839	5.9E-06
Clk3	-2.595357255	7.4E-06	Bola2	2.753651402	6.4E-06	Grwd1	2.482173026	6.0E-07
Fbxl12	-2.571608385	1.2E-05	Dennd3	2.753444767	1.7E-05	Gnl3	2.481614173	8.5E-08
Nhs1	-2.567932741	2.4E-05	Tubb2b	2.736518116	3.2E-05	Gins2	2.480681125	3.3E-05
C85492	-2.555978358	9.6E-05	Sall4	2.728923451	1.2E-04	Hn1l	2.477654095	8.8E-07
Vamp1	-2.538923208	5.6E-06	HK2	2.71757602	7.2E-07	Dlk1	2.46840138	1.9E-05
Sestd1	-2.531471795	7.6E-08	Gins2	2.717381768	7.8E-06	Gstz1	2.465783721	4.9E-08
Tmub1	-2.523309736	2.3E-09	Zcchc18	2.710574675	2.2E-05	Mybbp1a	2.457657061	8.6E-06
Afgf2	-2.51611242	4.4E-05	Anp32a	2.710130277	2.3E-05	Rilpl1	2.452106489	6.2E-08
Lypd6b	-2.51536588	1.4E-08	Vars	2.696592259	4.3E-06	Gylt1b	2.447447434	9.7E-08
Pstpip1	-2.513876355	1.1E-07	Nln	2.687249993	3.1E-08	Ncam1	2.44210722	1.5E-04
Arl5c	-2.513752483	2.1E-04	Oxct1	2.686963381	1.2E-06	Sdf2l1	2.439933175	2.1E-06
Tctex1d1	-2.497817479	8.5E-08	Hsp90ab1	2.684181927	2.0E-06	Hist1h4b	2.439405424	1.4E-05
Sin3b	-2.497106318	3.0E-06	Tfrc	2.680319278	4.4E-06	Vat1	2.438722656	4.3E-07

A5 continued. Deregulated genes ($F_c \geq 2$, adjusted P value <0.005). For a given transcript positive F_c values indicate an increase and negative values indicate a decrease in expression in HD1^{L/L};HD2^{L/WT} samples compared to WT LMCs.

downregulated			upregulated			upregulated		
gene symbols	FC	adj.P.Val	gene symbols	FC	adj.P.Val	gene symbols	FC	adj.P.Val
Fbxl12	-2.489832092	2.3E-05	Crtap	2.438612403	3.6E-06	Hspa9	2.251663431	4.8E-07
Gabarap1	-2.487638704	5.0E-05	Hspa2	2.435019555	5.9E-06	Cercam	2.249931658	5.7E-08
Arhgef11	-2.483537101	7.2E-07	Ahi1	2.426824049	6.8E-05	Pes1	2.24691981	1.2E-07
Hmha1	-2.482853695	4.4E-06	Rrp1b	2.416993314	1.7E-06	Micall1	2.245600216	3.8E-05
Ldoc1l	-2.468893518	1.3E-04	Syngn2	2.414395994	1.3E-07	Tctex1d2	2.244589709	2.3E-05
Itpr1	-2.458748313	9.0E-07	Poll	2.411379124	1.2E-07	NA	2.241934989	1.1E-04
Tnfrsf18	-2.440574098	1.3E-07	Dbp	2.41090671	3.6E-06	NA	2.241454801	4.4E-07
Gsdmc2	-2.439156748	2.7E-06	Hist1h3h	2.410499009	1.7E-05	Gm347	2.240662881	8.3E-07
Cd1d1	-2.430482863	1.9E-05	Syngn2	2.410494016	4.1E-08	Nasp	2.240470625	3.3E-06
Ppp1r9b	-2.427812379	6.9E-05	Aprt	2.409771232	7.5E-05	Pfkl	2.238269728	1.1E-07
Hmgcs2	-2.427076288	5.1E-05	Glt25d1	2.40252347	3.7E-06	Umps	2.234274226	6.5E-07
Sla2	-2.424238554	1.5E-06	Hist1h4j	2.399999929	1.9E-05	Ccdc86	2.232770701	1.5E-06
Marcks	-2.420959954	2.8E-05	Syngn2	2.397873182	1.3E-06	Eif5a	2.232335027	3.6E-06
Mier1	-2.413484159	6.4E-08	Sim2	2.396557902	1.2E-03	Pdlim7	2.231051455	4.3E-07
Trp53inp1	-2.403499845	4.0E-05	LOC641240	2.393957025	8.4E-06	Tjp3	2.226216031	8.5E-06
Tbc1d10c	-2.386424193	1.4E-06	Timm9	2.38074764	2.6E-06	NA	2.223836328	1.1E-07
Sri	-2.382677112	2.9E-07	Lmna	2.379704382	2.2E-05	Slc48a1	2.223386999	2.0E-06
Capn5	-2.373438162	4.8E-06	Ppap2c	2.37908584	8.1E-08	Liph	2.22319081	3.0E-05
Edaradd	-2.367020935	5.7E-04	Jdp2	2.373909887	3.9E-05	Blvrb	2.2216621	2.8E-07
AA960436	-2.364789903	4.2E-09	Acot7	2.373667528	4.7E-05	NA	2.221556454	8.7E-08
Ampd1	-2.364589694	3.1E-05	Dexi	2.373573298	3.7E-06	Gart	2.221085009	6.3E-06
Pip4k2a	-2.361955388	1.8E-05	Acot7	2.371136527	5.6E-05	Hspa9	2.219652435	2.5E-07
Egr1	-2.36108565	5.1E-05	Dexi	2.36664337	1.9E-06	Thg11	2.217725393	1.1E-07
Capn3	-2.36060119	1.0E-05	Hmga1	2.364848643	3.0E-06	Ahcy	2.217586834	2.4E-05
Dgka	-2.360478411	8.3E-05	Lmo4	2.360581239	2.3E-06	Nol12	2.214975322	4.1E-06
Chrna9	-2.357333693	2.1E-05	Ppm1l	2.357808328	4.4E-06	Adssl1	2.209080018	5.5E-06
Mad1l1	-2.356533808	6.1E-06	Pcyox1l	2.355594988	2.3E-07	Atad3a	2.205658626	6.1E-07
Slco4a1	-2.350633953	2.8E-05	Hist1h2bm	2.348534272	8.7E-05	Crel2	2.203232269	4.1E-07
Pdlim2	-2.342616069	2.7E-08	Tubb2b	2.346088384	2.1E-06	Tspan6	2.203136035	2.9E-07
Uaca	-2.338609469	2.8E-05	Ephb2	2.344094725	5.9E-07	2510009E07Rik	2.20216542	8.7E-08
Rag1	-2.336268292	3.1E-04	Acot7	2.344006755	2.8E-04	Rplp0	2.202109845	1.3E-06
Tigd2	-2.328819044	6.0E-07	Gale	2.342359883	1.7E-07	Tro	2.198575742	2.6E-06
Tbxa2r	-2.324572778	2.3E-06	Tro	2.340528628	6.0E-07	NA	2.197858658	1.1E-05
Al467606	-2.3218973	1.5E-05	Acaca	2.340197753	4.8E-05	Slc35b4	2.195904023	1.5E-06
Casp6	-2.320651468	1.2E-05	Tmem107	2.336526699	3.5E-06	Tuba8	2.193879416	3.8E-05
Gimap1	-2.316651008	1.5E-07	Etv5	2.33363545	9.6E-06	H2-Oa	2.190035127	2.1E-04
Arhgap25	-2.314713873	3.5E-08	Cd3eap	2.331983949	2.9E-05	Tubb2b	2.188429573	6.3E-05
NA	-2.31027009	1.3E-05	H2-Ab1	2.330257158	1.5E-07	Arsi	2.187769079	1.1E-05
Ly6d	-2.306240345	4.6E-03	Shmt1	2.329467376	4.4E-06	Tmed1	2.187422163	2.8E-08
Rnf167	-2.299455917	2.0E-06	Mif	2.329438447	5.2E-06	Nudc	2.185927321	8.2E-06
Ctu2	-2.295452381	1.1E-06	Hspd1	2.317956067	3.6E-07	E2f6	2.184660521	2.0E-06
Fbxl12	-2.295009964	2.1E-04	Pdgbf	2.308521385	6.7E-09	Rpl3l	2.18393724	4.3E-03
Fas	-2.291718809	1.9E-05	Rbpms	2.307900422	4.6E-06	Ttf2	2.183915571	4.5E-05
Dgke	-2.286228286	1.0E-04	Mcam	2.306629044	2.9E-08	Slc6a8	2.183030716	1.0E-09
Inpp5d	-2.283922967	3.4E-06	Dnajc21	2.303660603	1.8E-06	Ydjc	2.18271378	1.8E-05
Snn	-2.279861634	1.3E-06	Zfp704	2.303626515	9.6E-06	NA	2.182285795	1.7E-06
Casp6	-2.278760334	3.7E-07	Hyal2	2.300795891	2.0E-08	Rsph1	2.182185616	4.3E-07
2810021J22Rik	-2.274886344	5.2E-07	Mcm7	2.297018423	7.3E-05	Fam46c	2.181248066	2.3E-07
Degs1	-2.27312162	2.0E-06	Tpm4	2.29695886	1.5E-05	Sqle	2.177197309	1.4E-05
Ampd1	-2.272769279	1.7E-04	Fam38a	2.28986178	5.5E-07	Hist1h2ab	2.174902184	4.5E-05
Vopp1	-2.272663533	1.7E-05	Eif5a	2.284771198	1.5E-06	St3gal1	2.174221642	1.6E-05
Il17re	-2.271061376	9.5E-05	Mcm6	2.284031477	4.7E-05	Zfp41	2.172911588	4.1E-05
Rnf167	-2.270228603	7.3E-05	Gins2	2.283031321	1.9E-05	Naca	2.172391939	7.2E-06
Capn3	-2.265642883	6.2E-06	Rrp1b	2.282162695	1.1E-06	Kctd17	2.166051251	4.1E-05
S100a10	-2.255909334	2.3E-05	Esm1	2.279128114	9.7E-08	H2-Oa	2.165034237	5.6E-05
Vars2	-2.253109231	3.5E-06	NA	2.278917291	4.8E-07	Acot7	2.164501084	1.2E-04
Scarb2	-2.252813357	7.0E-08	Mpp6	2.27529481	1.6E-06	Med22	2.162607378	8.3E-09
6330406115Rik	-2.248949849	9.5E-06	Polr1a	2.275261366	2.4E-07	Pou2af1	2.162508983	2.1E-04
Usp10	-2.246232245	6.0E-04	Echdc2	2.268539713	1.8E-03	Nop58	2.158643214	7.2E-06
Mbnl2	-2.244126903	5.4E-06	Vegfb	2.25886148	6.1E-07	Kit	2.158538858	4.3E-03
Epc1	-2.241901631	7.9E-06	Gm8276	2.25565461	2.0E-06	Phf13	2.156437167	3.1E-07

A5 continued. Deregulated genes ($F_c \geq 2$, adjusted P value <0.005). For a given transcript positive F_c values indicate an increase and negative values indicate a decrease in expression in HD1^{L/L};HD2^{L/WT} samples compared to WT LMCs.

downregulated			upregulated			upregulated		
gene symbols	FC	adj.P.Val	gene symbols	FC	adj.P.Val	gene symbols	FC	adj.P.Val
Fam117a	-2.238475957	1.4E-05	Creld2	2.154950086	2.5E-07	Garnl3	2.066062709	4.0E-08
Cnp	-2.237850395	8.8E-06	NA	2.154941658	5.4E-06	Dock6	2.065531701	1.9E-05
Il16	-2.237620773	3.7E-05	Pold2	2.15480023	1.5E-04	Prickle1	2.064713966	5.1E-05
Sytl2	-2.235632919	5.9E-07	NA	2.153155935	9.7E-07	Naca	2.063897657	2.4E-06
Parp6	-2.228091657	3.9E-06	Tjp3	2.151766582	1.5E-05	Rbbp7	2.062018992	7.6E-04
Gm6776	-2.226037893	1.4E-04	Capn12	2.149036608	6.8E-05	NA	2.056539391	5.9E-07
LOC100047670	-2.225881489	2.2E-05	Adsl	2.148691418	1.2E-05	Chchd10	2.055745431	2.3E-07
Gm5107	-2.225842858	1.2E-05	Hsp90ab1	2.145857657	1.4E-06	Sfxn1	2.05402427	1.6E-07
Birc2	-2.22161653	6.0E-06	Dut	2.144355447	2.6E-05	Itgb7	2.052961958	4.7E-03
Cd97	-2.218227476	2.4E-07	Fnbp1l	2.144344101	4.9E-05	Ssx2ip	2.052551661	4.5E-08
Tbx6	-2.217986723	4.0E-05	Nap1l1	2.143805856	3.2E-06	Arid3a	2.052220003	2.4E-07
Sh3kbp1	-2.216291935	6.0E-08	Tpst1	2.142278054	4.5E-06	Prim2	2.051914472	4.5E-06
Rnf167	-2.213285885	5.9E-05	Arsi	2.141414583	2.7E-05	Mcm10	2.046573653	4.4E-04
Plxnd1	-2.208296887	2.5E-06	Zfp41	2.139487688	5.9E-06	Igsf3	2.045854072	3.1E-06
Tmem38b	-2.204676213	3.6E-05	Ppm1e	2.139145703	2.4E-06	Rps6ka1	2.043533275	3.0E-05
Ati2	-2.204525519	1.4E-05	Cdr2	2.138541031	1.4E-06	9430038101Rik	2.042450871	2.3E-07
Gm6552	-2.195822921	9.4E-07	Cdt1	2.136054405	5.7E-06	Rrp9	2.040903151	1.5E-05
Arpp21	-2.193232413	6.3E-04	A230050P20Rik	2.134102163	1.3E-03	Prpf19	2.040684743	9.3E-06
6330406115Rik	-2.189527948	3.7E-06	Efemp2	2.132438973	5.7E-09	Dyrk3	2.039721818	1.4E-07
Trat1	-2.18671786	1.4E-06	Akr7a5	2.131213019	5.2E-08	Iqgap2	2.038331002	2.0E-03
Exoc6b	-2.18359042	3.1E-05	Nr2f6	2.127329479	2.4E-08	NA	2.036764376	1.2E-04
Tnfrsf18	-2.1811732	1.2E-07	Rdbp	2.127124327	3.7E-04	Rad54l	2.03583139	4.1E-04
Mllt11	-2.179451464	2.7E-07	NA	2.125402562	3.6E-06	Ttc27	2.03372449	3.8E-06
Armcx1	-2.178687009	1.8E-04	Zfp608	2.119267218	2.6E-06	Lig1	2.031246624	1.8E-04
Sh3kbp1	-2.17803917	5.1E-07	Snx8	2.117204581	5.9E-07	Ppargc1b	2.030990251	1.6E-05
Dusp10	-2.167549856	4.6E-05	Cd276	2.115115976	2.0E-07	Shmt2	2.030868652	2.9E-05
Plxnd1	-2.167063496	1.5E-06	Rabl2a	2.114354918	8.4E-07	Elovl1	2.030677684	2.1E-07
Ankrd6	-2.165269155	1.5E-07	Rdbp	2.112769777	6.8E-04	Aimp2	2.030634222	4.4E-06
Dram2	-2.165259361	1.2E-06	Pa2g4	2.11227206	2.3E-06	2900010M23Rik	2.027679306	5.5E-07
Nedd9	-2.165009905	7.2E-07	Aldoa	2.112229565	2.8E-06	Lig1	2.027662816	1.3E-04
Ogt	-2.15777275	1.8E-04	Lgmn	2.111199427	1.2E-06	Bmp7	2.026720215	2.4E-05
O610010K14Rik	-2.151756226	1.8E-07	Tmem201	2.110566478	2.6E-08	Ncl	2.026107696	4.9E-05
Atpgd1	-2.15153856	1.9E-05	H1f0	2.109447119	1.4E-06	Fbxo10	2.02557921	1.4E-05
Whrn	-2.15048352	1.8E-04	NA	2.107913862	5.3E-06	Mybbp1a	2.025663174	8.7E-06
Themis	-2.147322336	1.9E-05	Nutf2	2.10639989	1.4E-06	Pabpc4	2.024290009	1.4E-06
Lpar6	-2.146168385	2.5E-03	Cxadr	2.106109801	1.7E-07	NA	2.024271069	1.8E-03
Fam49a	-2.145884644	5.6E-06	Ranbp1	2.104697521	7.3E-06	Prmt5	2.022289785	1.2E-05
Trpc4ap	-2.143719557	1.0E-05	Cox6b2	2.099888885	7.0E-05	Rars	2.020712473	5.6E-07
Def6	-2.141222526	4.6E-06	Fam169b	2.098143921	7.5E-05	Josd1	2.020459975	8.7E-08
Ati2	-2.140391754	5.2E-04	Mfap2	2.097055081	1.2E-08	Prmt8	2.019064283	8.9E-04
C85492	-2.138095015	1.6E-04	Gm6560	2.094149293	5.6E-06	Aebp2	2.016795816	5.6E-07
Spats2l	-2.136413787	1.4E-05	Apex1	2.092948054	2.7E-05	Ctpts	2.015095508	2.3E-05
Gimap6	-2.133518662	1.3E-05	2010317E24Rik	2.091760345	5.4E-05	NA	2.014873155	5.6E-06
Stx1a	-2.132190922	2.1E-07	Mfap2	2.090822652	8.4E-07	Bcap29	2.013665391	1.7E-04
Ap3m2	-2.129001218	8.4E-07	Pus1	2.090267115	6.5E-07	Cnnm1	2.013318328	1.8E-05
Sh3kbp1	-2.128580042	2.5E-07	NA	2.088664066	6.7E-09	Il7r	2.013312431	3.6E-03
Sri	-2.127441994	8.8E-06	Trio	2.087966703	2.3E-04	Tmem132a	2.012233245	1.5E-07
Myo1f	-2.124117459	1.3E-04	Fmc1	2.085134708	4.1E-05	Set	2.011211444	3.2E-04
Tmem229b	-2.123703985	1.1E-05	Rbbp7	2.083733147	2.4E-04	Cdc25b	2.009228548	2.5E-05
S100a13	-2.12253416	3.6E-05	Cdc42ep4	2.081577745	9.3E-06	Cd72	2.008674971	2.0E-04
Sbk1	-2.118464678	8.0E-06	Sfxn1	2.081301472	5.2E-07	NA	2.006410367	5.6E-04
Rasgrp1	-2.116667021	4.4E-07	Pprc1	2.07934993	3.2E-06	Med22	2.005369297	2.0E-07
NA	-2.11395986	1.2E-05	Syng1	2.079113911	2.0E-06	Prickle1	2.005036655	2.0E-05
Atg10	-2.112072015	6.0E-07	Ell3	2.078549957	4.7E-06	NA	2.004339001	5.5E-05
Arhgap24	-2.110705724	6.7E-07	Prpf19	2.073463496	2.3E-07	Atad2	2.003552432	6.0E-04
Arap2	-2.109731396	5.1E-04	Igsf3	2.071067886	1.7E-04	Wdr46	2.00344908	1.4E-05
Rbms1	-2.109372212	3.2E-06	Car12	2.070783758	2.2E-05	Nudc	2.002999738	2.3E-07
Lat	-2.108795786	4.6E-05	Slc25a1	2.070393089	5.5E-06	Nup43	2.002223346	1.9E-05
Igtp	-2.105267834	3.3E-04	Nup93	2.070383187	3.1E-05	Capsl	2.001995154	8.1E-04
Dclre1c	-2.102380971	1.6E-04	Cxcr5	2.070130709	6.5E-04			
Rorc	-2.100530051	2.0E-04	Fbxw8	2.068901777	2.3E-07			

A5 continued. Deregulated genes ($F_c \geq 2$, adjusted P value <0.005). For a given transcript positive F_c values indicate an increase and negative values indicate a decrease in expression in HD1^{L/L};HD2^{L/WT} samples compared to WT LMCs.

downregulated		
gene symbols	FC	adj.P.Val
Il17re	-2.099229688	6.9E-05
Whrn	-2.096066686	5.5E-05
5430411K18Rik	-2.091704352	4.0E-07
Rnf167	-2.090590189	8.7E-05
Cd27	-2.080333642	3.1E-07
Odf3b	-2.079572842	2.0E-03
Suv420h1	-2.079290956	1.9E-05
Acss1	-2.078766821	1.0E-07
Inpp5k	-2.077929997	4.6E-05
Zc3h12d	-2.076570863	2.5E-06
Nedd9	-2.075853336	2.1E-06
NA	-2.075621037	4.9E-08
Snrk	-2.07036693	1.4E-05
Inpp5k	-2.060354636	1.5E-05
Nsmaf	-2.059563254	1.1E-04
Tdrd5	-2.057565221	6.7E-04
Tnfai3	-2.0567007	1.6E-06
Irf6	-2.056221163	7.2E-08
Dusp11	-2.05447947	7.0E-06
Klf13	-2.054129358	1.9E-06
H2-T23	-2.05319177	5.3E-04
Znrf1	-2.048561277	4.9E-06
Tle6	-2.044198738	5.7E-04
Abcc5	-2.04340451	2.7E-05
Epc1	-2.042030933	3.9E-04
Mbnl2	-2.036328841	7.3E-06
Itk	-2.034561088	1.5E-06
Cd97	-2.031885378	2.0E-07
Synrg	-2.029825801	5.2E-06
Vps13c	-2.024459722	1.8E-05
Atp6v0a2	-2.02182477	2.2E-05
Plxdc1	-2.019902412	1.9E-04
Atl2	-2.019417273	9.5E-04
Tbxa2r	-2.018466922	1.2E-05
Zdhhc14	-2.015409478	7.9E-04
Fgf13	-2.014797683	1.4E-07
Slc25a45	-2.012470013	1.9E-06
Dntt	-2.007885275	1.9E-03
Fbxl12	-2.005109293	7.9E-04
Apobec1	-2.001661633	4.1E-06
Trpc4ap	-2.001592531	5.1E-07

B5. Genome-wide distribution of deregulated genes.

Chromosome	% deregulated	% array total	fold enrichment	EASE score (P value)
1	5.86	6.14	0.95	0.70
2	6.61	8.87	0.75	0.99
3	6.61	5.15	1.28	0.07
4	6.91	6.36	1.09	0.35
5	6.46	6.20	1.04	0.47
6	7.06	5.98	1.18	0.17
7	6.91	9.36	0.74	0.99
8	5.11	5.33	0.96	0.69
9	6.61	5.93	1.11	0.30
10	5.86	4.87	1.20	0.17
11	9.31	7.85	1.19	0.11
12	3.90	3.52	1.11	0.40
13	4.20	4.14	1.02	0.57
14	3.45	3.98	0.87	0.84
15	6.76	4.00	1.69	0.00
16	4.65	3.43	1.36	0.08
17	4.80	5.09	0.94	0.72
18	2.25	2.72	0.83	0.87
19	4.80	3.67	1.31	0.10

C5. Genome-wide distribution of upregulated genes.

Chromosome	% upregulated	% array total	fold enrichment	EASE score (P value)
1	5.64	6.14	0.76	0.92
2	5.64	8.87	1.00	0.64
3	5.64	5.15	0.44	1.09
4	7.35	6.36	0.29	1.16
5	5.15	6.20	0.89	0.83
6	5.39	5.98	0.79	0.90
7	7.60	9.36	0.93	0.81
8	5.88	5.33	0.42	1.10
9	6.86	5.93	0.30	1.16
10	6.62	4.87	0.10	1.36
11	10.05	7.85	0.08	1.28
12	4.90	3.52	0.13	1.39
13	5.15	4.14	0.25	1.24
14	3.43	3.98	0.83	0.86
15	10.05	4.00	0.00	2.51
16	5.15	3.43	0.07	1.50
17	4.66	5.09	0.76	0.92
18	1.96	2.72	0.93	0.72
19	4.66	3.67	0.24	1.27

D5. Genome-wide distribution of downregulated genes.

Chromosome	% downregulated	% array total	fold enrichment	EASE score (P value)
1	6.20	6.14	0.62	1.01
2	8.14	8.87	0.76	0.92
3	8.14	5.15	0.04	1.58
4	6.20	6.36	0.67	0.97
5	8.53	6.20	0.12	1.38
6	9.69	5.98	0.02	1.62
7	5.81	9.36	0.99	0.62
8	3.88	5.33	0.93	0.73
9	6.20	5.93	0.56	1.05
10	4.65	4.87	0.71	0.95
11	8.14	7.85	0.55	1.04
12	2.33	3.52	0.95	0.66
13	2.71	4.14	0.96	0.66
14	3.49	3.98	0.81	0.88
15	1.55	4.00	1.00	0.39
16	3.88	3.43	0.51	1.13
17	5.04	5.09	0.66	0.99
18	2.71	2.72	0.70	1.00
19	5.04	3.67	0.24	1.37

E5. Expression of *hdac2*, *mSin3a* and *mta-2* genes.

gene symbols	FC	adj.P.Val
MTA2	-1.194887599	7.9E-03
SIN3A	1.161269232	2.0E-01
SIN3A	1.326714594	1.3E-03
HDAC2	-1.237683323	2.1E-02
HDAC2	1.106876451	5.2E-02

References

Adkins, B., Mueller, C., Okada, C.Y., Reichert, R.A., Weissman, I.L. & Spangrude, G.J. 1987, "Early events in T-cell maturation", *Annual Review of Immunology*, vol. 5, pp. 325-365.

Adlam, M. & Siu, G. 2003, "Hierarchical interactions control CD4 gene expression during thymocyte development", *Immunity*, vol. 18, no. 2, pp. 173-184.

Allfrey, V.G., Faulkner, R. & Mirsky, A.E. 1964, "Acetylation and Methylation of Histones and their Possible Role in the Regulation of Rna Synthesis", *Proceedings of the National Academy of Sciences of the United States of America*, vol. 51, pp. 786-794.

Alvarez, J.D., Yasui, D.H., Niida, H., Joh, T., Loh, D.Y. & Kohwi-Shigematsu, T. 2000, "The MAR-binding protein SATB1 orchestrates temporal and spatial expression of multiple genes during T-cell development", *Genes & development*, vol. 14, no. 5, pp. 521-535.

Anderson, S.J., Levin, S.D. & Perlmutter, R.M. 1994, "Involvement of the protein tyrosine kinase p56lck in T cell signaling and thymocyte development", *Advances in Immunology*, vol. 56, pp. 151-178.

Andres, M.E., Burger, C., Peral-Rubio, M.J., Battaglioli, E., Anderson, M.E., Grimes, J., Dallman, J., Ballas, N. & Mandel, G. 1999, "CoREST: a functional corepressor required for regulation of neural-specific gene expression",

Proceedings of the National Academy of Sciences of the United States of America, vol. 96, no. 17, pp. 9873-9878.

Aronson, B.D., Fisher, A.L., Blechman, K., Caudy, M. & Gergen, J.P. 1997, "Groucho-dependent and -independent repression activities of Runt domain proteins", *Molecular and cellular biology*, vol. 17, no. 9, pp. 5581-5587.

August, A., Fischer, A., Hao, S., Mueller, C. & Ragin, M. 2002, "The Tec family of tyrosine kinases in T cells, amplifiers of T cell receptor signals", *The international journal of biochemistry & cell biology*, vol. 34, no. 10, pp. 1184-1189.

Avitahl, N., Winandy, S., Friedrich, C., Jones, B., Ge, Y. & Georgopoulos, K. 1999, "Ikaros sets thresholds for T cell activation and regulates chromosome propagation", *Immunity*, vol. 10, no. 3, pp. 333-343.

Azzam, H.S., Grinberg, A., Lui, K., Shen, H., Shores, E.W. & Love, P.E. 1998, "CD5 expression is developmentally regulated by T cell receptor (TCR) signals and TCR avidity", *The Journal of experimental medicine*, vol. 188, no. 12, pp. 2301-2311.

Badenhorst, P., Voas, M., Rebay, I. & Wu, C. 2002, "Biological functions of the ISWI chromatin remodeling complex NURF", *Genes & development*, vol. 16, no. 24, pp. 3186-3198.

Bain, G., Ray, W.J., Yao, M. & Gottlieb, D.I. 1996, "Retinoic acid promotes neural and represses mesodermal gene expression in mouse embryonic stem

cells in culture", *Biochemical and biophysical research communications*, vol. 223, no. 3, pp. 691-694.

Balasubramaniyan, V., Boddeke, E., Bakels, R., Kust, B., Kooistra, S., Veneman, A. & Copray, S. 2006, "Effects of histone deacetylation inhibition on neuronal differentiation of embryonic mouse neural stem cells", *Neuroscience*, vol. 143, no. 4, pp. 939-951.

Ballas, N., Battaglioli, E., Atouf, F., Andres, M.E., Chenoweth, J., Anderson, M.E., Burger, C., Moniwa, M., Davie, J.R., Bowers, W.J., Federoff, H.J., Rose, D.W., Rosenfeld, M.G., Brehm, P. & Mandel, G. 2001, "Regulation of neuronal traits by a novel transcriptional complex", *Neuron*, vol. 31, no. 3, pp. 353-365.

Barnden, M.J., Allison, J., Heath, W.R. & Carbone, F.R. 1998, "Defective TCR expression in transgenic mice constructed using cDNA-based alpha- and beta-chain genes under the control of heterologous regulatory elements", *Immunology and cell biology*, vol. 76, no. 1, pp. 34-40.

Barski, A., Cuddapah, S., Cui, K., Roh, T.Y., Schones, D.E., Wang, Z., Wei, G., Chepelev, I. & Zhao, K. 2007, "High-resolution profiling of histone methylations in the human genome", *Cell*, vol. 129, no. 4, pp. 823-837.

Beard, C., Hochedlinger, K., Plath, K., Wutz, A. & Jaenisch, R. 2006, "Efficient method to generate single-copy transgenic mice by site-specific integration in embryonic stem cells", *Genesis (New York, N.Y.: 2000)*, vol. 44, no. 1, pp. 23-28.

Bedford, M.T. & Clarke, S.G. 2009, "Protein arginine methylation in mammals: who, what, and why", *Molecular cell*, vol. 33, no. 1, pp. 1-13.

Bellard, M., Kuo, M.T., Dretzen, G. & Chambon, P. 1980, "Differential nuclease sensitivity of the ovalbumin and beta-globin chromatin regions in erythrocytes and oviduct cells of laying hen", *Nucleic acids research*, vol. 8, no. 12, pp. 2737-2750.

Berger, S.L. 2007, "The complex language of chromatin regulation during transcription", *Nature*, vol. 447, no. 7143, pp. 407-412.

Bernstein, B.E., Kamal, M., Lindblad-Toh, K., Bekiranov, S., Bailey, D.K., Huebert, D.J., McMahon, S., Karlsson, E.K., Kulbokas, E.J., 3rd, Gingeras, T.R., Schreiber, S.L. & Lander, E.S. 2005, "Genomic maps and comparative analysis of histone modifications in human and mouse", *Cell*, vol. 120, no. 2, pp. 169-181.

Bernstein, B.E., Meissner, A. & Lander, E.S. 2007, "The mammalian epigenome", *Cell*, vol. 128, no. 4, pp. 669-681.

Bernstein, B.E., Mikkelsen, T.S., Xie, X., Kamal, M., Huebert, D.J., Cuff, J., Fry, B., Meissner, A., Wernig, M., Plath, K., Jaenisch, R., Wagschal, A., Feil, R., Schreiber, S.L. & Lander, E.S. 2006, "A bivalent chromatin structure marks key developmental genes in embryonic stem cells", *Cell*, vol. 125, no. 2, pp. 315-326.

Bernstein, B.E., Tong, J.K. & Schreiber, S.L. 2000, "Genomewide studies of histone deacetylase function in yeast", *Proceedings of the National Academy of Sciences of the United States of America*, vol. 97, no. 25, pp. 13708-13713.

Bhaskara, S., Chyla, B.J., Amann, J.M., Knutson, S.K., Cortez, D., Sun, Z.W. & Hiebert, S.W. 2008, "Deletion of histone deacetylase 3 reveals critical roles in S phase progression and DNA damage control", *Molecular cell*, vol. 30, no. 1, pp. 61-72.

Bilic, I. & Ellmeier, W. 2007, "The role of BTB domain-containing zinc finger proteins in T cell development and function", *Immunology letters*, vol. 108, no. 1, pp. 1-9.

Bird, A. 2002, "DNA methylation patterns and epigenetic memory", *Genes & development*, vol. 16, no. 1, pp. 6-21.

Bird, A.P. 1986, "CpG-rich islands and the function of DNA methylation", *Nature*, vol. 321, no. 6067, pp. 209-213.

Birnboim, H.C. & Doly, J. 1979, "A rapid alkaline extraction procedure for screening recombinant plasmid DNA", *Nucleic acids research*, vol. 7, no. 6, pp. 1513-1523.

Boheler, K.R., Czyz, J., Tweedie, D., Yang, H.T., Anisimov, S.V. & Wobus, A.M. 2002, "Differentiation of pluripotent embryonic stem cells into cardiomyocytes", *Circulation research*, vol. 91, no. 3, pp. 189-201.

Bonner, W.M., Redon, C.E., Dickey, J.S., Nakamura, A.J., Sedelnikova, O.A., Solier, S. & Pommier, Y. 2008, "GammaH2AX and cancer", *Nature reviews.Cancer*, vol. 8, no. 12, pp. 957-967.

Borgulya, P., Kishi, H., Uematsu, Y. & von Boehmer, H. 1992, "Exclusion and inclusion of alpha and beta T cell receptor alleles", *Cell*, vol. 69, no. 3, pp. 529-537.

Boyes, J., Byfield, P., Nakatani, Y. & Ogryzko, V. 1998, "Regulation of activity of the transcription factor GATA-1 by acetylation", *Nature*, vol. 396, no. 6711, pp. 594-598.

Brehm, A., Miska, E.A., McCance, D.J., Reid, J.L., Bannister, A.J. & Kouzarides, T. 1998, "Retinoblastoma protein recruits histone deacetylase to repress transcription", *Nature*, vol. 391, no. 6667, pp. 597-601.

Brizzard, B.L., Chubet, R.G. & Vizard, D.L. 1994, "Immunoaffinity purification of FLAG epitope-tagged bacterial alkaline phosphatase using a novel monoclonal antibody and peptide elution", *BioTechniques*, vol. 16, no. 4, pp. 730-735.

Bruneau, B.G. 2002, "Transcriptional regulation of vertebrate cardiac morphogenesis", *Circulation research*, vol. 90, no. 5, pp. 509-519.

Brunmeir, R., Lagger, S. & Seiser, C. 2009, "Histone deacetylase HDAC1/HDAC2-controlled embryonic development and cell differentiation", *The International journal of developmental biology*, vol. 53, no. 2-3, pp. 275-289.

Buchholz, F., Angrand, P.O. & Stewart, A.F. 1998, "Improved properties of FLP recombinase evolved by cycling mutagenesis", *Nature biotechnology*, vol. 16, no. 7, pp. 657-662.

Ceballos, S.J. & Heyer, W.D. 2011, "Functions of the Snf2/Swi2 family Rad54 motor protein in homologous recombination", *Biochimica et biophysica acta*, vol. 1809, no. 9, pp. 509-523.

Chang, S., McKinsey, T.A., Zhang, C.L., Richardson, J.A., Hill, J.A. & Olson, E.N. 2004, "Histone deacetylases 5 and 9 govern responsiveness of the heart to a subset of stress signals and play redundant roles in heart development", *Molecular and cellular biology*, vol. 24, no. 19, pp. 8467-8476.

Chang, S., Young, B.D., Li, S., Qi, X., Richardson, J.A. & Olson, E.N. 2006, "Histone deacetylase 7 maintains vascular integrity by repressing matrix metalloproteinase 10", *Cell*, vol. 126, no. 2, pp. 321-334.

Chen, C.Y., Croissant, J., Majesky, M., Topouzis, S., McQuinn, T., Frankovsky, M.J. & Schwartz, R.J. 1996, "Activation of the cardiac alpha-actin promoter depends upon serum response factor, Tinman homologue, Nkx-2.5, and intact serum response elements", *Developmental genetics*, vol. 19, no. 2, pp. 119-130.

Chen, F., Kook, H., Milewski, R., Gitler, A.D., Lu, M.M., Li, J., Nazarian, R., Schnepf, R., Jen, K., Biben, C., Runke, G., Mackay, J.P., Novotny, J., Schwartz, R.J., Harvey, R.P., Mullins, M.C. & Epstein, J.A. 2002, "Hop is an unusual homeobox gene that modulates cardiac development", *Cell*, vol. 110, no. 6, pp. 713-723.

Chi, T.H., Wan, M., Zhao, K., Taniuchi, I., Chen, L., Littman, D.R. & Crabtree, G.R. 2002, "Reciprocal regulation of CD4/CD8 expression by SWI/SNF-like BAF complexes", *Nature*, vol. 418, no. 6894, pp. 195-199.

Chung, S., Andersson, T., Sonntag, K.C., Bjorklund, L., Isacson, O. & Kim, K.S. 2002, "Analysis of different promoter systems for efficient transgene expression in mouse embryonic stem cell lines", *Stem cells (Dayton, Ohio)*, vol. 20, no. 2, pp. 139-145.

Cowley, S.M., Iritani, B.M., Mendrysa, S.M., Xu, T., Cheng, P.F., Yada, J., Liggitt, H.D. & Eisenman, R.N. 2005, "The mSin3A chromatin-modifying complex is essential for embryogenesis and T-cell development", *Molecular and cellular biology*, vol. 25, no. 16, pp. 6990-7004.

Craig, J.M. 2005, "Heterochromatin--many flavours, common themes", *BioEssays : news and reviews in molecular, cellular and developmental biology*, vol. 27, no. 1, pp. 17-28.

Croft, M. 2009, "The role of TNF superfamily members in T-cell function and diseases", *Nature reviews.Immunology*, vol. 9, no. 4, pp. 271-285.

Das, C., Lucia, M.S., Hansen, K.C. & Tyler, J.K. 2009, "CBP/p300-mediated acetylation of histone H3 on lysine 56", *Nature*, vol. 459, no. 7243, pp. 113-117.

Dave, V.P., Allman, D., Keefe, R., Hardy, R.R. & Kappes, D.J. 1998, "HD mice: a novel mouse mutant with a specific defect in the generation of CD4(+) T cells", *Proceedings of the National Academy of Sciences of the United States of America*, vol. 95, no. 14, pp. 8187-8192.

de Bruijn, M.F. & Speck, N.A. 2004, "Core-binding factors in hematopoiesis and immune function", *Oncogene*, vol. 23, no. 24, pp. 4238-4248.

De Keersmaecker, K., Real, P.J., Gatta, G.D., Palomero, T., Sulis, M.L., Tosello, V., Van Vlierberghe, P., Barnes, K., Castillo, M., Sole, X., Hadler, M., Lenz, J., Aplan, P.D., Kelliher, M., Kee, B.L., Pandolfi, P.P., Kappes, D., Gounari, F., Petrie, H., Van der Meulen, J., Speleman, F., Paietta, E., Racevskis, J., Wiernik, P.H., Rowe, J.M., Soulier, J., Avran, D., Cave, H., Dastugue, N., Raimondi, S., Meijerink, J.P., Cordon-Cardo, C., Califano, A. & Ferrando, A.A. 2010, "The TLX1 oncogene drives aneuploidy in T cell transformation", *Nature medicine*, vol. 16, no. 11, pp. 1321-1327.

Desbaillets, I., Ziegler, U., Groscurth, P. & Gassmann, M. 2000, "Embryoid bodies: an in vitro model of mouse embryogenesis", *Experimental physiology*, vol. 85, no. 6, pp. 645-651.

Dillon, S.C., Zhang, X., Trievel, R.C. & Cheng, X. 2005, "The SET-domain protein superfamily: protein lysine methyltransferases", *Genome biology*, vol. 6, no. 8, pp. 227.

Du, Z., Song, J., Wang, Y., Zhao, Y., Guda, K., Yang, S., Kao, H.Y., Xu, Y., Willis, J., Markowitz, S.D., Sedwick, D., Ewing, R.M. & Wang, Z. 2010, "DNMT1 stability is regulated by proteins coordinating deubiquitination and acetylation-driven ubiquitination", *Science signaling*, vol. 3, no. 146, pp. ra80.

Duncan, E.M., Muratore-Schroeder, T.L., Cook, R.G., Garcia, B.A., Shabanowitz, J., Hunt, D.F. & Allis, C.D. 2008, "Cathepsin L proteolytically

processes histone H3 during mouse embryonic stem cell differentiation", *Cell*, vol. 135, no. 2, pp. 284-294.

Durst, K.L. & Hiebert, S.W. 2004, "Role of RUNX family members in transcriptional repression and gene silencing", *Oncogene*, vol. 23, no. 24, pp. 4220-4224.

Durst, K.L., Lutterbach, B., Kummalu, T., Friedman, A.D. & Hiebert, S.W. 2003, "The inv(16) fusion protein associates with corepressors via a smooth muscle myosin heavy-chain domain", *Molecular and cellular biology*, vol. 23, no. 2, pp. 607-619.

Dymecki, S.M. & Tomasiewicz, H. 1998, "Using Flp-recombinase to characterize expansion of Wnt1-expressing neural progenitors in the mouse", *Developmental biology*, vol. 201, no. 1, pp. 57-65.

Edmondson, D.G., Lyons, G.E., Martin, J.F. & Olson, E.N. 1994, "Mef2 gene expression marks the cardiac and skeletal muscle lineages during mouse embryogenesis", *Development (Cambridge, England)*, vol. 120, no. 5, pp. 1251-1263.

Egawa, T., Tillman, R.E., Naoe, Y., Taniuchi, I. & Littman, D.R. 2007, "The role of the Runx transcription factors in thymocyte differentiation and in homeostasis of naive T cells", *The Journal of experimental medicine*, vol. 204, no. 8, pp. 1945-1957.

Eissenberg, J.C., James, T.C., Foster-Hartnett, D.M., Hartnett, T., Ngan, V. & Elgin, S.C. 1990, "Mutation in a heterochromatin-specific chromosomal protein

is associated with suppression of position-effect variegation in *Drosophila melanogaster*", *Proceedings of the National Academy of Sciences of the United States of America*, vol. 87, no. 24, pp. 9923-9927.

Ekwall, K., Olsson, T., Turner, B.M., Cranston, G. & Allshire, R.C. 1997, "Transient inhibition of histone deacetylation alters the structural and functional imprint at fission yeast centromeres", *Cell*, vol. 91, no. 7, pp. 1021-1032.

ENCODE Project Consortium 2004, "The ENCODE (ENCyclopedia Of DNA Elements) Project", *Science (New York, N.Y.)*, vol. 306, no. 5696, pp. 636-640.

Farley, F.W., Soriano, P., Steffen, L.S. & Dymecki, S.M. 2000, "Widespread recombinase expression using FLPeR (flipper) mice", *Genesis (New York, N.Y.: 2000)*, vol. 28, no. 3-4, pp. 106-110.

Finch, J.T. & Klug, A. 1976, "Solenoidal model for superstructure in chromatin", *Proceedings of the National Academy of Sciences of the United States of America*, vol. 73, no. 6, pp. 1897-1901.

Finch, J.T., Lutter, L.C., Rhodes, D., Brown, R.S., Rushton, B., Levitt, M. & Klug, A. 1977, "Structure of nucleosome core particles of chromatin", *Nature*, vol. 269, no. 5623, pp. 29-36.

Fischle, W., Dequiedt, F., Fillion, M., Hendzel, M.J., Voelter, W. & Verdin, E. 2001, "Human HDAC7 histone deacetylase activity is associated with HDAC3 in vivo", *The Journal of biological chemistry*, vol. 276, no. 38, pp. 35826-35835.

Fischle, W., Dequiedt, F., Hendzel, M.J., Guenther, M.G., Lazar, M.A., Voelter, W. & Verdin, E. 2002, "Enzymatic activity associated with class II HDACs is

dependent on a multiprotein complex containing HDAC3 and SMRT/N-CoR", *Molecular cell*, vol. 9, no. 1, pp. 45-57.

Fu, G., Vallee, S., Rybakin, V., McGuire, M.V., Ampudia, J., Brockmeyer, C., Salek, M., Fallen, P.R., Hoerter, J.A., Munshi, A., Huang, Y.H., Hu, J., Fox, H.S., Sauer, K., Acuto, O. & Gascoigne, N.R. 2009, "Themis controls thymocyte selection through regulation of T cell antigen receptor-mediated signaling", *Nature immunology*, vol. 10, no. 8, pp. 848-856.

Fu, Y., Yan, W., Mohun, T.J. & Evans, S.M. 1998, "Vertebrate tinman homologues XNkx2-3 and XNkx2-5 are required for heart formation in a functionally redundant manner", *Development (Cambridge, England)*, vol. 125, no. 22, pp. 4439-4449.

Fujita, N., Watanabe, S., Ichimura, T., Tsuruzoe, S., Shinkai, Y., Tachibana, M., Chiba, T. & Nakao, M. 2003, "Methyl-CpG binding domain 1 (MBD1) interacts with the Suv39h1-HP1 heterochromatic complex for DNA methylation-based transcriptional repression", *The Journal of biological chemistry*, vol. 278, no. 26, pp. 24132-24138.

Fussner, E., Ching, R.W. & Bazett-Jones, D.P. 2011, "Living without 30nm chromatin fibers", *Trends in biochemical sciences*, vol. 36, no. 1, pp. 1-6.

Gaudet, F., Hodgson, J.G., Eden, A., Jackson-Grusby, L., Dausman, J., Gray, J.W., Leonhardt, H. & Jaenisch, R. 2003, "Induction of tumors in mice by genomic hypomethylation", *Science (New York, N.Y.)*, vol. 300, no. 5618, pp. 489-492.

Georgopoulos, K., Bigby, M., Wang, J.H., Molnar, A., Wu, P., Winandy, S. & Sharpe, A. 1994, "The Ikaros gene is required for the development of all lymphoid lineages", *Cell*, vol. 79, no. 1, pp. 143-156.

Germain, R.N. 2002, "T-cell development and the CD4-CD8 lineage decision", *Nature reviews.Immunology*, vol. 2, no. 5, pp. 309-322.

Gilbert, N., Boyle, S., Fiegler, H., Woodfine, K., Carter, N.P. & Bickmore, W.A. 2004, "Chromatin architecture of the human genome: gene-rich domains are enriched in open chromatin fibers", *Cell*, vol. 118, no. 5, pp. 555-566.

Glaser, K.B., Li, J., Staver, M.J., Wei, R.Q., Albert, D.H. & Davidsen, S.K. 2003, "Role of class I and class II histone deacetylases in carcinoma cells using siRNA", *Biochemical and biophysical research communications*, vol. 310, no. 2, pp. 529-536.

Godfrey, D.I., Kennedy, J., Suda, T. & Zlotnik, A. 1993, "A developmental pathway involving four phenotypically and functionally distinct subsets of CD3-CD4-CD8- triple-negative adult mouse thymocytes defined by CD44 and CD25 expression", *Journal of immunology (Baltimore, Md.: 1950)*, vol. 150, no. 10, pp. 4244-4252.

Goll, M.G. & Bestor, T.H. 2005, "Eukaryotic cytosine methyltransferases", *Annual Review of Biochemistry*, vol. 74, pp. 481-514.

Goto, T. & Monk, M. 1998, "Regulation of X-chromosome inactivation in development in mice and humans", *Microbiology and molecular biology reviews : MMBR*, vol. 62, no. 2, pp. 362-378.

Gregoretto, I.V., Lee, Y.M. & Goodson, H.V. 2004, "Molecular evolution of the histone deacetylase family: functional implications of phylogenetic analysis", *Journal of Molecular Biology*, vol. 338, no. 1, pp. 17-31.

Grewal, S.I., Bonaduce, M.J. & Klar, A.J. 1998, "Histone deacetylase homologs regulate epigenetic inheritance of transcriptional silencing and chromosome segregation in fission yeast", *Genetics*, vol. 150, no. 2, pp. 563-576.

Grewal, S.I. & Jia, S. 2007, "Heterochromatin revisited", *Nature reviews.Genetics*, vol. 8, no. 1, pp. 35-46.

Grow, M.W. & Krieg, P.A. 1998, "Tinman function is essential for vertebrate heart development: elimination of cardiac differentiation by dominant inhibitory mutants of the tinman-related genes, XNkx2-3 and XNkx2-5", *Developmental biology*, vol. 204, no. 1, pp. 187-196.

Growney, J.D., Shigematsu, H., Li, Z., Lee, B.H., Adelsperger, J., Rowan, R., Curley, D.P., Kutok, J.L., Akashi, K., Williams, I.R., Speck, N.A. & Gilliland, D.G. 2005, "Loss of Runx1 perturbs adult hematopoiesis and is associated with a myeloproliferative phenotype", *Blood*, vol. 106, no. 2, pp. 494-504.

Grozinger, C.M. & Schreiber, S.L. 2002, "Deacetylase enzymes: biological functions and the use of small-molecule inhibitors", *Chemistry & biology*, vol. 9, no. 1, pp. 3-16.

Gu, W. & Roeder, R.G. 1997, "Activation of p53 sequence-specific DNA binding by acetylation of the p53 C-terminal domain", *Cell*, vol. 90, no. 4, pp. 595-606.

Guan, J.S., Haggarty, S.J., Giacometti, E., Dannenberg, J.H., Joseph, N., Gao, J., Nieland, T.J., Zhou, Y., Wang, X., Mazitschek, R., Bradner, J.E., DePinho, R.A., Jaenisch, R. & Tsai, L.H. 2009, "HDAC2 negatively regulates memory formation and synaptic plasticity", *Nature*, vol. 459, no. 7243, pp. 55-60.

Haberland, M., Johnson, A., Mokalled, M.H., Montgomery, R.L. & Olson, E.N. 2009, "Genetic dissection of histone deacetylase requirement in tumor cells", *Proceedings of the National Academy of Sciences of the United States of America*, vol. 106, no. 19, pp. 7751-7755.

Haberland, M., Mokalled, M.H., Montgomery, R.L. & Olson, E.N. 2009, "Epigenetic control of skull morphogenesis by histone deacetylase 8", *Genes & development*, vol. 23, no. 14, pp. 1625-1630.

Haigis, M.C. & Guarente, L.P. 2006, "Mammalian sirtuins--emerging roles in physiology, aging, and calorie restriction", *Genes & development*, vol. 20, no. 21, pp. 2913-2921.

Hakimi, M.A., Bochar, D.A., Chenoweth, J., Lane, W.S., Mandel, G. & Shiekhattar, R. 2002, "A core-BRAF35 complex containing histone deacetylase mediates repression of neuronal-specific genes", *Proceedings of the National Academy of Sciences of the United States of America*, vol. 99, no. 11, pp. 7420-7425.

Han, D.W., Do, J.T., Arauzo-Bravo, M.J., Lee, S.H., Meissner, A., Lee, H.T., Jaenisch, R. & Scholer, H.R. 2009, "Epigenetic hierarchy governing Nestin expression", *Stem cells (Dayton, Ohio)*, vol. 27, no. 5, pp. 1088-1097.

Harker, N., Garefalaki, A., Menzel, U., Ktistaki, E., Naito, T., Georgopoulos, K. & Kioussis, D. 2011, "Pre-TCR signaling and CD8 gene bivalent chromatin resolution during thymocyte development", *Journal of immunology (Baltimore, Md.: 1950)*, vol. 186, no. 11, pp. 6368-6377.

Harker, N., Naito, T., Cortes, M., Hostert, A., Hirschberg, S., Tolaini, M., Roderick, K., Georgopoulos, K. & Kioussis, D. 2002, "The CD8alpha gene locus is regulated by the Ikaros family of proteins", *Molecular cell*, vol. 10, no. 6, pp. 1403-1415.

He, X., He, X., Dave, V.P., Zhang, Y., Hua, X., Nicolas, E., Xu, W., Roe, B.A. & Kappes, D.J. 2005, "The zinc finger transcription factor Th-POK regulates CD4 versus CD8 T-cell lineage commitment", *Nature*, vol. 433, no. 7028, pp. 826-833.

Hebert, J.M., Boyle, M. & Martin, G.R. 1991, "mRNA localization studies suggest that murine FGF-5 plays a role in gastrulation", *Development (Cambridge, England)*, vol. 112, no. 2, pp. 407-415.

Helbling Chadwick, L., Chadwick, B.P., Jaye, D.L. & Wade, P.A. 2009, "The Mi-2/NuRD complex associates with pericentromeric heterochromatin during S phase in rapidly proliferating lymphoid cells", *Chromosoma*, vol. 118, no. 4, pp. 445-457.

Hendriks, R.W., Nawijn, M.C., Engel, J.D., van Doorninck, H., Grosveld, F. & Karis, A. 1999, "Expression of the transcription factor GATA-3 is required for the development of the earliest T cell progenitors and correlates with stages of

cellular proliferation in the thymus", *European journal of immunology*, vol. 29, no. 6, pp. 1912-1918.

Hennet, T., Hagen, F.K., Tabak, L.A. & Marth, J.D. 1995, "T-cell-specific deletion of a polypeptide N-acetylgalactosaminyl-transferase gene by site-directed recombination", *Proceedings of the National Academy of Sciences of the United States of America*, vol. 92, no. 26, pp. 12070-12074.

Hernandez-Hoyos, G., Sohn, S.J., Rothenberg, E.V. & Alberola-Ila, J. 2000, "Lck activity controls CD4/CD8 T cell lineage commitment", *Immunity*, vol. 12, no. 3, pp. 313-322.

Herrmann, B.G. 1991, "Expression pattern of the Brachyury gene in whole-mount TWis/TWis mutant embryos", *Development (Cambridge, England)*, vol. 113, no. 3, pp. 913-917.

Hirota, T., Lipp, J.J., Toh, B.H. & Peters, J.M. 2005, "Histone H3 serine 10 phosphorylation by Aurora B causes HP1 dissociation from heterochromatin", *Nature*, vol. 438, no. 7071, pp. 1176-1180.

Hodges, E., Krishna, M.T., Pickard, C. & Smith, J.L. 2003, "Diagnostic role of tests for T cell receptor (TCR) genes", *Journal of clinical pathology*, vol. 56, no. 1, pp. 1-11.

Holliday, R. & Pugh, J.E. 1975, "DNA modification mechanisms and gene activity during development", *Science (New York, N.Y.)*, vol. 187, no. 4173, pp. 226-232.

Hong, S., Cho, Y.W., Yu, L.R., Yu, H., Veenstra, T.D. & Ge, K. 2007, "Identification of JmjC domain-containing UTX and JMJD3 as histone H3 lysine 27 demethylases", *Proceedings of the National Academy of Sciences of the United States of America*, vol. 104, no. 47, pp. 18439-18444.

Hooper, M., Hardy, K., Handyside, A., Hunter, S. & Monk, M. 1987, "HPRT-deficient (Lesch-Nyhan) mouse embryos derived from germline colonization by cultured cells", *Nature*, vol. 326, no. 6110, pp. 292-295.

Hsieh, J., Nakashima, K., Kuwabara, T., Mejia, E. & Gage, F.H. 2004, "Histone deacetylase inhibition-mediated neuronal differentiation of multipotent adult neural progenitor cells", *Proceedings of the National Academy of Sciences of the United States of America*, vol. 101, no. 47, pp. 16659-16664.

Hu, J., Qi, Q. & August, A. 2010, "Itk derived signals regulate the expression of Th-POK and controls the development of CD4 T cells", *PloS one*, vol. 5, no. 1, pp. e8891.

Huang da, W., Sherman, B.T. & Lempicki, R.A. 2009, "Bioinformatics enrichment tools: paths toward the comprehensive functional analysis of large gene lists", *Nucleic acids research*, vol. 37, no. 1, pp. 1-13.

Huang da, W., Sherman, B.T. & Lempicki, R.A. 2009, "Systematic and integrative analysis of large gene lists using DAVID bioinformatics resources", *Nature protocols*, vol. 4, no. 1, pp. 44-57.

Huang, Y., Fang, J., Bedford, M.T., Zhang, Y. & Xu, R.M. 2006, "Recognition of histone H3 lysine-4 methylation by the double tudor domain of JMJD2A", *Science (New York, N.Y.)*, vol. 312, no. 5774, pp. 748-751.

Hubbert, C., Guardiola, A., Shao, R., Kawaguchi, Y., Ito, A., Nixon, A., Yoshida, M., Wang, X.F. & Yao, T.P. 2002, "HDAC6 is a microtubule-associated deacetylase", *Nature*, vol. 417, no. 6887, pp. 455-458.

Humphrey, G.W., Wang, Y., Russanova, V.R., Hirai, T., Qin, J., Nakatani, Y. & Howard, B.H. 2001, "Stable histone deacetylase complexes distinguished by the presence of SANT domain proteins CoREST/kiaa0071 and Mta-L1", *The Journal of biological chemistry*, vol. 276, no. 9, pp. 6817-6824.

Ichikawa, M., Asai, T., Saito, T., Seo, S., Yamazaki, I., Yamagata, T., Mitani, K., Chiba, S., Ogawa, S., Kurokawa, M. & Hirai, H. 2004, "AML-1 is required for megakaryocytic maturation and lymphocytic differentiation, but not for maintenance of hematopoietic stem cells in adult hematopoiesis", *Nature medicine*, vol. 10, no. 3, pp. 299-304.

Inoue, A. & Fujimoto, D. 1969, "Enzymatic deacetylation of histone", *Biochemical and biophysical research communications*, vol. 36, no. 1, pp. 146-150.

Irie, H.Y., Mong, M.S., Itano, A., Crooks, M.E., Littman, D.R., Burakoff, S.J. & Robey, E. 1998, "The cytoplasmic domain of CD8 beta regulates Lck kinase activation and CD8 T cell development", *Journal of immunology (Baltimore, Md.: 1950)*, vol. 161, no. 1, pp. 183-191.

Ito, Y. 2008, "RUNX genes in development and cancer: regulation of viral gene expression and the discovery of RUNX family genes", *Advances in Cancer Research*, vol. 99, pp. 33-76.

Jacobs, S.A., Taverna, S.D., Zhang, Y., Briggs, S.D., Li, J., Eissenberg, J.C., Allis, C.D. & Khorasanizadeh, S. 2001, "Specificity of the HP1 chromo domain for the methylated N-terminus of histone H3", *The EMBO journal*, vol. 20, no. 18, pp. 5232-5241.

Janeway, C.A., Jr 1992, "The T cell receptor as a multicomponent signalling machine: CD4/CD8 coreceptors and CD45 in T cell activation", *Annual Review of Immunology*, vol. 10, pp. 645-674.

Jawerka, M., Colak, D., Dimou, L., Spiller, C., Lagger, S., Montgomery, R.L., Olson, E.N., Wurst, W., Gottlicher, M. & Gotz, M. 2010, "The specific role of histone deacetylase 2 in adult neurogenesis", *Neuron glia biology*, vol. 6, no. 2, pp. 93-107.

Jay, P.Y., Rozhitskaya, O., Tarnavski, O., Sherwood, M.C., Dorfman, A.L., Lu, Y., Ueyama, T. & Izumo, S. 2005, "Haploinsufficiency of the cardiac transcription factor Nkx2-5 variably affects the expression of putative target genes", *FASEB journal : official publication of the Federation of American Societies for Experimental Biology*, vol. 19, no. 11, pp. 1495-1497.

Jenuwein, T. & Allis, C.D. 2001, "Translating the histone code", *Science (New York, N.Y.)*, vol. 293, no. 5532, pp. 1074-1080.

Jepsen, K., Hermanson, O., Onami, T.M., Gleiberman, A.S., Lunyak, V., McEvilly, R.J., Kurokawa, R., Kumar, V., Liu, F., Seto, E., Hedrick, S.M., Mandel, G., Glass, C.K., Rose, D.W. & Rosenfeld, M.G. 2000, "Combinatorial roles of the nuclear receptor corepressor in transcription and development", *Cell*, vol. 102, no. 6, pp. 753-763.

Ji, Y., Resch, W., Corbett, E., Yamane, A., Casellas, R. & Schatz, D.G. 2010, "The in vivo pattern of binding of RAG1 and RAG2 to antigen receptor loci", *Cell*, vol. 141, no. 3, pp. 419-431.

Jin, C. & Felsenfeld, G. 2007, "Nucleosome stability mediated by histone variants H3.3 and H2A.Z", *Genes & development*, vol. 21, no. 12, pp. 1519-1529.

Johnson, C.A., White, D.A., Lavender, J.S., O'Neill, L.P. & Turner, B.M. 2002, "Human class I histone deacetylase complexes show enhanced catalytic activity in the presence of ATP and co-immunoprecipitate with the ATP-dependent chaperone protein Hsp70", *The Journal of biological chemistry*, vol. 277, no. 11, pp. 9590-9597.

Jorgensen, J.L., Reay, P.A., Ehrich, E.W. & Davis, M.M. 1992, "Molecular components of T-cell recognition", *Annual Review of Immunology*, vol. 10, pp. 835-873.

Kaji, K., Caballero, I.M., MacLeod, R., Nichols, J., Wilson, V.A. & Hendrich, B. 2006, "The NuRD component Mbd3 is required for pluripotency of embryonic stem cells", *Nature cell biology*, vol. 8, no. 3, pp. 285-292.

Kane, L.P., Lin, J. & Weiss, A. 2000, "Signal transduction by the TCR for antigen", *Current opinion in immunology*, vol. 12, no. 3, pp. 242-249.

Kasler, H.G., Young, B.D., Mottet, D., Lim, H.W., Collins, A.M., Olson, E.N. & Verdin, E. 2011, "Histone deacetylase 7 regulates cell survival and TCR signaling in CD4/CD8 double-positive thymocytes", *Journal of immunology (Baltimore, Md.: 1950)*, vol. 186, no. 8, pp. 4782-4793.

Kawabata, K., Sakurai, F., Yamaguchi, T., Hayakawa, T. & Mizuguchi, H. 2005, "Efficient gene transfer into mouse embryonic stem cells with adenovirus vectors", *Molecular therapy : the journal of the American Society of Gene Therapy*, vol. 12, no. 3, pp. 547-554.

Keefe, R., Dave, V., Allman, D., Wiest, D. & Kappes, D.J. 1999, "Regulation of lineage commitment distinct from positive selection", *Science (New York, N.Y.)*, vol. 286, no. 5442, pp. 1149-1153.

Keller, G.M. 1995, "In vitro differentiation of embryonic stem cells", *Current opinion in cell biology*, vol. 7, no. 6, pp. 862-869.

Kim, J., Sif, S., Jones, B., Jackson, A., Koipally, J., Heller, E., Winandy, S., Viel, A., Sawyer, A., Ikeda, T., Kingston, R. & Georgopoulos, K. 1999, "Ikaros DNA-binding proteins direct formation of chromatin remodeling complexes in lymphocytes", *Immunity*, vol. 10, no. 3, pp. 345-355.

Kioussis, D. & Ellmeier, W. 2002, "Chromatin and CD4, CD8A and CD8B gene expression during thymic differentiation", *Nature reviews.Immunology*, vol. 2, no. 12, pp. 909-919.

Klose, R.J., Yamane, K., Bae, Y., Zhang, D., Erdjument-Bromage, H., Tempst, P., Wong, J. & Zhang, Y. 2006, "The transcriptional repressor JHDM3A demethylates trimethyl histone H3 lysine 9 and lysine 36", *Nature*, vol. 442, no. 7100, pp. 312-316.

Knoepfler, P.S. & Eisenman, R.N. 1999, "Sin meets NuRD and other tails of repression", *Cell*, vol. 99, no. 5, pp. 447-450.

Kook, H. & Epstein, J.A. 2003, "Hopping to the beat. Hop regulation of cardiac gene expression", *Trends in cardiovascular medicine*, vol. 13, no. 7, pp. 261-264.

Kornberg, R.D. 1974, "Chromatin structure: a repeating unit of histones and DNA", *Science (New York, N.Y.)*, vol. 184, no. 4139, pp. 868-871.

Kouzarides, T. 2007, "Chromatin modifications and their function", *Cell*, vol. 128, no. 4, pp. 693-705.

Kouzarides, T. 2000, "Acetylation: a regulatory modification to rival phosphorylation?", *The EMBO journal*, vol. 19, no. 6, pp. 1176-1179.

Kruisbeek, A.M., Mond, J.J., Fowlkes, B.J., Carmen, J.A., Bridges, S. & Longo, D.L. 1985, "Absence of the Lyt-2-,L3T4+ lineage of T cells in mice treated neonatally with anti-I-A correlates with absence of intrathymic I-A-bearing antigen-presenting cell function", *The Journal of experimental medicine*, vol. 161, no. 5, pp. 1029-1047.

Kurdistani, S.K., Robyr, D., Tavazoie, S. & Grunstein, M. 2002, "Genome-wide binding map of the histone deacetylase Rpd3 in yeast", *Nature genetics*, vol. 31, no. 3, pp. 248-254.

Kurebayashi, S., Ueda, E., Sakaue, M., Patel, D.D., Medvedev, A., Zhang, F. & Jetten, A.M. 2000, "Retinoid-related orphan receptor gamma (RORgamma) is essential for lymphoid organogenesis and controls apoptosis during thymopoiesis", *Proceedings of the National Academy of Sciences of the United States of America*, vol. 97, no. 18, pp. 10132-10137.

Lachner, M., O'Carroll, D., Rea, S., Mechtler, K. & Jenuwein, T. 2001, "Methylation of histone H3 lysine 9 creates a binding site for HP1 proteins", *Nature*, vol. 410, no. 6824, pp. 116-120.

Lagger, G., O'Carroll, D., Rembold, M., Khier, H., Tischler, J., Weitzer, G., Schuettengruber, B., Hauser, C., Brunmeir, R., Jenuwein, T. & Seiser, C. 2002, "Essential function of histone deacetylase 1 in proliferation control and CDK inhibitor repression", *The EMBO journal*, vol. 21, no. 11, pp. 2672-2681.

Laherty, C.D., Yang, W.M., Sun, J.M., Davie, J.R., Seto, E. & Eisenman, R.N. 1997, "Histone deacetylases associated with the mSin3 corepressor mediate mad transcriptional repression", *Cell*, vol. 89, no. 3, pp. 349-356.

Lakso, M., Pichel, J.G., Gorman, J.R., Sauer, B., Okamoto, Y., Lee, E., Alt, F.W. & Westphal, H. 1996, "Efficient in vivo manipulation of mouse genomic sequences at the zygote stage", *Proceedings of the National Academy of Sciences of the United States of America*, vol. 93, no. 12, pp. 5860-5865.

Landry, J.W., Banerjee, S., Taylor, B., Aplan, P.D., Singer, A. & Wu, C. 2011, "Chromatin remodeling complex NURF regulates thymocyte maturation", *Genes & development*, vol. 25, no. 3, pp. 275-286.

LeBoeuf, M., Terrell, A., Trivedi, S., Sinha, S., Epstein, J.A., Olson, E.N., Morrisey, E.E. & Millar, S.E. 2010, "Hdac1 and Hdac2 act redundantly to control p63 and p53 functions in epidermal progenitor cells", *Developmental cell*, vol. 19, no. 6, pp. 807-818.

Ledbetter, J.A. & Seaman, W.E. 1982, "The Lyt-2, Lyt-3 macromolecules: structural and functional studies", *Immunological reviews*, vol. 68, pp. 197-218.

Ledbetter, J.A., Seaman, W.E., Tsu, T.T. & Herzenberg, L.A. 1981, "Lyt-2 and lyt-3 antigens are on two different polypeptide subunits linked by disulfide bonds. Relationship of subunits to T cell cytolytic activity", *The Journal of experimental medicine*, vol. 153, no. 6, pp. 1503-1516.

Lee, J.H., Hart, S.R. & Skalnik, D.G. 2004, "Histone deacetylase activity is required for embryonic stem cell differentiation", *Genesis (New York, N.Y.: 2000)*, vol. 38, no. 1, pp. 32-38.

Lee, J.H., Tate, C.M., You, J.S. & Skalnik, D.G. 2007, "Identification and characterization of the human Set1B histone H3-Lys4 methyltransferase complex", *The Journal of biological chemistry*, vol. 282, no. 18, pp. 13419-13428.

Lee, J.W., Blanco, L., Zhou, T., Garcia-Diaz, M., Bebenek, K., Kunkel, T.A., Wang, Z. & Povirk, L.F. 2004, "Implication of DNA polymerase lambda in

alignment-based gap filling for nonhomologous DNA end joining in human nuclear extracts", *The Journal of biological chemistry*, vol. 279, no. 1, pp. 805-811.

Lee, K.K. & Workman, J.L. 2007, "Histone acetyltransferase complexes: one size doesn't fit all", *Nature reviews.Molecular cell biology*, vol. 8, no. 4, pp. 284-295.

Lee, M.G., Wynder, C., Bochar, D.A., Hakimi, M.A., Cooch, N. & Shiekhattar, R. 2006, "Functional interplay between histone demethylase and deacetylase enzymes", *Molecular and cellular biology*, vol. 26, no. 17, pp. 6395-6402.

Lee, P.P., Fitzpatrick, D.R., Beard, C., Jessup, H.K., Lehar, S., Makar, K.W., Perez-Melgosa, M., Sweetser, M.T., Schlissel, M.S., Nguyen, S., Cherry, S.R., Tsai, J.H., Tucker, S.M., Weaver, W.M., Kelso, A., Jaenisch, R. & Wilson, C.B. 2001, "A critical role for Dnmt1 and DNA methylation in T cell development, function, and survival", *Immunity*, vol. 15, no. 5, pp. 763-774.

Leeb, M. & Wutz, A. 2007, "Ring1B is crucial for the regulation of developmental control genes and PRC1 proteins but not X inactivation in embryonic cells", *The Journal of cell biology*, vol. 178, no. 2, pp. 219-229.

Lemercier, C., Verdel, A., Galloo, B., Curtet, S., Brocard, M.P. & Khochbin, S. 2000, "mHDA1/HDAC5 histone deacetylase interacts with and represses MEF2A transcriptional activity", *The Journal of biological chemistry*, vol. 275, no. 20, pp. 15594-15599.

Lengauer, C., Kinzler, K.W. & Vogelstein, B. 1998, "Genetic instabilities in human cancers", *Nature*, vol. 396, no. 6712, pp. 643-649.

Lesourne, R., Uehara, S., Lee, J., Song, K.D., Li, L., Pinkhasov, J., Zhang, Y., Weng, N.P., Wildt, K.F., Wang, L., Bosselut, R. & Love, P.E. 2009, "Themis, a T cell-specific protein important for late thymocyte development", *Nature immunology*, vol. 10, no. 8, pp. 840-847.

Levanon, D., Goldstein, R.E., Bernstein, Y., Tang, H., Goldenberg, D., Stifani, S., Paroush, Z. & Groner, Y. 1998, "Transcriptional repression by AML1 and LEF-1 is mediated by the TLE/Groucho corepressors", *Proceedings of the National Academy of Sciences of the United States of America*, vol. 95, no. 20, pp. 11590-11595.

Li, B., Pattenden, S.G., Lee, D., Gutierrez, J., Chen, J., Seidel, C., Gerton, J. & Workman, J.L. 2005, "Preferential occupancy of histone variant H2AZ at inactive promoters influences local histone modifications and chromatin remodeling", *Proceedings of the National Academy of Sciences of the United States of America*, vol. 102, no. 51, pp. 18385-18390.

Li, J., Wang, J., Wang, J., Nawaz, Z., Liu, J.M., Qin, J. & Wong, J. 2000, "Both corepressor proteins SMRT and N-CoR exist in large protein complexes containing HDAC3", *The EMBO journal*, vol. 19, no. 16, pp. 4342-4350.

Liang, J., Wan, M., Zhang, Y., Gu, P., Xin, H., Jung, S.Y., Qin, J., Wong, J., Cooney, A.J., Liu, D. & Songyang, Z. 2008, "Nanog and Oct4 associate with unique transcriptional repression complexes in embryonic stem cells", *Nature cell biology*, vol. 10, no. 6, pp. 731-739.

Lin, Q., Schwarz, J., Bucana, C. & Olson, E.N. 1997, "Control of mouse cardiac morphogenesis and myogenesis by transcription factor MEF2C", *Science (New York, N.Y.)*, vol. 276, no. 5317, pp. 1404-1407.

Littau, V.C., Allfrey, V.G., Frenster, J.H. & Mirsky, A.E. 1964, "Active and Inactive Regions of Nuclear Chromatin as Revealed by Electron Microscope Autoradiography", *Proceedings of the National Academy of Sciences of the United States of America*, vol. 52, pp. 93-100.

Liu, P., Jenkins, N.A. & Copeland, N.G. 2003, "A highly efficient recombineering-based method for generating conditional knockout mutations", *Genome research*, vol. 13, no. 3, pp. 476-484.

Liu, Z., Li, T., Liu, Y., Jia, Z., Li, Y., Zhang, C., Chen, P., Ma, K., Affara, N. & Zhou, C. 2009, "WNT signaling promotes Nkx2.5 expression and early cardiomyogenesis via downregulation of Hdac1", *Biochimica et biophysica acta*, vol. 1793, no. 2, pp. 300-311.

Loonstra, A., Vooijs, M., Beverloo, H.B., Allak, B.A., van Drunen, E., Kanaar, R., Berns, A. & Jonkers, J. 2001, "Growth inhibition and DNA damage induced by Cre recombinase in mammalian cells", *Proceedings of the National Academy of Sciences of the United States of America*, vol. 98, no. 16, pp. 9209-9214.

Lu, J., McKinsey, T.A., Zhang, C.L. & Olson, E.N. 2000, "Regulation of skeletal myogenesis by association of the MEF2 transcription factor with class II histone deacetylases", *Molecular cell*, vol. 6, no. 2, pp. 233-244.

Lu, X., Kovalev, G.I., Chang, H., Kallin, E., Knudsen, G., Xia, L., Mishra, N., Ruiz, P., Li, E., Su, L. & Zhang, Y. 2008, "Inactivation of NuRD component Mta2 causes abnormal T cell activation and lupus-like autoimmune disease in mice", *The Journal of biological chemistry*, vol. 283, no. 20, pp. 13825-13833.

Lucas, J.A., Atherly, L.O. & Berg, L.J. 2002, "The absence of Itk inhibits positive selection without changing lineage commitment", *Journal of immunology (Baltimore, Md.: 1950)*, vol. 168, no. 12, pp. 6142-6151.

Luco, R.F., Pan, Q., Tominaga, K., Blencowe, B.J., Pereira-Smith, O.M. & Misteli, T. 2010, "Regulation of alternative splicing by histone modifications", *Science (New York, N.Y.)*, vol. 327, no. 5968, pp. 996-1000.

Luger, K., Mader, A.W., Richmond, R.K., Sargent, D.F. & Richmond, T.J. 1997, "Crystal structure of the nucleosome core particle at 2.8 Å resolution", *Nature*, vol. 389, no. 6648, pp. 251-260.

Luger, K., Rechsteiner, T.J., Flaus, A.J., Waye, M.M. & Richmond, T.J. 1997, "Characterization of nucleosome core particles containing histone proteins made in bacteria", *Journal of Molecular Biology*, vol. 272, no. 3, pp. 301-311.

Luger, K. & Richmond, T.J. 1998, "The histone tails of the nucleosome", *Current opinion in genetics & development*, vol. 8, no. 2, pp. 140-146.

Luke, J.J., Van De Wetering, C.I. & Knudson, C.M. 2003, "Lymphoma development in Bax transgenic mice is inhibited by Bcl-2 and associated with chromosomal instability", *Cell death and differentiation*, vol. 10, no. 6, pp. 740-748.

Luo, R.X., Postigo, A.A. & Dean, D.C. 1998, "Rb interacts with histone deacetylase to repress transcription", *Cell*, vol. 92, no. 4, pp. 463-473.

Lutterbach, B., Westendorf, J.J., Linggi, B., Isaac, S., Seto, E. & Hiebert, S.W. 2000, "A mechanism of repression by acute myeloid leukemia-1, the target of multiple chromosomal translocations in acute leukemia", *The Journal of biological chemistry*, vol. 275, no. 1, pp. 651-656.

Magnaghi-Jaulin, L., Groisman, R., Naguibneva, I., Robin, P., Lorain, S., Le Villain, J.P., Troalen, F., Trouche, D. & Harel-Bellan, A. 1998, "Retinoblastoma protein represses transcription by recruiting a histone deacetylase", *Nature*, vol. 391, no. 6667, pp. 601-605.

Malecki, M.J., Sanchez-Irizarry, C., Mitchell, J.L., Histen, G., Xu, M.L., Aster, J.C. & Blacklow, S.C. 2006, "Leukemia-associated mutations within the NOTCH1 heterodimerization domain fall into at least two distinct mechanistic classes", *Molecular and cellular biology*, vol. 26, no. 12, pp. 4642-4651.

Mann, B.S., Johnson, J.R., Cohen, M.H., Justice, R. & Pazdur, R. 2007, "FDA approval summary: vorinostat for treatment of advanced primary cutaneous T-cell lymphoma", *The oncologist*, vol. 12, no. 10, pp. 1247-1252.

Margueron, R. & Reinberg, D. 2011, "The Polycomb complex PRC2 and its mark in life", *Nature*, vol. 469, no. 7330, pp. 343-349.

Marinkovic, D., Marinkovic, T., Mahr, B., Hess, J. & Wirth, T. 2004, "Reversible lymphomagenesis in conditionally c-MYC expressing mice", *International journal of cancer. Journal international du cancer*, vol. 110, no. 3, pp. 336-342.

Marsden, M.P. & Laemmli, U.K. 1979, "Metaphase chromosome structure: evidence for a radial loop model", *Cell*, vol. 17, no. 4, pp. 849-858.

Martin, C. & Zhang, Y. 2005, "The diverse functions of histone lysine methylation", *Nature reviews.Molecular cell biology*, vol. 6, no. 11, pp. 838-849.

Medina, K.L., Garrett, K.P., Thompson, L.F., Rossi, M.I., Payne, K.J. & Kincade, P.W. 2001, "Identification of very early lymphoid precursors in bone marrow and their regulation by estrogen", *Nature immunology*, vol. 2, no. 8, pp. 718-724.

Merkenschlager, M., Graf, D., Lovatt, M., Bommhardt, U., Zamoyska, R. & Fisher, A.G. 1997, "How many thymocytes audition for selection?", *The Journal of experimental medicine*, vol. 186, no. 7, pp. 1149-1158.

Metivier, R., Penot, G., Hubner, M.R., Reid, G., Brand, H., Kos, M. & Gannon, F. 2003, "Estrogen receptor-alpha directs ordered, cyclical, and combinatorial recruitment of cofactors on a natural target promoter", *Cell*, vol. 115, no. 6, pp. 751-763.

Miller, K.M., Tjeertes, J.V., Coates, J., Legube, G., Polo, S.E., Britton, S. & Jackson, S.P. 2010, "Human HDAC1 and HDAC2 function in the DNA-damage response to promote DNA nonhomologous end-joining", *Nature structural & molecular biology*, vol. 17, no. 9, pp. 1144-1151.

Miller, T., Krogan, N.J., Dover, J., Erdjument-Bromage, H., Tempst, P., Johnston, M., Greenblatt, J.F. & Shilatifard, A. 2001, "COMPASS: a complex of proteins associated with a trithorax-related SET domain protein", *Proceedings*

of the National Academy of Sciences of the United States of America, vol. 98, no. 23, pp. 12902-12907.

Mizuguchi, G., Tsukiyama, T., Wisniewski, J. & Wu, C. 1997, "Role of nucleosome remodeling factor NURF in transcriptional activation of chromatin", *Molecular cell*, vol. 1, no. 1, pp. 141-150.

Mombaerts, P., Iacomini, J., Johnson, R.S., Herrup, K., Tonegawa, S. & Papaioannou, V.E. 1992, "RAG-1-deficient mice have no mature B and T lymphocytes", *Cell*, vol. 68, no. 5, pp. 869-877.

Montgomery, R.L., Davis, C.A., Potthoff, M.J., Haberland, M., Fielitz, J., Qi, X., Hill, J.A., Richardson, J.A. & Olson, E.N. 2007, "Histone deacetylases 1 and 2 redundantly regulate cardiac morphogenesis, growth, and contractility", *Genes & development*, vol. 21, no. 14, pp. 1790-1802.

Montgomery, R.L., Hsieh, J., Barbosa, A.C., Richardson, J.A. & Olson, E.N. 2009, "Histone deacetylases 1 and 2 control the progression of neural precursors to neurons during brain development", *Proceedings of the National Academy of Sciences of the United States of America*, vol. 106, no. 19, pp. 7876-7881.

Montgomery, R.L., Potthoff, M.J., Haberland, M., Qi, X., Matsuzaki, S., Humphries, K.M., Richardson, J.A., Bassel-Duby, R. & Olson, E.N. 2008, "Maintenance of cardiac energy metabolism by histone deacetylase 3 in mice", *The Journal of clinical investigation*, vol. 118, no. 11, pp. 3588-3597.

Morin, S., Charron, F., Robitaille, L. & Nemer, M. 2000, "GATA-dependent recruitment of MEF2 proteins to target promoters", *The EMBO journal*, vol. 19, no. 9, pp. 2046-2055.

Munsie, M.J., Michalska, A.E., O'Brien, C.M., Trounson, A.O., Pera, M.F. & Mountford, P.S. 2000, "Isolation of pluripotent embryonic stem cells from reprogrammed adult mouse somatic cell nuclei", *Current biology : CB*, vol. 10, no. 16, pp. 989-992.

Murry, C.E. & Keller, G. 2008, "Differentiation of embryonic stem cells to clinically relevant populations: lessons from embryonic development", *Cell*, vol. 132, no. 4, pp. 661-680.

Muto, M., Chen, Y., Kubo, E. & Mita, K. 1996, "Analysis of early initiating event(s) in radiation-induced thymic lymphomagenesis", *Japanese journal of cancer research : Gann*, vol. 87, no. 3, pp. 247-257.

Mutskov, V. & Felsenfeld, G. 2004, "Silencing of transgene transcription precedes methylation of promoter DNA and histone H3 lysine 9", *The EMBO journal*, vol. 23, no. 1, pp. 138-149.

Naito, T., Gomez-Del Arco, P., Williams, C.J. & Georgopoulos, K. 2007, "Antagonistic interactions between Ikaros and the chromatin remodeler Mi-2beta determine silencer activity and Cd4 gene expression", *Immunity*, vol. 27, no. 5, pp. 723-734.

Nakayama, K., Nakayama, K., Negishi, I., Kuida, K., Louie, M.C., Kanagawa, O., Nakauchi, H. & Loh, D.Y. 1994, "Requirement for CD8 beta chain in positive

selection of CD8-lineage T cells", *Science (New York, N.Y.)*, vol. 263, no. 5150, pp. 1131-1133.

Naoe, Y., Setoguchi, R., Akiyama, K., Muroi, S., Kuroda, M., Hatam, F., Littman, D.R. & Taniuchi, I. 2007, "Repression of interleukin-4 in T helper type 1 cells by Runx/Cbf beta binding to the Il4 silencer", *The Journal of experimental medicine*, vol. 204, no. 8, pp. 1749-1755.

Naruse, Y., Aoki, T., Kojima, T. & Mori, N. 1999, "Neural restrictive silencer factor recruits mSin3 and histone deacetylase complex to repress neuron-specific target genes", *Proceedings of the National Academy of Sciences of the United States of America*, vol. 96, no. 24, pp. 13691-13696.

Negishi, I., Motoyama, N., Nakayama, K., Nakayama, K., Senju, S., Hatakeyama, S., Zhang, Q., Chan, A.C. & Loh, D.Y. 1995, "Essential role for ZAP-70 in both positive and negative selection of thymocytes", *Nature*, vol. 376, no. 6539, pp. 435-438.

Nielsen, A.L., Oulad-Abdelghani, M., Ortiz, J.A., Remboutsika, E., Chambon, P. & Losson, R. 2001, "Heterochromatin formation in mammalian cells: interaction between histones and HP1 proteins", *Molecular cell*, vol. 7, no. 4, pp. 729-739.

Nielsen, T.K., Hildmann, C., Dickmanns, A., Schwienhorst, A. & Ficner, R. 2005, "Crystal structure of a bacterial class 2 histone deacetylase homologue", *Journal of Molecular Biology*, vol. 354, no. 1, pp. 107-120.

Nishimura, M., Fukushima-Nakase, Y., Fujita, Y., Nakao, M., Toda, S., Kitamura, N., Abe, T. & Okuda, T. 2004, "VWRPY motif-dependent and -

independent roles of AML1/Runx1 transcription factor in murine hematopoietic development", *Blood*, vol. 103, no. 2, pp. 562-570.

Niu, Z., Yu, W., Zhang, S.X., Barron, M., Belaguli, N.S., Schneider, M.D., Parmacek, M., Nordheim, A. & Schwartz, R.J. 2005, "Conditional mutagenesis of the murine serum response factor gene blocks cardiogenesis and the transcription of downstream gene targets", *The Journal of biological chemistry*, vol. 280, no. 37, pp. 32531-32538.

Niwa, H., Burdon, T., Chambers, I. & Smith, A. 1998, "Self-renewal of pluripotent embryonic stem cells is mediated via activation of STAT3", *Genes & development*, vol. 12, no. 13, pp. 2048-2060.

Nowicki, M.O., Falinski, R., Koptyra, M., Slupianek, A., Stoklosa, T., Gloc, E., Nieborowska-Skorska, M., Blasiak, J. & Skorski, T. 2004, "BCR/ABL oncogenic kinase promotes unfaithful repair of the reactive oxygen species-dependent DNA double-strand breaks", *Blood*, vol. 104, no. 12, pp. 3746-3753.

Okada, Y., Shimazaki, T., Sobue, G. & Okano, H. 2004, "Retinoic-acid-concentration-dependent acquisition of neural cell identity during in vitro differentiation of mouse embryonic stem cells", *Developmental biology*, vol. 275, no. 1, pp. 124-142.

O'Keefe, R.T., Henderson, S.C. & Spector, D.L. 1992, "Dynamic organization of DNA replication in mammalian cell nuclei: spatially and temporally defined replication of chromosome-specific alpha-satellite DNA sequences", *The Journal of cell biology*, vol. 116, no. 5, pp. 1095-1110.

Oki, M., Aihara, H. & Ito, T. 2007, "Role of histone phosphorylation in chromatin dynamics and its implications in diseases", *Sub-cellular biochemistry*, vol. 41, pp. 319-336.

Okuda, T., van Deursen, J., Hiebert, S.W., Grosveld, G. & Downing, J.R. 1996, "AML1, the target of multiple chromosomal translocations in human leukemia, is essential for normal fetal liver hematopoiesis", *Cell*, vol. 84, no. 2, pp. 321-330.

Olins, A.L. & Olins, D.E. 1974, "Spheroid chromatin units (v bodies)", *Science (New York, N.Y.)*, vol. 183, no. 4122, pp. 330-332.

Parthun, M.R. 2007, "Hat1: the emerging cellular roles of a type B histone acetyltransferase", *Oncogene*, vol. 26, no. 37, pp. 5319-5328.

Peng, J.C. & Karpen, G.H. 2008, "Epigenetic regulation of heterochromatic DNA stability", *Current opinion in genetics & development*, vol. 18, no. 2, pp. 204-211.

Perissi, V., Jepsen, K., Glass, C.K. & Rosenfeld, M.G. 2010, "Deconstructing repression: evolving models of co-repressor action", *Nature reviews.Genetics*, vol. 11, no. 2, pp. 109-123.

Peters, A.H., O'Carroll, D., Scherthan, H., Mechtler, K., Sauer, S., Schofer, C., Weipoltshammer, K., Pagani, M., Lachner, M., Kohlmaier, A., Opravil, S., Doyle, M., Sibilia, M. & Jenuwein, T. 2001, "Loss of the Suv39h histone methyltransferases impairs mammalian heterochromatin and genome stability", *Cell*, vol. 107, no. 3, pp. 323-337.

Pflum, M.K., Tong, J.K., Lane, W.S. & Schreiber, S.L. 2001, "Histone deacetylase 1 phosphorylation promotes enzymatic activity and complex formation", *The Journal of biological chemistry*, vol. 276, no. 50, pp. 47733-47741.

Pikaart, M.J., Recillas-Targa, F. & Felsenfeld, G. 1998, "Loss of transcriptional activity of a transgene is accompanied by DNA methylation and histone deacetylation and is prevented by insulators", *Genes & development*, vol. 12, no. 18, pp. 2852-2862.

Potthoff, M.J., Wu, H., Arnold, M.A., Shelton, J.M., Backs, J., McAnally, J., Richardson, J.A., Bassel-Duby, R. & Olson, E.N. 2007, "Histone deacetylase degradation and MEF2 activation promote the formation of slow-twitch myofibers", *The Journal of clinical investigation*, vol. 117, no. 9, pp. 2459-2467.

Pradhan, S., Bacolla, A., Wells, R.D. & Roberts, R.J. 1999, "Recombinant human DNA (cytosine-5) methyltransferase. I. Expression, purification, and comparison of de novo and maintenance methylation", *The Journal of biological chemistry*, vol. 274, no. 46, pp. 33002-33010.

Price, P.J. & Gregory, E.A. 1982, "Relationship between in vitro growth promotion and biophysical and biochemical properties of the serum supplement", *In vitro*, vol. 18, no. 6, pp. 576-584.

Purbey, P.K., Singh, S., Notani, D., Kumar, P.P., Limaye, A.S. & Galande, S. 2009, "Acetylation-dependent interaction of SATB1 and CtBP1 mediates transcriptional repression by SATB1", *Molecular and cellular biology*, vol. 29, no. 5, pp. 1321-1337.

Ray-Gallet, D. & Almouzni, G. 2010, "Nucleosome dynamics and histone variants", *Essays in biochemistry*, vol. 48, no. 1, pp. 75-87.

Reid, G., Metivier, R., Lin, C.Y., Denger, S., Ibberson, D., Ivacevic, T., Brand, H., Benes, V., Liu, E.T. & Gannon, F. 2005, "Multiple mechanisms induce transcriptional silencing of a subset of genes, including oestrogen receptor alpha, in response to deacetylase inhibition by valproic acid and trichostatin A", *Oncogene*, vol. 24, no. 31, pp. 4894-4907.

Robey, E. & Fowlkes, B.J. 1994, "Selective events in T cell development", *Annual Review of Immunology*, vol. 12, pp. 675-705.

Rowbotham, S.P., Barki, L., Neves-Costa, A., Santos, F., Dean, W., Hawkes, N., Choudhary, P., Will, W.R., Webster, J., Oxley, D., Green, C.M., Varga-Weisz, P. & Mermoud, J.E. 2011, "Maintenance of silent chromatin through replication requires SWI/SNF-like chromatin remodeler SMARCD1", *Molecular cell*, vol. 42, no. 3, pp. 285-296.

Rundlett, S.E., Carmen, A.A., Kobayashi, R., Bavykin, S., Turner, B.M. & Grunstein, M. 1996, "HDA1 and RPD3 are members of distinct yeast histone deacetylase complexes that regulate silencing and transcription", *Proceedings of the National Academy of Sciences of the United States of America*, vol. 93, no. 25, pp. 14503-14508.

Saha, A., Wittmeyer, J. & Cairns, B.R. 2006, "Chromatin remodelling: the industrial revolution of DNA around histones", *Nature reviews.Molecular cell biology*, vol. 7, no. 6, pp. 437-447.

Sakaguchi, S., Hombauer, M., Bilic, I., Naoe, Y., Schebesta, A., Taniuchi, I. & Ellmeier, W. 2010, "The zinc-finger protein MAZR is part of the transcription factor network that controls the CD4 versus CD8 lineage fate of double-positive thymocytes", *Nature immunology*, vol. 11, no. 5, pp. 442-448.

Santos-Rosa, H., Kirmizis, A., Nelson, C., Bartke, T., Saksouk, N., Cote, J. & Kouzarides, T. 2009, "Histone H3 tail clipping regulates gene expression", *Nature structural & molecular biology*, vol. 16, no. 1, pp. 17-22.

Sato, T., Ohno, S., Hayashi, T., Sato, C., Kohu, K., Satake, M. & Habu, S. 2005, "Dual functions of Runx proteins for reactivating CD8 and silencing CD4 at the commitment process into CD8 thymocytes", *Immunity*, vol. 22, no. 3, pp. 317-328.

Sawada, S. & Littman, D.R. 1991, "Identification and characterization of a T-cell-specific enhancer adjacent to the murine CD4 gene", *Molecular and cellular biology*, vol. 11, no. 11, pp. 5506-5515.

Schaeffer, E.M., Debnath, J., Yap, G., McVicar, D., Liao, X.C., Littman, D.R., Sher, A., Varmus, H.E., Lenardo, M.J. & Schwartzberg, P.L. 1999, "Requirement for Tec kinases Rlk and Itk in T cell receptor signaling and immunity", *Science (New York, N.Y.)*, vol. 284, no. 5414, pp. 638-641.

Schlesinger, J., Schueler, M., Grunert, M., Fischer, J.J., Zhang, Q., Krueger, T., Lange, M., Tonjes, M., Dunkel, I. & Sperling, S.R. 2011, "The cardiac transcription network modulated by Gata4, Mef2a, Nkx2.5, Srf, histone modifications, and microRNAs", *PLoS genetics*, vol. 7, no. 2, pp. e1001313.

Schmidt, E.E., Taylor, D.S., Prigge, J.R., Barnett, S. & Capecchi, M.R. 2000, "Illegitimate Cre-dependent chromosome rearrangements in transgenic mouse spermatids", *Proceedings of the National Academy of Sciences of the United States of America*, vol. 97, no. 25, pp. 13702-13707.

Scholzen, T. & Gerdes, J. 2000, "The Ki-67 protein: from the known and the unknown", *Journal of cellular physiology*, vol. 182, no. 3, pp. 311-322.

Senese, S., Zaragoza, K., Minardi, S., Muradore, I., Ronzoni, S., Passafaro, A., Bernard, L., Draetta, G.F., Alcalay, M., Seiser, C. & Chiocca, S. 2007, "Role for histone deacetylase 1 in human tumor cell proliferation", *Molecular and cellular biology*, vol. 27, no. 13, pp. 4784-4795.

Setoguchi, R., Tachibana, M., Naoe, Y., Muroi, S., Akiyama, K., Tezuka, C., Okuda, T. & Taniuchi, I. 2008, "Repression of the transcription factor Th-POK by Runx complexes in cytotoxic T cell development", *Science (New York, N.Y.)*, vol. 319, no. 5864, pp. 822-825.

Shapiro, M.J. & Shapiro, V.S. 2011, "Transcriptional repressors, corepressors and chromatin modifying enzymes in T cell development", *Cytokine*, vol. 53, no. 3, pp. 271-281.

Sharp, L.L. & Hedrick, S.M. 1999, "Commitment to the CD4 lineage mediated by extracellular signal-related kinase mitogen-activated protein kinase and Ick signaling", *Journal of immunology (Baltimore, Md.: 1950)*, vol. 163, no. 12, pp. 6598-6605.

Shechter, D., Dormann, H.L., Allis, C.D. & Hake, S.B. 2007, "Extraction, purification and analysis of histones", *Nature protocols*, vol. 2, no. 6, pp. 1445-1457.

Shi, X., Hong, T., Walter, K.L., Ewalt, M., Michishita, E., Hung, T., Carney, D., Pena, P., Lan, F., Kaadige, M.R., Lacoste, N., Cayrou, C., Davrazou, F., Saha, A., Cairns, B.R., Ayer, D.E., Kutateladze, T.G., Shi, Y., Cote, J., Chua, K.F. & Gozani, O. 2006, "ING2 PHD domain links histone H3 lysine 4 methylation to active gene repression", *Nature*, vol. 442, no. 7098, pp. 96-99.

Shilatifard, A. 2006, "Chromatin modifications by methylation and ubiquitination: implications in the regulation of gene expression", *Annual Review of Biochemistry*, vol. 75, pp. 243-269.

Shin, C.H., Liu, Z.P., Passier, R., Zhang, C.L., Wang, D.Z., Harris, T.M., Yamagishi, H., Richardson, J.A., Childs, G. & Olson, E.N. 2002, "Modulation of cardiac growth and development by HOP, an unusual homeodomain protein", *Cell*, vol. 110, no. 6, pp. 725-735.

Shinkai, Y., Koyasu, S., Nakayama, K., Murphy, K.M., Loh, D.Y., Reinherz, E.L. & Alt, F.W. 1993, "Restoration of T cell development in RAG-2-deficient mice by functional TCR transgenes", *Science (New York, N.Y.)*, vol. 259, no. 5096, pp. 822-825.

Siebzehnrubl, F.A., Buslei, R., Eyupoglu, I.Y., Seufert, S., Hahnen, E. & Blumcke, I. 2007, "Histone deacetylase inhibitors increase neuronal differentiation in adult forebrain precursor cells", *Experimental brain*

research. *Experimentelle Hirnforschung. Experimentation cerebrale*, vol. 176, no. 4, pp. 672-678.

Simpson, R.T. 1978, "Structure of chromatin containing extensively acetylated H3 and H4", *Cell*, vol. 13, no. 4, pp. 691-699.

Singer, A., Adoro, S. & Park, J.H. 2008, "Lineage fate and intense debate: myths, models and mechanisms of CD4- versus CD8-lineage choice", *Nature reviews. Immunology*, vol. 8, no. 10, pp. 788-801.

Siu, G., Wurster, A.L., Duncan, D.D., Soliman, T.M. & Hedrick, S.M. 1994, "A transcriptional silencer controls the developmental expression of the CD4 gene", *The EMBO journal*, vol. 13, no. 15, pp. 3570-3579.

Skorski, T. 2007, "Genomic instability: The cause and effect of BCR/ABL tyrosine kinase", *Current hematologic malignancy reports*, vol. 2, no. 2, pp. 69-74.

Smith, A.G. 2001, "Embryo-derived stem cells: of mice and men", *Annual Review of Cell and Developmental Biology*, vol. 17, pp. 435-462.

Sparrow, D.B., Miska, E.A., Langley, E., Reynaud-Deonauth, S., Kotecha, S., Towers, N., Spohr, G., Kouzarides, T. & Mohun, T.J. 1999, "MEF-2 function is modified by a novel co-repressor, MITR", *The EMBO journal*, vol. 18, no. 18, pp. 5085-5098.

Sridharan, R. & Smale, S.T. 2007, "Predominant interaction of both Ikaros and Helios with the NuRD complex in immature thymocytes", *The Journal of biological chemistry*, vol. 282, no. 41, pp. 30227-30238.

Srivastava, D. & Olson, E.N. 2000, "A genetic blueprint for cardiac development", *Nature*, vol. 407, no. 6801, pp. 221-226.

Starr, T.K., Jameson, S.C. & Hogquist, K.A. 2003, "Positive and negative selection of T cells", *Annual Review of Immunology*, vol. 21, pp. 139-176.

Sterner, D.E. & Berger, S.L. 2000, "Acetylation of histones and transcription-related factors", *Microbiology and molecular biology reviews : MMBR*, vol. 64, no. 2, pp. 435-459.

Stewart, M.D., Li, J. & Wong, J. 2005, "Relationship between histone H3 lysine 9 methylation, transcription repression, and heterochromatin protein 1 recruitment", *Molecular and cellular biology*, vol. 25, no. 7, pp. 2525-2538.

Strahl, B.D. & Allis, C.D. 2000, "The language of covalent histone modifications", *Nature*, vol. 403, no. 6765, pp. 41-45.

Strubing, C., Ahnert-Hilger, G., Shan, J., Wiedenmann, B., Hescheler, J. & Wobus, A.M. 1995, "Differentiation of pluripotent embryonic stem cells into the neuronal lineage in vitro gives rise to mature inhibitory and excitatory neurons", *Mechanisms of development*, vol. 53, no. 2, pp. 275-287.

Stucki, M. & Jackson, S.P. 2006, "gammaH2AX and MDC1: anchoring the DNA-damage-response machinery to broken chromosomes", *DNA repair*, vol. 5, no. 5, pp. 534-543.

Surh, C.D. & Sprent, J. 1994, "T-cell apoptosis detected in situ during positive and negative selection in the thymus", *Nature*, vol. 372, no. 6501, pp. 100-103.

Swain, S.L. 1983, "T cell subsets and the recognition of MHC class", *Immunological reviews*, vol. 74, pp. 129-142.

Taniuchi, I., Ellmeier, W. & Littman, D.R. 2004, "The CD4/CD8 lineage choice: new insights into epigenetic regulation during T cell development", *Advances in Immunology*, vol. 83, pp. 55-89.

Taniuchi, I., Osato, M., Egawa, T., Sunshine, M.J., Bae, S.C., Komori, T., Ito, Y. & Littman, D.R. 2002, "Differential requirements for Runx proteins in CD4 repression and epigenetic silencing during T lymphocyte development", *Cell*, vol. 111, no. 5, pp. 621-633.

Taniuchi, I., Sunshine, M.J., Festenstein, R. & Littman, D.R. 2002, "Evidence for distinct CD4 silencer functions at different stages of thymocyte differentiation", *Molecular cell*, vol. 10, no. 5, pp. 1083-1096.

Taplick, J., Kurtev, V., Kroboth, K., Posch, M., Lechner, T. & Seiser, C. 2001, "Homo-oligomerisation and nuclear localisation of mouse histone deacetylase 1", *Journal of Molecular Biology*, vol. 308, no. 1, pp. 27-38.

Taunton, J., Hassig, C.A. & Schreiber, S.L. 1996, "A mammalian histone deacetylase related to the yeast transcriptional regulator Rpd3p", *Science (New York, N.Y.)*, vol. 272, no. 5260, pp. 408-411.

Tell, G., Quadrioglio, F., Tiribelli, C. & Kelley, M.R. 2009, "The many functions of APE1/Ref-1: not only a DNA repair enzyme", *Antioxidants & redox signaling*, vol. 11, no. 3, pp. 601-620.

ten Berge, D., Koole, W., Fuerer, C., Fish, M., Eroglu, E. & Nusse, R. 2008, "Wnt signaling mediates self-organization and axis formation in embryoid bodies", *Cell stem cell*, vol. 3, no. 5, pp. 508-518.

Thoma, F., Koller, T. & Klug, A. 1979, "Involvement of histone H1 in the organization of the nucleosome and of the salt-dependent superstructures of chromatin", *The Journal of cell biology*, vol. 83, no. 2 Pt 1, pp. 403-427.

Thomas, J.O. & Kornberg, R.D. 1975, "An octamer of histones in chromatin and free in solution", *Proceedings of the National Academy of Sciences of the United States of America*, vol. 72, no. 7, pp. 2626-2630.

Tjeertes, J.V., Miller, K.M. & Jackson, S.P. 2009, "Screen for DNA-damage-responsive histone modifications identifies H3K9Ac and H3K56Ac in human cells", *The EMBO journal*, vol. 28, no. 13, pp. 1878-1889.

Trivedi, C.M., Luo, Y., Yin, Z., Zhang, M., Zhu, W., Wang, T., Floss, T., Goettlicher, M., Noppinger, P.R., Wurst, W., Ferrari, V.A., Abrams, C.S., Gruber, P.J. & Epstein, J.A. 2007, "Hdac2 regulates the cardiac hypertrophic response by modulating Gsk3 beta activity", *Nature medicine*, vol. 13, no. 3, pp. 324-331.

Tsukiyama, T. & Wu, C. 1995, "Purification and properties of an ATP-dependent nucleosome remodeling factor", *Cell*, vol. 83, no. 6, pp. 1011-1020.

Turner, B.M. 2005, "Reading signals on the nucleosome with a new nomenclature for modified histones", *Nature structural & molecular biology*, vol. 12, no. 2, pp. 110-112.

Turner, B.M. 1991, "Histone acetylation and control of gene expression", *Journal of cell science*, vol. 99 (Pt 1), no. Pt 1, pp. 13-20.

Urban, J.A. & Winandy, S. 2004, "Ikaros null mice display defects in T cell selection and CD4 versus CD8 lineage decisions", *Journal of immunology (Baltimore, Md.: 1950)*, vol. 173, no. 7, pp. 4470-4478.

Valamehr, B., Jonas, S.J., Polleux, J., Qiao, R., Guo, S., Gschwend, E.H., Stiles, B., Kam, K., Luo, T.J., Witte, O.N., Liu, X., Dunn, B. & Wu, H. 2008, "Hydrophobic surfaces for enhanced differentiation of embryonic stem cell-derived embryoid bodies", *Proceedings of the National Academy of Sciences of the United States of America*, vol. 105, no. 38, pp. 14459-14464.

Van den Wyngaert, I., de Vries, W., Kremer, A., Neefs, J., Verhasselt, P., Luyten, W.H. & Kass, S.U. 2000, "Cloning and characterization of human histone deacetylase 8", *FEBS letters*, vol. 478, no. 1-2, pp. 77-83.

van Hamburg, J.P., de Bruijn, M.J., Dingjan, G.M., Beverloo, H.B., Diepstraten, H., Ling, K.W. & Hendriks, R.W. 2008, "Cooperation of Gata3, c-Myc and Notch in malignant transformation of double positive thymocytes", *Molecular immunology*, vol. 45, no. 11, pp. 3085-3095.

van Oers, N.S., von Boehmer, H. & Weiss, A. 1995, "The pre-T cell receptor (TCR) complex is functionally coupled to the TCR-zeta subunit", *The Journal of experimental medicine*, vol. 182, no. 5, pp. 1585-1590.

Vannini, A., Volpari, C., Filocamo, G., Casavola, E.C., Brunetti, M., Renzoni, D., Chakravarty, P., Paolini, C., De Francesco, R., Gallinari, P., Steinkuhler, C. & Di

Marco, S. 2004, "Crystal structure of a eukaryotic zinc-dependent histone deacetylase, human HDAC8, complexed with a hydroxamic acid inhibitor", *Proceedings of the National Academy of Sciences of the United States of America*, vol. 101, no. 42, pp. 15064-15069.

Vega, R.B., Matsuda, K., Oh, J., Barbosa, A.C., Yang, X., Meadows, E., McAnally, J., Pomajzl, C., Shelton, J.M., Richardson, J.A., Karsenty, G. & Olson, E.N. 2004, "Histone deacetylase 4 controls chondrocyte hypertrophy during skeletogenesis", *Cell*, vol. 119, no. 4, pp. 555-566.

Vermeulen, M., Eberl, H.C., Matarese, F., Marks, H., Denissov, S., Butter, F., Lee, K.K., Olsen, J.V., Hyman, A.A., Stunnenberg, H.G. & Mann, M. 2010, "Quantitative interaction proteomics and genome-wide profiling of epigenetic histone marks and their readers", *Cell*, vol. 142, no. 6, pp. 967-980.

Vidal, M. & Gaber, R.F. 1991, "RPD3 encodes a second factor required to achieve maximum positive and negative transcriptional states in *Saccharomyces cerevisiae*", *Molecular and cellular biology*, vol. 11, no. 12, pp. 6317-6327.

Vidali, G., Boffa, L.C., Bradbury, E.M. & Allfrey, V.G. 1978, "Butyrate suppression of histone deacetylation leads to accumulation of multiacetylated forms of histones H3 and H4 and increased DNase I sensitivity of the associated DNA sequences", *Proceedings of the National Academy of Sciences of the United States of America*, vol. 75, no. 5, pp. 2239-2243.

von Boehmer, H. & Fehling, H.J. 1997, "Structure and function of the pre-T cell receptor", *Annual Review of Immunology*, vol. 15, pp. 433-452.

von Boehmer, H., Teh, H.S. & Kisielow, P. 1989, "The thymus selects the useful, neglects the useless and destroys the harmful", *Immunology today*, vol. 10, no. 2, pp. 57-61.

Vooijs, M., Jonkers, J. & Berns, A. 2001, "A highly efficient ligand-regulated Cre recombinase mouse line shows that LoxP recombination is position dependent", *EMBO reports*, vol. 2, no. 4, pp. 292-297.

Voss, A.K. & Thomas, T. 2009, "MYST family histone acetyltransferases take center stage in stem cells and development", *BioEssays : news and reviews in molecular, cellular and developmental biology*, vol. 31, no. 10, pp. 1050-1061.

Wang, J.H., Nichogiannopoulou, A., Wu, L., Sun, L., Sharpe, A.H., Bigby, M. & Georgopoulos, K. 1996, "Selective defects in the development of the fetal and adult lymphoid system in mice with an Ikaros null mutation", *Immunity*, vol. 5, no. 6, pp. 537-549.

Wang, L., Wildt, K.F., Zhu, J., Zhang, X., Feigenbaum, L., Tessarollo, L., Paul, W.E., Fowlkes, B.J. & Bosselut, R. 2008, "Distinct functions for the transcription factors GATA-3 and ThPOK during intrathymic differentiation of CD4(+) T cells", *Nature immunology*, vol. 9, no. 10, pp. 1122-1130.

Wang, L., Xiong, Y. & Bosselut, R. 2010, "Tenuous paths in unexplored territory: From T cell receptor signaling to effector gene expression during thymocyte selection", *Seminars in immunology*, vol. 22, no. 5, pp. 294-302.

Wang, Q., Stacy, T., Binder, M., Marin-Padilla, M., Sharpe, A.H. & Speck, N.A. 1996, "Disruption of the Cbfa2 gene causes necrosis and hemorrhaging in the

central nervous system and blocks definitive hematopoiesis", *Proceedings of the National Academy of Sciences of the United States of America*, vol. 93, no. 8, pp. 3444-3449.

Wang, Q., Stacy, T., Miller, J.D., Lewis, A.F., Gu, T.L., Huang, X., Bushweller, J.H., Bories, J.C., Alt, F.W., Ryan, G., Liu, P.P., Wynshaw-Boris, A., Binder, M., Marin-Padilla, M., Sharpe, A.H. & Speck, N.A. 1996, "The CBFbeta subunit is essential for CBFalpha2 (AML1) function in vivo", *Cell*, vol. 87, no. 4, pp. 697-708.

Wang, Z., Zang, C., Cui, K., Schones, D.E., Barski, A., Peng, W. & Zhao, K. 2009, "Genome-wide mapping of HATs and HDACs reveals distinct functions in active and inactive genes", *Cell*, vol. 138, no. 5, pp. 1019-1031.

Wang, Z., Zang, C., Rosenfeld, J.A., Schones, D.E., Barski, A., Cuddapah, S., Cui, K., Roh, T.Y., Peng, W., Zhang, M.Q. & Zhao, K. 2008, "Combinatorial patterns of histone acetylations and methylations in the human genome", *Nature genetics*, vol. 40, no. 7, pp. 897-903.

Ward, C.M. & Stern, P.L. 2002, "The human cytomegalovirus immediate-early promoter is transcriptionally active in undifferentiated mouse embryonic stem cells", *Stem cells (Dayton, Ohio)*, vol. 20, no. 5, pp. 472-475.

Weber, M., Davies, J.J., Wittig, D., Oakeley, E.J., Haase, M., Lam, W.L. & Schubeler, D. 2005, "Chromosome-wide and promoter-specific analyses identify sites of differential DNA methylation in normal and transformed human cells", *Nature genetics*, vol. 37, no. 8, pp. 853-862.

Wei, Y., Yu, L., Bowen, J., Gorovsky, M.A. & Allis, C.D. 1999, "Phosphorylation of histone H3 is required for proper chromosome condensation and segregation", *Cell*, vol. 97, no. 1, pp. 99-109.

Weidtkamp-Peters, S., Rahn, H.P., Cardoso, M.C. & Hemmerich, P. 2006, "Replication of centromeric heterochromatin in mouse fibroblasts takes place in early, middle, and late S phase", *Histochemistry and cell biology*, vol. 125, no. 1-2, pp. 91-102.

Weintraub, H. & Groudine, M. 1976, "Chromosomal subunits in active genes have an altered conformation", *Science (New York, N.Y.)*, vol. 193, no. 4256, pp. 848-856.

Weiss, A. & Littman, D.R. 1994, "Signal transduction by lymphocyte antigen receptors", *Cell*, vol. 76, no. 2, pp. 263-274.

Weng, A.P., Ferrando, A.A., Lee, W., Morris, J.P., 4th, Silverman, L.B., Sanchez-Irizarry, C., Blacklow, S.C., Look, A.T. & Aster, J.C. 2004, "Activating mutations of NOTCH1 in human T cell acute lymphoblastic leukemia", *Science (New York, N.Y.)*, vol. 306, no. 5694, pp. 269-271.

Weng, A.P., Millholland, J.M., Yashiro-Ohtani, Y., Arcangeli, M.L., Lau, A., Wai, C., Del Bianco, C., Rodriguez, C.G., Sai, H., Tobias, J., Li, Y., Wolfe, M.S., Shachaf, C., Felsher, D., Blacklow, S.C., Pear, W.S. & Aster, J.C. 2006, "c-Myc is an important direct target of Notch1 in T-cell acute lymphoblastic leukemia/lymphoma", *Genes & development*, vol. 20, no. 15, pp. 2096-2109.

Wheeler, J.C., Shigesada, K., Gergen, J.P. & Ito, Y. 2000, "Mechanisms of transcriptional regulation by Runt domain proteins", *Seminars in cell & developmental biology*, vol. 11, no. 5, pp. 369-375.

Whetstone, J.R., Nottke, A., Lan, F., Huarte, M., Smolikov, S., Chen, Z., Spooner, E., Li, E., Zhang, G., Colaiacovo, M. & Shi, Y. 2006, "Reversal of histone lysine trimethylation by the JMJD2 family of histone demethylases", *Cell*, vol. 125, no. 3, pp. 467-481.

Whitehurst, C.E., Chattopadhyay, S. & Chen, J. 1999, "Control of V(D)J recombinational accessibility of the D beta 1 gene segment at the TCR beta locus by a germline promoter", *Immunity*, vol. 10, no. 3, pp. 313-322.

Williams, C.J., Naito, T., Arco, P.G., Seavitt, J.R., Cashman, S.M., De Souza, B., Qi, X., Keables, P., Von Andrian, U.H. & Georgopoulos, K. 2004, "The chromatin remodeler Mi-2beta is required for CD4 expression and T cell development", *Immunity*, vol. 20, no. 6, pp. 719-733.

Wilson, P.A. & Hemmati-Brivanlou, A. 1995, "Induction of epidermis and inhibition of neural fate by Bmp-4", *Nature*, vol. 376, no. 6538, pp. 331-333.

Wilting, R.H., Yanover, E., Heideman, M.R., Jacobs, H., Horner, J., van der Torre, J., DePinho, R.A. & Dannenberg, J.H. 2010, "Overlapping functions of Hdac1 and Hdac2 in cell cycle regulation and haematopoiesis", *The EMBO journal*, vol. 29, no. 15, pp. 2586-2597.

Winandy, S., Wu, P. & Georgopoulos, K. 1995, "A dominant mutation in the Ikaros gene leads to rapid development of leukemia and lymphoma", *Cell*, vol. 83, no. 2, pp. 289-299.

Wirschubsky, Z., Tschlis, P., Klein, G. & Sumegi, J. 1986, "Rearrangement of c-myc, pim-1 and Mlvi-1 and trisomy of chromosome 15 in MCF- and Moloney-MuLV-induced murine T-cell leukemias", *International journal of cancer. Journal international du cancer*, vol. 38, no. 5, pp. 739-745.

Wysocka, J., Swigut, T., Milne, T.A., Dou, Y., Zhang, X., Burlingame, A.L., Roeder, R.G., Brivanlou, A.H. & Allis, C.D. 2005, "WDR5 associates with histone H3 methylated at K4 and is essential for H3 K4 methylation and vertebrate development", *Cell*, vol. 121, no. 6, pp. 859-872.

Wysocka, J., Swigut, T., Xiao, H., Milne, T.A., Kwon, S.Y., Landry, J., Kauer, M., Tackett, A.J., Chait, B.T., Badenhorst, P., Wu, C. & Allis, C.D. 2006, "A PHD finger of NURF couples histone H3 lysine 4 trimethylation with chromatin remodelling", *Nature*, vol. 442, no. 7098, pp. 86-90.

Xie, W., Song, C., Young, N.L., Sperling, A.S., Xu, F., Sridharan, R., Conway, A.E., Garcia, B.A., Plath, K., Clark, A.T. & Grunstein, M. 2009, "Histone h3 lysine 56 acetylation is linked to the core transcriptional network in human embryonic stem cells", *Molecular cell*, vol. 33, no. 4, pp. 417-427.

Xu, L., Glass, C.K. & Rosenfeld, M.G. 1999, "Coactivator and corepressor complexes in nuclear receptor function", *Current opinion in genetics & development*, vol. 9, no. 2, pp. 140-147.

Yamaguchi, T., Cubizolles, F., Zhang, Y., Reichert, N., Kohler, H., Seiser, C. & Matthias, P. 2010, "Histone deacetylases 1 and 2 act in concert to promote the G1-to-S progression", *Genes & development*, vol. 24, no. 5, pp. 455-469.

Yamashita, I., Nagata, T., Tada, T. & Nakayama, T. 1993, "CD69 cell surface expression identifies developing thymocytes which audition for T cell antigen receptor-mediated positive selection", *International immunology*, vol. 5, no. 9, pp. 1139-1150.

Yan, Q., Huang, J., Fan, T., Zhu, H. & Muegge, K. 2003, "Lsh, a modulator of CpG methylation, is crucial for normal histone methylation", *The EMBO journal*, vol. 22, no. 19, pp. 5154-5162.

Yang, W.M., Inouye, C., Zeng, Y., Bearss, D. & Seto, E. 1996, "Transcriptional repression by YY1 is mediated by interaction with a mammalian homolog of the yeast global regulator RPD3", *Proceedings of the National Academy of Sciences of the United States of America*, vol. 93, no. 23, pp. 12845-12850.

Yang, X.J. & Seto, E. 2008, "The Rpd3/Hda1 family of lysine deacetylases: from bacteria and yeast to mice and men", *Nature reviews.Molecular cell biology*, vol. 9, no. 3, pp. 206-218.

Ye, F., Chen, Y., Hoang, T., Montgomery, R.L., Zhao, X.H., Bu, H., Hu, T., Taketo, M.M., van Es, J.H., Clevers, H., Hsieh, J., Bassel-Duby, R., Olson, E.N. & Lu, Q.R. 2009, "HDAC1 and HDAC2 regulate oligodendrocyte differentiation by disrupting the beta-catenin-TCF interaction", *Nature neuroscience*, vol. 12, no. 7, pp. 829-838.

Ying, Q.L., Nichols, J., Chambers, I. & Smith, A. 2003, "BMP induction of Id proteins suppresses differentiation and sustains embryonic stem cell self-renewal in collaboration with STAT3", *Cell*, vol. 115, no. 3, pp. 281-292.

Ying, Q.L., Stavridis, M., Griffiths, D., Li, M. & Smith, A. 2003, "Conversion of embryonic stem cells into neuroectodermal precursors in adherent monoculture", *Nature biotechnology*, vol. 21, no. 2, pp. 183-186.

Yoshida, M., Kijima, M., Akita, M. & Beppu, T. 1990, "Potent and specific inhibition of mammalian histone deacetylase both in vivo and in vitro by trichostatin A", *The Journal of biological chemistry*, vol. 265, no. 28, pp. 17174-17179.

You, A., Tong, J.K., Grozinger, C.M. & Schreiber, S.L. 2001, "CoREST is an integral component of the CoREST- human histone deacetylase complex", *Proceedings of the National Academy of Sciences of the United States of America*, vol. 98, no. 4, pp. 1454-1458.

Zeller, K.I., Jegga, A.G., Aronow, B.J., O'Donnell, K.A. & Dang, C.V. 2003, "An integrated database of genes responsive to the Myc oncogenic transcription factor: identification of direct genomic targets", *Genome biology*, vol. 4, no. 10, pp. R69.

Zhang, C.L., McKinsey, T.A., Chang, S., Antos, C.L., Hill, J.A. & Olson, E.N. 2002, "Class II histone deacetylases act as signal-responsive repressors of cardiac hypertrophy", *Cell*, vol. 110, no. 4, pp. 479-488.

Zhang, W., Sloan-Lancaster, J., Kitchen, J., Tribble, R.P. & Samelson, L.E. 1998, "LAT: the ZAP-70 tyrosine kinase substrate that links T cell receptor to cellular activation", *Cell*, vol. 92, no. 1, pp. 83-92.

Zhang, X., Yuan, Z., Zhang, Y., Yong, S., Salas-Burgos, A., Koomen, J., Olashaw, N., Parsons, J.T., Yang, X.J., Dent, S.R., Yao, T.P., Lane, W.S. & Seto, E. 2007, "HDAC6 modulates cell motility by altering the acetylation level of cortactin", *Molecular cell*, vol. 27, no. 2, pp. 197-213.

Zhang, Y., Kwon, S., Yamaguchi, T., Cubizolles, F., Rousseaux, S., Kneissel, M., Cao, C., Li, N., Cheng, H.L., Chua, K., Lombard, D., Mizeracki, A., Matthias, G., Alt, F.W., Khochbin, S. & Matthias, P. 2008, "Mice lacking histone deacetylase 6 have hyperacetylated tubulin but are viable and develop normally", *Molecular and cellular biology*, vol. 28, no. 5, pp. 1688-1701.

Zhang, Y., LeRoy, G., Seelig, H.P., Lane, W.S. & Reinberg, D. 1998, "The dermatomyositis-specific autoantigen Mi2 is a component of a complex containing histone deacetylase and nucleosome remodeling activities", *Cell*, vol. 95, no. 2, pp. 279-289.

Zhang, Y., Ng, H.H., Erdjument-Bromage, H., Tempst, P., Bird, A. & Reinberg, D. 1999, "Analysis of the NuRD subunits reveals a histone deacetylase core complex and a connection with DNA methylation", *Genes & development*, vol. 13, no. 15, pp. 1924-1935.

Zhou, Y.B., Gerchman, S.E., Ramakrishnan, V., Travers, A. & Muyldermans, S. 1998, "Position and orientation of the globular domain of linker histone H5 on the nucleosome", *Nature*, vol. 395, no. 6700, pp. 402-405.

Zimmermann, S., Kiefer, F., Prudenziati, M., Spiller, C., Hansen, J., Floss, T., Wurst, W., Minucci, S. & Gottlicher, M. 2007, "Reduced body size and decreased intestinal tumor rates in HDAC2-mutant mice", *Cancer research*, vol. 67, no. 19, pp. 9047-9054.

Zippo, A., Serafini, R., Rocchigiani, M., Pennacchini, S., Krepelova, A. & Oliviero, S. 2009, "Histone crosstalk between H3S10ph and H4K16ac generates a histone code that mediates transcription elongation", *Cell*, vol. 138, no. 6, pp. 1122-1136.

Zou, Y.R., Sunshine, M.J., Taniuchi, I., Hatam, F., Killeen, N. & Littman, D.R. 2001, "Epigenetic silencing of CD4 in T cells committed to the cytotoxic lineage", *Nature genetics*, vol. 29, no. 3, pp. 332-336.

Zupkovitz, G., Grausenburger, R., Brunmeir, R., Senese, S., Tischler, J., Jurkin, J., Rembold, M., Meunier, D., Egger, G., Lagger, S., Chiocca, S., Propst, F., Weitzer, G. & Seiser, C. 2010, "The cyclin-dependent kinase inhibitor p21 is a crucial target for histone deacetylase 1 as a regulator of cellular proliferation", *Molecular and cellular biology*, vol. 30, no. 5, pp. 1171-1181.

Zupkovitz, G., Tischler, J., Posch, M., Sadzak, I., Ramsauer, K., Egger, G., Grausenburger, R., Schweifer, N., Chiocca, S., Decker, T. & Seiser, C. 2006, "Negative and positive regulation of gene expression by mouse histone deacetylase 1", *Molecular and cellular biology*, vol. 26, no. 21, pp. 7913-7928.

